

Paleoliquefaction Studies in Moderate Seismicity Regions with a History of Large Events

AVAILABILITY OF REFERENCE MATERIALS IN NRC PUBLICATIONS

NRC Reference Material

As of November 1999, you may electronically access NUREG-series publications and other NRC records at NRC's Library at www.nrc.gov/reading-rm.html. Publicly released records include, to name a few, NUREG-series publications; *Federal Register* notices; applicant, licensee, and vendor documents and correspondence; NRC correspondence and internal memoranda; bulletins and information notices; inspection and investigative reports; licensee event reports; and Commission papers and their attachments.

NRC publications in the NUREG series, NRC regulations, and Title 10, "Energy," in the *Code of Federal Regulations* may also be purchased from one of these two sources.

1. The Superintendent of Documents

U.S. Government Publishing Office
Washington, DC 20402-0001
Internet: bookstore.gpo.gov
Telephone: (202) 512-1800
Fax: (202) 512-2104

2. The National Technical Information Service

5301 Shawnee Road
Alexandria, VA 22312-0002
www.ntis.gov
1-800-553-6847 or, locally, (703) 605-6000

A single copy of each NRC draft report for comment is available free, to the extent of supply, upon written request as follows:

Address: **U.S. Nuclear Regulatory Commission**
Office of Administration
Multimedia, Graphics, and Storage &
Distribution Branch
Washington, DC 20555-0001
E-mail: distribution.resource@nrc.gov
Facsimile: (301) 415-2289

Some publications in the NUREG series that are posted at NRC's Web site address www.nrc.gov/reading-rm/doc-collections/nuregs are updated periodically and may differ from the last printed version. Although references to material found on a Web site bear the date the material was accessed, the material available on the date cited may subsequently be removed from the site.

Non-NRC Reference Material

Documents available from public and special technical libraries include all open literature items, such as books, journal articles, transactions, *Federal Register* notices, Federal and State legislation, and congressional reports. Such documents as theses, dissertations, foreign reports and translations, and non-NRC conference proceedings may be purchased from their sponsoring organization.

Copies of industry codes and standards used in a substantive manner in the NRC regulatory process are maintained at—

The NRC Technical Library

Two White Flint North
11545 Rockville Pike
Rockville, MD 20852-2738

These standards are available in the library for reference use by the public. Codes and standards are usually copyrighted and may be purchased from the originating organization or, if they are American National Standards, from—

American National Standards Institute

11 West 42nd Street
New York, NY 10036-8002
www.ansi.org
(212) 642-4900

Legally binding regulatory requirements are stated only in laws; NRC regulations; licenses, including technical specifications; or orders, not in NUREG-series publications. The views expressed in contractor prepared publications in this series are not necessarily those of the NRC.

The NUREG series comprises (1) technical and administrative reports and books prepared by the staff (NUREG-XXXX) or agency contractors (NUREG/CR-XXXX), (2) proceedings of conferences (NUREG/CP-XXXX), (3) reports resulting from international agreements (NUREG/IA-XXXX), (4) brochures (NUREG/BR-XXXX), and (5) compilations of legal decisions and orders of the Commission and Atomic and Safety Licensing Boards and of Directors' decisions under Section 2.206 of NRC's regulations (NUREG-0750).

DISCLAIMER: This report was prepared as an account of work sponsored by an agency of the U.S. Government. Neither the U.S. Government nor any agency thereof, nor any employee, makes any warranty, expressed or implied, or assumes any legal liability or responsibility for any third party's use, or the results of such use, of any information, apparatus, product, or process disclosed in this publication, or represents that its use by such third party would not infringe privately owned rights.

Paleoliquefaction Studies in Moderate Seismicity Regions with a History of Large Events

Manuscript Completed: January 2019

Date Published: June 2019

Prepared by:

M.P. Tuttle, L.W. Wolf, K. Dyer-Williams, P. Mayne,
R.H. Lafferty, K. Hess, M.E. Starr, M. Haynes,
J. Morrow, R. Scott, T. Busch, P. Villamor, J. Dunahue,
M. Rathgaber, K. Tucker, C. Karrenbauer, and C. Moseley

Rasool AnooShehpoor, NRC Project Manager

ABSTRACT

This report covers a multi-faceted paleoliquefaction project conducted between 2011 and 2018. The main focus of the report is the research component of the project, including a paleoliquefaction study in the New Madrid seismic zone (NMSZ) and surrounding region as well as post-earthquake survey for liquefaction features in the Central Virginia seismic zone following the 2011, magnitude (**M**) 5.7 Mineral, Virginia, earthquake. The report also summarizes two other components of the project including a NUREG/CR document and a training workshop on paleoliquefaction studies. NUREG/CR-7238 entitled, "Guidance Document: Conducting Paleoliquefaction Studies for Earthquake Source Characterization," captures today's best practices for conducting paleoliquefaction studies and includes an extensive bibliography. The training workshop was organized and held in the NMSZ for U.S. Nuclear Regulatory Commission (NRC) staff members and other members of the nuclear regulatory community.

The aim of paleoliquefaction research conducted in the NMSZ was to gather additional paleoliquefaction data that would help to reduce epistemic uncertainty in the seismic source model in this region, where seismic hazard is the highest in all of the central and eastern United States, and to evaluate the earthquake potential of other structural elements of the Reelfoot Rift system, including the Commerce Geophysical Lineament, the eastern and western Reelfoot Rift margins, and the Marianna area at the southern end of the eastern Reelfoot Rift margin. The research project involved conducting surveys for paleoliquefaction features in key areas that had not yet been systematically searched and constraining age estimates of previously and newly discovered sand blows to improve completeness of the paleoearthquake record in the region. Major discoveries include (1) a possible fault zone in western TN, delineated by northeast-oriented lineaments and large linear sand blows that formed during the A.D. 1811-1812 and A.D. 1450 New Madrid events; (2) sand blows near Paragould, AR, that suggest a previously unrecognized New Madrid earthquake about A.D. 0 ± 200 yr; (3) a sand blow near Blytheville, AR, that supports a previously recognized New Madrid earthquake about B.C. 1050 ± 250 yr and as one of three large earthquakes in a sequence; and (4) two to three generations of liquefaction features on Coldwater River in northwestern MS that may have formed during an ERM-S event in B.C. 300 ± 250 yr and/or during the Marianna events in B.C. 2850 ± 150 yr, B.C. 3550 ± 150 yr, or B.C. 4850 ± 150 yr. Overall, findings support prior interpretations that the NMSZ was the source of earthquake sequences in A.D. 1811-1812, A.D. 1450, and A.D. 900 and that the A.D. 1450 and A.D. 900 events included one or more earthquakes of **M** 7.5-7.8. With the addition of events in A.D. 0 ± 200 yr and B.C. 1050 ± 250 yr to the New Madrid earthquake chronology, an average recurrence time of ~1100 years is estimated for the period between 4400-1200 yr B.P. and of ~500 yr for the last 1200 years. However, given that sand blows that formed prior to the three most recent New Madrid events are still being found, it is likely that the paleoearthquake chronology is still incomplete prior to A.D. 900.

Following the 2011 **M** 5.7 Mineral, Virginia, earthquake, reconnaissance for liquefaction features was performed along 24 km of the South Anna River downstream from the epicenter. No modern liquefaction features were found either in the cutbanks or on the floodplains; however, possible paleoliquefaction features were found at eight sites along river. The dike sizes appeared to increase towards the east, suggesting that the paleoearthquake(s) responsible for their formation was larger, and/or located farther to the east, than the 2011 Mineral earthquake. This finding prompted a follow-on study supported by the National Earthquake Hazard Reduction Program managed by the U.S. Geological Survey. During that study, paleoliquefaction features were confirmed along the South Anna River and additional paleoliquefaction features found along other rivers in the region. The findings suggested that there were two paleoearthquakes in the

region during the past 4,500 years and that the older of the two events was of $M \geq 6$ and located farther to the east than the 2011 Mineral earthquake.

FOREWORD

The U.S. Nuclear Regulatory Commission (NRC) requires an evaluation to determine the Safe Shutdown Earthquake Ground Motion (SSE) for a nuclear power plant site as specified in 10 CFR Part 100. A performance-based approach to define site-specific earthquake ground motion is one component in the development and evaluation of the SSE. Regulatory Guide 1.208 provides guidance on this performance-based approach which implements a probabilistic seismic hazard analysis. The probabilistic seismic hazard analysis is dependent on the characterization of seismic (earthquake) sources, with the key parameters in characterizing seismic sources being their location, timing, and size. The historical record of measured earthquakes is limited; therefore, the study of prehistoric earthquakes is extremely valuable in characterizing seismic sources. The study of prehistoric liquefaction features, paleoliquefaction, is one method used to characterize seismic sources.

Regulatory Guide 1.208, A Performance-Based Approach to Define the Site-Specific Earthquake Ground Motion, and the Standard Review Plan for the Review of Safety Analysis Reports for Nuclear Power Plants: LWR Edition (NUREG-0800), Section 2.5.1, provides guidance to license applicants and NRC staff, respectively, on the review of seismic sources. This document provides updates on paleoliquefaction research in the New Madrid seismic zone (NMSZ), and to a lesser extent, the Central Virginia seismic zone (CVSZ), both of which serve as examples on how to conduct paleoliquefaction studies and to evaluate data with consideration of uncertainties encountered in the various phases of the study for seismic source characterization.

TABLE OF CONTENTS

ABSTRACT	iii
FOREWORD	v
TABLE OF CONTENTS	vii
LIST OF FIGURES	xi
LIST OF TABLES	xxix
EXECUTIVE SUMMARY	xxxiii
ACKNOWLEDGMENTS	xxxvii
ABBREVIATIONS AND ACRONYMS	xxxix
1 INTRODUCTION	1-1
2 NUREG/CR GUIDANCE DOCUMENT – TASK 1	2-1
3 TRAINING WORKSHOP – TASK 2	3-1
3.1 Workshop Presentations	3-2
3.2 Field Program	3-2
3.3 Workshop Wrap-Up: Discussion and Recommendations	3-3
3.3.1 Main Points.....	3-3
3.3.2 Recommendations for Research in Central and Eastern U.S.	3-3
4 PALEOLIQUEFACTION STUDIES IN MODERATE SEISMICITY REGIONS – TASK 3	4-1
4.1 Introduction	4-1
4.2 Methodology	4-1
4.2.1 Geological Methods	4-2
4.2.2 Geophysical Methods	4-3
4.2.3 Archaeological Methods.....	4-4
4.2.4 Geochronological Methods	4-5
4.2.5 Geotechnical Methods	4-7
4.3 Reconnaissance for Liquefaction Features Following the M 5.7, 2011, Mineral, Virginia, Earthquake	4-11
4.3.1 Introduction.....	4-11

4.3.2 Previous Paleoliquefaction Study	4-14
4.3.3 Results of Reconnaissance	4-14
4.3.4 Results of NEHRP-Funded Paleoliquefaction Study.....	4-15
4.4 Paleoliquefaction Study of the NMSZ and Surrounding Region.....	4-17
4.4.1 Background	4-17
4.4.2 NRC Project Plan	4-27
4.4.3 Revisiting Liquefaction Sites to Collect Additional Data and Samples.....	4-29
4.4.4 River Surveys to Identify Liquefaction Features in Key Areas	4-47
4.4.5 Site Investigations	4-90
4.4.6 Evaluation of Scenario Earthquakes.....	4-224
4.4.7 Summary and Discussion	4-239
4.4.8 Conclusion.....	4-258
4.4.9 Recommendations for Additional Research in the Greater New Madrid Region	4-261
5 REFERENCES	5-1
5.1 References for Main Body of Report and Archaeological Report (Appendix F).....	5-1
5.2 References for CEUS Paleoliquefaction Database	5-11
5.2.1 Charleston, South Carolina, Seismic Zone.....	5-11
5.2.1 New Madrid Seismic Zone	5-12
5.2.2 Marianna Area.....	5-15
5.2.3 St. Louis Region	5-15
5.2.4 New Madrid-Wabash Valley Region.....	5-15
5.2.5 Wabash Valley Seismic Zone	5-16
5.2.6 Central Virginia Seismic Zone.....	5-16
5.2.7 MA-NH Area	5-17
5.2.8 SE Quebec Region	5-17

5.3 References for CEUS Radiocarbon and OSL Dating Database	5-18
5.3.1 Charleston, South Carolina, Seismic Zone.....	5-18
5.3.2 New Madrid Seismic Zone	5-18
5.3.3 Marianna Area.....	5-21
5.3.4 St. Louis Region	5-21
5.3.5 New Madrid-Wabash Valley Region.....	5-21
5.3.6 Wabash Valley Seismic Zone	5-22
5.3.7 Central Virginia Seismic Zone.....	5-22
5.3.8 MA-NH Area.....	5-22
5.3.9 SE Quebec Region	5-22
APPENDIX A GEOLOGIC TIME SCALES	A-1
APPENDIX B FEDERAL REGULATIONS	B-1
APPENDIX C REVIEW OF FIELD DATA COLLECTION	C-1
APPENDIX D UPDATE OF CEUS PALEOLIQUEFACTION DATABASE	D-1
APPENDIX E CEUS RADIOCARBON AND OSL DATING DATABASES	E-1
APPENDIX F ARCHAEOLOGICAL REPORT FOR CARAWAY, WILDY, AND GARNER SITES	F-1
APPENDIX G EVALUATION OF SCENARIO EARTHQUAKES RESULTS TABLES	G-1

LIST OF FIGURES

Figure 4-1	Cross-Sectional Diagram Illustrating Sampling Strategies for Radiocarbon Dating and Age Estimation of Liquefaction Features (after NUREG-2115)	4-6
Figure 4-2	Illustrative sets of CRR curves for M 7.5 earthquakes for four in-situ tests: (a) standard penetration; (b) shear wave velocity; (c) cone penetration; and (d) flat plate dilatometer (after Schneider et al., 1998).....	4-8
Figure 4-3	Soil Behavioral Type for CPT Classification (after Robertson, 2004).....	4-10
Figure 4-4	Cyclic Resistance Ratio (CRR) for Evaluating Soil Liquefaction Potential from CPT	4-11
Figure 4-5	Map showing location of 23 August 2011 Mineral, Virginia, earthquake and its aftershocks relative to mapped piedmont faults and coastal faults, including Stafford fault system (from Powars et al., 2015).	4-12
Figure 4-6	Geologic map of epicentral area of 2011 M 5.7 Mineral, Virginia, earthquake and surrounding area, showing locations of sand blows that formed during that event as well as locations of possible paleoliquefaction features found in mid-1990s (gray squares) and during this study (black squares). Locations of towns and cities are indicated by black circles.	4-13
Figure 4-7	Photographs (left - unannotated; right - annotated) of paleoliquefaction features found along South Anna River downstream from sand blows that formed during 2011 M 5.7 Virginia earthquake. Lower in the section, the main dike is tabular and has distinct margins; higher in the section, the dike branches to form a sill and smaller dikes. The main dike appears to have intruded near-surface tubular root casts. Bioturbation and iron staining of their margins suggest that features are prehistoric in age. Black and white intervals on meter stick are 10 cm long.	4-15
Figure 4-8	Geologic map of the study region showing locations of the 2011 Virginia, earthquake sequence, small sand blows that formed in the epicentral area during that event, and paleoliquefaction features found during this and subsequent studies.	4-16
Figure 4-9	Earthquake magnitude-epicentral distance to liquefaction relation developed from worldwide liquefaction data set (modified from Castilla and Audemard, 2007).	4-17
Figure 4-10	Map of NM region, showing seismicity and major subsurface structural features, including Cottonwood-Ridgely fault system in western TN, and southeastern MO, Blytheville arch in northeastern AR, Reelfoot fault near New Madrid, MO, and Reelfoot rift margins (from NUREG-2115).....	4-18
Figure 4-11	Shaded relief map of NMSZ and surrounding region showing ages and measured sizes of earthquake-induced liquefaction features, previously recognized liquefaction field, inferred locations of historic earthquakes, and instrumental located earthquakes (modified from Tuttle et al., 2005). Note the location of Marianna about 80 km southwest of southern end of NMSZ.....	4-19

Figure 4-12	Generalized Surficial Geology Map of Mississippi River Alluvial Valley (modified from Saucier, 1994). MRF, Mississippi River Floodway.....	4-20
Figure 4-13	Diagram illustrating earthquake chronology for New Madrid seismic zone for past 5,500 years based on dating and correlation of liquefaction features at sites (listed at top) across region from north to south. Vertical bars represent age estimates of individual sand blows, and horizontal bars represent event times of 138 yr B.P. (A.D. 1811-1812); 500 yr B.P. (A.D. 1450 ± 150 yr); 1,050 B.P. (A.D. 900 ± 100 yr); and 4300 yr B.P. (2350 B.C. ± 200 yr) (from NUREG-2115).	4-22
Figure 4-14	Sand blow (upper photo - unannotated; lower - annotated) at site OR213 along Obion River near Midway, TN, composed of three sedimentary units separated by thin layers of silt (modified from Tuttle et al., 2002). Each unit probably formed as result of a large event in earthquake sequence. This sand blow is interpreted to have formed during 1811-1812 earthquakes. Dashed and dotted lines represent clear and inferred contacts, respectively. For scale, hoe is 1 m in length.....	4-24
Figure 4-15	Liquefaction fields for past three New Madrid events as interpreted from spatial distribution and stratigraphy of sand blows (from NUREG-2115). Liquefaction fields for 1811-1812 earthquakes are proportional in size to magnitudes derived by Bakun and Hooper (2004).....	4-25
Figure 4-16	Shaded relief map of Marianna area showing locations, estimated ages, and measured sizes of sand blows studied during previous NEHRP grants (modified from NUREG-2115).....	4-27
Figure 4-17	Map showing portions of rivers searched for earthquake-induced liquefaction features described in sections 4.4.3 and 4.4.4. Area of Figure 4-18 is outlined in black. Sources of earthquake information are cited in the figure explanation.	4-28
Figure 4-18	Map showing locations of site investigations of sand blows described in section 4.4.5.	4-29
Figure 4-19	Updated map of NMSZ and surrounding region showing ages and measured sizes of earthquake-induced liquefaction features studied during this project as well as previously studied liquefaction features, inferred locations of historic earthquakes, and instrumental located earthquakes (modified from NUREG-2115).	4-31
Figure 4-20	Map showing the surface projection of the Commerce geophysical lineament (horizontal hatch pattern) in northeastern Arkansas, southeastern Missouri, and southwestern Illinois (from Stephenson et al., 1999). Sites of paleoliquefaction found near the lineament (Vaughn, 1994) shown by triangles and areas of anomalous river drainage pattern identified along the Black and St. Francis Rivers (Fischer-Boyd and Schumm, 1995) shown by diagonal gray pattern. Seismicity from 1974-1995 shown by black dots.....	4-33

Figure 4-21	Map showing Quaternary deposits in the vicinity of Black, Current, St. Francis, and White Rivers along which survey for liquefaction features was performed (modified from Saucier, 1994; plates 4 and 6).	4-34
Figure 4-22	Map showing Quaternary deposits in the vicinity of the Obion River along which survey for liquefaction features was performed (modified from Saucier, 1994; plate 5).....	4-35
Figure 4-23	Photographs (upper - unannotated; lower - annotated) showing middle to upper part of sand dike intruding mottled silt exposed in cutbank at site CUR101a. Dike branches and narrows up section. Note iron staining and mottling of sand dike. Dashed lines represent clear contacts. For scale, white and black intervals on hoe represent 25 cm.....	4-38
Figure 4-24	Map showing liquefaction features along the Obion River and known geological structures that may have the potential to produce large earthquakes. Area outlined by black rectangle shown in Figure 4-55.	4-40
Figure 4-25	Photographs (left - unannotated; right - annotated) prior to cleaning of several dikes intruding mottled silt at OR507. The larger of the three dikes connected to the base of a sand blow in which a soil containing tree roots had formed. Dashed lines represent clear contacts; dotted lines represent inferred contacts.....	4-44
Figure 4-26	Photographs (upper - unannotated; lower - annotated) of two 23 cm wide sand dikes with multiple splays connected to the base of a large sand blow at OR601. The sand blow and dikes, that likely formed during the A.D. 1811-1812 earthquakes, are somewhat iron stained but otherwise showed no sign of soil development. Dashed lines represent clear contacts; dotted lines represent inferred contacts; solid lines represent clear contacts of sand blow units. Blue represents silt layer at top of sand blow unit. For scale, the black and white intervals on the meter stick represent 10 cm.	4-46
Figure 4-27	Map showing Quaternary deposits in the vicinity of the White and Coldwater Rivers along which survey for liquefaction features was performed (modified from Saucier, 1994; plate 7).....	4-49
Figure 4-28	Photograph showing pseudonodules at BR101. The smaller black and white intervals on the scale represent centimeters.....	4-50
Figure 4-29	Map showing liquefaction features along the Coldwater River downriver from the Arkabutla dam in northwestern Mississippi.	4-53
Figure 4-30	Photograph of small sand dike at CWR7. The black and white intervals on the meter stick represent 10 cm. S. Bastin points to the dike tip or termination.....	4-54
Figure 4-31	Photographs (left - unannotated; right - annotated) of two sand dikes at CWR9. Both dikes that were iron stained and cemented. The upper part of the dike that extends higher in the section is also bioturbated. Dashed lines represent clear contacts. The black and white intervals on the meter stick represent 10 cm.....	4-56

Figure 4-32	Photographs (upper - unannotated; lower - annotated) of site CWR12, showing source layers that liquefied at the base of the cutbank, sand dikes that crosscut overlying interbedded silt and sand layers and mottled silt, and sills that intrude along the basal contacts of silt layers. Dashed lines represent clear contacts; dotted lines represent inferred contacts. The black and white intervals on the meter stick represent 10 cm and those on the small scale next to dike termination represent 1 cm.	4-57
Figure 4-33	Photographs (left - unannotated; right - annotated) of portion of sand blow composed of two depositional units separated by a thin silt drape (blue), overlying a buried soil at LCD3. A 12-cm-thick soil A horizon had formed in the top of the sand blow and both depositional units, especially the upper one, exhibited iron staining. Radiocarbon dating of sample collected 1 cm below the sand blow provided a close maximum age of A.D. 1680, indicating that liquefaction features likely formed during the 1811-1812 A.D earthquake sequence. Dashed lines represent clear contacts; dotted lines represent inferred contacts. For scale, the shovel handle is 50 cm long.	4-60
Figure 4-34	Photographs (left - unannotated; right - annotated) showing large sand dike at LCD5. Development of a 24 cm soil in silt above the sand dike and soil lamellae within the top of the dike suggest that dike may have formed about 500 years ago, probably during the A.D. 1450 earthquakes. Dashed lines represent clear contacts; dotted lines represent inferred contacts; solid lines delineate flow structure and clast boundaries. Red and yellow intervals on shovel handle are 10 cm long.	4-62
Figure 4-35	Map showing liquefaction features along the St. Francis River and known geological structures that may have the potential to produce large earthquakes.	4-63
Figure 4-36	Map showing liquefaction features along the Chalk Bluff-Nimmons portion of the St. Francis River in northeastern Arkansas. Map area shown on Figure 4-35.	4-65
Figure 4-37	Photographs (left - unannotated; right - annotated) showing younger unweathered (grayish) dike intruding an older iron stained (reddish), larger sand dike at SFR8. Dashed and dotted lines represent clear and inferred contacts, respectively. Black and white intervals of meter stick represent 10 cm.	4-66
Figure 4-38	Photographs (left - unannotated; right - annotated) showing iron staining, mottling, and bioturbation in the upper part of older dike at SFR9. Dashed and dotted lines represent clear and inferred contacts, respectively. Shovel handle represents 50 cm.	4-67
Figure 4-39	Photograph of sand dike crosscutting mottled silt at site SFR12. Upper 1 m of dike is iron stained, mottled, and bioturbated. Black and white intervals of meter stick represent 10 cm.	4-68

Figure 4-40	Photographs (left - unannotated; right - annotated) showing sand dike originating in cross-bedded sand and forming dikes and sills at SFR16. Iron staining, mottling, and bioturbation occurs in the upper 1 m of an older dike. Dashed and dotted lines represent clear and inferred contacts, respectively. Black and white intervals represent 1 cm on small scale.....	4-71
Figure 4-41	Photograph showing relatively unweathered sand dikes at SFR15. Larger dike extends farther up section, where it splits to form two smaller dikes filled with small lignite clasts. Black and white intervals represent 10 cm on meter stick and 1 cm on small scale near split of dike into two smaller dikes.	4-72
Figure 4-42	Photographs (upper - unannotated; lower - annotated) showing sand dike originating in sand layer (left side) of interbedded silt and sand deposit, intruding adjacent silt, branching and extending up section at site SFR22. Black and white intervals on small scale represent 1 cm. Dashed lines represent clear contacts. Scale is placed adjacent to one of the dikes.	4-73
Figure 4-43	Photographs (left - unannotated; right - annotated) showing sand dike with blunt termination at SFR25. Large clasts of mottled silt appear to have collapsed into the dike from above. Horizontal layering as well as tubular flow structure occur within the dike. The upper part of the dike was iron stained, mottled, and contained small manganese nodules. Dashed lines represent clear contacts. Black and white intervals on hoe represent 25 cm.	4-74
Figure 4-44	Photographs (left - unannotated; right - annotated) showing sand dikes and sills originating in sand layer of interbedded silt and sand deposit at SFR31. Dashed lines represent clear contacts. M. Tuttle points to termination of dike 75 cm below the top of cutbank.	4-75
Figure 4-45	Map showing the Commerce geophysical lineament (CGL), Commerce fault zone (CF), and Commerce RLME fault zone in northeastern Arkansas and southeastern Missouri (from NUREG-2115). Sites of paleoliquefaction found near the lineament prior to this study indicated by red dots (Vaughn, 1994).....	4-76
Figure 4-46	Map showing liquefaction features along the Chalk Bluff-Fisk-Wilhelmina portion of the St. Francis River in southeastern Missouri. Map area shown on Figure 4-35.	4-78
Figure 4-47	Photographs (upper - unannotated; lower - annotated) showing very weathered sand dikes at SFR45. Dashed lines represent clear contacts. For scale, wooden handle of scraper is 36 cm long.	4-80
Figure 4-48	Photographs (left - unannotated; right - annotated) showing weathered sand dikes at SFR52. Dashed and dotted lines represent clear and inferred contacts, respectively. For scale, shovel handle is 25 cm long.	4-82
Figure 4-49	Photograph showing iron stained and cemented sand dike at SFR55. For scale, the cutbank is about 1.5-1.75 m high.....	4-83

Figure 4-50	Photograph of exposure along the White River near Oil Trough. At this site, recent silt overlies buried soil developed in silt underlain by interbedded silt and sand. No liquefaction feature was found at this or other sites despite conducive sedimentological conditions and very good to excellent exposure. For scale, the cutbank is about 4 m high.	4-84
Figure 4-51	Photograph of exposure along the White River near Clarendon. At this site, silt is underlain by interbedded silt and cross-bedded sand. For scale, shovel handle is 20 cm long.	4-86
Figure 4-52	Photographs (left - unannotated; right - annotated) of possible sand dikes originating in cross-bedded sand and intruding overlying mottled silt at WR105. Dashed and dotted lines represent clear and inferred contacts, respectively. Black and white intervals on meter stick represent 10 cm.	4-87
Figure 4-53	Photograph of Late Pleistocene sediment exposed at WR109. Pseudonodules shown in Figure 4-54 occur within interbedded sand and silt below the overhang (white arrow points to layer with pseudonodules). Portion of cutbank shown in photograph is 4.5-5.0 m high.	4-89
Figure 4-54	Photograph of pseudonodules in Late Pleistocene sediment exposed at WR109. For scale, white interval of meter stick is 10 cm long.	4-89
Figure 4-55	Enlargement of portion of shaded relief map of NMSZ and surrounding region, showing updated liquefaction data based on findings during this study, seismicity (red crosses), and previously recognized liquefaction field (white area) (modified from NUREG-2115). Area of enlargement shown on Figure 4-24.	4-92
Figure 4-56	Map of Quaternary deposits of portion of study area showing locations of selected study sites (modified from Saucier, 1994; plates 5 and 6). Faulkner and Wildy sites in AR, are located in Late Pleistocene valley-train deposits (light-brown unit - Pvl level 2; orange unit - Pvcl for relict channel deposits) of Mississippi River. Garner site in AR is located in Late Pleistocene valley-train deposits (brown unit - Pve level 3) just west of boundary with somewhat younger and lower terrace of Late Pleistocene valley-train deposits (light-brown unit - Pvl level 2; orange unit - Pvcl for relict channels). Stiles site in AR and Pritchett site in TN, are in located in Late Pleistocene valley-train deposits (light-brown unit - Pvl level 1) of Mississippi River but close to boundary with Holocene meander-belt deposits of Mississippi River (tan unit - Hpm 1 for point bar deposits; blue unit - Hchm for abandoned channels).	4-93
Figure 4-57	GE image of the Faulkner site, showing dark swath related to abandoned-channel deposit. Light-colored patches along the margins as well as within channel deposit are sand blows. Image acquired by US Geological Survey in April 2001.	4-95
Figure 4-58	Topographic map of Faulkner site, showing locations of point plotted artifacts, archeological site boundaries, geophysical grids, and paleoseismic trenches.	4-96

Figure 4-59	Layout of two resistivity survey grids at Faulkner (aka Caraway) site, AR. Grids consisted of multiple parallel profile lines, spaced at 5 m apart. Each line consisted of 24 electrodes at 2-m spacing. Distances indicate position along profile from first electrode. Numbers in circles indicate locations of paleoseismic trenches.	4-97
Figure 4-60	Composite resistivity images of Lines 1, 2 and 3 from Grid 1 at Faulkner site. Note view is to south.	4-99
Figure 4-61	Composite resistivity images of Lines 4, 5, and 6 from Grid 1 at Faulkner site. Note view is to the South.	4-100
Figure 4-62	Composite Resistivity Images of Lines 1, 2 and 3 from Grid 2 at Faulkner Site	4-101
Figure 4-63	Composite Resistivity Images of Lines 4, 5 and 6 from Grid 2 at Faulkner Site	4-102
Figure 4-64	Composite Resistivity Images of Lines 7, 8, and 9 from Grid 2 at Faulkner Site	4-103
Figure 4-65	Photograph of northwest wall of Trench 1 at Faulkner site, showing small iron-stained sand dike that pinched out at base of brownish soil and iron-stained sand blow above the soil. Dikes connected with base of sand blow in nearby Trench 2. For scale, shovel is 1 m long.	4-105
Figure 4-66	Log of Trench 2 at Faulkner site, showing sand blow and related sand dikes as well as radiocarbon and OSL dates on collected samples.	4-108
Figure 4-67	Photograph of southeast wall of Trench 2 at Faulkner site, showing large, sand- and clast-filled tubular structure below the base of the brownish soil, sand dikes emanating from the top of the structure, and iron-stained sand blow composed of two units (L1 and L2) with several v-shaped vent structures. For scale, wooden handle of scraper is 14 cm long.	4-109
Figure 4-68	Log of Trench 3 at Faulkner site, showing sand blow and related sand dikes as well as location of logs shown in Figure 4-69 and Figure 4-70.	4-111
Figure 4-69	Enlargement of western end of Trench 3 log at Faulkner site, showing sand blow and related sand dikes as well as OSL dates on sample of buried soil.	4-112
Figure 4-70	Paired photograph (A) and log (B) of portion of north wall of Trench 3 at Faulkner site, showing ~8 cm wide sand dike that intruded along tree root and sand blow that was deposited around tree trunk as well as radiocarbon dates on samples collected from the root and tree cast.	4-113
Figure 4-71	GE image of Wildy site, showing light-colored patches corresponding to sand blows. Large linear sand blow with northwest-oriented trend was selected for study. Image was acquired by US Geological Survey in January 2002.	4-117
Figure 4-72	Topographic map of Wildy site, showing locations of soil pits, geophysical grids, and paleoseismic trenches.	4-118

Figure 4-73	Layout of resistivity survey grid at Wildy site, AR, also showing positions of large northwest-oriented sand blow (shaded area), trench excavated through sand blow (solid black line), and portion of trench logged (open box).....	4-119
Figure 4-74	Composite Resistivity Images of Lines 4, 5, and 6 from Wildy Site	4-120
Figure 4-75	Composite Resistivity Images of Lines 4, 5, and 6 from Wildy Site	4-121
Figure 4-76	Resistivity Image of Lines 10 from Wildy Site	4-122
Figure 4-77	Photograph of northwest wall of Trench 1 at Wildy site, showing dipping surface of buried soil overlain by large sand blow, crosscut by a dark brown tree cast. For scale, trench is 16 m long and 2 m deep.	4-124
Figure 4-78	Log of Trench 1 at Wildy site, showing sand blow and related sand dikes as well as radiocarbon dates on collected samples.	4-125
Figure 4-79	Photographs (upper - unannotated; lower - annotated) of portion of sand blow shown in Figure 4-77 above large sand dike. Note flow lineations and large soil clast in the sand blow. Soil was displaced downward 90 cm across dike. Dashed and dotted lines represent clear and inferred contacts, respectively. Thin solid lines represent flow structure. For scale, red and yellow intervals on shovel handle are 10 cm long.	4-126
Figure 4-80	GE image showing location of Garner site outlined by solid white line, light-colored patches that cross site, and soil pits (indicated by blue flags) excavated in the patches to evaluate likelihood that they are sand blows. Fields have been graded making sand blows obvious. Lighthouse ditch is drainage south of site. Sand dikes were observed in banks of Lighthouse Ditch during reconnaissance of Late Pleistocene valley-train deposits in 2011. Satellite image was acquired by USDA Farm Service Agency on January 11, 2006.	4-129
Figure 4-81	Topographic map of Garner site and inset location map. Site map shows locations of soil pits, geophysical grid, archaeological site boundary, test units, point plotted artifacts, and proposed trench locations. Actual trench locations deviate from proposed locations as described in text.	4-130
Figure 4-82	Layout of resistivity survey grid at Garner site. Grid consisted of multiple parallel profile lines, spaced at 5 m apart. Each line consisted of 28 electrodes at 2-m spacing.	4-131
Figure 4-83	Composite Resistivity Images of Lines 1, 2, and 3 from Garner Site	4-133
Figure 4-84	Composite Resistivity Images of Lines 4, 5, and 6 from Garner Site	4-134
Figure 4-85	Photograph of Garner site (3CG1255). Field was fallow and visibility of ground surface was about 100%. View is towards northeast.....	4-135
Figure 4-86	Map of Garner site (3CG1255) showing location of controlled surface collection grid relative to geophysical survey area or grid, proposed trench locations, and archeological test units.	4-136

Figure 4-87	Points from Garner site (3CG1255), left to right, Early Archaic (possible Hardin) point, field specimen number (FSN) 29, Late Archaic stemmed point (FSN 37), two Late Archaic to Early Woodland expanding stem points (FSN 36, FSN 30).....	4-137
Figure 4-88	Artifact Density Map by Count of Chert Debitage at the Garner Site	4-139
Figure 4-89	Artifact Density Map by Count of Fire-Cracked Rock at Garner Site	4-139
Figure 4-90	Distribution of Retouched/Utilized Flakes at the Garner Site	4-140
Figure 4-91	Distribution of Chert Cores and Core Fragments at Garner Site.....	4-140
Figure 4-92	Garner Site, 3CG1255, Photograph of Test Unit 1, North Profile.....	4-141
Figure 4-93	Garner Site, 3CG1255, North and East-Wall Profile of Test Unit 1	4-141
Figure 4-94	Garner Site, 3CG1255, South- and West-Wall Profile of Test Unit 1	4-142
Figure 4-95	Chart showing the frequency of debitage and fire-cracked rock per level in Test Unit 1, Garner site (3CG1255).	4-143
Figure 4-96	Garner Site, 3CG1255, Photograph of Test Unit 2, North Profile.....	4-143
Figure 4-97	Garner Site, 3CG1255, North Wall Profile of Test Unit 2	4-144
Figure 4-98	Chart showing frequency of debitage and fire-cracked rock per level in Test Unit 2, Garner site (3CG1255).	4-145
Figure 4-99	Logs of Trenches 1 and 2 at Garner site, showing sand blows and related sand dikes, location of archeological test units excavated in the soil/cultural horizon buried by the sand blows, and radiocarbon and OSL dates on collected samples.....	4-147
Figure 4-100	Blister or surface mound that formed near Lincoln, southwest of Christchurch, during the 2010 M 7.1 Darfield, New Zealand, earthquake. Earthquake-induced liquefaction of subsurface sediment led to intrusion of dipping sand dikes (SD) into surface soil, lifting overlying soil to form blister. In this case, sand dikes reached ground surface and sand blow (SB) formed beside and on top of blister. Photograph by M. Tuttle.	4-148
Figure 4-101	3CG1255, Trench 1, TU 1, 5 cm below Base of Sand Blow	4-151
Figure 4-102	3CG1255, Trench 1, TU 1, 10 cm below and blow, showing increasing Fe-Mn concentration.	4-152
Figure 4-103	3CG1255, Trench 1, TU1, 15 cm below sand blow, showing fissures and/or root cast, with pronounced mottling or redoximorphic features.	4-152
Figure 4-104	3CG1255, Trench 1, TU 1, 20 cm below sand blow, fissure/root cast more pronounced but Fe-Mn concentration decreasing.	4-153
Figure 4-105	3CG1255, Trench 2, TU2, at 10 cm below Sand Blow.....	4-154
Figure 4-106	3CG1255, Trench 2, TU 2, 20 cm below Sand Blow.....	4-155
Figure 4-107	CG1255, Trench 2, TU 3, north wall and floor at 25 cm below sand blow, showing strata sloping from collapse after ejection of sand. 1: modern plow zone, 2: sand blow, 3: buried soil/cultural horizon.	4-156

Figure 4-108 3CG1255, Trench 2, TU3, at 25 cm below sand blow, unit excavated horizontally and so crosscutting sloping strata, shown by differential mottling.	4-156
Figure 4-109 3CG1255, Trench 2, TU 3, southeast corner of completed unit showing possible tree disturbance originating below sand blow.	4-157
Figure 4-110 3CG1255, Trench 2, TU 4, showings 50 cm x 50 cm fine-screen sample column in southwest corner.	4-158
Figure 4-111 3CG1255, Trench 2, TU 4, south wall, showing additional possible tree disturbance (soft, moist, dark stain in southeast corner).....	4-159
Figure 4-112 3CG1255, Trench 2, TU 5 completed at 25 cm below base of sand blow; backfilled 2013 test unit is visible to east/left.	4-160
Figure 4-113 Projectile point/knife bases from excavation. Left, 62 cmbs, top of old land surface; Right, TU 4, 5-10 below sand blow.	4-162
Figure 4-114 GE image showing location of Stiles site outlined by solid white line, light colored linear patches that cross site, and soil pits excavated during initial site visit to evaluate presence of sand blows. Pemiscot Bayou is drainage ditch south of site. Yarbro excavation, where historic and prehistoric sand blows were studied in 1990s, is located southeast of the Stiles site between Pemiscot Bayou and Route 150. Satellite image was acquired by USDA Farm Service Agency on October 14, 2010.....	4-165
Figure 4-115 Topographic map of Stiles site and inset location map. Site map shows locations of geophysical grids, archaeological test units, soil pits, and proposed trench locations. Actual trench locations deviate from proposed locations as described in text.....	4-166
Figure 4-116 Layout of resistivity survey grids at Stiles site. Grids consisted of multiple parallel profile lines, spaced at 5 m apart. Each line consisted of 28 electrodes at 2-m spacing.	4-167
Figure 4-117 Composite Resistivity Images of Lines 1, 2 and 3 from Grid 1 at Stiles Site.....	4-169
Figure 4-118 Composite Resistivity Images of Lines 4, 5, and 6 from Grid 1 at Stiles Site.....	4-170
Figure 4-119 Composite Resistivity Images of Lines 7 and 8 from Grid 1 at Stiles Site	4-171
Figure 4-120 Composite Resistivity Images of Line 1 from Grid 2 at Stiles Site	4-172
Figure 4-121 Composite Resistivity Images of Lines 2, 3, and 4 from Grid 2 at Stiles Site.....	4-173
Figure 4-122 Composite Resistivity Images of Lines 5, 6, and 7 from Grid 2 at Stiles Site.....	4-174
Figure 4-123 Photograph of Stiles location. Site was planted in north-south oriented rows of winter wheat and surface visibility was about 90%. View is towards southwest.....	4-175
Figure 4-124 Stiles Site, Photograph of North Profile of Test Unit 1, 0-30 cmbs.....	4-176
Figure 4-125 Stiles Site, Test Unit 1 North Profile, 0-30 cmbs.....	4-176

Figure 4-126 Stiles Site, Test Unit 2 North Profile, 0-46 cmbs.....4-177

Figure 4-127 Stiles Site, Photograph of Test Unit 3 North Profile, 0-40 cmbs.....4-178

Figure 4-128 Stiles Site, Test Unit 4, North Profile, 0-50 cmbs.....4-179

Figure 4-129 Logs of Trenches 1B and 1C at Stiles site, showing sand blows and related sand dikes. Radiocarbon dating of sample TR1b-S1 from top of buried soil suggests that overlying sand blow formed soon after B.C. 1010.....4-181

Figure 4-130 Photographs (upper - unannotated; lower - annotated) of vent area of compound sand blow above dike that crosscuts gray clayey soil in west wall of Stiles Trench 1C (see Figure 4-129). Note brown soil lamellae that formed in sand blow. Dashed lines represent clear contacts. For scale, black and white intervals on meter stick are 10 cm long.4-182

Figure 4-131 Log of Trench 2 at Stiles site, showing sand blows and related sand dikes. Radiocarbon dating of sample TR2-C2 from the top of the buried soil suggests that the overlying sand blow formed soon after A.D. 1450. Sample TR2-C4 probably from tree root that post dates the compound sand blow.4-184

Figure 4-132 Log of Trench 3 at Stiles site, showing sand blows and related sand dikes. Radiocarbon dating of samples C1 and C2 from the top of the buried soil suggest that the overlying sand blow formed soon after A.D. 1445-1465. This compound sand blow is similar in age to compound sand blow in nearby Trench 2.....4-186

Figure 4-133 Photographs (upper - unannotated; lower - annotated) of vent area with flow structure of compound sand blow above small dike in north wall of Stiles Trench 3 (see Figure 4-132). Dike observed in trench floor and lowermost trench wall did not connect with base of sand blow. Grayish brown soil and overlying units L1 (to left of small dike) and L2 of compound sand blow were offset across dike by 10 cm. Unit L1 was capped by silt and lignite and L2 was capped by silty, fine sand and lignite that fines away from dike to silty, very fine sand, and lignite. Dashed lines represent clear contacts. Thin solid white lines indicate flow structure. On scale, each black and white interval represents 1 cm.4-188

Figure 4-134 Map showing liquefaction features along the lower Obion River, including those at OR216/603 and the Pritchett site (P1-P4), previously mapped faults, including the Cottonwood Grove and Ridgely faults, and the postulated Obion River fault zone (indicated by two parallel dashed white lines).....4-191

Figure 4-135 GE image showing locations of the OR216/603 and Pritchett site as well as numerous lineaments along a zone extending from the old course of the Obion River near Midway to Chickasaw Bluffs northeast of Calvary, TN.4-192

Figure 4-136 Photograph of very large sand dike striking N35-46°E and overlying sand blow buried by fluvial deposits at Obion River 216 site. <i>In situ</i> tree trunk that yielded date of A.D. 1200-1320, A.D. 1350-1390 was in top of very dark brown soil to left of dike. Liquefaction features probably formed during A.D. 1450±150 yr earthquake(s). Large linear sand blows at Pritchett site southwest of Obion River 216 occur along strike of 1.6-m-wide dike.	4-193
Figure 4-137 GE image showing locations of Pritchett site outlined by solid white line, soil pits excavated during initial site visit to evaluate presence of sand blows, and Obion River 216 site northeast of Pritchett site. Light-colored linear patches are large sand blows and form lineaments that cross Pritchett site. Large sand dike at Obion River 216 has similar strike (N35-46°E) to and is along trend of northeast-oriented lineaments that cross western portion of site (red dashed lines). Other lineaments with north-northeastern trend cross eastern portion of site as well as field to east. Satellite image was acquired April 6, 1998, by USDA Farm Service Agency.....	4-194
Figure 4-138 Map of Pritchett site showing locations of scatter of historical artifacts near northern edge of site; subareas A and B; geophysical survey areas and GPR profiles within those subareas; Trench 3 relocated east of subarea A; and access routes and staging areas. Enlarged maps of subareas A and B are shown in Figure 4-139.	4-195
Figure 4-139 Pritchett site maps of Subareas A and B, showing locations of the geophysical survey area, GPR profiles, proposed trenches, and archaeological shovel tests. Trench 3 was located 80 m east of Trench 2 during fieldwork in fall of 2016.....	4-196
Figure 4-140 GPR profiles 1 and 2 collected across prominent sand blows at Pritchett site to verify presence of feeder dikes. On both profiles, strong dipping reflector represents contact between sand blow and underlying clayey soil and break in reflector represents feeder dike. Note ~0.5 m offsets of reflector across sand dike, which probably represents displacement of contact. Locations of profiles are shown on Figure 4-138 and Figure 4-139.....	4-197
Figure 4-141 Layout of north and south resistivity survey grids at Pritchett site. (A) North survey grid (Subarea A) consisted of three 96-m parallel profile lines, spaced at 5 m apart, with 48 electrodes at 2-m spacing. (B) South survey grid (Subarea B) consisted of four profile lines spaced at 5 m, with 24 electrodes at 2-m spacing.	4-198
Figure 4-142 Composite Resistivity Images of Lines 1, 2 and 3 from North Grid (Subarea A) Pritchett Site	4-200
Figure 4-143 Composite Resistivity Images of Lines 1 and 2 from South Grid (Subarea B) Pritchett Site	4-201
Figure 4-144 Composite Resistivity Images of Lines 3 and 4 from South Grid (Subarea B) Pritchett Site	4-202

Figure 4-145 View west in vicinity of Trenches 1 and 2 showing moderate to poor surface visibility (typically < 25%) at time of archeological surface survey.	4-203
Figure 4-146 Trench 1 shovel test profiles. Soil horizons: Ap (plow zone) 10YR4/3 loamy sand; C 10YR4/4 sand with clasts 10YR5/5; 2Ab (buried soil) 10YR6/2 clay.	4-205
Figure 4-147 Photo of Shovel Test 1	4-206
Figure 4-148 Trench 2 shovel test profiles. Soil horizons: Ap (plow zone) 10YR4/3 loamy sand; C 10YR4/4 sand with clasts 10YR5/5; 2Ab (buried soil) 10YR6/2 clay.	4-206
Figure 4-149 Photo of Shovel Test 5	4-207
Figure 4-150 Trench 3 shovel test profiles. Soil horizons: Ap (plow zone) 10YR4/3 loamy sand; C 10YR4/4 sand with clasts 10YR5/5; 2Ab (buried soil) 10YR6/2 clay.	4-207
Figure 4-151 Photo of Shovel Test 6	4-208
Figure 4-152 Trench 4 shovel test profiles. Soil horizons: Ap (plow zone) 10YR4/3-3/4 loamy sand; C 10YR5/4 coarse sand; 2Ab (buried soil) 7.5YR6/2-2.5YR6/0 clay.	4-208
Figure 4-153 Shovel Test 8.....	4-209
Figure 4-154 Shovel Test 9.....	4-210
Figure 4-155 Logs of Trenches 1 and 2 at Pritchett site, showing sand blows and related sand dikes. Radiocarbon dating of samples TR1-C1, TR1-C3, and TR2-C3 from buried soil suggest that overlying compound sand blows formed soon after A.D. 1450-1455.	4-213
Figure 4-156 Photographs (upper - unannotated; lower - annotated) of vent area of compound sand blow above 5-cm wide dike that crosscuts clayey soil in lower portion of south wall of Trench 1 at Pritchett site (see Figure 4-155). Note clast zones in vent area above sand dike. Dashed and dotted lines represent clear and inferred contacts, respectively. On scale next to dike, small black and white intervals represent 1 cm; black and white intervals on hoe are 10 cm long.	4-215
Figure 4-157 Photograph of Trench 2 at Pritchett site; view is slightly north of east. Larger dike and vent area are right (east) of hoe and smaller dike and vent area are left of hoe (see Figure 4-155). Compound sand blows are so large they are difficult to photograph in trenches. Also, low sun angle in November results in shadows in lower portion of trenches. For scale, black and white intervals on hoe are 10 cm long.....	4-217
Figure 4-158 Log of Trench 3 at Pritchett site, showing compound sand blow, related sand and lignite dikes, and vent structure. Radiocarbon dating of sample TR-C2 from buried soil suggests that overlying sand blow formed after A.D. 1440.	4-218

Figure 4-159	Photographs (upper - unannotated; lower - annotated) of portion of Trench 3 at Pritchett site showing sand dike crossing floor (to right of wooden handle of scarper) and lower portion of wall as well as overlying compound sand blow. Notice that clayey soil is displaced downward on left (east) side of dike relative to right side and that overlying compound sand blow, especially darker lower unit (L1), is thicker on left, filling in microtopography. Dashed lines represent clear contacts. For scale, black and white intervals on hoe are 10 cm long.....	4-219
Figure 4-160	Log of Trench 4 at Pritchett site, showing compound sand blow and related sand dikes. Radiocarbon dating of sample TR4-C5 from buried soil suggests that the overlying compound sand blow formed after A.D. 1660.....	4-222
Figure 4-161	Map of NMSZ and surrounding region, showing locations of historical earthquakes and RLMEs zones (from NUREG-2115) as well as borehole locations with geotechnical data used in liquefaction potential analysis.....	4-226
Figure 4-162	New Madrid earthquake chronology for past 5,500 years (from NUREG-2115), with events from Cox et al. (2006), Holbrooke et al. (2006), and results of site investigations from this project. New study sites listed at top across region from northeast to southwest. Vertical bars represent age estimates of individual sand blows, and horizontal bars represent event times of 138 yr BP (A.D. 1811-1812); 500 yr BP (A.D. 1450 ± 150 yr); 1,050 BP (A.D. 900 ± 150 yr); 1950 yr B.P. (A.D. 0 ± 200 yr); 3000 yr B.P. (B.C. 1050 ± 250 yr); and 4,300 yr BP (2350 B.C. ± 200 yr).....	4-247
Figure 4-163	Sand blow stratigraphy showing number and thickness of depositional units at previous sites (Tuttle et al., 2002) and new study sites, Faulkner, Stiles, and Wildy, for two offset sections along the southern and northern seismicity trends from southwest of Marked Tree, AR, to northeast Tiptonville, TN and from New Madrid, MO, to northeast of Charleston, MO. Vertical bars represent depositional units of individual sand blows, and horizontal lines represent New Madrid events, circa A.D. 1811-1812, A.D. 1450, and A.D. 900. The colored depositional unit might have formed during an earthquake in western TN. Site designations: L=Li, A=Amanda, Ar=Archway, Bg=Bugg, Br=Brooke, C=Central Ditch, D=Dodd, E=Eaker, ED=Eightmile Ditch, F=Faulkner, H=Hillhouse, J=Johnson, LD=Locust Creek Ditch, M=Marked Tree, S=Stiles, Y=Yarbro, W=Wildy. Earlier events are not shown since they are represented by few sand blows.	4-248

Figure 4-164	Sand blow stratigraphy showing number and thickness of depositional units at previous sites (Tuttle et al., 2002) and the Pritchett site, for a section parallel to and ~12 km east of the southern branch of the seismicity trend. Vertical bars represent depositional units of individual sand blows, and horizontal bars represent New Madrid events circa A.D. 1811-1812 and A.D. 1450. The colored depositional units might have formed during earthquakes centered in western TN. Site designations: FD=Forked Deer, L=Lowrance, H=Hatchie River, N=Nodena, O=Obion River, P=Pritchett, T=Tyronza. To date, none of the sand blows along this section can be unequivocally attributed to the A.D. 900 event. Earlier events are not shown since they are represented by few sand blows.....	4-252
Figure 4-165	Liquefaction fields for the past three New Madrid events as interpreted from spatial distribution and stratigraphy of sand blows (modified from Tuttle et al., 2002). The colored circles represent sand blows that formed during the A.D. 1811-1812 (red), A.D. 1450 (orange), and A.D. 900 (green) events and that are shown on Figure 4-19. Black circles indicate sand blows composed of 4 depositional units. Sand blows are shown relative to the preferred fault rupture scenario for the A.D. 1811-1812 earthquake sequence (from Johnston and Schweig, 1996). Earthquake magnitudes shown within 1811-1812 ellipses are those from Bakun and Hopper (2004).....	4-256
Figure 4-166	(A) Timeline showing timing of New Madrid events during the past 4,800 years. (B) Uncertainties in timing of New Madrid events leads to variability in estimates of their recurrence times. Average recurrence time for past three earthquake cycles is ~500 years and ~1100 years for the previous two earthquake cycles (modified from Tuttle et al., 2002).....	4-258
Figure A-1	Updated International Chronostratigraphic Chart (from Cohen et al., 2013).....	A-2
Figure A-2	Geologic column for the Quaternary period showing conceptual stages and generalized sea level curve indicating eustatic cycles (from Saucier, 1994).....	A-3
Figure C-1	Screenshot of MTA site form tested in GIS Kit app, showing site locations and attributes.	C-3
Figure C-2	Screenshot of MTA site form tested in GIS Kit app, showing site locations and geo referenced site photos.	C-4
Figure C-3	Comparison of Features Available in Garafa's GIS Pro and GIS Kit.....	C-5
Figure F-1	Faulkner Vicinity in 1977 (Ferguson 1979: Sheet 54)	F-2
Figure F-2	Google Earth Image of Faulkner (3CG1253 and 3CG1254) Vicinity, February 1997	F-3
Figure F-3	Google Earth Image of Faulkner (3CG1253 and 3CG1254) Vicinity, March 2001	F-3
Figure F-4	Google Earth Image of Faulkner (3CG1253 and 3CG1254) Vicinity, October 2010.....	F-4

Figure F-5	Google Earth Image of Faulkner (3CG1253 and 3CG1254) Vicinity, November 2013.....	F-4
Figure F-6	Wildy (3MS909) Vicinity ca. 1970 (Ferguson 1971: Sheet 24)	F-6
Figure F-7	Google Earth Image of Wildy (3MS909) Vicinity, April 1996.....	F-7
Figure F-8	Google Earth Image of Wildy (3MS909) Vicinity, January 2002	F-7
Figure F-9	Garner Vicinity in 1977 (Ferguson 1979: Sheet 6)	F-8
Figure F-10	Google Earth Image of Garner (3CG 1255) Vicinity, February 1994	F-9
Figure F-11	Google Earth Image of Garner (3CG 1255) Vicinity, February 2001	F-10
Figure F-12	Google Earth Image of Garner (3CG 1255) Vicinity, January 2006.....	F-10
Figure F-13	Google Earth Image of Garner (3CG 1255) Vicinity, October 2010.....	F-11
Figure F-14	Project Vicinity (Mitchell 1847)	F-17
Figure F-15	Project Vicinity (Colton 1855).....	F-17
Figure F-16	Project Vicinity (Cram 1876)	F-19
Figure F-17	Project Vicinity (Roeser 1878).....	F-19
Figure F-18	Project Vicinity (Hardesty 1883).....	F-20
Figure F-19	Project Vicinity (Cram 1887)	F-21
Figure F-20	Project Vicinity (Rand McNally 1889).....	F-22
Figure F-21	Project Vicinity (Branner 1889)	F-23
Figure F-22	Project Vicinity (Berthrong 1914)	F-24
Figure F-23	Project vicinity shown on Mississippi County soil survey (1914).....	F-25
Figure F-24	Project Vicinity (USGS 1916).....	F-25
Figure F-25	Caraway-Faulkner Vicinity (USDA 1916).....	F-26
Figure F-26	Garner Vicinity (USDA 1916)	F-27
Figure F-27	Project Vicinity (Cram 1920)	F-28
Figure F-28	Project Vicinity (Rand McNally 1921).....	F-29
Figure F-29	Project Vicinity (MidWest Map Co. 1931)	F-30
Figure F-30	Project Vicinity (USPO 1945).....	F-31
Figure F-31	Garner Site Project Vicinity (USGS Jonesboro 1958 and Leachville 1956).....	F-32
Figure F-32	Faulkner Site Project Vicinity (USGS Marked Tree 1956).....	F-32
Figure F-33	Wildy Site Project Vicinity on Manilla 1956 Quadrangle.....	F-33
Figure F-34	Project Vicinity Shown on 1983 Rivervale 7.5' Quadrangle	F-39
Figure F-35	Wildy Site Vicinity Shown on Manilla South 1983	F-40
Figure F-36	Wildy Site Barnes Series Ceramic Sherds	F-40
Figure F-37	Corner-Notched Base, cf. Dalton, 3CG1256	F-42

Figure F-38	Corner-Notched Dalton pp/k Base, 3CG1256	F-42
Figure F-39	Drill (Reworked pp/k?), 3CG1256	F-43
Figure F-40	Cores and Biface Preform, Archaic Period, 3CG1256, Right Possible Dalton adze	F-43
Figure F-41	Additional View of Core, 3CG1256	F-44
Figure F-42	Stemmed Points, Middle and/or Late Archaic Period, 3CG1256. Right, cf. Late Archaic Barbed.....	F-44
Figure F-43	Stemmed Point, Late Archaic Period, 3CG1256	F-45
Figure F-44	Stemmed Points, Late Archaic Period, 3CG1256. Left, cf. Gary	F-45
Figure F-45	Side-Notched Woodland Period pp/ks, 3CG1256. Right, similar to Jacks Reef	F-46
Figure F-46	Project Vicinity Shown on Dixie 7.5' Quadrangle (1983).....	F-47
Figure F-47	3CG1255, Trench 1, TU 1, 5 cm below Base of Sand Blow	F-49
Figure F-48	3CG1255, Trench 1, TU 1, 10 cm below Sand Blow, Showing Increasing Fe-Mg Concentration	F-49
Figure F-49	3CG1255, Trench 1, TU1, 15 cm below Sand Blow, Showing Fissures and/or Root Cast, with Pronounced Mottling	F-50
Figure F-50	3CG1255, Trench 1, TU 1, 20 cm below Sand Blow, Fissure/Rootcast more Pronounced but Fe-Mn Concentration Decreasing.....	F-51
Figure F-51	3CG1255, Trench 2, TU2, at 10cm below Sand Blow.....	F-52
Figure F-52	3CG1255, Trench 2, TU 2, 20 cm below Sand Blow.....	F-53
Figure F-53	3CG1255, Trench 2, TU 3, north wall and floor at 25 cm below sand blow, showing strata sloping from collapse after ejection of sand. A: modern plow zone, B: sand blow, C: buried land surface.	F-54
Figure F-54	3CG1255, Trench 2, TU3, at 25 cm below sand blow, unit excavated horizontally and so cross-cutting sloping strata, shown by differential mottling.	F-55
Figure F-55	3CG1255, Trench 2, TU 3, Southeast Corner of Completed Unit Showing Possible Tree Disturbance Originating below Sand Blow	F-56
Figure F-56	3CG1255, Trench 2, TU 4, showing 50 cm x 50 cm fine-screen sample column in southwest corner.	F-57
Figure F-57	3CG1255, Trench 2, TU 4, south wall, showing additional possible tree disturbance (soft, moist, dark stain in southeast corner) originating in/above sand blow.....	F-58
Figure F-58	3CG1255, Trench 2, TU 5 Completed at 25 cm below Base of Sand Blow	F-59
Figure F-59	Sketch of South Wall Trench 2, TU3, TU4, and TU5	F-60
Figure F-60	Projectile point/knife bases (cf. Snyders) from excavation. Left, 62 cmbs, top of old land surface; Right, TU 4, 5-10 cmbs.	F-62

Figure G-1	Results of liquefaction potential analysis for M 6.9 December 16, 1811 scenario earthquake at Marina-Lee #1 site, distance of 161 km. Original CPT sounding used in analysis is from Holzer, U.S. Geological Survey	G-21
Figure G-2	Results of liquefaction potential analysis for M 7.6 December 16, 1811 scenario earthquake at Marianna-Lee1 site, at distance 161 km. Original CPT sounding used in analysis is from Holzer, U.S. Geological Survey.....	G-22
Figure G-3	Results of liquefaction potential analysis for M 6.9 December 16, 1811 scenario earthquake at Wolf River site, distance of 104 km. Original CPT sounding used in analysis is from Schneider et al., 2001	G-23
Figure G-4	Results of liquefaction potential analysis for M 7.6 December 16, 1811 scenario earthquake at Wolf River site, distance of 104 km. Original CPT sounding used in analysis is from Schneider et al., 2001	G-24
Figure G-5	Results of liquefaction potential analysis at Wolf river site for M 6.9 on Eastern Rift margin-south and south river (picks) scenario earthquake at Wolf River site, distance of 60 km. Original CPT sounding used in analysis is from Schneider et al. (2001).....	G-25
Figure G-6	Results of liquefaction potential analysis at Wolf river site for M 6.9 on Eastern Rift margin-south and south river (picks) scenario earthquakes at Wolf River site, distance of 40 km. Original CPT sounding used in analysis is from Schneider et al. (2001).....	G-26
Figure G-7	Results of liquefaction potential analysis for M 7.1 on Eastern Rift margin-south and south river (fault) picks scenario earthquakes at Wolf River site, distance of 40 km. Original CPT sounding used in analysis is from Schneider et al. (2001).....	G-27

LIST OF TABLES

Table 4-1	Rivers Resurveyed and Liquefaction Sites Revisited (see Figure 4-10, Figure 4-11, Figure 4-17, Figure 4-19, Figure 4-20, Figure 4-21, and Figure 4-22)	4-30
Table 4-2	Radiocarbon Dating Results for Black River Sites.....	4-36
Table 4-3	Radiocarbon Dating Results for Current River Sites.....	4-37
Table 4-4	Radiocarbon Dating Results for Obion River Sites	4-42
Table 4-5	Optically Stimulated Luminescence Dating Results at Obion River Site OR507	4-44
Table 4-6	Rivers Surveyed for Liquefaction Features in Key Areas (Figure 4-10, Figure 4-11, Figure 4-19, Figure 4-20, Figure 4-21, and Figure 4-27).....	4-48
Table 4-7	Radiocarbon Dating Results for Black River Site.....	4-51
Table 4-8	Radiocarbon Dating Results for Coldwater River Sites	4-58
Table 4-9	Radiocarbon Dating Results for Locust Creek Ditch Sites	4-61
Table 4-10	Optically Stimulated Luminescence Dating Results at Locust Creek Ditch Site LCD3	4-61
Table 4-11	Radiocarbon dating results for St. Francis River sites between Chalk Bluff and Nimmons, Arkansas.....	4-69
Table 4-12	Radiocarbon Dating Results for St. Francis River Sites between Fisk and Wilhelmina, Missouri	4-79
Table 4-13	Optically Stimulated Luminescence Dating Results at St. Francis River Site StFR48	4-81
Table 4-14	Radiocarbon Dating Results for White River Sites	4-85
Table 4-15	Site Investigations (see Figure 4-56 for site locations)	4-90
Table 4-16	Cultural Periods, Time Spans, and Associated Diagnostic Artifacts (Modified from Lafferty, 1996; Tuttle et al., 1998).....	4-91
Table 4-17	Radiocarbon Dating Results for Faulkner (aka Caraway) Site	4-106
Table 4-18	Optically Stimulated Luminescence Dating Results for Faulkner Site.....	4-107
Table 4-19	Radiocarbon Dating Results for the Wildy Site	4-127
Table 4-20	Point Plotted and General Surface Artifacts.....	4-137
Table 4-21	Radiocarbon Dating Results for the Garner Site.....	4-149
Table 4-22	Optically Stimulated Luminescence Dating Results for the Garner Site	4-150
Table 4-23	3CG1255, Trench 1, TU 1 Artifact Recovery	4-153
Table 4-24	TU 2 Artifact Recovery.....	4-155
Table 4-25	TU 3 Artifact Recovery.....	4-157
Table 4-26	TU 4 Artifact Recovery.....	4-159
Table 4-27	TU 5 Artifact Recovery.....	4-160

Table 4-28	Radiocarbon Dating Results for the Stiles Site	4-183
Table 4-29	Site 1 Artifacts	4-204
Table 4-30	Radiocarbon Dating Results for the Pritchett Site.....	4-214
Table 4-31	Optically Stimulated Luminescence Dating Results for the Pritchett Site	4-216
Table 4-32	Scenario Earthquakes Evaluated Using Liquefaction Potential Analysis	4-225
Table 4-33	Distances (km) between Scenario Earthquakes or Source and Geotechnical Sites Used in analysis.....	4-228
Table 4-34	Locations of Geotechnical Data Used in Liquefaction Potential Analysis	4-229
Table 4-35	Summary of Results for M 6.9 December 16, 1811 Scenario Earthquake	4-230
Table 4-36	Summary of Results for M 7.6 December 16, 1811 Scenario Earthquake	4-231
Table 4-37	Summary of Results for M 7.0 January 23, 1812 Scenario Earthquake	4-232
Table 4-38	Summary of Results for M 7.5 January 23, 1812 Cscenario Earthquake	4-233
Table 4-39	Summary of Results for M 7.3 for February 7, 1812 Scenario Earthquake	4-234
Table 4-40	Summary of Results for M 7.8 for February 7, 1812 Scenario Earthquake	4-235
Table 4-41	Combined Results for M 7.6 December 16, 1811, M 7.5 January 23, 1812, and M 7.8 for February 7, 1812 Scenario Earthquakes	4-236
Table 4-42	Summary of Results for M 6.3 January 5, 1843 Scenario Earthquake	4-236
Table 4-43	Summary of Results for M 6.6 October 31, 1895 Scenario Earthquake	4-237
Table 4-44	Summary of Results for M 6.9 Commerce Fault Zone Scenario Earthquake	4-237
Table 4-45	Summary of Results for Eastern Rift Margin-North M 6.7 Scenario Earthquake South of Union City.....	4-238
Table 4-46	Summary of Results for Eastern Rift Margin-South M 6.9 Scenario Earthquakes West of Covington	4-238
Table 4-47	Summary of Results for Eastern Rift Margin-South M 6.9 Scenario Earthquakes Northwest of Memphis.....	4-238
Table 4-48	Summary of Results for Eastern Rift Margin-South M 7.1 Scenario Earthquakes Northwest of Memphis.....	4-238
Table 4-49	Summary of results for Eastern Rift margin-south river (fault) picks M 6.9 scenario earthquakes west of Memphis	4-238
Table 4-50	Summary of Results for Eastern Rift Margin-South River (Fault) Picks M 7.1 Scenario Earthquakes West of Memphis	4-238
Table 4-51	Summary of Results for Eastern Rift Margin-South River (fault) Picks M 6.9 Scenario Earthquakes near Tunica	4-238
Table 4-52	Summary of Results for Marianna Area Scenario Earthquakes.....	4-239
Table 4-53	Earthquake-Induced Liquefaction Features Studied along Rivers	4-241

Table 4-54	Earthquake-Induced Liquefaction Features at Study Sites	4-246
Table F-1	Population History Poinsett, Craighead, Greene and Mississippi Counties, Arkansas (Wikipedia).....	F-18
Table F-2	Archaic and Woodland Components in Poinsett, Craighead and Greene Counties.	F-33
Table F-3	Archaic and Woodland Components in Eastern Lowland Section of Poinsett, Craighead and Greene Counties.....	F-34
Table F-4	3CG1255, Trench 1, TU 1 artifact recovery	F-51
Table F-5	TU 2 artifact recovery	F-53
Table F-6	TU 3 Artifact Recovery	F-56
Table F-7	TU 4 Artifact Recovery	F-58
Table F-8	TU 5 Artifact Recovery	F-60
Table F-9	Bag List, 3 CG1255, 2015 Field Season.....	F-65
Table F-10	Artifact Tabulation.....	F-66
Table G-1	Results of Liquefaction Potential Analysis for M 6.9 and M 7.6 December 16, 1811 Scenario Earthquake	G-2
Table G-2	Results of Liquefaction Potential Analysis for M 7.0 and M 7.5 January 23, 1812 Scenario Earthquake	G-6
Table G-3	Results of Liquefaction Potential Analysis for M 7.3 and M 7.8 February 7, 1812 Scenario Earthquake	G-11
Table G-4	Results of Liquefaction Potential Analysis for M 6.3 January 5, 1843 Scenario Earthquake.....	G-15
Table G-5	Results of Liquefaction Potential Analysis for M 6.6 October, 31 1895 Scenario Earthquake.....	G-15
Table G-6	Results of Liquefaction Potential Analysis for Commerce fault zone M 6.9 scenario earthquake.....	G-16
Table G-7	Results of liquefaction potential analysis for Eastern Rift margin-north M 6.7 scenario earthquake.....	G-16
Table G-8	Results of liquefaction potential analysis for Eastern Rift margin-south M 6.9 scenario earthquake west of Covington	G-17
Table G-9	Results of liquefaction potential analysis for Eastern Rift margin-south scenario M 6.9 and M 7.1 earthquakes northwest of Memphis	G-17
Table G-10	Results of liquefaction potential analysis for Eastern Rift margin-south river (fault) picks M 7.1 scenario earthquake west of Memphis	G-18
Table G-11	Results of liquefaction potential analysis for Eastern Rift margin-south river (fault) picks M 6.9 scenario earthquake north of Tunisia	G-18
Table G-12	Results of liquefaction potential analysis for Marianna area M 6.7-M7.5 scenario earthquakes.....	G-19

EXECUTIVE SUMMARY

Paleoliquefaction, or the study of earthquake-induced liquefaction features preserved in the geologic record, provides valuable information about timing, location, and magnitude of large paleoearthquakes, particularly those with moment magnitude, **M**, greater than 6, during the past 50,000 years. Most paleoliquefaction studies have been conducted in intraplate geologic settings, but a few such studies have been carried out in interplate settings as well. In regions like the central and eastern United States (CEUS), where historical accounts of earthquakes date back only 300-400 years, paleoliquefaction studies provide a longer-term view of earthquake history. In the CEUS, paleoliquefaction studies have provided information that has been used in seismic source models of national probabilistic hazard maps and probabilistic seismic hazard analyses for nuclear facilities.

Although the results of paleoliquefaction studies have greatly increased the understanding of seismic hazards in several regions where Holocene (0.01 million years ago, or Ma, to present) and Late Pleistocene (0.126 to 0.01 Ma) age deposits occur, the specific type, level of detail, and quality of paleoliquefaction data vary from one study area to another. This variation is due, in part, to the lack of standardized procedures for paleoliquefaction studies. There is also a shortage of qualified and experienced paleoliquefaction experts and few comprehensive resources for new investigators or regulators interested in obtaining results from paleoliquefaction studies for characterizing earthquake sources and recurrence. This project advances the field of paleoliquefaction in several ways: by providing a NUREG/CR document on liquefaction studies; organizing a training workshop in paleoliquefaction studies for U.S. NRC staff; and conducting paleoliquefaction research in the New Madrid seismic zone (NMSZ) and surrounding areas, where seismic hazard is deemed the highest in the CEUS as well as searching for liquefaction features, or lack thereof, produced by the 2011, **M** 5.7 ± 0.1 Mineral, Virginia, earthquake.

This report summarizes information about NUREG/CR-7238 and the training workshop in Chapters 2 and 3, respectively, and covers, in detail, paleoliquefaction research in Chapter 4. Intended as a comprehensive resource for investigators and regulators interested in the field of paleoliquefaction, NUREG/CR-7238 includes background information on earthquake-induced liquefaction and related ground failures and on soft-sediment deformation features that may be preserved in the geologic record. It also reviews techniques used in paleoliquefaction studies, procedures for quantifying uncertainties of paleoliquefaction results, and approaches for incorporating paleoliquefaction data in seismic hazard assessments. The training workshop for NRC staff included classroom presentations on topics ranging from modern and historical analogues for interpreting paleoliquefaction features to incorporating paleoliquefaction data in probabilistic seismic hazard maps. In addition, the workshop included field trips to three liquefaction study sites. Workshop presentations are available as ML16221A590 and ML17019A240 through the Agency-wide Documents Access and Management System (ADAMS).

Most of this report is about the paleoliquefaction research conducted for this project. An introduction to the research and methodologies employed are presented in Sections 4.1 and 4.2. A review of the 2011 **M** 5.7 Mineral earthquake, reconnaissance for liquefaction features performed three months after the earthquake, and a follow-on study funded by National Earthquake Hazard Reduction Program (NEHRP) is given in Section 4.3. This is followed in Section 4.4 by detailed information about the NMSZ and the earthquake sequence of A.D. 1811-1812, the relationship between the NMSZ and the Reelfoot Rift, and previous paleoliquefaction studies conducted in the region. Field work, included reoccupying liquefaction sites to collect

additional data and samples for dating, searching river cutbanks to collect new information about liquefaction in key areas of interest, and conducting site investigations of sand blows are covered extensively in Sections 4.4.2-4.4.5. Evaluations of scenario earthquakes are summarized in Section 4.4.6 and results of liquefaction potential analysis performed for the evaluation are presented in figures and tables provided in Appendix G.

In Section 4.4.7, results of field work and various analyses are summarized, discussed, and interpreted in terms of timing, locations, magnitudes, and recurrence times of paleoearthquakes. The main advances and conclusions of the research are synthesized in the Section 4.4.8 and recommendations for additional research set forth in Section 4.4.9. For the convenience of the reader, geological time scales are provided in Appendix A. Federal regulations pertaining to the National Environmental Policy Act and the National Historic Preservation Act, and procedures developed during this project to comply with those regulations, are described in Appendix B. In addition, two hand-held data collectors were tested for their usefulness in paleoliquefaction data collection and management. The results of those tests are summarized in Appendix C. The information on liquefaction features studied during this project, as well as paleoliquefaction data that have become available in the past five years, were added to the CEUS paleoliquefaction database; the updated database is provided in Appendix D. Databases of radiocarbon and OSL results generated during this project, as well as readily available results from other regions, were created during this project and are presented in Appendix E. In addition, a detailed archeological report on the Caraway, Wildy, and Garner sites is provided in Appendix F. References for the main body of the report and the archeological report in Appendix F are in Section 5.1; references for the CEUS paleoliquefaction database, and CEUS radiocarbon and OSL databases are provided in Sections 5.2 and 3.3, respectively. A summary of results from paleoliquefaction research conducted during this project is provided below.

Paleoliquefaction research was aimed at reducing uncertainties in the mean recurrence time used in recent hazard models of large New Madrid earthquakes. In addition, the project sought to better understand the earthquake potential of seismic sources in the region surrounding the NMSZ and to evaluate migration of seismicity across the Reelfoot Rift system. In order to achieve these goals, surveys for liquefaction features were conducted along several rivers in the greater New Madrid region and detailed investigations were carried out at five sites within the New Madrid seismic zone. River segments and study sites were selected in key areas (Figures 4-17 and 4-18) that either had not yet been previously studied, that would help to constrain age estimates of previously and newly discovered sand blows, or that would improve completeness of the paleoearthquake record.

During the river surveys (Figure 4-17), many liquefaction features, including two to three generations of features, were found along the St. Francis River in northeastern AR, and southeastern MO. These are interpreted to have formed during the New Madrid events of A.D. 1811-1812, A.D. 1450, and A.D. 900. Along Locust Creek Ditch, also in northeastern AR, liquefaction features were found that likely formed during the A.D. 1811-1812 and A.D. 1450 New Madrid events. Similarly, liquefaction features that likely formed during the A.D. 1811-1812 and A.D. 1450 New Madrid events were found along the Obion River in western TN. No liquefaction features that predate the A.D. 900 New Madrid event were found in the Western Lowlands in the vicinity of the Commerce Geophysical Lineament. Similarly, no liquefaction features that predate the A.D. 1450 New Madrid event were found in western TN, in the vicinity of the eastern Reelfoot Rift margin. Two to three generations of liquefaction features that formed since 8340 yr B.P. were found along the Coldwater River in northwestern MS. These features probably were not related to New Madrid earthquakes. Instead Late Holocene features may have formed during the eastern Reelfoot Rift margin-south event of B.C. 300 and Middle Holocene features may have formed

during the Marianna events of B.C. 2850 ± 150 yr, B.C. 3550 ± 150 yr, or B.C. 4850 ± 150 yr. Few exposures of Late Pleistocene and Early Holocene deposits were found along the rivers surveyed and therefore limited our ability to assess the paleoearthquake record prior to 4000 yr B.P.

The detailed investigations at five sites (Figure 4-18; Garner, Faulkner, Wildy, Stiles, and Pritchett) involved review of surficial geology maps and aerial photographs and/or satellite imagery followed by site visits to locate sand blows in areas underlain by Late Pleistocene deposits, archaeological assessments of the presence or absence of intact cultural materials, geophysical surveys to profile the depth range of sand blows and to locate their feeder dikes, and excavation of selected sand blows to study the sand blows (e.g., number and thickness of depositional units, orientation of dikes and amount and style of ground failure) and to collect samples for dating. At the Garner site near Paragould, AR, weathered sand blows that buried a soil that contained Middle Woodland (A.D. 200-B.C. 200) artifacts likely formed in A.D. 0 ± 200 yr. Other sand blows, including one at the Eaker 2 site near Blytheville, AR, formed about the same time. These sand blows in the St. Francis Basin suggest that a previously unrecognized New Madrid earthquake may have occurred about A.D. 0. At the Faulkner site north of Marked Tree, AR, two generations of sand blows formed during the A.D. 1811-1812 and A.D. 1450 New Madrid events; at the Wildy site southwest of Blytheville, AR, a sand blow and large feeder dike formed during the A.D. 1450 New Madrid event. At the Stiles site near Blytheville, AR, two sand blows also formed during the A.D. 1450 New Madrid event, one of which was very large, northwest oriented, and composed of five depositional units. A third sand blow at the site was weathered, composed of three depositional units, and formed soon after B.C. 1010. The latter, in combination with another sand blow at Eaker 2, supports a previous finding from a river morphology study that there was a New Madrid earthquake about B.C. 1050 ± 250 yr. Results from the Stiles site suggest that the B.C. 1050 event was one of several large earthquakes in a sequence. At the Pritchett site southwest of Dyersburg, TN, three northeast-oriented sand blows formed during the A.D. 1450 New Madrid event. A fourth sand blow with a north-northeast orientation, formed during the A.D. 1811-1812. The sand blows at the site help to define, and occur along, a 32-km long, northeast-oriented zone of lineaments that might be the surface expression of an active fault zone.

The results of the river surveys and site investigations support prior interpretations that the New Madrid seismic zone was the source of three very large earthquakes in A.D. 1811-1812, A.D. 1450, and A.D. 900. Given the similarity in distribution and stratigraphy of sand blows that formed during the prehistorical and historical events, the A.D. 1450 and A.D. 900 earthquakes were likely similar in magnitude to the A.D. 1811-1812 earthquakes. Based on the evaluation of scenario events, the A.D. 1450 and A.D. 900 events likely included one or more earthquakes in the **M** 7.5-7.8 range (± 0.25 - 0.5 of a magnitude unit). The NMSZ is interpreted as the likely source of at least one large earthquake that induced liquefaction in the St. Francis Basin in A.D. 0 ± 200 yr and B.C. 1050 ± 250 yr, though additional information about both events would add confidence to this interpretation and help to identify their seismogenic sources. Previously, a recurrence time of about 500 yr for the past 1200 years was estimated for New Madrid events. This estimate is supported by additional liquefaction evidence for the A.D. 1450 event gained during this study. With the addition of the A.D. 0 and B.C. 1050 yr events to the New Madrid chronology, an average recurrence time of ~ 1100 years is estimated for the period between 4400-1200 yr B.P. However, it is likely that the paleoearthquake chronology is still incomplete prior to A.D. 900. Therefore, the recurrence time of 1100 years should be viewed as a maximum value for the 4400-1200 yr B.P. time period.

During the course of this project, the 2011, **M** 5.7 ± 0.1 Mineral, Virginia, earthquake struck the Mid-Atlantic region about 23 km southwest of the North Anna nuclear power station and 130 km

southwest of Washington, D.C. The earthquake is the largest earthquake in the Central Virginia seismic zone (CVSZ) during the historical period and raised concerns about the earthquake potential of the region. During the first few days following the earthquake, four small sand blows, which may have formed above animal burrows, were found in the stream bed and on the floodplain of the South Anna River in the epicentral area. The event thus provided an opportunity to document liquefaction induced by a moderate earthquake in the eastern United States. A decision was made to conduct post-earthquake survey for liquefaction features in the epicentral area as part of this project. The survey was conducted three months after the earthquake and involved searching river cutbanks and adjacent floodplains for 24 km of the South Anna River downstream from the earthquake epicenter. Despite careful looking, no additional modern liquefaction features were found. Small sand blows, like those documented within days of the earthquake may have been removed by a series of floods that occurred during the three months following the earthquake. However, paleoliquefaction features (i.e., sand dikes that have lateral continuity, branch upward, and are filled with sandy sediment containing clasts of the host deposit) were found at eight sites along the South Anna River river. Although it was a small sampling from which to draw definitive conclusions, the dike sizes appeared to increase towards the east, suggesting that the paleoearthquake(s) responsible for their formation may have been larger, and/or located farther to the east, than the 2011 **M** 5.7 Mineral earthquake. On the basis of this finding, a follow-on paleoliquefaction study was funded by NEHRP. During that study, systematic surveys of cutbank exposures were conducted along 119 km of six rivers, including the James, Mattaponi, North Anna, Pamunkey, Rivanna (and tributary Stigger Creek), and South Anna Rivers. Paleoliquefaction features were confirmed on the South Anna Rivers and Stigger Creek and fifteen additional features were found along the James, Mattaponi, and Pamunkey Rivers. The new observations supported the interpretations made during the initial post-earthquake survey. In addition, they observations suggested that there were two paleoearthquakes in the region during the past 4,500 years and that the older of the two events was of **M** ≥ 6 and located farther to the east than the 2011 Mineral earthquake.

ACKNOWLEDGMENTS

This multi-faceted project is sponsored by the U.S. Nuclear Regulatory Commission (NRC) under contract NRC-HQ-11-C-04-0041. The views and conclusions contained in the document are those of the authors and should not be interpreted as necessarily representing the official policies of the U.S. Government. Many thanks to Thomas Weaver, Sarah Tabatabai, and Rasool Anooshehpour who served as Project Managers at different times and provided valuable guidance and support during the course of the project. Others who encouraged the development and performance of this project include Annie Kammerer, Jon Ake, and Russ Wheeler. Numerous people participated in and contributed to different aspects of the project, including the development of a document on paleoliquefaction studies, organization of a training workshop in paleoliquefaction for NRC staff, and paleoliquefaction research primarily in the New Madrid seismic zone and surrounding region.

Co-authors of NUREG/CR-7238 entitled, "Guidance document: Conducting paleoliquefaction studies for earthquake source characterization," include Martitia Tuttle, Lorraine Wolf, Paul Mayne, Kathleen Dyer-Williams, and Robert Lafferty. Thomas Holzer contributed to the section on the liquefaction potential index. Others who helped with editing and map making include Taylor Busch, Caroline Moseley, Cameron Schroeder, and Kathleen Tucker. Reviewers Gail Atkinson, Russell Green, Thomas Holzer, Shannon Mahan, Julie Morrow, Alice Stieve, Gerry Stirewalt, Sarah Tabatabai, and Thomas Weaver provided comments and suggestions that improved the document.

The training workshop was organized by Martitia Tuttle and chaired by Lorraine Wolf and Martitia Tuttle. Kathleen Dyer-Williams, Jake Dunahue, Marion Haynes, and Pilar Villamor assisted with other aspects of the workshop including logistics, preparation of liquefaction sites, and presentations during the field trips. Presentations were given by Heather DeShon, Kathleen Dyer-Williams, Steven Forman, Russell Green, Darden Hood, Paul Mayne, Chuck Mueller, Haydar Al-Shukri, Mary Evelyn Starr, Martitia Tuttle, Pilar Villamor, Thomas Weaver, and Lorraine Wolf. Electronic files of workshop presentations are available through the Agency-wide Documents Access and Management System as ML16221A590 and ML17019A240.

The research component of the project, reported on in detail in this document, involved river surveys, site investigations, and various types of analyses. Martitia Tuttle as PI was responsible for managing the project and was also the lead on the paleoliquefaction aspects of the project. Robert Lafferty, Lorraine Wolf, and Paul Mayne were leads on archaeological, geophysical, and geotechnical aspects of the project, respectively. Taylor Busch, Marion Hayes, Alex MacKay, Sarah Tabatabai, and Martitia Tuttle, as well as Sarah Bastin and Monica Giona Bucci visiting from New Zealand, participated in searches for liquefaction features. Taylor Busch, Jake Dunahue, Kathy Hess, Robert Lafferty, Kathy Hess, Marion Haynes, Julie Morrow, Mary Evelyn Starr, Michelle Rathgaber, Robert Scott, Mert Su, Martitia Tuttle, Pilar Villamor, and Lorraine Wolf, and several Auburn University students participated in site investigations. Robert Scott made maps for the Faulkner, Garner, Stiles, Pritchett, and Wildy sites, and Michelle Rathgaber made the map for the Pritchett site. We are grateful to the property owners and farmers of the Faulkner, Garner, Stiles, Pritchett, and Wildy sites for granting us permission to work on their land. Kathleen Dyer-Williams and Paul Mayne collaborated on the liquefaction potential analysis. State Departments of Transportation in Arkansas, Illinois, Mississippi, Missouri, and Tennessee, Paul Mayne of Georgia Institute of Technology, and Tom Holzer of the US Geological Survey provided geotechnical data used in the analysis. Beta Analytic performed radiocarbon dating and Steven Forman and Shannon Mahan performed optically stimulated luminescence. Darden Hood of Beta

Analytic researched and provided information about samples dated more than ten years ago so that these data could be included in the radiocarbon database (Appendix E). Taylor Busch, Kathleen Dyer-Williams, Robert Lafferty, Paul Mayne, Julie Morrow, Robert Scott, Mary Evelyn Starr, Martitia Tuttle, and Lorraine Wolf contributed to various sections of the report. Mary Evelyn Starr, with input from Robert Lafferty, wrote the archaeological report for the Caraway, Wildy, and Garner sites in Appendix F. Kathy Tucker made project maps and report figures within a GIS framework. Cameron Karrenbauer, Caroline Moseley, Kathy Tucker, and Martitia Tuttle worked on the CEUS paleoliquefaction database as well as the CEUS radiocarbon and optically stimulated luminescence databases. Kathy Hess, Cameron Karrenbauer, Caroline Moseley, and Lorraine Wolf edited significant portions of the report. Many thanks to Rasool Anooshehpour, Gerry Stirewalt, Luisette Candelario, and Thomas Weaver for reviewing this very long report.

ABBREVIATIONS AND ACRONYMS

ADAMS	Agency-wide Documents Access and Management System
AGI	Advanced Geosciences Inc.
AMS	Accelerator mass spectrometry
AWL	Above water level
BTC	below top of cutbank
BR	Black River
CERI	Center of Earthquake Research and Information
CEUS	Central and Eastern United States
CFZ	Commerce fault zone
CGL	Commerce Geophysical Lineament
cmbs	cm below surface
CPT	Cone-penetration test
CRR	Cyclic resistance ratio
CSC	Controlled surface collection
CSR	Cyclic stress ratios
CVSZ	Central Virginia seismic zone
CW	Coldwater River
EPRI	Electric Power Research Institute
ER	Electrical resistivity
ERM	Eastern Reelfoot Rift margin
ERM-N	Eastern Reelfoot Rift margin-north
ERM-S	Eastern Reelfoot Rift margin-south
ERM-SCC	Eastern Reelfoot Rift margin-south Crittenden County
ERM-SRP	Eastern Reelfoot Rift margin-south river (fault) picks
FSN	Field Specimen Number
FCR	Fire-cracked rock
GE	Google Earth
GMPE	Ground motion prediction equations
GDRL	Geoluminescence Dating Research Laboratory
GPR	Ground-penetrating radar
ICP-MS	Inductively coupled plasma-mass spectrometry
LCD	Locust Creek Ditch
MA	Marianna area
MMI	Modified Mercalli Intensity
MTA	M.Tuttle & Associates
NEHRP	National Earthquake Hazard Reduction Program
NMSZ	New Madrid seismic zone
M, M_w	Moment magnitude
MRF	Mississippi River Floodway
NRC	Nuclear Regulatory Commission
NRHP	National Register of Historic Places
OR	Obion River
OSL	Optically stimulated luminescence
Ppk	Projectile point/knives
PGA	Peak ground acceleration
RLME	Repeated large magnitude earthquakes

SAR	Single aliquot regeneration
SFR	St. Francis River
SHPO	State Historic Preservation Office
SPT	Standard penetration test
SSC	Seismic source characterization
TL	Thermal luminescence
TU	Test unit
WR	White River
WRM	Western Reelfoot Rift margin

1 INTRODUCTION

Paleoliquefaction studies focus on soft-sediment deformation structures and related ground failures resulting from earthquake-induced liquefaction and preserved in the geological record. Paleoliquefaction studies are inherently regional in scope, requiring observations and interpretations of liquefaction features at many sites over a large area, and provide information about the timing, location, magnitude, and recurrence times of paleoearthquakes, particularly those of moment magnitude, **M**, greater than 6, that occurred during the past 50,000+ years. Paleoliquefaction has emerged as a significant contributor to the understanding of earthquake hazard in the intraplate settings of the Central and Eastern United States (CEUS) and southeastern Canada where active faults rarely rupture the ground surface and where the recurrence time of large earthquakes is longer than the historic record of seismicity. Increasingly, paleoliquefaction studies are being conducted in interplate settings, where recent earthquakes, such as the 22 February 2011, **M** 6.2, earthquake in Christchurch, New Zealand, induced liquefaction over large areas but were not associated with surface ruptures.

Recognizing their usefulness for extending the record of earthquakes back in time by thousands to tens of thousands of years, paleoliquefaction data were used in the seismic source models for the CEUS seismic source characterization (SSC) for nuclear facilities (NUREG-2115). As part of the CEUS SSC project, a paleoliquefaction database including all major regional datasets was developed and a technical report written that summarized the state of knowledge for each region and reviewed uncertainties associated with the identification and interpretation of earthquake-induced liquefaction features (NUREG-2115). During the course of that effort, it became evident that the type, level of detail, and quality of paleoliquefaction data are uneven from one region to another and that significant uncertainties remain, even in regions where large paleoearthquakes have been recognized, largely related to insufficient data.

This project was designed to rectify some of the shortcomings identified during the CEUS SSC paleoliquefaction effort. The project objectives are three-fold: to standardize procedures used in paleoliquefaction studies, to provide guidance for those who wish to conduct or evaluate paleoliquefaction studies, and to reduce uncertainties in the recurrence estimates and source model for an intraplate region where large paleoearthquakes have been previously identified. To achieve these objectives, the project included three main tasks including the following: Task 1 - the development of a NUREG/CR document, Task 2 - a training workshop for the Nuclear Regulatory commission (NRC) staff members and other members of the nuclear regulatory community, and Task 3 - paleoliquefaction research in the New Madrid seismic zone (NMSZ) and surrounding region.

Three months after the project began, the 23 August 2011, **M**, 5.7 ± 0.1 Mineral, Virginia, earthquake, occurred 130 km southwest of Washington, D.C. and only 23 km southwest of the North Anna nuclear power plant. There were early reports that sand blows had formed in the epicentral area of the earthquake. Responding to the opportunity presented by the Mineral, Virginia, earthquake, post-earthquake survey for liquefaction features was added to Task 3. The goals of the survey were to document liquefaction features that formed during the moderate earthquake and to compare these features with paleoliquefaction features previously found in the Central Virginia seismic zone (CVSZ). Also, development of a radiocarbon and optically stimulated luminescence (OSL) database for CEUS liquefaction sites was added to Task 3. The radiocarbon and OSL database complement the CEUS paleoliquefaction database developed during the CEUS SSC project, providing the actual data on which age estimates of liquefaction features are based in the paleoliquefaction database.

2 NUREG/CR GUIDANCE DOCUMENT – TASK 1

NUREG/CR-7238 entitled, “Guidance document: Conducting paleoliquefaction studies for earthquake source characterization,” was prepared as part of this project. The primary goal of the document is to provide detailed and practical guidance for conducting paleoliquefaction studies that result in high-quality data for use in seismic source characterization and seismic hazard assessment. Towards this end, the document includes a review of geological, geophysical, and geotechnical techniques used in paleoliquefaction studies, procedures for quantifying uncertainties of paleoliquefaction results, and approaches for incorporating paleoliquefaction data in seismic hazard assessment. The intended audience includes geoscientists who want to learn about paleoliquefaction studies, government and consulting personnel who want to use paleoliquefaction data in seismic hazard assessments, regulators who want to evaluate the results of specific studies, and paleoliquefaction practitioners planning future research and studies. The document was written by an interdisciplinary team with more than ninety years of combined experience in paleoliquefaction and the related fields of paleoseismology, Quaternary geology, structural geology, neotectonics, seismology, geophysics, geotechnical engineering, archaeology, and soil science. The document went through an extensive review by NRC staff as well as an external reviewer. The final version of the report was submitted in June 7, 2016 and was published in January 2018.

As mentioned in the Introduction, the development of the NUREG document was conceived during the CEUS seismic source characterization (SSC) project, a multi-year project, funded by the Electric Power Research Institute (EPRI), the U.S. Department of Energy, and the NRC, and completed in 2012. The NUREG document was designed as a comprehensive resource for investigators and regulators and intended to help standardize methodologies, to promote paleoliquefaction studies in areas where new or additional data are needed to better characterize seismic sources, and to encourage further development of the field through multidisciplinary research.

The document presents background information on paleoseismology, earthquake-induced liquefaction and related ground failures, and soft-sediment deformation structures that form as a result of liquefaction. It also provides guidance on all aspects of paleoliquefaction studies, including selection of study areas and the various types of information that should be consulted, performance of site investigations and surveys of river cutbanks and other exposures, relative and absolute dating techniques used to constrain ages of liquefaction features and thus important for estimating the timing and recurrence of paleoearthquakes, and geological and geotechnical approaches to estimating source areas and magnitudes of paleoearthquakes. The report identifies factors that contribute to uncertainty in paleoliquefaction data and observations and analyses that can help to reduce those uncertainties. In addition, procedures are described for the quantification and expression of uncertainty in estimates of timing, location, magnitude, and recurrence of paleoearthquakes.

The NUREG document includes a discussion of the use of paleoliquefaction data in seismic hazard assessment through the development of regional seismic source models. An example is given of a paleoliquefaction study conducted in the NMSZ and the use of the resulting paleoliquefaction data in seismic source models of the NMSZ. The document concludes with recommendations for future research, including case studies of liquefaction induced by recent earthquakes, geophysical methods for mapping buried sand blows and sand dikes, and geotechnical *in situ* testing devices and procedures, as well as improved methodologies, for assessing liquefaction potential. In addition, there are five appendices that present recent

advances in understanding earthquake-induced liquefaction and ground deformation, the data form used to record information during documentation of liquefaction features and sites, and the archaeological excavation protocol used at paleoseismic sites where cultural materials are present.

3 TRAINING WORKSHOP – TASK 2

The primary goals of the workshop were to provide training for NRC staff and other members of the nuclear regulatory community on various aspects of paleoliquefaction studies including collection and interpretation of geological, geophysical, and geotechnical data and their use in seismic source characterization and to promote discussion on various aspects of paleoliquefaction studies among investigators and regulators. The training workshop took place on November 10-13, 2015 in the NMSZ, where paleoliquefaction research had been conducted in the past and where liquefaction sites were under investigation as part of this NRC-funded project (Task 3). The New Madrid region, which hosts a broad range of liquefaction features from compound, very large sand blows and related feeder dikes in the NMSZ proper to small sand dikes at distal sites and soft-sediment deformation structures in their source layers, is an excellent learning laboratory for the training workshop.

The workshop included classroom presentations on a range of pertinent topics. The titles of the presentations and the experts who delivered them are listed below. In addition, there were daily field trips to liquefaction sites, where aerial photographs and satellite images were reviewed, cultural history discussed, examples of artifacts viewed, electrical resistivity and ground-penetrating radar surveys demonstrated, liquefaction features including sand dikes and sand blows examined, and dating strategies and sampling techniques debated. A canoe trip along a portion of the St. Francis River where sand dikes and source beds were exposed had been planned for the workshop. However, the canoe trip had to be abandoned due to a rainstorm the day before that dropped several inches of rain resulting in high river level, which covered the liquefaction sites. Instead, the R.P. Haynes and Locust Creek sites were visited where previously documented sand dikes and sand blows were searched for and examined in drainage ditch cutbanks. In addition, the group visited two Native American mounds and the Delta Gateway Museum that has exhibits on the natural, cultural, agricultural, and industrial history of the region, including information on earthquakes and floods. Activities during the field program are also listed below. At the conclusion of the workshop, there was a wrap-up session during which main topics and priorities for future paleoliquefaction research were discussed by presenters and participants. The topics and priorities that were discussed are summarized in bulletized form below.

There were 10 participants in the workshop from the NRC Office of Nuclear Regulatory Research, Office of New Reactors, NRC Region IV, NRC Office of Nuclear Reactor Regulation, and the Defense Nuclear Safety Board. M. Tuttle organized the workshop, L. Wolf and M. Tuttle chaired the workshop, K. Dyer-Williams, P. Villamor, J. Dunahue, and M. Haynes assisted with other aspects of the workshop including logistics, preparation of liquefaction sites, and presentations during the field trips.

During the course of the project, it was decided that an electronic file of workshop presentations would be provided to the US NRC and posted on the Agencywide Documents Access and Management System (ADAMS). Presentations were edited so that they could be made available online and the pdf file of the workshop presentations was submitted to the US NRC on February 2, 2016. The presentations are available as ML16221A590 and ML17019A240 in ADAMS.

3.1 Workshop Presentations

1. "Complex faulting, seismicity, and swarm activity within the New Madrid seismic zone," by Heather R. DeShon, Southern Methodist University
2. "Paleoliquefaction studies: Learning from historical and modern cases of liquefaction and dating paleoliquefaction features," by Martitia Tuttle, M. Tuttle & Associates
3. "Geophysical imaging techniques at paleoliquefaction sites," by Lorraine Wolf, Auburn University
4. "Paleoseismology of Marianna, Arkansas, area: Application of ground-penetrating radar," by Haydar Al-Shukri, Hanan Mahdi, University of Arkansas at Little Rock, and Martitia Tuttle, M. Tuttle & Associates
5. "NHPA, NEPA, and ESA: Federal regulations affecting paleoseismology studies," by Thomas Weaver, U.S. Nuclear Regulatory Commission
6. "Seismic geotechnics," by Paul W. Mayne, Georgia Institute of Technology
7. "New in-situ test developments 2014," by Paul W. Mayne, Georgia Institute of Technology
8. "Evaluation of scenario earthquakes," by Kathleen Dyer-Williams, M. Tuttle & Associates
9. "Radiocarbon dating and its use in paleoliquefaction studies," by Darden Hood, Beta Analytic
10. "Optically stimulated luminescence dating for paleoseismology," by Steven L. Forman, Liliana C. Marin, Xiaohua Gua, Ashley Ramsey, Chris Dickey, Connor Mayhut, Baylor University
11. "Archaeology and its uses in earthquake studies," by Mary Evelyn Starr, Consulting Archaeologist
12. "2010-2011 Canterbury earthquake sequence: hidden faults, liquefaction, rock fall, economic impact, and government response," by Pilar Villamor, GNS-New Zealand
13. "Recent advances in paleoliquefaction back-calculation procedures," by Russell A. Green and Brett Maurer, Virginia Institute of Technology
14. "The USGS seismic hazard maps," by Chuck Mueller and members of the USGS NSHM Project, U.S. Geological Survey
15. "NRC Training Workshop Wrap up: Discussion and recommendations," facilitated by Lorraine Wolf, Auburn University, and Martitia Tuttle, M. Tuttle & Associates

3.2 Field Program

1. Land-based investigations (Stiles and Garner sites)
 - identifying sand blows using aerial photographs and satellite images
 - identifying sand blows and dikes using geologic and geophysical techniques
 - logging sand blows exposed in trench walls
 - collecting samples for radiocarbon and OSL dating
2. River-based investigation (St. Francis River; if rained out - visit R.P. Haynes and Locust Creek liquefaction sites, Delta Gateway Museum, and Native American Mounds)
 - searching for liquefaction features along cutbanks of rivers and drainage ditches
 - documenting liquefaction features and collecting samples for dating

3.3 Workshop Wrap-Up: Discussion and Recommendations

3.3.1 Main Points

1. Purpose of paleoliquefaction studies is to support PSHA
 - Identification of Recurrent Large Magnitude Earthquakes (RLME) sources and their characteristics
 - Provides critical information for evaluating nuclear power plant site safety
2. Modern and historical analogs of eq-induced liquefaction
 - Valuable learning opportunities for interpreting past events
 - Serve as targets for paleoliquefaction studies
3. Dating of liquefaction features
 - Well constrained ages of features are essential for correlating features across a seismic region & for estimating timing, source areas, magnitudes, and recurrence times of paleoearthquakes
 - Poorly constrained ages can lead large uncertainties of paleoearthquake characteristics

3.3.2 Recommendations for Research in Central and Eastern U.S.

1. Studies of RLME source zones
 - New Madrid seismic zone and Marianna area – infrequent, high impact events; blind faults buried under basin sediments
 - Central Virginia seismic zone – any kind of surface deformation would be helpful
 - Eastern Tennessee seismic zone – is it a source of RLMEs?
 - Other potentially active zones (e.g., Charleston – need further, comprehensive evaluation)
2. Priorities
 - a. Central Virginia seismic zone – very high priority due to proximity to North Anna nuclear power plant and Washington D.C.; refine techniques for locating and dating sand dikes
 - b. Marianna area – more complete characterization of earthquake potential, timing, and related uncertainties; better understanding of relationship to NMSZ and active seismicity
 - c. Eastern Tennessee seismic zone – did changing conditions over time (e.g., water table) affect the record of past earthquakes?
 - d. Modern earthquakes – positive and negative evidence (e.g., Christchurch earthquake induced liquefaction in some places and not in others)
 - e. New technology and data to identify active faults (e.g., LIDAR, potential field data - magnetics and gravity, ambient noise studies, high-resolution seismic data)
 - f. Drivers of seismicity – still a big question

4 PALEOLIQUEFACTION STUDIES IN MODERATE SEISMICITY REGIONS – TASK 3

4.1 Introduction

On the basis of its very large earthquakes in A.D. 1811-1812 and earlier paleoearthquakes, the NMSZ is recognized as having the highest hazard in the CEUS but large uncertainties in the hazard models have spurred considerable debate and controversy. Sensitivity analysis of seismic sources associated with the Reelfoot Rift fault system suggests that earthquake rate has the greatest effect on hazard estimates, with uncertainties being greatest for the central New Madrid fault zone. For example, the range of uncertainty in the mean recurrence interval for recent source models of large New Madrid earthquakes exceeds a factor of 7 and leads to a range of mean probabilities of occurrence (over the next 50 years) that exceeds a factor of 500 (Excelon Generating Company, 2003). Mean recurrence interval estimates for this region are more dependent on paleoseismology than anywhere else in the CEUS. Therefore, it is imperative to recover critical information and to derive the best possible estimates before much of the near-surface record of past earthquakes is lost to land leveling and other agricultural practices.

This paleoliquefaction study in the NMSZ and surrounding region encompasses a large area including the St. Francis Basin and the Western Lowlands (Mississippi River floodplain west of Crowley's Ridge) in southeastern Missouri and northeastern and eastern-central Arkansas, as well as parts of western Tennessee, and northwestern Mississippi. The study involved surveying key areas for paleoliquefaction features that had not yet been systematically searched, constraining age estimates of previously and newly discovered prehistoric sand blows, and conducting detailed investigations of sand blows in areas underlain by Late Pleistocene fluvial deposits where there may be a longer liquefaction record of paleoearthquakes. With new information about the age, size, and areal distribution of paleoliquefaction features and by evaluating scenario earthquakes using liquefaction potential analysis, we reinterpret the timing, locations, and magnitudes of paleoearthquakes as well as update the paleoearthquake chronology, recurrence estimates, and source models for the region.

New information gathered during this study is also relevant to three hypotheses regarding seismic source characterization in the CEUS: (1) the NMSZ is characterized by bimodal recurrence with an average recurrence interval of 500 years during active periods separated by periods of quiescence lasting 1,700 years or more; (2) faults in western Tennessee that are spatially associated with the eastern margin of the Reelfoot Rift (referred to as the Eastern Reelfoot margin) have repeatedly produced very large earthquakes during the Holocene; (3) seismicity migrates from one part of the Reelfoot Rift fault system to another with a periodicity of 5,000-15,000 years. By gathering new data about paleoearthquakes in the region, this project will advance the effort to characterize the long-term deformation along the Reelfoot Rift that may have implications for other aulocogens (or failed rift that is no longer active) in intraplate settings.

4.2 Methodology

Paleoliquefaction studies are interdisciplinary in nature and therefore draw upon methods in the geosciences, geoengineering, and related fields. Generally, paleoliquefaction studies begin with a review of modern and historical seismicity, surficial and bedrock geology, geotechnical properties of soil or sediment, aerial photographs and satellite images, as well as conditions in the field in order to select areas of study across a region of interest. This is followed by field studies that often include searching for and documenting earthquake-induced liquefaction features in river

cutbanks, or other exposures such as sand and gravel pits, as well as conducting detailed investigations of liquefaction sites. Detailed investigations often involve imaging liquefaction features with geophysical techniques and trenching liquefaction features to study their characteristics. During field studies, organic and sediment samples are collected for radiocarbon and OSL dating to estimate the age of host sediment where liquefaction features do and do not occur as well as the age of the liquefaction features. Geotechnical testing might be conducted at liquefaction sites, or previously collected geotechnical data used, to evaluate scenario earthquakes and to help estimate the source areas and magnitudes of earthquakes that best explain the regional distribution of observed liquefaction. All data are compiled and considered in a regional context to interpret the timing, location, magnitude, and recurrence times of large earthquakes. Below, the geological, geophysical, archaeological, geochronological, and geotechnical methods are summarized that were used in this study. Additional discussion of these and other methods in paleoliquefaction studies can be found in NUREG/CR-7238.

4.2.1 Geological Methods

On the basis of previous paleoliquefaction and paleoseismological studies in the NMSZ, areas of interest were identified where additional paleoliquefaction data would be helpful to improve the understanding of known paleoearthquakes, to fill spatial and temporal gaps in the paleoseismic record, and to test hypotheses about the earthquake potential of various earthquake sources. Quaternary geology as well as aerial photographs and satellite imagery of those areas were reviewed to select sections of rivers as well as agricultural fields for reconnaissance. In particular, river sections and fields were selected where Holocene and Late Pleistocene fluvial deposits had been mapped and where light-tonal patches likely to represent sand blows were identified on aerial photographs and satellite imagery.

During reconnaissance, river sections were inspected to assess whether or not geologic conditions were favorable for the formation and preservation of liquefaction features and cutbank exposures adequate to warrant searches for liquefaction features. Also, light-tonal patches in agricultural fields were visited to further assess whether or not they were likely to be sand blows. Surface soils were inspected and soil pits were hand dug in light-tonal patches that were characterized by sandy soils and surrounded by dark-tonal areas characterized by silty or clayey soils. Sandy deposits that contained soil clasts and that buried soils similar to those that surrounded the light-tonal patches were likely to be sand blows. On the basis of findings during reconnaissance, river sections were selected for systematic surveys and likely sand blows in agricultural fields were selected for site investigations.

During the river surveys, all exposures were examined for the presence of liquefaction features and other deformation related to earthquakes. Sedimentary conditions, buried soils, and other marker beds, and amount of exposure were noted on topographic maps of the river sections. Features that appeared to be sand dikes were tracked up section to determine if they terminated within the host deposit or were connected to sand blows. Lenticular sandy layers that might be sand blows were also examined. Liquefaction features were cleared with a trowel and/or shovel and described in terms of their sediment type, sedimentary structures, soil development, size (width of dikes, thickness and lateral extent of sand blows and sills), orientation, vertical and horizontal displacements, crosscutting relations, and stratigraphic context. Liquefaction features, and their context and relationships, were photographed. Wood, charcoal, and other organic samples were collected for radiocarbon dating, and at some sites, sediment samples were collected for OSL dating by first excavating a small area to remove dried out and cracked soil and then driving sampling tubes horizontally into the cutbank. The locations of liquefaction sites were

measured with a global positioning system (GPS) unit and marked on topographic maps. All the information gathered at the sites was recorded on site description forms.

During the site investigations, trenches were excavated in likely sand blows. Trenches were excavated with a backhoe with a ~1 m wide bucket fitted with a smooth blade. The trenches were mostly 1 to 1.5 m deep. Shoring was used in trenches more than 1.5 m deep or in cases where the trench walls were prone to caving. Plow zones were removed with the backhoe in thin, 2-5-cm thick cuts until the base of the plow zone was reached. The contacts with the underlying sand blows were carefully cleaned with hand tools and examined for intruding root casts and/or cultural features. Intruding features were documented, photographed, and sampled. The excavations continued through the sand blows, with frequent cleaning and examination of the trench walls and floor, until the soil buried beneath the sand blow was reached. The upper contacts of the buried soils were carefully examined for and samples collected of leaves, tree debris, *in situ* tree trunk or root casts, and other organic materials. In cases where cultural artifacts were found in the buried soil, backhoe excavation ceased and archaeological test units were excavated in the buried soil by a project archaeologist (see section 4.2.3 below). In cases where no cultural artifacts were found in the buried soil, backhoe excavation continued to reveal the feeder dikes of the sand blows.

After trench excavations were completed, trench walls and floors were cleaned with shovels and trowels, level lines were established, metric tapes hung as vertical lines, and walls logged at an appropriate scale (2.54 cm on log = 25 cm or 50 cm on trench wall) depending on the complexity of the features. During logging, liquefaction features were described in terms of sediment type, sedimentary structures, weathering characteristics and/or soil development, cross-cutting relations, orientation, vertical and horizontal displacements, and stratigraphic context. The characteristics of the buried soils were documented, including color, texture, and redoximorphic features (color patterns in soil formed by the processes of reduction, translocation, and oxidation of Fe and Mn oxides), as were characteristics of host sediment, including sediment type, bedding, lateral continuity, and weathering characteristics. Organic samples were collected for radiocarbon dating, and in a few circumstances, for OSL dating. The locations of the samples were noted on the trench logs.

4.2.2 Geophysical Methods

Geophysical techniques offer a non-invasive tool to locate sand dikes and sand blows in the subsurface and to map the three-dimensional morphology of these features. Although sand blow deposits are often previously identified by careful examination of surface deposits and natural exposures, geophysical techniques can afford an understanding of subsurface sedimentary properties and structural relationships and can help guide future trench excavations. The ability of geophysical techniques to detect vertical and lateral changes in sedimentary properties makes them an effective mapping tool in paleoliquefaction studies. The techniques are used to locate the feeder dikes of sand blows (diagnostic features of earthquake-induced liquefaction) that crosscut soil horizons, to map the extent of sand blows, and to identify cultural features in association with sand blows. By imaging subsurface relationships, geophysical surveys help to identify and target critical relationships thus maximizing results from trenching while minimizing any impact to archeological sites.

Electrical resistance tomography was used to investigate the five sites selected for paleoseismological trenching studies. Electrical resistivity (ER) methods use a low-frequency alternating current that is introduced through an electrode pair, while a potential difference is measured by another electrode pair. The ratio of the voltage at the receiver electrodes to the

current input by the transmitting pair is the impedance. The ability for current to travel through the subsurface is a function of the medium's physical properties. Resistivity (the inverse of conductivity) is a measure of the resistance of a volume to the applied electric current. In general, rocks are associated with high resistivity, whereas sediments, due to their higher porosity, can be associated with either high or low resistivity depending upon their degree of saturation or clay content. Saturated sediments or those containing salts or clays are associated with low resistivity because their ionic content increases the ability for current to flow and thus decreases the material's resistivity. Compared to silty and clayey soils with high moisture content, sandy well-drained sand dikes and sand blows will have higher resistivity.

Although electrical methods have been in use for resource exploration since Schlumberger's early work in the last century (Oristaglio et al., 2009), the method was first applied to studies of earthquake-induced liquefaction in the mid-1990's (Wolf et al., 1998; Tuttle et al., 1999). The time required to perform surveys and their imaging capability have improved with the use of equipment with multichannel, automated switching capability and 3-D inversion algorithms for estimating the true subsurface distribution of resistivities (Wolf et al., 2006). When done correctly in suitable environs, the imaging capability of the ER method is excellent.

The calculation of apparent resistivity is based on the style of array, or electrode configuration selected. The factors affecting the measured values are the input current, the spacing between electrodes, and the physical properties of the material. If 3-D data acquisition is not employed, profile lines should be oriented perpendicular to the strike of elongated sand blows and underlying sand dikes, if observed at the surface. In map view, sand dikes and related sand blows often form *en echelon* patterns, and parallel profile lines help to determine their orientation and approximate (± 0.5 m using electrode spacings of 2 m) location. If a 3-D geometry for data acquisition is possible and desirable, the electrode cables are laid out in snake-wise fashion within a rectangular grid, with spacing between the lines at 2-electrode spacing. The 3-D data acquisition provides a true 3-D picture of the subsurface rather than a pseudo 3-D image that interpolates between parallel lines. This is because in the 3-D acquisition, current is being measured across the array instead of simply along a 2-D line. Although 3-D data acquisition provides a more accurate representation of the subsurface, the data acquisition time can easily increase by a factor of 3. In addition, although a 3-D approach results in greater resolution, the imaging depths are shallower given a fixed number of electrodes because of the line spacing requirement.

4.2.3 Archaeological Methods

Archaeological methods were employed at sites where cultural artifacts were found in association with liquefaction features. Under such circumstances, archaeological methods were used during both site evaluations and site investigations (Phases 1 and 2, respectively, as described in Appendix B).

During site evaluations, surface surveys for artifacts were performed in the gridded areas of the geophysical surveys. A total station was used to establish base lines of the north, south, east, and west sides of the survey areas. Corners of artifact collection units within the survey areas were established by using a 100 m fiberglass surveyor tape. The gridded areas were visually inspected in systematic transects spaced 3 m apart or less. All artifacts within each grid were collected, bagged, and tagged. The artifacts were later cleaned and identified and the artifact data tabulated. Artifact density maps were generated showing the distribution of cultural materials within the collection areas. These maps were made using Surfer® 10 from Golden Software

(<http://www.goldensoftware.com>), which uses an interpolation grid to create a contour map based on artifact counts and using data values centered in the collection cells. In addition, archeological test units or shovel test units, measuring 33 cm x 66 cm, were set up at 10 m intervals within the footprint of the proposed trench locations. The locations of the shovel tests were measured with a hand-held GPS device, surveyed with a total station, and/or recorded on the field maps of the geophysical grids. The test units were excavated by hand and all fill from the test units was screened through ¼ inch hardware cloth. All materials retained on the screen were collected and returned to the laboratory for analysis. Profiles of the shovel test units were sketched and photographed and soil and sedimentary units were described and recorded on the sketches. In the laboratory, artifacts from the test units were cleaned and identified and the artifact data tabulated.

During site investigations, the plow zones were removed with a backhoe in thin, 2-5-cm-thick, cuts until the base of the plow zone was reached. The contact with the underlying sand blow was carefully cleaned with hand tools and examined for intruding cultural features such as post molds, pits, and wall trenches. Excavations continued through the sand blows until the soils buried beneath the sand blows were reached. The contacts of the buried soils were carefully examined for cultural materials and archeological test units, measuring 33 cm x 66 cm, were excavated in the buried soils until they became devoid of cultural material. Locations of the test units were measured relative to the ends of the trenches. Otherwise, similar procedures were followed to those described above for site evaluations, including excavation of test units, screening fill, collecting cultural material, recording soil and sedimentary units, analyzing artifacts, and reporting data.

4.2.4 Geochronological Methods

Liquefaction features are dated to estimate the ages of the paleoearthquakes that were responsible for their formation. It is important to constrain the ages of liquefaction features as narrowly as possible to differentiate closely timed events and to correlate similar-age features across a region (Tuttle, 2001). Sand blows usually provide the best opportunity for estimating the ages of paleoearthquakes with relatively small uncertainties, because it is often possible to determine close maximum age constraints and sometimes both maximum and minimum age constraints for the deposits (Figure 4-1). Under circumstances where sand dikes and sills may have formed (e.g., moderate earthquakes or distal site of liquefaction), age estimates of liquefaction features often have greater uncertainties. This is because sand dikes and sills terminated below the ground surface at the time of the paleoearthquake. Also, maximum age constraints are based on dating of the uppermost stratigraphic units intruded by the features which may be much older than the liquefaction features themselves (Tuttle, 2001).

In this study, approaches to dating liquefaction features include soil development and weathering characteristics, stratigraphic context, archeological context, radiocarbon dating, and OSL dating. (See NUREG/CR-7238 for detailed descriptions of these approaches.) Soil development is used as a relative dating tool to distinguish young, unweathered features from significantly older, weathered features. Stratigraphic context and structural relationships of liquefaction features are used to estimate their relative ages and to correlate liquefaction features between exposures. Along river cutbanks with laterally continuous stratigraphy or prominent marker beds, age equivalence can be established between different exposures or sites. By establishing the ages of the continuous strata or marker beds with a numerical dating technique such as radiocarbon dating, these ages can be extrapolated to other nearby sites where liquefaction features may occur. Similarly, cultural artifacts, especially if the artifacts are diagnostic of a cultural period,

found in prominent marker beds or in cultural horizons and features directly associated with liquefaction features, can help to estimate their ages.

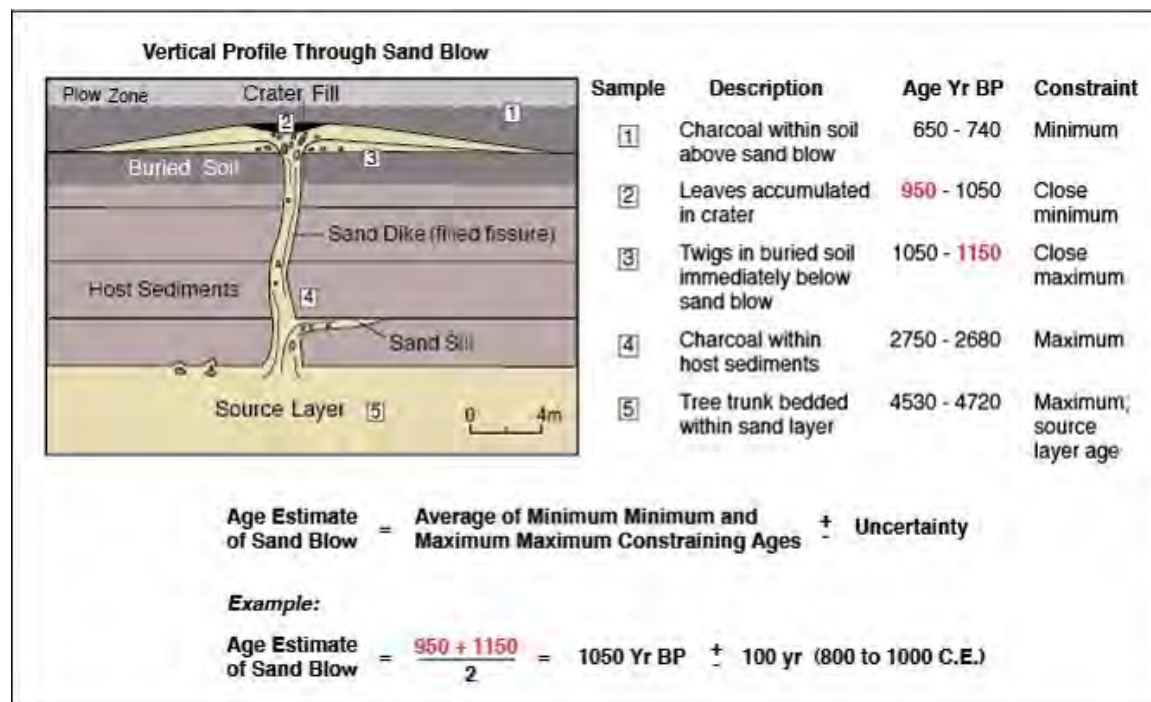


Figure 4-1 Cross-Sectional Diagram Illustrating Sampling Strategies for Radiocarbon Dating and Age Estimation of Liquefaction Features (after NUREG-2115)

Radiocarbon dating, or ^{14}C dating, was the most common technique used to estimate the ages of sand blows and dikes in this study. Ideally, samples collected above and below sand blows were dated in order to bracket the age of the features. In many cases, however, only samples collected below the sand blows from buried soils were available. Organic samples collected in close association with liquefaction features were sent to Beta Analytic, Inc. radiocarbon laboratory for accelerator mass spectrometry (AMS) dating. This technique was chosen for analysis because it requires only smaller samples (charcoal ≥ 20 milligrams, wood ≥ 20 milligrams, and soil ≥ 2 grams) and has a precision of better than $\pm 1\%$, corresponding to ± 80 radiocarbon years, for samples that are less than 10000 years in age (Aiken, 1990). Radiocarbon ages were calibrated using the Pretoria procedure (Talma and Vogel, 1993; Vogel et al., 1993). Two-sigma calibrated dates were used to estimate the ages of liquefaction features to assure with a high probability that the actual ages of the liquefaction features fall within the estimated age range.

OSL dating has been used in several paleoliquefaction studies over the past ten years. It offers the advantage of dating sediment itself; so potentially provides a means of dating liquefaction features at sites where organic samples used in radiocarbon dating are not found. However, the application of OSL dating in paleoliquefaction studies remains a substantial challenge and uncertainties in ages often range between 4 and 10%. The most common problem is that the sediment has not received enough sunlight exposure prior to burial to rid the sample of previously acquired luminescence (Lian, 2007; Forman, 2015). During venting following liquefaction, sediment of various apparent ages may be entrained and mixed. In addition, the paleosurface onto which the slurry of water and entrained sediment vent may be eroded, disturbed, or mixed. Other factors that can contribute to uncertainties include bioturbation, diagenesis and post-

depositional weathering, accumulation of secondary minerals (silica, calcium carbonate, and clay), and water-content fluctuations (Aitken, 1998; Forman et al., 2000; Forman, 2015).

During this project in order to compare OSL and radiocarbon results, OSL samples were collected in close proximity to organic samples used in radiocarbon dating. As discussed in detail in section 4.4, OSL ages were often older and sometimes much older than radiocarbon ages. At sites where sand blows were trenched, OSL samples were collected of the buried surfaces immediately below the sand blows. During river reconnaissance, OSL samples were collected of the contact between the sand blow and buried surface and of the host sediment crosscut by sand dikes. Two samples collected at the Faulkner (aka Caraway) site and one sample each collected at the Obion River 507 and Locust Creek Ditch 3 sites were sent to the US Geological Survey's OSL Dating Laboratory. Two samples each collected at the Garner and Pritchett sites and one sample collected at the St. Francis River 48 site were sent to the Geoluminescence Dating Research Laboratory (GDRL) Lab at Baylor University. Both laboratories used single aliquot regeneration (SAR) protocols for dating quartz sand grains (e.g., Wintle and Murray, 2006; Forman, 2015). The US Geological Survey's lab used an automated Risø TL/Luminescence-DA-15/20 in the SAR analyses while GDRL used an automated Risø TL/OSL-DA-15 system. A determination of the environmental dose rate is needed to render an optical age. This dose rate is an estimate of sediment exposure to ionizing radiation from U and Th decay series, ⁴⁰K, (sometimes including ⁸⁷Rb) and cosmic sources during the burial period. The US Geological Survey's lab determined U and Th content of sediment, assuming secular equilibrium in the decay series, by high-resolution gamma spectrometry (Ge detector). For the GDRL lab, U and Th content of the dose rate samples and ⁴⁰K were determined by inductively coupled plasma-mass spectrometry (ICP-MS) analysed at ALS Laboratories in Reno, Nevada.

4.2.5 Geotechnical Methods

The cyclic-stress method of liquefaction potential analysis, also known as the simplified procedure, is used in the evaluation of paleoearthquakes. This method is well established, remains the standard in engineering practice, and is suitable for many field and tectonic settings (e.g., Seed and Idriss, 1971, 1981, and 1982; Youd et al., 2001; Cetin et al., 2004; Moss et al., 2006; Robertson, 2004 and 2009; Idriss and Boulanger, 2004, 2008, and 2010; Boulanger and Idriss, 2014). In the analysis, peak ground accelerations (PGA) are estimated for scenario earthquakes of moment magnitudes at distances from known or suspected sources by employing regionally appropriate ground motion prediction equations (GMPEs). In this study, medium GMPEs developed for use in the new generation of seismic hazard maps (Atkinson and Boore, 2011; Atkinson et al., 2012; Atkinson and Assatourians, 2012) are used to calculate peak ground accelerations for the scenario earthquakes. After determining the accelerations, cyclic stress ratios (CSR) generated by scenario earthquakes are calculated using Equation 4-1,

$$CSR_{7.5} = \frac{\tau_{ave}}{\sigma'_{v0}} = 0.65 \cdot \left(\frac{a_{max}}{g} \right) \cdot \left(\frac{\sigma_{v0}}{\sigma'_{v0}} \right) \cdot r_d \cdot \frac{1}{MSF} \quad (4-1)$$

where a_{max} = PGA (horizontal component), (a_{max}/g) is PGA divided by the acceleration due to gravity; σ_{v0} and σ'_{v0} are the total and effective vertical overburden stresses, respectively; r_d is a stress reduction coefficient; and MSF is the magnitude scaling factor. The $CSR_{7.5}$ represents the normalized shear stress (τ_{ave}/σ_v) induced in the soil by the earthquake event (i.e., the seismic demand) and commonly referenced to a benchmark case with $M = 7.5$.

Variations in standard penetration test (SPT) procedure are corrected by adjusting the measured blow count (N_m) using Equation 4-2:

$$N_{1(60)} = C_N C_E C_B C_R C_S N_m \quad (4-2)$$

where $N_{1(60)}$ is normalized blow count corrected for hammer energy (C_E), effective confining stress (C_N), borehole diameter (C_B), rod length (C_R), and sampler configuration (C_S), with N_m being the measured SPT resistance or "blow count" reported in blows/foot (or blows/0.3m). In this way, the measured N value is standardized to 60% of the potential energy.

Following the computations of the cyclic stress ratio and the adjusted and normalized blow count, the liquefaction potential of representative layers at borehole sites is determined by plotting CSR versus normalized blow count [$(N_1)_{60}$] on charts such as that shown in Figure 4-2a for M 7.5 earthquakes. If CSR is greater than or equal to CRR , the value plots on or above the curve, the soil is likely to liquefy. Conversely, if CSR is less than CRR , the value plots below the curve, and liquefaction is considered unlikely.

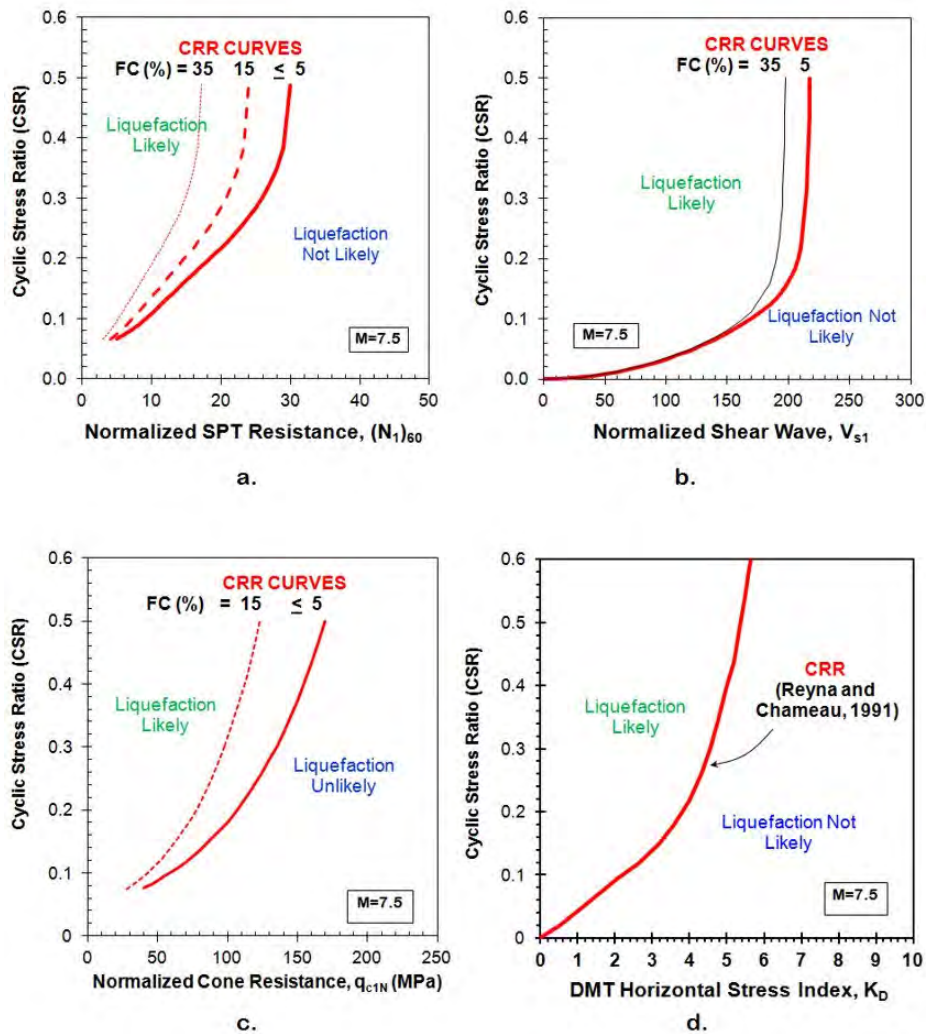


Figure 4-2 Illustrative sets of CRR curves for M 7.5 earthquakes for four in-situ tests: (a) standard penetration; (b) shear wave velocity; (c) cone penetration; and (d) flat plate dilatometer (after Schneider et al., 1998).

As an approximation to the base curve, for clean sands which are tested in boreholes using the standard penetration test (SPT), the cyclic resistance ratio (CRR) for an **M** 7.5 event proposed by Youd et al. (2001) is given by Equation 4-3:

$$CRR_{7.5} = \frac{1}{34 - (N_1)_{60-cs}} + \frac{(N_1)_{60-cs}}{135} + \frac{50}{[10 \cdot (N_1)_{60-cs} + 45]^2} - \frac{1}{200} \quad (4-3)$$

for $(N_1)_{60-cs} < 30$; $(N_1)_{60-cs}$ refers to equivalent clean sand. In this study we use the approximation to the base curve.

The CRR for magnitudes other than 7.5 is calculated by multiplying $CSR_{7.5}$ by the appropriate MSF , which is given by Equation 4-4 where M_w represents moment magnitude:

$$MSF = (M_w/7.5)^{-3.3} \quad (4-4)$$

As a means to better quantify uncertainty, stress-based methods have been re-evaluated using probabilistic analysis. In lieu of a single CRR curve, a family of CRR curves is derived to indicate the probability (P_L) that liquefaction may occur. Sets of probability curves have been developed for the SPT with ranges generally given from $P_L = 5\%$ up to $P_L = 95\%$ (Liao et al., 1988; Youd and Noble, 1997; Toprak et al., 1999; Juang et al., 2002; Cetin et al., 2004; Boulanger and Idriss, 2012).

Alternatively, the calculated factor of safety (FS) can be used to approximately assess the P_L . For example, in their approach, Juang and Jiang (2000) suggest (Equation 4-5):

$$P_L = \frac{1}{1 + (FS / 1.0)^{3.34}} \quad (4-5)$$

where P_L is the probability of liquefaction and F_s is the factor of safety. If P_L is greater than or equal to 50%, a layer is likely to liquefy. This approach is taken in this study due to its simplicity and ease of use for inclusion in spread sheets.

Unlike the SPT, the CPT provides no physical sample for determining soil type. We understand that the CPT material index, I_c , as defined by Robertson (2004) is adequate for evaluating soil type when CPT is used and collection of soil samples is not deemed necessary. With I_c , soil behavioral types and fines content are determined from CPT measurements of tip resistance and sleeve friction. The available soil resistance (i.e., cyclic resistance ratio, CRR) is estimated from the stress-normalized cone resistance (Q_{tn}) which is compared with the level of seismic ground motions (i.e., cyclic stress ratio, CSR) to calculate FS and/or probability of liquefaction (P_L) at the location.

The soil type is evaluated from the CPT material index, I_c (Robertson, 2004):

$$I_c = \sqrt{[3.47 - \log Q_{tn}]^2 + [1.22 + \log F_r]^2} \quad (4-6)$$

where Q_{tn} = stress-normalized cone tip resistance and F_r = normalized sleeve friction are calculated from the cone penetrometer readings (Equations 4-7 and 4-8):

$$Q_{tn} = \frac{(q_t - \sigma_{vo})/\sigma_{atm}}{(\sigma_{vo}'/\sigma_{atm})^n} \quad (4-7)$$

$$F_r(\%) = 100 \cdot \frac{f_s}{(q_t - \sigma_{vo})'} \quad (4-8)$$

where σ_{vo} = total vertical overburden stress, σ_{vo}' = effective vertical stress, and σ_{atm} = a reference stress equal to atmospheric pressure (1 atm \approx 1 bar \approx 100 kPa). In the initial evaluation, the exponent n is set to $n = 1$ to find the soil behavioral type (SBT) which is based on a 9-zonal chart developed by Robertson (1990). The SBT was modified by Robertson and Wride (1998) and Zhang et al. (2002), as shown in Figure 4-3.

Normalized CPT Soil Behavioral Type (SBTn)

(after Robertson 2009)

$I_c \leq 2.6$: Sand-like
 $I_c > 2.6$: Clay-like

Liquefaction of Sands is applicable when $I_c \leq 2.6$

Steps for SBT Zones (Z)

- Find sensitive soils of zone 1 when: $Q_{tn} < 12 \exp(-1.4 F_r)$
- Zone 8 ($1.5 < F_r < 4.5\%$) and Zone 9 ($F_r > 4.5\%$): $Q_{tn} \geq \frac{1}{+0.006(F_r - 0.9) - 0.0004(F_r - 0.9)^2 - 0.002}$
- Use CPT index I_c for Zones 2 through 7

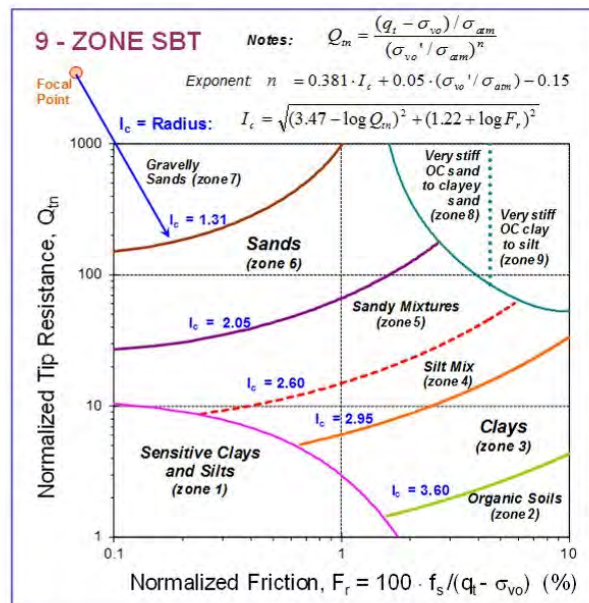


Figure 4-3 Soil Behavioral Type for CPT Classification (after Robertson, 2004)

During testing, the level of seismic ground motion, CSR is compared with the normalized cone tip resistance for clean sand to determine whether liquefaction will or will not occur. A critical level of seismic loading is designated by the cyclic resistance ratio (CRR). If the CSR > CRR, then liquefaction is likely, otherwise if the CSR < CRR, liquefaction is unlikely (Figure 4-4). For clean sand, the CRR can be expressed by Equations 4-9 and 4-10 for an **M** 7.5 earthquake (Youd et al., 2001; Robertson and Wride, 1998):

For $(Q_{tn})_{cs} < 50$:

$$CRR_{7.5} = 8.33 \left[\frac{(Q_{tn})_{cs}}{1000} \right] + 0.05 \quad (4-9)$$

For $50 \leq (Q_{tn})_{cs} < 160$:

$$CRR_{7.5} = 93 \left[\frac{(Q_{tn})_{cs}}{1000} \right] + 0.08 \quad (4-10)$$

Again, the calculated safety factor FS was used to estimate the liquefaction probability.

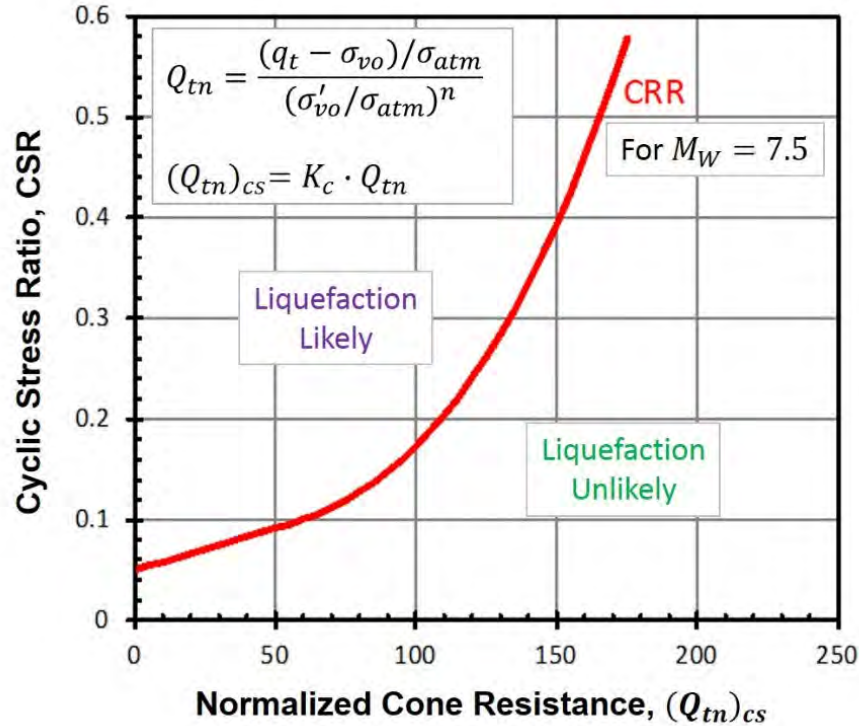


Figure 4-4 Cyclic Resistance Ratio (CRR) for Evaluating Soil Liquefaction Potential from CPT

4.3 Reconnaissance for Liquefaction Features Following the M 5.7, 2011, Mineral, Virginia, Earthquake

4.3.1 Introduction

On August 23, 2011, an **M**, 5.7 ± 0.1 earthquake occurred near Mineral, Virginia, about 50 km east of Charlottesville, 60 km northwest of Richmond, and 130 km southwest of Washington, D.C. (Figure 4-5 and Figure 4-6; Horton et al., 2015). The m_{bLg} (magnitude derived from the displacement amplitude of L_g waves) of the earthquake was 6.28 ± 0.26 (Chapman, 2015). The earthquake was felt along most of the eastern seaboard from Georgia to Canada. The mainshock and some aftershocks were characterized by high stress drops in the 50-100 MPa range comparable to those of the 1988 **M** 5.9 Saguenay, Canada, 2010 **M** 7.1 Darfield, New Zealand, and 2011 **M** 6.3 Christchurch, New Zealand, earthquakes (Ellsworth et al., 2011).

The 2011 **M** 5.7 Mineral earthquake occurred in the central Virginia seismic zone (CVSZ), an area of diffuse seismicity with most earthquakes occurring within ~60 km of the James River between Richmond and Charlottesville (e.g., Chapman, 2015). The Mineral earthquake is the largest main

shock to have occurred in the CVSZ during the historical period and raised concerns about the earthquake potential of the seismic zone located only 130 km from the nation's capital. Peak ground acceleration (PGA) of 0.27 g, measured 23 km northeast of the epicenter at the North Anna nuclear power plant, was greater than the 2% probability of exceedance in 50 yr for hard rock shown on the seismic hazard maps for the CVSZ (Petersen et al., 2008). Seismicity in the CVSZ ranges in depth from near surface to 12 km (Bollinger et al., 1985). Because the southern Appalachian detachment is at least 12 km deep in this part of the Piedmont, seismicity of the CVSZ is thought to occur on the Paleozoic and Mesozoic faults above the Precambrian basement though there is no clear association with any particular mapped fault (e.g., Pratt et al., 1988 and 2015; Chapman, 2015; Figure 4-5).

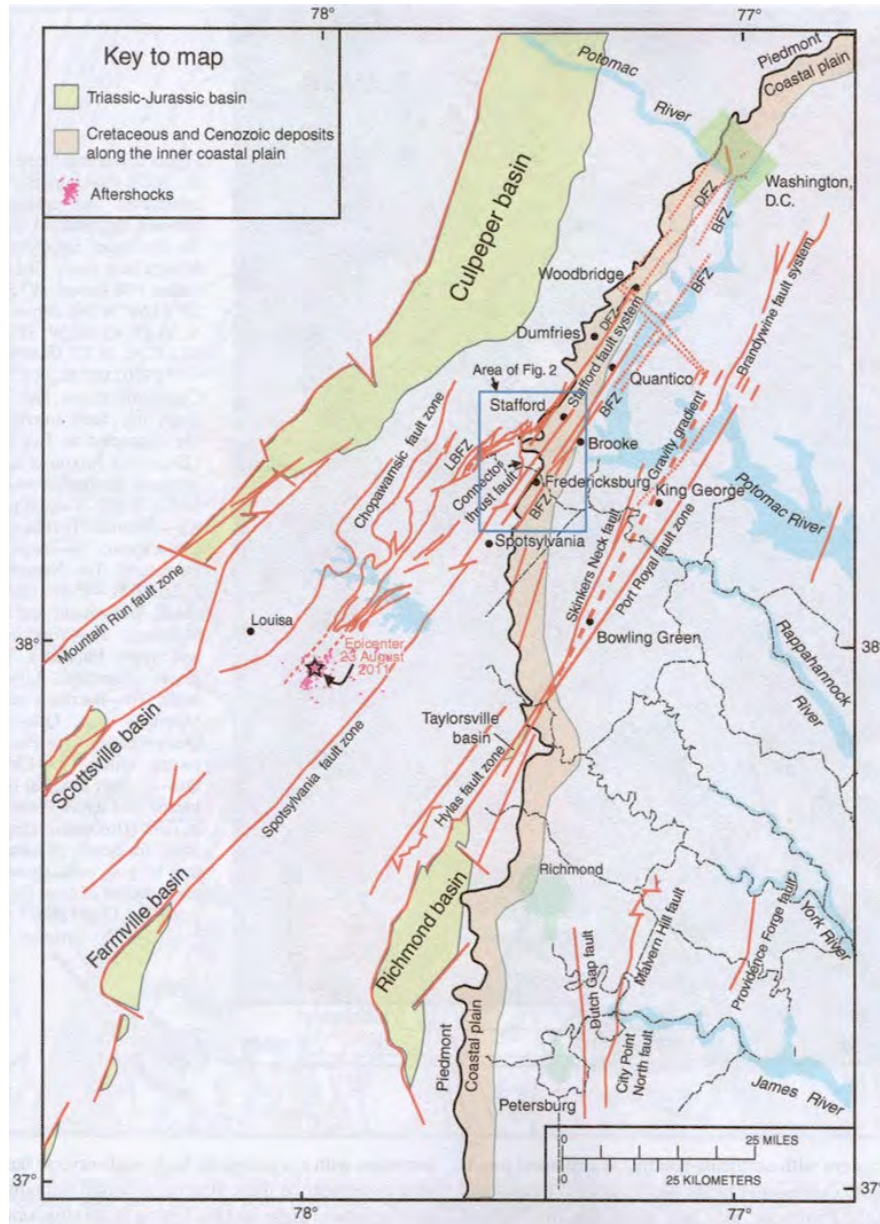


Figure 4-5 Map showing location of 23 August 2011 Mineral, Virginia, earthquake and its aftershocks relative to mapped piedmont faults and coastal faults, including Stafford fault system (from Powars et al., 2015).

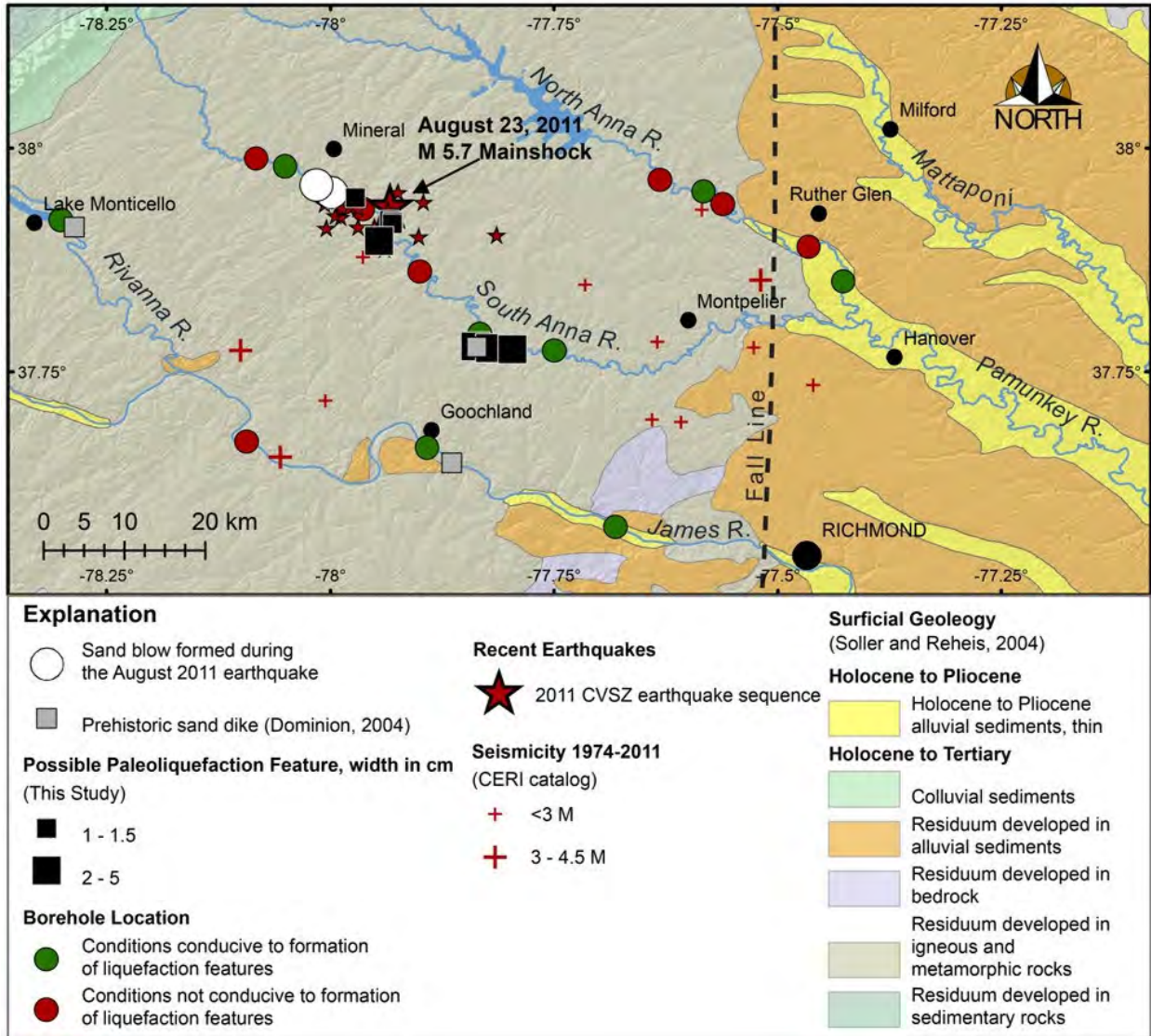


Figure 4-6 Geologic map of epicentral area of 2011 M 5.7 Mineral, Virginia, earthquake and surrounding area, showing locations of sand blows that formed during that event as well as locations of possible paleoliquefaction features found in mid-1990s (gray squares) and during this study (black squares). Locations of towns and cities are indicated by black circles.

The 2011, M 5.7, Mineral earthquake provided the rare opportunity to document liquefaction induced by a moderate earthquake in the eastern United States. During the first few days following the earthquake, four small sand blows were found in the epicentral area near the South Anna River in Yancy Mill and about 5 km upstream near the Bend of River Road (e.g., Green et al., 2015). In two cases, sand blows formed as the result of water and entrained sand venting through animal holes or burrows. Much of the sediment in the epicentral area is clayey residuum developed in igneous and metamorphic rock (Figure 4-6; Soller and Reheis, 2004), though Holocene terraces occur along portions of the South Anna River. Given the paucity of liquefiable sediment, it is not surprising that liquefaction was not more common in the epicentral area. It should be noted, that the initial survey for liquefaction features was limited to a few floodplains and bridge crossings of the South Anna River in the epicentral area. An aerial reconnaissance of the

broader epicentral region, including portions of the James River to the southeast, found no evidence of liquefaction or lateral spreading; however, the aerial reconnaissance was hampered by heavy forest and vegetative cover across much of the region (Green et al., 2015). In addition, Hurricane Irene struck Virginia, four days after the earthquake and was followed about a week later by heavy rain from remnants of tropical storm Lee. High river levels resulting from precipitation during these storms washed away the sand blows that had been found in and near the South Anna River, and possibly in other locations as well.

4.3.2 Previous Paleoliquefaction Study

During a paleoliquefaction study conducted in the mid-1990s, cutbank exposures of rivers in the CVSZ were searched for paleoliquefaction features. Several weathered sand dikes (1 to 10 cm wide) were found at one site each on the James, Rivanna, and South Anna Rivers (Obermeier and McNulty, 1998; Dominion, 2004). These sites range from 18 to 30 km from the epicenter of the 2011 **M** 5.7 Virginia, earthquake (Figure 4-6; gray squares). Along some of the rivers that were searched, liquefiable sediment was rare or absent. Where liquefiable sediment was present, it ranged from 1,000-3,000 years in age (Dominion, 2004), limiting the length of the paleoseismic record. The paleoliquefaction features were attributed to at least one, and possibly three, moderate earthquakes during the Holocene. The apparent lack of widespread liquefaction features was interpreted as evidence that an earthquake of **M** > 7 had not occurred in the CVSZ during the past 10000 years, though an earthquake in the **M** 6 to 7 range was not ruled out (Obermeier and McNulty, 1998; Dominion, 2004). Therefore, the 2011 Mineral earthquake provides an opportunity to compare paleoliquefaction features with modern features and thereby improve understanding of paleoearthquake(s) in the CVSZ.

4.3.3 Results of Reconnaissance

Reconnaissance conducted for this project was performed during the week of November 16-23, 2011, three months after the mainshock. Unfortunately, it rained during the field trip causing many of the rivers in the area to rise 0.6-1.8 meters, obscuring most of the cutbanks. Only the South Anna River was low enough to warrant searching for liquefaction features along its banks. Cutbank exposures of the South Anna River were carefully examined for liquefaction features in the Yanceyville area and downstream for a distance of 24 kilometers. In addition, several flood plains flanking the river were searched for sand blows. No modern liquefaction features were found either in the cutbanks or on the floodplains. However, possible paleoliquefaction features were found at eight sites along the South Anna River (Figure 4-6, black squares). One of these sites occurs in the vicinity of a possible liquefaction feature found during the mid-1990s paleoliquefaction study described above.

The features identified in 2011 that are most likely to be the result of earthquake-induced liquefaction are dike-like structures that have lateral continuity, branch upward, and are filled with sandy sediment containing clasts of the host deposit (Figure 4-7). At a couple of the South Anna River sites, animal burrows and root casts appeared to have been utilized as near-surface pathways for liquefied and fluidized sediment. Also, the possible liquefaction features were somewhat bioturbated and weathered suggesting that they are prehistoric, probably Holocene, in age. In general, the dike-like features appeared to increase in width, from 1-1.5 cm to 2-5 cm, towards the east. Given that no recent liquefaction features were found along the South Anna River and that the paleoliquefaction features appeared to be getting larger in size towards the east, the prehistoric earthquake(s) responsible for the paleoliquefaction features may have been larger, and/or located farther to the east, than the 2011 **M** 5.7 event.

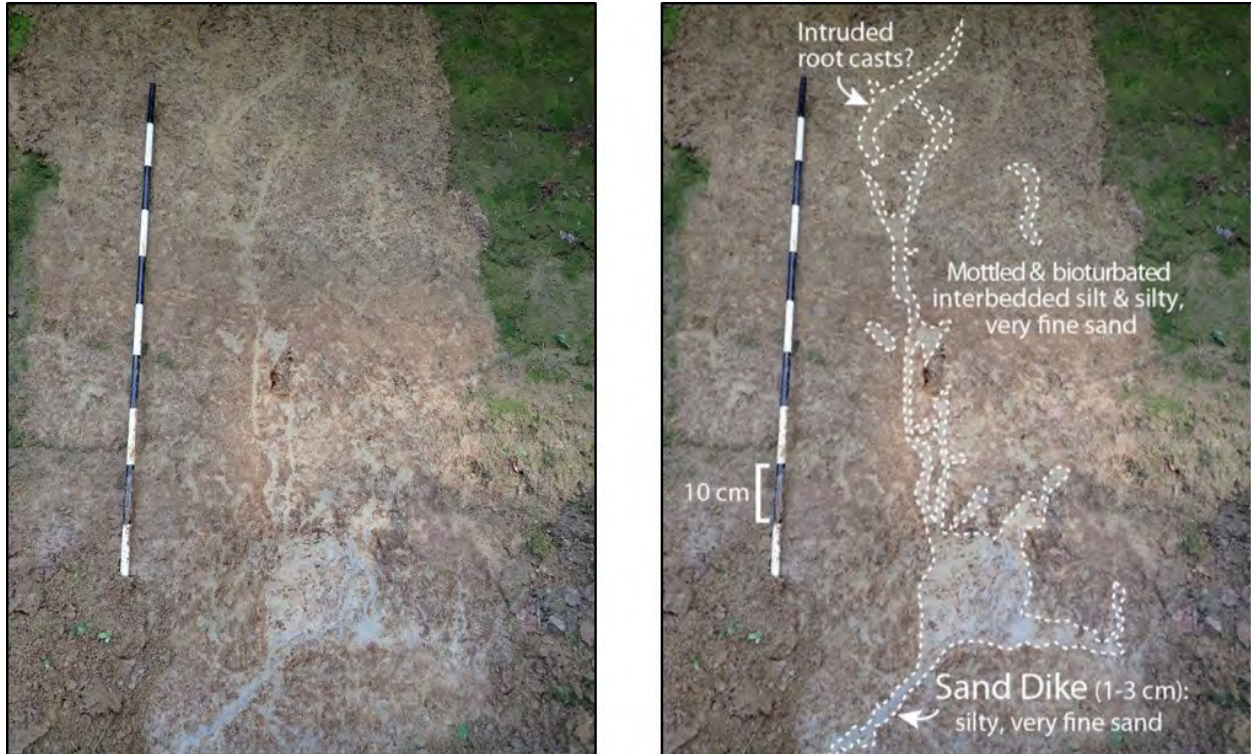


Figure 4-7 Photographs (left - unannotated; right - annotated) of paleoliquefaction features found along South Anna River downstream from sand blows that formed during 2011 M 5.7 Virginia earthquake. Lower in the section, the main dike is tabular and has distinct margins; higher in the section, the dike branches to form a sill and smaller dikes. The main dike appears to have intruded near-surface tubular root casts. Bioturbation and iron staining of their margins suggest that features are prehistoric in age. Black and white intervals on meter stick are 10 cm long.

The findings of the 2011 post-earthquake surveys for liquefaction features along the South Anna River were very promising, suggesting that a liquefaction record of paleoearthquakes is more prevalent than previously thought. Additional study of the possible paleoliquefaction features found at eight sites on the South Anna River in 2011, as well as those found at one site each on the James, Rivanna, and South Anna Rivers in the mid 1990s, seemed warranted. Furthermore, reconnaissance along other rivers in the region, including several to the east of the epicentral area of the Mineral earthquake where liquefiable sediments are common and conditions are suitable for the formation of liquefaction features, would help to test the hypothesis that at least one paleoearthquake larger, and/or located farther to the east, than the 2011 M 5.7 Mineral earthquake struck the region during the Holocene.

4.3.4 Results of NEHRP-Funded Paleoliquefaction Study

During a subsequent study funded by the National Earthquake Hazard Reduction Program (NEHRP) managed by the US Geological Survey, the presence of paleoliquefaction features was verified along the South Anna River and Stigger Creek, a tributary to the Rivanna River, and additional liquefaction features were found along the James, Mattaponi, and Pamunkey Rivers during reconnaissance of 119 km of six rivers in the meizoseismal area (area of strongest shaking and maximum damage) of the 2011 Mineral earthquake (Figure 4-8).

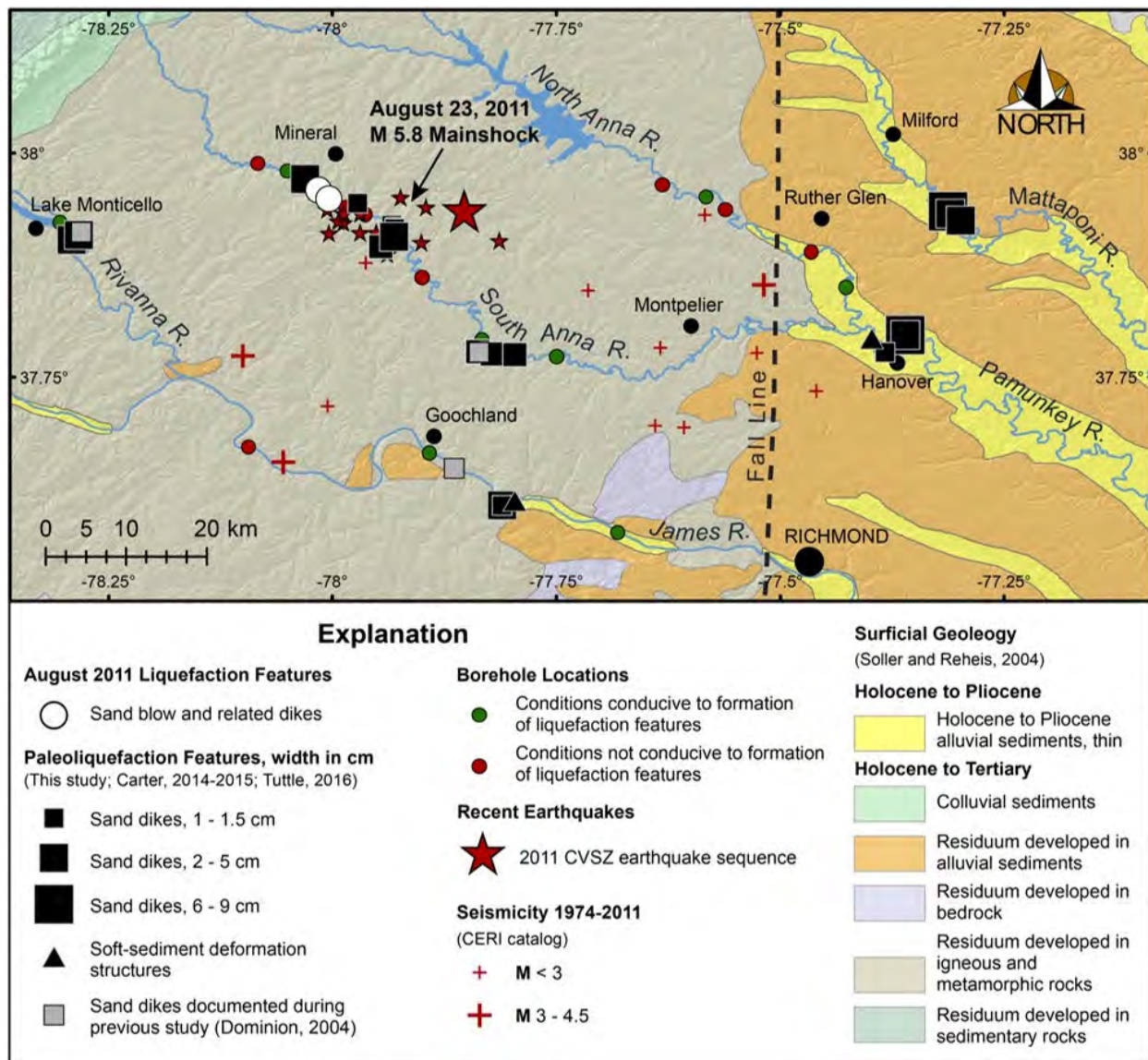


Figure 4-8 Geologic map of the study region showing locations of the 2011 Virginia, earthquake sequence, small sand blows that formed in the epicentral area during that event, and paleoliquefaction features found during this and subsequent studies.

On the basis of weathering characteristics of the liquefaction features as well as radiocarbon and OSL dating of sediment in which liquefaction features occur, at least two episodes of earthquake-induced liquefaction were inferred. A few small (≤ 3 cm) sand dikes and strata-bound soft-sediment deformation structures at three sites on the James and Pamunkey Rivers probably formed during a recent earthquake in the past 500 years. The three sites occur in the southeastern part of the study area suggesting that the earthquake may have been located in this area or farther to the southeast. Bioturbated and weathered sand dikes (≤ 7 cm) and sills at sites on the Mattaponi, Pamunkey, and South Anna Rivers, as well as Stigger Creek, are likely to be prehistoric in age and are currently assumed to have formed during a single Late Holocene earthquake in the past 4,500 years. The size and areal distribution of the liquefaction features suggest that the Late Holocene event was an $M \geq 6$ and located farther to the east than the 2011 Mineral earthquake (Figure 4-9). Additional study is needed to map the full extent and to

constrain the ages of liquefaction features in order to better assess the earthquake potential of the Central Virginia seismic zone. See Tuttle (2016) for details of the study.

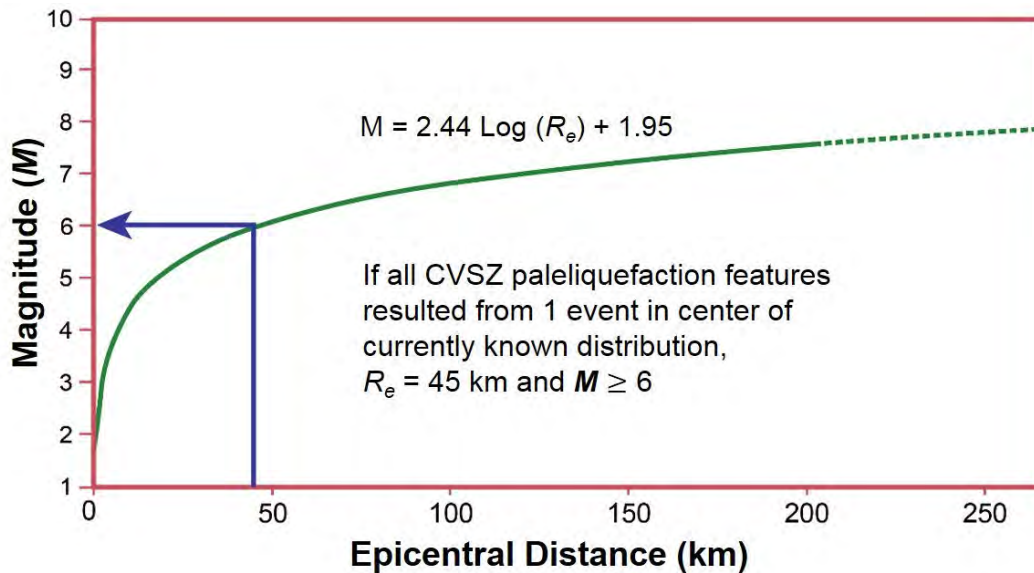


Figure 4-9 Earthquake magnitude-epicentral distance to liquefaction relation developed from worldwide liquefaction data set (modified from Castilla and Audemard, 2007).

4.4 Paleoliquefaction Study of the NMSZ and Surrounding Region

4.4.1 Background

In the winter of 1811-1812, a major earthquake sequence including three mainshocks with **M** 7 to 8 and several large aftershocks, struck the central United States (e.g., Johnston, 1996; Hough et al., 2000; Bakun and Hooper, 2004). These earthquakes are inferred to have been centered in the NMSZ and to include some of the largest known intraplate earthquakes in the world (Johnston and Kanter, 1990). The 1811-1812 New Madrid earthquakes induced liquefaction and related ground failures across the New Madrid region and up to 250 km from their inferred epicenters (Figure 4-10 and Figure 4-11; Fuller, 1912; Saucier, 1977; Obermeier, 1989; Johnston and Schweig, 1996). The large liquefaction field produced by the 1811-1812 mainshocks supports the interpretation that they were very large magnitude earthquakes (Ambraseys, 1988; Tuttle et al., 2002). A repeat of a New Madrid event in the central U.S. would be very damaging to urban centers such as Memphis, Little Rock, and St. Louis (combined population of about 4 million) and to engineered structures across the region.

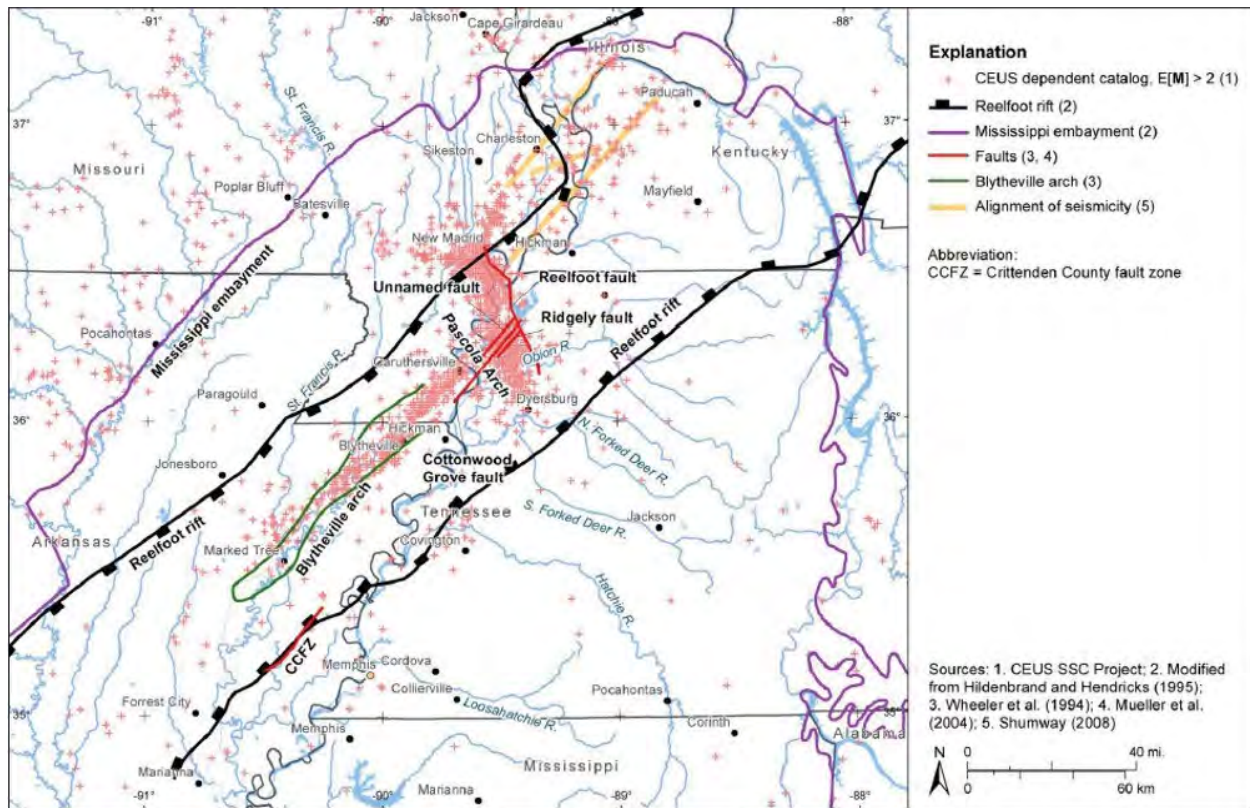


Figure 4-10 Map of NM region, showing seismicity and major subsurface structural features, including Cottonwood-Ridgely fault system in western TN, and southeastern MO, Blytheville arch in northeastern AR, Reelfoot fault near New Madrid, MO, and Reelfoot rift margins (from NUREG-2115).

Paleoseismological studies have begun to decipher the earthquake history of the NMSZ and have changed the perception of the hazard it poses. 1811-1812-type earthquake sequences, or New Madrid events, in A.D. 900 ± 100 years, A.D. 1450 ± 150 years, and 2350 ± 200 years B.C., have been recognized largely through the study of earthquake-induced liquefaction features primarily in the Holocene meander-belt deposits in the New Madrid region (Figure 4-11, Figure 4-12, and Figure 4-13; e.g., Tuttle et al., 2002 and 2005). From these paleoseismic data, a mean recurrence time of 500 years has been estimated for New Madrid events. Although it is based on only two earthquake cycles, this estimate of mean recurrence time has been incorporated into and changed assessments of the regional earthquake hazard and the National Probabilistic Seismic Hazard Maps (Petersen et al., 2008 and 2014).

A study of the morphology of the Mississippi River deposits northeast of the Reelfoot fault found that the river channel experienced abrupt changes that coincided with the A.D. 900 and 2350 B.C. New Madrid events (Holbrooke et al., 2006). In addition, a third abrupt change to the river channel apparently occurred about B.C. 1000. Liquefaction features that formed about this time have been found at a couple of sites in the vicinity of Blytheville, Arkansas (Tuttle, 1999) and support the interpretation that there may have been another New Madrid earthquake about 3 ka (thousand years ago). Taken together, the various types of data provide evidence that the NMSZ produced sequences of very large earthquakes every 500-1800 years during the past 4.5 ka.

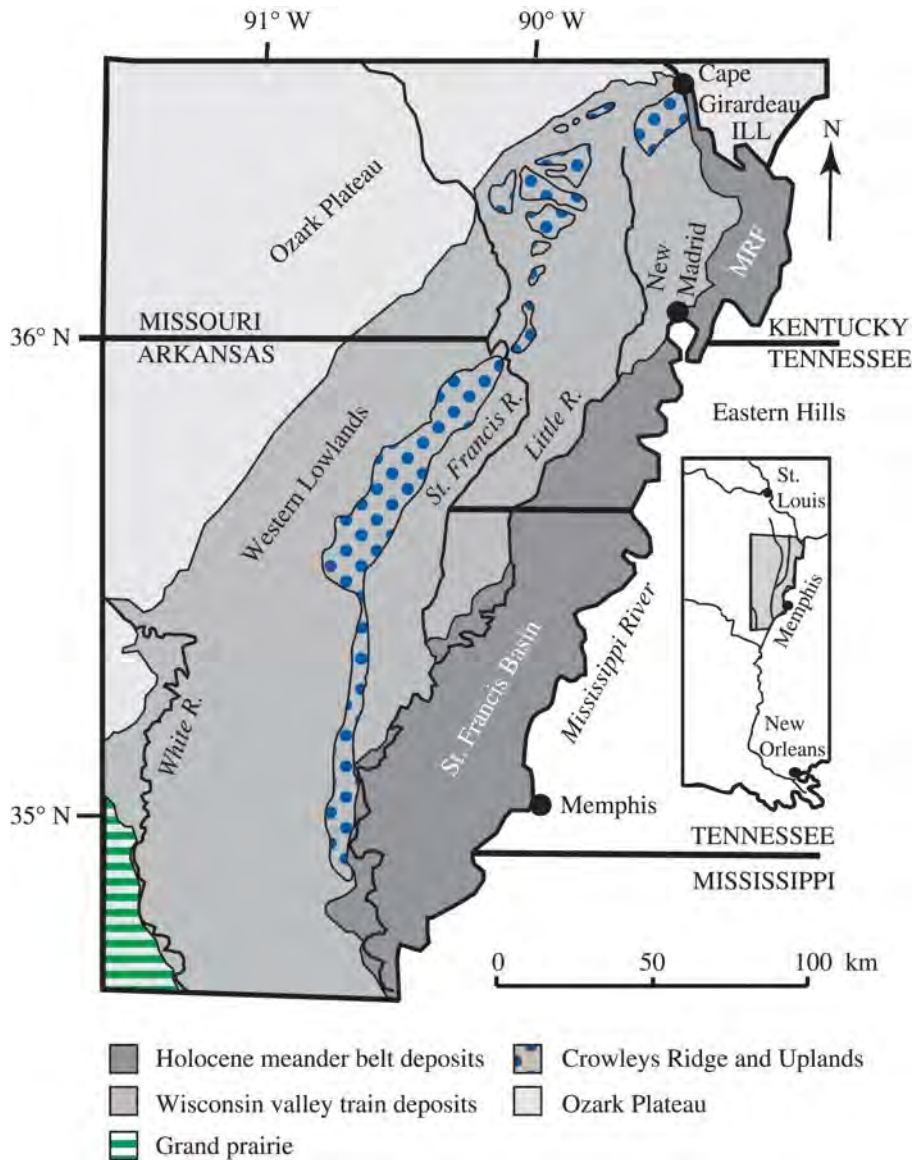


Figure 4-12 Generalized Surficial Geology Map of Mississippi River Alluvial Valley (modified from Saucier, 1994). MRF, Mississippi River Floodway

On the basis of paleoseismic data, Holbrooke et al. (2006) hypothesized that the NMSZ is characterized by active periods separated by periods of quiescence lasting about 1700 years. Bimodal recurrence would have important implications for seismic hazards.

4.4.1.1 Relationship of the New Madrid Seismic Zone to the Reelfoot Rift

The NMSZ is located in the northern part of the Reelfoot Rift, a continental failed rift of Late Precambrian-Early Cambrian age (Figure 4-10). From south to north, the NMSZ is composed of a southwest-northeast trend of earthquakes from about Marked Tree to Caruthersville, a northwest-southeast trend of epicenters from about Dyersburg to New Madrid, and a second northeastern alignment of epicenters from New Madrid to about Charleston (Figure 4-10 and Figure 4-11). The focal mechanisms of earthquakes along the two northeast-trending belts of seismicity are almost pure right-lateral strike-slip, while those in the northwestern-trending belt show almost pure thrust faulting. Thus, the northwest-trending seismicity seems to indicate a compressive step within a

regional strike-slip regime. In addition to the seismicity belts in the center of the Reelfoot Rift, there are also less distinct but nevertheless noticeable northeasterly trends in the modern earthquake epicenters such as along the southeastern margin of the rift in western Tennessee and along the Commerce fault zone in southwestern Illinois and southeastern Missouri. The Commerce fault zone crosses Crowley's Ridge between Sikeston and Poplar Bluff and is thought to be an active fault related to the Reelfoot Rift (Baldwin et al., 2006 and 2014; Figure 4-10 and Figure 4-11).

Although New Madrid seismicity has been correlated with various structural elements, the controlling factors of its location and geodynamic processes affecting its long-term behavior remain uncertain. The most common interpretation is that seismicity may be controlled by inherited structures of the northeast-oriented Reelfoot Rift fault system and an even older northwest-oriented fault system that are being reactivated in the current stress regime (Johnston and Schweig, 1996; Braile et al., 1997; Csontos et al., 2008). In the vicinity of the southwest branch of the seismic zone, shallow seismic reflection and borehole data show a spatial correlation between earthquakes and the Blytheville arch, a Paleozoic structural high of fractured rock (McKeown et al., 1990; Williams et al., 2007). The Bootheel lineament crossing southeastern Missouri and northeastern Arkansas is thought to reflect faulting at depth and to have slipped during the 1811-1812 New Madrid sequence (Schweig and Marple, 1991; Johnston and Schweig, 1996). Hildenbrand and Hendricks (1995) noted that a 100-km wide, southeast trending gravity low, which they interpreted as a Precambrian batholith, intersects the Reelfoot Rift. They postulate that the intersection of the batholith and the Reelfoot Rift may represent an especially weak zone susceptible to earthquake activity and that the batholith may limit the lateral extent of the seismic activity along the rift axis. Another hypothesis is that the Reelfoot Rift may have been significantly weakened by its passage over the Bermuda hotspot during the Cretaceous, making it especially prone to seismic activity (Cox and Van Arsdale, 1997).

4.4.1.2 *Previous Paleoliquefaction Studies in the New Madrid Region*

Previously, Tuttle and collaborators studied liquefaction features at more than two hundred sites and conducted detailed investigations of sand blows at more than fifty sites primarily in the NMSZ (Figure 4-11; e.g., Tuttle et al., 1996, 2002, 2005; Li et al., 1998). During these studies, the ages of liquefaction features were estimated and information gathered regarding the size, sedimentary characteristics, and spatial distribution of both historic and prehistoric liquefaction features. In addition, liquefaction potential analysis was performed to help constrain locations and magnitudes of historic and prehistoric earthquakes.

The age estimates of liquefaction features across the region clustered around A.D. 1810 \pm 130 years, A.D. 1450 \pm 150 years, A.D. 900 \pm 100 years, interpreted as the dates of causative earthquakes (Figure 4-13; Tuttle et al., 2002). In addition, there were large sand blows in northeastern Arkansas and southeastern Missouri, that formed in 2350 B.C. \pm 200 yr (Tuttle et al., 2005). There was a close size and spatial correlation of both historic and prehistoric sand blows within the NMSZ, which was almost certainly the source of earthquakes responsible for most of the liquefaction features (Figure 4-11). The findings indicated that the NMSZ generated sequences including very large, **M** 7 to 8, earthquake every 500 years on average during the past 1,200 years. The estimated uncertainties on the timing of each New Madrid event allow for the intervals to be as short as 160 years and as long as 1200 years (Cramer, 2001).

There is no *a priori* reason to assume a constant recurrence rate anywhere, and certainly not in intraplate areas such as the NMSZ, where driving forces are not well understood. However, some of the variability in earthquake recurrence in the NMSZ is due to uncertainties associated with radiocarbon dating itself and with dating horizons that bound, and therefore pre- and post-date, sand blows. By collecting samples that provide close maximum and minimum age constraints of sand blows, it might be possible to reduce uncertainties associated with their age estimates and thus timing of prehistoric earthquakes. Also, by finding and dating older liquefaction features in areas underlain by Early-Middle Holocene and Late Wisconsin deposits (Figure 4-12), it might be possible to extend the chronology of earthquakes in the New Madrid region back in time to 10,000, possibly 12,000, years B.P.

Many historic sand blows in the New Madrid region were compound structures attributed to the three to four largest earthquakes in the 1811-1812 sequence (Saucier, 1989; Tuttle et al., 2002). Most of these sand blows ranged in thickness from 0.2 to 1.4 m. They were composed of 1 to 4, fining-upward sedimentary units that were 30 to 60 cm thick, tens of meters wide, and hundreds of meters long (Figure 4-14). Occasionally, the units were capped by silt or clay resulting from quiet water deposition following the cessation of ground shaking. Sand blows in the New Madrid region were unusually large features compared to sand blows worldwide. This was due in part to their compound nature. But even individual units composing the sand blows were large, suggesting very large earthquakes. For comparison, sand blows that formed during the M 6.6, 1895 Charleston, Missouri, earthquake, were relatively small, ranging from 0.15 m to 3 m in length (Metzger et al., 1998). Liquefaction-related ground failures resulting from the 1895 earthquake were limited to a 15 km² area surrounding the inferred epicenter.

Like those that formed in 1811-1812, many sand blows attributed to prehistoric earthquakes also were compound structures composed of multiple, fining upward units. Individual sedimentary units of the prehistoric sand blows were similar in thickness and lateral extent to sand blow units that formed in 1811-1812, suggesting that the A.D. 1450 and A.D. 900 events caused similar levels of ground shaking, and therefore were similar in magnitude, to the 1811-1812 earthquakes. The compound nature of the prehistoric sand blows suggested that several very large earthquakes clustered in time, characterized the prehistoric events. Sedimentary characteristics of prehistoric sand blows argued for liquefaction induced by a few very large earthquakes over a period of months, rather than more numerous, smaller earthquakes over a period of hundreds of years.

The spatial distribution of sand blows that formed in 1811-1812 was explained by three liquefaction fields, taking into account the internal stratigraphy or number and thickness of the major depositional units constituting sand blows across the region (Figure 4-15). Many of the sand blows that formed in 1811-1812 are composed of three major sedimentary units. Sand blows in the Dyersburg-Blytheville area have a fourth unit that may have formed as a result of a large aftershock on December 16, 1811. In a review of intensity data, the December 16th aftershock was located northwest of Dyersburg and attributed to the southeastern segment of the Reelfoot fault (Hough and Martin, 2002). It will be interesting to see if a fourth field in the Dyersburg-Blytheville area is corroborated as additional data is gathered in the area and incorporated into the regional liquefaction maps.

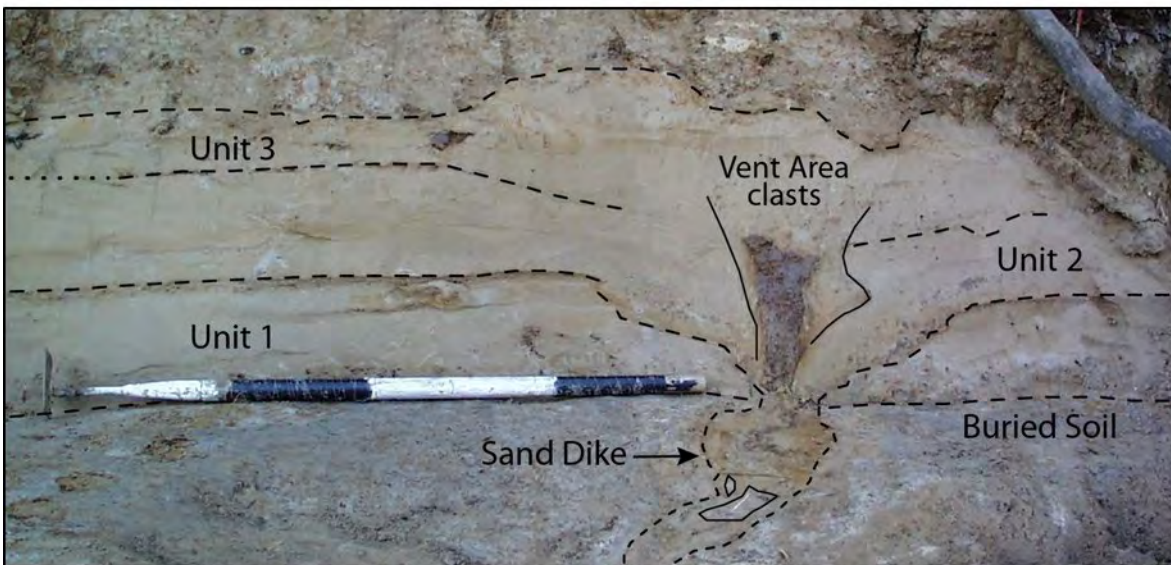


Figure 4-14 Sand blow (upper photo - unannotated; lower - annotated) at site OR213 along Obion River near Midway, TN, composed of three sedimentary units separated by thin layers of silt (modified from Tuttle et al., 2002). Each unit probably formed as result of a large event in earthquake sequence. This sand blow is interpreted to have formed during 1811-1812 earthquakes. Dashed and dotted lines represent clear and inferred contacts, respectively. For scale, hoe is 1 m in length.

The liquefaction fields for the 1811-1812 earthquakes were constrained by field data on sand blows collected prior to 2001 and encompassed the preferred fault-rupture scenario for the 1811-1812 event proposed by Johnston and Schweig (1996) (Figure 4-15). Prehistoric liquefaction features were modeled in a similar manner as the 1811-1812 earthquake sequence. For example, the spatial distribution and internal stratigraphy of sand blows attributed to the A.D. 900 event were similar to sand blows that formed in 1811-1812. Therefore, the liquefaction fields encompassing sand blows attributed to the A.D. 900 event were similar to the 1811-1812 liquefaction fields, except in the southern part of the seismic zone, where one field is smaller in size because sand blows of this age had not yet been identified near Dyersburg or Paragould

(Figure 4-15). Sand blows that formed about A.D. 900 near Blytheville and Caruthersville were composed of three depositional units, and therefore, were attributed to three different events whose liquefaction fields overlap in that area. The distribution and internal stratigraphy of sand blows attributed to the A.D. 1450 event also were fit with three liquefaction fields. Other interpretations of sand blow distribution and stratigraphy were possible, but those presented above seemed the most reasonable based on the data available in 2001.

The preferred interpretation of prehistoric sand blows suggested at least two earthquakes occurred in A.D. 1450 and A.D. 900 that were similar in locations and magnitudes to the 1811-1812 mainshocks. In addition, it was suggested that (1) faults, associated with the northwest-oriented, central branch of the NMSZ, such as the Reelfoot fault, were the source of similar-size earthquakes during all three sequences, (2) faults associated with the southern branch of the seismic zone may have ruptured during each sequence, but produced a smaller magnitude earthquake in A.D. 900, and (3) faults associated with the northern branch of the NMSZ may have ruptured in A.D. 900 and 1812, but not in A.D. 1450. This approach of using sand blow distribution and stratigraphy to map the liquefaction fields of multiple large events in an earthquake sequence may prove a powerful tool for identifying earthquake sources and studying the behavior of a complex fault system such as that in the New Madrid region.

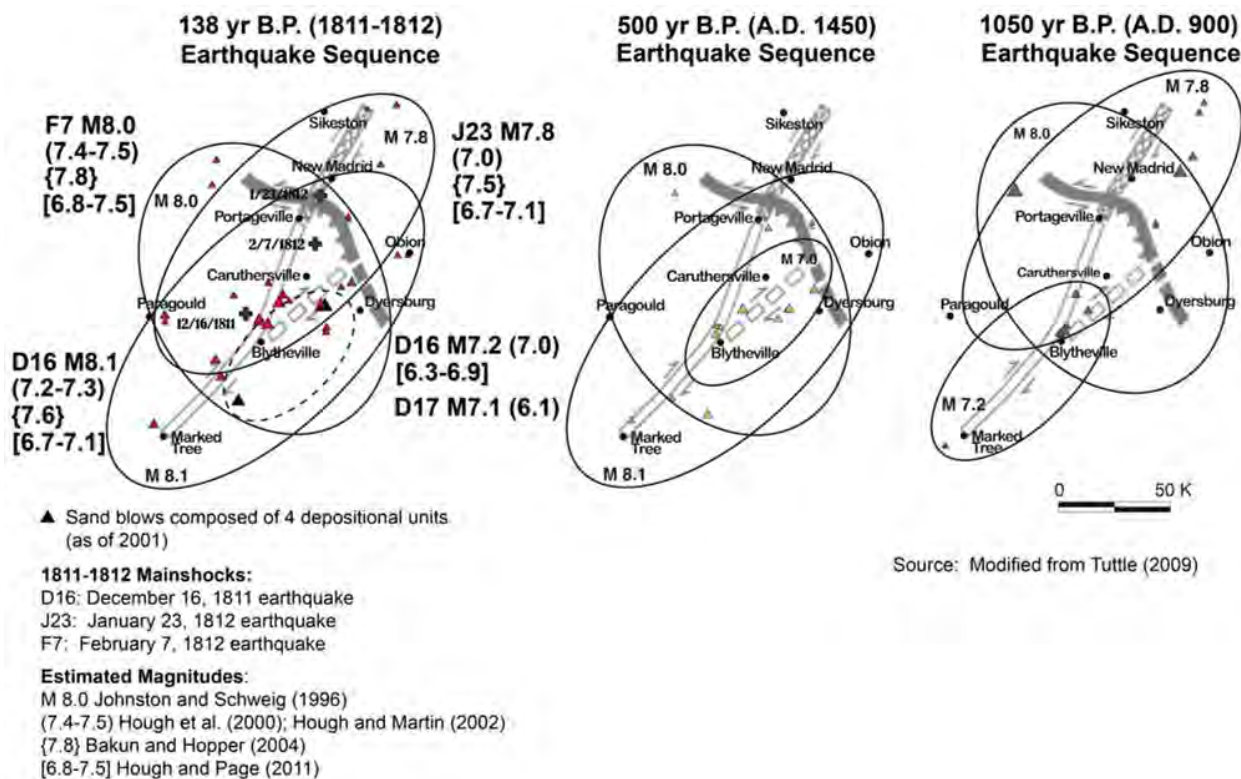


Figure 4-15 Liquefaction fields for past three New Madrid events as interpreted from spatial distribution and stratigraphy of sand blows (from NUREG-2115). Liquefaction fields for 1811-1812 earthquakes are proportional in size to magnitudes derived by Bakun and Hooper (2004).

In general, results of liquefaction potential analysis were consistent with interpretations of the locations and magnitudes of historic and prehistoric earthquakes. Liquefaction analysis performed for sites along the Hatchie River near Covington, TN, suggests that the December 16th and February 7th mainshocks were of **M** 7.6 and 7.8, respectively, and that the January 23rd

event was located too far away to induce liquefaction in this area, even if it were of **M** 7.8 (Tuttle and Schweig, 2004). These magnitude estimates are similar to those derived for the 1811-1812 mainshocks by a reanalysis of intensity data (Bakun and Hopper, 2004). Interestingly, several 1811-1812 sand blows found along Hatchie River were composed of two sedimentary units, probably related to the December 16th and February 7th events. Several Hatchie River sand blows thought to have formed during the A.D. 1450 event also were composed of two units.

Paleoliquefaction studies in the Marianna area of east-central Arkansas about 80 km southwest of the southern end of the NMSZ suggested that other faults of the Reelfoot Rift fault system may have been active during the Holocene (Al-Shukri et al., 2006; Tuttle et al., 2006; Al-Shukri et al., 2015). During those studies, very large sand blows were found in both the Saint Francis Basin and the Western Lowlands near the southern end of the Reelfoot Rift, where few modern or historic earthquakes have been centered (Al-Shukri et al., 2006; Tuttle et al., 2006; Figure 4-11 and Figure 4-16). Radiocarbon and OSL dating indicated that the sand blows are Middle to Late Holocene in age (4.8, 5.5, 6.8, and 9.8 ka). Initial liquefaction potential analysis suggested that earthquakes of **M** 6-6.5 located 5-10 km below the sand blows could account for liquefaction at the sites (for details on methodology and results, see Al-Shukri et al., 2015). Therefore, **M** 6-6.5 was considered a minimum magnitude estimate for the Marianna paleoearthquakes. Small sand blows found near Marked Tree and Blytheville, Arkansas, are similar in age (about 3500 B.C. or 5450 years B.P.) to an exceptionally large sand blow at the Daytona Beach site. The similar-aged sand blows near Marked Tree and Blytheville may be distal liquefaction features resulting from a large earthquake centered near Marianna (Figure 4-11). According to empirical relations between earthquake magnitude and greatest distance to sand blows (Ambraseys, 1988; Castilla and Audemard, 2007), an earthquake centered near the Daytona Beach site would have to be of **M** \geq 7.2 to produce sand blows 140 km away, the distance between Marianna and the Blytheville site (Tuttle et al., 2006).

An earthquake sequence in the Marianna area, like the 1811-1812 New Madrid earthquake sequence, may have resulted from interaction of northeast- and northwest-trending faults. In the Marianna area, the southern end of the Eastern Reelfoot margin intersects the White River fault zone (Figure 4-10 and Figure 4-16). The Eastern Reelfoot margin is thought to be at least 300 km in length, to be seismically active (Hough and Martin, 2002), to have produced Late Wisconsin-Holocene fault displacements in western Tennessee (Cox et al., 2001 and 2006), and to deform and offset Quaternary deposits where it has been imaged below the Mississippi River about 10 km northwest of Memphis (Magnani and McIntosh, 2009; Hao et al., 2013). The fault zone is thought to extend from western Tennessee, southwestward across the floodplains of the Mississippi and St. Francis Rivers, across Crowley's Ridge near the Marianna Gap, and into the Western Lowland just north of Marianna (Figure 4-10 and Figure 4-16). Additional paleoliquefaction data collected in western Tennessee, east-central Arkansas, and northwestern Mississippi, may help to evaluate a possible relationship between the large Late-Middle Holocene sand blows near Marianna and activity along the Eastern Reelfoot margin to the northeast.

Paleoseismic data gathered across the greater New Madrid region support the hypothesis that seismicity migrated across the Reelfoot Rift fault system during the past several tens of thousands of years and most recently shifted to the NMSZ (McBride et al., 2002). It appears that the Commerce fault and Eastern Reelfoot margin may have been active during the Late Wisconsin-Early Holocene, that the southern portion of the Eastern Reelfoot margin near Marianna, Arkansas may have been active between 9.8-4.8 ka, and that the New Madrid fault zone became active about 4.5 ka and remains active today. It seems that seismicity may migrate from one part of the rift to another with a periodicity of 5-15 kyr.

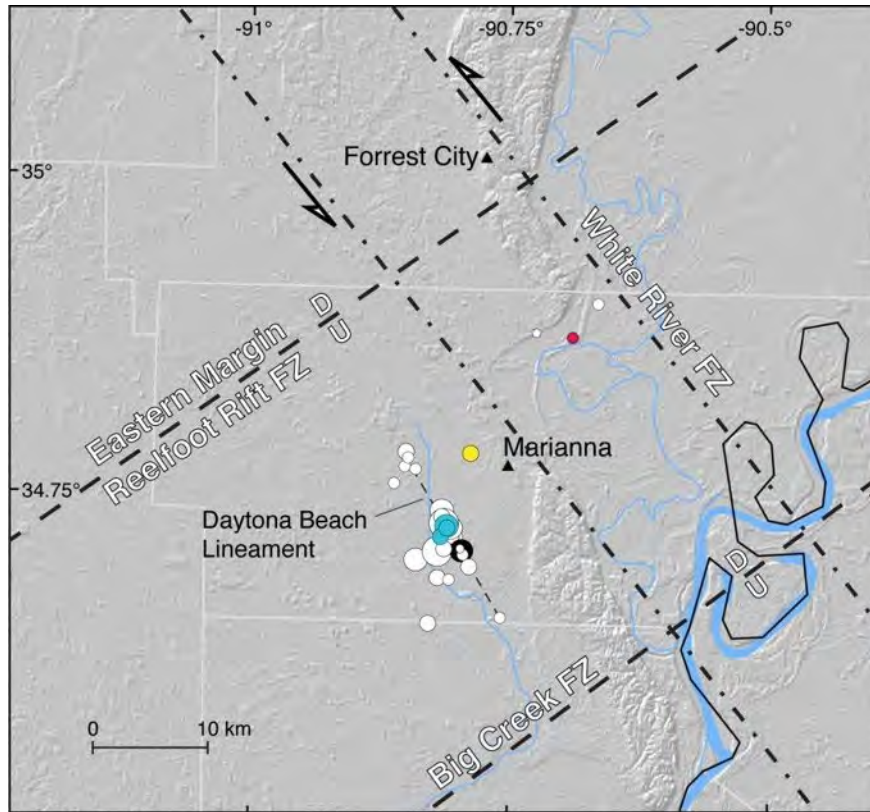


Figure 4-16 Shaded relief map of Marianna area showing locations, estimated ages, and measured sizes of sand blows studied during previous NEHRP grants (modified from NUREG-2115).

4.4.2 NRC Project Plan

This NRC paleoliquefaction study is regional in scope and designed to fill spatial and temporal gaps in the existing paleoliquefaction data. Previously identified liquefaction sites were targeted along the Black and Current Rivers in the Western Lowlands and along the Obion River in western Tennessee (Figure 4-17). River surveys were conducted in search of earthquake-induced liquefaction features in key areas that had not been searched previously and that occur in close proximity to possible earthquake sources, such as the Commerce Geophysical Lineament, eastern Reelfoot Rift margin, western Reelfoot Rift margin, and the Marianna area. These areas include portions of Locust Creek Ditch and the Black, Coldwater, St. Francis, and White Rivers. Reconnaissance was also conducted along Tallahatchie River in northwestern Mississippi, Lighthouse Ditch in northeastern Arkansas, and a short stretch of the Black River in northeastern Arkansas, upriver from its confluence with the Current River. Sand blows were identified in areas underlain by Late Pleistocene deposits, and subsequent investigations were conducted at selected sites (Faulkner, Garner, Stiles, Pritchett, and Wildy) in northeastern Arkansas and western Tennessee (Figure 4-18). Various scenario earthquakes were evaluated using

liquefaction potential analysis to help interpret the distribution of liquefaction features. All results are considered together in order to estimate the timing, locations, magnitudes, and recurrence times of paleoearthquakes. The results of this study are presented below in sections 4.4.3 to 4.4.7.



Figure 4-17 Map showing portions of rivers searched for earthquake-induced liquefaction features described in sections 4.4.3 and 4.4.4. Area of Figure 4-18 is outlined in black. Sources of earthquake information are cited in the figure explanation.

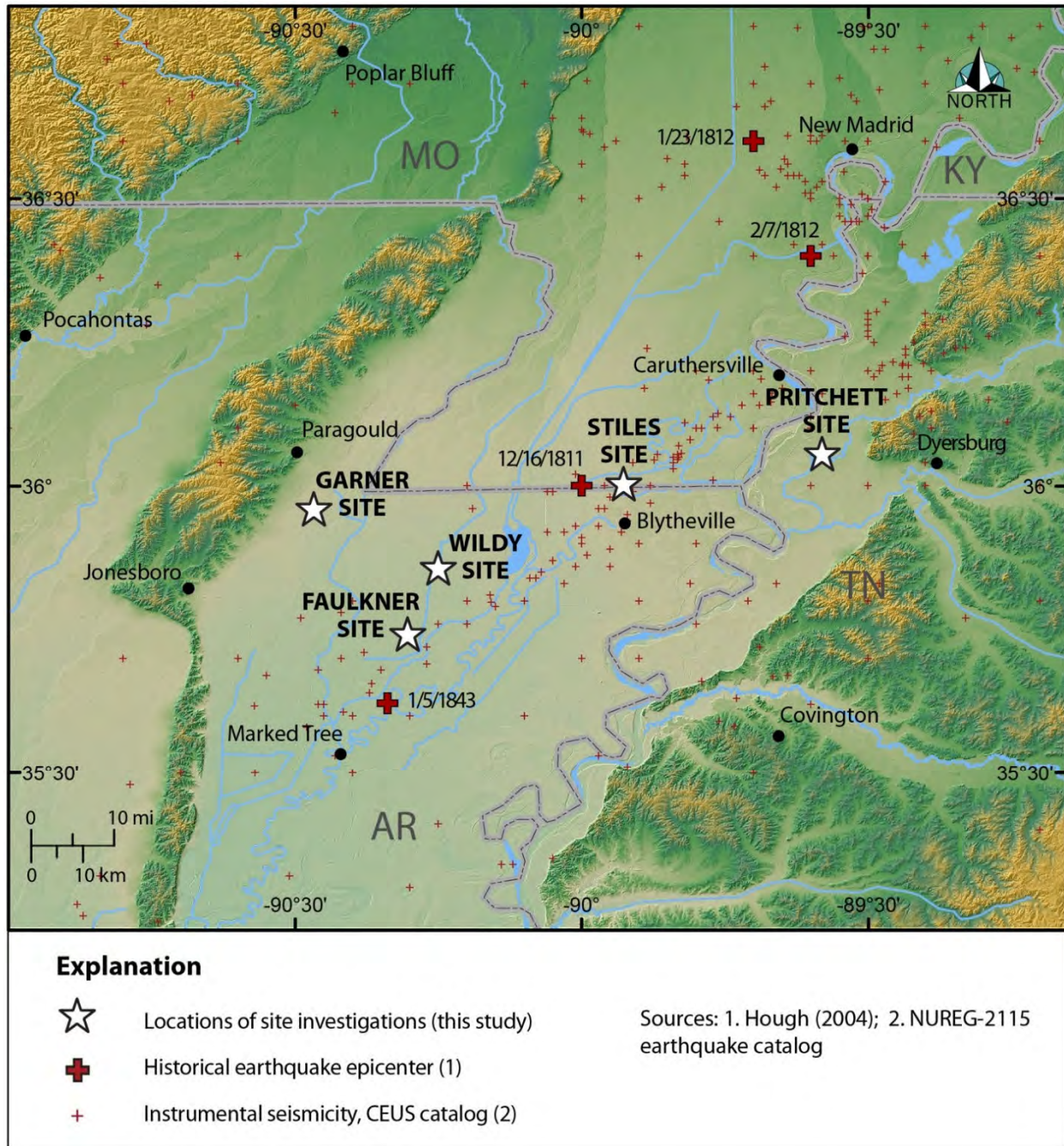


Figure 4-18 Map showing locations of site investigations of sand blows described in section 4.4.5.

4.4.3 Revisiting Liquefaction Sites to Collect Additional Data and Samples

Using the CEUS paleoliquefaction database (NUREG-2115), paleoliquefaction data were reviewed and liquefaction sites selected for further study along the Black and Current Rivers near Pocahontas and Reyno, Arkansas, respectively, and along the Obion River near Obion and Midway, Tennessee (Table 4-1; Figure 4-11, Figure 4-17, Figure 4-19, Figure 4-20, Figure 4-21, and Figure 4-22). Sand blows at these sites were potentially prehistoric in age but additional

dating was needed to estimate the age of the sand blows and their causative paleoearthquakes. Using GPS coordinates of the sites and topographic maps on which the site had been marked, we returned to the approximate locations of the sites, relocated the liquefaction features if possible, documented the features that we found, and collected samples for dating. Liquefaction features described in this section are shown on Figure 4-19 and included in Appendix D. Radiocarbon and OSL dates are included in Appendix E. Radiocarbon dating results generated during this study and cited below are 2-sigma calibrated dates and ages, and ages in years B.P. are relative to years before A.D. 1950.

Table 4-1 Rivers Resurveyed and Liquefaction Sites Revisited (see Figure 4-10, Figure 4-11, Figure 4-17, Figure 4-19, Figure 4-20, Figure 4-21, and Figure 4-22)

River Name	Location	Length (km)	Survey Type	Reasons for Selection
Black River	Near Pocahontas, Arkansas	9.5	Continuous	Liquefaction features previously found along river but ages poorly constrained; Holocene fluvial inset in Late Pleistocene valley-train deposits (level 2); proximity to Commerce Geophysical Lineament
Current River	Near Pocahontas, Arkansas	3	Continuous	Liquefaction features previously found along river but ages poorly constrained; Holocene fluvial inset in Late Pleistocene valley-train deposits (level 2); proximity to Commerce Geophysical Lineament
Obion River	Near Obion & Midway, Tennessee	11.5 11.5	Continuous	Liquefaction features previously found along both sections of river but ages of most features poorly constrained; near Obion, Holocene point bar deposits inset in Late Pleistocene valley train, natural levee, and backswamp deposits; near Midway, Holocene point bar deposits inset in point bar and abandoned channel deposits of Mississippi River and flanked by Late Pleistocene valley train deposits; also between Cottonwood-Ridgely fault system and eastern Reelfoot Rift margin

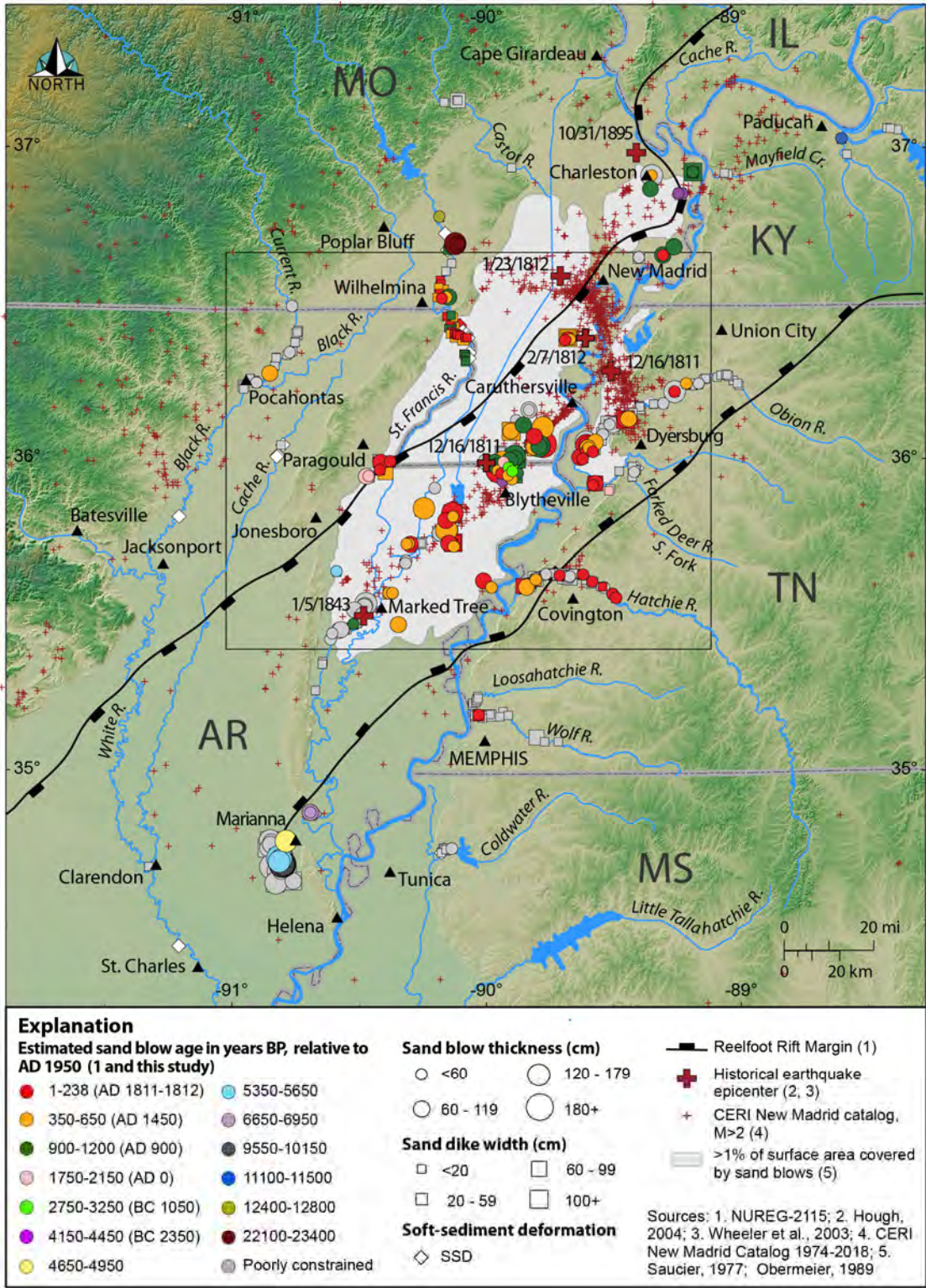


Figure 4-19 Updated map of NMSZ and surrounding region showing ages and measured sizes of earthquake-induced liquefaction features studied during this project as well as previously studied liquefaction features, inferred locations of historic earthquakes, and instrumental located earthquakes (modified from NUREG-2115).

4.4.3.1 *Black River near Pocahontas, Arkansas*

The Black River was searched for earthquake-induced liquefaction features along a 9.5 km section upstream from the boat ramp in Pocahontas while revisiting BR5 and BR7 liquefaction sites previously documented in 1997 (Tuttle, 1999; Figure 4-11, Figure 4-17, and 4-19). No new liquefaction sites were found, but BR5 and BR7 were relocated and samples collected for dating. Both liquefaction sites had been altered by erosion. As described in more detail below, radiocarbon dating at BR5 provides a maximum constraining age of 1740 B.C. (3690 yr B.P.) for the sand dikes that intruded a channel-fill deposit at this site. Radiocarbon dating at BR7 provides a minimum constraining age of A.D. 1930 (or 20 yr B.P.) for the sand blow and related sand dikes at that site. Although the additional dating helps to limit them somewhat, the age estimates of the liquefaction features remain poorly constrained. Liquefaction features at both sites are Late Holocene in age and could have formed during one of several New Madrid earthquakes known to have been responsible for liquefaction features in this area.

The surficial geology along the resurveyed portion of the Black River is mapped as Holocene point bar deposits inset in Late Pleistocene valley train deposits on which sand dunes occur in some locations (Figure 4-21). There was very good exposure of fluvial deposits along the river with most cutbanks on the order of 3.5 to 5 m high. Sediment exposed in the cutbanks was typically unweathered silt underlain by weathered silt with redoximorphic features (aka mottles) followed by interbedded silt and sand or cross-bedded sand or by channel-fill deposits of gray silt embedded in cross-bedded sand. In a few locations, unweathered silt was underlain by iron-stained clayey sand containing buried soils and large krotovina casts. These sediments are likely Late Pleistocene in age.

During the previous survey, two iron-stained sand dikes, 2 and 4 cm wide, were found at BR5 that originated in cross-bedded sand and intruded the southern edge of a channel-fill deposit exposed in the cutbank just downstream from the mouth of the Fourche River. The sand dikes within the channel-fill deposit extended above the contact of the cross-bedded sand and overlying weathered silt with redoximorphic features. Despite careful examination of the site, no organic sample was found that would help estimate the age of the liquefaction features. Therefore, we returned to this site to try to find samples for dating the sand dikes.

During this study, BR5 was easily relocated since the cutbank was well exposed downstream from the mouth of the Fourche River. The contact between cross-bedded sand and the southern edge of the channel-fill deposit was closely examined for the previously discovered sand dikes, but they could not be found. They likely had been removed by erosion along this cutbank. Nevertheless, the stratigraphic relations were the same as before. We found a tree trunk and associated leaf litter horizontally bedded within the channel-fill deposit and near its southern edge. A leaf, sample BR5-L2, collected from this context yielded a date of 1740-1610 B.C. (3690-3560 yr B.P.) (Table 4-2). This date provides an age estimate for the channel-fill deposit and thus a maximum constraining age of 1740 B.C. (3690 yr B.P.) for the sand dikes that intruded the deposit. The liquefaction features previously recorded at this site are Late Holocene in age.

During the previous survey, several sand dikes, up to 9 cm wide, and two overlying lenticular sand bodies were found at BR7. The lenticular sand bodies, 10 and 15 cm thick and 1.1 and 1.7 m wide, were interpreted as small sand blows, though there was no direct connection observed between the sand dikes and the lenticular sand bodies. This lack of connectivity contributed to uncertainty in the interpretation. The liquefaction features occurred in Holocene deposits of the Black River, and therefore, clearly formed during the Holocene. The stratigraphic position of the

sand blows about 4 m below the surface, as well as iron staining and mottling of the likely sand blows and related sand dikes, suggested that they formed prior to the A.D. 1811-1812 New Madrid earthquakes.

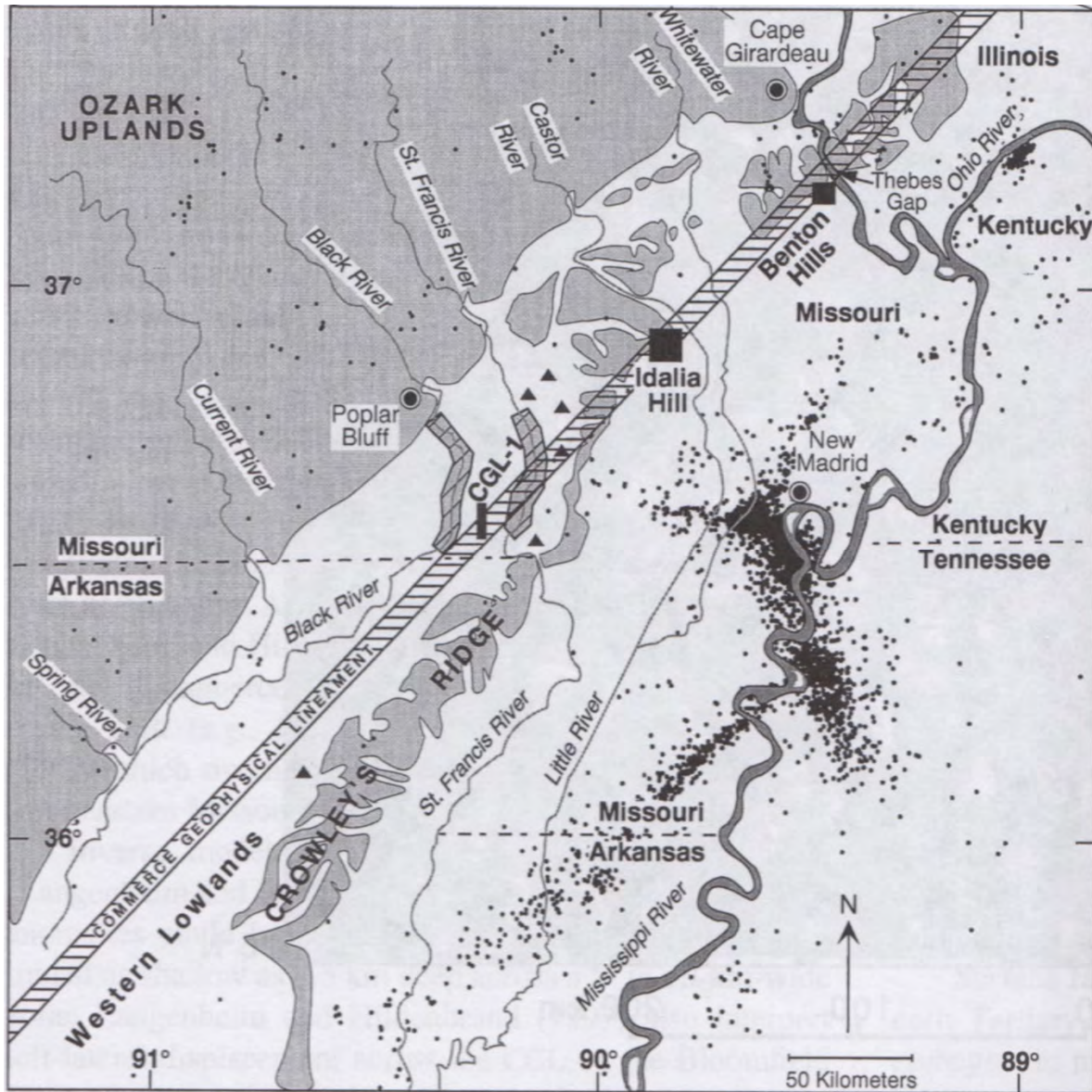
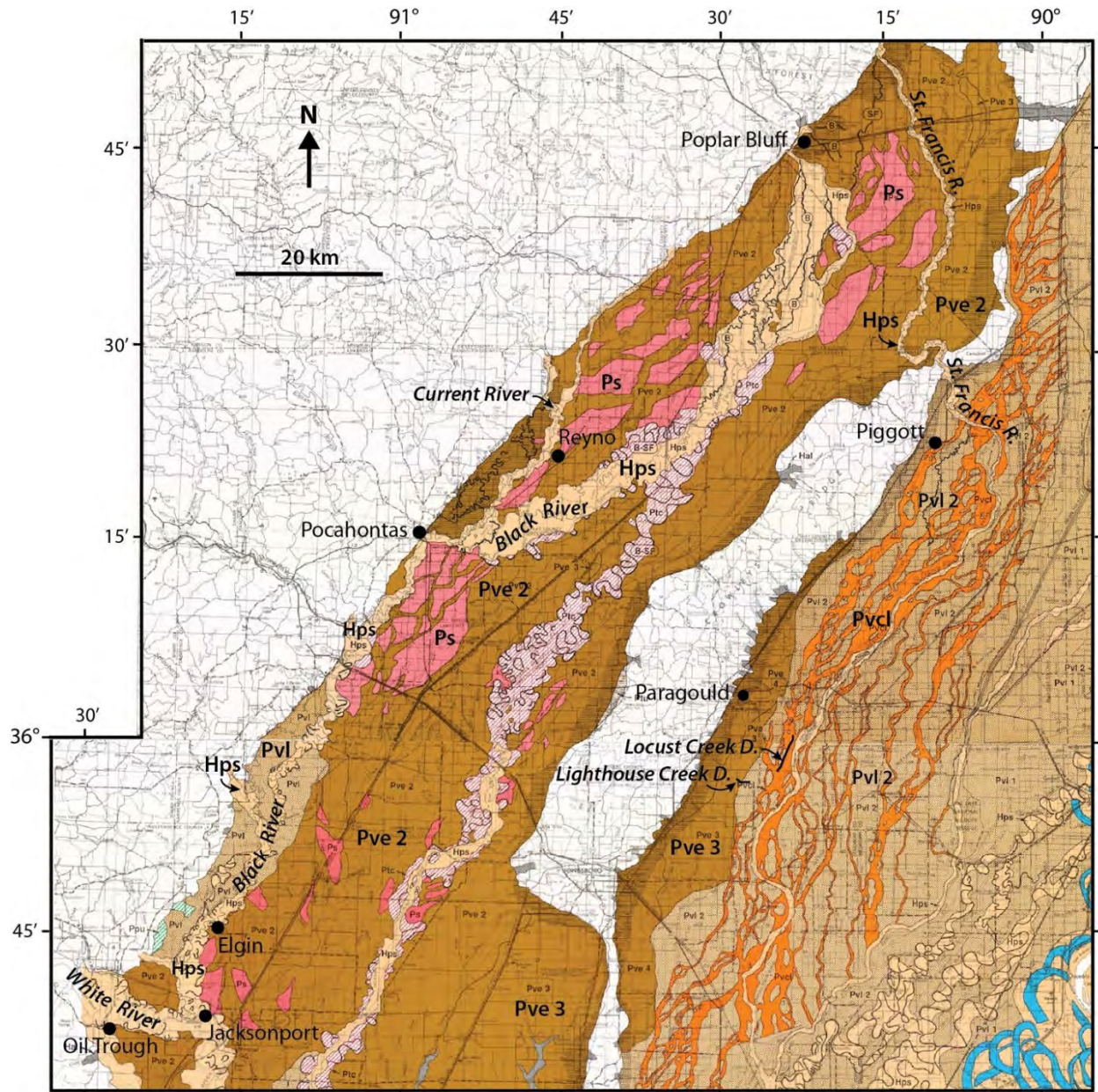


Figure 4-20 Map showing the surface projection of the Commerce geophysical lineament (horizontal hatch pattern) in northeastern Arkansas, southeastern Missouri, and southwestern Illinois (from Stephenson et al., 1999). Sites of paleoliquefaction found near the lineament (Vaughn, 1994) shown by triangles and areas of anomalous river drainage pattern identified along the Black and St. Francis Rivers (Fischer-Boyd and Schumm, 1995) shown by diagonal gray pattern. Seismicity from 1974-1995 shown by black dots.



Explanation

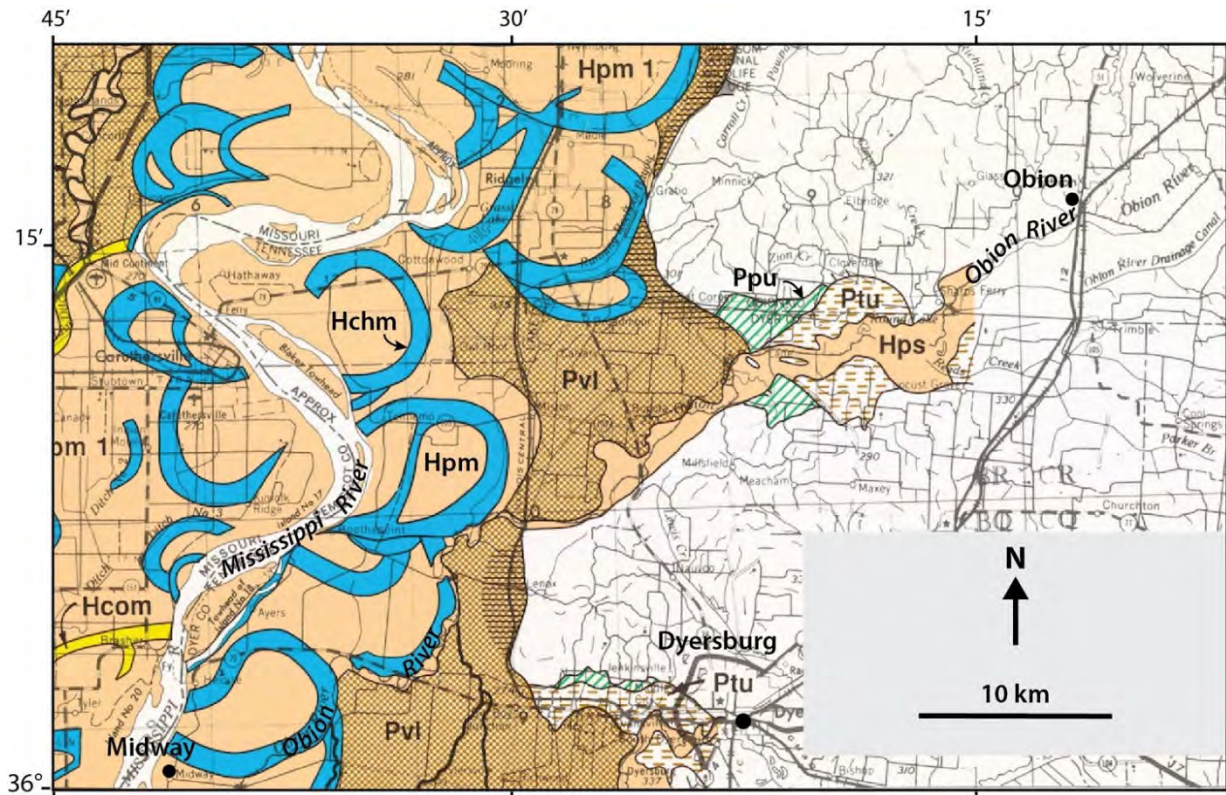
Holocene Units

Hps - Point bar deposits of small streams

Pleistocene Units

- Pvl - Late Pleistocene (Late Wisconsin) valley train (levels 1 & 2)
- Pvc - Relict channels of Late Pleistocene (Late Wisconsin) valley train
- Pve - Late Pleistocene (Early Wisconsin) valley train (levels 1-5)
- Ps - Sand dune fields and eolian deposits on valley trains

Figure 4-21 Map showing Quaternary deposits in the vicinity of Black, Current, St. Francis, and White Rivers along which survey for liquefaction features was performed (modified from Saucier, 1994; plates 4 and 6).



Explanation

Holocene Units

Hps - Point bar deposits of small streams
 Hpm - Point bar deposits of Mississippi R.
 Hchm - Abandoned channels of Mississippi R.
 Hcom - Abandoned courses of Mississippi R.

Pleistocene Units

Pvl - Late Pleistocene (Late Wisconsin) valley train (levels 1 & 2)
 Pve - Late Pleistocene (Early Wisconsin) valley train (levels 1-5)
 Ptu - Fluvial deposits (probably Early Wisconsin or earlier)
 Ppu - Fluvial deposit; mostly natural levee and backswamp

Figure 4-22 Map showing Quaternary deposits in the vicinity of the Obion River along which survey for liquefaction features was performed (modified from Saucier, 1994; plate 5).

During this study, BR7 was revisited to see if the relationship between sand dikes and likely sand blows were any clearer with further erosion of the site and to collect samples for dating. The site was relocated but only one of the likely sand blows and several small sand dikes remained. The sand blow was 4 cm thick and 1.11 m wide. The sand dikes were about 1 to 4 cm wide, crosscut weathered silt, and pinched upward. The larger sand dike became discontinuous about 15 cm below the likely sand blow but domains of the dike could be traced to the base of the sand blow, where a small sand-filled vent structure was observed, indicating that the dike and sand blow are connected and thus related. As before, iron staining and mottling were noted in the sand blow and sand dikes.

A piece of charred material, sample BR7-C1, was collected 30 cm above the sand blow from mottled silt. The sample yielded a date with three ranges of A.D. 1680-1730 (270-220 yr B.P.), 1810-1930 (140-20 yr B.P.) and post-A.D. 1950 (Table 4-2) and provides an age estimate of the silt deposited above the sand blow. The date indicates that the liquefaction features formed before A.D. 1930 (or 20 yr B.P.); thus, either the 1811-1812 or A.D. 1450 ± 150 yr New Madrid

earthquakes could be responsible for the liquefaction features. The weathering of the liquefaction features suggests that they may have formed during the earlier of the two events but this is not certain.

Table 4-2 Radiocarbon Dating Results for Black River Sites

Sample # Lab #	¹³ C/ ¹² C Ratio	Radiocarbon Age Yr B.P. ¹	Calibrated Radiocarbon Age Yr B.P. ²	Calibrated Calendar Date A.D./B.C. ²	Sample Description
BR5-L2 BA-338294	-28.3	3370 ± 30	3690-3560	BC 1740-1610	Leaf from silty, channel fill that dikes intruded; leaf litter adjacent to buried tree at water level
BR7-C1 BA-338295	-26.5	90 ± 30	270-220 140-20	AD 1680-1730 AD 1810-1930 AD Post 1950	Charred material 30 cm above possible sand blow & 1.5 m above water level (AWL) from mottled silt

¹ Conventional radiocarbon ages in years B.P. or before present (1950) determined by Beta Analytic, Inc. Errors represent 1 standard deviation statistics or 68% probability.

² Calibrated age ranges as determined by Beta Analytic, Inc., using the Pretoria procedure (Talma and Vogel, 1993; Vogel et al., 1993). Ranges represent 2 standard deviation statistics or 95% probability.

4.4.3.2 Current River near Reyno, Arkansas

The Current River was resurveyed along a 3 km section downstream from a boat ramp near Reyno while trying to relocate previously documented liquefaction sites CurR7 and CurR8a that had been previously documented (Tuttle, 1999; Figure 4-11, Figure 4-17, and Figure 4-19). CR7 could not be relocated and was presumed removed by erosion. CurR8a was relocated but had been greatly altered by erosion. As described in more detail below, only one sand dike remained at CurR8a. This sand dike and three others were found along a 70 m stretch of cutbank (Cur101a, 101b, and 100). The sand dikes were iron stained and mottled and likely to be prehistoric in age. Radiocarbon dating of a sample from one of the sites provides a maximum constraining age of 1660 B.C. (3610 yr B.P.) for three of the four dikes. Unfortunately, we were not able to establish a minimum constraining age for any of the dikes. Like the liquefaction features along the Black River described above, the liquefaction at CUR101 and 100 are Late Holocene in age. Given their weathering characteristics, these sand dikes likely formed during one of the prehistoric New Madrid earthquakes.

The surficial geology along the resurveyed portion of the Current River is mapped as Holocene point bar deposits inset in Late Pleistocene (Early Wisconsin) valley train deposits (level 2) on which sand dunes occur in some locations (Figure 4-21). There was very good exposure of fluvial deposits along the river with most cutbanks on the order of 5 to 5.5 m high. Sediment exposed in the cutbanks was typically unweathered silt underlain by weathered silt with redoximorphic features followed by gray silt or interbedded silt and sand.

Previously, seven dikes, two sills, and one sand blow were documented at CurR8a (Tuttle, 1999). The site occurred along 14 m of the southern cutbank of the Current River near the western margin of a north-northwest trending abandoned river channel. The sand blow occurred low in the section and was as much as 12 cm thick and about 8 m wide. The sand blow was crosscut by

one or two generations of younger dikes. One of the dikes extended to within 1.3 m of the ground surface. The upper 50 cm of the dike was weathered, suggesting that it formed prior to 1811. Radiocarbon dating, structural and stratigraphic relations, and varying degrees of weathering of the liquefaction features indicate that at least two, and possibly as many as four, paleoearthquakes induced liquefaction at this site since B.C. 3490 or in the past 5440 yr B.P. We returned to CurR8a to collect additional samples for dating the liquefaction features at this site in hopes of further constraining the timing of paleoearthquakes in the Pocahontas area.

During this study, CurR8a was relocated near the western margin of a north-northwest trending abandoned river channel. However, the site had been so altered that it was given a new site number, CurR101a. The sand blow had been completely removed by erosion, but a 5 cm wide sand dike remained. It intruded mottled silt, branched upward, and extended to 1.9 m below the terrace surface where it became a discontinuous dike for another 20 cm (Figure 4-23). The sand dike fined upward from fine sand to very fine sandy, silt. The upper part of the dike was mottled and the middle part slightly iron stained. The weathering characteristics of the dike suggest that it is prehistoric in age. A sample of charred material, CurR101a-C2, was collected 38 cm below the termination of dike and about 2.1 m below the surface. The date of this sample is 1660-1650 B.C. and 1640-1500 B.C. (3610-3600 yr B.P. and 3590-3450 yr B.P.) (Table 4-3). The sample provides a maximum constraining age of B.C. 1660 (3610 yr B.P.) for the sand dike.

Table 4-3 Radiocarbon Dating Results for Current River Sites

Sample # Lab #	¹³ C/ ¹² C Ratio	Radiocarb on Age Yr B.P. ¹	Calibrated Radiocarbon Age Yr B.P. ²	Calibrated Calendar Date A.D./B.C. ²	Sample Description
CurR101a-C2 BA-338297	-24.5	3300 ± 30	3610-3600 3590-3450	BC 1660-1650 BC 1640-1500	Charred material 28- 38 cm below dike termination from silt

¹ Conventional radiocarbon ages in years B.P. or before present (1950) determined by Beta Analytic, Inc. Errors represent 1 standard deviation statistics or 68% probability.

² Calibrated age ranges as determined by Beta Analytic, Inc., using the Pretoria procedure (Talma and Vogel, 1993; Vogel et al., 1993). Ranges represent 2 standard deviation statistics or 95% probability.

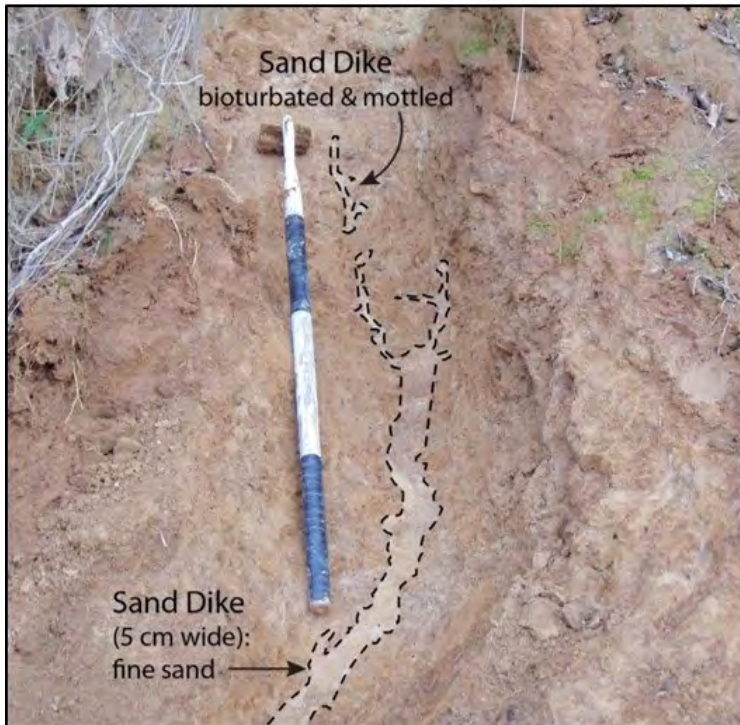


Figure 4-23 Photographs (upper - unannotated; lower - annotated) showing middle to upper part of sand dike intruding mottled silt exposed in cutbank at site CUR101a. Dike branches and narrows up section. Note iron staining and mottling of sand dike. Dashed lines represent clear contacts. For scale, white and black intervals on hoe represent 25 cm.

Only 22 m downstream, two sand dikes were found close together. Their location was given the site designation CurR101b. One dike, 2.5 cm wide, was observed near the base of the cutbank and pinched out 4.5 m below the surface. It was composed of very fine sand and was iron-stained near its termination. The other dike was 2 cm wide, had a strike and dip of N9°W, 85° SW, pinched out 2 m below the surface in mottled silt, and extended up section as a discontinuous dike to 1 m below the surface. This dike was composed of very fine to fine sand and was iron-stained. Given the proximity of CurR101a, sample CurR101a-C2, collected about 2.1 m below the surface, also provides a maximum constraining age of 1660 B.C. (3610 yr B.P.) for the second dike that terminates about 1 m below the surface.

A third dike was found 45 m upstream from CurR101a. Its location was given the site designation CurR100. The dike was 5 cm wide near the base of the cutbank, also intruded mottled silt, and pinched out about 2 m below the surface. This dike was also iron-stained and mottled. Given its similarity in weathering characteristic, this dike is probably similar in age to the dikes at CurR101a and CurR101b and likely formed since 1660 B.C. (3610 yr B.P.) as well.

4.4.3.3 *Obion River near Obion and Midway, Tennessee*

The Obion River was resurveyed along two portions of the river, including 11.5 km near Obion and 11.5 km near Midway, where sand blows had been previously documented in 1995 and 2000, respectively, but whose ages were poorly constrained (Tuttle, 1999; Tuttle and Schweig, 2001; Figure 4-11, Figure 4-17, and Figure 4-19). For the Obion section, the river was resurveyed for 5.5 km upstream and 6 km downstream from the boat ramp south of the town of Obion (Figure 4-24). For the Midway section, the river was resurveyed for 11.5 km upstream from the boat ramp east of the town of Midway. The two sections of the river were resurveyed to locate the sand blows and collect samples for dating as well as to document any additional liquefaction features that had been revealed since the previous surveys. Despite changes to cutbanks due to erosion and deposition, several sand blows were relocated and additional sand blows and sand dikes discovered.

As described in more detail below, it was determined that the sand blow and related feeder dikes at OR6 (renamed OR502) likely formed during the A.D. 1450 New Madrid earthquakes, whereas the newly discovered sand blow and related dikes at OR 507 probably formed during the A.D. 1811-1812 earthquakes. Sand dikes at OR503 likely formed during two different events since B.C. 1010 (2960 yr B.P.). At site OR214, renamed OR602, no new organic samples were found for additional radiocarbon dating, but soil development within and above the sand blow was carefully examined. On the basis of previous dating and amount of soil development, the sand blow and feeder dike could have formed during either the A.D. 1450 ± 150 yr or A.D. 900 ± 150 yr New Madrid events. For OR216, renamed OR603, additional radiocarbon dating provides a minimum constraining age and supports the previous interpretation that the liquefaction features at this site formed during the A.D. 1450 earthquakes. At a newly discovered liquefaction site, OR600, there was a compound sand blow and related feeder dikes. Radiocarbon dating at this site provided a close maximum constraining age of A.D. 1668 (282 yr B.P.) for the sand blow, indicating that the liquefaction features at this site formed during the A.D. 1811-1812 earthquakes.

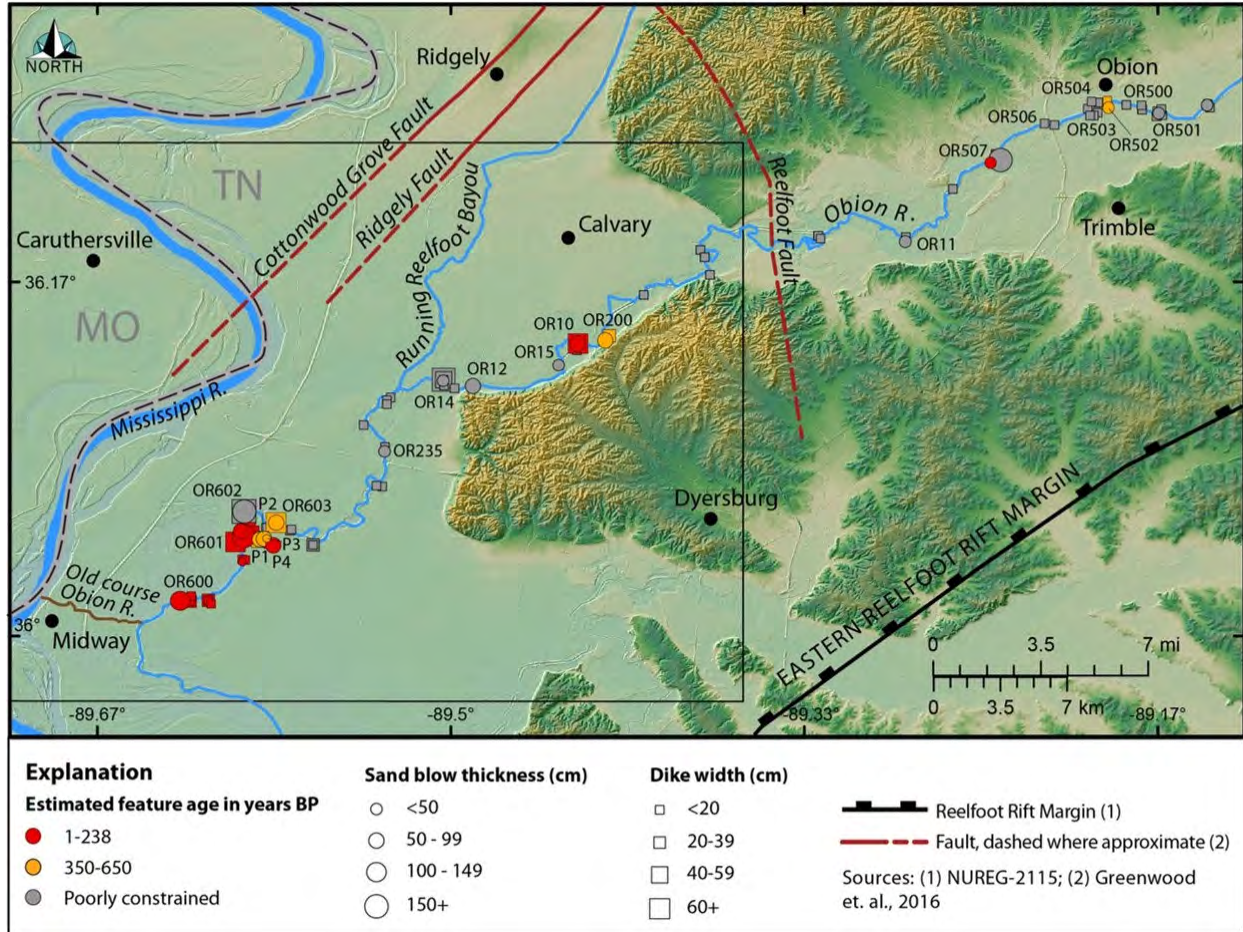


Figure 4-24 Map showing liquefaction features along the Obion River and known geological structures that may have the potential to produce large earthquakes. Area outlined by black rectangle shown in Figure 4-55.

The surficial geology along the Obion section of the river is mapped as Holocene point bar deposits inset in Late Pleistocene valley train, natural levee, and backswamp deposits (Figure 4-22). At the time of the survey, there was very good exposure of fluvial deposits of the lower 2 m of the 4 to 5 m high cutbanks. The upper 2 to 3 m of most cutbanks were often heavily vegetated. Sediment exposed in the cutbanks was typically interbedded silt and sand underlain by weathered silt characterized by redoximorphic features and containing lignite. Using a soil probe to 1.5 m below the river level, silt was underlain by interbedded silt and sand followed by sand.

During the previous survey along the Obion section, two sand blows and related sand dikes had been documented at OR3 and OR6 and sand dikes had been documented at OR4, OR5, OR7, and OR8. During this study, OR3 and OR6 were relocated and given new site names OR501 and OR502, respectively. OR4, OR5, OR7 and OR8 could not be relocated and may have been removed by erosion. Four additional liquefaction sites were found and designated OR500, OR503, OR504, OR506, and OR507. Sand dikes had formed at all of these sites and a sand blow had formed at OR507. OR504 and OR505 were found nearby the previous locations of OR5 and OR7, respectively.

Previously at liquefaction site OR3/501, a sand blow, about 30 cm thick and 5.5 m wide, and two sand dikes, 5.5 and 2 cm wide, were found. The sand blow was overlying and overlain by silt.

The overlying silt and the upper part of the sand blow had been subjected to soil development. A piece of wood (B-86192) collected from the silty loam above the sand blow yielded dates of A.D. 1500 to 1700, 1730 to 1820, and 1920 to 1950. A piece of charcoal (B-86193) collected from 28 cm below the sand blow and 4.3 m below the ground surface yielded a date of B.C. 1680 to 1500. Since no large earthquakes have occurred in the area between A.D. 1920 and A.D. 1950, this range can be excluded. Therefore, the sand blow formed sometime between B.C. 1680 and A.D. 1820 (3630-130 yr B.P.).

During this study, OR3/501 was relocated but had been significantly altered by erosion. Unfortunately, the sand blow had been completely removed by erosion and only one 4-cm-wide sand dike remained. The dike intruded mottled silt, had a strike and dip of N10°E, 75° NW, pinched out 0.8 m above the river level or 4.2 m below the top of the cutbank. The sand dike had clear margins and was composed of very fine to fine sand. A similar sand dike, 3-cm wide, with strike and dip of N14°E, 97° NW, that pinched out 4 m below top of the cutbank, was found along the same bank about 20 m upstream.

At OR6/502, a small sand blow, 12 cm thick and 3 m wide, and a feeder dike, 6 cm wide, were documented. The sand blow was overlain by a silt deposit exhibiting soil development and containing charcoal and burned soil. Two different pieces of charcoal from this horizon (B-91639, B-86194) yielded modern radiocarbon ages. Charcoal collected 42 cm below the sand blow (B-86195) yielded a date of A.D. 1280 to 1400 (670-550 yr B.P.). The sand blow clearly formed after A.D. 1280 (670 yr B.P.) but it was uncertain whether the liquefaction features formed during the A.D. 1450 or A.D. 1811-1812 earthquakes.

During this study, OR6/502 was relocated and found to be somewhat modified by erosion. Most of the sand blow, 12 cm thick and 2.3 m wide, remained. The sand dike had been mostly removed and was only 1 cm wide and pinched out below the base of the sand blow. However, there was a vent structure at the base of the sand blow, suggesting it had been connected to a feeder dike. A 22-cm-thick soil had developed above the sand blow and the entire thickness of the sand blow was iron-stained. On the basis of the rate of soil development of 0.5 ± 0.1 mm/yr estimated for sand blows in the New Madrid region (Tuttle et al., 2000), the 22 cm thick soil above the sand blow suggests that it had formed about A.D. 1510 ± 100 yr. Radiocarbon dating of charred material (OR502-C2) collected 4 cm below the base of sand blow from weathered silt provides a close maximum constraining age of A.D. 1290-1410 (660-540 yr B.P.) (Table 4-4). Given the amount of soil development above the sand blow and the close maximum constraining age of A.D. 1290 (660 yr B.P.), the liquefaction features at this site likely formed during the A.D. 1450 earthquakes.

Three more sand dikes were found 24 m upstream along the same cutbank. This liquefaction site was designated OR503. The two larger dikes, 6 cm and 3 cm wide, extended about 1 m above the river, and were iron stained, especially along their margins. The smaller dike, 1 cm wide, extended 1.37 m above the water table, became silty in its tip, and was unweathered. The difference in weathering characteristics suggested that the dikes formed during two different events. A sample of charred material (OR503-C1) collected 70 cm above the river level, or 3.7 m below the top of the cutbank, yielded a date of B.C. 1010-890 and B.C. 880-850 (2960-2840 and 2820-2800 yr B.P.) (Table 4-4). Since all three dikes extend higher in the section than the position of the sample, the two generations of sand dikes formed since B.C. 1010 (2960 yr B.P.).

Table 4-4 Radiocarbon Dating Results for Obion River Sites

Sample # Lab #	¹³C/¹²C Ratio	Radiocarbon Age Yr B.P.¹	Calibrated Radiocarbon Age Yr B.P.²	Calibrated Calendar Date A.D./B.C.²	Sample Description
OR502-C2 BA-315738	-27.3	610 ± 30	660-540	AD 1290-1410	Charred material 4 cm below sand blow from weathered silt
OR502-C3 BA-306978	-25.7	134.2 ± 0.5 pMC	Modern 0+	Modern AD Post 1950	Charred material from soil developed in sand blow 7 cm below upper contact of soil
OR503-C1 BA-315739	-27.1	2790 ± 30	2960-2840 2820-2800	BC 1010-890 BC 880-850	Charred material 3.7 m BTC & 70 cm AWL from weathered silt crosscut by sand dikes
OR505-W1 BA-306979	-25.4	80 ± 40	270-210 190 150-10	AD 1680-1740 AD 1760 AD 1880-1940 AD Post 1950	Wood, outer 3 cm of Cypress stump rooted in layered silt near WL
OR507-W1 BA-306980	-23.6	40 ± 30	240 60-40 0	AD 1710 AD 1880-1910 AD 1950-1960+	Charred material from upper 1 cm of soil developed in sand blow
OR600-C5 BA-399639	-27.9	130 ± 30	282-169 152-Post 0	AD 1668-1781 AD 1798-Post 1950	Charred material 3 cm below base of sand blow from buried clay
OR601-C2 BA-399642	-28.3	150 ± 30	285-165 155-60 45-Post 0	AD 1665-1785 AD 1795-1890 AD 1905-Post 1950	Twig 70 cm below sand blow from silty clay
OR603-C2 BA-399646	-25.5	80 ± 30	265-220 140-25 Post 0	AD 1685-1730 AD 1810-1925 AD Post 1950	Charred material, angular piece, 19 cm above upper contact of sand blow, from silt layer in interbedded silt and sand deposit
OR604-W4 BA-399647	-27.0	700 ± 30	685-650 580-570	AD 1265-1300 AD 1370-1380	Twig, horizontally bedded, from clayey channel fill, 94 cm below top of deposit

¹ Conventional radiocarbon ages in years B.P. or before present (1950) determined by Beta Analytic, Inc. Errors represent 1 standard deviation statistics or 68% probability.

² Calibrated age ranges as determined by Beta Analytic, Inc., using the Pretoria procedure (Talma and Vogel, 1993; Vogel et al., 1993). Ranges represent 2 standard deviation statistics or 95% probability.

At OR507, there were three sand dikes and one sand blow (Figure 4-25). The largest dike, 10 cm wide at the base of the cutbank, was composed of very fine to fine sand, had a strike and dip of N30°E, 90°, respectively, and was iron stained especially along its margins. The 27-cm-thick sand blow also was composed of very fine to fine sand. It was bioturbated and slightly iron

stained in its upper few centimeters. The sand blow was at least 3.1 m wide. Part of sand blow was covered by tree roots and other vegetation. A soil, about 12-15 cm thick, had developed above the sand blow, suggesting that it could have formed during the 1811-1812 earthquakes. Radiocarbon dating of charred material (OR507-W1) collected from that soil horizon provides a minimum constraining age of A.D. 1710, A.D. 1880-1910, and A.D. 1950+ (240, 60-40, and 0 yr B.P.). Optically stimulated luminescence dating of the sediment (OSL1) immediately below the sand blow provides a maximum age constraint of 5560-4700 yr B.P. (Table 4-5). This OSL date is considerably older than the radiocarbon date of the soil above the sand blow and of radiocarbon dates of sediment exposed elsewhere along the river. The radiocarbon dating results are given more weight since they are thought to be more reliable. The liquefaction features at this site probably formed during the A.D. 1811-1812 earthquakes, given the relatively small amount of soil development above the sand blow, the young minimum constraining age of the sample from the soil, and the minimal weathering of the sand blow.

The sand dikes documented at OR 500, OR504, OR506 ranged from 1-4 cm in width, intruded weathered silt and extended no more than 1 m above the river level. Some of the dikes were weathered while others were not, suggesting that the dikes formed during at least two different events separated in time.

The surficial geology upriver from Midway is mapped as Holocene point bar deposits inset in point bar and abandoned channel deposits of the Mississippi River and flanked by Late Pleistocene valley train deposits (Figure 4-22). At the time of the survey, there was very good exposure of fluvial deposits in the middle portion of the 5-6 m high cutbanks. The upper 1 m of the cutbanks was often vegetated and the lower 1 m was usually covered with recently deposited mud. Sediment exposed in the cutbanks was typically layered silt underlain by silt with redoximorphic features followed by silty clay. At a few locations, cross-bedded sand was exposed below silty clay above the base of the cutbank. From 0-1.5 m below the river level, silt sometimes transitioned to interbedded silt and sand and was underlain by sand, as determined with a soil probe.

During the previous survey along the Midway section, sand blows and related sand dikes were documented at OR209, OR210, and OR211 and thought to have formed during the A.D. 1811-1812 earthquakes (Tuttle and Schweig, 2001). Age estimates of the liquefaction features at these three sites were constrained by radiocarbon dating. On the basis of minimal weathering similar to the other three sand blows, a fourth sand blow and related sand dike at OR213 was interpreted to have formed during the 1811-1812 earthquakes as well. However, sand blows and related sand dikes at two other sites, OR214 and 216, were thought to have formed during previous earthquakes, possibly the event in A.D. 1450 ± 150 years, based on initial radiocarbon dating. These two sites were revisited during this study to collect additional samples for radiocarbon dating in order to better constrain the age estimates of the sand blows. OR214 and OR216 were given new site names, OR602 and OR603, respectively. During resurvey of the river section, OR212 was also relocated and renamed OR601. Previously, three sand dikes had been documented at the site, but erosion of the cutbank had revealed a new sand blow and related sand dikes. In addition, a new liquefaction site was found and designated OR600.

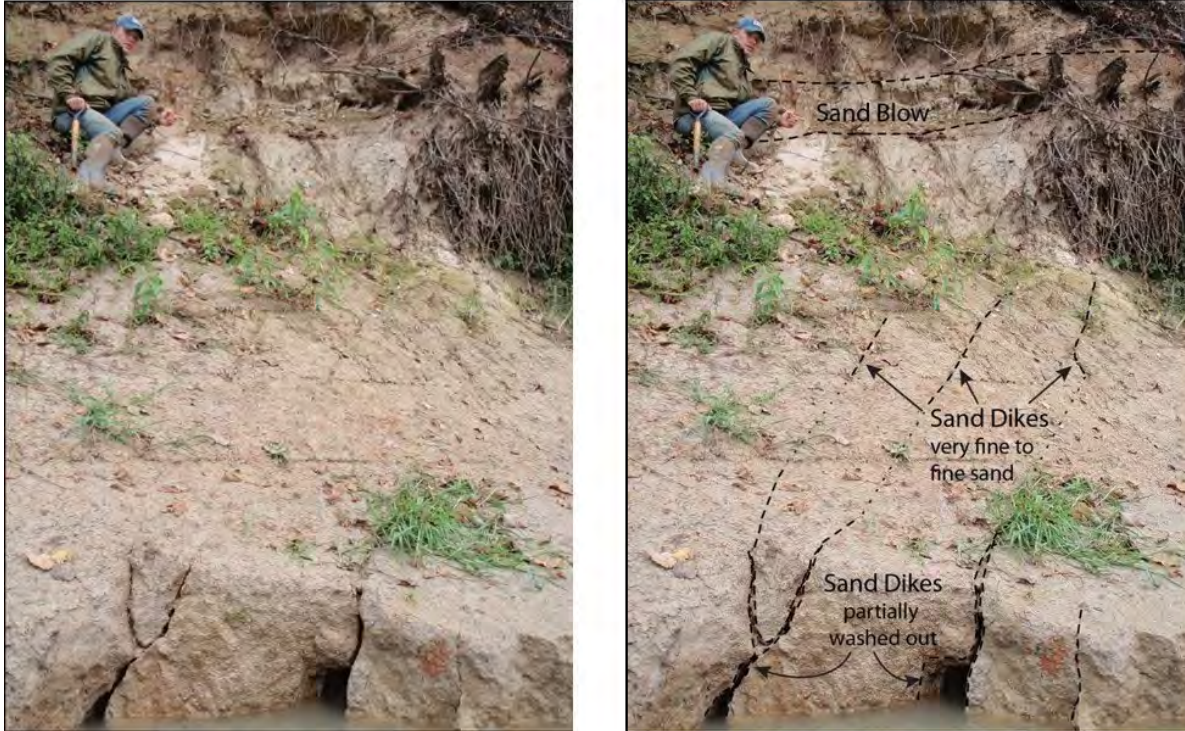


Figure 4-25 Photographs (left - unannotated; right - annotated) prior to cleaning of several dikes intruding mottled silt at OR507. The larger of the three dikes connected to the base of a sand blow in which a soil containing tree roots had formed. Dashed lines represent clear contacts; dotted lines represent inferred contacts.

Table 4-5 Optically Stimulated Luminescence Dating Results at Obion River Site OR507

Sample Number	Lab	Cosmic Dose Rate (Gy/ka) ¹	Total Dose Rate (Gy/ka)	OSL Age (Yr) ²	Calendar Age (Yr) ³	Sample Description
OSL1	USGS	0.16 ± 0.01	2.16 ± 0.05	5190 ± 430	5560-4700	From cutbank, quartz grains from buried soil below sand blow

¹ Cosmic dose rate calculated using methods of Prescott and Hutton (1994).

² Linear and exponential fit used on equivalent dose at one standard deviation. Datum year is A.D. 2010.

³ Years B.P. or before present (1950).

Previously at liquefaction site OR214/602, a sand blow, about 87 cm thick and 50 m wide, and two sand dikes, 14 and 7.5 cm wide, were found. The sand blow was composed of two normally graded depositional units, 43 cm and 44 cm thick, that were separated by a thin (<0.5 cm) layer of silt to either side of the vent structures above the dikes. The vent structures contained clasts of silty clay. Both depositional units were iron stained and cemented, especially the upper portion of the upper unit. The sand blow was about 1.8 m below the top of the cutbank, beneath recent silt containing horizontally bedded logs and weathered silt with redoximorphic features in which a 20-cm-thick A soil horizon had formed. The sand blow was underlain by silty clay. A piece of charred material collected from the base of the soil developed in the silt above the sand blow yielded a date with two ranges of A.D. 1290-1520 and A.D. 1580-1630 (660-430 and 380-320 yr

B.P.) and provided minimum age constraint of A.D. 1620 (320 yr B.P.), indicating that the liquefaction features formed before the A.D. 1811-1812 earthquakes.

During this study, site OR214/602 was relocated but had been altered somewhat by erosion of the cutbank. In the recent exposure, the sand blow was 150 cm thick, 30 m wide, and connected via a vent structure, containing clasts of silty clay, to a 1.4 m-wide sand dike. The sand blow was composed of two normally graded depositional units, 30 cm and 47 cm thick, separated by a thin silt layer, plus a third basal unit, 17 cm thick but of limited lateral extent adjacent to the sand dike. Loose white sand appeared to have been injected along the contact between the basal and overlying units of the sand blow, suggesting a subsequent and more recent episode of earthquake-induced liquefaction. The upper 10 cm of the sand blow had been subjected to soil development, as evidenced by the presence of root pores and organic and iron staining of sand grains. Despite careful looking, no organic samples were found for additional radiocarbon dating to help constrain the age of the sand blow. Several samples were collected but were determined to be either lignite or manganese nodules upon examination with a microscope. On the basis of the rate of soil development of 0.5 ± 0.1 mm/yr estimated for sand blows in the New Madrid region (Tuttle et al., 2000), the 10-cm-thick soil developed in the top of the sand blow suggests that it was exposed for about 166-250 years prior to burial by the overlying silt and therefore predates the overlying silt by this much time. Subtracting this amount of time from the previously determined radiocarbon date of A.D. 1290-1520 and A.D. 1580-1630 (660-430 and 380-320 yr B.P.) from organic material in the soil developed in the overlying silt, the sand blow could date to any time between A.D. 1040 and A.D. 1464 (910-486 yr B.P.). Given the uncertainty in the dating at this site, the large compound sand blow and large dike could have formed during either the A.D. 1450 ± 150 yr or A.D. 900 ± 150 yr New Madrid events.

A very large sand dike, 1.6 m wide, and related sand blow, at least 60 cm thick, previously were found at OR216 (Tuttle and Schweig, 2001). The upper part of the sand blow had been reworked by fluvial processes and subsequently buried by about 4 m of fluvial deposits. A buried soil with *in situ* tree trunks, as well as other sedimentary layers, were offset by about 1 m across the dike. Radiocarbon dating of a sample collected from the *in situ* tree trunk in the buried soil yielded a date of A.D. 1200-1320 and A.D. 1350-1390 (750-630 and 600-560 yr B.P.), providing a close maximum constraining age for the liquefaction features. It seemed likely that these features formed during the A.D. 1450 ± 150 yr earthquakes; however, there was some uncertainty about this interpretation given that there was no minimum constraining age for the liquefaction features.

During this study, site OR216 was relocated in order to collect additional samples for dating. The site was assigned a new number, OR603. The site had been significantly changed by erosion and the lower portion of the cutbank was covered by recently deposited silt. An angular piece of charred material (OR603-C2) was collected 19 cm above the upper contact of the sand blow from a silt layer within an interbedded silt and sand deposit. The sample yielded a date with three ranges of A.D. 1685-1730, A.D. 1810-1925, and post A.D. 1950 (265-220, 140-25, and Post 0 yr B.P.). It is reasonable to discard the two more recent ranges, given that the previously determined date of A.D. 1200-1320 and A.D. 1350-1390 (750-630 and 600-560 yr B.P.) from the *in situ* tree trunk is thought to provide a close maximum constraining age for the liquefaction features. Using both the maximum and minimum constraining ages, the age estimate of the large sand dike and related sand blow is A.D. 1465 ± 265 yr (or 485 ± 265 yr B.P.). This age estimate further suggests that the liquefaction features at this site formed during the A.D. 1450 ± 150 yr earthquakes.

Previously, three sand dikes, ranging from 1.5 to 5 cm in width, had been documented at OR212/601. During this study, the site was found to be significantly altered by erosion, revealing

a large sand blow and two main sand dikes (Figure 4-26). The recently revealed sand blow was 95 cm thick, 40 m wide, and had been fed by multiple branching sand dikes, the two larger dikes both being 23 cm wide. The sand blow was composed of four depositional units of medium to fine sand that varied in thickness and were separated by either thin silt or lignite layers. The sand blow was slightly iron stained throughout but otherwise showed no sign of soil development.

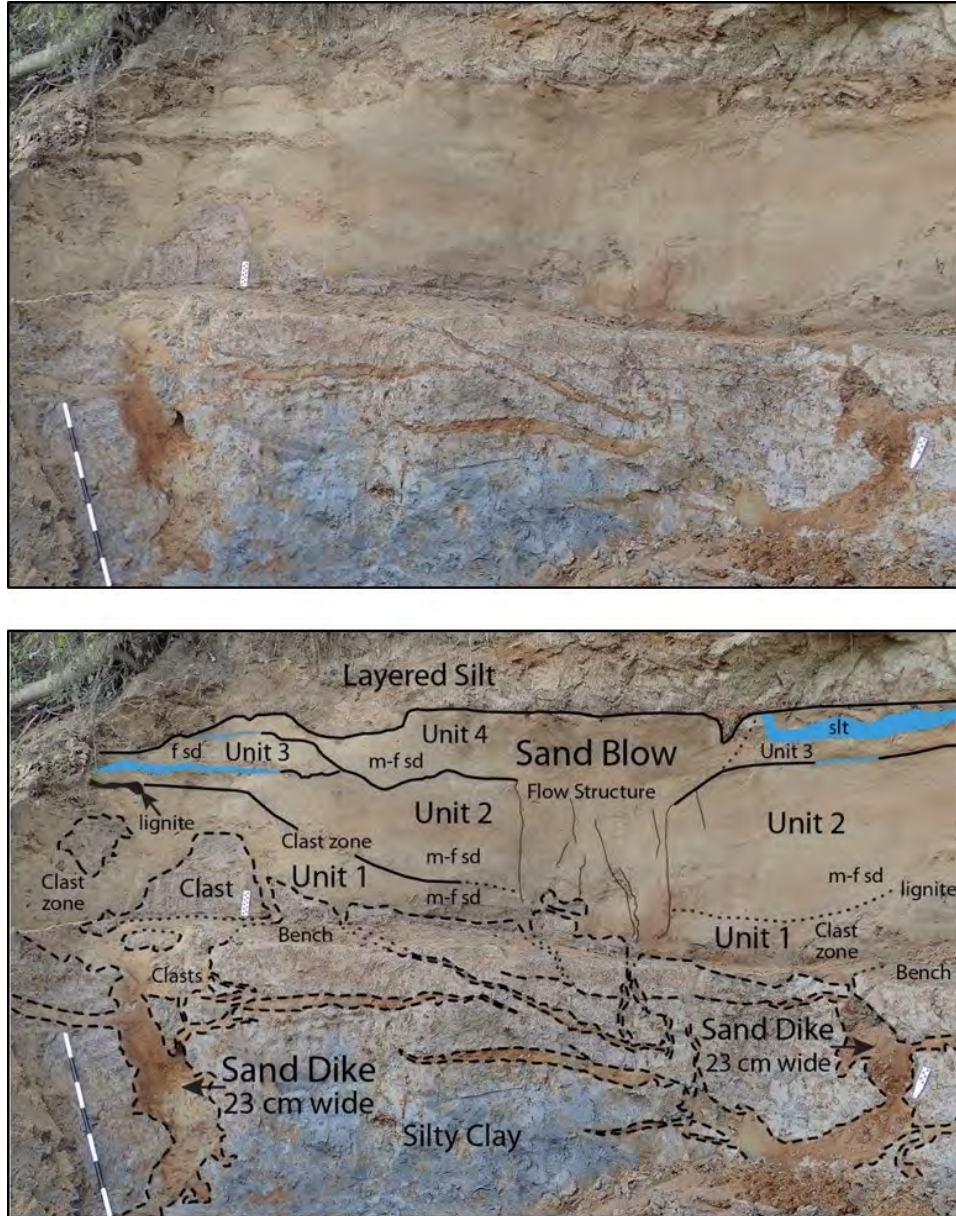


Figure 4-26 Photographs (upper - unannotated; lower - annotated) of two 23 cm wide sand dikes with multiple splays connected to the base of a large sand blow at OR601. The sand blow and dikes, that likely formed during the A.D. 1811-1812 earthquakes, are somewhat iron stained but otherwise showed no sign of soil development. Dashed lines represent clear contacts; dotted lines represent inferred contacts; solid lines represent clear contacts of sand blow units. Blue represents silt layer at top of sand blow unit. For scale, the black and white intervals on the meter stick represent 10 cm.

The sand dikes were also iron stained, especially along their margins. A twig (OR601-C2) collected 70 cm below the sand blow from silty clay yielded a date of A.D. 1665-1785, A.D. 1795-1890, and A.D. 1905-post 1950 (285-165, 155-60, and 45-Post 0 yr B.P.). The date provides a maximum constraining age, indicating that the liquefaction features at this site formed after A.D. 1665 (285 yr B.P.), and therefore, during the A.D. 1811-1812 earthquakes.

A new liquefaction site, designated OR600, was found during the resurvey of this section of the river. At this site, we found a compound sand blow, 105 cm thick and 30 m wide, and a compound sand dike composed of three phases. The sand blow was composed of five depositional units of fine to very fine sand that ranged from 7 to 50 cm in thickness and were separated by either thin layers of silt, silty fine sand, or lignite. The upper 7 cm of the sand blow were weathered. The compound sand dike was composed of three dikes that ranged from 4 to 24 cm in width. One dike was composed primarily of silt and the other two dikes were composed mostly of fine sand. All three dikes exhibited iron staining. The sandy dikes were especially iron stained along their margins. A piece of charred material (OR600-C5) collected 3 cm below the sand blow from silty clay yielded a date of A.D. 1668-1781, A.D. 1798-post 1950 (282-169, 152-Post 0 yr B.P.). The date provides a close maximum constraining age, indicating that the liquefaction features at this site formed after A.D. 1668 (282 yr B.P.). This sand blow and its feeder dikes formed during the A.D. 1811-1812 earthquakes like many of the other liquefaction features along this section of the river.

4.4.4 River Surveys to Identify Liquefaction Features in Key Areas

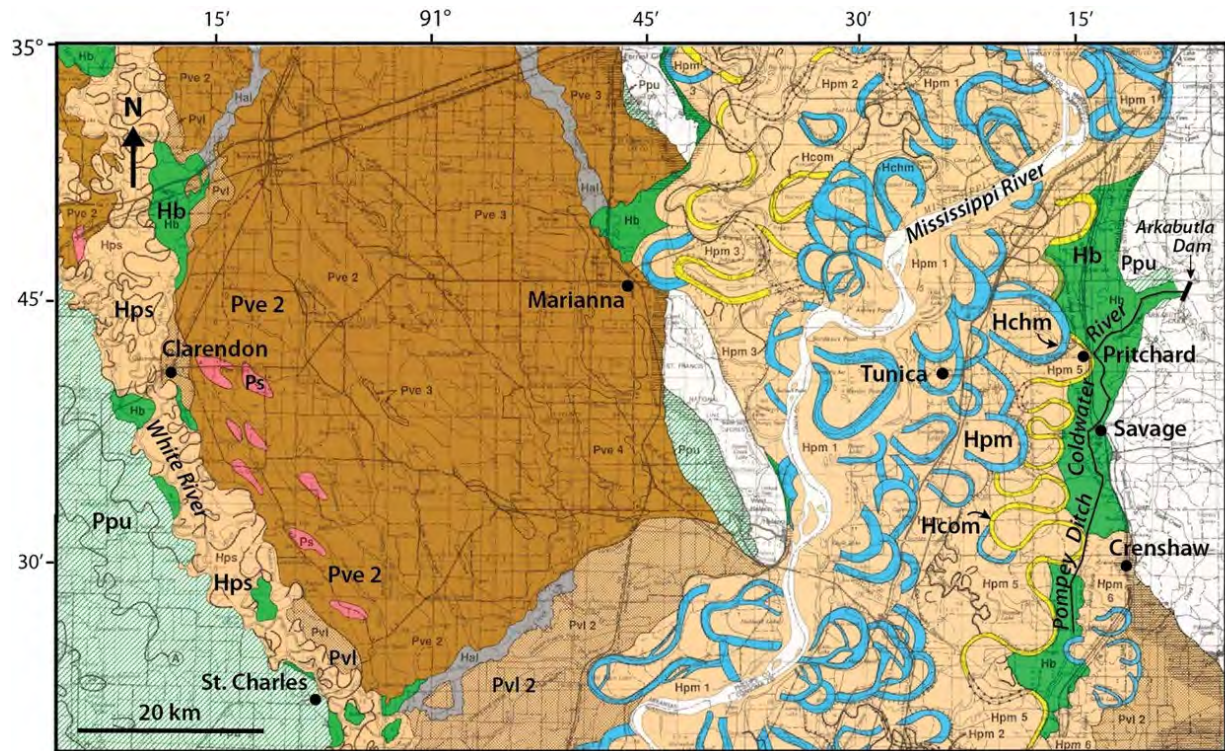
Systematic surveys for earthquake-induced liquefaction features were conducted along selected portions of rivers in key areas for interpreting locations and magnitudes of paleoearthquakes and for assessing certain faults as earthquake sources (Table 4-6). Most of the selected river segments had not been previously surveyed for liquefaction features. These segments included the following: Coldwater River in northeastern Mississippi, east of the Marianna source area and near the eastern margin of the Reelfoot Rift; Locust Creek Ditch and the St. Francis River near the western margin of the Reelfoot Rift in northeastern Arkansas; the St. Francis River near the Commerce fault zone in southeastern Missouri; the White River near Clarendon and St. Charles west and southwest of the Marianna source area in east-central Arkansas, respectively. The Black and White Rivers near Jacksonport, Arkansas, had been searched before but at a time when the river level was relatively high (Tuttle, 1999). Previously, paleoliquefaction features had been found in drainage ditches and fields near the St. Francis River in southeastern Missouri, but a systematic survey had not been conducted along the river (Vaughn, 1994).

4.4.4.1 Black River near Jacksonport and Elgin, Arkansas

We conducted systematic surveys for liquefaction features along two portions of the lower Black River, including 6.5 km upstream from its confluence with the White River near Jacksonport and 26.5 km upstream from Elgin, Arkansas (Figure 4-11, Figure 4-17, and Figure 4-19). Much of the lower Black River had been searched previously in the late 1990s; at the time, the river level was fairly high due to severe rainstorms during fieldwork (Tuttle, 1999). Although no liquefaction features were found at that time, there was concern that the apparent absence was due to lack of exposure of the lower part of the cutbanks. The river was resurveyed in October 2013 when the river level was relatively low.

Table 4-6 Rivers Surveyed for Liquefaction Features in Key Areas (Figure 4-10, Figure 4-11, Figure 4-19, Figure 4-20, Figure 4-21, and Figure 4-27)

River Name	Location	Length (km)	Survey Type	Reasons for Selection
Black River	Upstream from Elgin & Jacksonport, Arkansas	26.5 6.5	Two continuous segments	Liquefaction features not previously found but river level had been high; Holocene point bar deposits inset in Late Pleistocene (Early & Late Wisconsin) valley-train deposits; proximity to WRM and southwest extension of CGL
Coldwater River	Near Arkabutla Dam & Savage, Mississippi	6.5 13	Two continuous segments	Not previously searched; Holocene backswamp deposits inset in Pleistocene fluvial deposits, including natural levee and backswamp deposits; proximity to ERM (southern extension - river fault picks); east of Marianna area
Locust Creek Ditch	Southeast of Paragould, Arkansas	5	Spot checked cutbanks	Little liquefaction data in area except for 1811-1812; Late Pleistocene (Late Wisconsin) valley-train deposits; proximity to WRM
St. Francis River	Between Chalk Bluff & Nimmons, Arkansas	29	Continuous	Not previously searched; geographical gap in paleoliquefaction data; Holocene point bar deposits inset in Late Pleistocene (Late Wisconsin) valley train, including relict channels, and Holocene alluvial fans and aprons adjacent to Crowley's Ridge; between WRM and CGL
St. Francis River	Between Fisk & Wilhelmina, Missouri	33	Continuous	Late Pleistocene and Holocene liquefaction features previously found in area; Holocene point bar deposits inset in Late Pleistocene (Early Wisconsin) valley train deposits; crosses CGL
White River	Oil Trough, Arkansas	10.5	Continuous	Liquefaction features not previously found but river level was high at time; Holocene point bar deposits inset in Late Pleistocene (Early Wisconsin) valley-train deposits; proximity to WRM and southwest extension of CGL
White River	Clarendon, Arkansas	10	Continuous	Not previously searched; Holocene point bar and backswamp deposits inset in Late Pleistocene (Early & Late Wisconsin) valley-train deposits and other fluvial deposits; west of Marianna area
White River	St. Charles, Arkansas	20	Continuous	Not previously searched; Holocene point bar and backswamp deposits inset in Late Pleistocene (Early & Late Wisconsin) valley-train deposits and other fluvial deposits; southwest of Marianna area and north-northeast of Desha County



Explanation

Holocene Units

Hps - Point bar deposits of small streams
 Hpm - Point bar deposits of Mississippi R.
 Hchm - Abandoned channels of Mississippi R.
 Hcom - Abandoned courses of Mississippi R.
 Hb - Backswamp deposits

Pleistocene Units

Pvl - Late Pleistocene (Late Wisconsin) valley train (levels 1 & 2)
 Pve - Late Pleistocene (Early Wisconsin) valley train (levels 1-5)
 Ps - Sand dune fields and eolian deposits on valley trains
 Ppu - Fluvial deposits; mostly natural levee and backswamp

Figure 4-27 Map showing Quaternary deposits in the vicinity of the White and Coldwater Rivers along which survey for liquefaction features was performed (modified from Saucier, 1994; plate 7).

The surficial geology along the resurveyed portions of the Black River is mapped as Holocene point bar deposits inset in Late Pleistocene (Late Wisconsin) valley train deposits and Late Pleistocene (Early Wisconsin) valley train deposits (level 2) on which sand dunes occur in some locations (Saucier, 1994; Figure 4-21). During the survey, there were good to excellent exposures provided by many long cutbanks that ranged from 3-6 m in height, with most in the 4-4.5 m range. The lower cutbanks likely revealed Late Holocene deposits while the few higher cutbanks may have revealed Late Pleistocene deposits. Along the Jacksonport section of the river, sediment exposed in the cutbanks was typically reddish weathered silt underlain by interbedded iron-stained sand and mottled silt that continued below the water level for at least 1.5 m, as determined with a soil probe. In a few locations, where abandoned tributaries intersected the course of the river, reddish weathered silt was underlain by gray massive silt.

At Paroquet Bluff, a 6-m-high cutbank revealed weathered silt underlain by silty rhythmites followed by weathered silt with a pebbly layer near the base of the cutbank. Along the Elgin section of the river, the sediment was somewhat coarser grained. The sediment sections ranged from reddish weathered silt underlain by interbedded iron-stained sand and mottled silt, followed by cross-bedded sand to iron-stained sand underlain by interbedded silt and sand or gray clay with manganese nodules followed by bioturbated cross-bedded sand. Again, where abandoned

tributaries intersected the course of the river, weathered silt was underlain by gray massive silt. The sediment conditions were conducive to the formation of earthquake-induced liquefaction features. Most of the exposures were likely of Late Holocene deposits.

As described in more detail below, soft-sediment deformation structures were found at one location, BR101, along the Elgin section of the river (Figure 4-17 and Figure 4-19). Otherwise, no other liquefaction feature was found along either surveyed section. Although not required, the soft-sediment deformation structures may have formed as the result of earthquake-induced liquefaction. If they did, they would indicate that ground shaking was just barely strong enough (MMI ~VIII) to induce liquefaction at the site. Given the likely Late Holocene age of the sediment in which they occur, the soft-sediment deformation structures may have formed during one of the Late Holocene earthquake sequences centered in the New Madrid seismic zone.

Three more sand dikes were found 24 m upstream along the same cutbank. This liquefaction site was designated OR503. The two larger dikes, 6 cm and 3 cm wide, extended about 1 m above the river, and were iron stained, especially along their margins. The smaller dike, 1 cm wide, extended 1.37 m above the water table, became silty in its tip, and was unweathered. The difference in weathering characteristics suggested that the dikes formed during two different events. A sample of charred material (OR503-C1) collected 70 cm above the river level, or 3.7 m below the top of the cutbank, yielded a date of B.C. 1010-890 and B.C. 880-850 (2960-2840 and 2820-2800 yr B.P.) (Table 4-4). Since all three dikes extend higher in the section than the position of the sample, the two generations of sand dikes formed since B.C. 1010 (2960 yr B.P.).

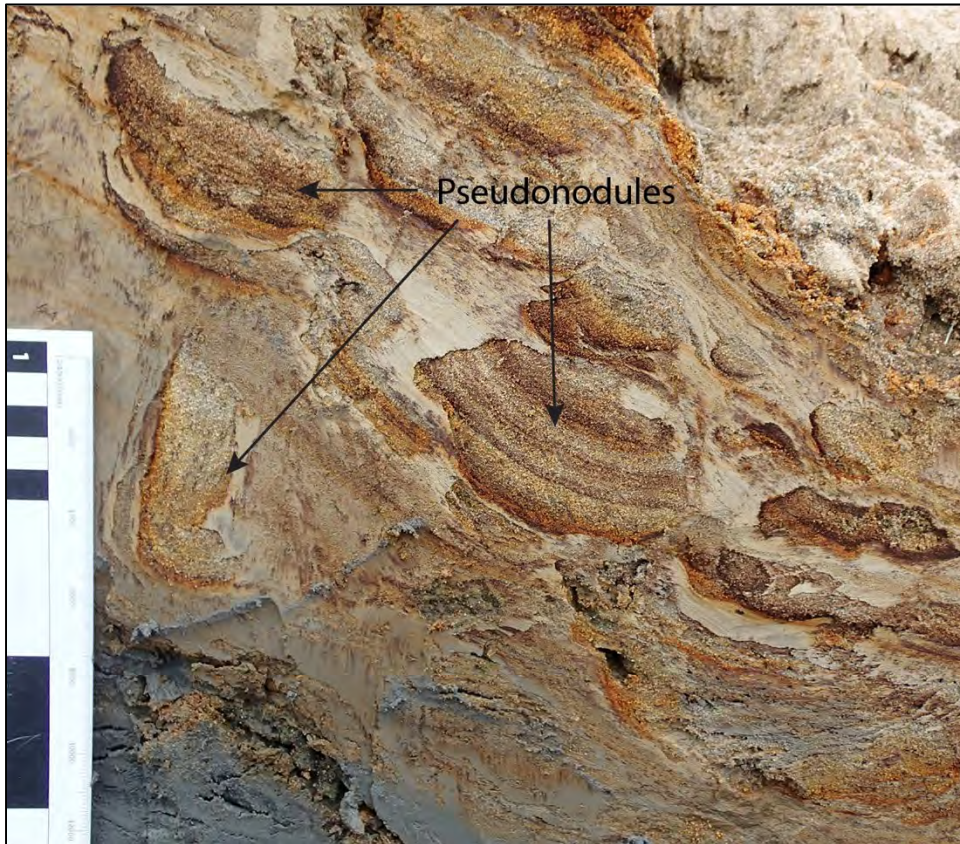


Figure 4-28 Photograph showing pseudonodules at BR101. The smaller black and white intervals on the scale represent centimeters.

Unfortunately, no organic samples were found at the site that could help estimate the age of the deposit in which the pseudonodules formed. An organic sample was collected about 2.5 km upriver, at site BR102, but the sample proved to be modern (Table 4-7). The sample was taken from a tree trunk horizontally bedded at the contact of layered silt above and weathered sand below. Given its modern date, the tree and overlying layered silt appear to have been recently deposited on the cutbank. There is no other dating along the lower Black River that could help to estimate the age of the deposit that may have liquefied. However, it is likely to be Late Holocene in age, based on dating (B.C.1740-1610 or 3690-3560 yr B.P.) of similar deposits along the Black River near Pocahontas.

Table 4-7 Radiocarbon Dating Results for Black River Site

Sample # Lab #	¹³ C/ ¹² C Ratio	Radiocarbon Age Yr B.P. ¹	Calibrated Radiocarbon Age Yr B.P. ²	Calibrated Calendar Date A.D./B.C. ²	Sample Description
BR102-W1 BA-368212	-28.5	152.7 ± 0.4 % Modern Carbon (pMC)	Modern 0+	Modern AD Post 1950	Wood, outer 1 cm of tree, 3.25 m below top of cutbank (BTC) & 25 cm AWL, horizontally bedded below silt

¹ Conventional radiocarbon ages in years B.P. or before present (1950) determined by Beta Analytic, Inc. Errors represent 1 standard deviation statistics or 68% probability.

² Calibrated age ranges as determined by Beta Analytic, Inc., using the Pretoria procedure (Talma and Vogel, 1993; Vogel et al., 1993). Ranges represent 2 standard deviation statistics or 95% probability.

4.4.4.2 Coldwater River-Pompey Ditch east of Tunica, Mississippi

During initial reconnaissance of the Coldwater River and related ditches in August 2013, sedimentary conditions appeared conducive to the formation of liquefaction features and liquefaction features were found at several sites (CWR2, CWR4, and CWR5) downstream from the Arkabutla Dam (Figure 4-17, Figure 4-19, and Figure 4-27). We returned the following year to perform a systematic survey along two sections of the Coldwater River system, including 6.5 km immediately downstream from the dam and another 13 km farther downstream between the towns of Savage and Crenshaw (Figure 4-17 and Figure 4-27). For the Arkabutla Dam section, the river was surveyed from a boat ramp just below the spillway downstream towards the town of Prichard. For the downstream section, the river was surveyed from a boat ramp on Pompey Ditch west of Crenshaw upstream to the intersection with the Coldwater River, and from there, along the Coldwater River towards Savage.

Surficial geology immediately downstream of the Arkabutla Dam is mapped as Holocene backswamp deposits inset in Pleistocene fluvial deposits, including natural levee and backswamp deposits (Saucier, 1994; Figure 4-27). About 4 km downstream from the dam, the river valley opens up into the broader Mississippi River valley. Here, the Coldwater River turns south and flows along the eastern margin of the Mississippi River valley. Holocene backswamp deposits have been mapped along the eastern margin of the valley until about Crenshaw. Holocene point bar, abandoned courses, and abandoned channel deposits of the Mississippi River are mapped between the backswamp and the current course of the Mississippi River to the west and along the eastern margin of the valley in the Crenshaw area.

The lower portion of the Coldwater River and Pompey Ditch were surveyed in September 2014. At that time, exposure was limited due to heavy vegetation of the upper banks and recent

deposition of silt on the lower banks. In exposure provided by occasional cutbanks, 30-50 m long and 4-5 m high, tan silt was underlain by silt with reddish redoximorphic features or clay with calcium carbonate nodules. Silt or clay extended another 1.5 m below the cutbank as determined with a soil probe. No sand was encountered within 1.5 m below the cutbank.

No liquefaction features were found along the lower portion of the Coldwater River and Pompey Ditch. Several silt-filled cracks were found but they narrowed downward and were likely due to slumping of the cutbank. The apparent absence of liquefaction features in this area may be due to relatively poor exposure of the banks and/or to the sedimentary conditions characterized by thick silt and clay and apparent absence of sand at least in the upper 6 m of the fluvial deposits.

The upper portion of the Coldwater River was surveyed in October 2014 when the river level was relatively low (Figure 4-17). At the time, there were excellent exposures of fluvial deposits in the lower 1.5-2 m of 3.5-6 m-high cutbanks. The upper 2-4 m of most cutbanks were vegetated. Sediment exposed in the cutbanks was typically tan silt to very fine sand underlain by clayey silt to silt with reddish redoximorphic features. At a few locations, interbedded silt and cross-bedded sand were exposed near the base of the cutbank. Elsewhere, interbedded silt and sand was encountered with a soil probe within 1.5 m depth below the cutbank.

During the 2014 survey downstream from the Arkabutla Dam, the liquefaction sites CWR2 and CWR4, that had been found during initial reconnaissance, were revisited (Figure 4-29). At CWR2, additional information and samples were collected under the new site designation, CWR7. Liquefaction site CWR5 was not relocated but a new site, designated CWR9, was found nearby and documented as were six additional liquefaction sites, CWR8, CWR11, CWR12, CWR14, CWR15, and CWR16. We documented one sand blow, thirty-three sand dikes, and six sand sills at eleven sites. Dikes ranged in width from 0.2 to 24 cm and the one sand blow was 27 cm thick. At two of the sites, the source layer of the sand dikes and sills were exposed and exhibited disturbed bedding and foundered clasts of the overlying sediment. Weathering characteristics of liquefaction features ranged from slight iron staining to very iron stained, cementation, and bioturbation. Cross-cutting relationships and weathering characteristics of liquefaction features suggest there may be three generations of liquefaction features.

Radiocarbon dating performed on samples collected from five sites (CWR2/CWR7, 8, 9, 12, and 16) helped to estimate the ages of some of the liquefaction features. All of the liquefaction features appear to have formed during the Holocene. Based on radiocarbon dating of sediment crosscut by dikes at the various sites, the three generations were assigned to three categories: <8340 yr B.P., <4965 yr B.P., and <3715 yr B.P. and are shown on Figure 4-29 by different shades of gray. The oldest generation of liquefaction features (<8340 yr B.P.) pre-dates earthquakes centered in the NMSZ but could be similar in age to earthquakes in the Marianna area (6650-6950 yr B.P. and 5350-5650 yr B.P.). The youngest generation of features (<3715 yr B.P.) post-dates Marianna earthquakes but could be similar in age to New Madrid earthquakes (2600-2900 yr B.P., 900-1200 yr B.P., 350-650 yr B.P.). The middle generation of features overlaps the ages of Marianna (4650-4950 yr B.P.) and New Madrid (4150-4450 yr B.P.) earthquakes. The liquefaction sites are discussed below.

At CWR2, three dikes, composed of silty, very fine sand and ranging from 0.5-1 cm wide, pinched out in gray silt about 2 m below the top of the cutbank. The dikes were iron stained along their margins. Radiocarbon dating of a sample of charred material (CWR2-C1) collected from gray silt crosscut by the dikes yielded a date of B.C. 3370-3330, 3220-3180, 3160-3120 (or 5320-5280, 5170-5130, 5110-5070 yr B.P.) (Table 4-8). This site was revisited and renamed CWR7. At that time, two additional dikes were found that were 2 cm and 0.4 cm wide that also pinched out in

gray silt about 2 m below the top of the cutbank (Figure 4-30). A sample of plant material (CWR7-W3) collected slightly higher in the silty section than the previous sample yielded a date of B.C. 2835-2815, 2665-2550, and 2535-2490 (or 4785-4765, 4615-4500, 4485-4440 yr B.P.). This date is younger than that for CWR2-C1 and provides a maximum constraining age of B.C. 2835 (or 4785 yr B.P.) for all the dikes at the site.

At CWR4, seven sand dikes were found along a 10 m section of the river. The dikes were composed of either fine sand or medium-fine sand, ranged from 1-8 cm in width, and pinched out in mottled silt about 4-4.5 m below the top of the cutbank. Two of the less iron-stained dikes crosscut a very iron-stained dike, suggesting two, possibly three, generations of liquefaction features at the site. One of the dikes appeared to originate in a sand layer exposed at the base of the cutbank. No organic samples were found at CWR4 that could be used to date the dikes. However, a sample (CWR12-C3) was collected from mottled silt about 4.4 m below the top of cutbank at site CWR12 only 58 m upstream from CWR4. The sample yielded a date of B.C. 3015-2895 (4965-4845 yr B.P.) (Table 4-8) for the silt deposit crosscut by the sand dikes at CWR4. Given the proximity and similarity of the sites, sample CWR12-C3 provides a maximum constraining age of B.C. 3015 (or 4965 yr B.P.) for the dikes.

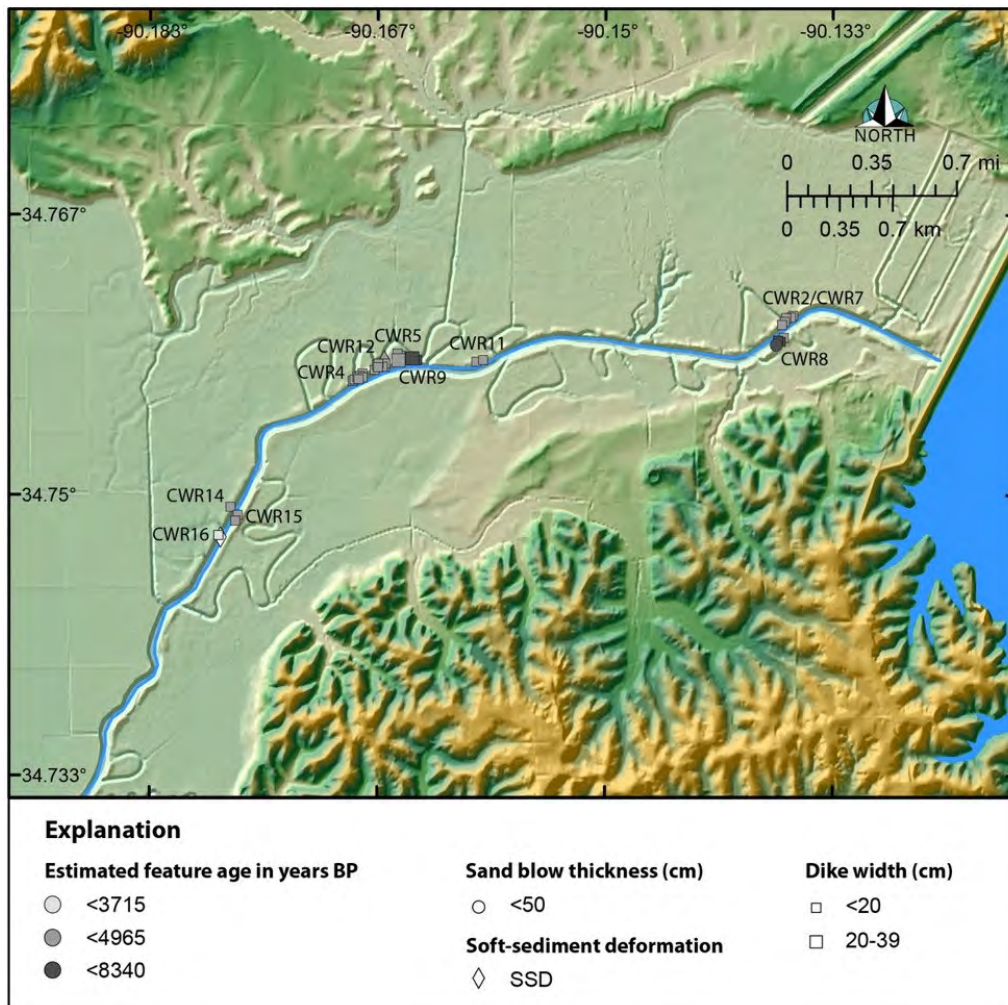


Figure 4-29 Map showing liquefaction features along the Coldwater River downriver from the Arkabutla dam in northwestern Mississippi.

At CWR5, three sand dikes were found that were composed of fine sand, ranged from 3-20 cm in width, and pinched out in silt about 1-1.5 m above the water level or 4-4.5 m below the top of the cutbank. The degree of weathering was not noted for these dikes. A thick sand bed was encountered with the soil probe 10 cm below the base of the cutbank and may have been the source bed of the sand dikes. No organic samples were found at this site. However, sample CWR12-C3 collected from silt with redoximorphic features at site CWR12 about 68 m downstream from CWR5 again provides an age estimate of the silt deposit and a maximum constraining age of B.C. 3015 (or 4965 yr B.P.) for the dikes at CWR5.



Figure 4-30 Photograph of small sand dike at CWR7. The black and white intervals on the meter stick represent 10 cm. S. Bastin points to the dike tip or termination.

At CWR8, there were three sand dikes and one sand blow within silt characterized by redoximorphic features and manganese nodules. The sand blow, 27 cm thick and at least 1.9 m wide, was composed of silty, fine sand and was very iron stained and bioturbated, especially its upper contact. The sand blow thinned away from the feeder dike and the flanks of the sand blow were covered by vegetation. The largest dike, up to 6.5 cm wide, was composed of fine sand with small silt clasts, had a strike and dip of N20°W, 79 NE°, was iron stained and cemented throughout, especially along its margins, and was connected to the base of the sand blow. A

second vent structure at the base of the sand blow suggested that there had been another feeder dike most of which had been removed by erosion. A second dike, only 0.8 cm wide, also composed of fine sand and iron stained and cemented throughout, terminated at 1.16 m above the water level, approximately level with the base of the sand blow. A third dike, 2.3 cm wide, composed of fine sand with granule-size silt clasts, crosscut the sand blow and extended at least 1.3 m above the water level or 3.7 m below the top of the cutbank. The termination of the dike was covered with vegetation including tree roots. This sand dike was much less weathered than the other two and had iron staining only along its margins. Radiocarbon dating of charred material (CWR8-C13) in weathered silt about 25 cm below the sand blow provides a maximum constraining age of B.C. 6390-6230 (or 8340-8180 yr B.P.) (Table 4-8) for the very weathered sand dikes and related sand blow. The less weathered dike that crosscuts the sand blow is clearly younger and may be similar in age (<4785 yr B.P.) to the relatively unweathered sand dikes at nearby site CWR2/7, only 75 m away.

At CWR9, in close proximity to CWR5 and CWR12, two sand dikes were found that were composed of medium-fine sand, ranged from 8-24 cm in width, and pinched out in silt with redoximorphic features between 0.4-2.4 m above the water level or 3.1-5.1 m below the top of the cutbank (Figure 4-31). The dike that extended higher in the section fined up section from medium-fine sand with silt clasts to very fine sandy silt and became discontinuous towards its tip. Both dikes were iron stained and cemented, and the dike that extended farther up section was also bioturbated. The weathering characteristics of these dikes were similar to the older dikes at CWR8. Radiocarbon dating of sample CWR9-C5, in weathered silt and about 10 cm above the discontinuous dike tip, provides an age estimate (6305-6275, 6235-6215 yr B.P.) (Table 4-8) for the sediment above the dike. This date does not necessarily provide a minimum age for the dikes since the ground level at the time of the causative earthquake is not known. However, the date is consistent with the interpretation that the very weathered dikes at CWR9 may have formed during the same event as the liquefaction features at CWR8 (<8340 yr B.P.).

At CWR11, two small sand dikes, both 0.2 cm wide, composed of very fine sandy silt, crosscut silt with redoximorphic features and extended 1-1.1 m above the water table or 1.9-2 m below the top of the cutbank. Both dikes were iron stained and partially cemented. No organic samples could be found for radiocarbon dating. This site is about 0.6 km from CWR12 and has a similar geological setting to that site. In addition, the weathering characteristics of sand dikes at the two sites are similar. Therefore, the sand dikes at CWR11 are inferred to be similar in age (< 4965 yr B.P.) to those at CWR12.

CWR12 was one of the more interesting liquefaction sites along the Coldwater (Figure 4-32). There were multiple sand dikes at this site that ranged from 2.5-7.5 cm wide. There were no crosscutting relationships between the liquefaction features suggesting that they all formed during the same event. The dikes originated in three different sand layers within an interbedded silt and cross-bedded sand deposit exposed towards the base of the cutbank. The bedding of the source layers was disturbed. Sand dikes and sills had formed within the interbedded deposit and sills had been intruded below the overlying massive silt deposit. Clasts of the overlying silt had foundered into the sills. Several sand dikes intruded the overlying silt deposit and one of the dikes extended 1.75 m above the water level or to 4.25 m below the top of the cutbank. Sand dikes lower in the section were unweathered, whereas dikes that extended higher in the section were iron stained and partially cemented. Sample CWR12-C3 collected about 13 cm below the dike tip provides a maximum constraining age of B.C. 3015 (or 4965 yr B.P.) (Table 4-8) for the dikes at this site. Sample CWR12-C1 collected from the interbedded silt and cross-bedded sand deposit from which the dikes originated provides an age estimate of the deposit of B.C. 7025-6960, 6950-6930, 6915-6880, and 6845-6680 (or 8975-8910, 8900-8880, 8865-8830, and 8795-8630 yr B.P.).

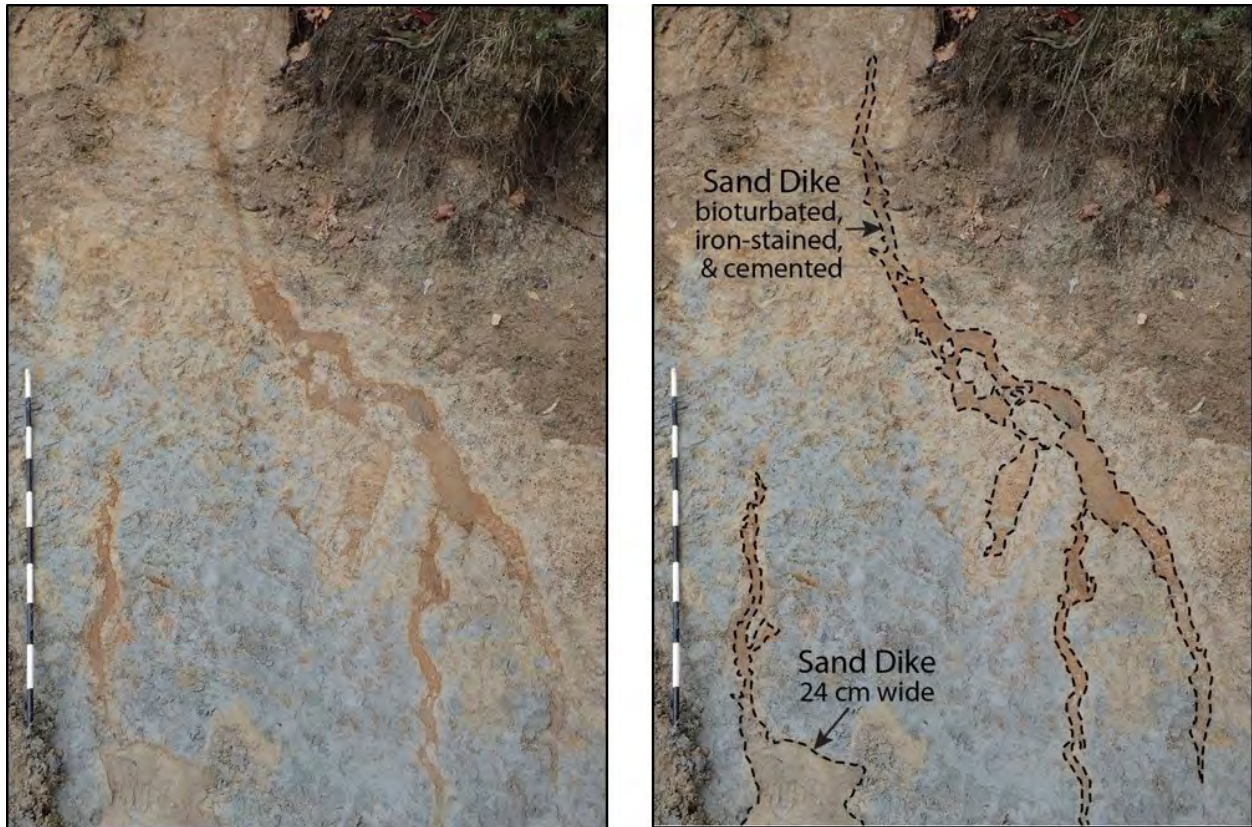


Figure 4-31 Photographs (left - unannotated; right - annotated) of two sand dikes at CWR9. Both dikes that were iron stained and cemented. The upper part of the dike that extends higher in the section is also bioturbated. Dashed lines represent clear contacts. The black and white intervals on the meter stick represent 10 cm.

At CWR14, there was only one dike, 5 cm wide, composed of fine sand with silt clasts that crosscut silt with redoximorphic features. The dike was subparallel to the cutbank and its upper extent had been removed by erosion. The dike was iron stained and cemented. No organic samples were found for dating. This site is ~1.4 km from CWR12. The liquefaction features at this site are inferred to be similar in age to those at CWR12 given the similarities in the weathering characteristics of the liquefaction features and geological setting of the two sites.

At CWR15, only ~25 m downstream from CWR14, there were two sand dikes, 13.5 and 2 cm wide, that crosscut silt with redoximorphic features and extended 70 cm and 76 cm above the water level, respectively. These dikes were also subparallel to the cutbank so their upper extent could not be determined. The larger dike was a compound dike composed of 2-3 phases of medium sand with silt clasts separated by laminations of silty very fine sand. Where the dike was composed of only two phases, the compound dike was iron stained throughout and cemented. Where the dike was widest and composed of three phases, the inner phase was less weathered. The multiple phases suggest multiple episodes of intrusion; however, degree of weathering maybe related to proximity to the host sediment. No organic samples were found for dating. Like the dikes at CWR14, the dikes at this site are inferred to be similar in age to those at CWR12.

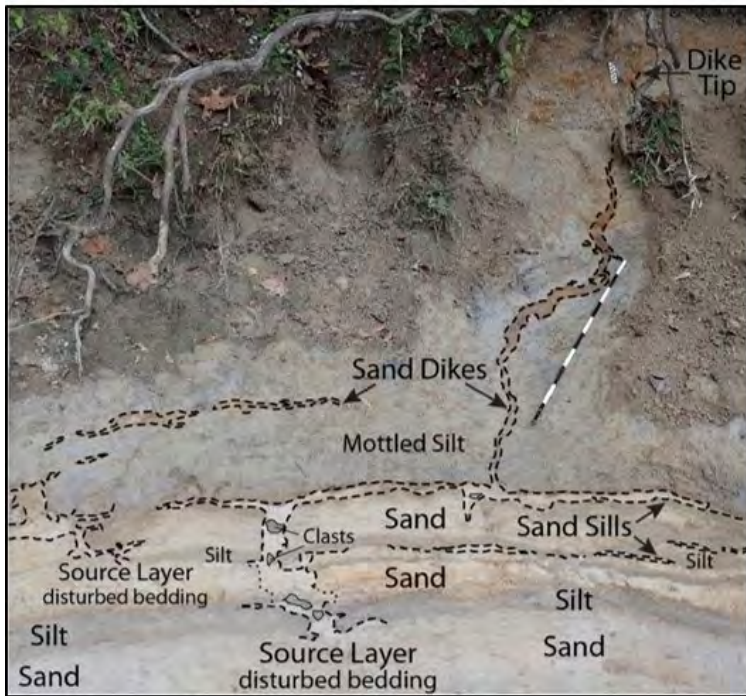


Figure 4-32 Photographs (upper - unannotated; lower - annotated) of site CWR12, showing source layers that liquefied at the base of the cutbank, sand dikes that crosscut overlying interbedded silt and sand layers and mottled silt, and sills that intrude along the basal contacts of silt layers. Dashed lines represent clear contacts; dotted lines represent inferred contacts. The black and white intervals on the meter stick represent 10 cm and those on the small scale next to dike termination represent 1 cm.

Table 4-8 Radiocarbon Dating Results for Coldwater River Sites

Sample # Lab #	¹³ C/ ¹² C Ratio	Radiocarbon Age Yr B.P. ¹	Calibrated Radiocarbon Age Yr B.P. ²	Calibrated Calendar Date A.D./B.C. ²	Sample Description
CWR2-C1 BA-368213	-22.1	4560 ± 30	5320-5280 5170-5130 5110-5070	BC 3370-3330 BC 3220-3180 BC 3160-3120	Charred material 37 cm below dike tip from gray silt
CWR7-W3 BA-399631	NA ³	4060 ± 30	4785-4765 4615-4500 4485-4440	BC 2835-2815 BC 2665-2550 BC 2535-2490	Plant material 31 cm below dike tip from gray silt
CWR8-C13 BA-401790	-26.8	7430 ± 30	8340-8180	BC 6390-6230	Charred material ~25 cm below sand blow from mottled silt
CWR9-C5 BA-401787	-28.4	5480 ± 30	6305-6275 6235-6215	BC 4355-4325 BC 4285-4265	Charred material ~10 cm above discontinuous dike & ~3 m below top of cutbank from mottled silt
CWR12-C1 BA-399636	-27.5	7920 ± 30	8975-8910 8900-8880 8865-8830 8795-8630	BC 7025-6960 BC 6950-6930 BC 6915-6880 BC 6845-6680	Charred material ~5.8 m below top of cutbank from sand layer, source of sand dikes
CWR12-C3 BA-401788	-26.0	4330 ± 30	4965-4845	BC 3015-2895	Charred material 13cm below dike tip & ~4.4 m below top of cutbank from mottled silt
CWR16-W3 BA-399638	-27.1	3410 ± 30	3715-3580	BC 1765-1630	Wood, sub-horizontally bedded, level with dike tip in layered silty clay

¹ Conventional radiocarbon ages in years B.P. or before present (1950) determined by Beta Analytic, Inc. Errors represent 1 standard deviation statistics or 68% probability.

² Calibrated age ranges as determined by Beta Analytic, Inc., using the Pretoria procedure (Talma and Vogel, 1993; Vogel et al., 1993). Ranges represent 2 standard deviation statistics or 95% probability.

³ The original sample was too small to provide a ¹³C/¹²C ratio on the original material. However, a ratio including both natural and laboratory effects was measured during the ¹⁴C detection to calculate the true conventional radiocarbon age.

At CWR16, one small, 1-cm-wide, sand dike originated in a deposit of interbedded fine sandy silt and medium-fine sand towards the base of the cutbank and extended about 10 cm into the overlying layered silty clay containing many organics. The dike was iron stained throughout but only its margins were iron cemented. The base of the silty clay had delaminated and clasts had foundered into the underlying sand deposit and a sill of medium-fine sand had intruded along the base of the silty clay. Below the base of the cutbank, sand extended for another 1.5 m as determined with a soil probe. Radiocarbon dating of a piece of wood (CWR16-W3) horizontally bedded in the layered silty clay at the level of the dike tip provides a maximum constraining age of B.C. 1765 (or 3715 yr B.P.) (Table 4-8).

4.4.4.3 *Locust Creek Ditch southeast of Paragould, Arkansas*

We examined cutbank exposures along a 5-km stretch of Locust Creek Ditch southeast of Paragould, Arkansas (Figure 4-11, Figure 4-17, and Figure 4-19). The U.S. Army Corps of Engineers had recently cleaned the ditch. Even so, vegetation had regrown on most of the banks, except where Big Slough Ditch joined Locust Creek Ditch and downstream from the Rt 932 bridge. This portion of Locust Creek Ditch is about 1.5-3.5 km east of the western Reelfoot Rift margin. Few liquefaction features had been previously studied in this area except for two sand blows and related sand dikes that were documented along Eightmile Ditch, 3-4 km west of Locust Creek Ditch (Tuttle, 1999; Figure 4-11). Both those sand blows were attributed to the A.D. 1811-1812 earthquake sequence.

Along Locust Creek Ditch, surficial geology is mapped as Late Pleistocene (Late Wisconsin) valley train deposits (level 2), including relict channels (Saucier, 1994; Figure 4-21). Holocene point bar deposits are mapped along the St. Francis River, only 0.5-2.0 km east of the ditch. The area along Locust Creek Ditch has been affected by flooding of the St. Francis River, especially before construction of drainage ditches by the Army Corps of Engineers in the 1900s. Exposure along the surveyed portion of Locust Creek Ditch was generally poor due to vegetation growing on the ditch banks. However, erosion had carved cutbanks that provided good exposure in several locations. Those cutbanks ranged from 2.5-3.5 m high and revealed 1.0-1.5 m of ditch spoil underlain by a buried soil developed in silt followed by interbedded silt and sand with large lenses of clayey silt-clay (abandoned channel deposits). Below the cutbank, interbedded silt and sand was underlain by sand that coarsened with depth to 1.5 m below the water level, as determined with a soil probe.

During this study, we documented one sand blow and five sand dikes at four sites. The sand blow was composed of two depositional units and was fed by at least two dikes. A 12-cm-thick soil had developed in the top of the sand blow and its two depositional units exhibited only slight iron staining, as did its feeder dikes. The degree of soil development and weathering suggested that these liquefaction features were historic in age. This was supported by radiocarbon dating of organic material from the soil buried by the sand blow. Therefore, these features likely formed during the A.D. 1811-1812 New Madrid earthquakes. The sand dikes at the other three sites exhibited a greater degree of soil development and weathering, including iron and manganese staining, suggesting that they are prehistoric in age. A 24-cm thick soil A horizon as well as soil lamellae had formed in the top of one of these dikes. This dike likely formed during the A.D. 1450 New Madrid event. The two more significant liquefaction sites are discussed below.

At site LCD3, two sand dikes, 20 cm and 5 cm wide, intruded and crosscut a large lens of gleyed (reduction of iron in anaerobic environment which creates grey or blue colors) clay, a likely channel-fill deposit, overlain by slightly mottled silt that coarsens upward to a silty, fine sand in which a thin soil A horizon had formed. The larger dike was intruded along the southwestern contact of a channel-fill deposit and adjacent weathered sand deposit. The lower portions of the dikes were composed of medium-fine sand and fined upward to very fine sand and contained clasts of silt and clay. The sand blow, at least 55 cm thick and 9.7 m long, was composed of two depositional units of very fine to fine sand with silt clasts (Figure 4-33).



Figure 4-33 Photographs (left - unannotated; right - annotated) of portion of sand blow composed of two depositional units separated by a thin silt drape (blue), overlying a buried soil at LCD3. A 12-cm-thick soil A horizon had formed in the top of the sand blow and both depositional units, especially the upper one, exhibited iron staining. Radiocarbon dating of sample collected 1 cm below the sand blow provided a close maximum age of A.D. 1680, indicating that liquefaction features likely formed during the 1811-1812 A.D earthquake sequence. Dashed lines represent clear contacts; dotted lines represent inferred contacts. For scale, the shovel handle is 50 cm long.

The lower unit was 27 cm thick and the upper unit 28 cm thick. A 12-cm-thick A horizon had formed in the top of the upper unit with another 9 cm of organic staining below. The upper and lower units both exhibited slight iron staining. Only the southern margin of the sand blow was exposed and the rest of the sand blow, and possibly other feeder dikes, were covered by vegetated bank spoil. The thickness of the A horizon developed in the sand blow was similar to that of other sand blows that formed during the A.D. 1811-1812 New Madrid earthquakes. Dating of two samples, LCD3-C2 and LCD3-C106, of charred material also indicated that this sand blow likely formed during the A.D. 1811-1812 event. Sample LCD3-C2 collected 11 cm below the sand blow from mottled silt yielded a date of A.D. 1040-1100, 1120-1140, 1150-1220 (910-850, 830-810, 800-730 yr B.P.) (Table 4-9). Sample LCD3-C105 collected 1 cm below the sand blow from the buried soil yielded a date of A.D. 1680-1730, 1810-1930, post-1950 (270-220, 140-20, post-0 yr B.P.). This date represents a close maximum age of A.D. 1680 (270 yr B.P.). A sediment sample, OSL2, was collected of the upper contact of the soil buried by the sand blow. It yielded a calendar age of 3980-3280 yr B.P. (Table 4-10), much older than the two radiocarbon ages of the soil and silt below the sand blow. The radiocarbon ages are consistent with the weathering characteristics of the sand blow. Again, the radiocarbon ages are given preference over the OSL

age. The A.D. 1811-1812 earthquakes, the only historic earthquakes in the region capable of producing large sand blows, were likely responsible for the liquefaction features at this site.

At site LCD5, one dike, 76 cm wide near the base of the exposure and 30 cm wide near the top of the dike, intruded and crosscut interbedded silt and sand, and extended to 1.5 m above the water level or 24 cm below the topsoil that had been buried by ditch spoil (Figure 4-34). The dike was composed of medium-fine sand with silt and lignite clasts and exhibited flow structure near its base. A contact within the host deposit was displaced by 22 cm across the dike, south side down. The upper 76 cm of the dike was slightly iron stained and the lower 76 cm was manganese stained. In addition, soil lamellae had formed in the upper 30 cm of the dike. The dike was overlain by silt in which a 24-cm-thick silt loam had formed. Soil lamellae is thought to take at least several hundred years to form. Therefore, the presence of soil lamellae in the upper part of the dike suggests that it pre-dates the A.D. 1811-1812 earthquakes. This is supported by the degree of iron and manganese staining of the dike. It is unlikely that such a large dike would have approached the ground surface without breaking through, especially given the 22 cm of vertical displacement across the dike. Therefore, the overlying silt probably was deposited and the silty loam soil developed after the dike formed. Given the rate of soil development in the region, the 24-cm-thick soil above the sand dike suggests that the dike formed about A.D. 1450 ± 100 yr, consistent with earthquake-induced liquefaction during the A.D. 1450 event.

Table 4-9 Radiocarbon Dating Results for Locust Creek Ditch Sites

Sample # Lab #	¹³ C/ ¹² C Ratio	Radiocarbon Age Yr B.P. ¹	Calibrated Radiocarbon Age Yr B.P. ²	Calibrated Calendar Date A.D./B.C. ²	Sample Description
LCD3-C2 BA-306977	-25.0	880 ± 30	910-850 830-810 800-730	AD 1040-1100 AD 1120-1140 AD 1150-1220	Charred material 11 cm below sand blow from mottled silt
LCD3-C106 BA-338298	-24.1	90 ± 30	270-220 140-20 Post 0	AD 1680-1730 AD 1810-1930 AD Post 1950	Charred material 1 cm below base of sand blow from buried soil

¹ Conventional radiocarbon ages in years B.P. or before present (1950) determined by Beta Analytic, Inc. Errors represent 1 standard deviation statistics or 68% probability.

² Calibrated age ranges as determined by Beta Analytic, Inc., using the Pretoria procedure (Talma and Vogel, 1993; Vogel et al., 1993). Ranges represent 2 standard deviation statistics or 95% probability.

Table 4-10 Optically Stimulated Luminescence Dating Results at Locust Creek Ditch Site LCD3

Sample Number	Lab	Cosmic Dose Rate (Gy/ka) ¹	Total Dose Rate (Gy/ka)	OSL Age (Yr) ²	Calendar Age (Yr) ³	Sample Description
OSL2	USGS	0.17 ± 0.01	1.84 ± 0.08	3690 ± 350	3980-3280	From cutbank, quartz grains from buried soil below sand blow

¹ Cosmic dose rate calculated using methods of Prescott and Hutton (1994).

² Linear and exponential fit used on equivalent dose at one standard deviation. Datum year is A.D. 2010.

³ Years B.P. or before present (1950).

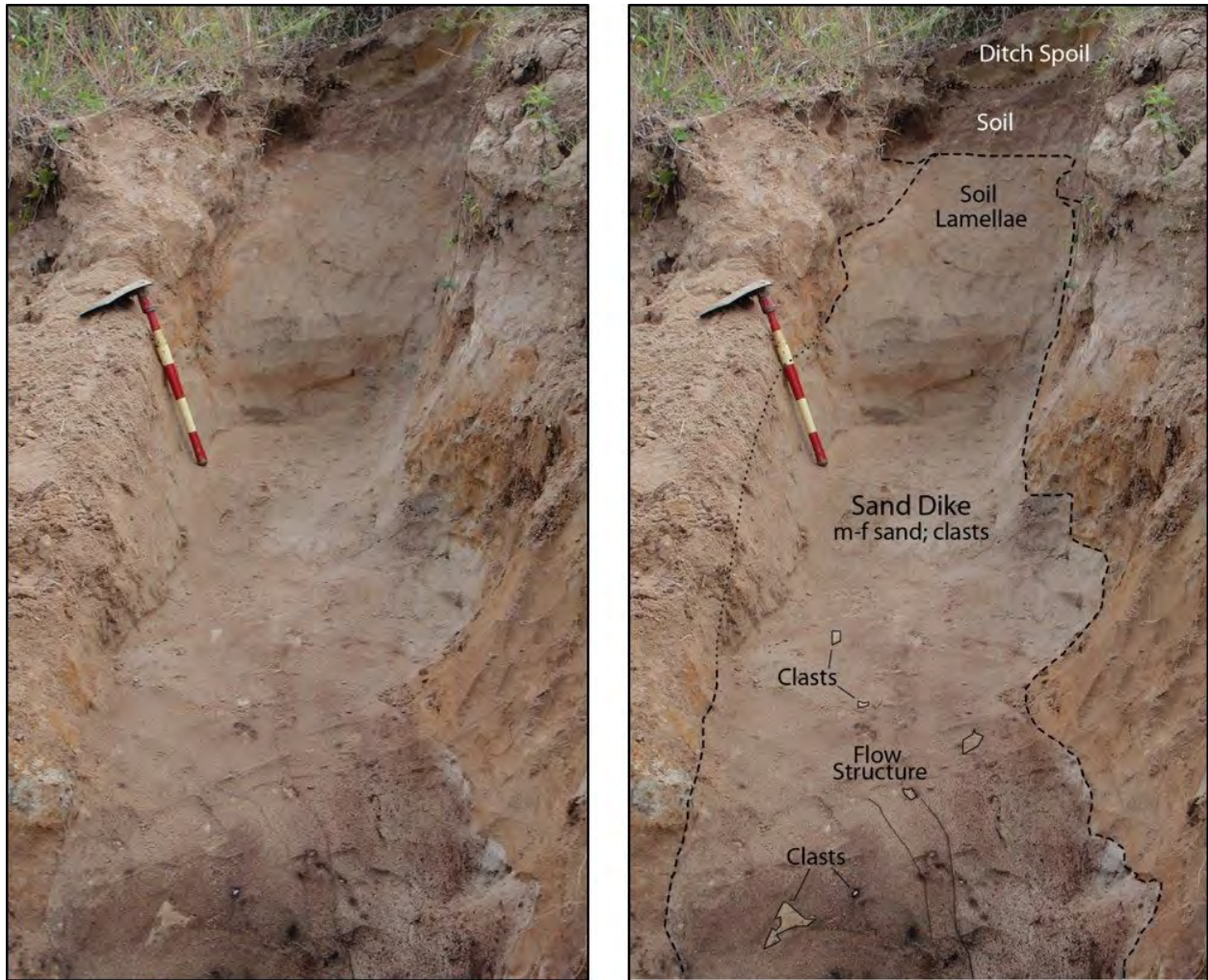


Figure 4-34 Photographs (left - unannotated; right - annotated) showing large sand dike at LCD5. Development of a 24 cm soil in silt above the sand dike and soil lamellae within the top of the dike suggest that dike may have formed about 500 years ago, probably during the A.D. 1450 earthquakes. Dashed lines represent clear contacts; dotted lines represent inferred contacts; solid lines delineate flow structure and clast boundaries. Red and yellow intervals on shovel handle are 10 cm long.

4.4.4.4 *St. Francis River between Chalk Bluff and Nimmons, Arkansas*

We performed a systematic survey along 29 km of the St. Francis River between Chalk Bluff, where the river flows through Crowley's Ridge, and Nimmons, Arkansas (Figure 4-11, Figure 4-17, Figure 4-19, Figure 4-35, and Figure 4-36). More than once, the river survey had to be Surficial geology is mapped as Holocene point-bar deposits inset in Late Pleistocene (Late Wisconsin) valley train (level 2), including relict channels, and Holocene alluvial fans and aprons adjacent to Crowley's Ridge (Saucier, 1994; Figure 4-21). Exposure along this portion of the St. Francis River was good to excellent, limited only by vegetation including tree roots on the upper 0.5-1.5 m of the banks and sometimes by a thin coat of silt deposited on the lower 0.5-1.0 m of the banks. Cutbank exposure ranged from 3-5 m high and was almost continuous along meandering sections of the river, but sparser along straighter sections.

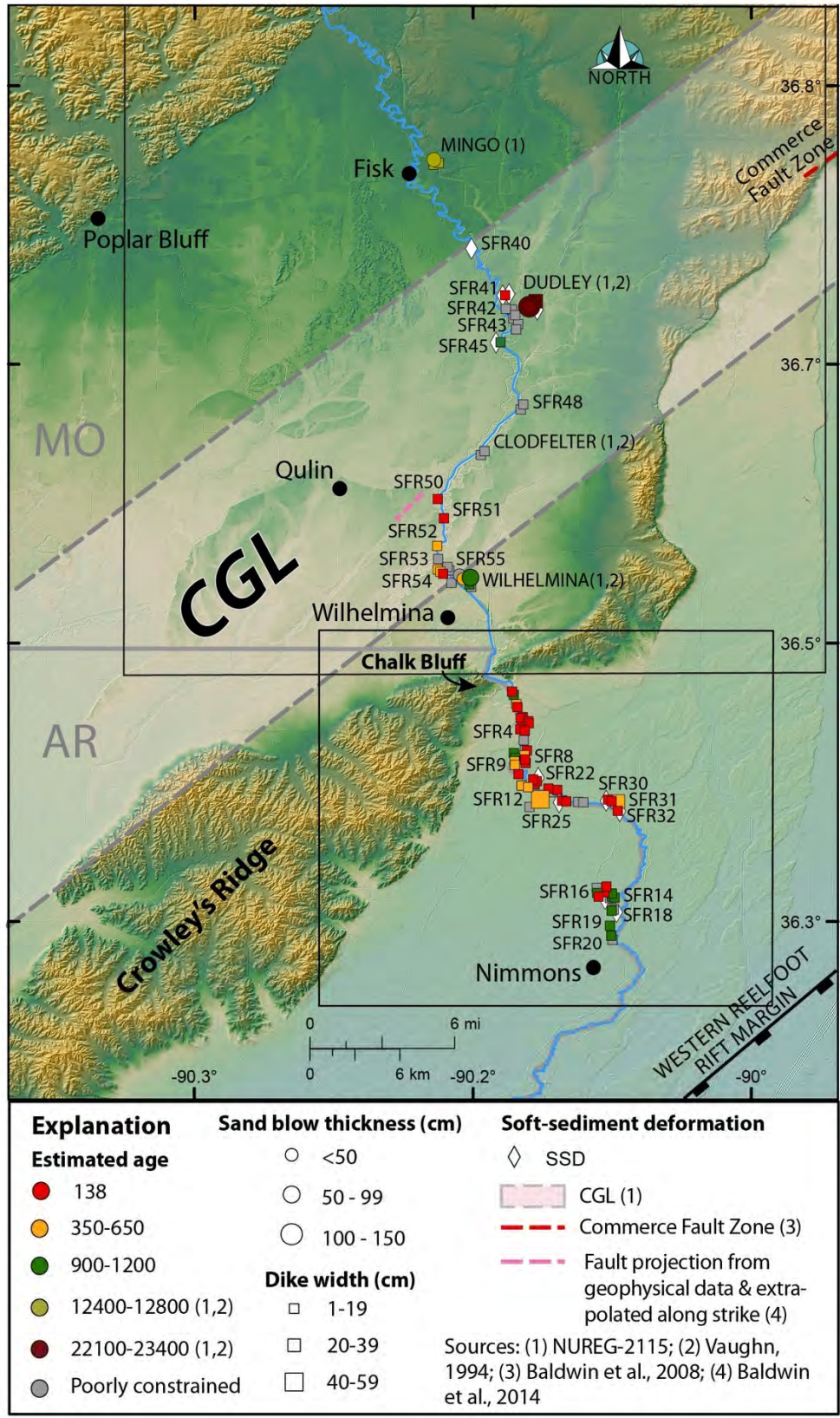


Figure 4-35 Map showing liquefaction features along the St. Francis River and known geological structures that may have the potential to produce large earthquakes.

Along the straighter north-south section immediately downstream from Chalk Bluff, cutbanks revealed recently deposited layered silt and sand overlying silt to fine sandy silt with redoximorphic features, CaCO₃ nodules, manganese staining, and krotovina. Occasionally, there were buried soils within the mottled silt or within lenses of clay loam embedded in the mottled silt. As determined with a soil probe, the silt deposit transitioned to interbedded silt and sand and then to sand at ~1.0-1.5 m below the water level. Along the meandering northwest-southeast section of the river, cutbanks exposed buff silt overlying silt with redoximorphic features. At some locations, interbedded silt and sand underlain by cross-bedded sand were exposed near the base of the cutbank. At other locations, this sequence of sediment occurred below the water level as determined with a soil probe. Along the straighter north-south section farther downstream, most cutbanks revealed buff silt overlying silt with redoximorphic features followed by bioturbated clayey silt, silty clay, or clay with iron and manganese nodules underlain by sand, in places cross-bedded. The contact between the clayey silt, silty clay, or clay and underlying sand was very irregular due to bioturbation that created a mixed zone.

Along the Chalk Bluff-Nimmons portion of the St. Francis River, we documented fifty-four sand dikes and seven sand sills at twenty-eight sites. Dikes ranged in width from 0.2-21 cm, with the exception of one dike that was 41 cm wide. At six of the sites, source layers of the sand dikes and sills were exposed and exhibited disturbed bedding, soft-sediment deformation, flow structure, and foundered clasts of the overlying sediment. Unfortunately, no sand blows were found along the river. Crosscutting relationships at SFR8, 13, and 16 indicate at least two generations of liquefaction features. Radiocarbon dating was performed on samples collected at eight sites (SFR2, 4, 9, 12, 14, 17, 30 and 32). Weathering characteristics of liquefaction features ranged from little to no iron staining to iron staining, mottling, silt accumulation, cementation, and bioturbation. Crosscutting relationships, radiocarbon dating, and degree of weathering were used to interpret the ages of many of the liquefaction features. Almost all of the features can be attributed to the New Madrid events of A.D. 1811-1812, A.D. 1450, and A.D. 900. The most significant liquefaction sites are discussed below.

At site SFR4, two small sand dikes, 1 cm and 0.5 cm wide, composed of very fine to fine sand, crosscut silt characterized by redoximorphic features, calcium carbonate nodules, and krotovina. The dikes extended 1 m above the water level or 3 m below the top of the cutbank. The upper 45 cm of the dikes were iron stained but showed no other signs of advanced weathering, suggesting that they are historic in age and probably formed during the A.D.1811-1812 New Madrid earthquakes. Sample SFR4-C2 of charred material collected from the silt deposit about 75 cm above the water level and 25 cm below the tip of the dikes, yielded a date of B.C. 6640-6470 (8590-8420 yr B.P.) (Table 4-11). This date provides an age estimate for the silt and a maximum constraining age of B.C. 6640 (or 8590 yr B.P.) for the dikes. At nearby site SFR2, located 0.5 km upstream from SFR4, sample SFR2-C2 collected from the silt deposit, but stratigraphically lower than SFR4-C2, yielded an older date of B.C. 9740-9720, 9670-9300 (11690-11680, 11620-11250 yr B.P.).

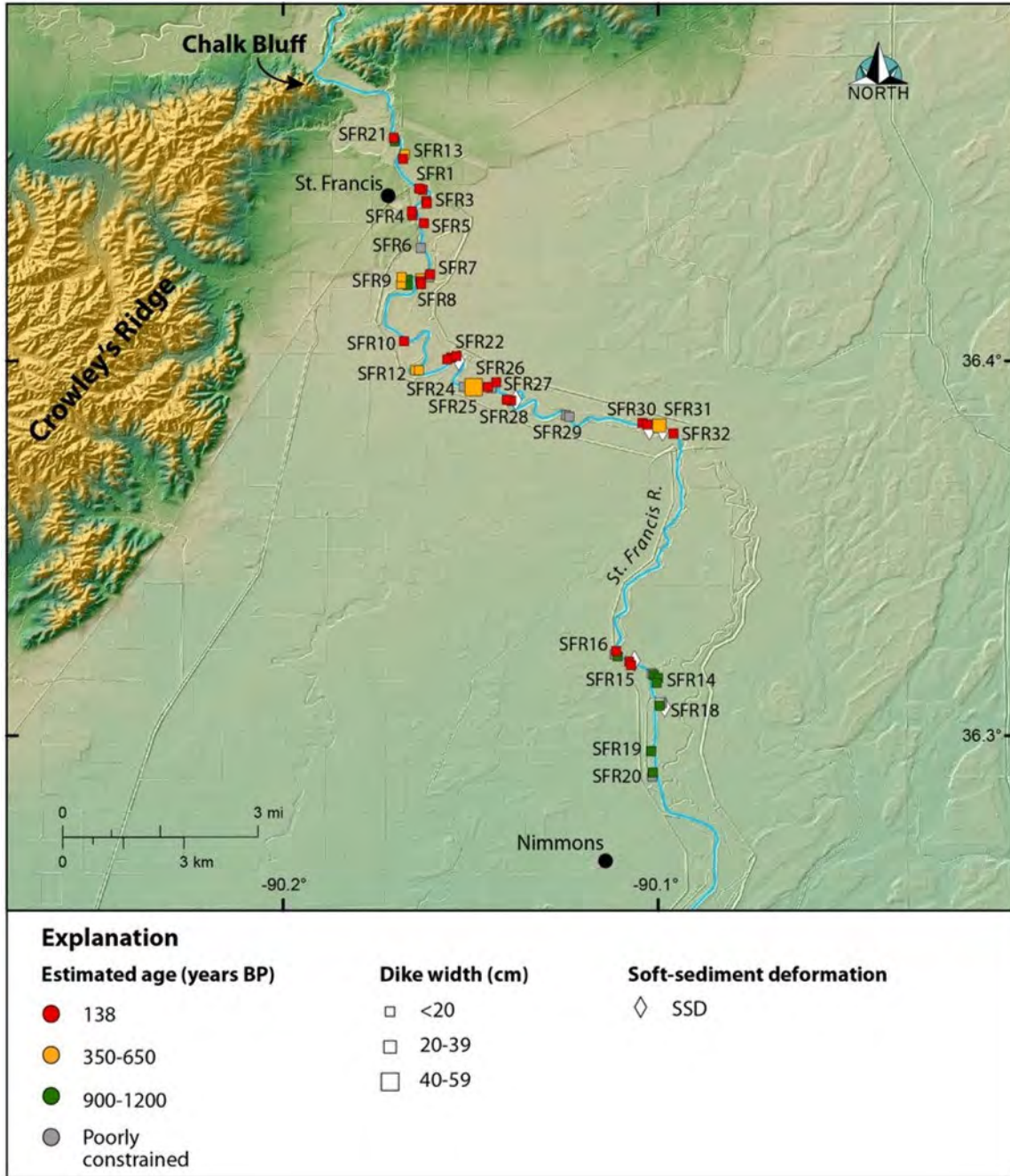


Figure 4-36 Map showing liquefaction features along the Chalk Bluff-Nimmons portion of the St. Francis River in northeastern Arkansas. Map area shown on Figure 4-35.

At site SFR8, three sand dikes, ranging from 0.3-2.0 cm wide, intruded clayey silt with redoximorphic features. One dike, 2.0 cm wide, was composed of fine to medium sand and extended 1.3 m up section to the contact with an overlying sand deposit. The dike was iron stained throughout and mottled near its termination. An unweathered dike, 0.3 cm wide and composed of fine sand, intruded the iron-stained dike and terminated within it ~25 cm above the water level (Figure 4-37). Another 2 cm wide dike, composed of very fine to fine sand, also extended 1.3 m up section to the contact between the clayey silt and overlying sand.

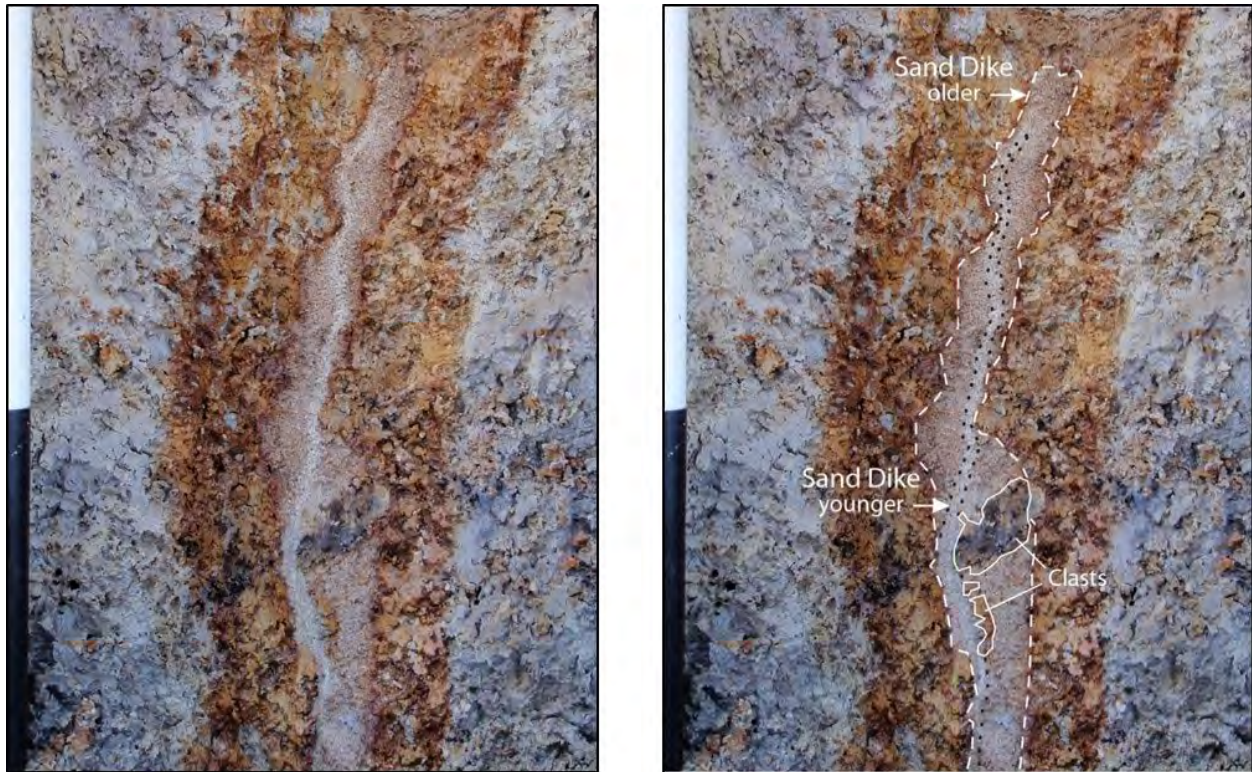


Figure 4-37 Photographs (left - unannotated; right - annotated) showing younger unweathered (grayish) dike intruding an older iron stained (reddish), larger sand dike at SFR8. Dashed and dotted lines represent clear and inferred contacts, respectively. Black and white intervals of meter stick represent 10 cm.

The dike appeared to intrude the overlying sand deposit but it became very difficult to follow up section. Like the 0.3 cm wide dike, this dike exhibited no iron staining and likely formed during the same event. Crosscutting relationships and differences in weathering indicate that there are two generations of liquefaction features at this site. The unweathered dikes may have formed during the A.D. 1811-1812 event, whereas the weathered dike is likely prehistoric in age. Its weathering characteristics are similar to weathered dikes at SFR9 and SFR12 described below and thought to have formed during the A.D. 1450 New Madrid event.

At site SFR9, four sand dikes, ranging from 2-8 cm wide and composed of fine sand containing silt clasts, intruded and crosscut silt with redoximorphic features. Three of the dikes extended 2.5 m above the water level to 2 m below the top of the cutbank. The largest dike extended higher in the cutbank to 2.75 m above the water level and 1.75 m below the top of the cutbank. Two of the dikes exhibited iron staining and mottling in their upper 0.5 m, whereas the other two dikes were more weathered and exhibited iron staining, mottling, and bioturbation in their upper 1 m (Figure 4-38). Degree of weathering suggests that the dikes are prehistoric in age and that they may have formed during two different events. Sample SFR9-C1 of charred material was collected from the mottled silt about 2 m below the surface and adjacent to the tip of one of the dikes. The sample yielded a date of B.C. 1880-1680 (3830-3630 yr B.P.) (Table 4-11) and suggests that the dikes at SFR9 formed sometime after B.C. 1880 B.C. (3830 yr B.P.). Based on weathering characteristics, the less weathered dikes at SFR9 may be similar in age to those at SFR12 described below and thought to have formed during the A.D. 1450 event. The more weathered dike would have formed earlier, possibly during the A.D. 900 event.

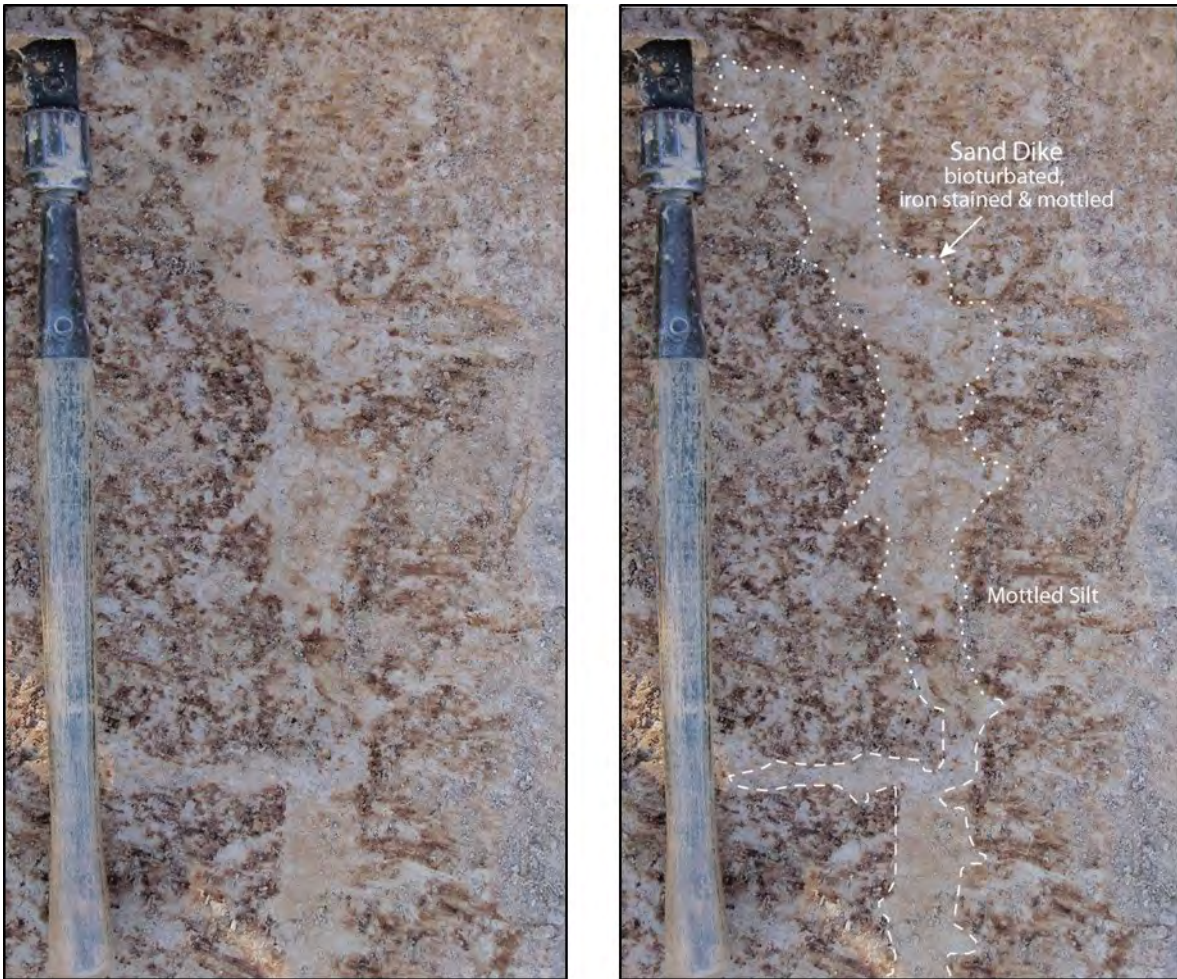


Figure 4-38 Photographs (left - unannotated; right - annotated) showing iron staining, mottling, and bioturbation in the upper part of older dike at SFR9. Dashed and dotted lines represent clear and inferred contacts, respectively. Shovel handle represents 50 cm.

At site SFR12, an 8-cm-wide dike, composed of fine-very fine sand containing silt clasts, crosscuts interbedded sand and silt and overlying mottled silt, extending 2 m above the water level to 2 m below the top of the cutbank (Figure 4-39). Several dikes and sills branched off of the main dike. The upper 1 m of the main dike was iron stained and mottled and therefore likely prehistoric in age. Radiocarbon dating of sample SFR12-C2, charred material from the mottled silt about 1.5 above water level and 0.5 m below the dike tip, yielded a date of A.D. 1020-1160 (930-790 yr B.P.) (Table 4-11). Sample SFR12-L2, leaves collected from a silt layer about 0.8 m above water level and 1.2 m below the dike tip, gave a date of A.D. 780-900, 910-970 (1170-1050, 1040-980 yr B.P.) and is stratigraphically consistent with the younger date for sample SFR12-C2 collected higher in the section. Sample SFR12-C2 provides a maximum constraining age of A.D. 1020 (930 yr B.P.) for all the liquefaction features. Based on weathering characteristics and radiocarbon dating, liquefaction features at this site formed between A.D. 1811 and A.D. 1020, probably during the A.D. 1450 earthquake sequence.

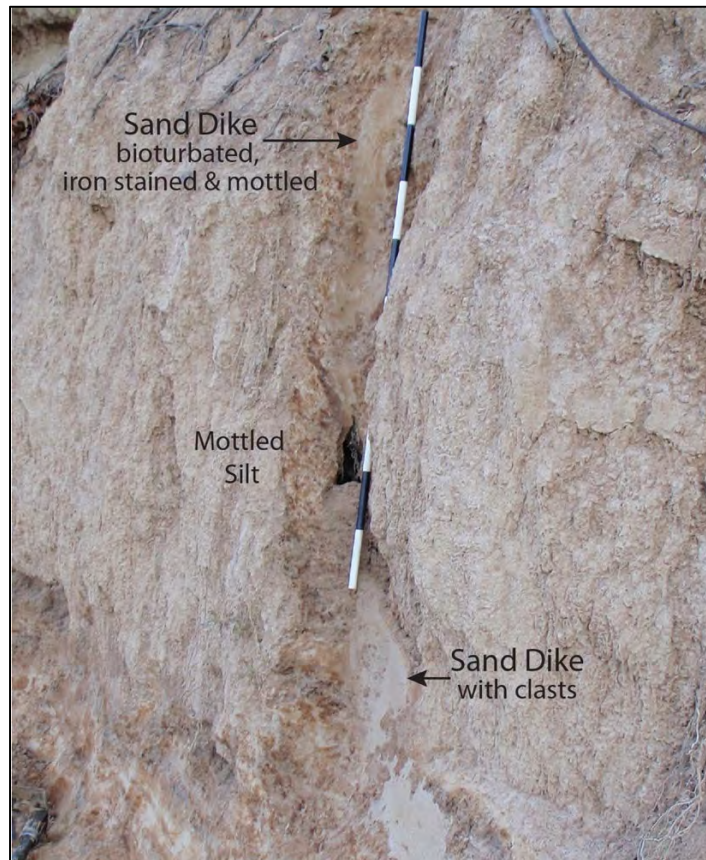


Figure 4-39 Photograph of sand dike crosscutting mottled silt at site SFR12. Upper 1 m of dike is iron stained, mottled, and bioturbated. Black and white intervals of meter stick represent 10 cm.

At SFR14, three sand dikes, all 3 cm wide, and a fourth dike, 0.4 cm wide, were found along a 110 m long cutbank. The dikes were observed originating in a sand layer occurring at the base of the cutbank and intruding the overlying sequence of sediment with bioturbated and mixed clay and sand, overlain by bioturbated silty clay in which a soil and iron and manganese nodules had formed, followed by mottled silt. The dikes were composed of medium to fine sand containing clay and silt clasts. The three larger dikes extended 1.6 m above the sandy source layer to 1.5 m below the top of the cutbank. These three dikes all exhibited iron staining, mottling, and fines accumulation. The upper part of one the dikes was also bioturbated and another one was cemented. The degree of weathering of the three dikes suggests that they are prehistoric in age. Radiocarbon dating of sample SFR14a-C3, charred material collected near the top of bioturbated clayey silt and 0.75 m below the dike tip yielded a date of A.D. 780-785, 880-990 (1170-1165, 1070-980 yr B.P.) (Table 4-11). Across the river from SFR14, sample SFR17-W1 collected near the base of the bioturbated clayey silt yielded a date of A.D. 85-255, 300-315 (1865-1695, 1650-1635 yr B.P.), stratigraphically consistent with the younger date of sample SFR14a-C3 collected higher in the deposit. Sample SFR14a-C3 provides a maximum constraining age of A.D. 780 (1170 yr B.P.) for the liquefaction features. The weathering of the liquefaction features at this site seems greater than dikes at SFR12, which probably formed during the A.D. 1450 event, and similar to the more weathered dikes at SFR9 that probably formed during the A.D. 900 event. Therefore, the dikes at this site are interpreted as having formed during the A.D. 900 New Madrid event.

Table 4-11 Radiocarbon dating results for St. Francis River sites between Chalk Bluff and Nimmons, Arkansas

Sample # Lab #	$^{13}\text{C}/^{12}\text{C}$ Ratio	Radiocarbon Age Yr B.P.¹	Calibrated Radiocarbon Age Yr B.P.²	Calibrated Calendar Date A.D./B.C.²	Sample Description
SFR2-C2 BA-315741	-26.7	9970 ± 50	11690-11670 11620-11250	BC 9740-9720 BC 9670-9300	Charred material from mottled silt at base of 3.5-m high cutbank
SFR4-C2 BA-315742	-26.1	7720 ± 40	8590-8420	BC 6640-6470	Charred material 3.25 m BTC (below top of cutbank), 25 cm below dike tip, & 75 cm AWL, from mottled silt
SFR9-C1 BA-338302	-27.0	3440 ± 30	3830-3790 3770-3750 3730-3630	BC 1880-1840 BC 1820-1800 BC 1780-1680	Charred material from mottled silt ~2 m BTC & adjacent to dike tip
SFR12-C2 BA-338303	-26.0	950 ± 30	930-790	AD 1020-1160	Charred material 0.5 m below dike tip & 1.5 m AWL from mottled silt
SFR12-L2 BA-338304	-26.5	1160 ± 30	1170-1050 1040-980	AD 780-900 AD 910-970	Leaves 1.2 m below dike tip & 0.8 cm AWL from silt layer crosscut by sand dikes
SFR14a-C3 BA-422149	-25.1	1120 ± 30	1170-1165 1070-960	AD 780-785 AD 880-990	Charred material 2.25 m BTC & 75 cm below dike tip from bioturbated clayey silt
SFR17-W2 BA-422148	-25.9	550 ± 30	635-595 560-520	AD 1315-1355 AD 1390-1430	Wood from tree trunk ~1.4 m BTC bedded in sand overlying weathered clay
SFR17-W1 BA-422147	-26.7	1830 ± 30	1865-1695 1650-1635	AD 85-255 AD 300-315	Wood ~2.9 m BTC from base of bioturbated, clayey silt
SFR22-C2 BA-452744	-24.7	31340 ± 210	35655-34805	BC 33705- 32855	Plant material, likely lignite, 2.03 m BTC & 97 cm AWL from mottled silt
SFR30-C1 BA-452749	-25.3	1510 ± 30	1515-1460 1415-1340	AD 435-490 AD 535-610	Charred material 2.5 m BTC & 70 cm AWL from sand layer; source of dikes
SFR32-W1 BA-452745	-29.2	640 ± 30	665-620 610-555	AD 1285-1330 AD 1340-1395	Leaves, horizontally bedded in layered silt, 2.15 m BTC & 10 cm AWL

¹ Conventional radiocarbon ages in years B.P. or before present (1950) determined by Beta Analytic, Inc. Errors represent 1 standard deviation statistics or 68% probability.

² Calibrated age ranges as determined by Beta Analytic, Inc., using the Pretoria procedure (Talma and Vogel, 1993; Vogel et al., 1993). Ranges represent 2 standard deviation statistics or 95% probability.

At SFR16, three sand dikes, composed of medium to fine sand with clasts of silt and cross-bedded sand, were found along a 60-m-long cutbank. The largest dike, 5.8 cm wide, and the smallest dike, 0.2 cm wide, originated in a sand layer at the base of the cutbank (Figure 4-40). The source bed of the dikes exhibited disturbed bedding and contained founder clasts from the overlying unit. The largest dike extended 2.5 m above the water table, and 1.5 m above the sandy source bed, to 2 m below the top of the cutbank. The dike crosscut a sequence of sediment with weathered cross-bedded sand overlain by mottled silt with manganese nodules, followed by mottled sand. The dike had a 7-cm-wide bulbous termination in the weathered sand. The upper 1.0 m of the dike was very iron-stained and the upper 0.6 m was also mottled and bioturbated. Weathering characteristics of this dike were similar to those of very weathered dikes at SFR14 suggesting that this dike might also have formed during the A.D. 900 New Madrid event. There was a domain of relatively unweathered and loose sand along one of the dike margins, suggesting intrusion during a more recent event. The third dike, only 3 m upstream from the largest dike, was 2 cm wide and extended 3.1 m above the water table to 1.4 m below the top of cutbank. It terminated at the contact of the weathered sand and overlying silt deposit, 60 cm above the largest dike. The third dike was essentially unweathered and loose, suggesting that it formed during the A.D. 1811-1812 New Madrid event. A similarly unweathered dike was found at nearby SFR15 (Figure 4-41).

Downstream from SFR14, the main dikes at SFR18, SFR19, and SFR20 were 4, 10, and 6 cm wide, respectively. They extended from 1.2 to 2.4 m above the water level and crosscut a sequence of sediment, including sand overlain by bioturbated clay and sand, followed by clay, and mottled silt. The dikes exhibited iron staining, fines accumulation, and cementation. A portion of one of the dikes was also bioturbated. The bioturbated clay and sand at these three sites are thought to be correlative with bioturbated clayey silt and sand at SFR17 (not shown on Figure 4-36 because it is not a liquefaction site) located near SFR18. Radiocarbon dating of sample SFR17-W1 from the bioturbated clay and sand provided a maximum age of A.D. 85 (1865 yr B.P.) (Table 4-11) for the dikes at the three sites. Like the dikes at SFR14, the very weathered dikes at SFR18, SFR19, and SFR20 may have formed during the A.D. 900 New Madrid event.

At SFR22, three sand dikes, 19, 3.5, and 2 cm wide, had formed at the edge of a lense of interbedded silt and sand embedded within mottled silt (Figure 4-42). The largest dike originated in a layer of medium-fine sand at the base of the cutbank, the lowest observable layer of the lense of interbedded silt and sand, likely a point-bar deposit. The bedding of the sandy source bed was slightly disturbed. Also, soft-sediment deformation structures, specifically small pillows, had formed in the overlying sand layer within the lense. Parallel bedding was not disturbed within the two other overlying sand layers within the lense. It seems that the lower two sand layers had liquefied, whereas the upper two layers had not. This may be indicative of the water level at the time of the earthquake that induced liquefaction. The dike, composed of loose, medium-fine sand with silt clasts, intruded the mottled silt adjacent to the edge of the likely point-bar deposit. Up section, the strike of the dike became subparallel to the cutbank and the upper portion of the dike had been removed by bank erosion. The dike showed no signs of weathering. The 3.5 cm wide dike, was also composed of medium-fine sand, intruded the mottled silt, extending to 2.25 m above the water level where it pinched out within 0.75 m of the top of the cutbank. The upper part of the dike was only slightly iron stained. The 2 cm wide dike intruded the mottled silt, extending to 1.58 m above the water level, where it became discontinuous, and pinched out at 1.75 m above the water. This dike was also loose and only slightly iron stained. Given that there was little to no weathering in all three dikes including the two that extended higher in the cutbank, these dikes are likely to be historic in age and to have formed during the A.D. 1811-1812 New Madrid events.

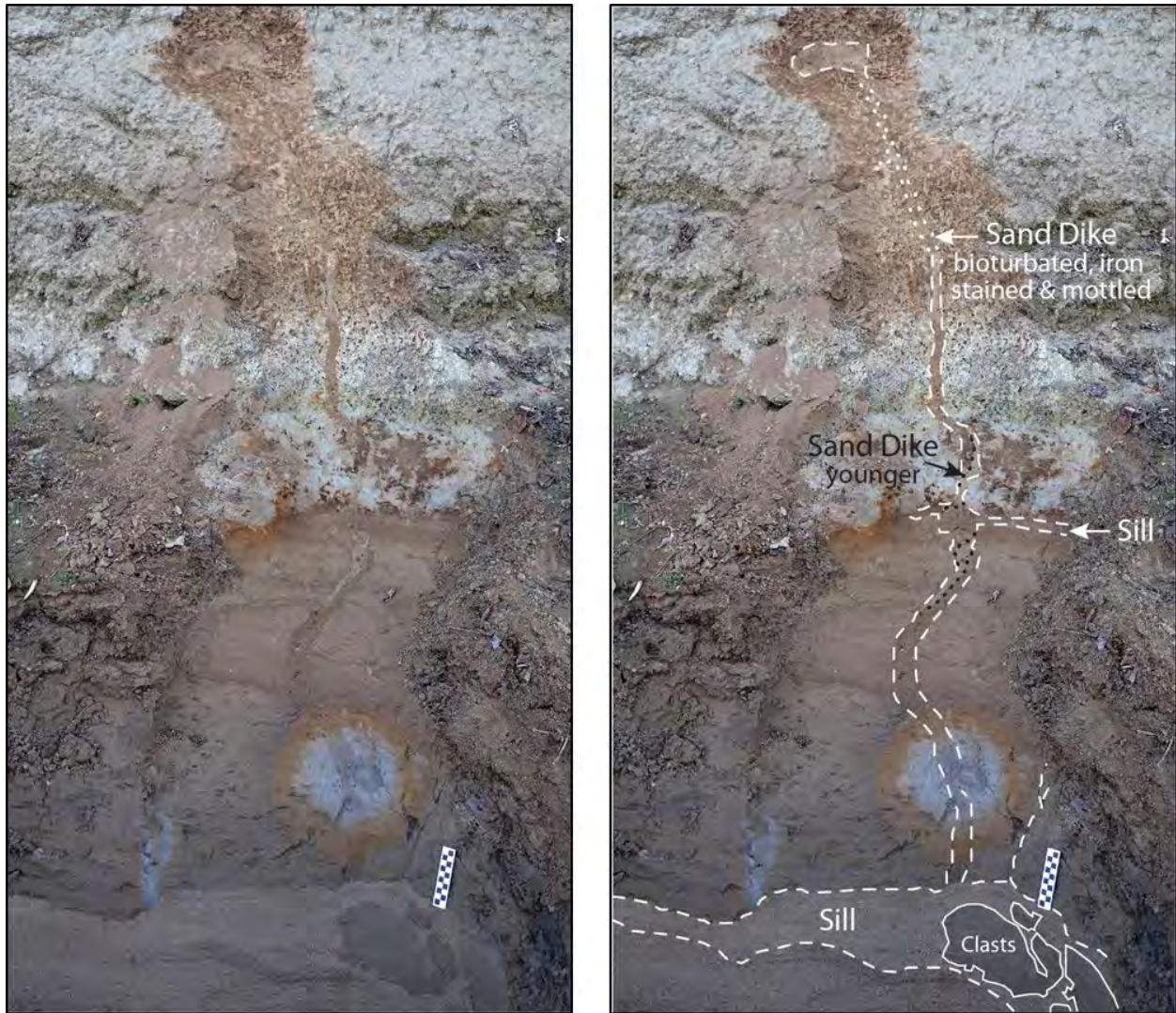


Figure 4-40 Photographs (left - unannotated; right - annotated) showing sand dike originating in cross-bedded sand and forming dikes and sills at SFR16. Iron staining, mottling, and bioturbation occurs in the upper 1 m of an older dike. Dashed and dotted lines represent clear and inferred contacts, respectively. Black and white intervals represent 1 cm on small scale.



Figure 4-41 Photograph showing relatively unweathered sand dikes at SFR15. Larger dike extends farther up section, where it splits to form two smaller dikes filled with small lignite clasts. Black and white intervals represent 10 cm on meter stick and 1 cm on small scale near split of dike into two smaller dikes.

At SFR25, there was one dike, 41-cm wide, that intruded mottled silt and extended 2.25 m above the water level to 0.75 m below the top of the cutbank (Figure 4-43). The dike had a blunt termination that was composed of many small lignite clasts and was underlain by iron stained and mottled silt containing a large clast of mottled silt with manganese nodules. The silt was underlain by iron-stained and mottled fine sand with small manganese nodules. Below the fine sand, there was a chunk of silt that spanned the width of the dike, exhibited reddish brown mottles, and appeared to be sheared along the dike margins. The coloring of the mottles matched that of the host silt near the tip of the dike. The chunk of silt appeared to have collapsed into the dike from above. Below the chunk of silt, there was layered silt and sand followed by iron-stained sand with small silt clasts and occasional lenses of silt and sand. With depth, the dike became less iron stained and was composed of tubular domains of light gray, coarse-medium sand within dark gray, medium-fine sand. The horizontal layering within the dike suggested that there had been lateral flow within the dike, whereas the tubular domains of coarser sand suggested vertical flow. The size of the dike, much wider than other dikes along this portion of the river, the collapse of overlying mottled silt into the dike, and the bedding indicative of lateral flow within the dike suggest that lateral spreading was involved in the formation of this dike. The degree of weathering suggests that the dike is prehistoric in age. Based on similarity in degree of weathering with SFR12, this dike may have formed during A.D. 1450 event.

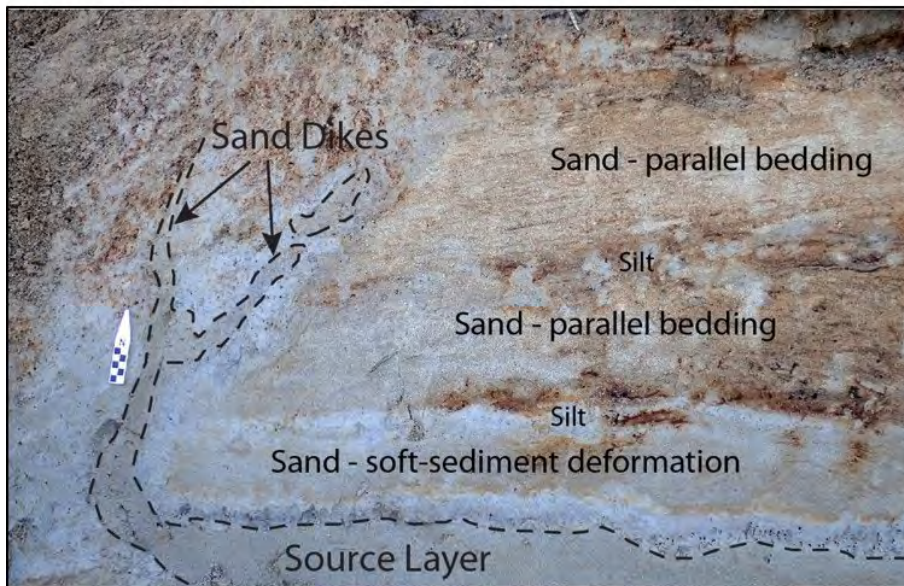


Figure 4-42 Photographs (upper - unannotated; lower - annotated) showing sand dike originating in sand layer (left side) of interbedded silt and sand deposit, intruding adjacent silt, branching and extending up section at site SFR22. Black and white intervals on small scale represent 1 cm. Dashed lines represent clear contacts. Scale is placed adjacent to one of the dikes.

At SFR30, two sand dikes, 6 and 3 cm wide, originated in a sandy source bed, intruded the overlying sequence of sediment with interbedded silt and silty sand, overlain by layered silt, followed by mottled silt. The sandy source bed exhibited disturbed bedding and flow structure below the base of the dikes. In addition, the source bed contained clasts of the overlying deposit that appeared to have experienced basal erosion. The larger dike extended 1.5 m above the water table where it became a sill and low-angle dike. The sill/dike was iron stained, especially along its margins; however, the dike below was loose and not iron stained. The smaller dike extended 1.55 m above the water table, where it became discontinuous for another 10 cm and

terminated 1.35 m below the top of cutbank. This dike exhibited little to no iron staining. Radiocarbon dating of sample SFR30-C1, charred material, collected from the source bed of the dikes provides an age estimate (A.D. 435-490, 535-610 or 1515-1460, 1415-1340 yr B.P.) (Table 4-11) of the sandy layer. At nearby site SFR32, where the sequence of sediment was similar to that at SFR30 and SFR31, sample SFR32-W1 (horizontally bedded leaves) was collected from layered silt between mottled silt above and interbedded silt and silty sand below. The sample yielded a radiocarbon date of A.D. 1285-1330, 1340-1395 (665-620, 610-555 yr B.P.) and provides a maximum constraining age of A.D. 1285 for the sand dikes at SFR30. Given that there was little to no weathering of the dikes, it is likely they are historic in age and formed during A.D. 1811-1812 New Madrid earthquakes.



Figure 4-43 Photographs (left - unannotated; right - annotated) showing sand dike with blunt termination at SFR25. Large clasts of mottled silt appear to have collapsed into the dike from above. Horizontal layering as well as tubular flow structure occur within the dike. The upper part of the dike was iron stained, mottled, and contained small manganese nodules. Dashed lines represent clear contacts. Black and white intervals on hoe represent 25 cm.

At SFR31, a 21-cm-wide sand dike, originating in a fine sand layer near the base of the cutbank, intruded overlying interbedded silt and silty sand, layered silt, and mottled silt (Figure 4-44). The dike extended 1.5 m above the water level to 0.75 m below the top of the cutbank. The upper 1.0 m of the dike exhibited iron staining, fines accumulation, and cementation, and therefore is almost certainly older than the dikes at SFR30. Sample SFR32-W1, collected from layered silt at nearby site SFR31, provides a maximum constraining age of A.D. 1285 (Table 4-11) for the sand dike at SFR31. Therefore, the weathered dike at this site is interpreted as having formed during the A.D. 1450 event.



Figure 4-44 Photographs (left - unannotated; right - annotated) showing sand dikes and sills originating in sand layer of interbedded silt and sand deposit at SFR31. Dashed lines represent clear contacts. M. Tuttle points to termination of dike 75 cm below the top of cutbank.

At SFR32, a 14-cm-wide sand dike, originating in a fine sand layer near the base of the cutbank, intruded overlying layered silt and silty fine sand, layered silt, and mottled silt. The dike extended 1.5 m above the water level to 0.75 cm below the top of the cutbank. The upper portion of the dike was slightly iron-stained, whereas the lower part was loose and unweathered. Sample SFR32-W1, already described above, was collected 1.4 m below the dike tip from the layered silt and yielded a date of A.D. 1285-1330, 1340-1395 (665-620, 610-555 yr B.P.) (Table 4-11). This date provides a maximum constraining age of A.D. 1285 for the sand dike. Because it exhibited little to no weathering, similar to the dike at SFR30, and was much less weathered than the dike at SFR31, the dike at SFR32 is interpreted as having formed during the A.D. 1811-1812 event.

4.4.4.5 *St. Francis River between Fisk and Wilhelmina, Missouri*

We performed a systematic survey along 33 km of the St. Francis River between Fisk and Wilhelmina in southeastern Missouri (Figure 4-11, Figure 4-17, Figure 4-19, Figure 4-35, Figure 4-45, and Figure 4-46). The survey began about 10 km downstream from Fisk and ended at the Rt. 228 bridge east of Wilhelmina. This portion of the St. Francis River crosses the Commerce Geophysical Lineament (CGL; NUREG-2115). Southeast of Quin, Missouri, Quaternary faulting associated with the CGL has been interpreted from seismic reflection and refraction profiles about 2-4 km northwest of the St. Francis River (Stephenson et al., 1999; Baldwin et al., 2014). In

addition, several liquefaction features had been found in drainage ditches associated with the St. Francis River (Vaughn, 1994). At two sites, the liquefaction features were thought to be Late Pleistocene in age, and at a third site features were Late Holocene in age and may have formed during the A.D. 1811-1812, A.D. 1450, and A.D. 900 New Madrid earthquakes.

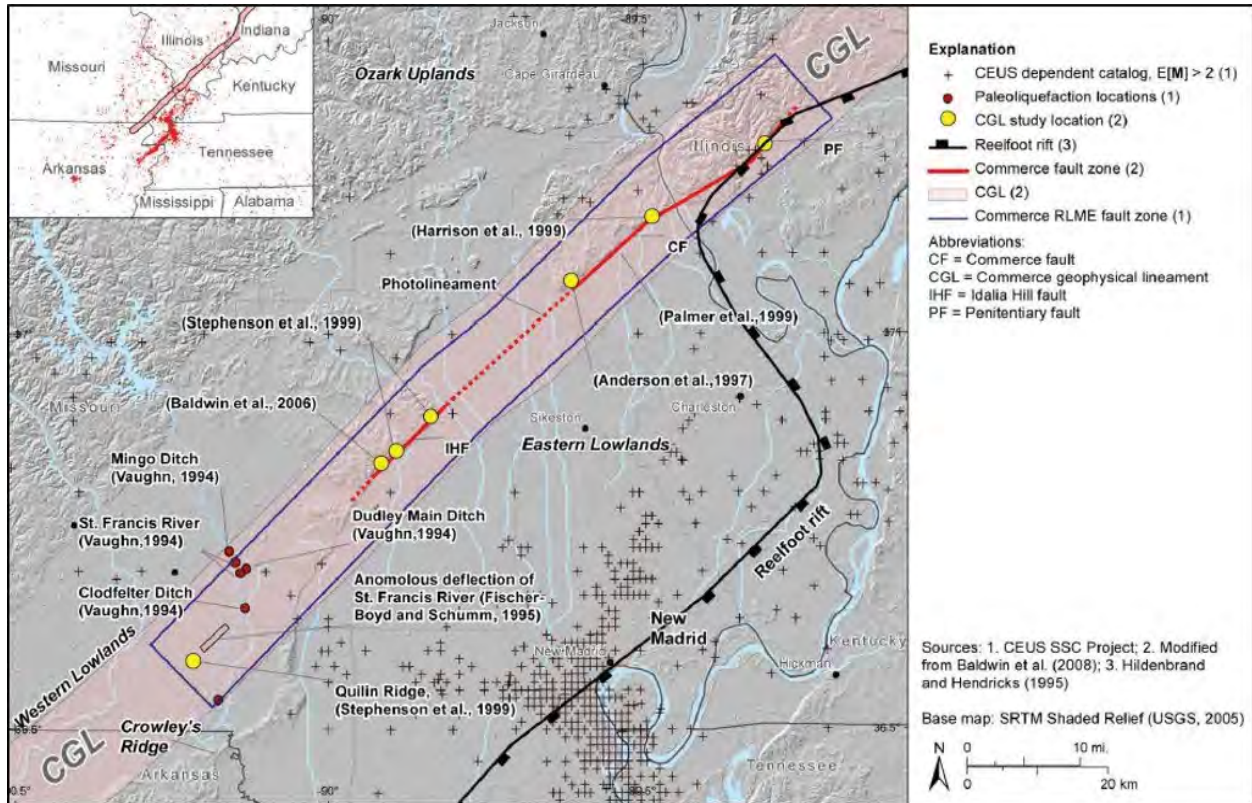


Figure 4-45 Map showing the Commerce geophysical lineament (CGL), Commerce fault zone (CF), and Commerce RLME fault zone in northeastern Arkansas and southeastern Missouri (from NUREG-2115). Sites of paleoliquefaction found near the lineament prior to this study indicated by red dots (Vaughn, 1994).

Surficial geology along this portion of the St. Francis River is mapped as Holocene point-bar deposits inset in Late Pleistocene (Early Wisconsin) valley train (level 2), including interfluvial and relict channels (Saucier, 1994; Figure 4-21). Most, if not all, of this portion of the river had been channelized. Exposure was poor along the straight sections; however, there was good to excellent exposure in most bends where cutbanks had formed due to erosion. Cutbanks ranged from 3-9 m high, with most cutbanks in the 4-6 m range. The upper 0.5-2.0 m of the cutbanks was often vegetated and sometimes the lower 0.5-1.0 m was covered by recent deposits or slumped sediment.

Along the northernmost, northwest-southeast-oriented section of the St. Francis River, most cutbanks were 6 m high and revealed buff-colored silt overlying interbedded or laminated silt and sand. Sand layers tended to get thicker and coarser with depth. At a couple of locations, buff-colored silt was underlain by clay in which a soil had developed. In a large river bend just upstream from Dudley Main Ditch, there were two terrace levels, and sediment was exposed only in 3 m high cutbanks of the lower terrace. The cutbanks revealed recent layered silt overlying bioturbated and weathered sand with redoximorphic features and silty krotovina. Along the middle section from Dudley Main Ditch to Wilhelmina Cutoff Ditch, most cutbanks were 4-6 m high and

revealed buff-colored silt overlying interbedded silt and sand or mottled silt followed by interbedded silt and sand. The interbedded silt and sand deposit often contained organic debris, ranging from leaf litter to tree trunks. In a few locations, gray sandy silt with large lenses of gray silt occurred between mottled silt and interbedded silt and sand. North of Wilhelmina, the Wilhelmina Cutoff Ditch heads southeast towards Crowley's Ridge, diverging from the old abandoned channel of the St. Francis River. The survey was conducted along the Wilhelmina Cutoff Ditch since the river now flows along it. Between the old channel and Rt. 207 bridge crossing, cutbanks were 4.5 m high and exposed buff silt underlain by mottled silt followed by bioturbated and weathered sand with redoximorphic features and silty krotovina. From Rt. 207 to Rt. 228 bridge crossing, there were only a few cutbank exposures that were 4.5 m high and revealed a thick deposit of brownish silt.

Along the Fisk-Wilhelmina portion of the St. Francis River, we documented twenty-one sand dikes at fourteen sites. Dikes ranged in width from 0.2-15 cm. At two of the sites, source layers of the sand dikes were exposed and exhibited soft-sediment deformation including pseudonodules, load casts, foundered clasts and associated delamination of overlying silt. In addition, soft-sediment deformation was noted in interbedded silt and sand crosscut by dikes.

Unfortunately, no sand blows were found along the river. At two sites, SFR50 and 53, sand dikes were composed of two phases of sediment with different weathering characteristics, suggesting that they formed during two different events. Radiocarbon dating was performed on samples collected at three sites (SFR41, 50, and 52) and OSL dating was performed at one site (SFR48). As demonstrated at site SFR50, even very weathered dikes probably formed since B.C. 3020 (or 4970 yr B.P.). Radiocarbon dating and degree of weathering were used to interpret the ages of liquefaction features at six of the sites. These features can be attributed to the New Madrid events of A.D. 1811-1812, A.D. 1450, and A.D. 900. If radiocarbon dating had been performed for more sites, it might have been possible to interpret the ages of additional liquefaction features. The most significant liquefaction sites are discussed below.

At site SFR41, one sand dike, 5 cm wide, composed of medium-fine sand with silt clasts, crosscut laminated and interbedded silt and sand and extended at least 1.7 m above the water level to 1.3 m below the top of the cutbank. The termination of the dike could not be seen because it was covered by vegetated sediment. The upper 50 cm of the visible dike was somewhat iron stained, especially its margins, but otherwise was loose and showed no other signs of weathering, suggesting that it is historic in age. Sample SFR41-L1, leaves, collected from the laminated silt and sand about 1.45 m below the top of the dike and 20 cm above the base of the dike, yielded a date of A.D. 1525-1555, 1630-1665, and 1780-1795 (425-395, 320-285, 170-155 yr B.P.) (Table 4-12). This date provides an age estimate for the laminated silt and sand and a maximum constraining age of A.D. 1525 (or 425 yr B.P.) for the dike. On the basis of radiocarbon dating and minimal weathering, this dike likely formed during the historic New Madrid earthquakes of A.D. 1811-1812.

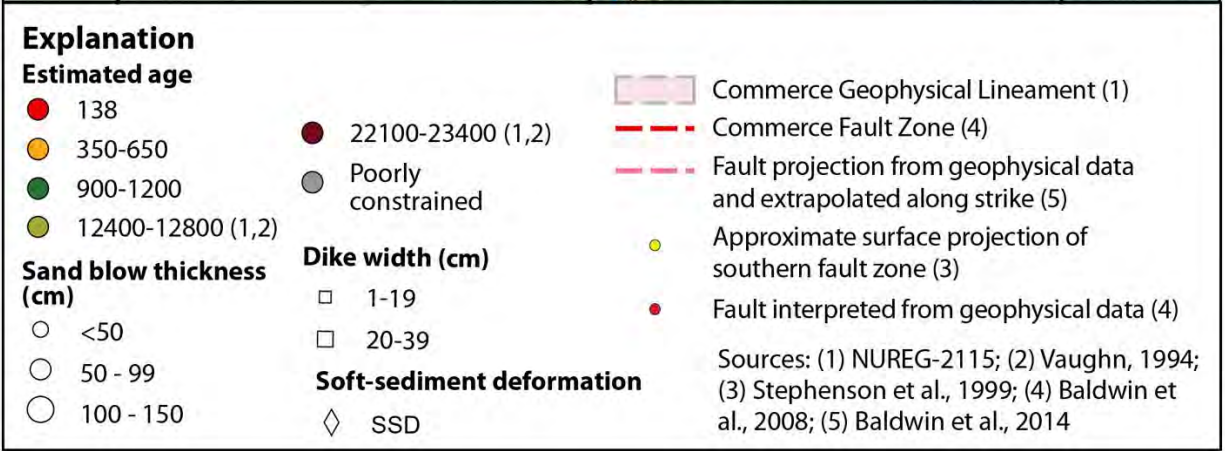
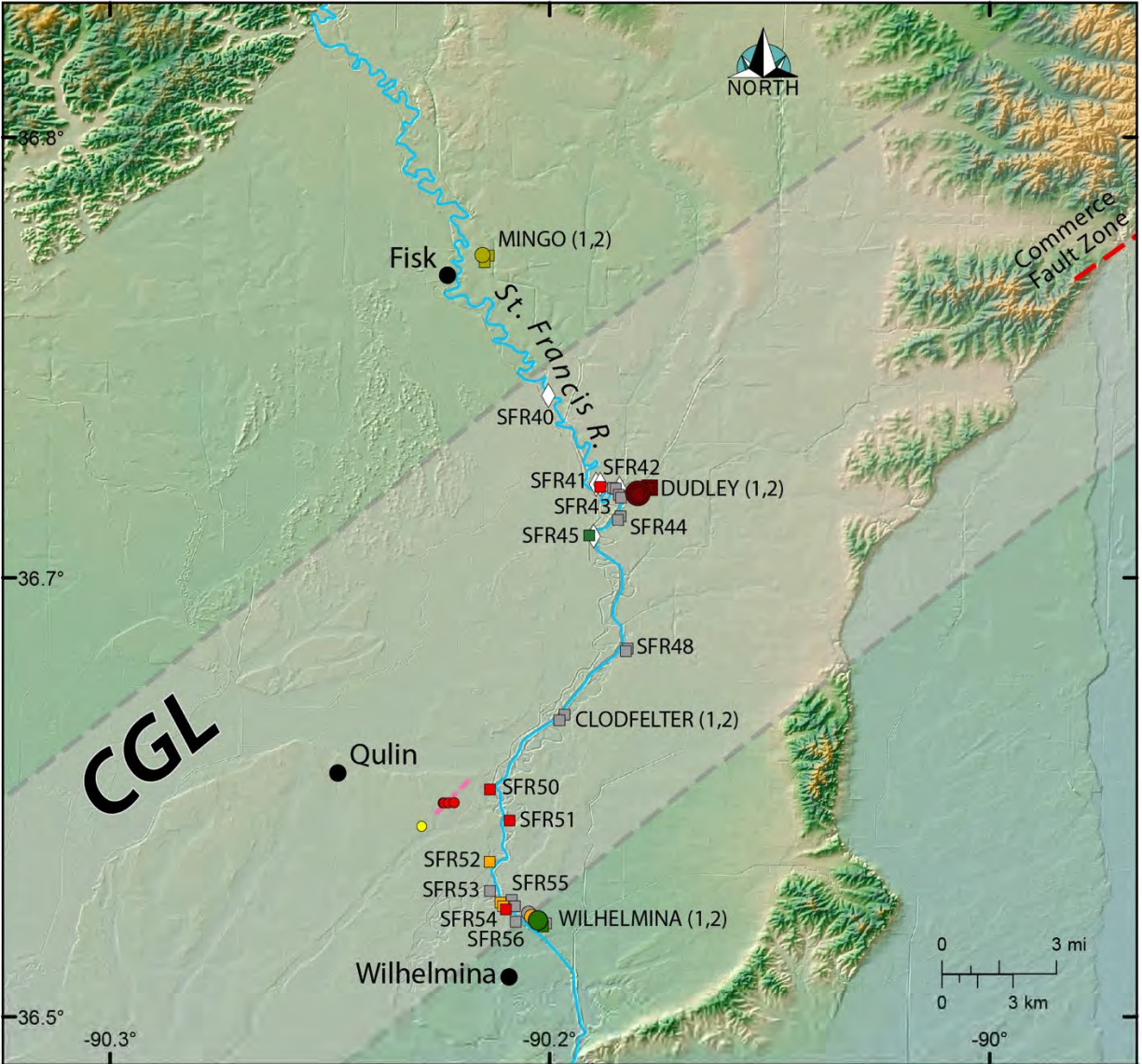


Figure 4-46 Map showing liquefaction features along the Chalk Bluff-Fisk-Wilhelmina portion of the St. Francis River in southeastern Missouri. Map area shown on Figure 4-35.

Table 4-12 Radiocarbon Dating Results for St. Francis River Sites between Fisk and Wilhelmina, Missouri

Sample # Lab #	¹³ C/ ¹² C Ratio	Radiocarbon Age Yr B.P. ¹	Calibrated Radiocarbon Age Yr B.P. ²	Calibrated Calendar Date A.D./B.C. ²	Sample Description
SFR41-L1 BA-452746	-28.5	260 ± 30	425-395 320-285 170-155	AD 1525-1555 AD 1630-1665 AD 1780-1795	Leaves 1.45 m below top of dike, 20 cm above base of dike, & 45 cm AWL; horizon-tally bedded in laminated silt with sandy interbeds
SFR50-W1 BA-452748	-28.1	4340 ± 30	4970-4845	BC 3020-2895	Wood 1 m below dike tip & 70 cm AWL; from layered silt with thin interbeds of sand
SFR52-C1 BA-452747	-28.2	440 ± 30	525-480	AD 1425-1470	Charred material 56 cm below dike tip & 1.8 m AWL; from mottled silt

¹ Conventional radiocarbon ages in years B.P. or before present (1950) determined by Beta Analytic, Inc. Errors represent 1 standard deviation statistics or 68% probability.

² Calibrated age ranges as determined by Beta Analytic, Inc., using the Pretoria procedure (Talma and Vogel, 1993; Vogel et al., 1993). Ranges represent 2 standard deviation statistics or 95% probability.

Sites SFR42 and 43 occurred within 30 m of each other and had the same sedimentological setting. At both sites, two dikes crosscut weathered and bioturbated sand with silty krotovina. The dikes at SFR42 were 2 and 1 cm wide and the dikes at SFR43 were 15 and 2 cm wide. The dikes were truncated at the upper contact of the weathered sand, between 40 cm and 70 cm above the water level, and were overlain by recent layered silt. Nearby, a known Paleoindian (12000-14000 yr B.P.) archeological site occurred in the weathered and bioturbated sand, indicating that the deposit crosscut by the dikes is at least 12000 years old. All four dikes were only slightly iron stained, suggesting that they may be fairly young; however, there is much uncertainty about their age because the upper parts of the dikes had been truncated.

At site SFR45, one sand dike, up to 8 cm wide, originated in interbedded sand and silt exposed in the lower 1.2 m of the cutbank (Figure 4-47). The source beds exhibited soft-sediment deformation structures including pseudonodules and load casts. The dike intruded and crosscut the overlying very weathered and mottled silt, branched upward, and terminated at the base of a buried soil about 3.1 m above the water level and about 4.9 m below the top of the cutbank. The dike was composed of medium-fine sand and was very weathered. The entire height (1.9 m) was iron stained and cemented and the upper part of the dike was also bioturbated and exhibited fines accumulation. The degree of weathering suggests that the dike is prehistoric in age. Given that its weathering characteristics are similar to those of very weathered dikes at SFR14, this dike also may have formed during the A.D. 900 New Madrid event.



Figure 4-47 Photographs (upper - unannotated; lower - annotated) showing very weathered sand dikes at SFR45. Dashed lines represent clear contacts. For scale, wooden handle of scraper is 36 cm long.

At site SFR48, three dikes, 5, 3, and 2.5 cm wide, composed of very fine to fine sand, intruded cross-bedded, silty, medium-fine sand overlain by weathered, gray, sandy silt. Up section, two of the dikes became subparallel to the cutbank and their terminations had been removed by erosion. The third dike extended to 2.5 m above the water level or 1.5 m below the top of the cutbank. The upper 1 m of the dike was iron stained, especially its margins. Iron staining of the margins continued to the base of the cutbank. No organic samples could be found at the site for radiocarbon dating. A sediment sample was collected from the cross-bedded, silty, medium-fine sand about 20 cm below the contact with the overlying weathered, gray, sandy silt. OSL dating of the sample suggests that the cross-bedded sand at the base of the cutbank was deposited

88090-77230 yr B.P. (Table 4-13). However, it should be noted that OSL dating consistently has given older dates than radiocarbon dating of co-located organic samples during the course of this study. Therefore, the sediment might not be as old as the OSL date suggests.

Table 4-13 Optically Stimulated Luminescence Dating Results at St. Francis River Site StFR48

Sample Number	Lab	Cosmic Dose Rate (mGray/yr) ¹	Dose Rate (mGray/yr)	OSL Age (Yr) ²	Calendar Age (Yr) ³	Sample Description
OSL1	BG4323	0.12 ± 0.01	1.80 ± 0.09	82720 ± 5430	88090-77230	From cross-bedded silty sand near base of cutbank overlain by weathered sandy silt; both crosscut by dikes

¹ Cosmic dose rate calculated from parameters in Prescott and Hutton (1994).

² Systematic and random errors calculated in a quadrature at one standard deviation. Datum year is A.D. 2010.

³ Years B.P. or before present (1950).

At site SFR50, an *en echelon* sand dike, 8 cm wide and composed of very fine to fine sand with silt clasts, intruded layered silt with thin interbeds of sand and overlying mottled silt. The dike terminated at 1.7 m above the water level or 4.3 m below the top of the cutbank. The upper portion of the dike was composed of two phases: a more weathered phase that was iron-stained and cemented, with fines coating sand grains and a less weathered phase that was loose and only slightly iron stained. The lower part of the dike was composed of a less weathered phase as well. Most of the dike was loose and only slightly weathered and may have formed during the A.D. 1811-1812 New Madrid earthquakes. The small weathered portion of the dike likely predates the historic earthquakes. Sample SFR50-W1, wood, collected from the layered silt with interbeds of sand about 70 cm above the water level and 1 m below the dike tip, yielded a date of B.C. 3020-2895 (4970-4845 yr B.P.) (Table 4-12). This date provides an age estimate for the layered silt and a maximum constraining age of B.C. 3020 (or 4970 yr B.P.) for both generations of liquefaction features.

At site SFR52, a sand dike, 7 cm wide, crosscut interbedded clayey silt and sand as well as overlying mottled silt and terminated at 2.4 m above the water level or 2.1 m below the top of the cutbank (Figure 4-48). The dike fined upward from very fine to fine sand to silty, very fine sand. The upper 90 cm of the dike was iron stained and the upper 8 cm exhibited some coating of sand grains by fines. Sample SFR52-C1, charred material, collected from mottled silt 1.8 m above the water level and 56 cm below the dike tip, yielded a date of A.D. 1425-1470 (525-480 yr B.P.) (Table 4-12). This date provides an age estimate for the mottled silt and a maximum constraining age of A.D. 1425 (or 525 yr B.P.) for the dike. Given the radiocarbon dating and weathering characteristics, the dike probably formed during the A.D. 1450 New Madrid event.

At site SFR53, a sand dike, up to 14 cm wide, intruded very weathered, iron stained sand and overlying mottled silt. Up section, the dike trended subparallel to the cutbank and was removed by erosion above 1.4 m above the water table or 3.1 m below the top of the cutbank. The dike was composed of two phases of medium-fine sand with small silt clasts, suggesting intrusion during two different earthquakes. One phase appeared slightly more iron stained than the other. The compound dike fined up section to fine sand. The upper 57 cm of the dike was only

somewhat iron-stained, suggesting that the dike may be historical in age. However, since the upper part of the dike had eroded away, there is considerable uncertainty regarding the relative age of the dike.

At site SFR54, three dikes, 8.5, 4.0, and 1.5 cm wide, were exposed along a 25-m-long cutbank. The largest dike was composed of coarse-medium sand, the second largest of medium-fine sand, and the smallest of fine sand and silty very fine sand near its termination. The largest dike intruded bioturbated clayey silt, extended to 1.2 m above the water level, where it was covered by a slump of mottled silt. This dike was iron-stained throughout, especially along its margins. The second largest dike, intruded weathered sand with manganese staining and overlying mottled silt, where it terminated at 2 m above the water level or 2.5 m below the surface. This dike also was iron-stained throughout, especially along its margins. The smallest dike intruded bioturbated clayey silt, where it terminated 3 m above the water level or 1.5 m below the surface. The upper 1 m of the dike was slightly iron-stained. On the basis of little to no weathering of the smallest dike, it probably formed during the A.D. 1811-1812 New Madrid event. The weathering characteristics of the other two dikes are more similar to the dike at SFR52 than the very weathered dike at SFR45 and therefore is interpreted to have formed during the A.D. 1450 event.

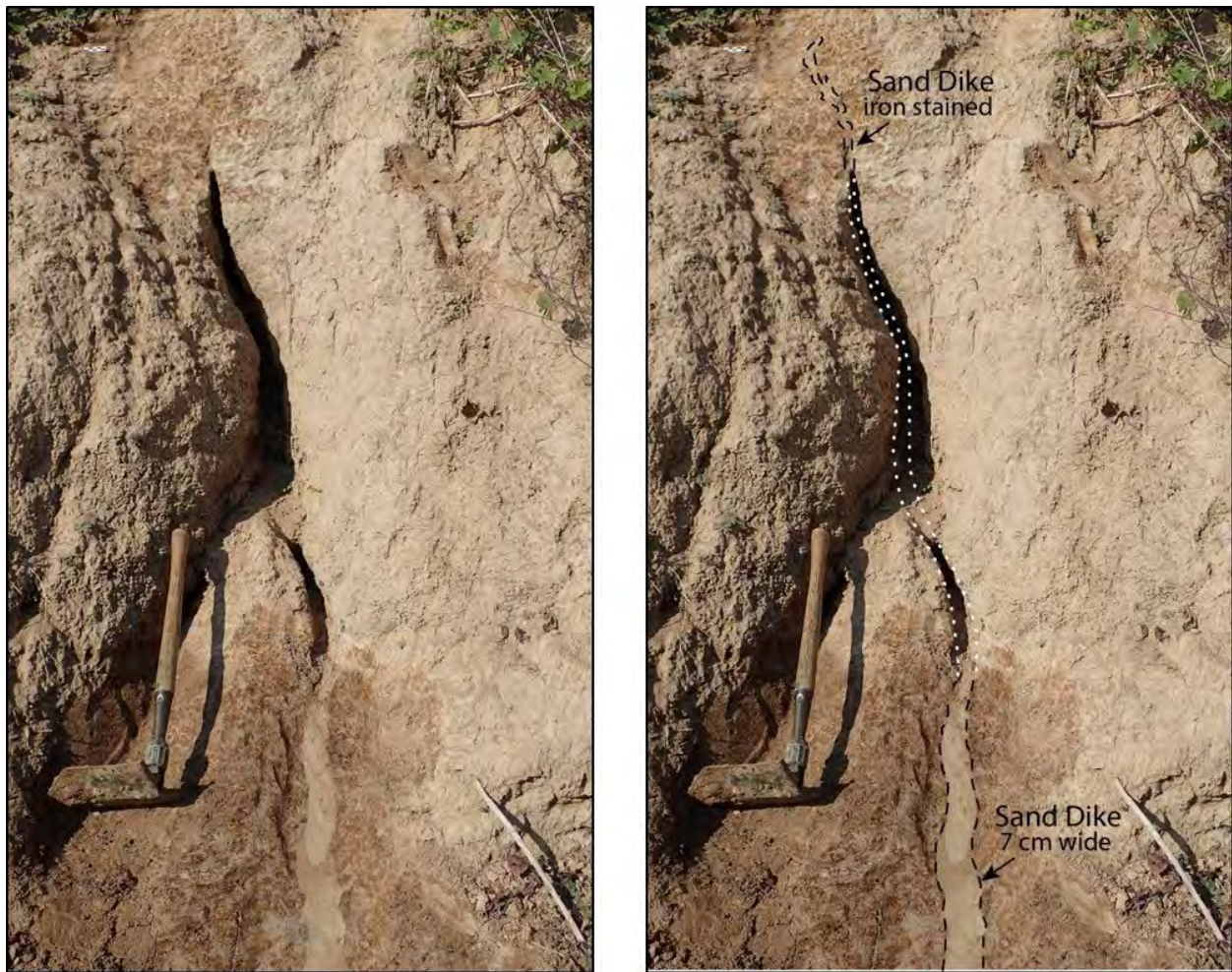


Figure 4-48 Photographs (left - unannotated; right - annotated) showing weathered sand dikes at SFR52. Dashed and dotted lines represent clear and inferred contacts, respectively. For scale, shovel handle is 25 cm long.

At sites SFR55, two dikes 12 and 8 cm wide, were exposed along a 20-m cutbank. The dikes crosscut weathered and bioturbated sand and overlying gray silt, extended to 2 m and 1.5 m, respectively, above the water level, where they were covered by vegetated sediment (Figure 4-49). The dikes were iron stained and cemented, suggesting that they are prehistoric in age. Across the river at SFR56, there was a 6-cm-wide dike that also crosscut weathered and bioturbated sand and overlying gray silt and may have reached a buried soil developed in the silt. This dike was washed out and the cutbank was too steep climb in order to examine the termination of the dike. These sites warrant further examination when the upper parts of the dikes are more accessible.



Figure 4-49 Photograph showing iron stained and cemented sand dike at SFR55. For scale, the cutbank is about 1.5-1.75 m high.

4.4.4.6 *White River near Oil Trough, Arkansas*

We conducted systematic surveys for liquefaction features along 10.5 km of the White River upstream from the Rt. 122 bridge near Elgin, Arkansas (Figure 4-11, Figure 4-17, and Figure 4-19). This portion of the White River had been searched previously in the late 1990s but at the time the river level was fairly high due to recent rainstorms (Tuttle, 1999). The river was resurveyed in November 2013 when the river level was relatively low. This portion of the river was selected to resurvey because it occurs in the vicinity of the southwest extension of Commerce Geophysical Lineament and not far from the western Reelfoot Rift margin.

The surficial geology along the resurveyed portions of the White River is mapped as Holocene point-bar deposits inset in Late Pleistocene (Early Wisconsin) valley train (level 2) (Saucier, 1994; Figure 4-21). During the survey, there were very good to excellent exposures provided by 4.0-5.5 m high cutbanks in most river bends. Sediment exposed in the cutbanks was typically silt with one or two buried soils underlain by interbedded silt and iron stained sand followed by cross-

bedded sand that coarsened downward to pebbly sand (Figure 4-50). The transition to pebbly sand usually occurred below the water level but was observed at the base of the cutbank at a few sites. Previously, radiocarbon dating of charcoal (BA-86196) collected from the lower of two buried soils within silt at WR1, located upstream from Oil Trough, indicated the silt in which two soils had developed was deposited during the past 600 years. In a few locations, where abandoned tributaries intersected the course of the river, depositional units dipped towards the abandoned tributary and layered silt and sand was deposited above the silt. In addition, there was one 5.0-5.5 m high exposure of silt loam developed in reddish weathered silt. The more weathered sediment exposed in the higher cutbanks is likely Late Pleistocene in age, whereas the less weathered sediment exposed in the lower cutbanks is probably Late Pleistocene in age.



Figure 4-50 Photograph of exposure along the White River near Oil Trough. At this site, recent silt overlies buried soil developed in silt underlain by interbedded silt and sand. No liquefaction feature was found at this or other sites despite conducive sedimentological conditions and very good to excellent exposure. For scale, the cutbank is about 4 m high.

At one site upstream from Oil Trough, silt loam was underlain by interbedded silt and sand to the base of the cutbank. Interbedded silt and sand continued for at least another 1.5 m below the cutbank as determined with a soil probe. Radiocarbon dating was performed on a sample of leaf mat (WR103-L1) collected 25 cm above the water level from a silt layer. It yielded a date of A.D. 1680-1760, 1770-1780, 1800-1940, post 1950 (270-190, 180-170, 150-10, post 0 yr B.P.) (Table 4-14). This date provides an age estimate for the layered silt and sand, indicating that it was deposited in the past 350 years.

The sedimentological conditions, including interbedded silt and sand and fine-grained abandoned channel deposits inset in coarse-grained channel deposits, were conducive to the formation of earthquake-induced liquefaction features. However, no liquefaction features were found along this resurveyed section of the river. The large, meandering White River is actively eroding and depositing sediment along its course. Much of the sediment exposed in the river cutbanks is fairly young, perhaps less than 1000 years old; but old enough to record the New Madrid earthquakes of A.D. 1811-1812 and A.D. 1450. The apparent absence of liquefaction features, even soft-sediment deformation structures, suggests that ground shaking during these events was not strong enough (generally MMI < VIII) in this area to induce liquefaction. Given the apparent young age of much of the exposed sediment, it is unlikely that large earthquakes generated prior to A.D. 1000 would be recorded in the White River sediment.

Table 4-14 Radiocarbon Dating Results for White River Sites

Sample # Lab #	¹³ C/ ¹² C Ratio	Radiocarbon Age Yr B.P. ¹	Calibrated Radiocarbon Age Yr B.P. ²	Calibrated Calendar Date A.D./B.C. ²	Sample Description
WR103-L1 Beta- 368233	-30.2	110 ± 30	270-190 180-170 150-10 Post 0	AD 1680-1760 AD 1770-1780 AD 1800-1940 AD Post 1950	Leaf mat 3.75 m BTC & 25 cm AWL from layered silt and sand deposit
WR104-L1 Beta- 368234	-30.8	1960 ± 30	1990-1960 1950-1860	BC 40-10 0-AD 80	Leaf mat and stems 3.75 m BTC & 25 cm AWL from silt layer within cross-bedded sand
WR107-L1 Beta- 368235	-29.9	740 ± 30	720 710-660	AD 1230 AD 1240-1290	Leaf mat and stems at water level, ~4 m BTC, from organic layer within interbedded sand and silt deposit

¹ Conventional radiocarbon ages in years B.P. or before present (1950) determined by Beta Analytic, Inc. Errors represent 1 standard deviation statistics or 68% probability.

² Calibrated age ranges as determined by Beta Analytic, Inc., using the Pretoria procedure (Talma and Vogel, 1993; Vogel et al., 1993). Ranges represent 2 standard deviation statistics or 95% probability.

4.4.4.7 White River near Clarendon, Arkansas

We surveyed 10 km of the White River upstream from the Rt 79 bridge in Clarendon, Arkansas (Figure 4-11, Figure 4-17, and Figure 4-19). This portion of the White River had never before been searched for liquefaction features. It was selected because it occurs about 45-50 km west of the very large sand blows near Marianna, Arkansas.

The surficial geology along the White River near Clarendon is mapped as Holocene point-bar and backswamp deposits inset in Late Pleistocene (Late Wisconsin) valley train deposits, Late Pleistocene (Early Wisconsin) valley train deposits (level 2), and other Pleistocene fluvial deposits, mostly natural levee and backswamp (Saucier, 1994; Figure 4-27).

During the survey, there was almost continuous exposure provided by 4.0-4.5 m high cutbanks on one side of the river or the other. Overall, the exposure was excellent. Sediment exposed in the cutbanks was typically recent layered silt overlying a buried soil developed in mottled silt or clayey

silt underlain by interbedded silt and cross-bedded sand (Figure 4-51). The contact of interbedded silt and cross-bedded sand occurred within 1 m above or below the water level.

At site WR105, one possible small (1-2 cm) dike was observed originating in cross-bedded sand and intruding the overlying clayey silt (Figure 4-52). However, the sediment looked like it might have been disturbed leading to some uncertainty about the origin of the feature. Radiocarbon dating was performed on a sample of leaf mat and stems (WR104-L1) collected 25 cm above the water level from a silt layer within cross-bedded sand at site WR104 about 230 m from WR105. The sample yielded a date of B.C. 40-10, 0-A.D. 80 (1990-1960, 1950-1860 yr B.P.) (Table 4-14). This date provides an age estimate for interbedded silt and cross-bedded sand and a maximum constraining age of B.C. 40 (or 1990 yr B.P.) for the possible dike.



Figure 4-51 Photograph of exposure along the White River near Clarendon. At this site, silt is underlain by interbedded silt and cross-bedded sand. For scale, shovel handle is 20 cm long.

The sedimentological conditions were conducive to the formation of earthquake-induced liquefaction features. Much of the sediment exposed in its cutbanks is likely to be 2000 years old or less. The sediment is old enough to record the New Madrid earthquakes of A.D. 1811-1812, A.D. 1450, and A.D. 900. Perhaps the small dike formed during one of these events. The sediments exposed along this part of the river were too young to record the very large Marianna sand blows.

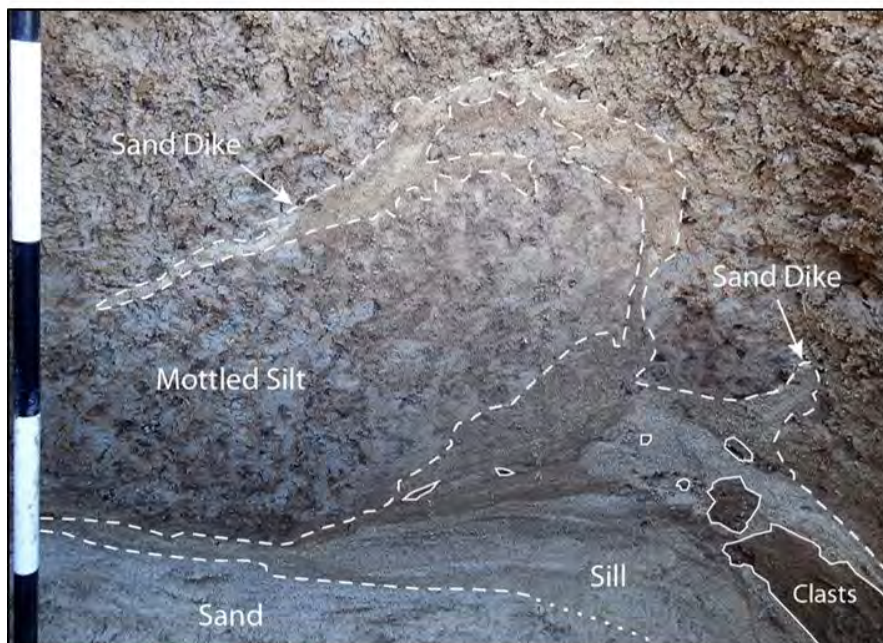


Figure 4-52 Photographs (left - unannotated; right - annotated) of possible sand dikes originating in cross-bedded sand and intruding overlying mottled silt at WR105. Dashed and dotted lines represent clear and inferred contacts, respectively. Black and white intervals on meter stick represent 10 cm.

4.4.4.8 *White River near St. Charles, Arkansas*

We surveyed another 20 km of the White River upstream from St. Charles, Arkansas (Figure 4-11, Figure 4-17, and Figure 4-19). Like the Clarendon section, this section had not been previously searched. It too was selected because it occurs about 45-50 km but southwest of the Marianna sand blows. In addition, it occurs about 50-80 km north-northeast of the proposed Desha County liquefaction field (Cox et al., 2007).

The surficial geology mapped along this portion of the White River is similar to that mapped along the Clarendon section; Holocene point-bar and backswamp deposits inset in Late Pleistocene (Late Wisconsin) valley train deposits, Late Pleistocene (Early Wisconsin) valley train deposits (level 2), and other Pleistocene fluvial deposits, mostly natural levee and backswamp (Saucier, 1994; Figure 4-27).

Along this portion of the river, as well there was almost continuous exposure provided by 4.0-4.5 m high cutbanks on one side of the river or the other. Overall, the exposure was excellent. Sediment exposed in the cutbanks was typically recent layered silt overlying a buried soil developed in mottled silt that contained large lenses of clayey silt and was underlain by bioturbated and interbedded silt and iron-stained sand. The interbedded silt and sand became sandier with depth and the sand became cross-bedded. The contact of interbedded silt and cross-bedded sand occurred within 1-3 m above or below the water level. Radiocarbon dating was performed on a sample of leaf mat and stems (WR107-L1) collected at the water level from an organic layer within cross-bedded sand and silt. The sample yielded a date of A.D. 1230, 1240-1290 (720, 710-660 yr B.P.) (Table 4-14). This date provides an age estimate for interbedded silt and sand and indicates that much of the sediment observed along this portion of the river, and beneath the 4-m high terrace, was deposited during the past 800 years. In places where the river intercepted abandoned channels or tributaries, cutbanks were only 3 m high and exposed layered silt that would have been young as well. No liquefaction feature was found in the Late Holocene deposits.

There were also several 10-12 m high cutbanks exposing very weathered and presumably Late Pleistocene deposits. At one location near St. Charles, the high cutbank exposed very weathered silt underlain by layered silt followed by mottled silt. At another location near Crockett's Bluff, loess underlain by weathered silt was followed by a paleosol developed in interbedded sand and silt (Figure 4-53).

At WR109 near Crockett's Bluff, pseudonodules had formed about 6 m above the water layer in interbedded very fine sand and very fine sandy silt (Figure 4-54). Pseudonodules are thought to form close to the sediment-water interface or soon after deposition. Therefore, if the pseudonodules are related to earthquake-induced liquefaction, they likely formed during the Late Pleistocene. These features might have formed during a Late Pleistocene Marianna earthquake; however, this interpretation is tenuous but could be strengthened if additional features were found in the area and their ages better constrained. These features are probably much older than the proposed paleoearthquakes (roughly 1000 and 6000 yr ago) in Desha County.



Figure 4-53 Photograph of Late Pleistocene sediment exposed at WR109. Pseudonodules shown in Figure 4-54 occur within interbedded sand and silt below the overhang (white arrow points to layer with pseudonodules). Portion of cutbank shown in photograph is 4.5-5.0 m high.



Figure 4-54 Photograph of pseudonodules in Late Pleistocene sediment exposed at WR109. For scale, white interval of meter stick is 10 cm long.

4.4.5 Site Investigations

Detailed investigations were conducted at five liquefaction sites that held promise for constraining the timing and locations of paleoearthquakes in areas where additional information would help to reduce uncertainties in estimates of location, magnitude, and recurrence of large earthquakes in the New Madrid region (Figure 4-18). The study sites - Garner, Caraway, Wildy, Stiles, and Pritchett - were selected because they occur in areas with little to no previous paleoliquefaction data, on Late Pleistocene landforms that have the potential to contain a record of pre-A.D. 800 earthquakes, and for several sites, because they occur in the vicinity of possible earthquake sources (Table 4-15). The presence of sand blows was suggested by interpretation of aerial photographs and/or satellite imagery and by observations made during site visits.

Table 4-15 Site Investigations (see Figure 4-56 for site locations)

Site	Trench	Latitude & Longitude (Degrees)	Reasons for Selection
Faulkner	1 & 2 3	35.7383 -90.3017 35.7372 -90.3033	Geographical gap in paleoliquefaction data; Late Pleistocene valley-train deposits (level 2); surface scatters of sand-tempered sherds (Woodland period) and lithics in vicinity of sand blow; difference in characteristics of sand blows on Google earth (GE) imagery suggests two generations of features
Wildy	1 & 2	35.8508 -90.2479	Geographical gap in paleoliquefaction data; Late Pleistocene valley-train deposits (level 2); surface scatter of sand-tempered sherds (Woodland) and lithics in vicinity of sand blow
Garner	1 2	35.9543 -90.4725 35.9542 -90.4728	Geographical gap in paleoliquefaction data; Late Pleistocene valley-train deposits (level 3); surface scatter of lithics and several projectile points (Early Archaic, Late Archaic, Late Archaic-Early Woodland) above sand blow; other archaeological sites in vicinity with Dalton, Early and Late Archaic components; sand dikes observed in cutbank of nearby Lighthouse Ditch; proximity to the western margin of the Reelfoot Rift
Stiles	1 2 3	35.9875 -89.9350 35.9876 -89.9354 35.9857 -89.9349	Late Pleistocene valley-train deposits (level 1); different orientations of sand blows on GE imagery; possibly two generations of features; absence of cultural artifacts
Pritchett	1 2 3 4	36.0461 -89.5911 36.0461 -89.5906 36.0462 -89.5896 36.0439 -89.5870	Late Pleistocene valley-train deposits (level 1); long linear sand blows along northeastern trend of large dike previously observed in cutbank of Obion River suggesting possible surface expression of active fault

Initially, sites were sought where sand blows occur in association with intact archaeological horizons, since past studies had had good success with constraining the age of sand blows by dating abundant organic materials from these horizons (e.g., Tuttle et al., 1999 and 2005). In particular, sand blows were sought that occurred with pre-Mississippian sites (Table 4-16). However, this approach was somewhat altered after the Arkansas State Historic Preservation Office requested that the NRC implement a process according to section 106 of the National Historic Preservation Act. This process was developed after the investigations at the Faulkner and Wildy sites in October-November 2011 and followed during the investigations of the Garner and Stiles sites in 2012-2015 and the Pritchett site in 2015-2016.

Table 4-16 Cultural Periods, Time Spans, and Associated Diagnostic Artifacts (Modified from Lafferty, 1996; Tuttle et al., 1998)

Cultural Periods	Years (A.D./ B.C.)	Diagnostic Artifacts
Historic	A.D. 1673- present	Iron, glass, glazed pottery, plastic
Late Mississippian	A.D. 1400-1673	Shell-tempered pottery - Parkin Punctate, Campbell Applique, Matthews Incised, Bell Plain, and Memphis rim mode; Nodena points
Middle Mississippian	A.D.1000-1400	Shell-tempered pottery - Parkin Punctate and Old Town Red (exterior slipped); Madison points
Early Mississippian	A.D. 800-1000	Pottery transition - shell-tempered pottery, Varney Red Filmed pottery (interior slipped) and mixed temper wares; Madison points
Late Woodland	A.D. 400-1000	Cordmarked and plain, sand- (Barnes) and grog- (Baytown, Mulberry Creek) tempered pottery; Madison points and Table Rock stemmed points
Middle Woodland	200 B.C.-A.D. 400	Sand- and grog-tempered pottery; dentate, stamped, and fabric-marked pottery
Early Woodland	500-200 B.C.	Punctated pottery; baked clay objects
Late Archaic	3000-500 B.C.	Stemmed projectile points; baked clay objects
Middle Archaic	7000-3000 B.C.	Grooved axes
Early Archaic	8000-7000 B.C.	Corner-notched projectile points
Dalton	8500-8000 B.C.	Dalton projectile points

As described in more detail in Appendix B, a Section 106 process was developed and implemented that included a two-phased approach: phase 1 site evaluation and excavation plan and a phase 2 excavation and subsurface investigation. Before executing phase 2, State Historic Preservation Offices or Tribal State Historic Preservation Offices must not reject the excavation plan outlined in a phase 1 report. Due to uncertainties related to this process, liquefaction sites were selected that were devoid of archaeological material or where sand blows occurred in association with archaeological sites that were unlikely to qualify for National Register of Historic Places (NRHP) due to site disturbance related to farming practices. Site evaluation reports prepared for the Garner, Stiles, and Pritchett sites were submitted to the U.S. Nuclear Regulatory Commission (Tuttle et al., 2014 and 2016).

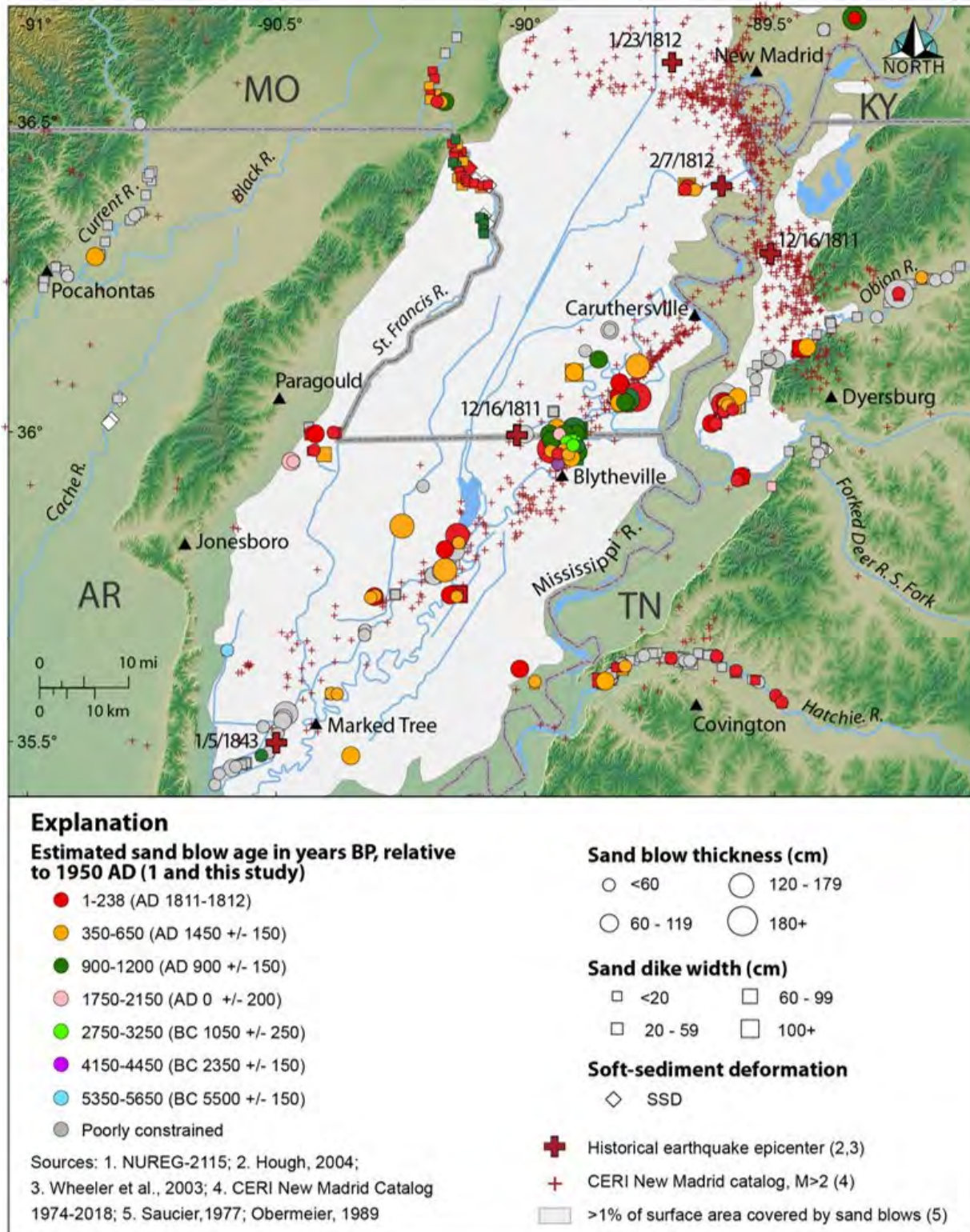


Figure 4-55 Enlargement of portion of shaded relief map of NMSZ and surrounding region, showing updated liquefaction data based on findings during this study, seismicity (red crosses), and previously recognized liquefaction field (white area) (modified from NUREG-2115). Area of enlargement shown on Figure 4-24.

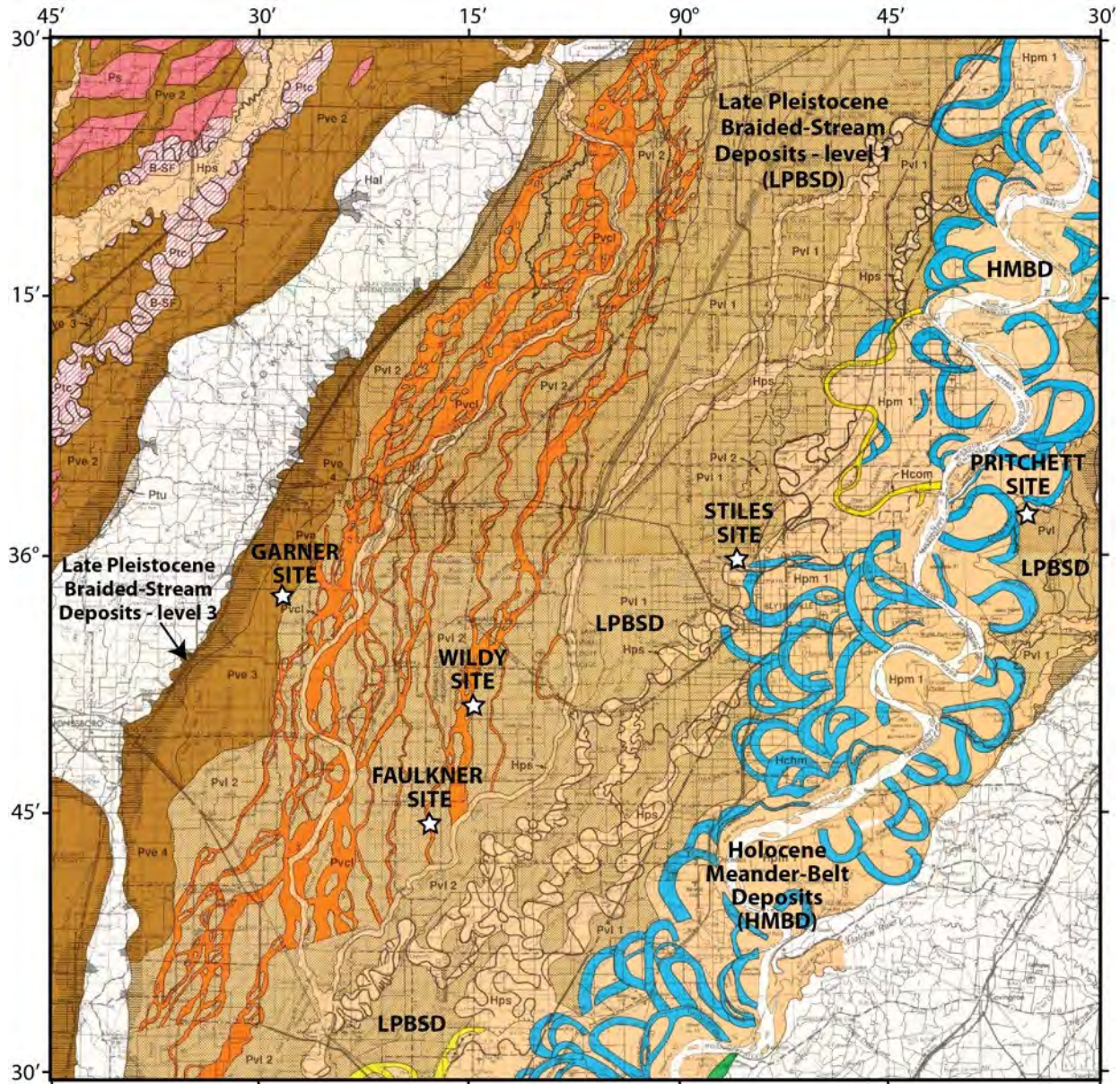


Figure 4-56 Map of Quaternary deposits of portion of study area showing locations of selected study sites (modified from Saucier, 1994; plates 5 and 6). Faulkner and Wildy sites in AR, are located in Late Pleistocene valley-train deposits (light-brown unit - Pvl level 2; orange unit - Pvc1 for relict channel deposits) of Mississippi River. Garner site in AR is located in Late Pleistocene valley-train deposits (brown unit - Pve level 3) just west of boundary with somewhat younger and lower terrace of Late Pleistocene valley-train deposits (light-brown unit - Pvl level 2; orange unit - Pvc1 for relict channels). Stiles site in AR and Pritchett site in TN, are in located in Late Pleistocene valley-train deposits (light-brown unit - Pvl level 1) of Mississippi River but close to boundary with Holocene meander-belt deposits of Mississippi River (tan unit - Hpm 1 for point bar deposits; blue unit - Hchm for abandoned channels).

4.4.5.1 *Faulkner (aka Caraway) Site*

The Faulkner site is located between the southern branch of the NMSZ and the western margin of the Reelfoot Rift and between the Little River and St. Francis River (Figure 4-18 and Figure 4-19). The site is located within the liquefaction field (1% of the surface area covered with sand blows) mapped on the basis of aerial photograph interpretation (Obermeier, 1989) and about 3 km west of the Little River Ditch, where many sand blows have been found during previous studies (Tuttle et al., 2002 and 2005; Tuttle and Hartleb, 2012). The Faulkner site occurs in Late Pleistocene valley-train deposits (Pv1 level 2) and straddles a relict channel deposit (Pvcl) of the Mississippi River (Figure 4-56; Saucier, 1994). Given the age of the deposits, the site has the potential to contain a record of known Late Holocene New Madrid events as well as earlier paleoearthquakes. Prior to this NRC-funded project, no paleoliquefaction features had been studied in the area between the Little and St. Francis Rivers.

4.4.5.1.1 *Reconnaissance*

In 2011, the U.S. Army Corps of Engineers provided information about recently cleaned drainage ditches in the New Madrid region, including several ditches in the area between Little River and Crowley's Ridge to the west. Satellite imagery was reviewed to identify possible sand blows that may have been exposed in the recently cleaned ditches. Reconnaissance for sand dikes and sand blows was performed along selected portions of cleaned ditches. During reconnaissance, Mr. Faulkner, a property owner and farmer in the Caraway area, encouraged us to check out sandy patches in one of his fields southeast of the town of Caraway, where he and others had found Native American artifacts. Cultural materials can be useful for getting an idea of the age of land surfaces and any sand blows that may be present.

On Google Earth satellite imagery of the Faulkner site, light-colored patches interpreted to be sand blows occur along the margins of and within a northwest-oriented dark-colored swath that is likely to be the relict, or abandoned, channel deposit mapped by Saucier (1994; Figure 4-57). There appear to be two types of sand blows that vary from one another in shape, size, and reflectance. Sand blows that occur along the margins of the abandoned channel deposit tend to be linear in plan view, relatively small, and faint in reflectance whereas sand blows that occur within the abandoned channel deposit or cross the channel margin appear to be elliptical in plan view, relatively large, and bright in reflectance. The differences between the two-types of sand blows suggest that they formed at different times, with the brighter sand blows likely to be younger than the fainter sand blows.

In October 2011, the Faulkner site was visited to check for the presence of sand blows and associated cultural materials. Several soil pits were dug along two transects (along which Trenches 1 and 3 were later excavated) crossing light-colored patches on the northeast and southwest sides of the field (Figure 4-58). The soil pits revealed that the light-colored patches were underlain by sandy sediment with silt clasts, lignite and flow structure, all characteristics of sand blows, and the dark-colored swath interpreted to be an abandoned channel deposit was underlain by clayey sediment. Iron staining of the sandy sediment was more pronounced along the northeastern transect and the western end of the southwestern transect than along most of the southwestern transect where there was little to no iron staining. Differences in iron staining may be related to the amount of time sediment has been exposed to weathering processes. Therefore, these initial observations suggested that the more weathered linear sand blows along the northeastern and southwestern margins of the abandoned channel deposit may be older than the less weathered elliptical sand blow that crosses the southwestern margin of the abandoned channel fill. In addition, sand-tempered potsherds of the Woodland cultural period (Table 4-16)

were found in the northeast part of the field near a linear sand blow along the eastern margin of the abandoned channel deposit (Figure 4-58). Given the Late Pleistocene age of the sediment, the likely presence of one or two generations of sand blows, and the association of Woodland artifacts with the sand blows, the Faulkner site was selected for further investigation.

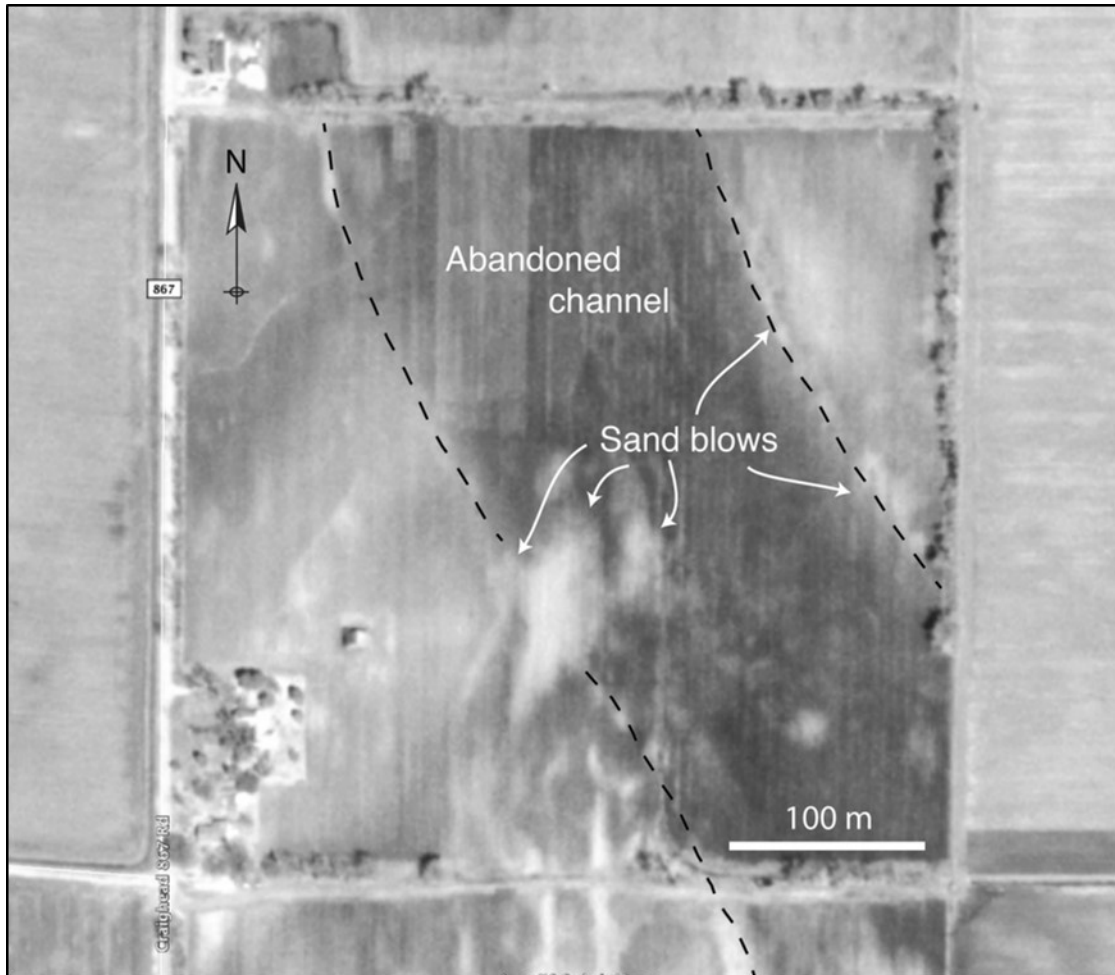


Figure 4-57 GE image of the Faulkner site, showing dark swath related to abandoned-channel deposit. Light-colored patches along the margins as well as within channel deposit are sand blows. Image acquired by US Geological Survey in April 2001.

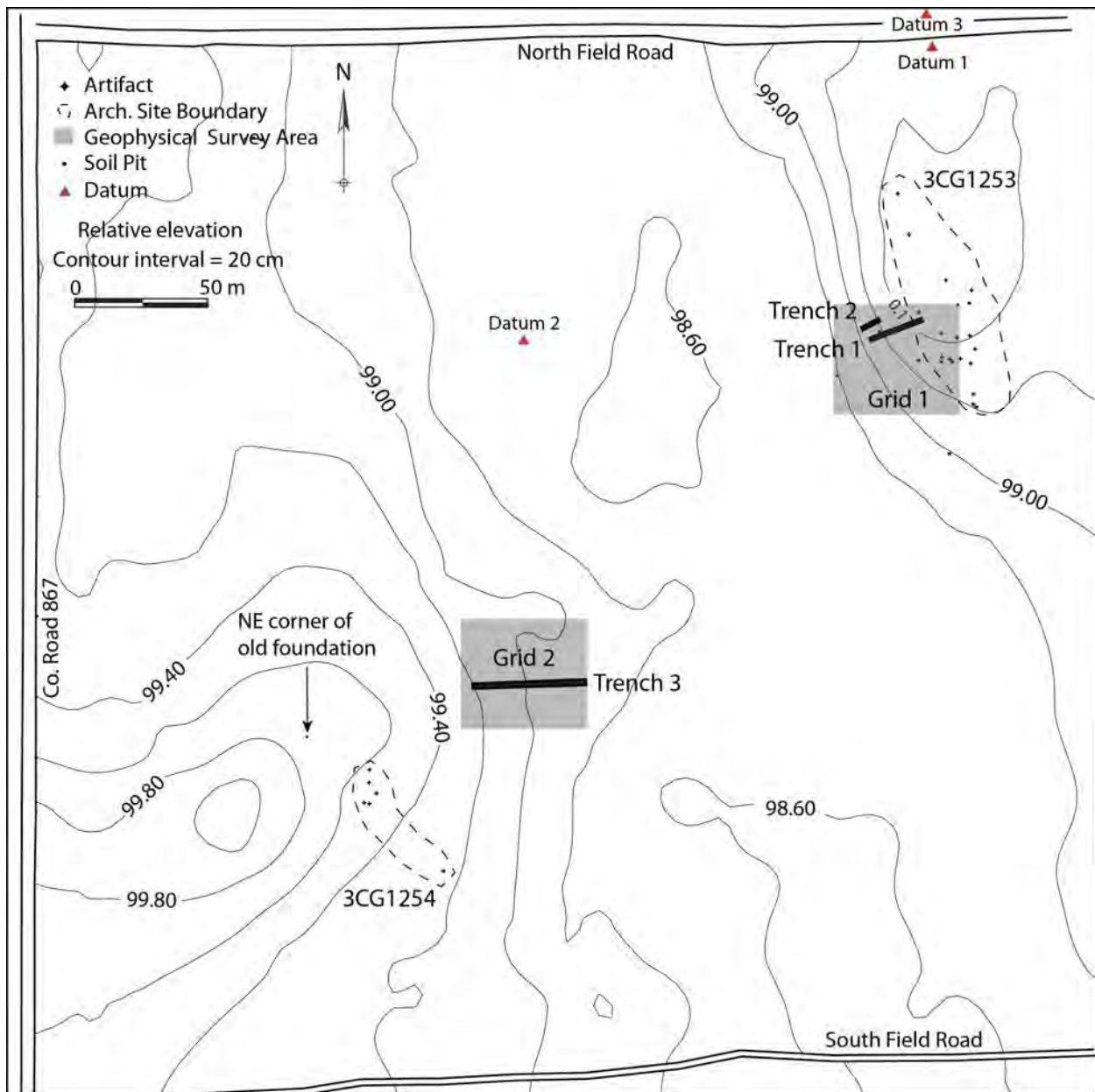


Figure 4-58 Topographic map of Faulkner site, showing locations of point plotted artifacts, archeological site boundaries, geophysical grids, and paleoseismic trenches.

4.4.5.1.2 *Electrical Resistivity Surveys*

In late October 2011, geophysical surveys using electrical resistance (ER) tomography were conducted at the Faulkner site. Two survey areas were selected on the basis of the interpretation of GE imagery and field inspection of likely sand blows. The locations of the geophysical survey areas are shown on the topographic map made of the site (Figure 4-58). Figure 4-59 shows the layout of two survey grids at the Faulkner site, AR. Each grid consisted of multiple parallel profile lines within a rectangular area. All lines were 46 m in length. Data were collected using an Advanced Geosciences Inc. (AGI) SuperSting resistivity meter, with automatic electrode-switching capability. Each line consisted of 24 electrodes at 2-m spacing. An AGI mixed dipole array

(similar to a conventional dipole-dipole configuration) was chosen for the data acquisition because this array provides optimal resolution for near-surface features and sufficient depth penetration to guide future trench excavations. Measurement errors in all surveys did not exceed 0.2%.

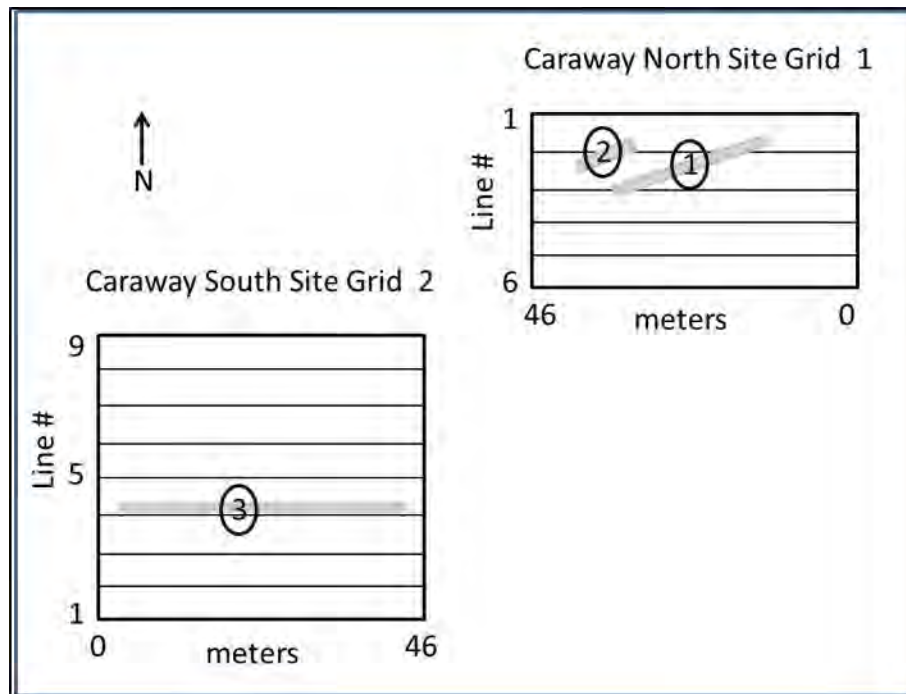


Figure 4-59 Layout of two resistivity survey grids at Faulkner (aka Caraway) site, AR. Grids consisted of multiple parallel profile lines, spaced at 5 m apart. Each line consisted of 24 electrodes at 2-m spacing. Distances indicate position along profile from first electrode. Numbers in circles indicate locations of paleoseismic trenches.

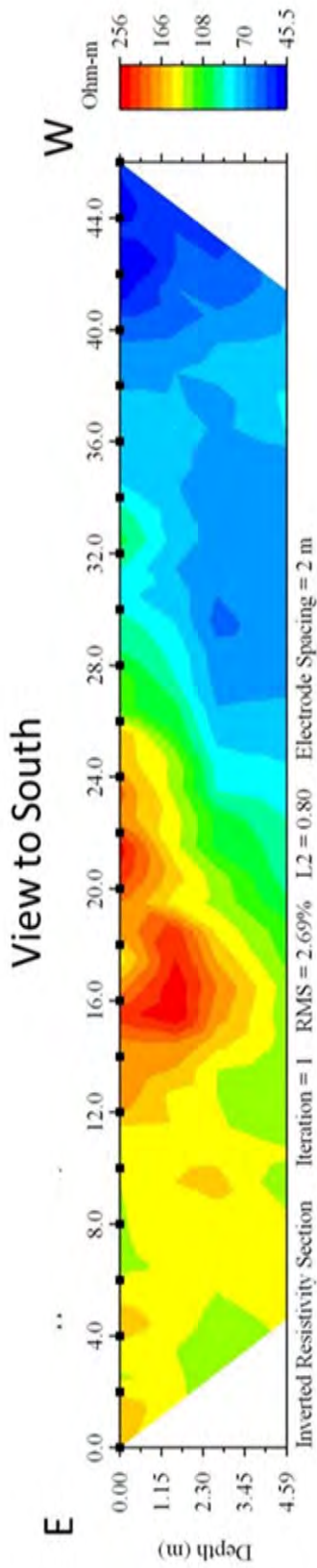
Raw data observations of apparent resistivity from all profile measurements were processed using AGI's 2-D EarthImager inversion software to produce cross-sections of the true subsurface resistivity distribution. The model is validated by using a forward-modeling technique to predict the apparent resistivity distribution if one assumes that the calculated true resistivity distribution in the subsurface model is correct. Statistical measures of the solution are thus obtained. The maximum RMS data error in the inversions was less than 5%.

4.4.5.1.3 *Electrical Resistivity Results*

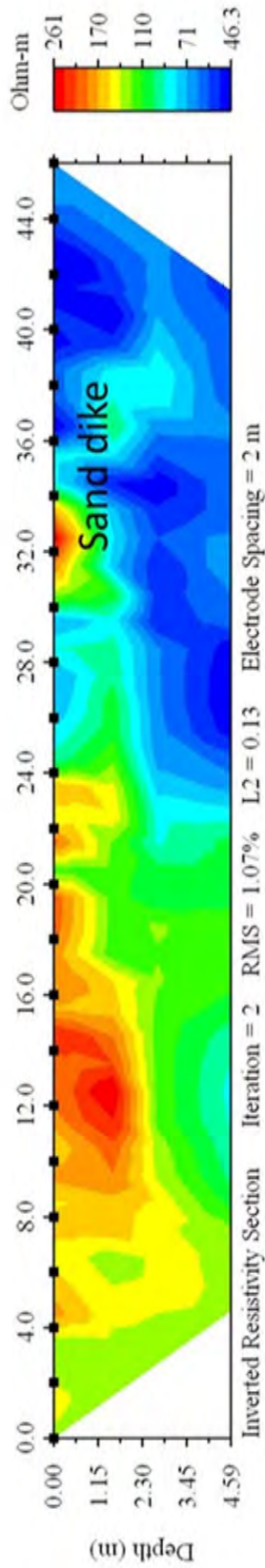
Figure 4-60 and Figure 4-61 contain composite images, each showing three profile lines for survey Grid 1 at the Faulkner site. Grid 1 consisted of six parallel profile lines, shown with views towards the south (east to left side of profile). The line numbers increase to the south. Hot colors (red-orange) represent areas of sediment with relatively high resistivity (usually indicating sandy or silty sand sediment that can be associated with fluvial features, such as channel deposits, or liquefaction features, such as sand blows and sand dikes). Cool colors indicate subsurface areas that are relatively more conductive, usually containing finer-grained sediment with varying amounts of clay. These areas can be associated with fluvial features such as channel fill and overbank deposits. In Figure 4-60, a large area of high resistivity (~ 0 to 26 m along the profile) is evident on the eastern side of Line 1. This area corresponds with a large sand deposit on the

surface that extends southward to Line 4 and beyond (Figure 4-61). Two isolated areas of high resistivity are noted on Line 2 (at ~ 32 m) and Line 3 (at ~28 to 30 m) (Figure 4-60). These areas connect to a deeper deposit (moderately high resistivity shown in green) within a more conductive area (blue) that is associated with finer-grained host sediments. Interpolating between the small, high-resistivity areas seen in Lines 2 and 3, we interpret this deposit as a narrow sand-filled fissure or dike that trends northwest-southeast. On Line 5, the large sand deposit seen on the east side of Line 1 is replaced by more conductive (finer-grained) sediment below 2.5 m depth. This is consistent with the southeast trend of the sand deposit observed on the surface in aerial photos. A small sandy patch interpreted as a sand-filled feeder dike is seen on Lines 5 and 6 at approximately 16 to 24 m along the geophysical profile.

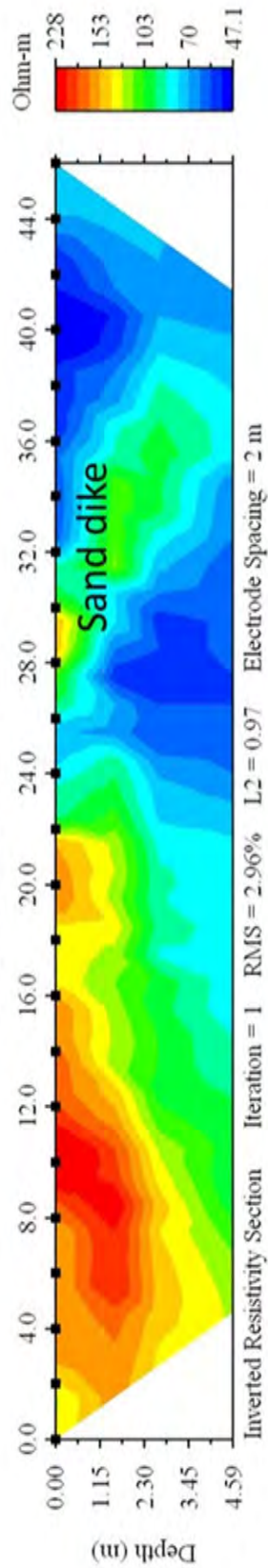
Grid 2 at the Faulkner site consisted of nine parallel profiles shown in Figure 4-62 to Figure 4-64. Line 9 is located farthest to the north, and cross-sections are north-facing (east to the right side of the profiles). Line 1 shows the presence of two areas with high resistivity (interpreted as sand deposits), a large one on the western side of the profile and a small one on the easternmost end (~ 40 to 46 m in the profile). Based on its size and characteristics, the large deposit may be a fluvial feature. On Lines 2, 3, 4, 5, and 6, a small high-resistivity area (between 8 m and 12 m) that extends upward from the large sandy deposit to the surface is interpreted to be a sand dike. From the intersection of the dike with the surface, an area of high resistivity extends eastward, thickening to ~2 m in the center of the cross sections of Lines 4 and 5. This deposit (between 8-30 m on Line 4) is interpreted as a sand blow. In Lines 7 and 8, the sand blow is less pronounced. Towards the eastern end (~ 30 to 48 m) of Line 9, a large area of high resistivity is likely related to another sand blow. Supported by GE imagery and surface observations, this sand blow may intersect with, or be related to, the large sand blow to the southwest.



10282011-Grid 1 Line 1



10282011-Grid 1 Line 2



10282011-Grid 1 Line 3

Figure 4-60 Composite resistivity images of Lines 1, 2 and 3 from Grid 1 at Faulkner site. Note view is to south.

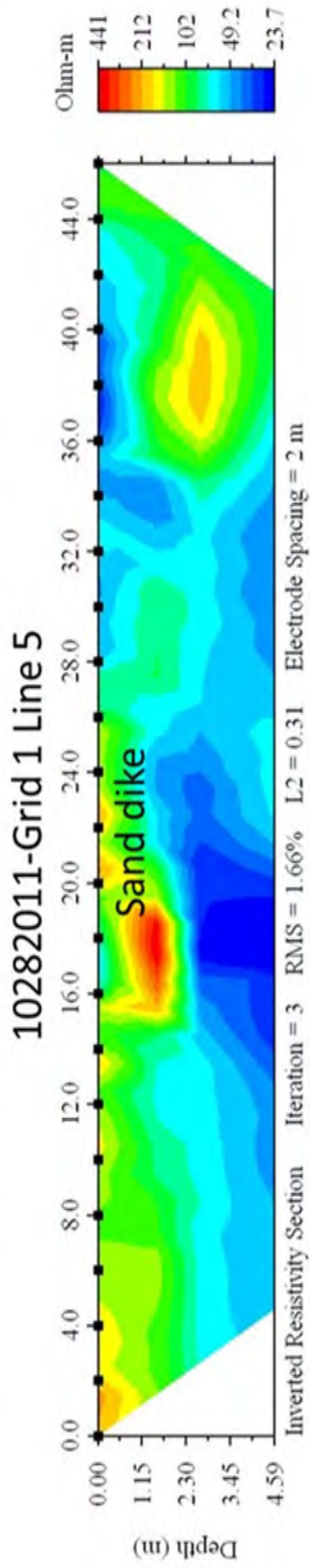
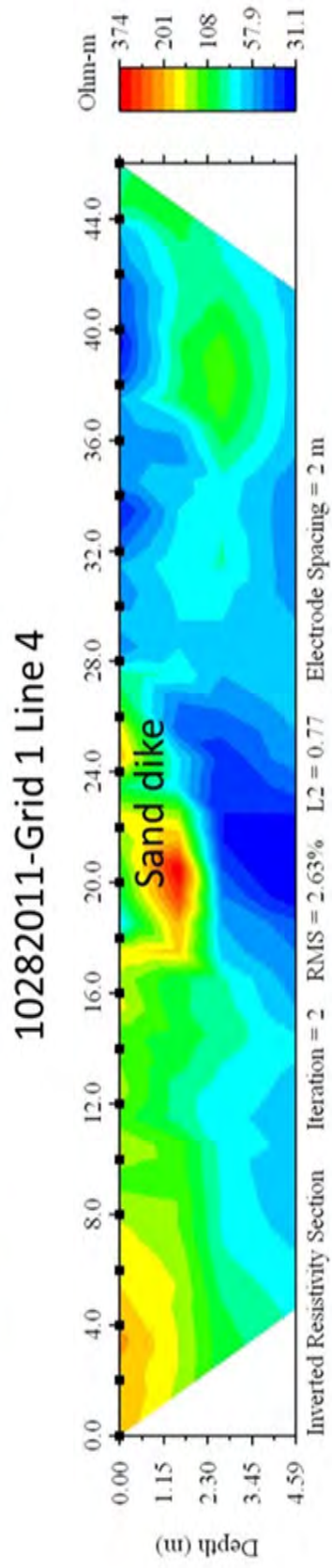
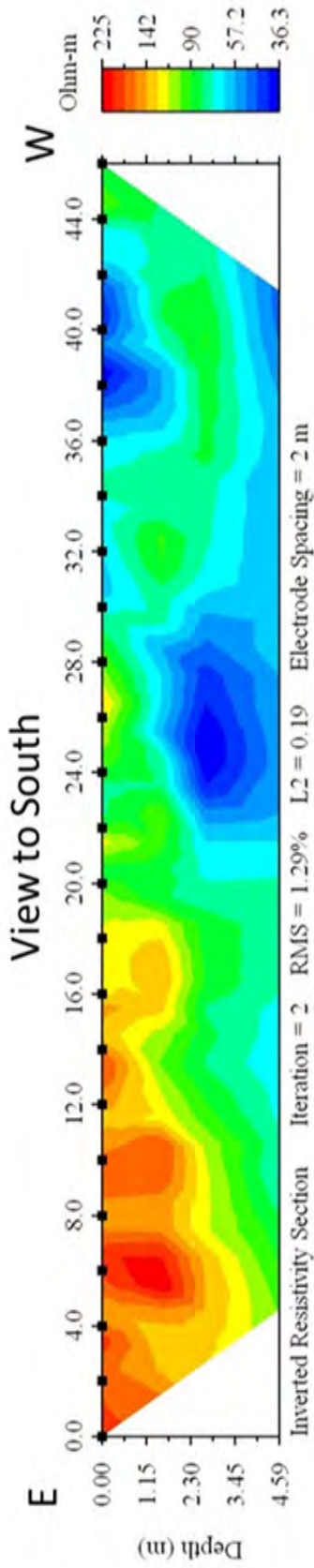


Figure 4-61 Composite resistivity images of Lines 4, 5, and 6 from Grid 1 at Faulkner site. Note view is to the South.

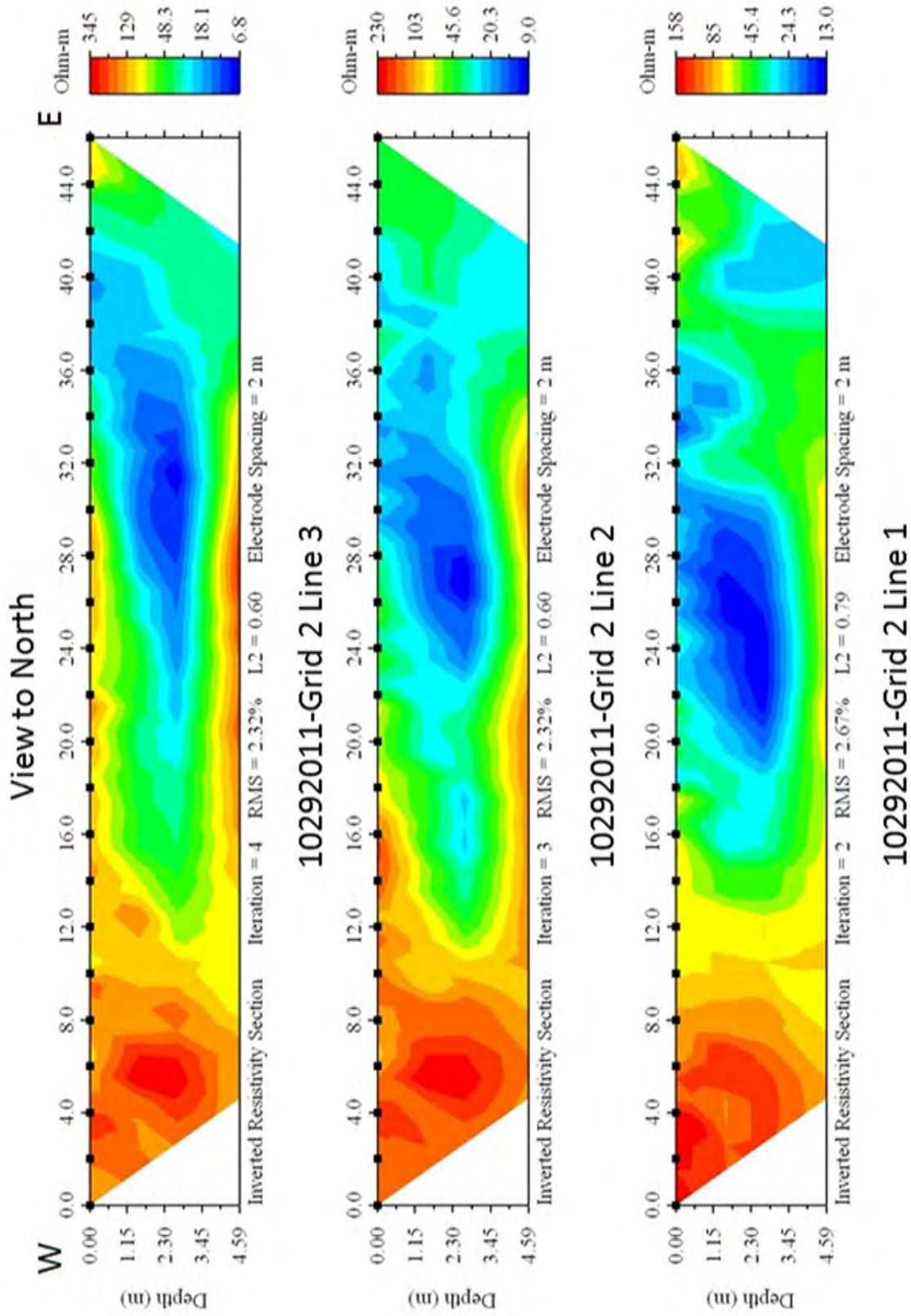


Figure 4-62 Composite Resistivity Images of Lines 1, 2 and 3 from Grid 2 at Faulkner Site

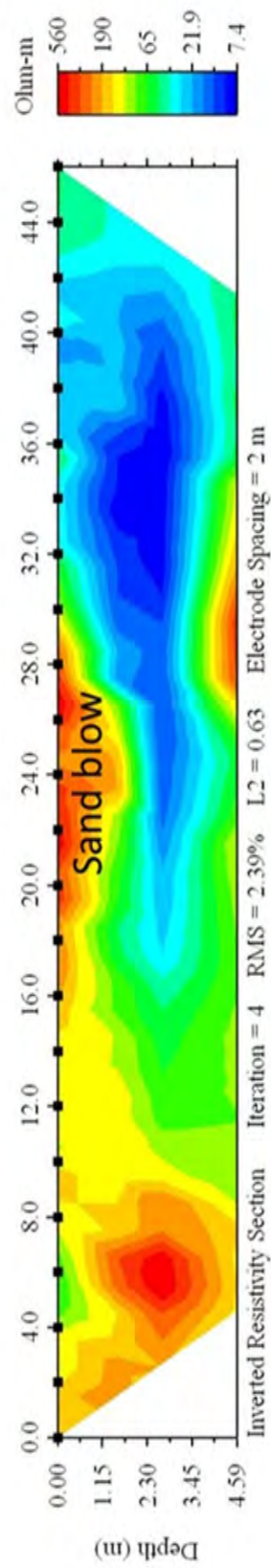
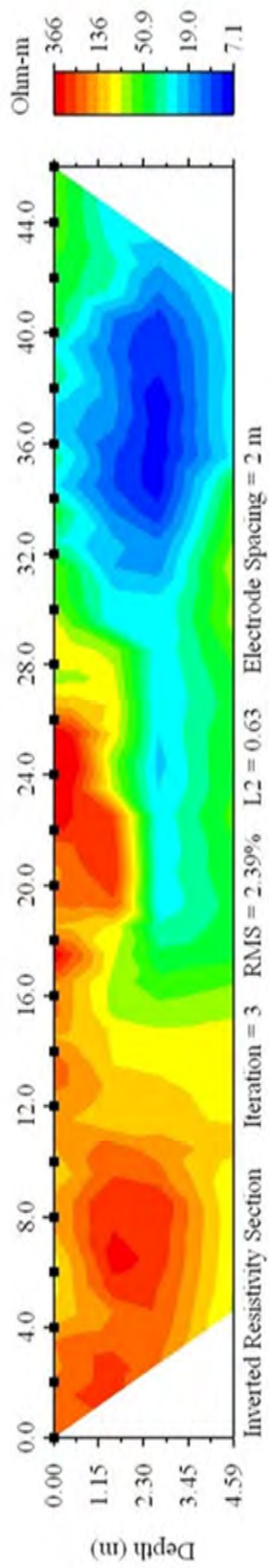
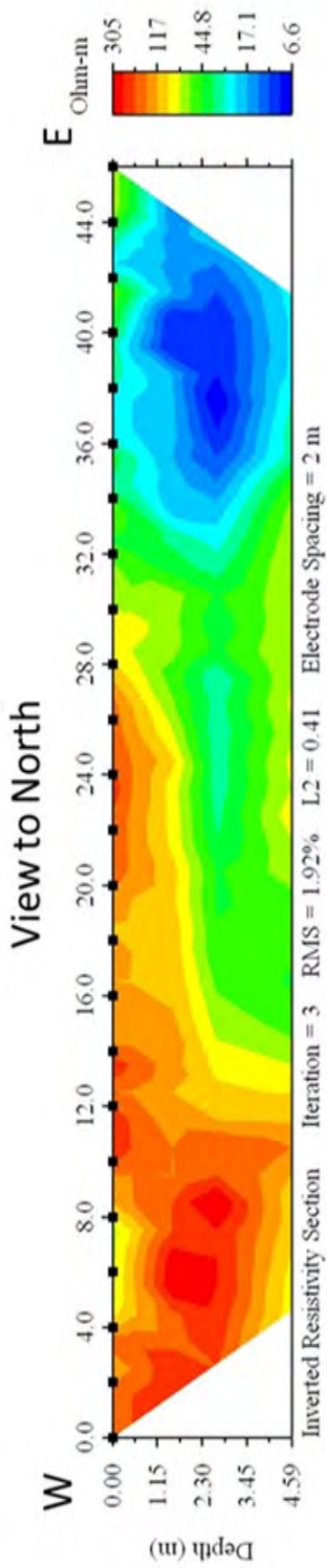
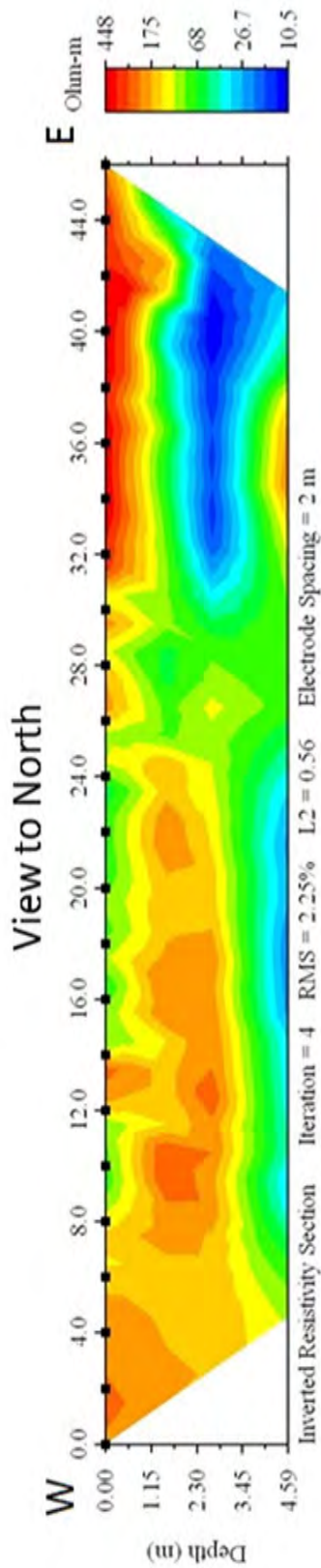
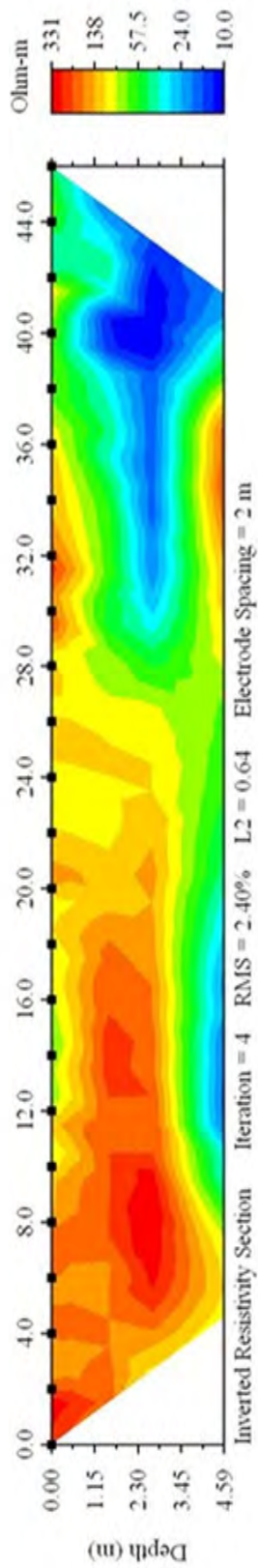


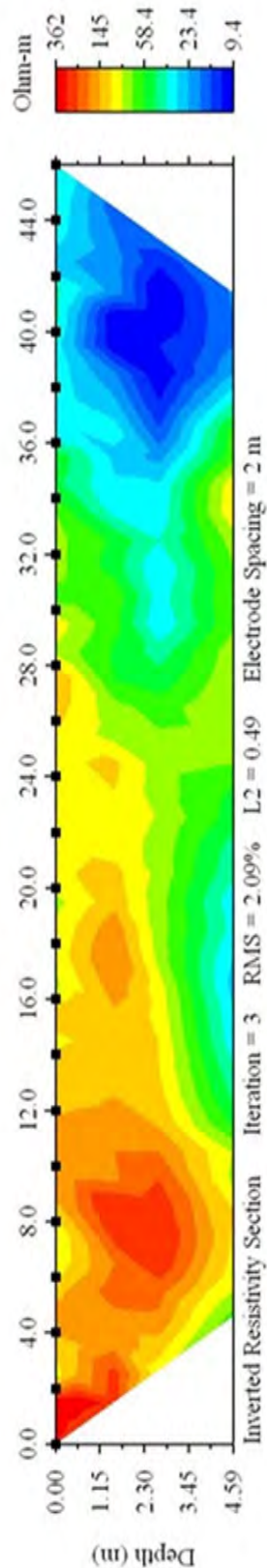
Figure 4-63 Composite Resistivity Images of Lines 4, 5 and 6 from Grid 2 at Faulkner Site



10292011-Grid 2 Line 9



10292011-Grid 2 Line 8



10292011-Grid 2 Line 7

Figure 4-64 Composite Resistivity Images of Lines 7, 8, and 9 from Grid 2 at Faulkner Site

4.4.5.1.4 *Pre-Trenching Archaeological Evaluation*

Also, in October 2011 and prior to trench excavation, a surface survey for cultural material was conducted at the Faulkner site. At the time, the crop had been harvested and visibility of the ground surface was good (50%-75%). Two archeological sites were delineated during the survey, 3CG1253 in the northeastern quadrant of the field and east of the abandoned channel and 3CG1254 in the southwest quadrant of the field and west of the abandoned channel (Figure 4-58).

Archeological site 3CG1253 was a relatively small, low-density surface scatter of artifacts indicative of Woodland Period occupation (Table 4-16). Material collected in the surface collection was limited to lithics and ceramics. These were 10 pieces of chert debitage, 7 small, eroded sand-tempered (Barnes series) sherds and two pieces of other fired clay. Similarly, archeological site 3CG1254 was a small, elongate, low-density surface scatter of artifacts also from the Woodland Period. This site was very limited, as only 3 artifacts were recovered. The artifacts included a small sand-tempered (Barnes series) sherd and two non-diagnostic flakes of Crowley's Ridge gravel.

No subsurface archaeological investigations were conducted within the boundaries of 3CG1253 and 3CG1254. Project archaeologists monitored excavation of nearby paleoseismic trenches described below but no cultural material was found in the trenches.

4.4.5.1.5 *Siting Paleoseismic Trenches*

In late October 2011, three trenches were sited at the Faulkner on the basis of GE imagery, field observations of likely sand blows, geophysical observations of likely sand blows and related sand dikes, and proximity to surface scatter of artifacts (Figure 4-58). The trenches were sited so that they that would expose sand blows and intersect likely feeder dikes. Trenches 1 and 2 were cited in geophysical grid 1 in the northeastern part of the site. Trench 1 was excavated at an oblique angle to and intersecting resistivity Lines 2 and 3. Trench 2 was excavated 5 m northwest of and parallel to Trench 1 and intersected a high-resistivity area interpreted to be a sand dike at 32 m on Line 2. Trench 3 was excavated in geophysical grid 2 in the southwestern part of the site and along resistivity Line 4 to intersect a small high-resistivity area at 8 m interpreted to be a sand dike and another area of high resistivity between 14-30 m interpreted to be a sand blow.

4.4.5.1.6 *Paleoseismic Observations*

In late October-early November 2011, three trenches were excavated at the Faulkner site in the locations described above. All three trenches exposed sand blows and one or more sand dikes and confirmed the interpretations of the geophysical profiles.

Trench 1

Trench 1 was about 14 m long and oriented about N68°E, roughly perpendicular to the northeastern margin of the abandoned channel and the linear light-colored patch interpreted as a sand blow that formed along the channel margin. Much of the trench was about 1 m in depth but was deepened to 1.5 m to examine a sand dike (Figure 4-65).

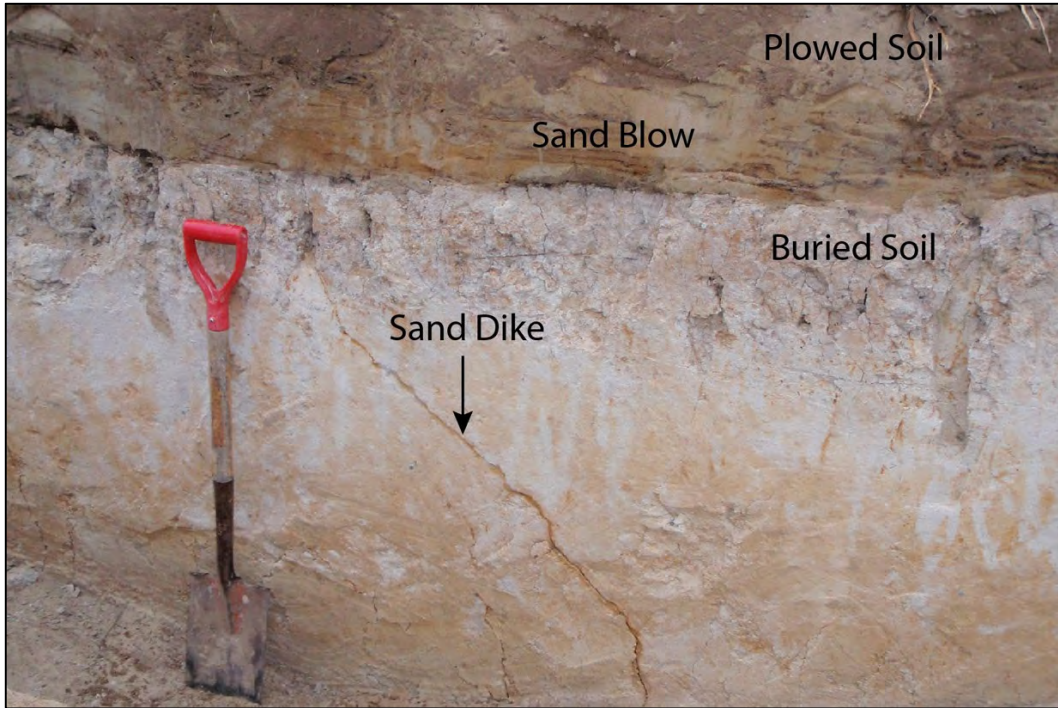


Figure 4-65 Photograph of northwest wall of Trench 1 at Faulkner site, showing small iron-stained sand dike that pinched out at base of brownish soil and iron-stained sand blow above the soil. Dikes connected with base of sand blow in nearby Trench 2. For scale, shovel is 1 m long.

The sand dike, 3 cm wide with clear margins, was observed in the trench floor and walls crosscutting weathered silty clay loam. In one wall, the dike narrowed up section, extended to within 15 cm of the base of the sand blow, and terminated at the base of a brownish soil (Figure 4-65). The entire exposed height (~1 m) of the sand dike was iron stained, suggesting that it is prehistoric in age. In the other wall, the sand dike intersected and intruded a tree-root cast. Overlying the brownish soil, an iron-stained sand deposit, about 3 m across, was thickest above the feeder dike and was characterized by vent structures near the upward projection of the sand dike. The sand deposit corresponds with the linear light-colored patch along the northeastern margin of the abandoned channel and is interpreted to be a sand blow. A sample of charred material (CWY-T1-C1) was collected from the soil adjacent to the dike termination. The sample yielded a two-sigma calibrated date of A.D. 1260-1290 (Table 4-17). Because the sand dike did not extend through the soil and connect with the sand blow above, we excavated Trench 2 about 5 m to the northwest of and roughly parallel to Trench 1. As described below, several sand dikes connected with the sand blow in the cross-section provided by Trench 2. The sand dike and sand blow in Trench 1 were photographed, but the trench was not logged.

Table 4-17 Radiocarbon Dating Results for Faulkner (aka Caraway) Site

Sample # Lab #	¹³ C/ ¹² C Ratio	Radiocarbon Age Yr B.P. ¹	Calibrated Radiocarbon Age Yr B.P. ²	Calibrated Calendar Date A.D./B.C. ²	Sample Description
CWY-T1-C1 BA-330164	-24.3	730 ± 30	690-660	AD 1260-1290	Charred material 15 cm below sand blow and adjacent to dike termination
CWY-T2-C2 BA-315736	-27.0	350 ± 30	500-310	AD 1450-1640	Charred material 5 cm below sand blow from buried soil
CWY-T3- W1 BA-315737	-28.2	90 ± 30	270-220 140-20	AD 1680-1730 AD 1810-1930 AD Post 1950	Wood from outer 1 cm of tree trunk buried by sand blow
CWY-T3- C10 BA-330165	-26.4	210 ± 30	300-270 220-140 20-0+	AD 1650-1680 AD 1730-1810 AD 1930-1950+	Charred material from root cast in sand blow

¹ Conventional radiocarbon ages in years B.P. or before present (1950) determined by Beta Analytic, Inc. Errors represent 1 standard deviation statistics or 68% probability.

² Calibrated age ranges as determined by Beta Analytic, Inc., using the Pretoria procedure (Talma and Vogel, 1993; Vogel et al., 1993). Ranges represent 2 standard deviation statistics or 95% probability.

Trench 2

Trench 2 was 7 m long and orientated N64°E. Much of the Trench was 1.0-1.2 m in depth but was deepened to 1.4 m to further expose sand dikes crosscutting weathered silty clay loam.

Ten sand dikes ranging from 0.25-7 cm wide, and a large sandy structure to which many of the dikes are related, crosscut soil horizons exposed in the southeast wall of the trench (Figure 4-66 and Figure 4-67). The large sandy structure (between meter marks 2.75 and 4 on the trench log) was about 95 cm wide by 50 cm high and was composed of domains of two distinct sediment compositions - fine to very fine sand (L1) and medium to fine sand (L2), both somewhat iron stained and containing clasts of silty clay. The top of the sandy structure coincides with the base of the brownish sandy loam (soil horizon IIA in Figure 4-66). Several dikes connected to the base of the sandy structure were traced several centimeters across the trench floor where they intersected a semi-circular sandy structure. The large sandy structures in the trench wall and trench floor are interpreted as parts of a large tubular structure, possibly a large void formed by a decayed tree root system, filled with intruded sand. Two of the sand dikes in the lower part of the wall were also tubular in morphology and may have been part of the tree root system. Three dikes extended from the top of the large sandy structure through the brownish sandy loam to the base of a sand deposit composed of two major depositional units and interpreted to be a sand blow (Figure 4-66).

A small dike directly above the large sandy structure and composed of fine to very fine sand (L1) was connected to the base of the lower unit of the sand blow (below meter mark 3 on the trench log). The lower unit, also composed of L1 but more iron stained than the dikes below, was about 6 m across and was thickest, 20 cm, above the sand dike where the unit was composed of two to three subunits. The lower unit extended about 2 m to the northeast of the dike and for at least 4 m to the southwest of the dike in the downslope direction. A thin layer of silt drapes the upper

surface of the lower unit towards the northeastern end of the trench. Vent structures in the lower unit likely formed during the second episode of venting during which the upper unit was deposited.

A shallow-dipping dike composed of medium to fine sand (L2) was connected to the base of the upper unit of the sand blow (between meter marks 2 and 2.25). The dike contained clasts of the soil horizons and was characterized by lignite banding and flow lineations. The upper unit of the sand blow, also composed of L2 but more iron stained than its feeder dike, was up to 15 cm thick and more than 7 m across. It extended the entire length of the trench and thinned in both directions away from the dike. Soil clasts were concentrated in the sand blow above the dike.

Radiocarbon dating was performed on a sample (CWY-T2-C2) of charred material collected from the brownish soil 5 cm below the base of the sand blow. The sample yielded a two-sigma calibrated date of A.D. 1450-1640 (Table 4-17). OSL dating was performed on quartz grains extracted from a sediment sample (OSL2) taken of the upper contact of the soil buried by the sand blow (Table 4-18). The OSL age was 3150 ± 300 (or 3390-2790 yr B.P.), considerably older than the two radiocarbon dates.

Table 4-18 Optically Stimulated Luminescence Dating Results for Faulkner Site

Sample Number	Lab	Cosmic Dose Rate (Gy/ka) ¹	Total Dose Rate (Gy/ka)	OSL Age (Yr) ²	Calendar Age (Yr) ³	Sample Description
OSL1	USGS	0.20 ± 0.01	2.49 ± 0.06	3460 ± 330	3730-3070	From Trench 3, west end-south wall, quartz grains from buried soil below sand blow
OSL2	USGS	0.20 ± 0.01	2.74 ± 0.08	3150 ± 300	3390-2790	From Trench 2, southeast wall, quartz grains from buried soil below sand blow

¹ Cosmic dose rate calculated using methods of Prescott and Hutton (1994).

² Linear and exponential fit used on equivalent dose at one standard deviation. Datum year is A.D. 2010.

³ Years B.P. or before present (1950).

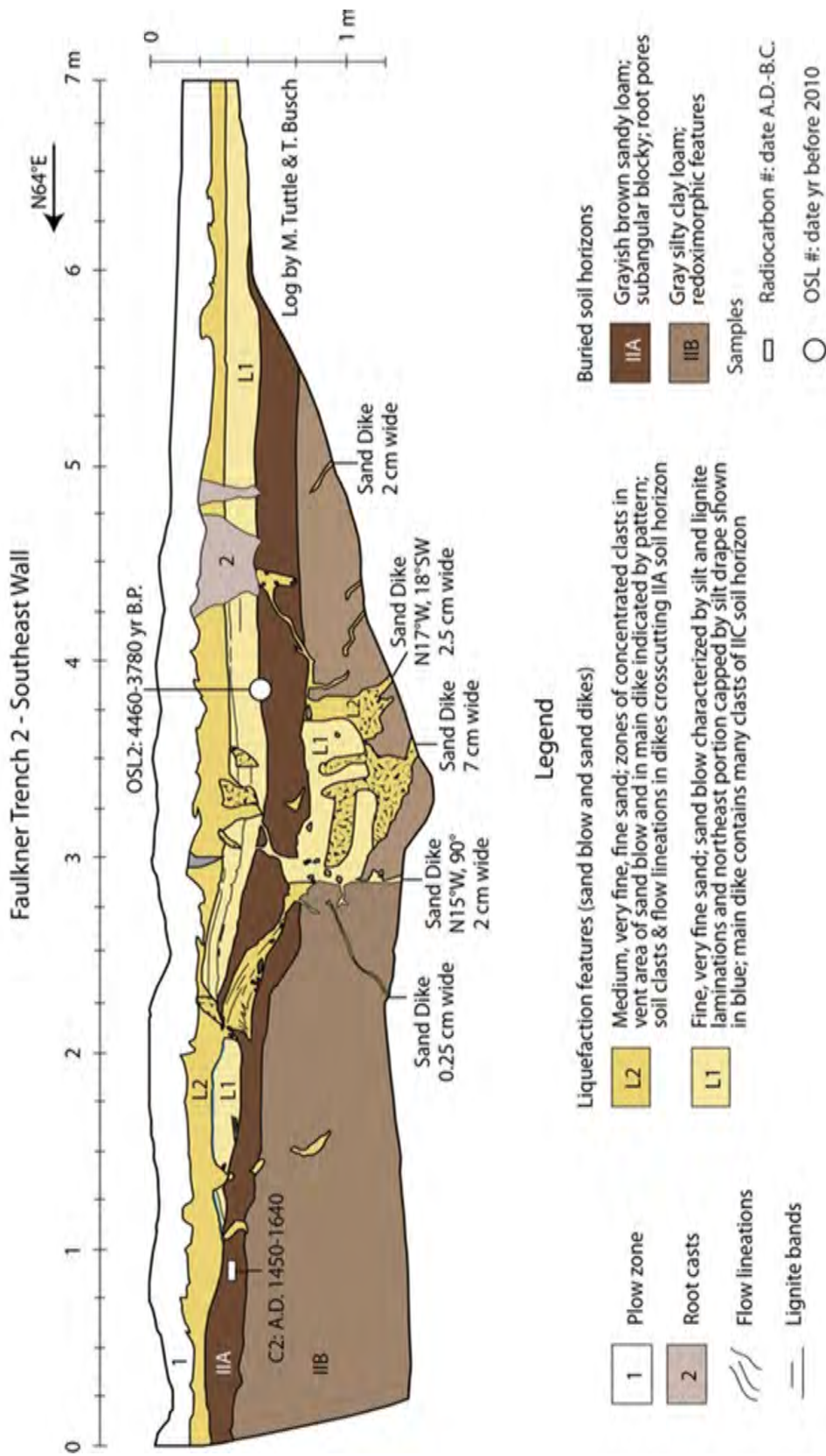


Figure 4-66 Log of Trench 2 at Faulkner site, showing sand blow and related sand dikes as well as radiocarbon and OSL dates on collected samples.

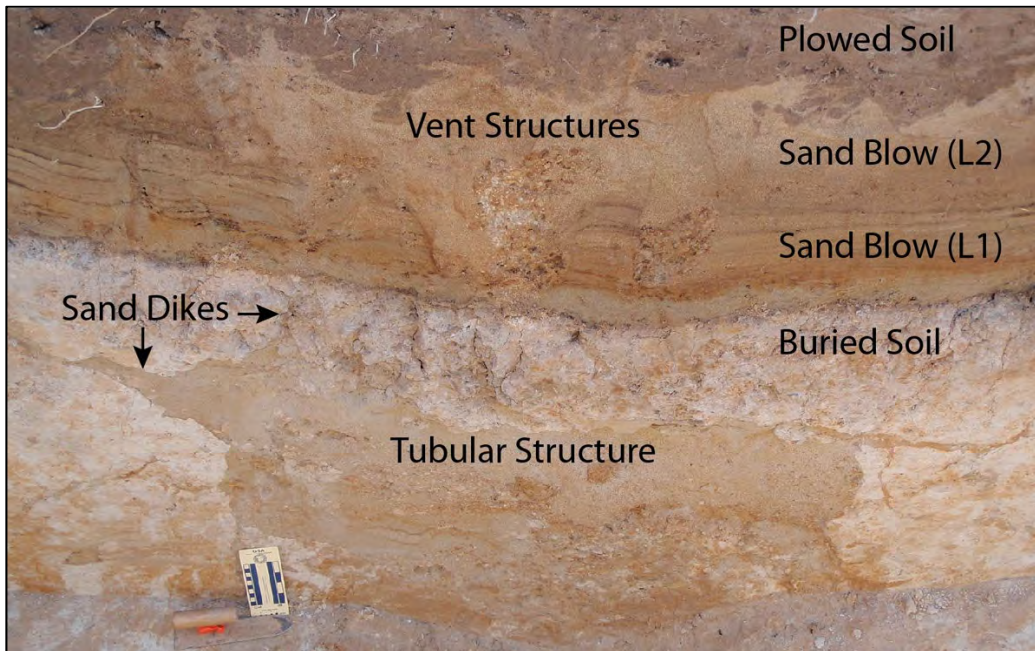


Figure 4-67 Photograph of southeast wall of Trench 2 at Faulkner site, showing large, sand- and clast-filled tubular structure below the base of the brownish soil, sand dikes emanating from the top of the structure, and iron-stained sand blow composed of two units (L1 and L2) with several v-shaped vent structures. For scale, wooden handle of scraper is 14 cm long.

Trench 3

Trench 3 was about 33 m long, oriented N85°W, and crossed two types light-colored patches observed on GE imagery and interpreted to be related to two generations of sand blows (Figure 4-57). Most of the trench was less than 1.5 m in depth but was deepened to 2 m at the western end in order to further view sand dikes.

In the south wall of Trench 3, six sand dikes were exposed that ranged up to 14 cm wide and crosscut predominantly silty and clayey soils (Figure 4-68 and Figure 4-69). Two sand dikes occurred at the western end of the trench between meter marks 0 and 4. The larger of the two dikes, was 14 cm wide as measured in the trench floor and narrowed up section. It was composed of loose but iron-stained sand, containing lignite pebbles and clasts of clay and iron-cemented sand. The dike appeared to have been intruded along the margin of a more weathered dike composed of iron-stained and cemented sand, also containing lignite pebbles and clasts (Figure 4-69). The large and less weathered dike had a strike and dip of N22°W, 78°SW near the base of the trench wall and changed orientation up section, where the strike and dip became N3°W, 35°NE. The lower portion of the more weathered dike may have been removed during the intrusion of the larger dike. This is supported by the presence of clasts of iron-cemented sand in the larger dike. The more weathered dike had a strike and dip of N3°W, 35°NE, where it was adjacent to the less weathered dike. Two smaller dikes branch off the weathered dike. One of these dikes, with a strike and dip of N4°W, 39°SW, extended up section to the base of brownish silty clay soil, crosscutting sandy clay loam and an embedded wedge of brown clay (Figure 4-69). Although not observed in the trench wall, the connection of the dike to the overlying sand deposit almost certainly occurred nearby, therefore suggesting that the overlying sand deposit was a sand blow. A partial vent structure occurred in the brown silty clay soil and in the lower unit of the sand deposit above the dike tip (below meter mark 3). The sand deposit was composed of two

depositional units, both about 30 cm thick. Basal Unit L1 was composed of coarse to medium sand that fined upwards to very fine sand and characterized by lignite bands and flow lineations. Unit L2 was a very fine to medium sand that fined upwards to very fine sand and contained clasts of the underlying soil horizons. The two depositional units of the sand blow filled what would have been a small surface depression at the time of the event. The depression occurs above the wedge of brown clay embedded in the subsoil. Although now partially destroyed by the modern plow zone, both units thin away from and probably pinch out within several meters of the dike. It should be noted that the brownish silty clay soil below the sand blow also thins to the east and has been removed between meter marks 4.5 and 5.0.

Also exposed in the south wall of Trench 3, four small (~1 cm wide) sand dikes occurred between meter marks 16 and 23. In contrast to the dikes at the western end of the trench, these small dikes exhibited no iron staining or other evidence of weathering. Although none of these dikes made a clear connection with a sand deposit above, other nearby sand dikes, intruded along a tree root exposed in the floor and north wall of the trench, did connect with the overlying sand deposit interpreted as a sand blow (Figure 4-68 and Figure 4-70). The sand blow exposed in both the southern and northern trench walls was composed of multiple depositional units. The lowermost unit, Unit L3, was composed of medium to very fine sand and contained numerous clay clasts above the sand dike. The unit was up to 32 cm thick and more than 15 m across, extending from meter mark 17 eastward past the end of the trench (Figure 4-68). Unit L4 was composed of coarse to medium sand that fined upwards to very fine to fine sand, containing clasts and exhibiting lignite bands and flow lineations. L4 was up to 42 cm thick and about 21 m across, extending between meter marks 5 and 26. The uppermost unit, L5, was composed of medium to very fine sand, slightly weathered, and reworked adjacent to the crater fill and tree cast exposed in the north wall of the trench. The unit was up to 12 cm thick and of very limited extent, about 3-4 m across, in both walls of the trench.

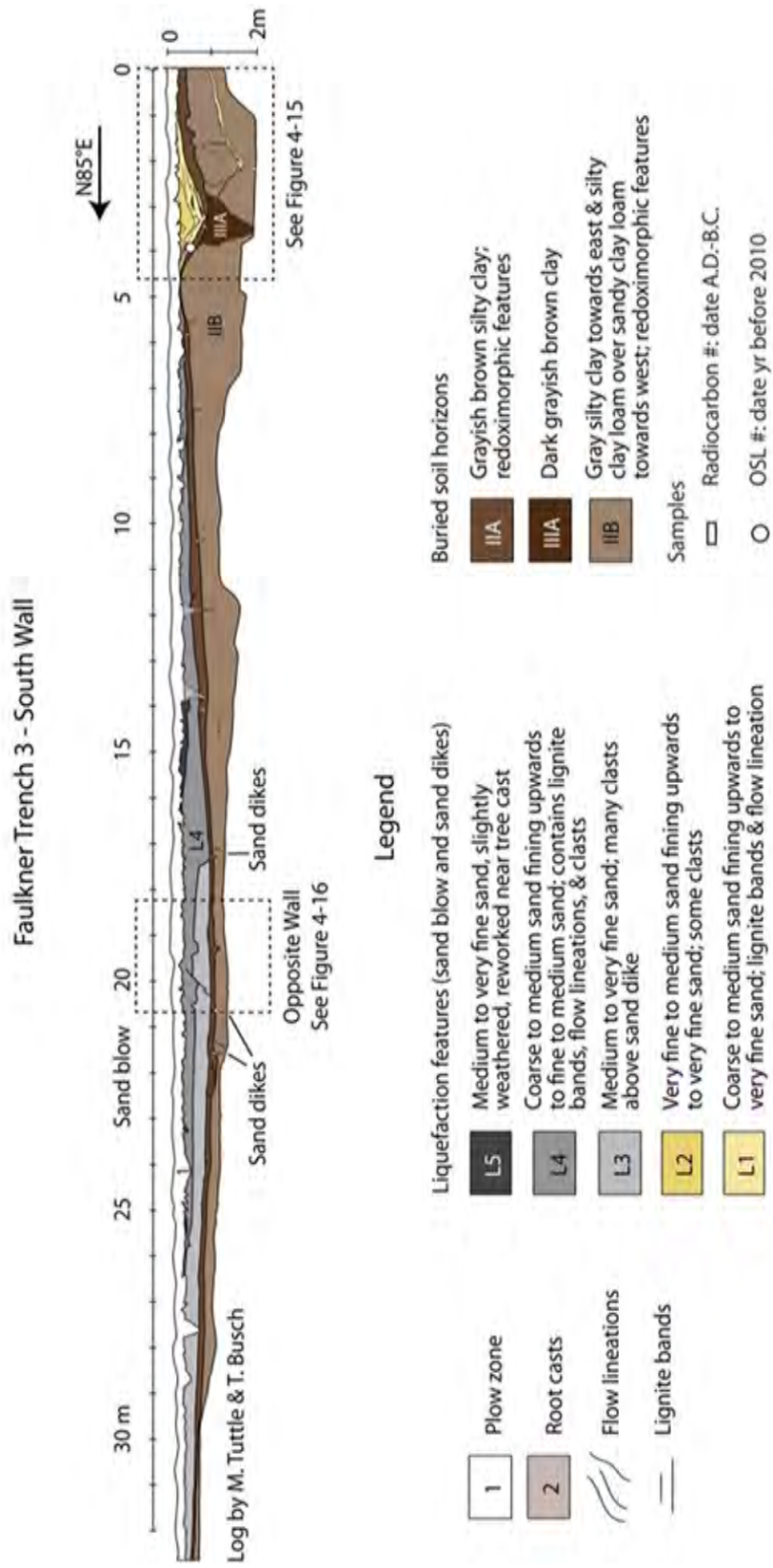
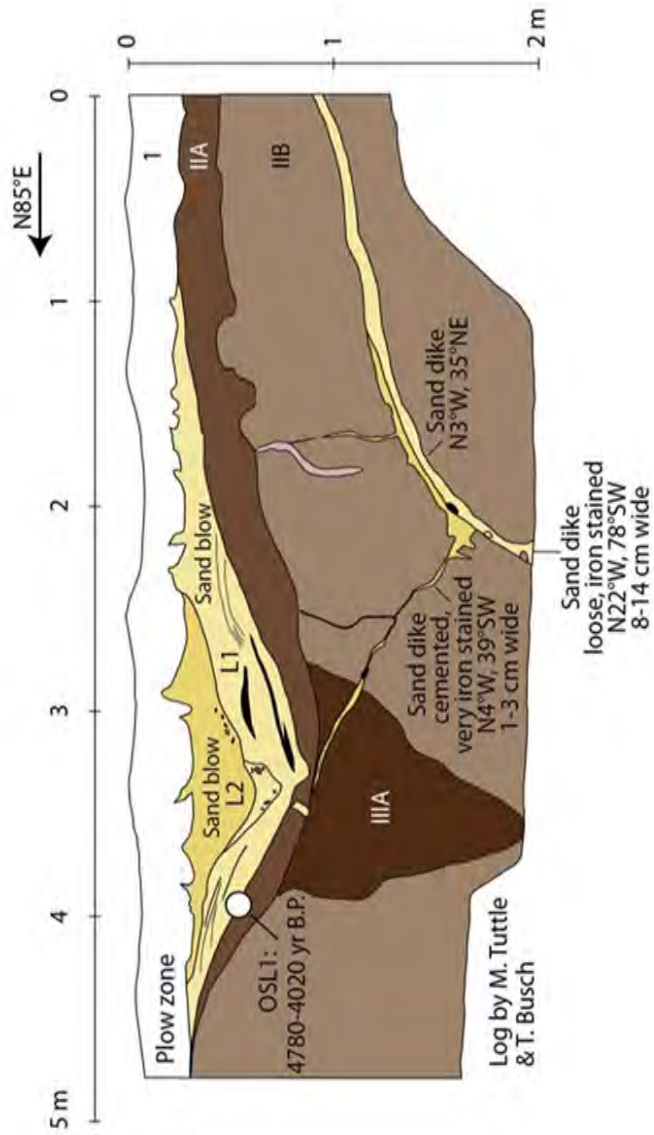


Figure 4-68 Log of Trench 3 at Faulkner site, showing sand blow and related sand dikes as well as location of logs shown in Figure 4-69 and Figure 4-70.

Faulkner Trench 3 - South Wall

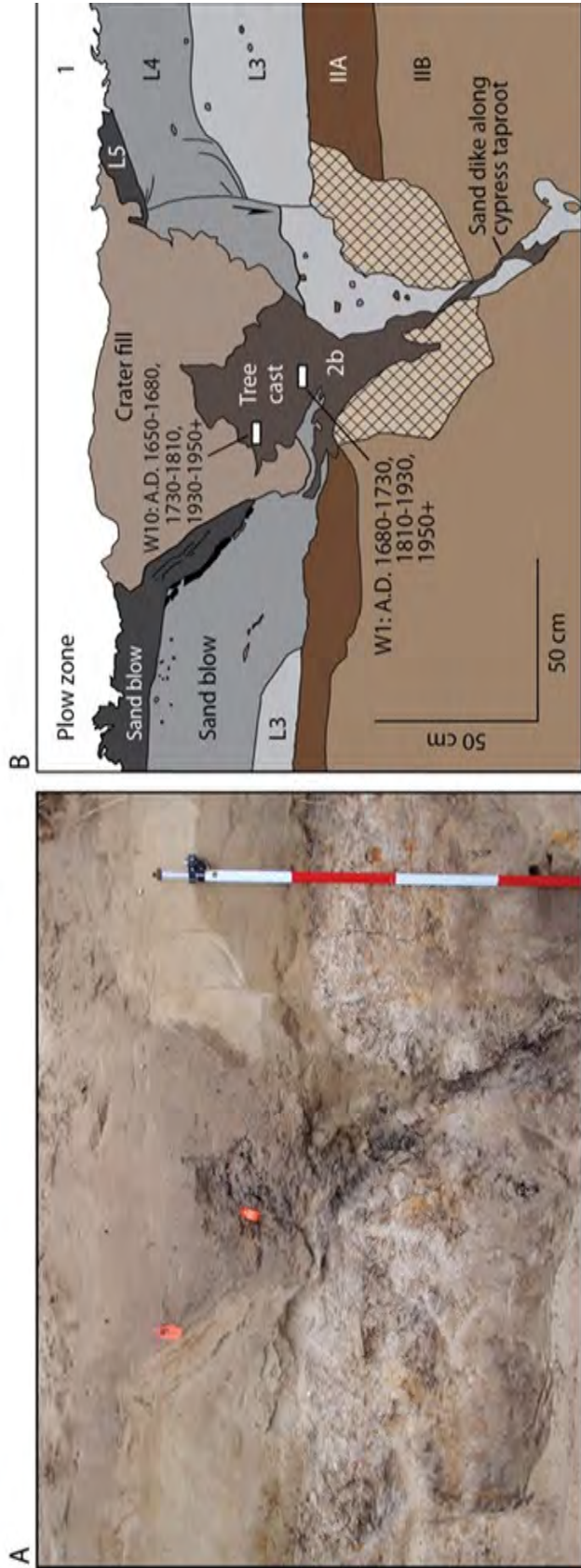


Legend

Liquefaction features (sand blow and sand dikes)		Buried soil horizons			
1	Plow zone	L2	Very fine to medium sand fining upwards to very fine sand; some clasts	IIA	Grayish brown silty clay; redoximorphic features
2	Root casts	L1	Coarse to medium sand fining upwards to very fine sand; lignite bands & flow lineation	IIIA	Dark grayish brown clay
○	OSL #: date yr before 2010	☁	Clasts	IIB	Gray silty clay towards east & silty clay loam over sandy clay loam towards west; redoximorphic features
		—	Flow lineations		
		—	Lignite bands		
		—	Lignite pebbles		

Figure 4-69 Enlargement of western end of Trench 3 log at Faulkner site, showing sand blow and related sand dikes as well as OSL dates on sample of buried soil.

Faulkner Trench 3 - North Wall



Log by T. Busch and M. Tuttle

Legend

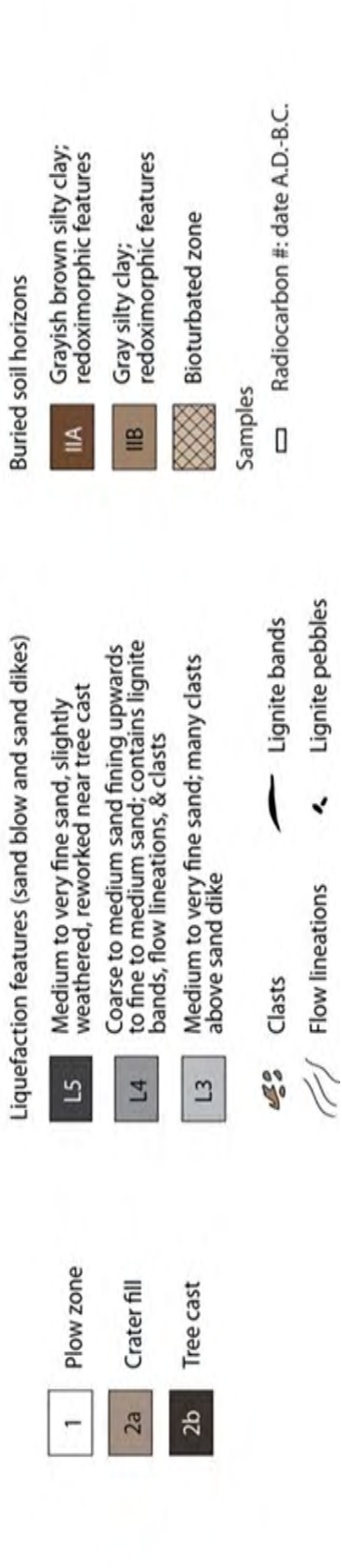


Figure 4-70 Paired photograph (A) and log (B) of portion of north wall of Trench 3 at Faulkner site, showing ~8 cm wide sand dike that intruded along tree root and sand blow that was deposited around tree trunk as well as radiocarbon dates on samples collected from the root and tree cast.

Units L3 and L4 were thickest between meter marks 15 and 22, coinciding with the lowest elevation of the buried surface below the sand blow. The buried surface was inclined towards the east between meter mark 5 and 20 at which point it reversed dip and was inclined very slightly towards the west between meter mark 20 and 20 and 32. As seen in the north wall, the upper contacts of L3, L4, and L5 all dip towards the tree cast and associated crater fill (Figure 4-70). The rooting habit of the tree, including a deep taproot and shallow lateral roots, is suggestive of cypress. Part of the remaining tree root was collected from the trench floor and was later confirmed to be cypress (N. Lopinot, pers. comm., 2012). There was a heavily bioturbated zone in the soil adjacent to the base of the tree cast. Root casts occurred in and along the top of the buried soil, but not in the sand blow units.

The soils below sand blows exposed in both trench walls were carefully examined for organic material for radiocarbon dating. Several samples were collected; but upon closer inspection with a microscope, they all proved to be small manganese nodules. Luckily, the tree cast exposed in the north wall contained plenty of organic material. Radiocarbon dating was performed on two samples collected from the tree cast (Figure 4-70). Sample CWY-T3-W1 was a piece of wood collected from the outer centimeter of an intact portion of the tree trunk just above the root system. The sample yielded a two-sigma calibrated date of A.D. 1680-1730 A.D., 1810-1930, and post-1950 (Table 4-17). Sample CWY-T3-C10 was charred material collected from the tree cast. The two-sigma calibrated date of this sample was A.D. 1650-1680, 1730-1810, and 1930-post 1950 A.D. In addition, a sediment sample (OSL1) was collected of the upper contact of the soil beneath sand blow unit L1 towards the western end of the trench for OSL dating. Analysis was performed on quartz grains extracted from the sample. It yielded an OSL age of 3460 ± 330 (or 3730-3070 yr B.P.) (Table 4-18).

4.4.5.1.7 *Paleoseismic Interpretations*

Trenches 1 and 2

Given the proximity of Trenches 1 and 2, the sand blows and sand dikes observed in the two trenches are probably related. The sand blow corresponds with the light-colored linear patch along the northeastern margin of the abandoned channel that crosses the Faulkner site. The sand blow in Trench 2 was composed of two depositional units separated in part by a silt drape. The presence of the silt drape, but no indication of soil development, suggests a period of quiescence during which silt settled out of vented water on the surface before the upper unit was deposited. Therefore, the compound sand blow may have formed during two closely timed earthquakes. The liquefaction features in both trenches are somewhat iron stained suggesting that they are prehistoric in age. The radiocarbon dates of two samples from the soil buried by the compound sand blow are stratigraphically consistent and provide maximum age constraint for the formation of the liquefaction features. The date of A.D. 1450-1640 from 5 cm below the sand blow provides a close maximum age and suggests that the liquefaction features formed soon after A.D. 1450. The OSL date is much older than the radiocarbon date and probably does not reflect the time of burial of the soil by the sand blow. Perhaps the luminescence clock had not been completely reset in the surface soil due to heavy vegetative cover; or perhaps the soil had been mixed through the process of bioturbation with deeper sediment whose luminescence clock had not been reset. In the New Madrid seismic zone, numerous compound sand blows are thought to have formed during a New Madrid event about A.D. 1450 ± 150 yr. The liquefaction features in Trenches 1 and 2 likely formed during the A.D. 1450 event. The sand blows in Trenches 1 and 2 are not particularly large but are consistent in size with similar-aged sand blows along the Little River south of Big Lake and near Marked Tree (NUREG-2115). Sand dikes in both trenches are fairly small except where they appear to have intruded a large void formed by a decayed tree root system.

Trench 3

There appear to be two generations of sand blows in Trench 3 based primarily on the degree of weathering. The small sand blow at the western end of the trench is composed of two depositional units, is iron-stained, and corresponds with the smaller, fainter, linear sand blow along the southwestern margin of the abandoned channel deposit as seen on GE imagery (Figure 4-57). The large sand blow that extends much of the length of the trench is composed of three depositional units, is only slightly weathered in its uppermost unit, and corresponds with the larger, brighter, elliptical sand blow that crosses the channel margin and overlies the abandoned channel deposit. The weathered sand blow at the western end of the trench is similar to the compound sand blow in Trench 2. Both sand blows are relatively small, composed of two depositional units, are iron stained, and formed along the margins of the abandoned channel deposit. Unfortunately, no organic material was found in the soil beneath the western sand blow to provide maximum age constraint. However, based on its similarities with the sand blow in Trench 2, the small, weathered, compound sand blow in Trench 3 probably formed during the A.D. 1450 event. Similar to Trench 2, the OSL date of the soil buried by the sand blow is on the order of 4 kyr and probably does not reflect the time of the event.

The large, relatively unweathered sand blow in Trench 3 is likely to be younger than the smaller, more weathered sand blows at the site. The cypress tree, whose remains were exposed in the north wall of Trench 3, was probably alive when a sand dike intruded along its taproot and units L3, L4, and L5 were deposited around the base. This interpretation is supported by the presence of root casts in and along the top of the buried soil and absence of root casts in the sand blow units. In addition, the upper contacts of L3, L4, and L5 that dip towards the tree cast suggest that a standing tree trunk likely affected deposition of the sand blow units. Turbulence caused by the tree, as vented water flowed around it, would have caused scouring of the depositional units. Therefore, radiocarbon dating of organic material from the cypress tree provides a maximum constraining age for the liquefaction features and indicates that they formed after A.D. 1680, probably during the A.D. 1811-1812 New Madrid earthquake sequence. The younger sand blow exposed in Trench 3 is larger than those thought to have formed during the 1450 event. This is due in part to its greater number of depositional units. The size of the younger sand blow at this site is consistent with other sand blows that formed in A.D. 1811-1812 and were found along Kochtitzky Ditch (NUREG-2115). The number of the units composing the sand blows suggest that three earthquakes during the A.D. 1811-1812 event were strong enough to induced liquefaction at the site, compared to two earthquakes during the 1450 event.

As mentioned above, the buried land surface beneath the large sand blow was inclined towards the east but then reversed its inclination slightly towards the west. The eastward inclination of the buried surface likely reflected the natural slope towards the abandoned channel. This is supported by the change in texture of the subsoil from sandy clay loam at the western end of the trench to silty clay towards the eastern end of the trench. The reversal in inclination may be related to the microtopography of the buried surface or possibly to a small amount of subsidence related to the venting of a large quantity of sand. Either way, units L3 and L4 of the large sand blow filled in the low area as defined by the buried surface.

The wedge of brown clay at the western end of Trench 3 is interpreted as a small channel, perhaps a tributary to the main river channel that was partially filled with fine-grained sediment prior to the earthquakes that induced liquefaction. The surface depression above the small

abandoned channel caught and helped to preserve the small compound sand blow composed of units L1 and L2. Thinning of brownish silty clay soil between the small compound sand blow towards the west and the large compound sand blow towards the east occurred before deposition of the sand blows. This area may well have been an interfluvium between the main channel and the tributary that was subjected to erosion.

4.4.5.2 *Wildy (aka Busch) Site*

The Wildy site is located about 13 km northeast of the Faulkner site (Figure 4-56). The Wildy site also occurs between the southern branch of the NMSZ and the western margin of the Reelfoot Rift and is within the liquefaction field (1% of the surface area covered with sand blows) interpreted from aerial photographs (Figure 4-55; Obermeier, 1989). It is located between the Little and St. Francis Rivers and about 10 km northwest of the Little River Ditch, where sand blows south of Big Lake are thought to have formed during the A.D. 1811-1812 and A.D. 1450 ± 150 yr New Madrid events (Tuttle et al., 2002 and 2005; Tuttle and Hartleb, 2012). The Wildy site occurs in Late Pleistocene valley-train deposits (Pv1 level 2) and just 1 km east of the Buffalo Creek Ditch excavated in an abandoned channel (Pvcl) of the Mississippi River (Figure 4-56; Saucier, 1994). The site has the potential to provide additional information about known Late Holocene New Madrid events as well as earlier paleoearthquakes in an area where no paleoliquefaction features had been studied in the past.

4.4.5.2.1 *Reconnaissance*

As mentioned above in Section 4.4.4.1, the U.S. Army Corps of Engineers provided information about cleaned and excavated ditches in the area between Little River and Crowley's Ridge. Satellite imagery was reviewed to identify sections of the ditches where sand blows might have been exposed and selected ditch sections were inspected for sand blows and sand dikes. During that reconnaissance in September 2011, a sand blow and related sand dike were found in a recently cleaned ditch along the south side of West County Rd 378. The sand blow was thickest, 30 cm, above its feeder dikes, 2 and 3 cm wide, and thinned laterally in both directions away from the dikes. The dikes crosscut and the sand blow overlaid a brown soil horizon. Several sand-tempered (Barnes series) potsherds from the Woodland cultural period were found in the soil horizon beyond the western end of the sand blow.

Following the initial find of the liquefaction features at the Wildy site, GE satellite imagery was reviewed and several northwest-orientated, light-colored patches likely to be sand blows were identified in the field south of the road ditch (Figure 4-71). In October 2011, an additional reconnaissance was performed in the field adjacent to the ditch, targeting the light-colored patches seen on GE imagery. Stunted cotton delineated the light-colored patches that were sandy in contrast to surrounding silty soils. A soil pit (SP2 on Figure 4-72) dug in a prominent northwest-orientated sandy patch revealed a 60-cm-thick sand deposit below a 30-cm-thick plow zone. The sand deposit was composed of two units separated by a thin layer of lignite. The upper unit was somewhat weathered fine to medium sand and the lower unit was unweathered fine to coarse sand. In contrast, a soil pit (SP1 on Figure 4-72) dug beyond the margins of the sandy patches revealed a very weathered silt loam below the plow zone. The observations in the soil pits supported the interpretation that the sandy patches were sand blows. The Wildy site was selected for further investigation given the likely presence of sand blows, the possible association with a Woodland site, and the Late Pleistocene age of the underlying sediment.

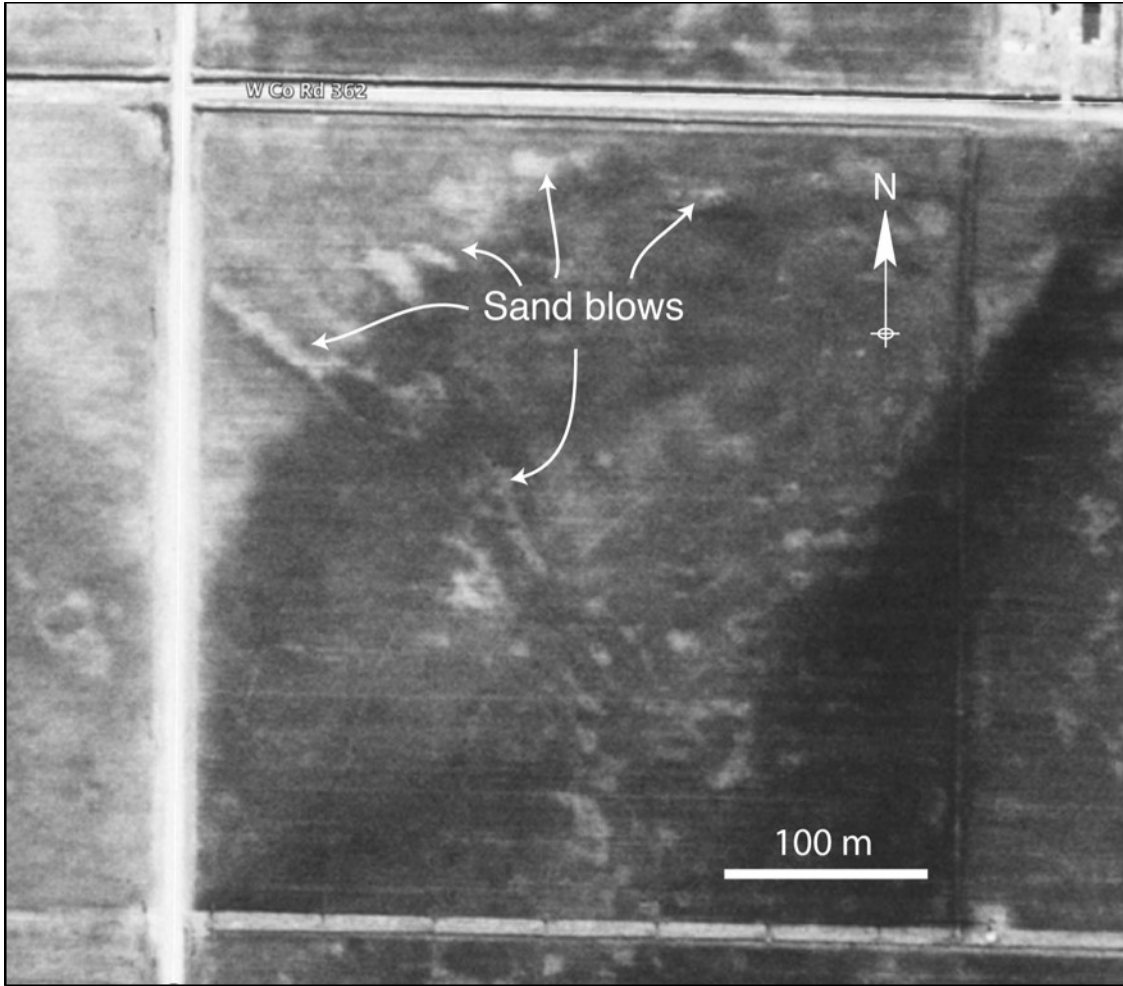


Figure 4-71 GE image of Wildy site, showing light-colored patches corresponding to sand blows. Large linear sand blow with northwest-oriented trend was selected for study. Image was acquired by US Geological Survey in January 2002.

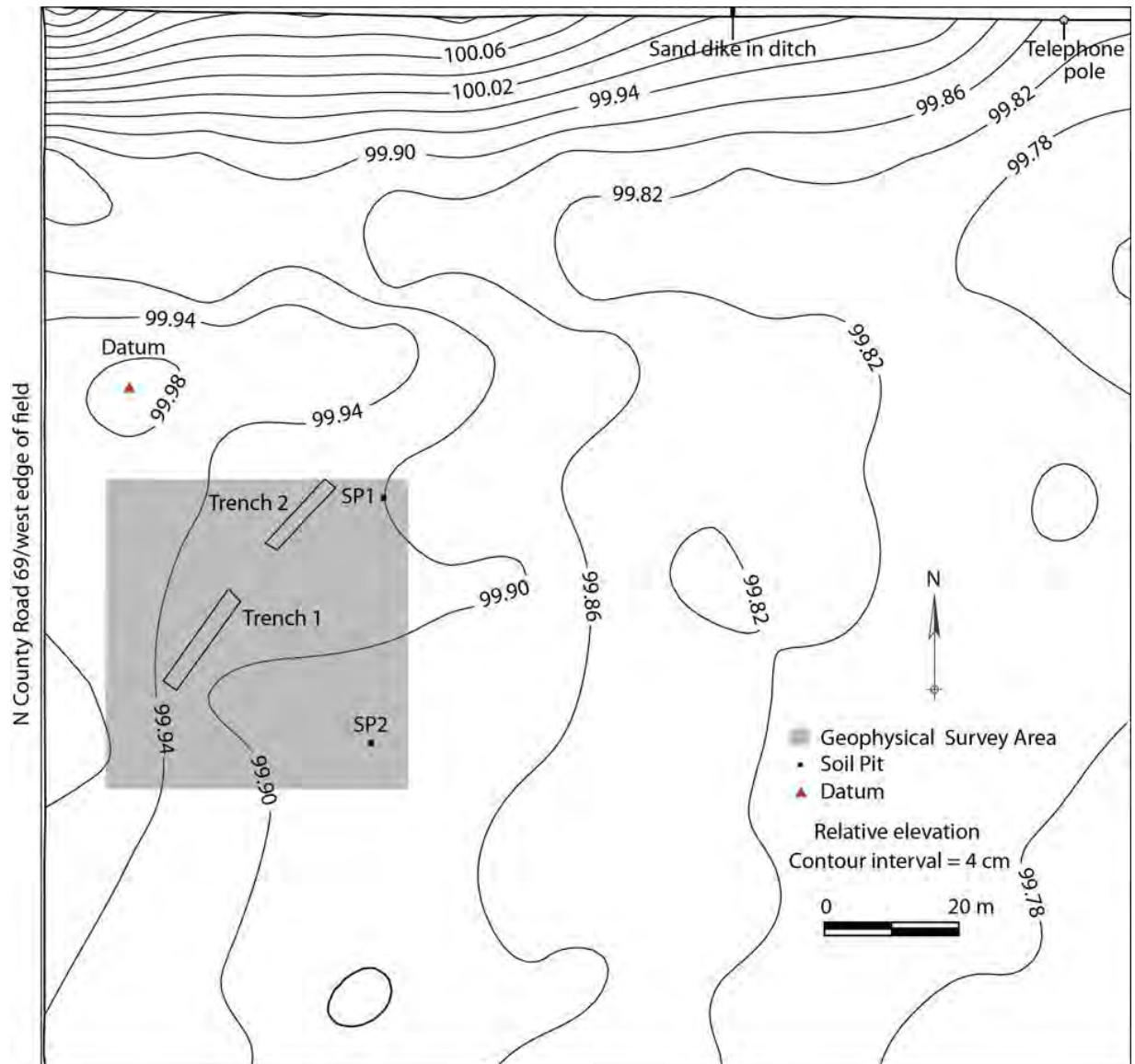


Figure 4-72 Topographic map of Wildy site, showing locations of soil pits, geophysical grids, and paleoseismic trenches.

4.4.5.2.2 *Electrical Resistivity Surveys*

Also, in October 2011, a geophysical survey using ER tomography was conducted at the Wildy site. The area of the geophysical survey was selected to cover the large northwest-oriented sandy patch interpreted to be a sand blow. The survey area is shown on the topographic map made of the site (Figure 4-72). Figure 4-73 shows the ER survey layout at the Wildy site. The grid consisted of multiple parallel lines within a rectangular area. All lines were 46 m in length. Data were collected using an AGI SuperSting resistivity meter, with automatic electrode-switching capability. Each line consisted of 24 electrodes at 2-m spacing. An AGI mixed dipole array (similar to a conventional dipole-dipole configuration) was chosen for the data acquisition because this array provides optimal resolution for near-surface features and sufficient depth penetration to guide future trench excavations. Measurement errors in all surveys did not exceed 0.2%.

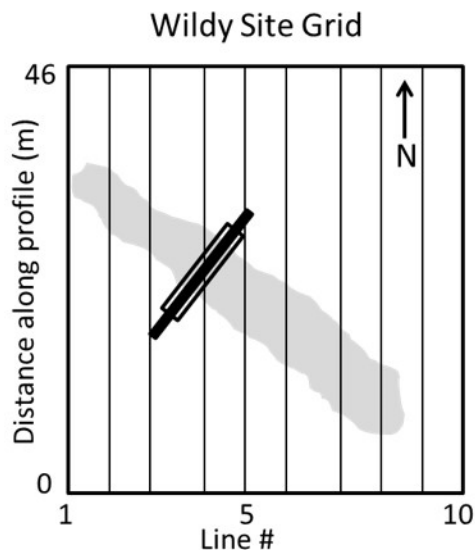
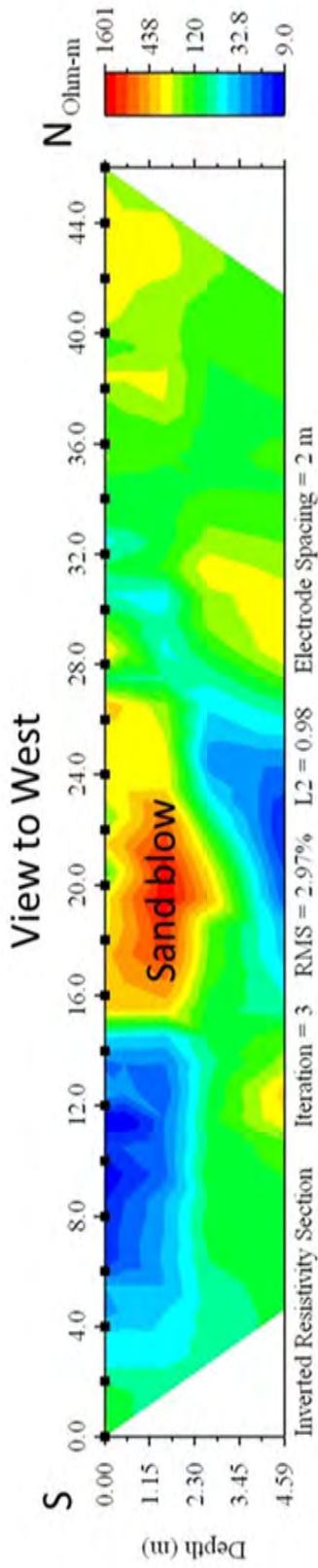


Figure 4-73 Layout of resistivity survey grid at Wildy site, AR, also showing positions of large northwest-oriented sand blow (shaded area), trench excavated through sand blow (solid black line), and portion of trench logged (open box).

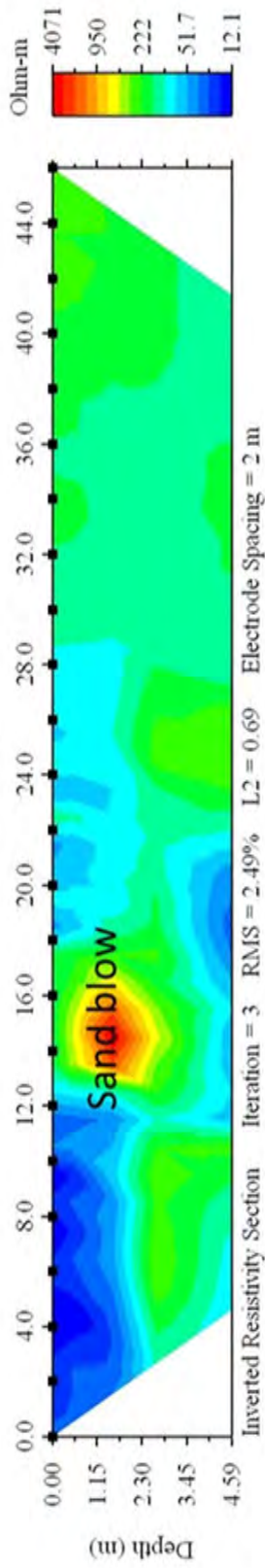
As for the Faulkner site, raw data observations of apparent resistivity from all profile measurements were processed using AGI's 2-D EarthImager inversion software to produce cross-sections of the true subsurface resistivity distribution. The model is validated by using a forward-modeling technique to predict the apparent resistivity distribution if one assumes that the calculated true resistivity distribution in the subsurface model is correct. Statistical measures of the solution are thus obtained. The maximum RMS data error in the inversions was less than 5%.

Electrical Resistivity Results

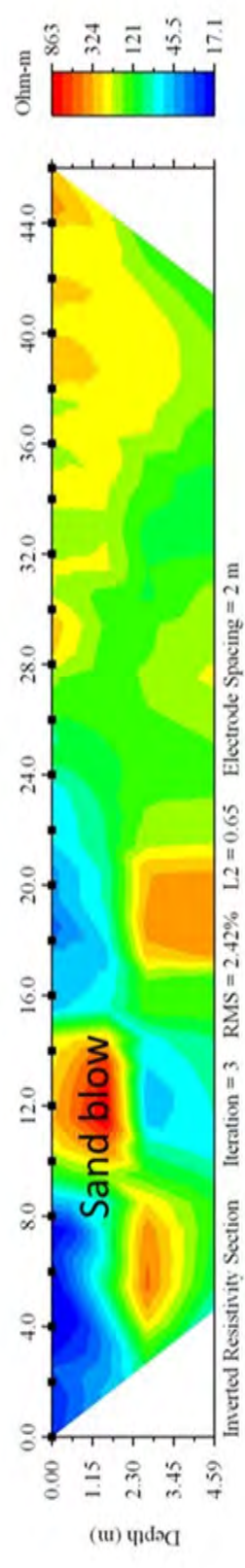
Figure 4-74 to Figure 4-76 contain images of the data acquired at the Wildy site. The grid contained ten parallel profile lines numbered from west to east (Figure 4-73). A northwest trending sand blow deposit identified on the surface is clearly seen in the geophysical profiles (Line 1, 25 m to 35 m along profile, to Line 8, 0 m to 10 m along profile). On Lines 9 and 10, a very large high-resistivity area is seen on the northern two-thirds of the profiles, reflecting a large sand deposit. A high resistivity area in the central part of the profile along Line 3 (~ 19 m to 27 m) connects to a deeper high-resistivity feature (11 m to 17 m). This feature is interpreted to be a sand dike connecting the sand blow at the surface to a source of sand at depth. This interpretation was substantiated by observations made in Trench 1 described below. Eastward of Line 3, the sand blow location moves southward, until Line 10, where a large sand body is present on the northern two-thirds of the grid.



10302011-Wildy Line 4



10302011-Wildy Line 5



10302011-Wildy Line 6

Figure 4-74 Composite Resistivity Images of Lines 4, 5, and 6 from Wildy Site

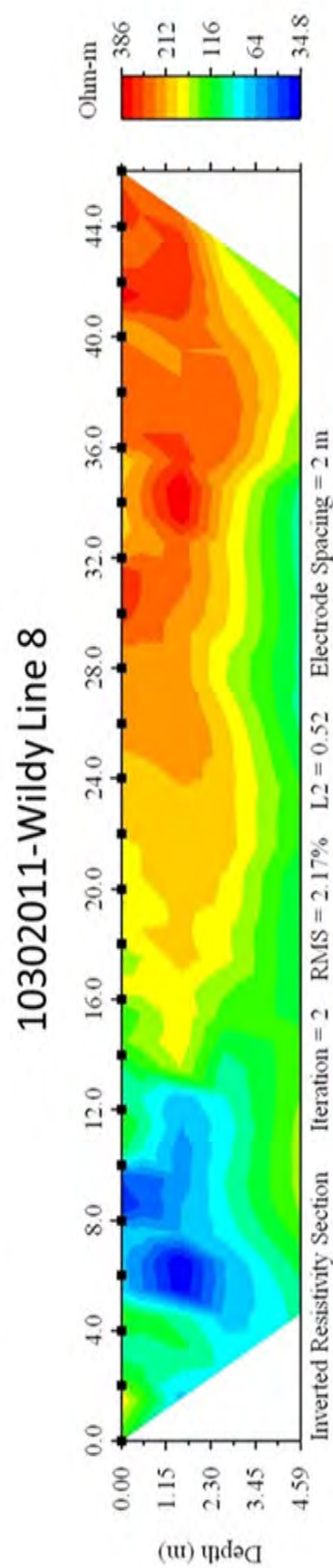
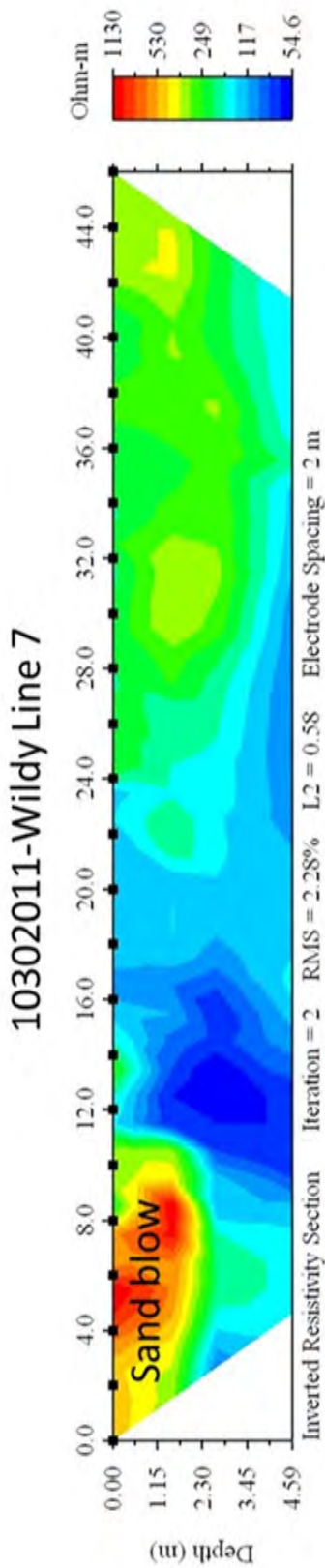
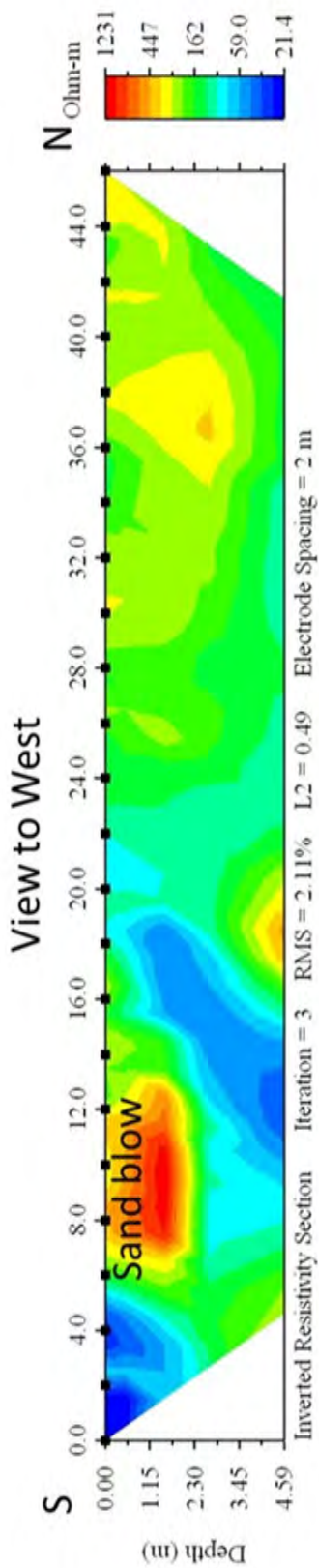


Figure 4-75 Composite Resistivity Images of Lines 4, 5, and 6 from Wildy Site

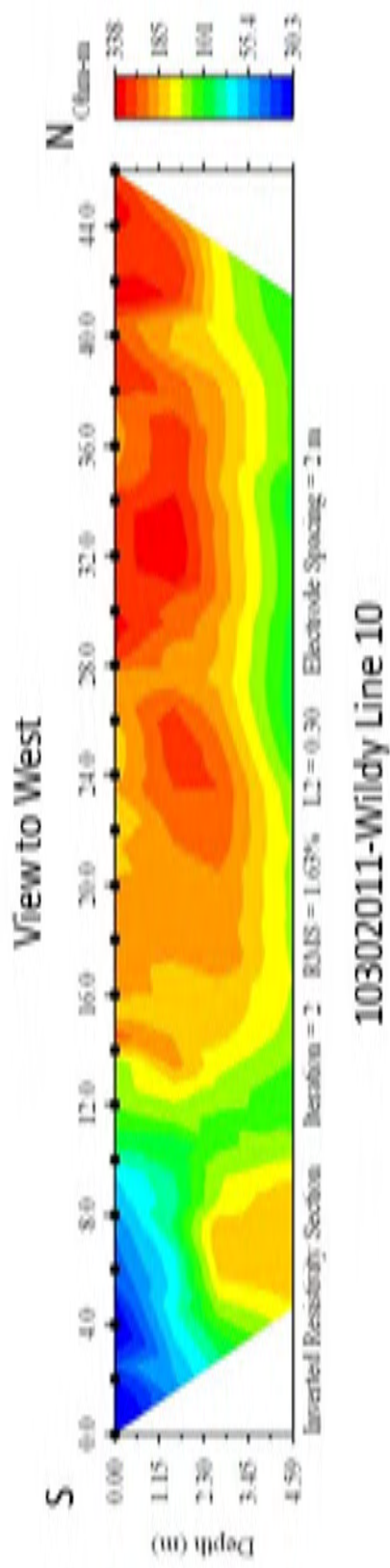


Figure 4-76 Resistivity Image of Lines 10 from Wildy Site

4.4.5.2.3 *Pre-Trenching Archaeological Evaluation*

Prior to trenching, project archaeologists conducted a surface survey in the field south of the ditch and found a small, sparse ceramic scatter. Two paleoseismic trenches, describe in detail below, were excavated outside the area of identified artifact scatter. Archaeologists monitored excavation, but no archaeological deposits or artifacts were encountered in the trenches.

4.4.5.2.4 *Siting of Trenches*

Trench 1 was sited on the basis of interpretations of GE images, field observations, and geophysical profiles in order to study the large northwest-oriented sand blow (Figure 4-72). The trench was oriented at an oblique angle to the geophysical profiles, intersecting Line 3 at about 18 m along the profile and Line 5 at about 28 m along the profile in order to intersect the sand dike (Figure 4-73). A second trench was cited northeast of Trench 1 where no sand blow or sand dike had been interpreted on the profiles. Trench 2 would serve as a control and test of the geophysical methodology.

4.4.5.2.5 *Paleoseismic Observations*

In late October-early November 2011, two trenches were excavated at the Wildy site as described above. Trench 1 exposed a sand blow and related sand dikes described below. Trench 2 revealed no sand blow or sand dike, only sandy loam. Because there were no liquefaction features exposed in Trench 2, it was not logged. Findings in both trenches confirmed the interpretations of the geophysical profiles.

Trench 1

The trench was about 16 m long, extending beyond the margins of the sand blow, and was orientated N54°E, roughly perpendicular to the long dimension of the sand blow and the trend of the feeder dike (Figure 4-77 and Figure 4-78). Most of the trench was less than 1.5 m deep. However, the trench was deepened to 2 m to observe the top of the soil horizon below the sand blow as well as its feeder dikes. In order to safely examine and log the liquefaction features, the southeastern wall of the trench was removed and an inclined ramp excavated.

A large sand blow, up to 120 cm thick, and three feeder dikes, ranging up to 146 cm wide, were exposed in the trench (Figure 4-77). The largest sand dike (between 4.5 and 6 meters on the trench log) and the overlying sand blow appeared to be composed of two depositional units (Figure 4-78). Unit L1 was up to 100 cm thick and was composed of coarse, medium, and fine sand immediately above the dike. The unit fined to very fine and fine sand and thinned towards the northeast. There may have been 2-3 subunits within Unit 1, but they were discontinuous so it was difficult to be sure. The unit exhibited thin discontinuous laminations of silt as well as lignite stringers and contained soil clasts especially in the lower portion of the sand blow. A portion of the upper contact of Unit 1 was capped by a silt drape. Unit 2 was up to 20 cm thick, composed of coarse and medium sand immediately above the dike, and also fined as well as thinned towards the northeast. The unit exhibited flow structure and clasts of soil above the sand dike and was somewhat weathered immediately below the plow zone (Figure 4-79).

The western margin of the largest sand dike was orientated N64°W, 85°SW and a small (3 cm) sand dike between meter marks 8 and 9 on the log was orientated N35°W, 80°W (Figure 4-78). The tilted soil between the 6 and 7-meter marks may be a large clast within the feeder dike. If so, the dike was even wider (~300 cm). Between meter marks 16 and 7, the soil beneath the sand

blow dipped towards the large sand dike and was displaced downward by about 90 cm across the dike. The sand blow, overlying the dipping surface, essentially filled the topographic low created by ground failure.



Figure 4-77 Photograph of northwest wall of Trench 1 at Wildy site, showing dipping surface of buried soil overlain by large sand blow, crosscut by a dark brown tree cast. For scale, trench is 16 m long and 2 m deep.

Towards the northeastern end of the trench, the sand blow was crosscut by a tree cast and associated bioturbated zone. The tree cast was funnel-shaped, extended into the soil buried by the sand blow, and composed of organic material. The morphology of the tree cast suggested that it had a taproot. There were no remnant tree stump or roots that could be used for identification. Adjacent to the tree cast, the sand blow was structureless and contained root casts, indicating that it had been bioturbated. Beyond the bioturbated zone, bedding dipped shallowly towards the large sand dike at the southwestern end of the trench.

Radiocarbon dating was performed on two organic samples collected from Trench 1. A piece of wood (Busch-T1-C1) collected from the brown silt loam about 1 m southwest of the large dike and about 4 cm below the sand blow yielded a two-sigma calibrated date of A.D. 1320-1340 and 1390-1440 (Table 4-19). A sample of charred material from the tree cast (Busch-T1-C13) gave a two-sigma calibrated date with four ranges of A.D. 1670-1780, 1800-1900, 1900-1940, and post-1950.

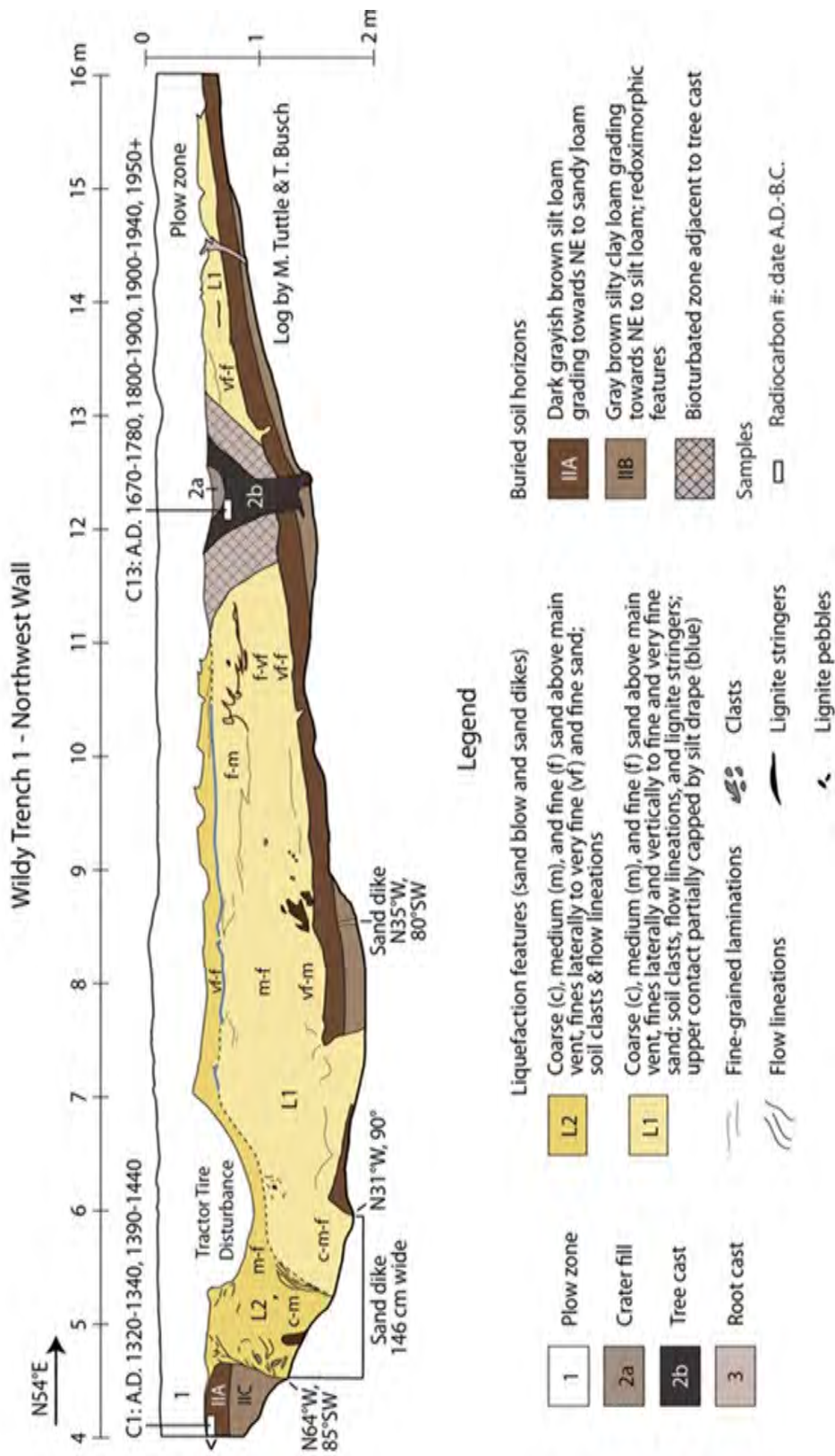


Figure 4-78 Log of Trench 1 at Wildy site, showing sand blow and related sand dikes as well as radiocarbon dates on collected samples.

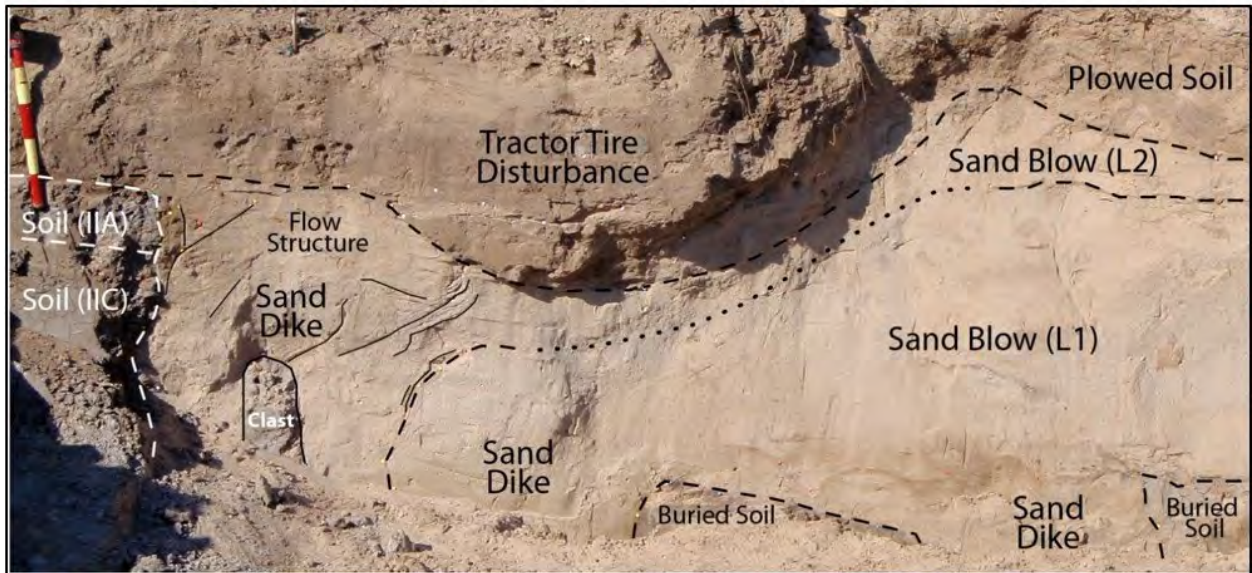


Figure 4-79 Photographs (upper - unannotated; lower - annotated) of portion of sand blow shown in Figure 4-77 above large sand dike. Note flow lineations and large soil clast in the sand blow. Soil was displaced downward 90 cm across dike. Dashed and dotted lines represent clear and inferred contacts, respectively. Thin solid lines represent flow structure. For scale, red and yellow intervals on shovel handle are 10 cm long.

Table 4-19 Radiocarbon Dating Results for the Wildy Site

Sample # Lab #	¹³ C/ ¹² C Ratio	Radiocarbon Age Yr B.P. ¹	Calibrated Radiocarbon Age Yr B.P. ²	Calibrated Calendar Date A.D./B.C. ²	Sample Description
Busch-T1- C1 BA-315735	-26.2	530 ± 30	630-610 560-510	AD 1320-1340 AD 1390-1440	Charred material 4 cm below sand blow from buried soil
Busch-T1- C13 BA-330163	-25.9	130 ± 30	280-170 150-50 50-0 0+	AD 1670-1780 AD 1800-1900 AD 1900-1940 AD 1950-1950+	Charred material 3 cm below crater fill in tree root cast in sand blow

¹ Conventional radiocarbon ages in years B.P. or before present (1950) determined by Beta Analytic, Inc. Errors represent 1 standard deviation statistics or 68% probability.

² Calibrated age ranges as determined by Beta Analytic, Inc., using the Pretoria procedure (Talma and Vogel, 1993; Vogel et al., 1993). Ranges represent 2 standard deviation statistics or 95% probability.

4.4.5.2.6 Paleoseismic Interpretations

Trench 1

Observations in Trench 1 confirm that the light-colored northwest-oriented linear patch on GE imagery was a sand blow. The sand blow, composed of two depositional units, is interpreted to be a compound sand blow that formed during two earthquakes in a sequence. The site suffered asymmetrical ground failure, including 90 cm vertical displacement of the ground surface, related to earthquake-induced liquefaction. As previously described for other liquefaction sites in the region, the sand blow filled the topographic low as the ground subsided due to venting of sediment from below (Tuttle and Barstow, 1996). The upper unit of the sand blow was somewhat weathered, suggesting that it may be prehistoric in age. The radiocarbon date of a piece of wood collected from the soil below the sand blow provides a close maximum age constraint and suggests that the liquefaction features formed soon after A.D. 1320. The tree cast that crosscuts the sand blow and related bioturbated zone within the sand blow are thought to be related to a tree that grew in the sand blow after it had been deposited. This interpretation is supported by bedding of the compound sand blow that shows no sign of turbulence and scouring around the base of a tree. Therefore, the radiocarbon date of the charred material from the tree cast provides minimum age constraint. Unfortunately, the date has four possible ranges, spanning the time period A.D. 1670 to post-A.D. 1950. The date from the sample collected from the soil buried by the sand blow is given more weight since it was essentially locked in time, whereas the tree from which the second sample was collected could have grown into the sand blow any time after it was deposited. There are two earthquake sequences, the A.D. 1450 and A.D. 1811-1812 events, known to have induced severe liquefaction in the region between A.D. 1320 and today. Although the later event cannot be ruled out, the A.D. 1450 event is more likely responsible for liquefaction and ground failure at the site based on the weathered nature of the sand blow and the date of the sample from the buried soil.

4.4.5.3 Garner Site

The Garner site is located about 30 km northwest of the southern branch of the NMSZ and very close to the western margin of the Reelfoot Rift, another possible source of large earthquakes (Figure 4-18 and Figure 4-19). The site is located west of the liquefaction field (1% of the surface area covered with sand blows) interpreted from aerial photographs (Obermeier, 1989) and about 5 km southwest of sand blows found along Eightmile Ditch and thought to have formed during the

1811-1812 earthquakes (Tuttle, 1999). The Garner site occurs in Late Pleistocene valley-train deposits (Pve level 3) just west of the mapped boundary with Late Pleistocene valley-train deposits (Pvl level 2 and Pvc1) to the east (Figure 4-56; Saucier, 1994). An escarpment between the two paleosurfaces is still obvious in the field and is located east of the Garner site. Given the age of the deposits, the site has the potential to contain an exceptionally long paleoseismic record. Prior to this NRC-funded project, no paleoliquefaction features had been studied in this area of Late Pleistocene valley-train deposits along the eastern margin of Crowleys Ridge.

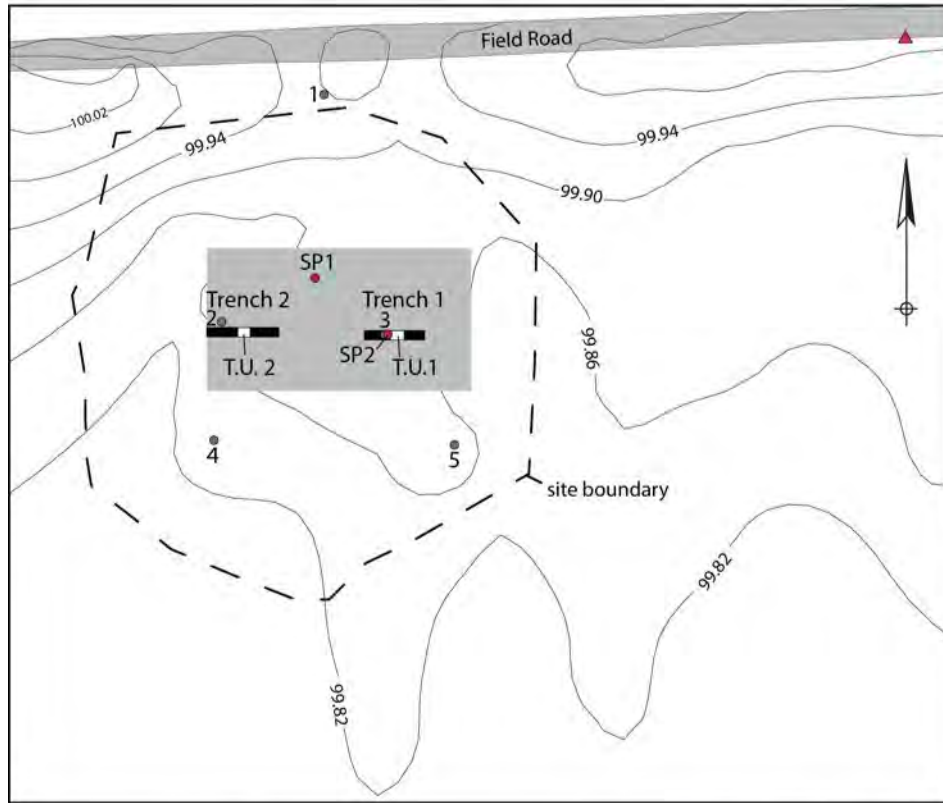
4.4.5.3.1 *Reconnaissance*

In the fall of 2011, a portion of Lighthouse Ditch, which was dry at the time, was walked and sediment exposed along the ditch banks examined for earthquake-induced liquefaction features. Several sand dikes, but no sand blows, were found and documented along the ditch. A time series of GE satellite imagery was examined in the vicinity of the sand dikes along Lighthouse Ditch in the hopes of finding surficial sand blows since they would have a greater potential for dating paleoearthquakes. On the satellite imagery, light-colored patches that persist through time and may represent sand blows were identified in the farmed fields north and south of Lighthouse Ditch (Figure 4-80). A cluster of large (roughly 120 m by 40 m) light-colored patches resembling sand blows occurs in the fields north of Lighthouse Ditch and east of a lateral ditch that drains from the north into Lighthouse Ditch. The bright tone of the patches suggests that the upper portion of the likely sand blows may have been truncated by land leveling. The patches appear elongated in the north-northeast direction and the overall trend of the cluster is along the same orientation. If these patches are in fact sand blows, their feeder dikes are likely to be oriented north-northeast as well.

In October 2012, the fields north of Lighthouse Ditch were visited to verify whether the north-northeast oriented light-colored patches seen in the satellite imagery are large sand blows. At the time of the site visit, the crops had been recently harvested and the soil surface was well exposed. The light-colored patches were found to be sandy on the surface and to be surrounded by silty soils. Lithic artifacts including an intact point (Late Archaic-Early Woodland expanding stem), the base of a broken point (Late Archaic stemmed), and flakes were found in association with two likely sand blows immediately south of the east-west farm road (Figure 4-81).

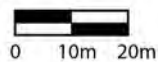


Figure 4-80 GE image showing location of Garner site outlined by solid white line, light-colored patches that cross site, and soil pits (indicated by blue flags) excavated in the patches to evaluate likelihood that they are sand blows. Fields have been graded making sand blows obvious. Lighthouse ditch is drainage south of site. Sand dikes were observed in banks of Lighthouse Ditch during reconnaissance of Late Pleistocene valley-train deposits in 2011. Satellite image was acquired by USDA Farm Service Agency on January 11, 2006.



Legend

- soil pit in likely sand blow (SP#)
 - geophysical survey area
 - ▬ proposed trench locations
 - ▭ test unit (T.U.)
 - piece plotted artifact
 - 1 = projectile point/knife (FSN 30)
 - 2 = biface (FSN 32)
 - 3 = groundstone fragment
 - 4 = projectile point/knife (FSN 29)
 - 5 = biface (FSN 34)
 - ▲ datum: N500 E500
- countour interval = 4 centimeters



Location Index Map



Figure 4-81 Topographic map of Garner site and inset location map. Site map shows locations of soil pits, geophysical grid, archaeological site boundary, test units, point plotted artifacts, and proposed trench locations. Actual trench locations deviate from proposed locations as described in text.

We hand dug one small soil pit in each of these two likely sand blows to observe their sedimentological characteristics (Figure 4-81). The soil pits revealed sandy layers containing lignite and small silt clasts, typical of sand blows in the region. Soil pit 1 was dug along the eastern flank of the western sand blow. The pit was 63 cm deep and almost entirely in sandy

sediment. As observed in the soil pit, the upper 28 cm are massive and mixed sandy loam interpreted as a plow zone. The plow zone is underlain by 28 cm of mottled red and gray fine to very fine sand, containing a few pieces of lignite and exhibiting some layering. The sand is underlain by gray silt. About 16 m southeast of soil pit 1, soil pit 2 was excavated to a depth of 40 cm in another likely sand blow. As observed in the soil pit, the upper 12 cm are a massive sandy loam and a plow zone. The plow zone is underlain by 8 cm of fine sand containing small clasts of silt. The sand layer overlies a thin soil developed in a gray silt. The gray silt extends to 35 cm below the surface. Below the gray silt is a 3 cm thick fine to very fine sand, which in turn is underlain by gray silt. The origin of the sandy units is difficult to interpret in such a small exposure, but they could represent one or two liquefaction events. Given the age of the sediments, the likely presence of one or two generations of sand blows, and the association of Late Archaic-Early Woodland artifacts with the sand blows, the Garner site was selected for further investigation.

4.4.5.3.2 Electrical Resistivity Surveys

In March 2013, geophysical surveys using electrical resistance tomography were conducted at the Garner site. On the basis of interpretation of satellite imagery and field inspection of likely sand blows described above in Section 2, one area was surveyed. The location of the geophysical survey area is shown on the topographic map of the site (Figure 4-81). Figure 4-82 shows the survey grid, consisting of multiple parallel profile lines within a rectangular area. All lines were 46 m in length. Data were collected using an AGI SuperSting resistivity meter, with automatic electrode switching capability. Each line consisted of 28 electrodes at 2-m spacing. An AGI mixed dipole array (similar to a conventional dipole-dipole configuration) was chosen for the data acquisition because this array provides optimal resolution for near-surface features and sufficient depth penetration to guide trench excavations. Measurement errors in the survey did not exceed 0.2%.

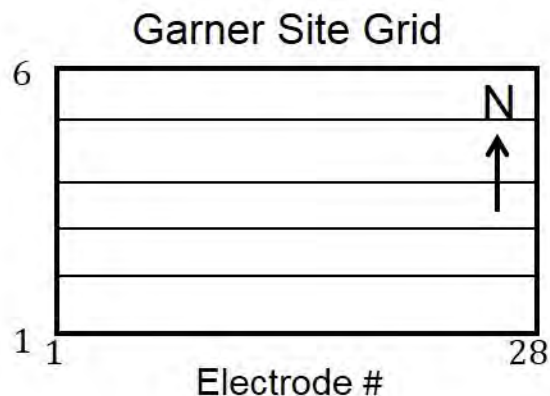


Figure 4-82 Layout of resistivity survey grid at Garner site. Grid consisted of multiple parallel profile lines, spaced at 5 m apart. Each line consisted of 28 electrodes at 2-m spacing.

Raw data observations of apparent resistivity from all profile measurements were processed using AGI's 2D EarthImager software to produce cross-sections of the true subsurface resistivity distribution. If one assumes that the true resistivity distribution in the subsurface is correct, the model is validated by using a forward-modeling technique to predict the apparent resistivity distribution. Statistical measures of the solution are thus obtained. The maximum RMS data error in the inversions was less than 5%.

Survey Results

Figure 4-83 to Figure 4-84 contain composite images of the resistivity data acquired at the Garner site. The grid contained six parallel profile lines numbered from south to north (Figure 4-82). Several profile lines contain features that indicate possible feeder dikes that connect a deeper zone of high resistivity to likely sand blow deposits at the surface, making this site particularly intriguing. Line 2 shows a possible westward dipping sand dike at ~29 to 30 m along the profile (Figure 4-83). The feature appears to connect with the deeper deposit as seen in the cross-section of Line 3 to the north. A similar, though less resistive, feature is evident in Lines 4 and 5 (Figure 4-84). On Line 3, a resistive area along the surface, a likely sand blow, and a linear feature extending downward from the base of the resistive area (~3 to 4 m), a possible sandy feeder dike, are seen on the western end of the profile. The higher resistivity area along the surface expands eastward to cover the central portion of the grid in Line 6 to the north (Figure 4-84).

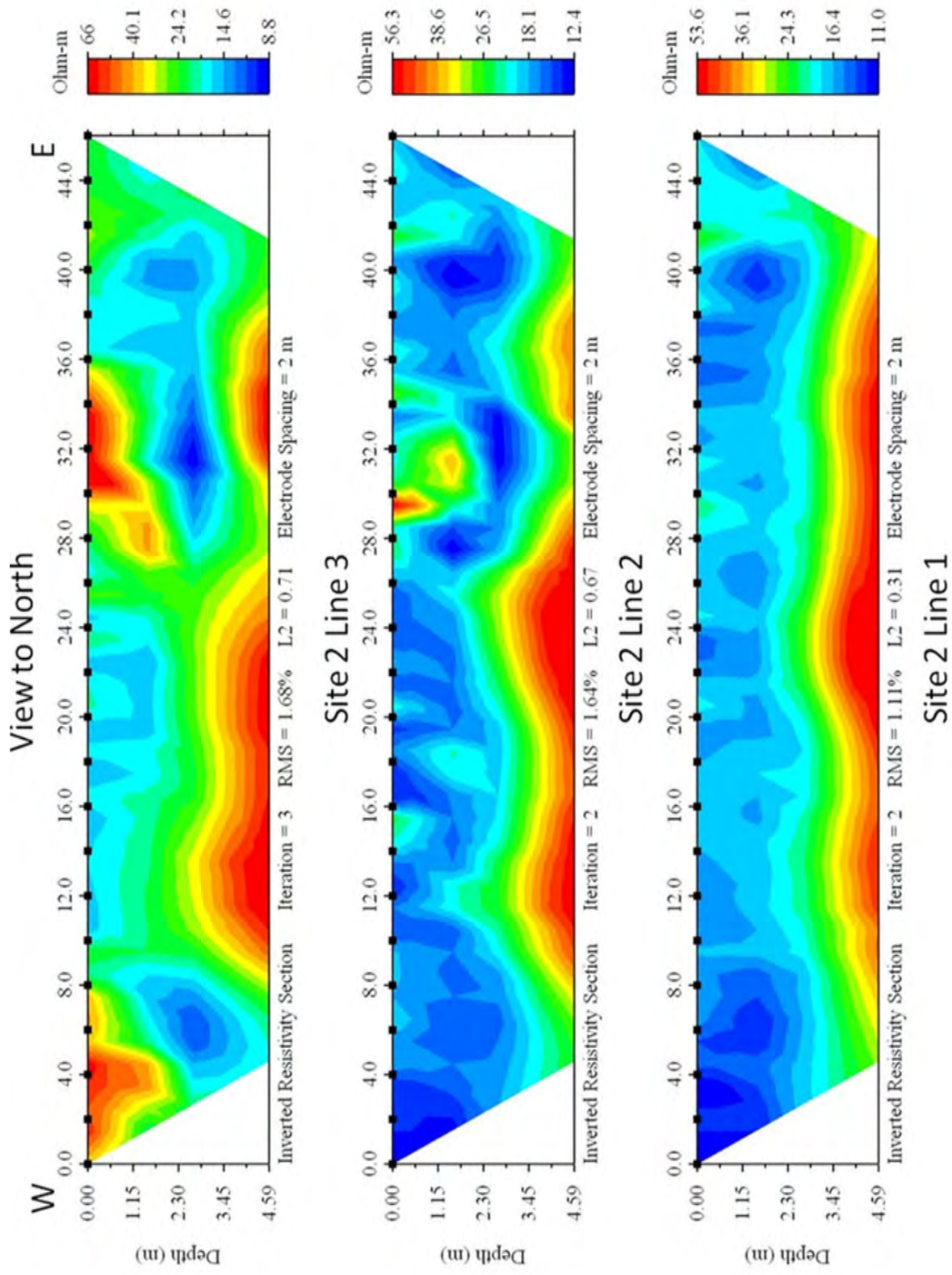


Figure 4-83 Composite Resistivity Images of Lines 1, 2, and 3 from Garner Site

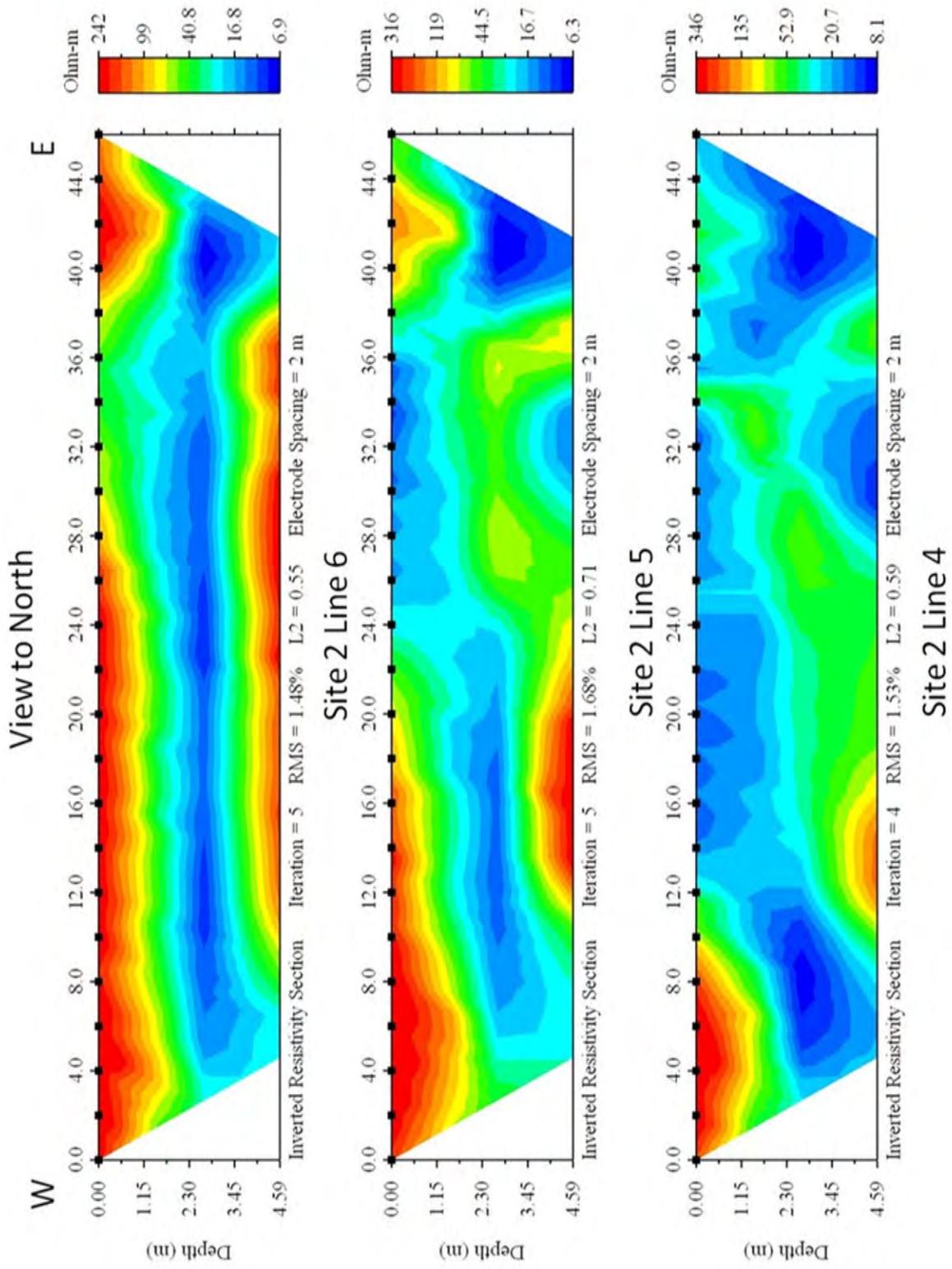


Figure 4-84 Composite Resistivity Images of Lines 4, 5, and 6 from Garner Site

4.4.5.3.3 *Pre-Trenching Archaeological Evaluation*

The Garner site was evaluated in March 2013. At the time, the field was fallow with the 2012 crop plowed under and surface visibility approaching 100 percent (Figure 4-85). A controlled surface collection (CSC) was conducted at the Garner site (3CG1255) in order to map the distribution of artifacts on the surface. This was followed by excavation of archaeological test units, also known as shovel tests, within the footprint of the proposed trenches.



Figure 4-85 Photograph of Garner site (3CG1255). Field was fallow and visibility of ground surface was about 100%. View is towards northeast.

Controlled Surface Collection

An 80 m by 100 m grid with twenty 400 m² collection cells was established. It was oriented relative to magnetic north with its northeast corner at N494.265 E430.497. This grid effectively covered the archaeological site as defined by the surface artifact distribution (Figure 4-86).

A 20 m x 20 m grid cell size (400 m²) was used because of the relative low density of the artifact scatter and the likelihood that land leveling had altered the distribution of surface and near surface material in the agricultural field. This grid size reduced the number of collection units while maintaining enough horizontal control to facilitate the identification of potential artifact concentrations.

All obvious and all suspected prehistoric artifacts were collected, including fire-cracked rock (FCR), as well as historic artifacts, unmodified rock, cannel coal, and concretions. The majority of the prehistoric materials consisted of chipped stone artifacts (e.g., chert debitage, bifaces and biface fragments, unifacial tools, utilized/retouched flakes, cores) but also included a small number of groundstone tool fragments and small pieces of fired clay. Only samples of the historic artifacts found in collection units were collected in the field.

Diagnostic artifacts were collected from the site prior to the March 2013 assessments. These include projectile points, bifaces, and a groundstone tool that are point plotted on the site map (Figure 4-81 and Table 4-20).

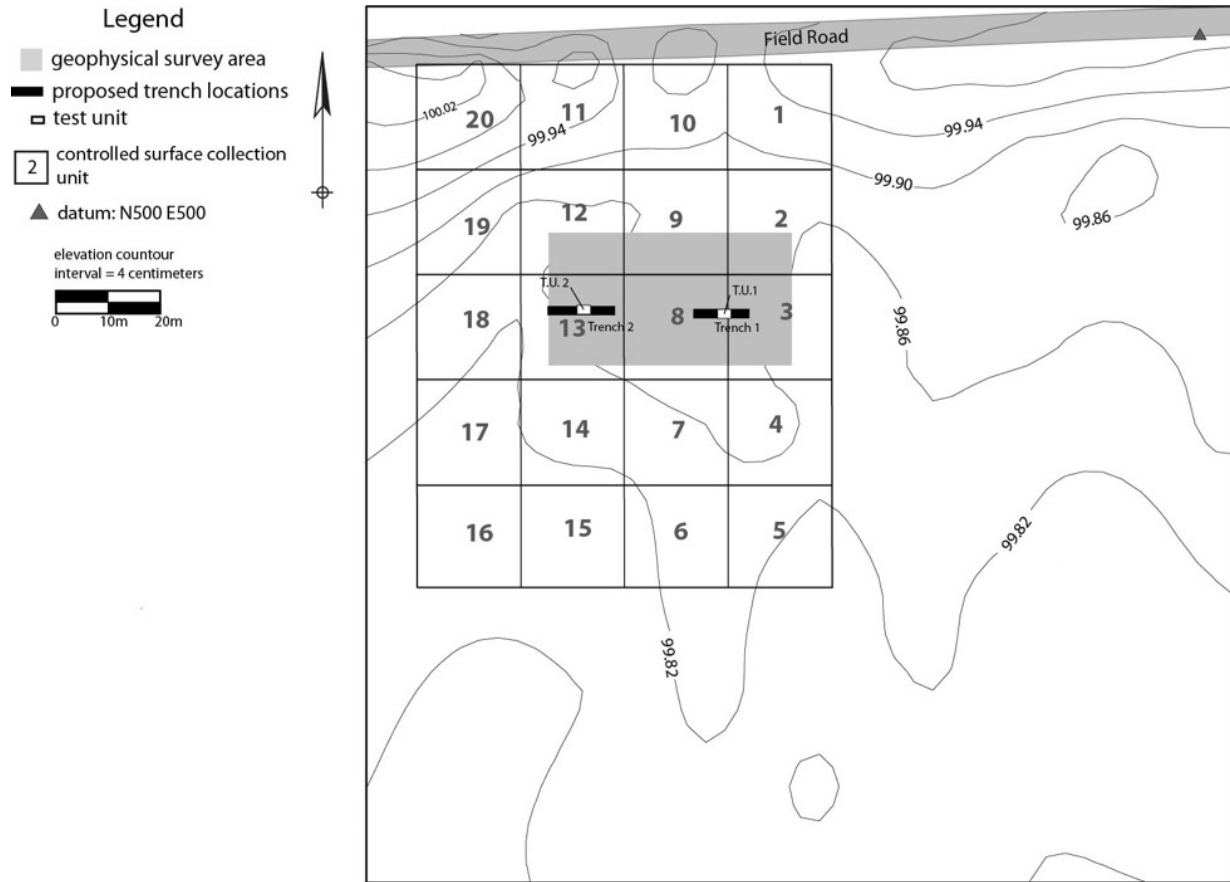


Figure 4-86 Map of Garner site (3CG1255) showing location of controlled surface collection grid relative to geophysical survey area or grid, proposed trench locations, and archeological test units.

Table 4-20 Point Plotted and General Surface Artifacts

FSN	Description	Ct	Wt	Location
2013-456-29	projectile point/knife	1	11.3	P.P. on site map
2013-456-30	projectile point/knife	1	10.7	P.P. on site map
2013-456-36	projectile point/knife	1	10.8	W.P. 977 general surface
2013-456-37	projectile point/knife	1	13.4	W.P. 895 general surface
2013-456-31	biface fragment	1	6.2	P.P. general surface
2013-456-32	biface fragment	1	4.8	P.P. on site map
2013-456-33	biface fragment	1	10.2	P.P. general surface
2013-456-34	biface fragment	1	7.3	P.P. on site map
2013-456-35	groundstone tool fragment	1	280.0	W.P. 975 on site map

Four hafted projectile point/knives (ppks) were recovered from the surface (see Figure 4-81). These include a possible Hardin ppk of Early Archaic period age, a stemmed ppk of probably Late Archaic age, and two basal fragments of what are possibly Late Archaic to Early Woodland expanding stem ppks (Figure 4-87).



Figure 4-87 Points from Garner site (3CG1255), left to right, Early Archaic (possible Hardin) point, field specimen number (FSN) 29, Late Archaic stemmed point (FSN 37), two Late Archaic to Early Woodland expanding stem points (FSN 36, FSN 30).

A total of 879 pieces of chert debitage (flakes and shatter) and tools (bifaces, unifaces, and cores) were retrieved within the collection area, with a mean density of 43.9 chipped stone artifacts per 20 x 20 m collection square, or 0.1095/ m² (43.9/400). Individual unit counts for chipped stone artifacts range from 9 to 157. The collection grid also yielded a total of 103 pieces of FCR with a

mean density of 5.2 pieces per 20 m collection square, with individual square counts ranging from 0 to 22. See Tuttle et al. (2014) for data tables of artifacts recovered during the controlled surface collection.

Artifact density maps for chert debitage (Figure 4-88) and FCR (Figure 4-89) were generated to show distribution of prehistoric materials within the collection area. Two additional maps were created showing the distribution of expedient chert tools (retouched/utilized flakes) (Figure 4-90) and cores and core fragments (Figure 4-91) by shading each collection block a different color based on the number of artifacts found in each block.

The distribution of chipped stone debitage generally matches that of FCR. The pattern consists of two high density concentrations of chert debitage and FCR that overlap in collection unit 8 at the center of the grid. The distribution of expedient chert tools, consisting of retouched and/or utilized flakes, largely corresponds to areas with high density of chipped stone debitage. Chert cores and core fragments occur in higher numbers in collection units 13 and 12 immediately west and northwest of collection unit 8, which marks the north end of the high-density distribution of chert debitage. The chert cores from units 13 and 12 were found on the east side of both units. In general, artifact density is higher in collection cells on the east side of the grid.

Test Units

Two archaeological test units, designated 1 and 2, were excavated in the footprint of proposed Trenches 1 and 2 (Figure 4-81). Test Unit 1 was excavated at 33 m and Test Unit 2 at 6 m along the geophysical profile 3 to expose the sand blows and the buried soils below. Since the proposed Trenches 1 and 2 were only 10 and 12 m long, respectively, the test units were placed at the midpoints of the footprints. A groundstone artifact had been recovered from the surface in the center of the footprint of proposed Trench 1 and near Test Unit 1. A biface was collected from the surface of the site and in the center of the footprint of proposed Trench 2 and near Test Unit 2. After removing the plow zone as a single stratum, both test units were excavated in 10 cm levels. See Tuttle et al. (2014) for data tables of artifacts recovered from the test units.

Test Unit 1 (TU1) was excavated to 60 cm below the surface (cmbs) (Figure 4-92 to Figure 4-94). The 10-20 cm thick plow zone is a dark grayish brown (10YR4/2) sandy loam. Two plow scars are present in the north and south profiles. The slope of the scars suggest that the plow was a turning plow. A few plow scars extend deeper into the underlying units. Below the plow zone, there is 10-20 cm of light yellowish brown (10 YR 6/4) fine-medium sand with some lignite that is likely to be part of a sand blow. Below the sand blow is a very dark gray brown (10YR6/3) to pale brown (10YR6/3) silt. The upper 1-2 cm is darker (10YR6/3) in places and likely represents a buried soil. One flake was recovered from the upper few centimeters of the buried soil. The lowest layer, from 45-60 cmbs, is a light brownish gray (10 YR 6/4) silt with brownish yellow (10YR6/6) mottles, also known as redoximorphic features, that form as the result of reduction, movement, and oxidation of iron and manganese oxides in seasonal saturated soils (Veprakas, 1992).

The frequency of artifacts per level recovered from Test Unit 1 is presented in Figure 4-95. Most of the artifacts were recovered from levels 3 and 4, at a depth of 30-50 cmbs. These two levels occur in the upper 20 cm of the very dark grey brown to pale brown silt beneath the likely sand blow.

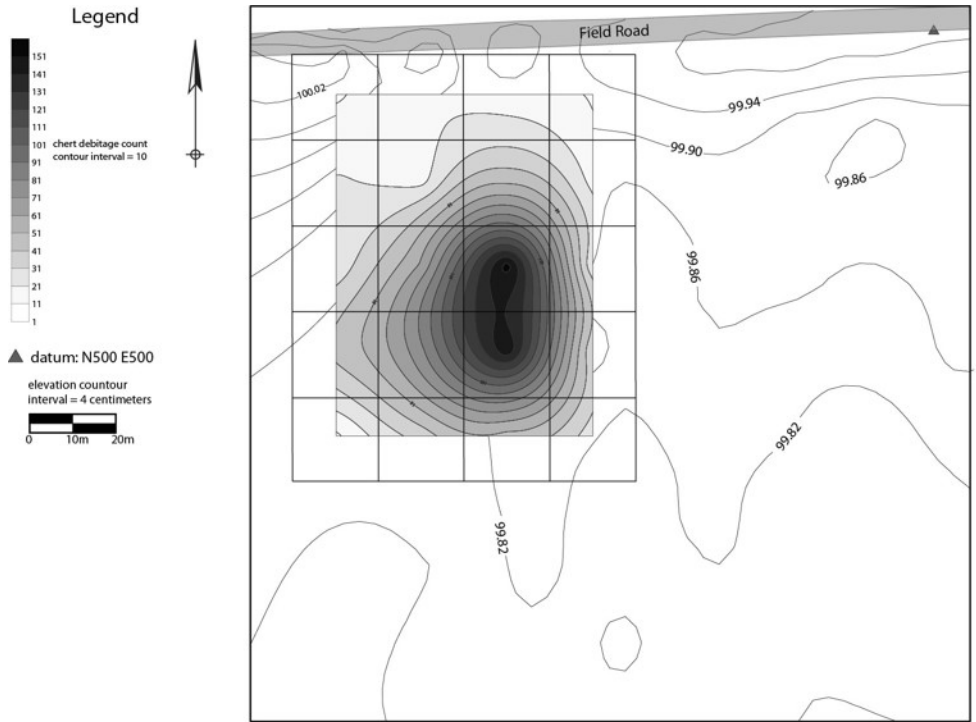


Figure 4-88 Artifact Density Map by Count of Chert Debitage at the Garner Site

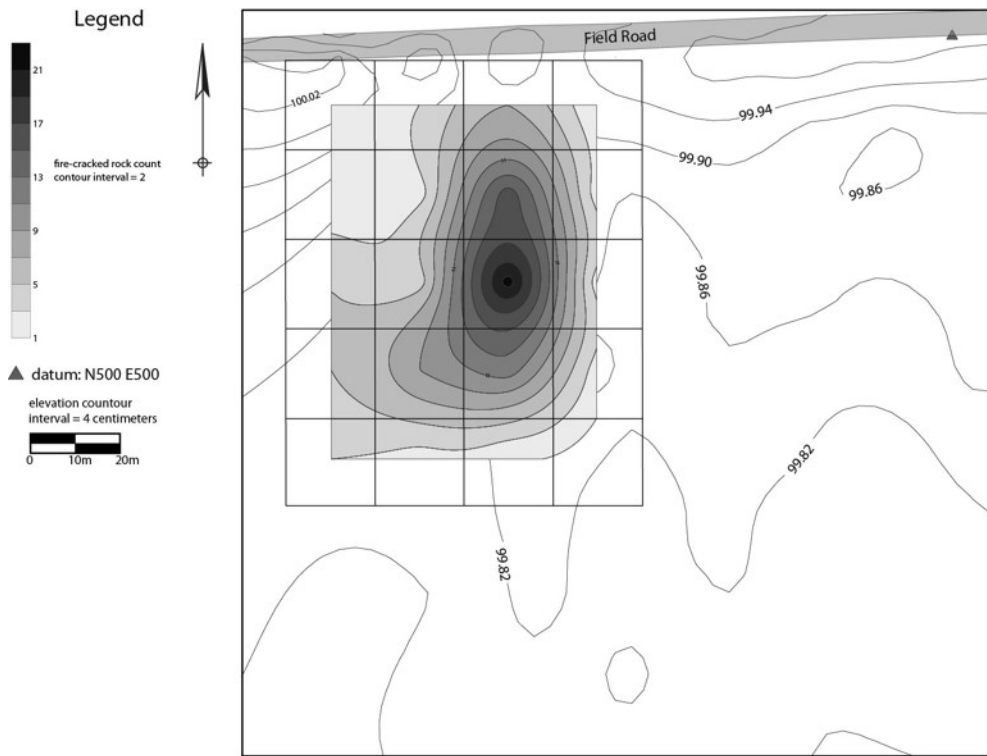


Figure 4-89 Artifact Density Map by Count of Fire-Cracked Rock at Garner Site



Figure 4-90 Distribution of Retouched/Utilized Flakes at the Garner Site

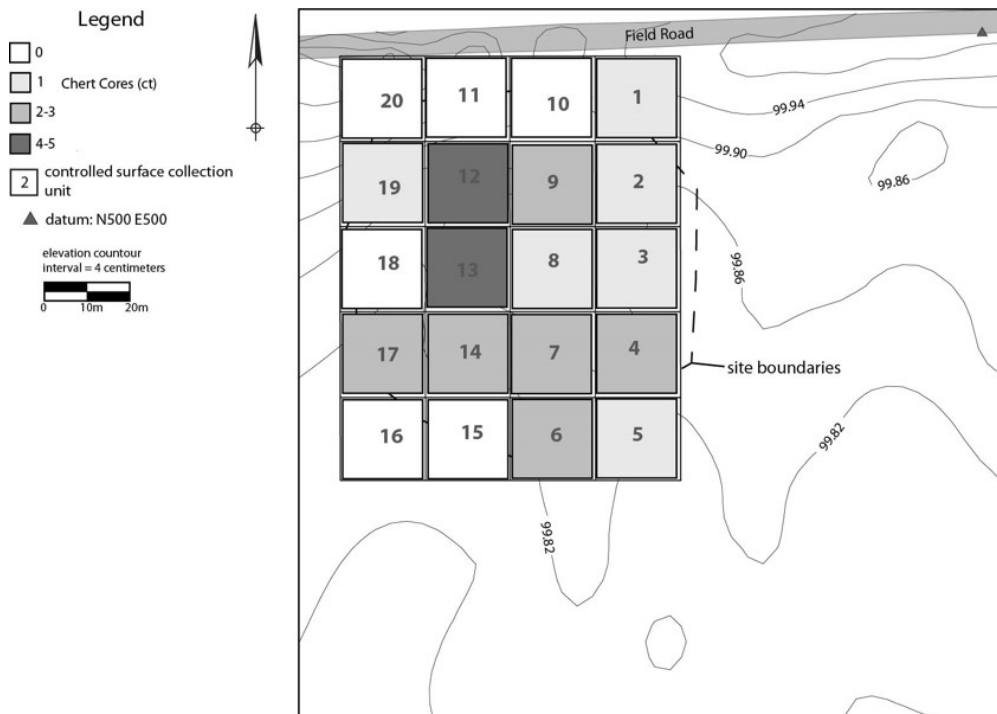


Figure 4-91 Distribution of Chert Cores and Core Fragments at Garner Site



Figure 4-92 Garner Site, 3CG1255, Photograph of Test Unit 1, North Profile

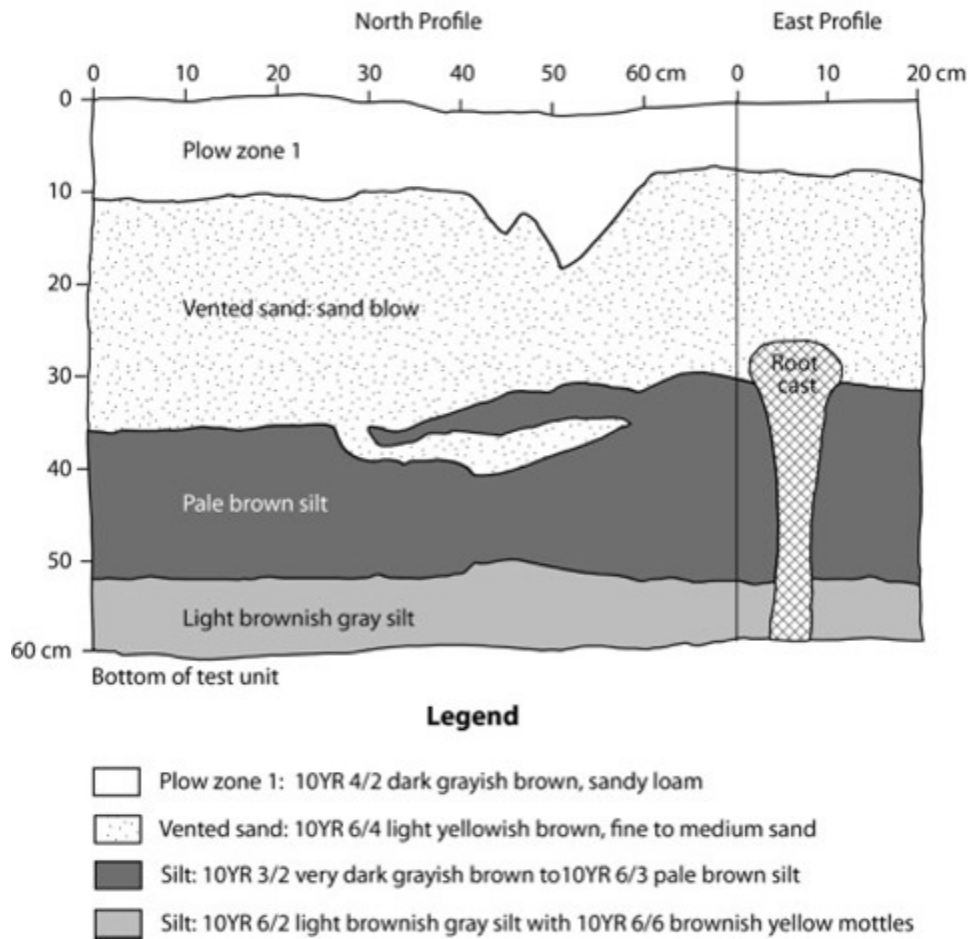


Figure 4-93 Garner Site, 3CG1255, North and East-Wall Profile of Test Unit 1

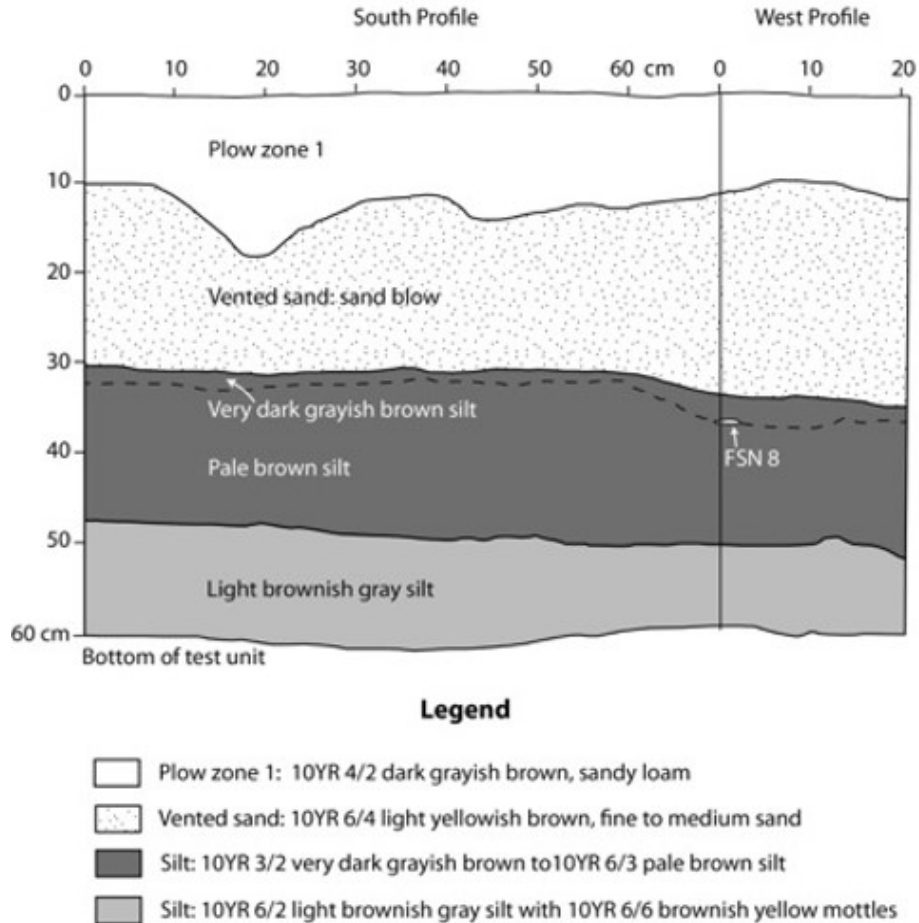


Figure 4-94 Garner Site, 3CG1255, South- and West-Wall Profile of Test Unit 1

Test Unit 2 was excavated to 50 cmbs and exposed six layers (Figure 4-96 and Figure 4-97). The plow zone has upper and lower zones. The upper zone is from 8-10 cm thick and is a massive dark brown (7.5YR 3/2) sandy loam. The lower plow zone is a slightly lighter brown (10YR 4/3) sandy loam to a depth of 15-24 cm. At the base there is a sloping plow scar similar to others found in most of the test units excavated in this project. The plow zone is underlain by a light yellowish brown (10YR 4/6) silty fine sand, with brownish yellow (10YR 6/8) redoximorphic features, that is likely to be part of a sand blow. It is underlain by a brown (10YR 4/3) to pale brown (10YR 6/3) silt with few yellowish red (5YR5/8) redoximorphic features. The upper 1-2 cm of the silt is slightly darker and likely represents a buried soil. The lower portion of the silt is brown (10YR 5/3) with numerous yellowish red redoximorphic features. The layering exposed in Test Units 1 and 2 are similar.

Artifacts frequency per level recovered from Test Unit 2 is presented in Figure 4-98. Similar to Test Unit 1, most of the Test Unit 2 artifacts were from the brown to pale brown silt below the likely sand blow. The presence of some artifacts in the plow zone above the vented sand raises the possibility that there may have been occupation both above and below the sand blow. Alternatively, the artifacts had been brought to the surface by plowing or moved to the area by land leveling.

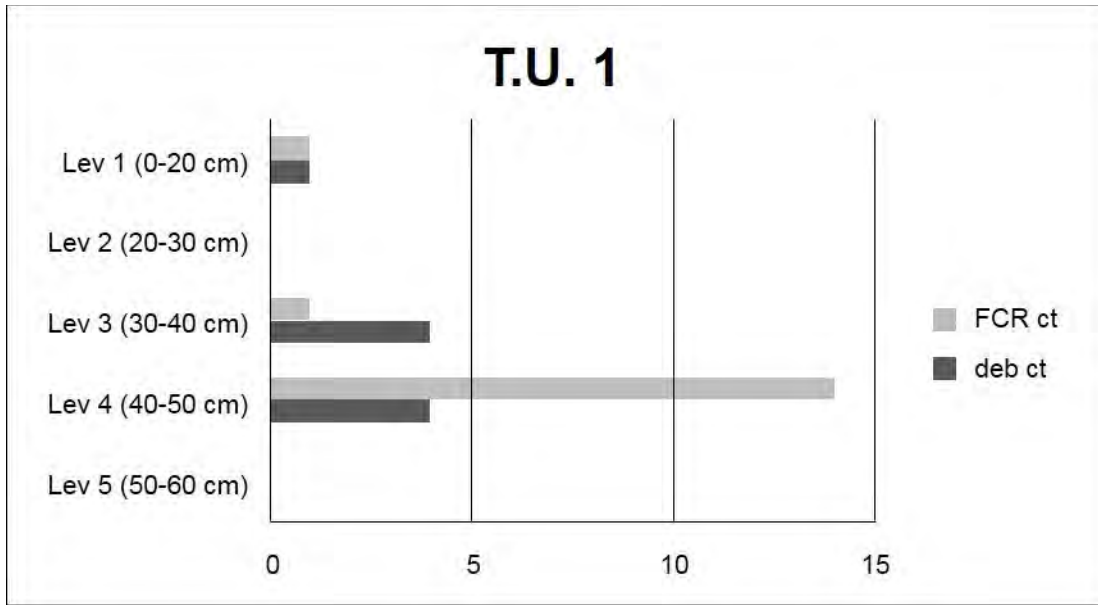


Figure 4-95 Chart showing the frequency of debitage and fire-cracked rock per level in Test Unit 1, Garner site (3CG1255).



Figure 4-96 Garner Site, 3CG1255, Photograph of Test Unit 2, North Profile

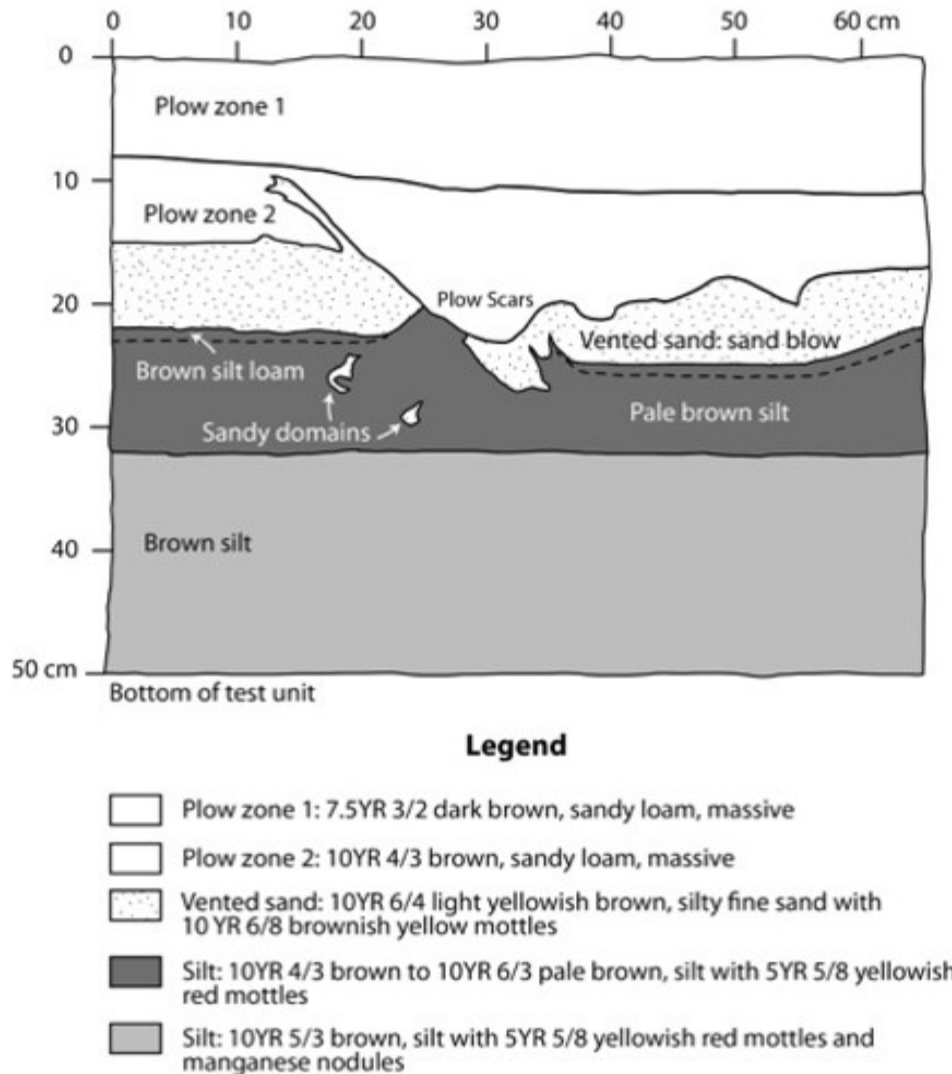


Figure 4-97 Garner Site, 3CG1255, North Wall Profile of Test Unit 2

Initial Assessment

The surface collections at the Garner site (3CG1255) revealed a low intensity scatter of artifacts over a rather wide area. There is an apparent strong correlation between debitage and FCR distributions suggesting continuity in the spatial and functional use of the surface of site. The projectile points from the surface collection suggest that the site was periodically reoccupied from perhaps as early as 10,000 to about 2,000 or 3,000 years ago. Hafted ppks include implements that are Archaic and Woodland in age, but none of these were collected within the overlapping artifact concentrations in the east half of the collection area.

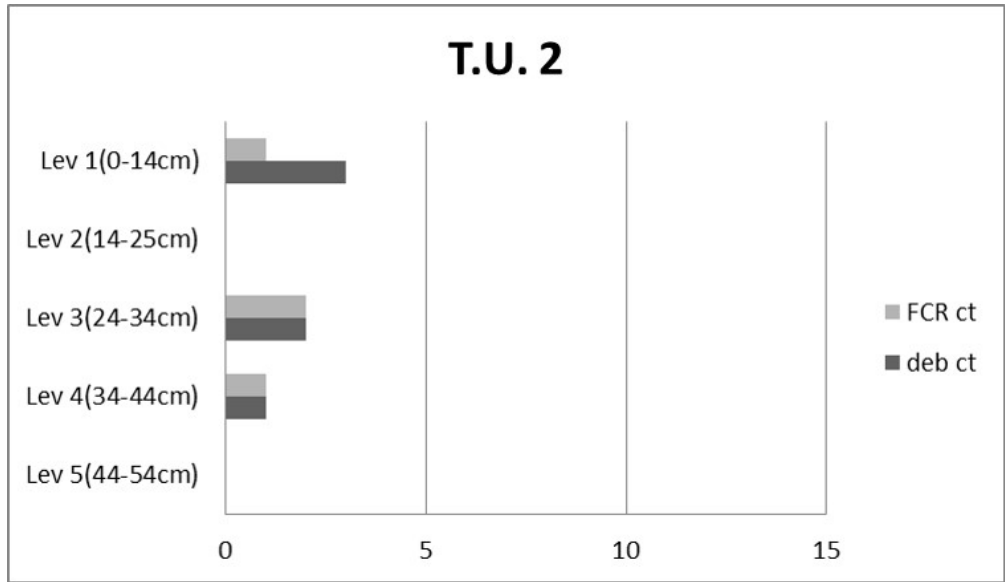


Figure 4-98 Chart showing frequency of debitage and fire-cracked rock per level in Test Unit 2, Garner site (3CG1255).

The similarity in the spatial distribution of debitage and FCR suggests that subsurface cultural remains may be present in the upper stratum the site. In other documented cases, similar patterns in the surface distribution of cultural materials have been found to overlies intact subsurface features (Lafferty et al., 1996 and 1987; Hargrave and Butler, 1992; DelCastello and Butler, 2000). These data alone, however, cannot be used as evidence of intact cultural remains immediately below the surface at Garner.

Other evidence supporting the possibility that subsurface cultural remains exist at the site was recovered in Test Units 1 and 2. The majority of the cultural material recovered from the test units was found in the soil horizons immediately beneath a sand layer that is likely to be a sand blow. It is possible that prehistoric sand blows covered a portion of the site, which has helped to preserve the archaeological deposits. Such a situation was encountered at the Dodd site in Pemiscot County (Tuttle et al., 1999) and at the Manly-Usery site in Mississippi County (Rathgeber, 2012).

4.4.5.3.4 Siting Paleoseismic Trenches

As described in Section 4.4.4.3.1, likely sand blows were located at the Garner site on the basis of interpretation of satellite imagery and field inspection including excavation of small soil pits. The presence of sand blows at the site was further supported by the results of electrical resistance tomography that imaged the likely sand blows and related feeder dikes. The electrical resistivity images provided vertical profiles of the likely liquefaction features that helped to select locations for the paleoseismic trenches. Resistivity profile number 3 was especially compelling with two high resistive areas on the surface, likely sand blows that appear to be connected by westward dipping resistive zones, likely feeder dikes, to a deeper high resistive area, likely sandy source beds. Therefore, Trenches 1 and 2 were proposed from 28-38 m and 0-12 m, respectively, along resistivity profile number 3 (upper profile in Figure 4-83; Figure 4-81).

4.4.5.3.5 Paleoseismic Observations

In November 2015, two trenches were excavated in exposed sand blows and associated sand dikes at the Garner site as proposed in the site evaluation report (Tuttle et al., 2014).

Trench 1

Trench 1 was 10.75 m long and varied from 0.25 to 0.85 m in depth (Figure 4-99). The eastern half of the trench was very shallow since excavation stopped at the contact between the sand blow and the soil/cultural horizon below. For the western half of the trench, excavation went deeper to expose the feeder dike of the sand blow. The contact between the sand blow and the soil was more than 15 cm higher west of the vent area of the sand dike than it was east of the vent area and apparently had been truncated by plowing. In fact, both IIA1 and IIA2 soil horizons with a combined thickness of 15 cm appear to have been removed west of the vent. Therefore, the surface of the soil/cultural horizon may have been 30 cm higher west of the vent area.

Beneath the plow zone, the sand blow, up to 25 cm thick, was composed of one depositional unit (L1) of fine to very fine sand that exhibited normal grading and contained a few stringers of lignite and scattered clasts of silt. The sand blow thinned towards the eastern end of the trench and was absent west of the vent area. It is possible that the sand blow had extended towards the west but had been destroyed by plowing. The sand blow was stained throughout by iron and manganese. Manganese staining was especially prominent in the lower 5 cm of the layer.

A sand dike (also unit L1) was connected to the base of the sand blow near its western end (below the 3 m mark on Figure 4-99). As measured across the trench, the dike had a strike and dip of N46°E and 10°NW. The dike was only 5-7 cm wide where it breached the A horizon but was up to 30 cm within the underlying B horizon. The dike was composed mostly of medium and fine sand but also contained a lens of pebbly sand. There were many clasts of silt within the dike, especially near the vent area, where the dike appears to have branched as it approached the surface. Domains of sand were observed near and along the base of the A horizon on both sides of the vent and may have been part of a sill intruded along the A/B horizon contact. The upper 1.5 m of the dike was stained by iron and manganese. The lower 1.5 m of the dike exhibited very light iron and manganese staining.

In Trench 1, the sand dike dips towards the northwest suggesting the source sand that liquefied is northwest of the trench. At this location, the ground surface at the time of the event, represented by the thin IIA1 soil horizon breached by the dike and buried by the sand blow, does not appear to have subsided as a result of venting of subsurface material but on the contrary to have been raised above the shallowly dipping sand dike. In fact, the amount of uplift is similar to the width of the dike. Ground deformation observed in Trench 1 resembles “blisters” that formed during the 2010 **M** 7.1 Darfield, New Zealand, earthquake (Villamor et al., 2016). The blisters were circular to elliptical mounds that formed as the result of uplift of the soil above dipping sand dikes. In cases where the sand dikes reached the ground surface, sand blows formed in association with the mounds (Figure 4-100).

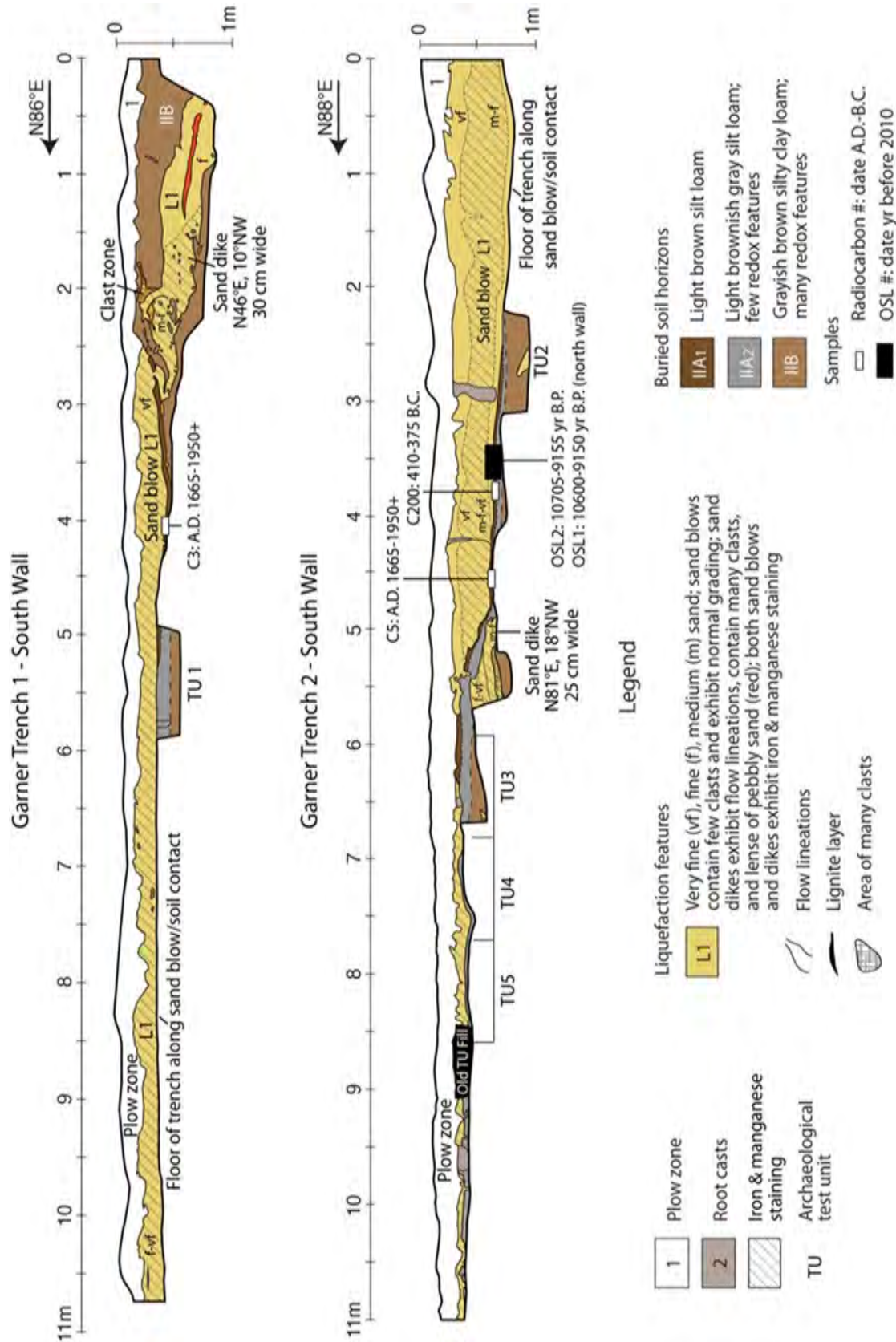


Figure 4-99 Logs of Trenches 1 and 2 at Garner site, showing sand blows and related sand dikes, location of archeological test units excavated in the soil/cultural horizon buried by the sand blows, and radiocarbon and OSL dates on collected samples.



Figure 4-100 Blister or surface mound that formed near Lincoln, southwest of Christchurch, during the 2010 M 7.1 Darfield, New Zealand, earthquake. Earthquake-induced liquefaction of subsurface sediment led to intrusion of dipping sand dikes (SD) into surface soil, lifting overlying soil to form blister. In this case, sand dikes reached ground surface and sand blow (SB) formed beside and on top of blister. Photograph by M. Tuttle.

Radiocarbon dating was performed on one organic sample from Trench 1. A sample of charred material collected (TR1-C3) from the soil/cultural horizon below the sand blow yielded a calibrated date of A.D. 1665-1785, 1795-1890, 1905-1950+ (Table 4-21). This is a very young date and two of the three ranges post-date the 1811-1812 earthquakes. Unfortunately, the sample was probably from a plant root that had grown through the sand blow and into the silty soil below; and therefore, does not help to estimate the age of the liquefaction features or the earthquake that produced them.

Table 4-21 Radiocarbon Dating Results for the Garner Site

Sample # Lab #	¹³ C/ ¹² C Ratio	Radiocarbon Age Yr B.P. ¹	Calibrated Radiocarbon Age Yr B.P. ²	Calibrated Calendar Date A.D./B.C. ²	Sample Description
Garner- TR1-C3 BA-434561	-23.6	150 ± 30	285-165 155-60 45-0+	AD 1665-1785 AD 1795-1890 AD 1905-1950+	Charred material from cultural horizon buried by sand blow
Garner- TR2-C200 BA-452736	-25.3	2330 ± 30	2360-2325	BC 410-375	Buried soil 0-1.5 cm below sand blow
Garner- TR2-C5 BA-434562	-29.3	180 ± 30	295-255 225-135 115-110 95-85 30-0+	AD 1665-1695 AD 1725-1815 AD 1835-1840 AD 1855-1865 AD 1920-1950+	Plant material 0.5 cm below sand blow from buried soil

¹ Conventional radiocarbon ages in years B.P. or before present (1950) determined by Beta Analytic, Inc. Errors represent 1 standard deviation statistics or 68% probability.

² Calibrated age ranges as determined by Beta Analytic, Inc., using the Pretoria procedure (Talma and Vogel, 1993; Vogel et al., 1993). Ranges represent 2 standard deviation statistics or 95% probability.

Trench 2

While excavating Trench 2, its western end was extended 2.5 m towards the west to expose more of the sand blow and the surface of the intact buried soil and cultural horizon beneath the sand blow. The trench was stopped 3.5 m short on its eastern end, since the sand blow was only a few centimeters thick and mostly disturbed by plowing. Some plow scars extended through the sand blow and into the cultural horizon below. When excavation was completed, Trench 2 was 11 m long and it varied in depth from 0.2 to 0.87 m in depth (Figure 4-99). Similar to Trench 1, the eastern half of the trench was very shallow because the sand blow was thin and excavation stopped at the contact with the soil/cultural horizon below. For the western half of Trench 2, excavation went deeper to expose the feeder dike and the sand blow, which thickened towards the west. The western end of the trench was excavated to the contact between the sand blow and the buried soil/cultural horizon. Care was taken not to disturb the underlying soil/cultural horizon.

Beneath the plow zone, the sand blow, up to 65 cm thick, was composed of one depositional unit (L1) of medium, fine, and very fine sand that exhibited normal grading and contained a few scattered clasts of silt. The upper 10-20 cm of the sand blow were bleached and underlain by a 20-30 cm thick zone of iron and manganese staining. Small manganese nodules had formed in this zone. The lower 10-15 cm of the sand blow were less stained and the bottom few centimeters did not appear stained at all. The characteristics of staining suggest that iron and manganese had been leached from the upper part of the sand blow probably by rainwater and had accumulated in the middle part of the sand blow. The absence of staining in the lowest part of the sand blow was probably due to wet reducing conditions immediately above the relatively impermeable silty soil.

A large sand dike, and several small sandy domains, (also part of L1) were observed crosscutting the soil below the sand blow. The large dike had a strike and dip of N81°E and 18°NW and ranged up to 25 cm wide. In the exposures provided by the trench walls, the large sand did not connect with the sand blow above but was very close, within 2 cm in the southern wall, to making that connection (below the 5 m mark on Figure 4-99). Since the dike dips towards the

north-northwest, the dike likely connects with the sand blow south of the trench wall. The dike was composed of a lower layer of medium and fine sand with many silt clasts in the lowermost 5-8 cm and an upper layer of fine and very fine sand. The upper 5-10 cm of the dike were bleached similar to the upper part of the sand blow, suggesting that the two are indeed connected, facilitating the down-section movement of rainwater. Otherwise, the lower 20 cm of the dike exhibited light iron and manganese staining.

In Trench 2, the sand dike dipped towards the north-northwest, suggesting the source sand that liquefied is north of the trench. The ground surface at the time of the event, represented by the thin IIA1 soil horizon, dipped abruptly and then shallowly towards the northwest (between 6 m mark to 0 m mark on Figure 4-99). The sand blow, overlying the dipping surface, essentially filled the topographic low. It appears that the ground subsided as a result of removal of subsurface sediment due to liquefaction and venting. This style of ground failure at liquefaction sites is common in the New Madrid seismic zone (Tuttle and Barstow, 1996).

Radiocarbon dating was performed on two organic samples from Trench 2. A soil sample (TR2-C200) of the uppermost 1.5 cm of the soil buried by the sand blow yielded a calibrated date of B.C. 410-375 (Table 4-21). A sample of charred material (TR2-C5) collected from the soil/cultural horizon below the sand blow yielded a calibrated date of A.D. 1665-1695, 1725-1815, 1835-1840, 1855-1865, 1920-1950+ (Table 4-21). This is a very young date and three of the five ranges post-date the 1811-1812 earthquakes. A few root casts and modern roots were observed extending through the entire thickness of the sand blow. Unfortunately, the sample was probably from a plant root that had grown through the sand blow and into the silty soil below, and therefore, does not help to estimate the age of the liquefaction features or the earthquake that produced them. Two sediment samples collected of the soil buried by the sand blow yielded similar OSL ages of 9875 ± 725 yr (or 10540-9090 yr B.P.) and 9930 ± 775 yr (or 10645-9095 yr B.P.) (Table 4-22). These ages are much older than any of the radiocarbon dates.

Table 4-22 Optically Stimulated Luminescence Dating Results for the Garner Site

Sample Number	Lab Number	Cosmic Dose Rate (mGray/yr) ¹	Dose Rate (mGray/yr)	OSL Age (Yr) ²	Calendar Age (Yr) ³	Sample Description
OSL-1	BG4254	0.14 ± 0.01	2.27 ± 0.12	9875 ± 725	10540-9090	From Trench 2, north wall, quartz grains from buried soil below sand blow
OSL2-1	BG4253	0.14 ± 0.01	2.26 ± 0.12	9930 ± 775	10645-9095	From Trench 2, south wall, quartz grains from buried soil below sand blow

¹ Cosmic dose rate calculated from parameters in Prescott and Hutton (1994).

² Systematic and random errors calculated in a quadrature at one standard deviation. Datum year is A.D. 2010.

³ Years B.P. or before present (1950).

4.4.5.3.6 Archaeological Investigation

Excavation of Trenches 1 and 2 were conducted in accordance with the procedure developed for this project in order to comply with Section 106 of the National Historic Preservation Act (Appendix B). For both trenches, the plow zone was removed and the sand blow surface scraped in search

of intruding contexts. Then the sand blow was removed to the buried land surface, which was scraped by shovel and trowel. Test units were then excavated into the soil that had been buried by the sand blows (Figure 4-99). Cultural materials collected from the test units were later analyzed in the laboratory.

Test Units

In Trench 1, removal of the 15 cm thick, dark brown (10 YR 3/3) fine sandy loam plow zone failed to reveal any archaeological features intruding into the sand blow. After examination of the sub-plow zone surface, the sand blow was removed to the top of the light brownish gray (10 YR 6/2) silt below. This buried surface was marked by occasional plow scars and strong redoximorphic features, including weak 1-2 mm Fe-Mn concretions. Chert debitage and fire cracked rock also became immediately evident as this buried surface was cleared of remaining sand.

A test unit (TU) was laid out at 5 to 6 m east of the west end of Trench 1 (Figure 4-81) and excavation began in 5 cm arbitrary levels with soil removed screened through ¼" hardware cloth (Figure 4-99). Four levels were excavated: 0-5 cm below sand, 5-10 cm, 10-15 cm and 15-20 cm. The last level was culturally sterile. Soil development in the homogeneous light brownish grey silt was weak and the concretion formation appeared to be the result of water percolating through the sand blow, reaching a perched water table that formed above the rather impervious silt. In contrast to the 1-2 mm concretions at the contact, by 5-10 cmbs there were more and larger (2-4 mm) concretions (Figure 4-101). By 10-15 cmbs, there were fewer concretions and the soil was heavily mottled (Figure 4-102 and Figure 4-103). Excavation ended at 20 cmbs, where mottling and mineral concentration were decreasing but evidence of biological activity was still clear (Figure 4-104). As a potential indication of disturbance, a very small fragment of iron/steel wire was recovered from the 10-15 cm level; downward filtration of such a relatively heavy, very small, bi-pointed item is not unexpected and is not considered an indication of a significant level of disturbance. Artifacts from TU 1 are summarized below (Table 4-23). Fire-cracked rock (FCR) was the dominant artifact class recovered (n=50), with only 8 pieces of chert debitage.



Figure 4-101 3CG1255, Trench 1, TU 1, 5 cm below Base of Sand Blow



Figure 4-102 3CG1255, Trench 1, TU 1, 10 cm below and blow, showing increasing Fe-Mn concentration.



Figure 4-103 3CG1255, Trench 1, TU1, 15 cm below sand blow, showing fissures and/or root cast, with pronounced mottling or redoximorphic features.

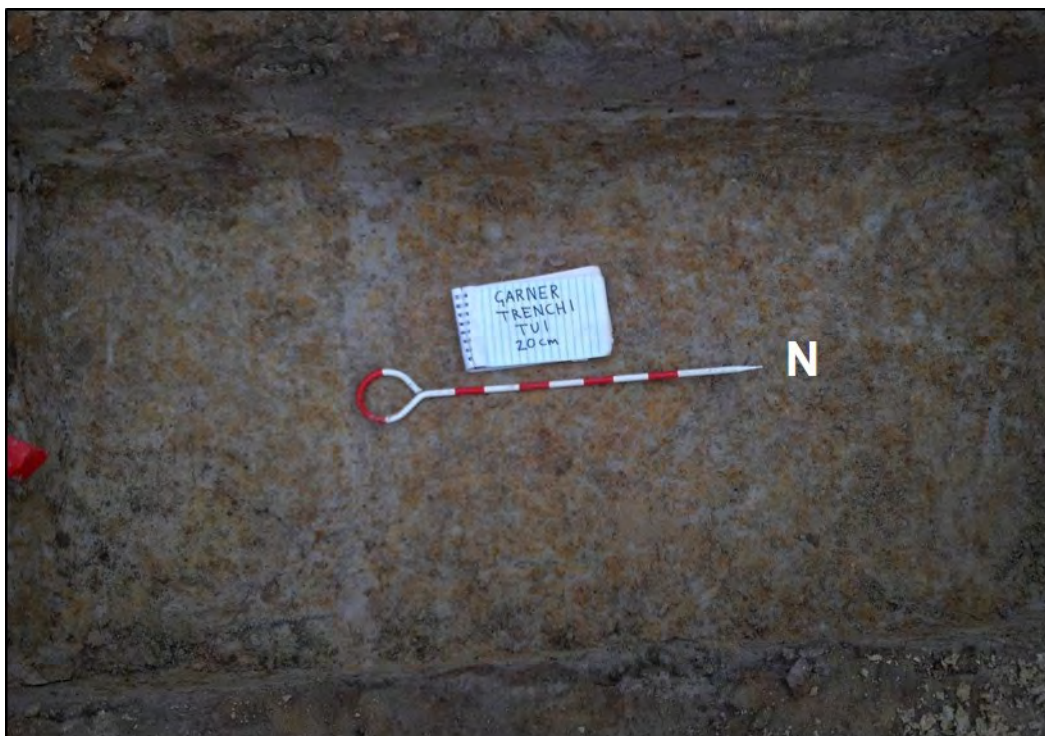


Figure 4-104 3CG1255, Trench 1, TU 1, 20 cm below sand blow, fissure/root cast more pronounced but Fe-Mn concentration decreasing.

Table 4-23 3CG1255, Trench 1, TU 1 Artifact Recovery

Level	Debitage	Other	Totals
0-5 cm	1 secondary decortication flake 1 flake fragment	14 FCR 1 quartz pebble 1 concretion	18
5-10 cm	2 biface thinning flakes 1 core fragment/shatter	23 FCR 1 quartz pebble 1 concretion	28
10-15 cm	2 biface thinning flakes 1 flake fragment	13 FCR 1 wire	17
15-20 cm			No artifacts
Totals	8debitage	50 FCR 2 pebbles 2 concretions 1 wire	63

Trench 2 was excavated in the same manner as Trench 1. Artifacts were again recovered at the contact between the sand blow and the buried land surface. In particular, a side-notched projectile point basal fragment was recovered immediately below the sand blow on the top of the old land surface (62 cmbs). Diffuse charcoal was again noted at the contact, but without any clear cultural context. There was abundant Fe-Mn concentration in small, weak concretions at the contact.

Test Unit 2 was placed at the originally mapped west end of Trench 2, which was subsequently expanded to the west (Figure 4-99). TU 2 was excavated in 5 cm thick arbitrary levels. Level 1 (0-5 cm below sand) was loamy silt noticeably darker (10 YR 5/2 greyish brown) than subsequent levels. Level 2 (5-10 cm, Figure 4-105) and Level 3 (10-15 cm) were excavated through blocky subangular silt with heavy redoximorphic features and pronounced clay skins on soil ped surfaces. Concretions began at about 10 cm, where other redoximorphic features were also noted. Level 4 (15-20 cm; Figure 4-106) was blocky, heavily mottled grey (2.5 Y5/0) to grayish brown (2.5 Y 5/2) silt with abundant evidence of root casts and sand filled fissures. This unit produced 12 artifacts, including 5 debitage and 4 fire-cracked rock (Table 4-24).

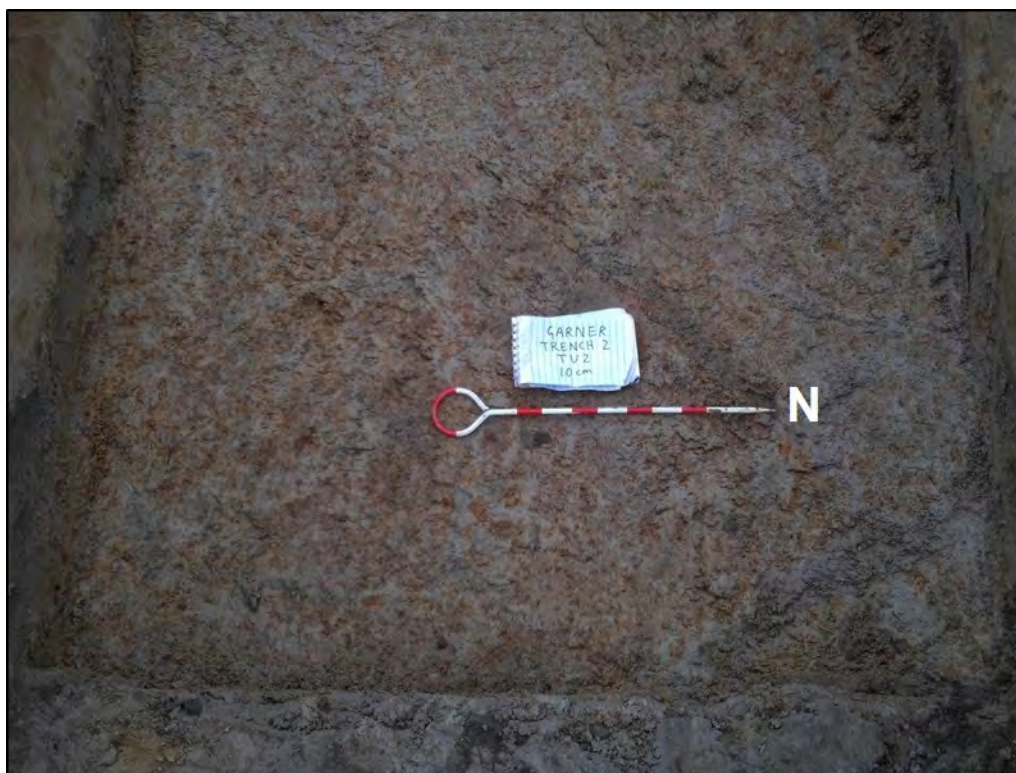


Figure 4-105 3CG1255, Trench 2, TU2, at 10 cm below Sand Blow



Figure 4-106 3CG1255, Trench 2, TU 2, 20 cm below Sand Blow

Table 4-24 TU 2 Artifact Recovery

Level	Debitage	Other	Totals
0-5 cm	1 primary decortication flake 2 secondary decortications flakes 1 flake fragment	3 FCR 1 quartz pebble 1 bone	9
5-10 cm			No artifacts
10-15 cm	1 core fragment	1 FCR 1 concretion	3
15-20 cm			No artifacts
Totals	5 debitage	4 FCR 1 pebble 1 bone 1 concretion	12

Test Unit 3 was placed east of TU 2. A little partially carbonized wood and fibrous material that appeared to be Johnson grass rhizomes was noted in scraping away remnants of the sand. It is not unusual to find Johnson grass rhizomes at several meters depth. The old land surface of this unit sloped downward to the west due to subsidence as sand was ejected (Figure 4-99). The unit was excavated to 25 cmbs (Figure 4-107 and Figure 4-108). The southeast corner of this test unit contained a poorly defined 15 cm x 15 cm concentration of oxidized, weakly fired soil interlaced with sand veins (Figure 4-109).



Figure 4-107 CG1255, Trench 2, TU 3, north wall and floor at 25 cm below sand blow, showing strata sloping from collapse after ejection of sand. 1: modern plow zone, 2: sand blow, 3: buried soil/cultural horizon.



Figure 4-108 3CG1255, Trench 2, TU3, at 25 cm below sand blow, unit excavated horizontally and so crosscutting sloping strata, shown by differential mottling.



Figure 4-109 3CG1255, Trench 2, TU 3, southeast corner of completed unit showing possible tree disturbance originating below sand blow.

Examination of the overlying sand blow provided no indication that this ill-defined burned area extended from above. It was not evident at the surface of the old soil when excavation began and was only noted at about 15 cm below the buried land surface; this material extended to 25 cm below the sand. This vaguely disturbed area is interpreted as non-cultural, probably a tree stump, and was not further treated as an archaeological feature. An OSL column producing dates indicating burial ca. 9000 to 10,000 years ago was excavated in the north wall of this test unit; while the natural disturbance in the unit was limited to the south wall. The old land surface-sand blow contact in this unit also produced a radiocarbon date (C200) indicating carbonization ca. 410-375 B.C. Artifacts from TU 3 are summarized in Table 4-25 material recovered included 8 pieces of debitage and 10 fragments of fire-cracked rock.

Table 4-25 TU 3 Artifact Recovery

Level	Debitage	Other	Totals
0-5 cm	1 secondary decortication flake 1 core trimming flake 2 utilized flakes		4
5-10 cm	1 biface thinning flake 2 flake fragments	9 FCR 1 burned earth	13
10-15 cm	1 biface thinning flake	1 FCR	2
15-20 cm			No artifacts
Totals	8 debitage	10 FCR 1 burned earth	19

Test Unit 4 was placed east adjacent to TU3 to attempt to further define the indistinct area with weakly burned clods of clayey silt soil. Similar materials were recovered from an area extending 40 cm along the south wall of the trench and 30 cm north into the unit but again they were diffuse,

poorly consolidated and not clearly of cultural origin. This “feature” is interpreted as a tree stump burned out prior to deposition of the sand blow and prior to or perhaps contemporaneously with the deposition of the archaeological materials, rather than as a cultural feature in and of itself. TU 4 was excavated in four 5-cm thick levels. The southwest corner of the unit (50 cm x 50 cm) where burned soil was noted (Figure 4-110) was bagged as a soil sample for water screening in the same levels as the dry screen excavation; the few artifacts (1 flake and burned earth) recovered from the water screening were returned to the level bags. Little or no carbon was recovered and none was noted during excavation. A further potential feature, an area of homogeneous, lighter brown (10 YR 5/4) soil was noted in the southeast corner of TU 4 (Figure 4-111). It was distinguished primarily by the fact that the general matrix of TU 4 from 10 cm down was markedly mottled and blocky, while this soil area was homogeneous and finely granular. No artifacts were associated with this poorly defined area. It could not be defined in the overlying sand blow. It too is interpreted as a non-cultural, pre-sand blow tree root disturbance. Artifacts from TU 4 are summarized in Table 4-26. TU 4 produced 36 artifacts, including 4 debitage, 8 fire-cracked rock and a second projectile point/knife (ppk) fragment. This possibly corner-notched pp/k base from the 5-10 level is of material and manufacture similar to that recovered in clearing the top of the old land surface at 62 cm below the present surface.



Figure 4-110 3CG1255, Trench 2, TU 4, showings 50 cm x 50 cm fine-screen sample column in southwest corner.



Figure 4-111 3CG1255, Trench 2, TU 4, south wall, showing additional possible tree disturbance (soft, moist, dark stain in southeast corner).

Table 4-26 TU 4 Artifact Recovery

Level	Debitage	Other	Totals
0-5 cm	1 flake fragment	3 FCR 7 burned earth 1 charcoal	12
5-10 cm	1 biface thinning flake 1 ppk base	6 burned earth 3 charcoal	11
10-15 cm	2 biface thinning flakes	5 FCR 7 burned earth	14
15-20 cm			No artifacts
Totals	4debitage 1 ppk base	8 FCR 20 burned earth 3 charcoal	36

Test Unit 5 was placed east adjacent to TU4, to attempt to further define the possible tree stump stain. The unit was excavated in 5 cm levels to 25 cm below the sand blow (Figure 4-112). The sand blow thinned over this unit, so that the old land surface was marked by plow scars diagonal to the current north-south direction of cultivation (i.e., running northwest-southeast). TU 5 intersected a previous 1 ft x 2 ft test unit from 2013. It also produced the deepest deposits encountered, with materials recovered from 20-25 cm below the base of the sand blow. While adjacent units produced 5 (TU 2), 8 (TU 3) and 4 (TU 4) pieces ofdebitage, TU 5 produced 11 pieces ofdebitage, a pp/k tip, and 23 pieces of fire-cracked rock (Table 4-27).



Figure 4-112 3CG1255, Trench 2, TU 5 completed at 25 cm below base of sand blow; backfilled 2013 test unit is visible to east/left.

Table 4-27 TU 5 Artifact Recovery

Level	Debitage	Other	Totals
0-5 cm	2 bifacethinning flakes 1 flake fragment	1 FCR 1 burned sandstone 1 pebble	6
5-10 cm	1 biface thinning flake	3 FCR 1 concretion	5
10-15 cm	1 secondary decortication flake 2 biface thinning flakes 1 flake fragment 1 ppk tip	7 FCR	12
15-20 cm	1 secondary decortications flake 1 flake fragment	8 FCR 2 burned sandstone 2 burned earth	14
20-25 cm	1 biface thinning flake	4 FCR	5
Totals	11debitage 1 ppk tip	23 FCR 3 burned sandstone 1 pebble 1 concretion	42

Artifact Analysis

In addition to the projectile point/knife (ppk) base fragment recovered in clearing the sand blow base/old land surface contact in Trench 2, a second pp/k base of similar material and style was recovered from TU 4, 5-10 cm, and a nondiagnostic pp/k tip from TU 5, 10-15 cm (Figure 4-113).

The first specimen, from 62 cmbs, is 23 mm wide at the remaining section of blade, with a 16 mm wide stem. The notches are 4 mm wide. The basal margin is uneven, but markedly convex. Flaking is broad and random. There is no basal grinding, but the biface has a thin (6 mm), lenticular cross-section. The material is slightly chalky, smooth, high-quality white (5 YR 8/1) chert with faint pink banding. This biface may have failed in manufacture or use, with a transverse fracture originating at one notch. The second pp/k base is a stem only, but it may be from a corner-notched point. The stem is 25 mm wide at the convex base, 17 mm wide at the deepest preserved point of the notches, and 6 mm thick at the thickest point. The base is not ground. The material is again white (5 YR 8/1) somewhat weathered and stained, smooth, high-quality chert.

Regional projectile point morphology and chronology are discussed in Appendix F and are summarized here as it pertains to the admittedly speculative typology of the two fragmentary specimens. Notching (side, corner or intermediate) is typical of two widely separated periods - the Early Archaic and the Middle Woodland. Middle Archaic and Late Archaic/Early Woodland forms in our area are almost exclusively stemmed rather than notched (Table 4-16). First, we will discuss the Early Archaic forms. Consideration of the notched bases of well-thinned, white (Burlington/Crescent?) chert, along with the absence of pottery and the high density of fire-cracked rock, indicates that the sealed deposit at the Garner site may date to the Archaic period; however, it should be noted that this interpretation is open to question due to the fragmented nature of the two ppk bases as well as the limited area investigated. The fragmentary bases resemble the St. Charles (9000-8500 B.P.; McGahey, 2000) form, in that they are well-thinned and have expanding, convex bases, but are atypical of the heavily ground early Archaic form in having little or no evidence of basal grinding. The Cypress Creek pp/k (8000-7500 B.P.; McGahey, 2000) also has wide corner notches, expanding stems and broad, random flaking but these points are typically thicker and have a straight basal margin. While our specimens are well-thinned, an identification with the Early Archaic is improbable due to the lack of highly diagnostic basal grinding.

Since Early Archaic types probably can be dismissed, another typology to consider for the notched projectile point/knife base fragments is the Middle Woodland period, Hopewell-Marksville culture, Snyder cluster stem. The Snyder form proper (200 B.C.-A.D. 200; Justice and Kudlaty, 1999; 100 B.C.-A.D. 300; Perino, 1985) is also well thinned, with broad, random flaking; lenticular to flattened cross sections; excurvate bases on expanding stems and deep corner notches, and they too often occur on Crescent quarry type cherts and are found throughout the midcontinent from the Great Lakes to the Ozarks and Southern Plains margins. The form is allowed considerable morphological variation. The Gibson type (A.D. 250-350; Perino, 1985) is a later Snyders cluster variant with excurvate base and notched placed slightly higher (i.e. side-notched). Gibson points are typical of the Illinois Valley, eastern Missouri and regions to the north. A final type to consider is the Jack's Reef and Racoon points (Late Woodland, AD 800-1000), which are made on a very thin, flattened pentagonal biface with wide and irregular flaking. The Jack's Reef forms are considered corner-notched while the Racoon variant is side-notched (the actual difference being small and best determined from intact specimens). These last two Late Woodland notched forms are uncommon in the project area. All of the forms considered can be expected on the high-grade white cherts of the midcontinent, and all have Midwestern and Central Mississippi Valley affiliations. The lack of basal grinding is the strongest argument for a Middle Woodland, rather than Early Archaic, affiliation for the 3CG1255 buried component.



Figure 4-113 Projectile point/knife bases from excavation. Left, 62 cmbs, top of old land surface; Right, TU 4, 5-10 below sand blow.

While it is difficult to argue from negative evidence, it should be pointed out that no pottery was recovered from any sub-sand blow contexts in the approximately 5 square meters excavated in 2015. An aceramic component does not, however, in and of itself argue for pre-Woodland occupation, as Early and even Middle Woodland hunting and other extraction or non-habitation camps may not have required pottery. It should be noted that the records review (see Appendix F) indicated that, after Late Woodland, Late Archaic components are the most common occupation period reported for this portion of the Eastern Lowland. The fact that Early and Middle Woodland components are so poorly represented in the area may be the result of pottery being used on few sites of the period, leaving them to appear to be Archaic rather than Woodland sites. Other diagnostic artifact classes besides Tchula (Early Woodland) and Marksville (Middle Woodland) ceramics are poorly defined for the interval. Given (1) the low-density nature of the buried deposit and the sparse recovery of any material besides fire cracked rock and debitage, (2) the wide range of dates indicated by the CSC materials (Early Archaic through Middle Woodland), and (3) the ambiguous nature of our two most-diagnostic artifacts, it is difficult to assign a cultural period of the Garner site at the time of burial. Lack of pottery and local ubiquity suggests a Late Archaic/Early Woodland date, but the ppk morphology indicates a Middle Woodland date is more likely.

4.4.5.3.7 *Paleoseismic Interpretations*

Both sand blows exposed in Trenches 1 and 2 are composed of only one depositional unit and are characterized by similar degree of weathering suggesting that they formed during one and the same earthquake. In fact, they may even be part of the same sand blow with the intervening portion removed. In addition, the liquefaction features observed in both trenches may have had the same source, given the proximity of the two trenches, the dips of the feeder dikes, and similarity in grain-size.

In the thicker sand blow in Trench 2, iron and manganese appeared to have been leached from the upper 10-20 cm and to have accumulated deeper in the profile. In the thinner sand blow in Trench 1, the entire profile was stained by iron and manganese. Below both sand blows, the upper portion of the feeder dikes also exhibited iron and manganese staining. Although iron staining can occur quite quickly, the degree of weathering, including the depletion and accumulation of cations within the liquefaction features, suggest that they formed prior to A.D. 1811.

The calibrated date of 410-375 B.C. from the upper 1.5 cm of the soil buried by the sand blow in Trench 2 provides close maximum age constraint and suggests that the liquefaction features formed soon after 410 B.C. The archaeological interpretation that the artifacts, primarily the projectile point /knife base fragments, recovered from the soil buried by the sand blows most likely represent the Middle Woodland period, Marksville culture (200 B.C.-A.D. 200) is consistent with the radiocarbon date of the buried soil. Artifacts recovered from the ground surface during the pre-trenching archeological assessment included Late Archaic and Late Archaic to Early Woodland points with the highest concentrations of chert debitage, fire-cracked rock, retouched/utilized flakes in cell 8 of the collection grid (Figure 4-88 to Figure 4-90). The high concentration of artifacts in cell 8 coincides with the western end of Trench 1 where the soil was uplifted above the shallowly dipping dike. As this slightly uplifted (~15 cm) area was eroded and plowed, artifacts in the upper 10-15 cm of the uplifted soil would be concentrated at the surface and reflect artifacts for that depth range. Therefore, the artifacts in cell 8 and possibly other artifacts across the Garner site provide something similar to a maximum constraining age of Late Archaic-Early Woodland for the cultural horizon whereas the Middle Woodland projectile point/knife base fragments recovered from the soil beneath the sand blows better reflect the time of burial. Therefore, the sand blows likely formed during an earthquake between 200 B.C.-A.D. 200.

An alternative age for this event is obtained if the OSL dates are used. The OSL dates of 8590-7140 B.C. yr (10540-9090 yr B.P.) and 8695-7145 B.C. (10645-9095 yr B.P.) of the soil buried by the Garner sand blows suggest that the liquefaction features formed soon after 8695-8590 B.C. An alternative archaeological interpretation of the artifacts from the buried soil is that they are from the Early Archaic period 8000-7000 B.C.; however, this seems very unlikely given the lack of basal grinding of the projectile points. The only known paleoearthquake in the region to have occurred at this time is a Marianna earthquake between 8200-7600 B.C. (or 10150-9550 yr B.P.) located about 140 km south of the Garner site. If the Marianna event (B.C. 7900 ± 300 yr or 9850 ± 300 yr B.P.) were responsible for liquefaction at the Garner site, it would have to be of $M \geq 7.1$ to produce sand blows at that distance (Castilla and Audemard, 2007). However, it seems highly unlikely that the OSL dates reflect the true age of the land surface at the time of burial. The OSL dates are much older than the radiocarbon date of the same buried soil and the projectile point /knife base fragments recovered from the buried soil are more likely from the Middle Woodland period. Perhaps the older OSL dates are due to incomplete resetting of luminescence of the soil prior to burial or to mixing of the soil by bioturbation.

4.4.5.4 *Stiles Site*

The Stiles site is located near the epicenter of the December 16, 1811 mainshock and is underlain by the southwestern branch of the NMSZ as well as the Blytheville Arch, a possible source of the historical and modern seismicity (Figure 4-18 and Figure 4-19). The site straddles the mapped boundary between Holocene meander-belt deposits and Late Pleistocene valley-train deposits (level 1) of the Mississippi River (Figure 4-56; Saucier, 1994). The Pemiscot Bayou, a distributary channel of the Mississippi that was active from about 2500-5000 years B.P. and largely infilled by

2200 years B.P. (Guccione et al., 1999), is located along the southern border of the site. It is likely that the northern portion of the site is underlain by Late Pleistocene valley-train deposits and that Pemiscot Bayou deposits are inset into and onlap the valley-train deposits beneath the southern portion of the site. Previously, liquefaction sites in the Holocene meander-belt, south and east of the Stiles site, provided paleoseismic data that helped to estimate the timing, location, and magnitudes of New Madrid events in A.D. 1450 ± 150 yr, A.D. 900 ± 150 yr, and B.C. 2350 ± 200 yr (Tuttle et al., 2002 and 2005; Tuttle and Hartleb, 2012). Therefore, the Stiles site may provide additional information about Late Holocene earthquakes as well as new information about older events.

Sand blows were recognized at the Stiles site during a helicopter survey along Pemiscot Bayou in 2007. From the air, several prominent, light-colored linear patches were observed crossing the site. Examining a time series of GE satellite imagery acquired between 1994 and 2012, the light colored-linear patches persisted through time indicating that they reflect the physical properties of the soil and are not ephemeral features related to agricultural practices (e.g., misapplication of fertilizers and herbicides). One of the linear patches is oriented northwest-southeast, an unusual orientation for sand blows in the area, and several others linear patches are oriented roughly east-west, subparallel to the nearby Pemiscot Bayou (Figure 4-114 and Figure 4-115). Two large, east-west-oriented linear patches cross the center of the site, are subparallel to one another, and appear to have formed along the margins of a sediment-filled abandoned channel. Given its size, orientation, and location, the abandoned channel may be an ancestral channel of Pemiscot Bayou. There are several smaller linear patches that are oriented northeast-southwest. In a few places, linear patches of different orientations intersect one another, suggesting that there were multiple episodes of liquefaction at the site. Therefore, it may be possible to examine structural and stratigraphic relations of different generations of liquefaction features that will help to establish their relative time of formation.

4.4.5.4.1 *Reconnaissance*

The initial site visit was conducted in November 2011 to field check interpretations of aerial observations and satellite imagery and to look for cultural artifacts on the ground surface. At the time of the visit, the crops had been recently harvested and the soil surface was well exposed. The light-colored patches were found to be sandy in contrast to the surrounding darker-colored soils that were silty in the northern portion of the site and clayey in the southern portion of the site closer to Pemiscot Bayou.

We hand dug three small soil pits in the light-colored patches to observe the sedimentological characteristics of the likely sand blow deposits (Figure 4-114 and Figure 4-115). The soil pits revealed sandy layers containing lignite and silt clasts, similar to known sand blows in the area. Soil pit 1 was dug in the large northwest-southeast oriented patch. The pit was 74 cm deep and entirely in sandy sediment. As observed in the soil pit, the upper 18 cm was massive sandy loam interpreted as a plow zone. Beneath the plow zone were two depositional units composed of medium to fine sand. The upper sandy unit contained silt clasts and its upper 12 cm were iron-stained. Soil pit 2 was excavated at the southeastern end of the large northwest-southeast oriented patch near its intersection with an east-west oriented patch. The pit was 55 cm deep and entirely in sandy sediment. As observed in the pit, the upper 20 cm were massive sandy loam interpreted as a plow zone. The plow zone was underlain by 30 cm of silty sand containing lignite followed by 5 cm of sand. Soil pit 3 was excavated near the intersection of the southern member of the pair of large, east-west-oriented linear patches and a smaller, northeast-southwest-oriented linear patch. The pit was 70 cm deep and revealed a 25-cm-thick plow zone of silty sand,

underlain by a 45-cm-thick deposit of medium to fine sand containing a thin layer of lignite towards its base. The sand is underlain by clay at 70 cm below the surface.



Figure 4-114 GE image showing location of Stiles site outlined by solid white line, light colored linear patches that cross site, and soil pits excavated during initial site visit to evaluate presence of sand blows. Pemiscot Bayou is drainage ditch south of site. Yarbrow excavation, where historic and prehistoric sand blows were studied in 1990s, is located southeast of the Stiles site between Pemiscot Bayou and Route 150. Satellite image was acquired by USDA Farm Service Agency on October 14, 2010.

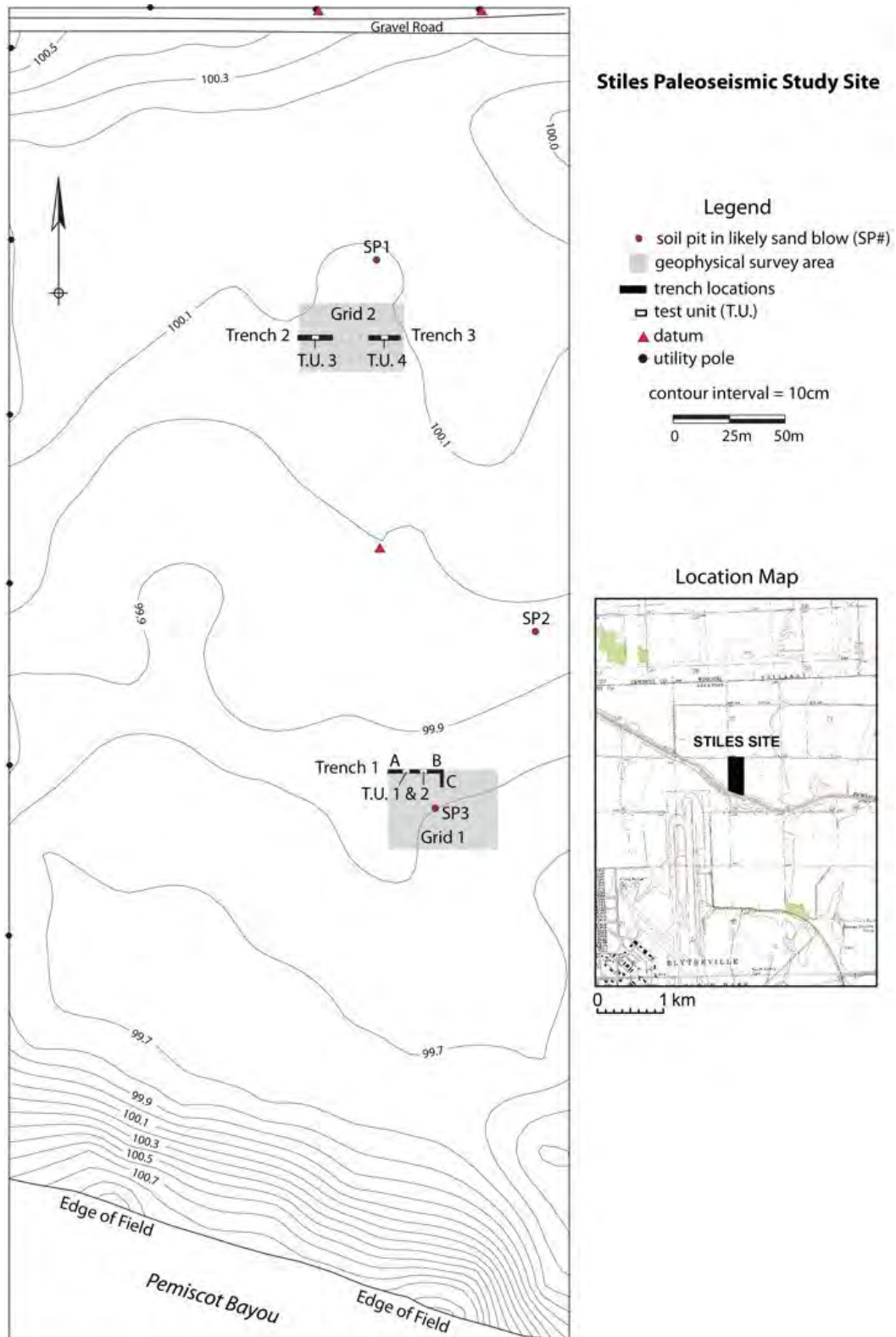


Figure 4-115 Topographic map of Stiles site and inset location map. Site map shows locations of geophysical grids, archaeological test units, soil pits, and proposed trench locations. Actual trench locations deviate from proposed locations as described in text.

The field observations of sandy surface soils compared to adjacent silty soils of the floodplain and of sedimentological characteristics of the deposits exposed in the soil pits support the interpretation that the light-colored patches are sand blows resulting from earthquake-induced liquefaction. No artifacts were found on the ground surface or in the soil pits. Given the presence of both Holocene and Late Pleistocene deposits as well as sand blows of different orientations that appeared to intersect one another, this was an intriguing site that might provide insights into liquefaction and ground failure in different types of deposits as well as a long record of paleoearthquakes. Also, given that the site appeared to be devoid of archaeological material, it presented a potential location for conducting excavations for the training workshop task of this project. Therefore, this site was selected for further investigation.

4.4.5.4.2 Electrical Resistivity Surveys

In March 2013, geophysical surveys using electrical resistance tomography also were conducted at the Stiles site. On the basis of interpretation of satellite imagery and field inspection of likely sand blows described above in Section 2, two areas were surveyed at the site. The location of the geophysical survey area is shown on the topographic map of the site (Figure 4-115). Figure 4-116 shows the layout of the survey grids at the Stiles site. Each grid consisted of multiple parallel profile lines within a rectangular area. All lines were 46 m in length. Data were collected using an AGI SuperSting resistivity meter, with automatic electrode switching capability. Each line consisted of 28 electrodes at 2-m spacing. An AGI mixed dipole array (similar to a conventional dipole-dipole configuration) was chosen for the data acquisition because this array provides optimal resolution for near-surface features and sufficient depth penetration to guide future trench excavations. Measurement errors in all surveys did not exceed 0.2%

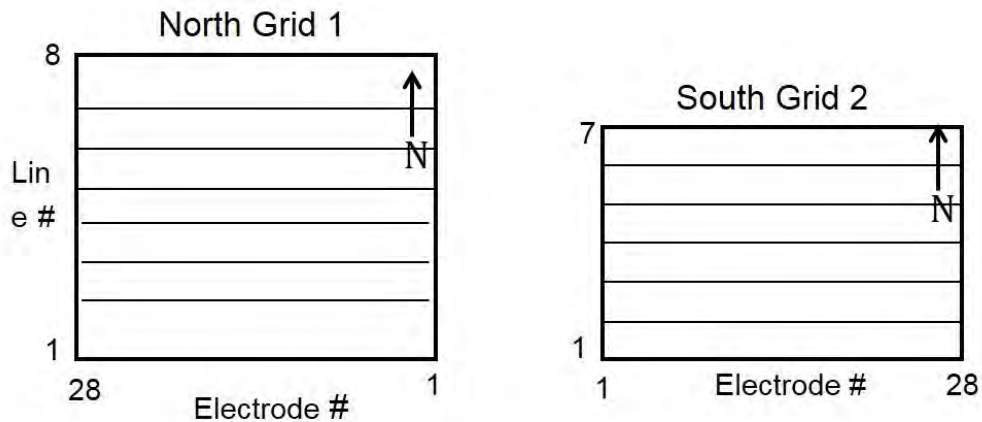


Figure 4-116 Layout of resistivity survey grids at Stiles site. Grids consisted of multiple parallel profile lines, spaced at 5 m apart. Each line consisted of 28 electrodes at 2-m spacing.

As for the Garner site, raw data observations of apparent resistivity from all profile measurements were processed using AGI's 2D EarthImager software to produce cross-sections of the true subsurface resistivity distribution. If one assumes that the true resistivity distribution in the subsurface is correct, the model is validated by using a forward-modeling technique to predict the apparent resistivity distribution. Statistical measures of the solution are thus obtained. The maximum RMS data error in the inversions was less than 5%.

Survey Results

Figure 4-117 to 4-122 contain composite images, each showing three profile lines, for grids 1 and 2 at the Stiles site. Grid 1 consisted of eight profile lines, shown in Figure 4-117 to Figure 4-119, with views towards the south (east to left side of profile). The line numbers increase to the north. Hot colors (red-orange) represent areas of sediment with relatively high resistivity (usually indicating sandy or silty-sand deposits often associated with sand blows and sand dikes). Cool colors indicate subsurface areas that are more conductive, usually containing finer-grained sediments with varying amounts of clay. In Figure 4-117, an area of high resistivity (~20 to 34 m along the profile) evident in Line 1 increases in size to the west as seen in profile locations farther to the north (e.g., Line 3). The area reaches its maximum size on Line 4. In Line 5, there appears to be two areas of high resistivity, one in the central section of the profile and one on the western edge, which were interpreted as sand blows during initial field reconnaissance. The area in the central part of the profile expands eastward in Line 7 (14 m to 33 m along profile), whereas the area on the western side retains similar dimensions to that in Line 6. Line 8 shows a narrow vertical zone of high resistivity (26 to 28 m along the profile) and a broader eastward dipping zone of high resistivity (38 to 42 m along the profile) interpreted as possible sand dikes that connect a larger area at depth (possibly a source unit) with the two likely sand blows at the surface.

Grid 2 consisted of seven profiles shown in Figure 4-120 to Figure 4-122. Line 7 is located farthest to the north, and cross-sections are north-facing (east to the right side of the profiles). Line 1 shows the presence of two areas with high resistivity (sand blows) on the western and eastern ends of the profile. These two areas of high resistivity can be tracked towards the north on Lines 2, 3, 4, and 5. On Lines 5 and 6, the area of high resistivity on the western end of the profiles is much diminished. On Line 4, both eastern and western areas of high resistivity are prominent and a deeper unit is present. Two linear features, possibly sandy feeder dikes, are seen at the base of the resistive area on the east side of the profile (~34 m and 42 m along the profile) and a similar linear feature is seen at the base of the resistive area on the west side of the profile (~4 m along the profile) (Figure 4-121). Similar features suggestive of sandy feeder dikes are seen in Line 6 (Figure 4-122).

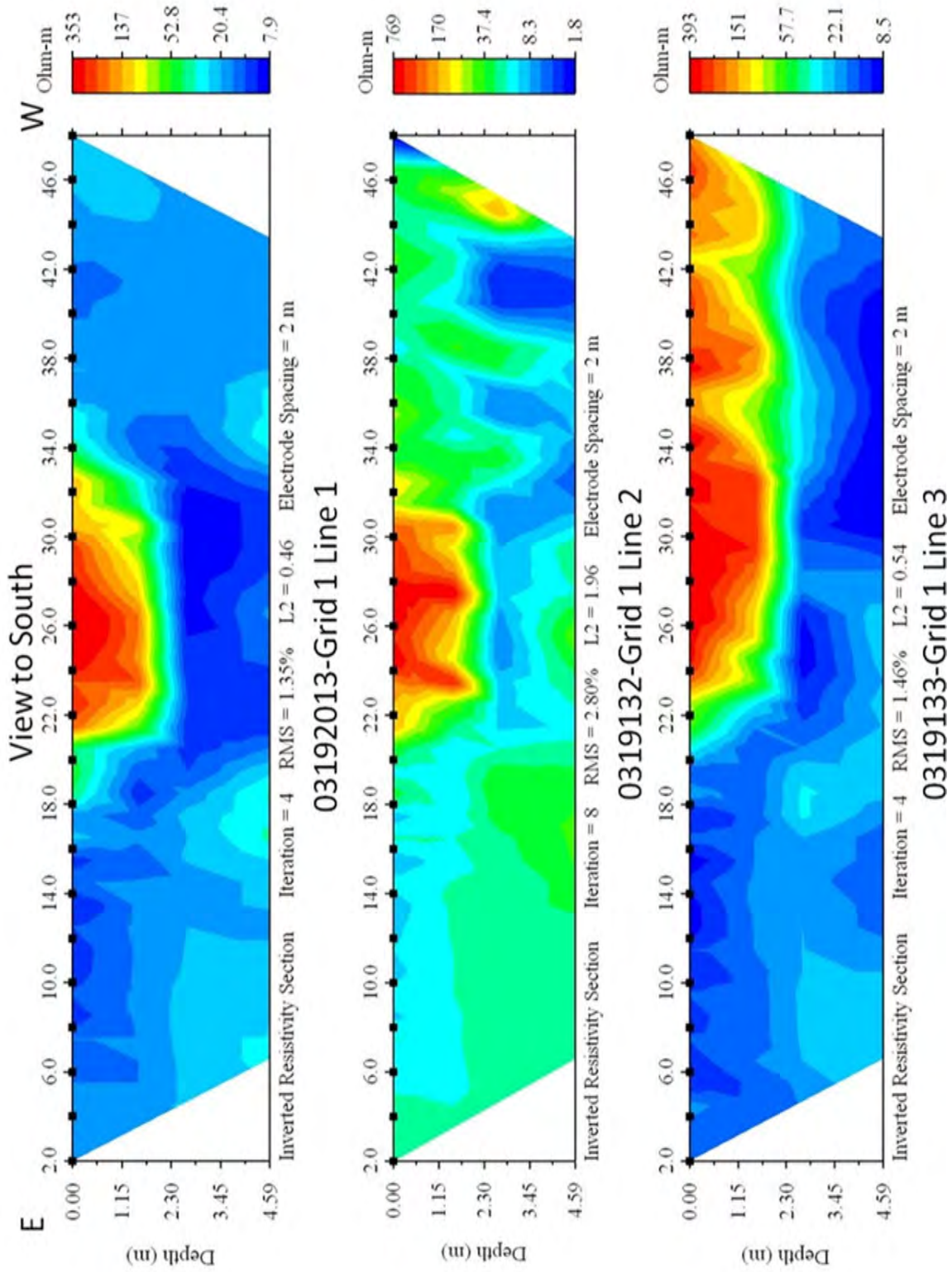


Figure 4-117 Composite Resistivity Images of Lines 1, 2 and 3 from Grid 1 at Stiles Site

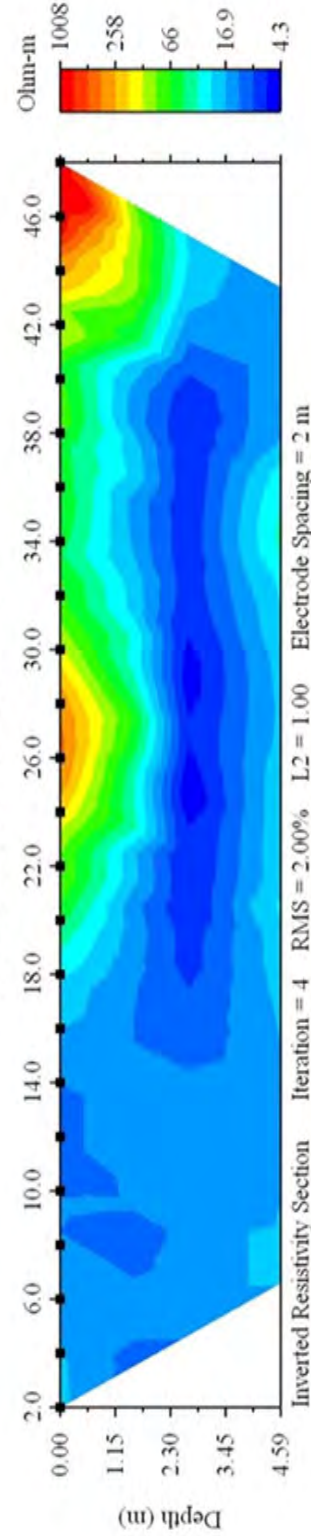
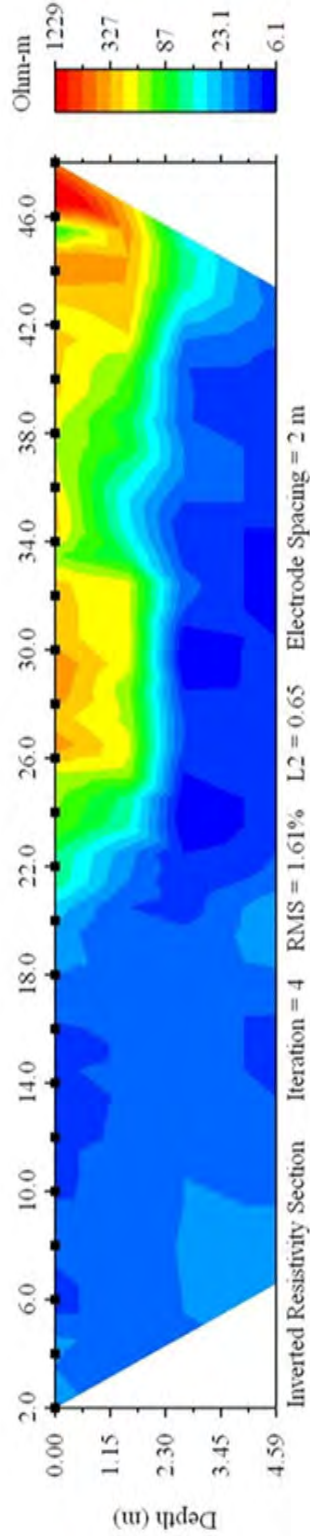
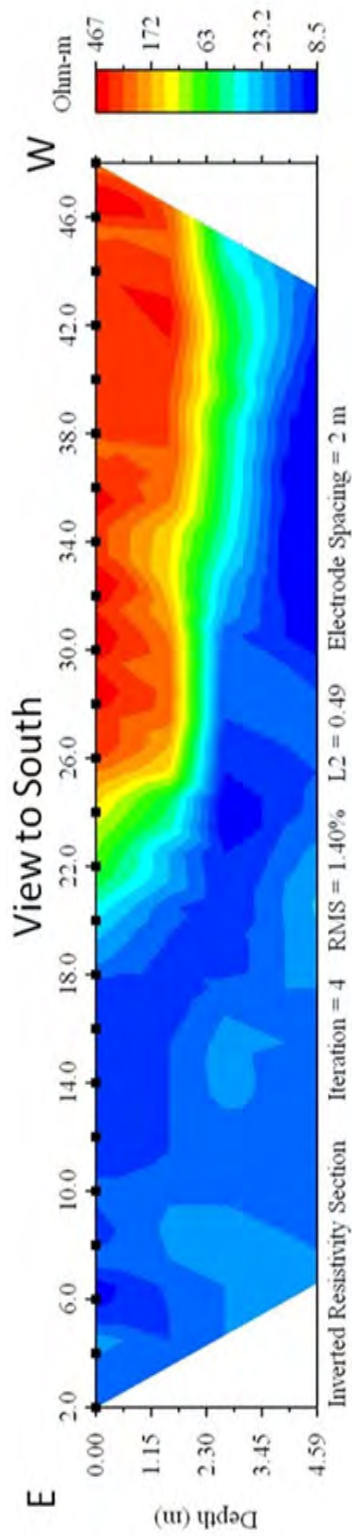


Figure 4-118 Composite Resistivity Images of Lines 4, 5, and 6 from Grid 1 at Stiles Site

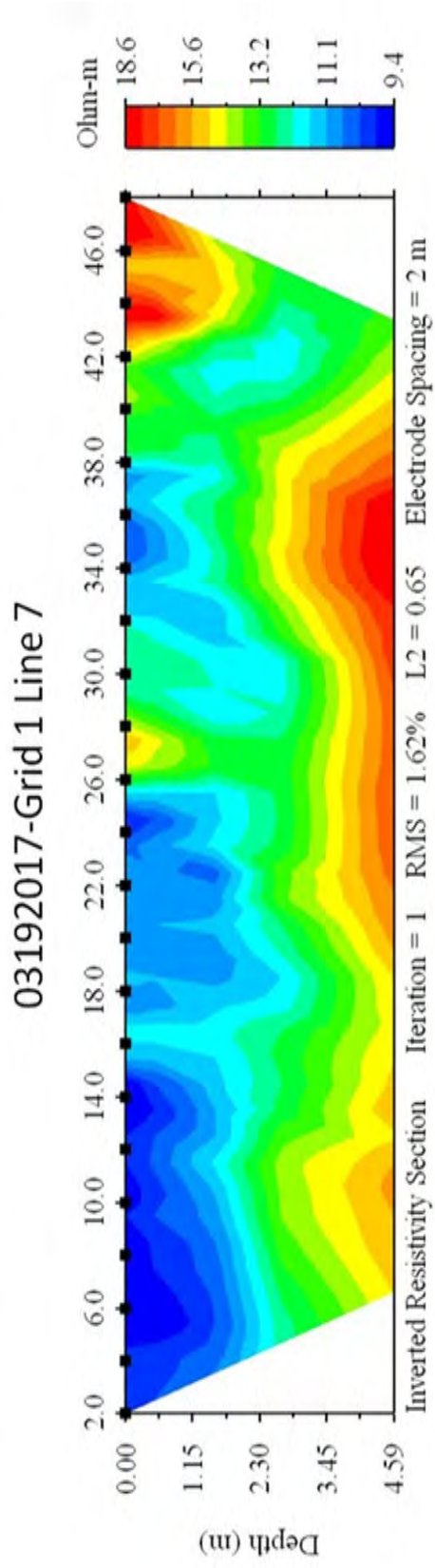
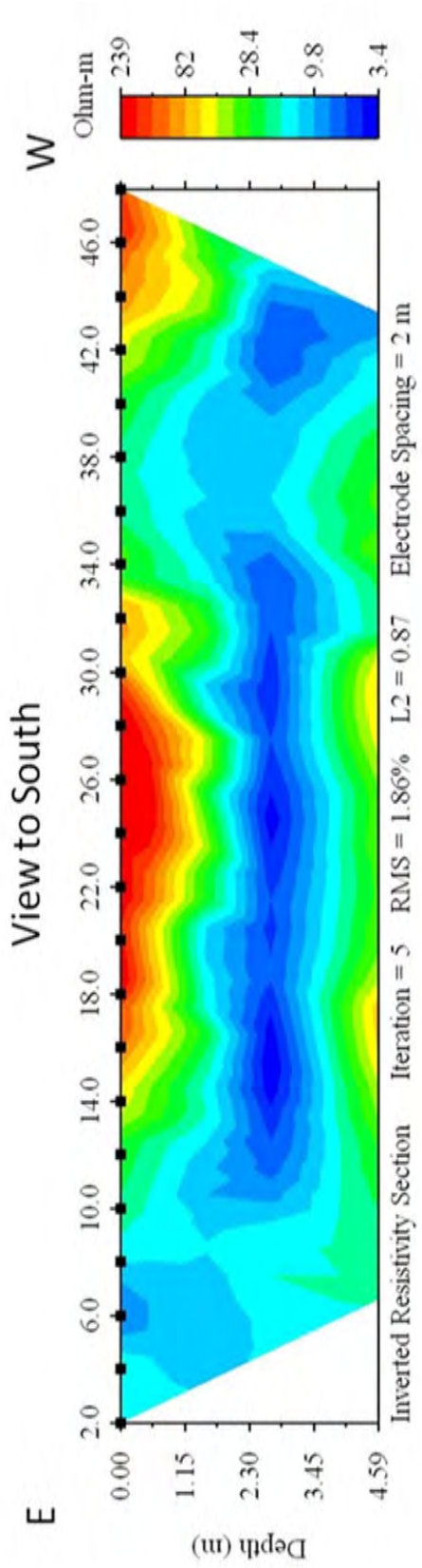


Figure 4-119 Composite Resistivity Images of Lines 7 and 8 from Grid 1 at Stiles Site

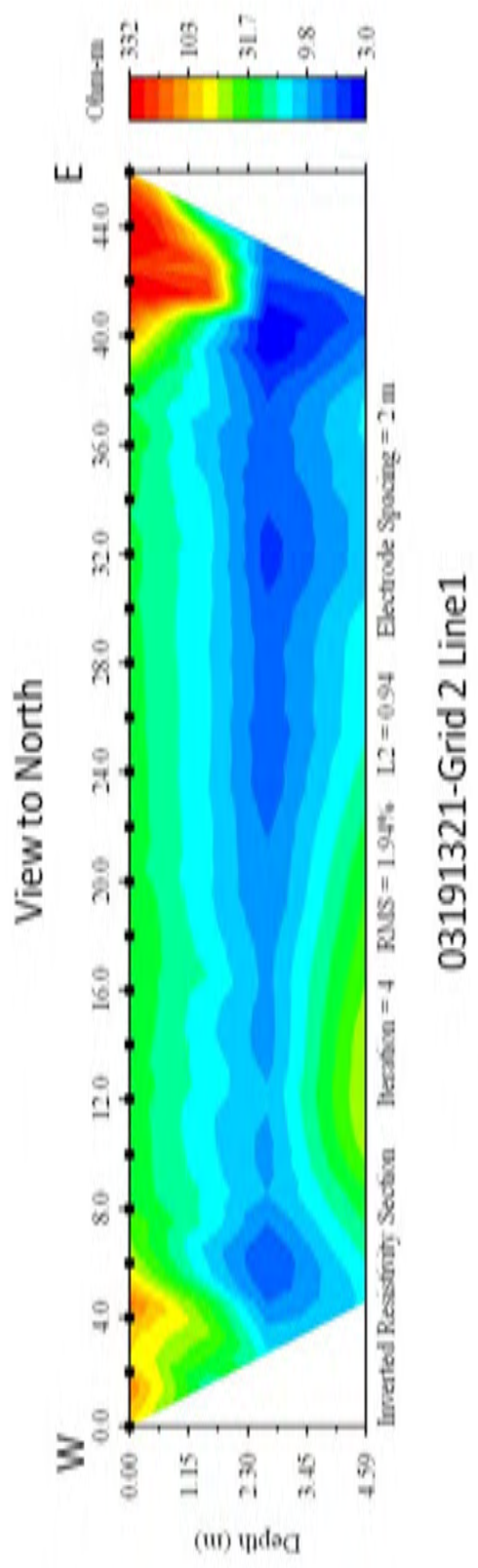


Figure 4-120 Composite Resistivity Images of Line 1 from Grid 2 at Stiles Site

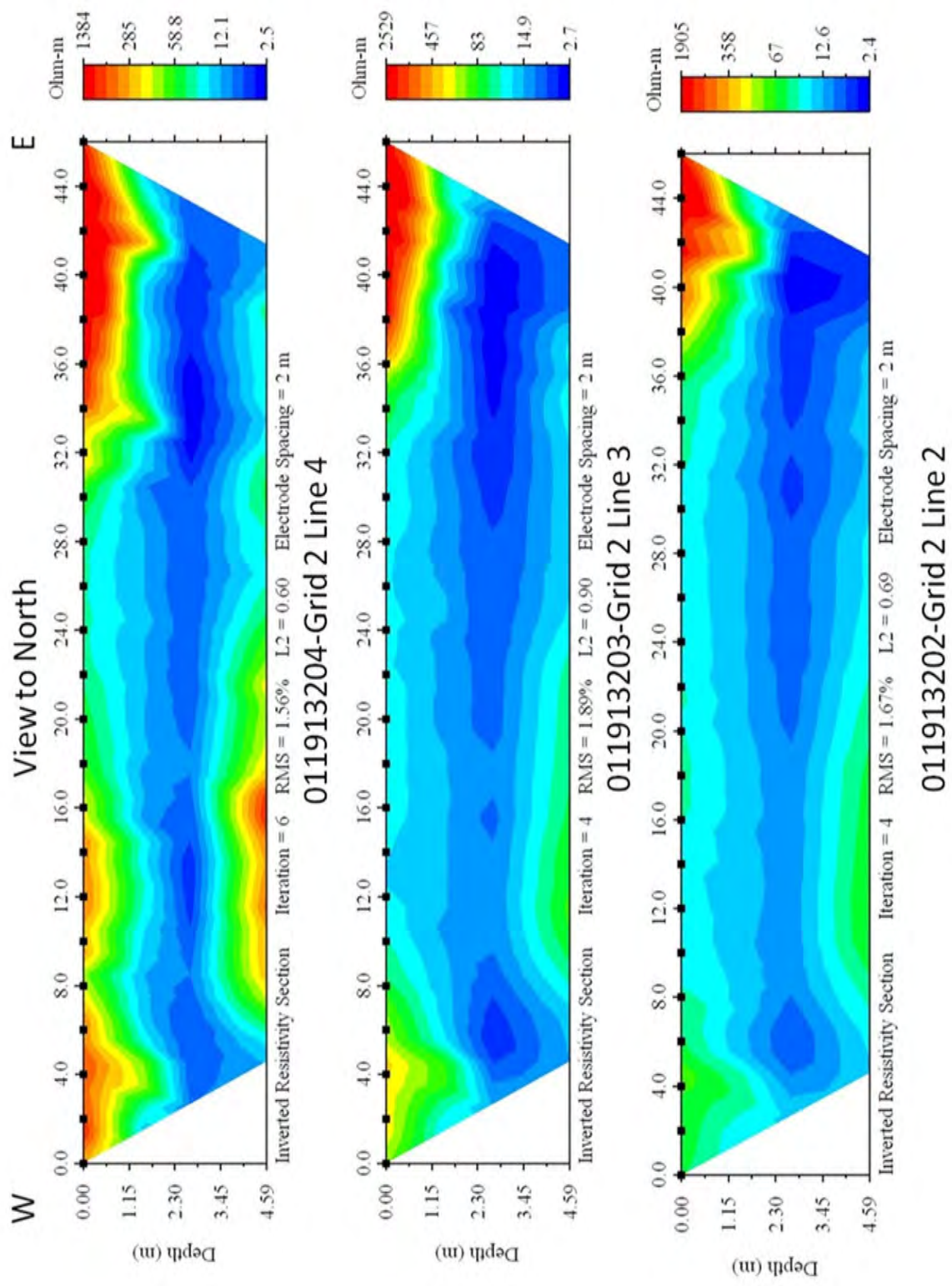


Figure 4-121 Composite Resistivity Images of Lines 2, 3, and 4 from Grid 2 at Stiles Site

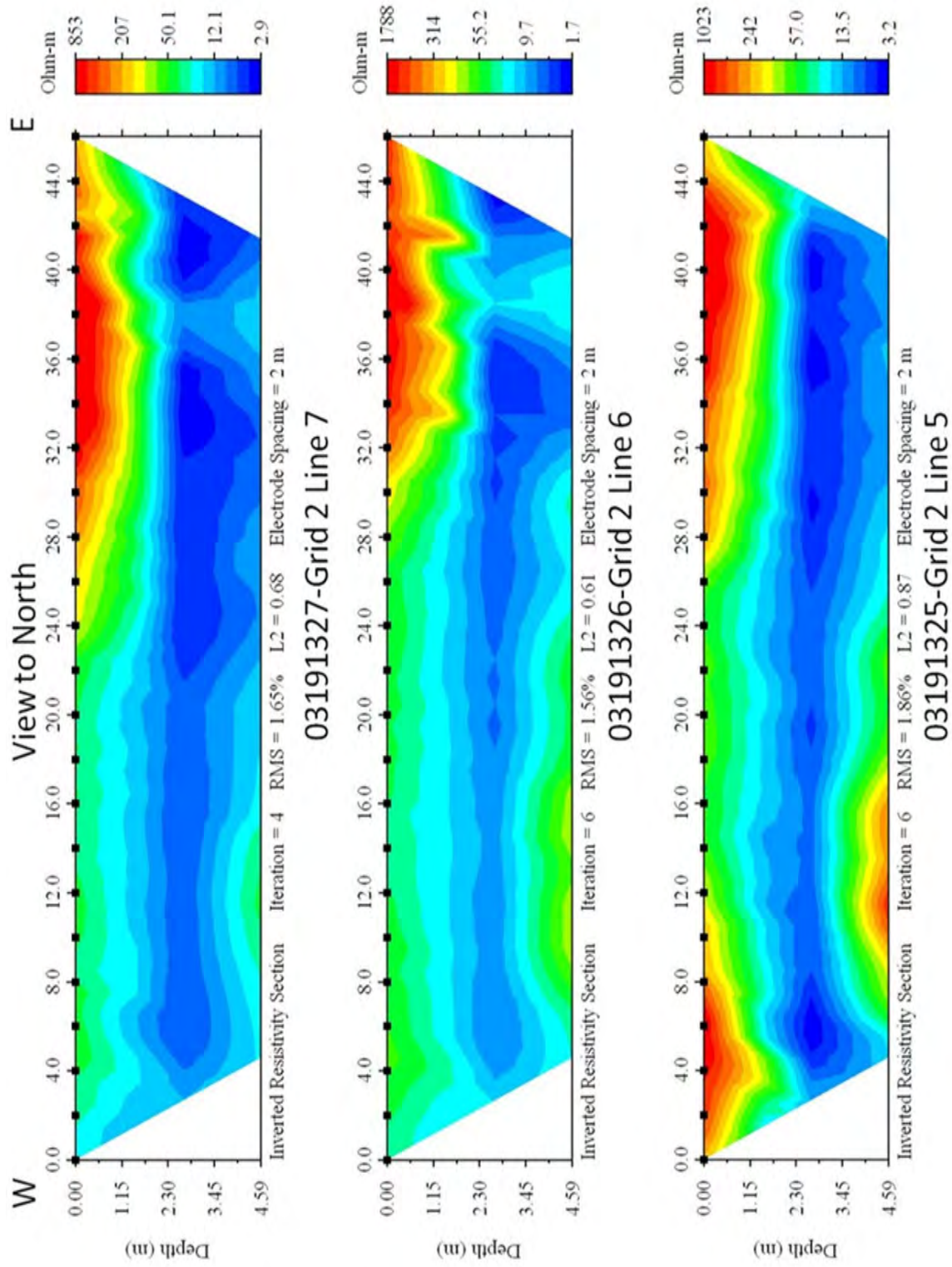


Figure 4-122 Composite Resistivity Images of Lines 5, 6, and 7 from Grid 2 at Stiles Site

4.4.5.4.3 Pre-Trenching Archaeological Assessment

The Stiles site was evaluated between March 18 and March 22, 2013. At the time, the site was planted in winter wheat and visibility of the ground surface was approximately 90 percent (Figure 4-123). The ground surface was surveyed in transects spaced ca. 3 m apart. No artifacts were found during the surface survey.



Figure 4-123 Photograph of Stiles location. Site was planted in north-south oriented rows of winter wheat and surface visibility was about 90%. View is towards southwest.

Test Units

In order to assess presence or absence of intact cultural deposits in the proposed trench locations, shovel Test Units 1 and 2 were excavated in the footprint Trench 1, Test Unit 3 was excavated in the footprint Trench 2, and Test Unit 4 was excavated in the footprint of Trench 3. More specifically, Test Units 1 and 2 were excavated at 40 m and 32 m along resistivity profile number 8 in geophysical grid 1 (Figure 4-115; lower profile in Figure 4-119) and shovel Test Units 3 and 4 were excavated at 7 m and 38 m along resistivity profile number 4 in geophysical grid 2 (Figure 4-115; upper profile in Figure 4-121). Since proposed Trenches 2 and 3 are only 14 and 12 m long, respectively, the test units were placed at the midpoints of the footprints.

Trench 1, Test Unit 1 (T.U. 1) was excavated to a depth of 30 cm. There are three strata (Figure 4-124 and Figure 4-125). The plow zone extends to a depth of 22 cm and has an upper and lower part. The upper part (Plow zone 1) goes from the surface to 7-8 cmbs. It is composed of dark brown (7.5YR3/2) sandy loam. The lower plow zone (Plow zone 2) is a dark grayish brown sandy loam with ~10 percent clay. Below the plow zone, there is a grayish brown very fine sandy silt with strong brown redoximorphic features. The silt is intruded by a dike of yellowish brown,

silty, medium to fine sand that contains lignite and clasts of silty clay. In addition, two apparently horizontal layers of the same yellowish brown, silty, medium to fine sand occurs between 25 and 30 cmbs on either side of the dike and may be portions of an earlier sand blow. The sandy layer on the east (right) side of the profile is underlain by dark gray silty clay. No artifacts were found in Test Unit 1.



Figure 4-124 Stiles Site, Photograph of North Profile of Test Unit 1, 0-30 cmbs

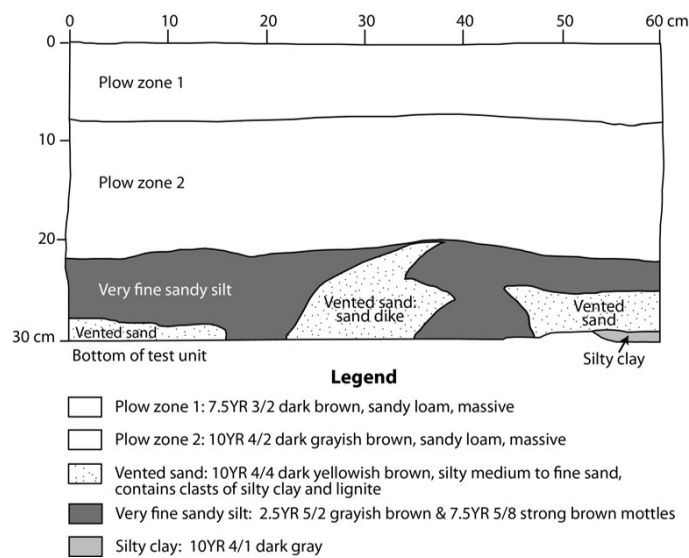
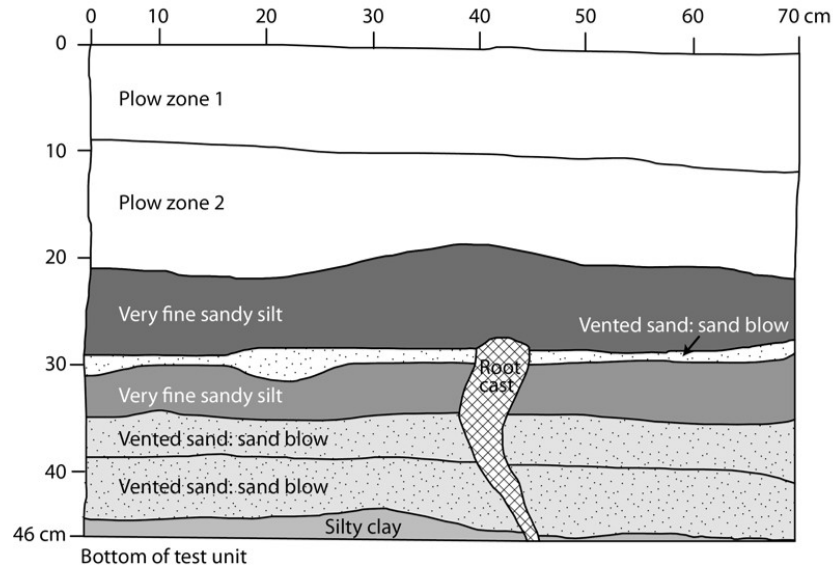


Figure 4-125 Stiles Site, Test Unit 1 North Profile, 0-30 cmbs



Legend

- Plow zone 1: 7.5YR 3/2 dark brown, sandy loam, massive
- Plow zone 2: 10YR 4/2 dark grayish brown, sandy loam, massive
- Very fine sandy silt: 2.5YR 5/2 grayish brown & 7.5YR 5/8 strong brown mottles
- Vented sand: 10YR 4/4 dark yellowish brown, silty medium to fine sand, contains clasts of silty clay and lignite
- Very fine sandy silt: 2.5YR 5/2 grayish brown & 7.5YR 5/6 strong brown mottles
- Vented sand: 7.5YR 5/4 brown, silty medium to fine sand, contains clasts of silty clay and lignite
- Silty clay: 10YR 4/1 dark gray

Figure 4-126 Stiles Site, Test Unit 2 North Profile, 0-46 cmbs

Trench 1, Test Unit 2 (T.U. 2) was excavated to a depth of 46 cmbs. The plow zone is 22 cm thick and is composed of upper and lower parts differentiated primarily by coloration (Figure 4-126). The 9-11 cm thick upper plow zone (Plow zone 1) is a dark brown (7.5YR 3/2) massive sandy loam. The 11-13 cm thick lower plow zone (Plow zone 2) is a grayish brown (10YR 4/2) massive sandy loam. Below the plow zone, are six layers between 21 cm to 46 cmbs. The upper layer (21-29 cmbs) is a grayish brown very fine sandy silt with strong brown (7.5YR 5/8) redoximorphic features. Underlying this layer is a thin (1-3 cm thick) dark yellowish brown, silty, medium to fine sand that contains clasts of silty clay and lignite. This layer appears to be very similar to the possible sand blow in Test Unit 1. It is underlain by a grayish brown very fine sandy silt with strong brown (7.5YR 5/8) redoximorphic features, which in turn is underlain by two layers of brown, silty, medium to fine sand also containing fine-grained clasts and lignite. These two layers are similar to the uppermost sandy layer, except that they are darker in color, contain more lignite, and appear to fine upward. They too are likely to be sand blows. The lowest layer exposed in the test unit is a dark gray silty clay. No artifacts were found in Test Unit 2.

Trench 2, Test Unit 3 (T.U. 3) was excavated to 40 cmbs (Figure 4-127). At the base of the plow zone, about 17 cmbs, sand dikes crosscut dark brown sandy clay loam with small orange redoximorphic features. The dikes are composed of yellowish brown fine to medium sand with clasts of clay loam and pieces of lignite. Two sand dikes, possibly a compound dike, at the

western end of the test unit are about 4 and 8 cm wide. The sand dike crossing the middle part of the test unit is 5-11 cm wide. No artifacts were found in Test Unit 3.



Figure 4-127 Stiles Site, Photograph of Test Unit 3 North Profile, 0-40 cmbs

Trench 3, Test Unit 4 (T.U. 4) was excavated to 50 cmbs and is composed of three layers (Figure 4-128). The 16 cm thick upper plow zone (Plow Zone 1) is a brown sandy loam. It is underlain by a lower plow zone (Plow Zone 2) with an irregular lower contact that is up to 8 cm thick and composed of lenses of brown sandy loam and sand containing lignite. The plow zones are underlain by yellowish brown sand that is at least 30 cm thick interpreted as a sand blow. No artifacts were found in Test Unit 4.

At the Stiles site, no intact cultural deposits were found in the test units excavated in the proposed trench locations. In addition, no artifacts were recovered during the surface survey. There is no evidence, based on this assessment, of an archaeological site in the vicinity of the proposed trenches. Although the excavated area of the test units is small, involving only 0.87 m², the lack of carbon, burned/fired clay, and artifacts as well as lack of artifacts on the ground surface makes it unlikely that there are any shallowly (e.g., between 5-40 cm) buried intact deposits. There are no archaeological characteristics at this location.

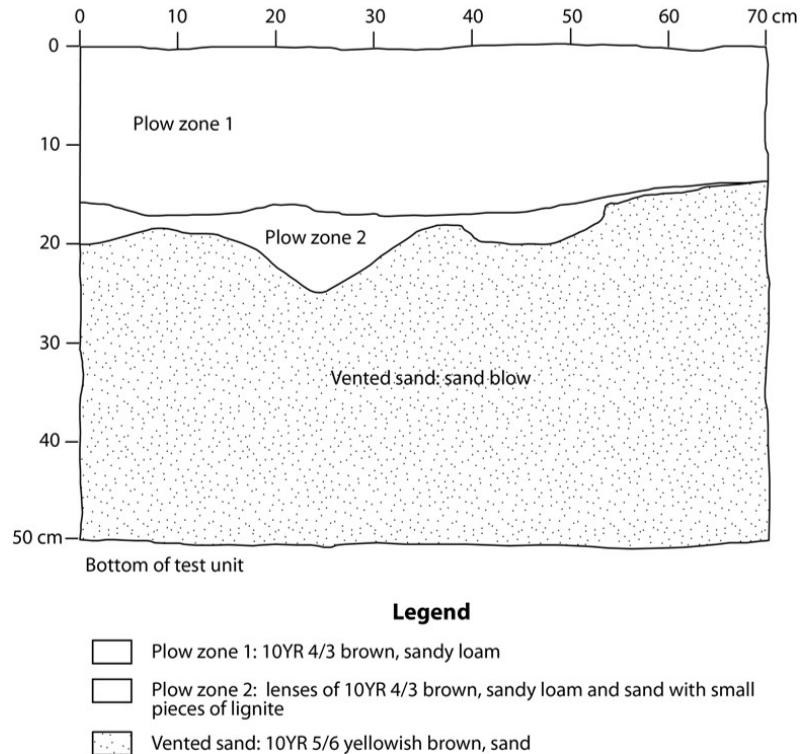


Figure 4-128 Stiles Site, Test Unit 4, North Profile, 0-50 cmbs

Archaeological Assessment

On the basis of the evaluation, there are no archaeological materials at the Stiles site. Surface survey and test units in the footprint of the proposed trenches did not yield any evidence of past human occupation. The proposed trenches at the Stiles site are unlikely to encounter cultural horizons or features and therefore there would be no adverse effects from trenching.

4.4.5.4.4 Siting Paleoseismic Trenches

As described in Section 2, likely sand blows were located at the Sites site on the basis of interpretation of satellite imagery and field inspection including excavation of small soil pits. The presence of sand blows was further supported by the results of electrical resistance tomography. Resistivity profile number 8 in grid 1 and resistivity profile number 4 in grid 2 provided excellent targets for paleoseismic trenching. On profile number 8 in grid 1, two high resistive areas on the surface, likely sand blows, appear to be connected by somewhat less resistive zones, likely feeder dikes, to a deeper high resistive area, likely source beds of the liquefaction features. On profile number 4 in grid 2, there are two prominent high resistive areas on the surface that are likely related to sand blows. Several high resistive linear features that extend downward from the base of the high resistive areas are likely related to feeder dikes of the sand blows. A deeper high resistive area may represent the sandy source bed from which the liquefaction features were derived. Trench 1 was proposed from 24-48 m along resistivity profile number 8 (lower profile in Figure 4-115, Figure 4-117) and Trenches 2 and 3 were proposed from 0-14 m and 32-44 m along resistivity profile number 4 (upper profile in Figure 4-121; Figure 4-115) in order to reveal the relationship between sand blows and their feeder dikes.

4.4.5.4.5 *Paleoseismic Observations*

In November 2015, three trenches were excavated at the Stiles site as proposed in the site evaluation report and described above. All three trenches exposed sand blows and associated sand dikes.

Trench 1

Trenches 1A and 1B crossed a sand blow associated with a linear east-west oriented sand blow that is subparallel to the nearby Pemiscot Bayou and along the southern flank of what appears to be an abandoned channel fill (Figure 4-114 and Figure 4-115). While excavating the western end of proposed Trench 1, it was quickly discovered that little remained of what had been a thin sand blow. The sand blow had been almost completely destroyed by plowing. Therefore, Trench 1A at the western end of the proposed trench was abandoned (Figure 4-115). We excavated 6.5 m of the eastern end of the proposed trench which became Trench 1B. As observed in the trench walls, the sand blow appeared to be thickening towards the south. Therefore, we also excavated Trench 1C, perpendicular to Trench 1B and extending 7.6 m towards the south from the eastern end of Trench 1B.

In Trenches 1B and 1C, the plow zone ranged from 18-25 cm and a few plow scars extended up to 15 cm into the sand blow (Figure 4-129). In Trench 1C, the sand blow, up to 55 cm thick, was composed of three depositional units; L1, L2, and L3. Unit L1 was the lowest unit and had three subunits: a sand with many clay clasts that fines to silt towards the north and away from the dike, a medium sand with a few clasts that pinches out also towards the north, and an uppermost lignite layer which contains clay clasts and exhibits a few desiccation cracks. Unit L2 overlies unit L1 and was composed of fine to medium sand in which soil lamellae had developed in the upper 20 cm. Towards the north end of the trench and away from the dike, unit L2 thinned and fined becoming interbedded sand and lignite capped by silt. Unit L3 overlies L2, was composed of fine, medium, and coarse sand, with clasts of clay and sand, and occurred above a sand dike (Figure 4-130). Soil lamellae had formed in the upper 30 cm of L3. The sand dike was 28 cm wide, had a strike and dip of N86°E and 76°NW, and was composed of two depositional units, L1 and L3, which were continuous with their equivalent sand blow components. The surface of the clayey soil beneath the sand blow was inclined towards the south and the sand blow thickened in that direction as well, suggesting another sand dike farther towards the south.

In Trench 1B, the sand blow, about 30 cm thick, was composed also of three depositional units. Units L1 and L2 were similar in character to their equivalent units observed towards the northern end of Trench 1C. Unit L1 was a thin silt layer that pinched out towards the west (Figure 4-129; below meter mark 3). Unit L2 was composed of interbedded sand, lignite, and silt and extended along the length of the trench except where truncated by L3. Unit L3 was composed of coarse and medium sand, with clasts of clay and lignite pebbles, and occurred above a semi-circular vent exposed in the trench floor. The vent contained coarse sand with clay clasts. Portions of L3 were overlying L2 and became finer grained (medium and fine sand) towards the western end of the trench.

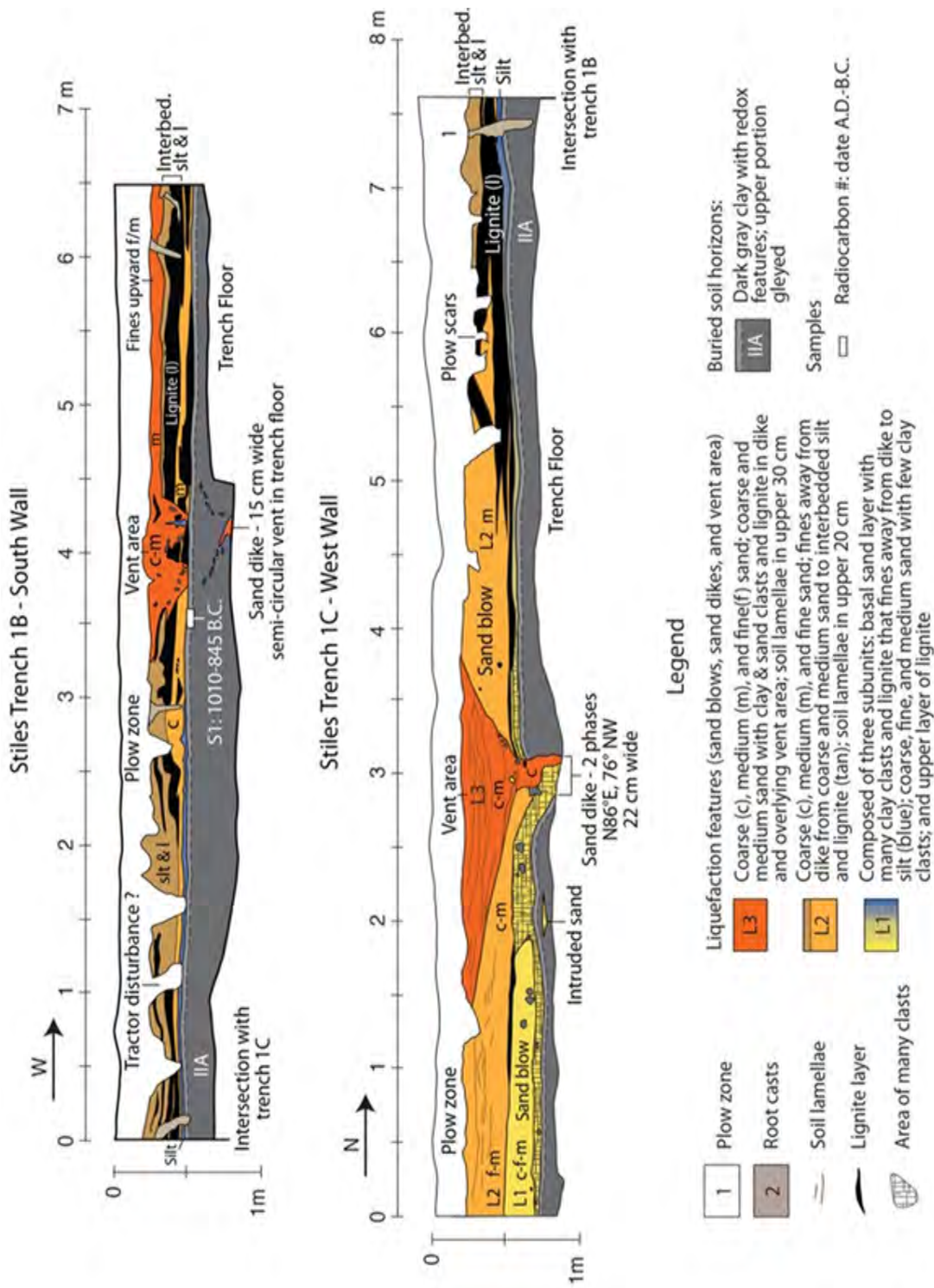


Figure 4-129 Logs of Trenches 1B and 1C at Stiles site, showing sand blows and related sand dikes. Radiocarbon dating of sample TR1b-S1 from top of buried soil suggests that overlying sand blow formed soon after B.C. 1010.

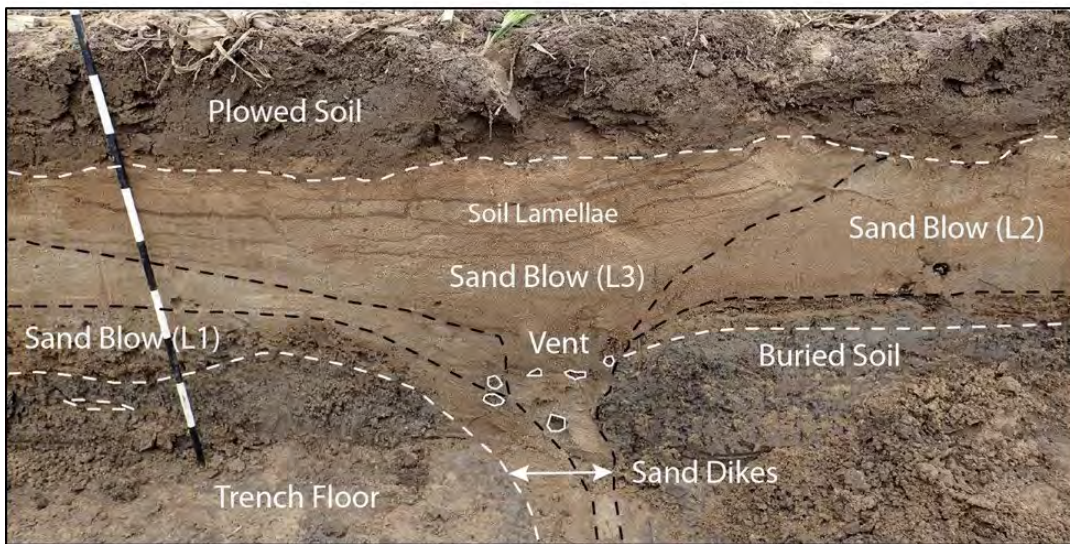


Figure 4-130 Photographs (upper - unannotated; lower - annotated) of vent area of compound sand blow above dike that crosscuts gray clayey soil in west wall of Stiles Trench 1C (see Figure 4-129). Note brown soil lamellae that formed in sand blow. Dashed lines represent clear contacts. For scale, black and white intervals on meter stick are 10 cm long.

Given its strike of N86°E, the sand dike exposed in Trench 1B is probably related to one of the large linear east-west oriented sand blows near soil pit 3 (Figure 4-114). The ground surface buried by the compound sand blow is 25 cm deeper on the south end of the trench than on the north end of the trench whereas the present ground surface is 12 cm lower on the south end than on the north end. This difference may be due to differential ground failure related to liquefaction; however, it may also reflect the pre-event topography that would have sloped southward towards the Pemiscot Bayou.

Despite much looking, no wood or charcoal samples for dating could be found in any of the walls of Trenches 1C and 1B. Therefore, a sample (TR1b-S1) of the buried soil below the sand blow in Trench 1B was collected and submitted for radiocarbon dating. The sample yielded a calibrated date of B.C. 1010-890, 875-845 (Table 4-28).

Table 4-28 Radiocarbon Dating Results for the Stiles Site

Sample # Lab #	¹³ C/ ¹² C Ratio	Radiocarbon Age Yr B.P. ¹	Calibrated Radiocarbon Age Yr B.P. ²	Calibrated Calendar Date A.D./B.C. ²	Sample Description
Stiles- TR1b-S1 BA-434564	-24.5	2790 ± 30	2960-2840 2825-2795	BC 1010-890 BC 875-845	Buried soil 1-2 cm below sand blow
Stiles-TR2- C2 BA-434565	-28.6	350 ± 30	500-310	AD 1450-1640	Charred material 1 cm below sand blow from buried soil
Stiles-TR2- C4 BA-434566	-25.3	70 ± 30	260-220 140-20 0+	AD 1690-1730 AD 1810-1920 AD 1950+	Charred material 40 cm below sand blow from silty clay; near root cast
Stiles-TR3- C1 BA-434567	-25.4	330 ± 30	485-305	AD 1465-1645	Charred material 2 cm below sand blow from buried soil
Stiles-TR3- C2 BA-434568	-28.6	380 ± 30	505-425 395-320	AD 1445-1525 AD 1555-1630	Charred material 3 cm below sand blow from buried soil

¹ Conventional radiocarbon ages in years B.P. or before present (1950) determined by Beta Analytic, Inc. Errors represent 1 standard deviation statistics or 68% probability.

² Calibrated age ranges as determined by Beta Analytic, Inc., using the Pretoria procedure (Talma and Vogel, 1993; Vogel et al., 1993). Ranges represent 2 standard deviation statistics or 95% probability.

Trench 2

Trench 2 crossed an isolated semi-circular sand blow and was 13.5 m long, 0.5 m shorter on its western end than originally proposed. The trench was stopped short because the feeder dike had been exposed at the eastern end of the trench and the sand blow was thinning towards the west. The trench varied in depth from 0.65-1.05 m.

The plow zone ranged from 10-30 cm thick with several plow scars extending another 8-15 cm into the sand blow. Beneath the plow zone, the sand blow, up to 45 cm thick, was composed of two depositional units, L1 and L2 (Figure 4-131). Unit L1 was discontinuous, ranged up to 10 cm thick, and was composed of fine and very fine sand with clay clasts and capped by lignite, silty very fine sand, and silt. L1 was observed only west of the dike. Unit L2 overlay L1, ranged up to 38 cm thick, and changed character with distance from the feeder dike. In the upper 10-20 cm of L2, sand grains were coated with fines that probably washed into the sand blow from the overlying soil by rainwater. Above and adjacent to the feeder dike, L2 was composed of fine and medium sand containing several large clay clasts. Towards the west, L2 divides into two subunits. The lower subunit was composed of coarse, fine, and medium sand with numerous clay clasts and lignite pebbles, and the upper subunit was composed of fine and medium sand with only a few small clay clasts. The boundary between the two subunits was primarily textural though it may have been enhanced by the accumulation of translocated fines. Towards the western end of the trench, the lower subunit further divides into three thinner layers separated by silt. A large sand dike crosscut the buried soil and connected with the sand blow towards the eastern end of the trench. The dike was about 25 cm wide, was composed of fine and medium sand (unit L2) containing a subvertical zone of clay clasts, and had a strike and dip of N70°W and 72°SW.

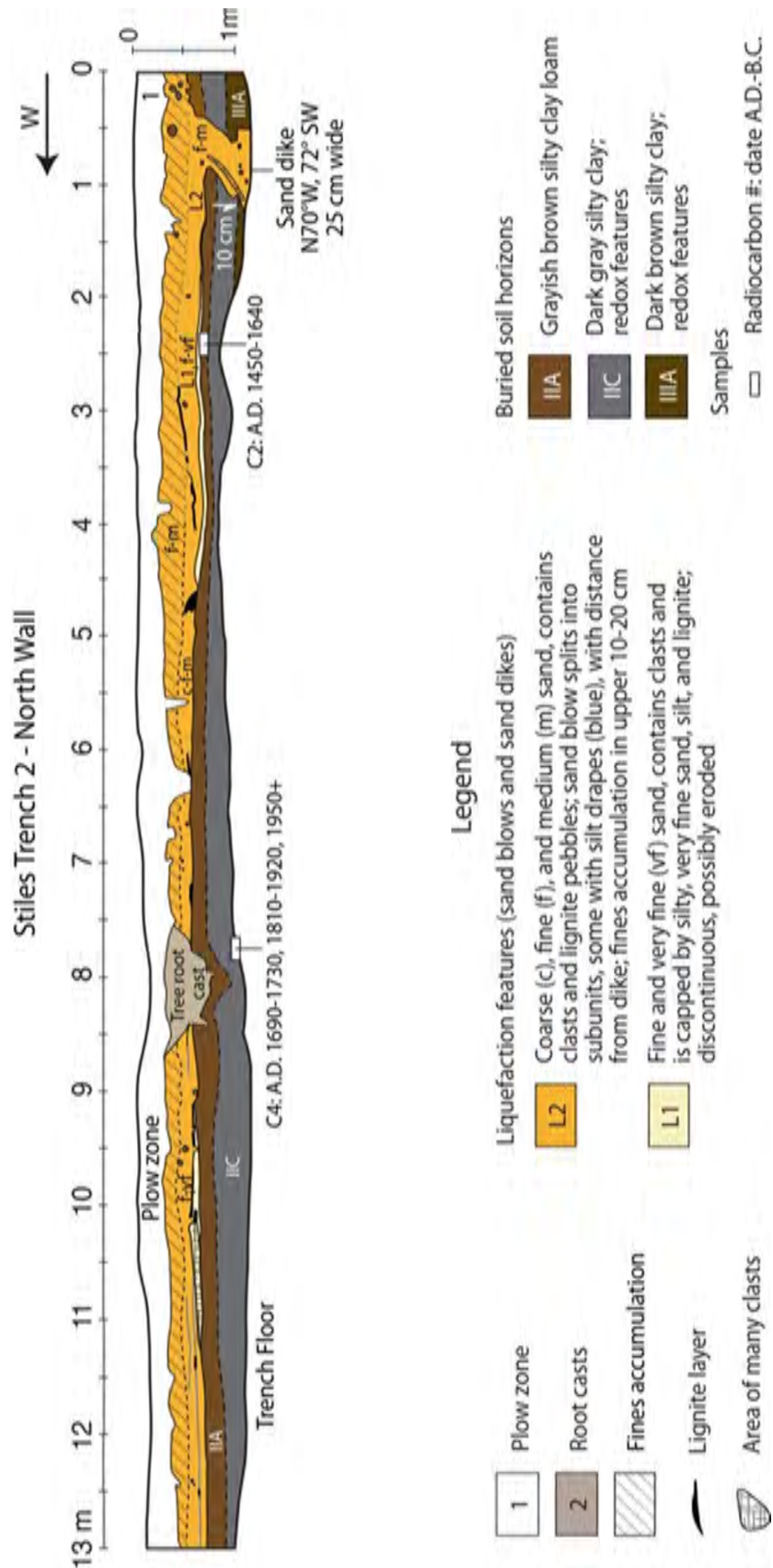


Figure 4-131 Log of Trench 2 at Stiles site, showing sand blows and related sand dikes. Radiocarbon dating of sample TR2-C2 from the top of the buried soil suggests that the overlying sand blow formed soon after A.D. 1450. Sample TR2-C4 probably from tree root that post dates the compound sand blow.

Between trench meter marks 7.5 and 8.5, the entire thickness of the sand blow and upper 20 cm of the buried soil are disturbed. The disturbed zone is crater shaped and contains mixed sand and soil and clasts of soil. Below the crater, root casts extend 15-20 cm into the soil. The disturbance was likely caused by tree throw, or toppling of a tree, creating a crater that was filled with chunks of soil as well as sand that washed in over time. The deposition of the subunits of L2 did not appear to have been affected by the presence of a tree, unlike the historical sand blow at the Faulkner site, suggesting that the tree at the Stiles site had grown through the sand blow after its formation.

The surface of the buried soil was 10 cm lower on the west side of the dike than on the east side. Similarly, boundaries of underlying soil horizons were displaced downward on the west side of the dike. The down-dropped surface of the buried soil remained at about the same depth (~70 cm below the surface) for about 3 m at which point it was inclined slightly upward towards the western end of the trench. Given that the buried surface is offset across the dike and that the dike is subparallel to the nearby Pemiscot Bayou, ground failure and dike formation may have been related to lateral spreading towards the southwest. As with others in the region, this sand blow filled the topographic low created by ground subsidence resulting from liquefaction and venting of subsurface sediment.

Radiocarbon dating was performed on two organic samples from Trench 2. A sample of charred material (TR2-C2) collected 1 cm below the sand blow from the buried soil yielded a calibrated date of A.D. 1450-1640. A second sample of charred material (TR2-C4) was collected 40 cm below the sand blow but yielded a much younger date of A.D. 1690-1730, 1810-1920, and 1950+ (Table 4-28). Given its young age and proximity to the tree throw cast, the sample was likely from tree roots that had grown through the sand blow.

Trench 3

Trench 3 crossed the large northwest-southeast oriented sand blow and was 13 m long, 1 m longer on its western end than originally proposed. The trench varied in depth from 0.65-1.25 m. The water table was encountered at this depth.

The plow zone ranged from 18-30 cm thick with several plow scars extending another 8-10 cm into the sand blow. Beneath the plow zone, the sand blow, up to 108 cm thick, was composed of five depositional units, L1-L5 (Figure 4-132). Unit L1 was discontinuous, ranged up to 12 cm thick, and was composed predominantly of fine sand with a few clay clasts and capped by silty, very fine sand, silt, and lignite. L1 was observed primarily between the main dike and the smaller dike towards the eastern end of the trench (between trench meter marks 1 and 4). L1 did not occur east of the smaller dike. Discontinuous domains of L1 occurred west of the main dike (between trench meter marks 5.5 and 10). Unit L2 overlay L1, ranged up to 35 cm thick, and changed character with distance from the feeder dike. Adjacent to the main feeder dike, L2 was composed of fine and medium sand containing clay clasts and was capped by silty, fine and very fine sand and lignite. Towards the west, L2 divides into two subunits. The lower subunit was composed of fine and medium sand with clay clasts and lenses of lignite and was capped by silty, very fine sand, lignite, and silt. The upper subunit was composed of medium and fine sand with few clay clasts and was capped by silty, very fine sand and lignite. The upper subunit pinched out or was difficult to follow west of meter mark 10.5. The upper boundary of L2 was iron-stained.

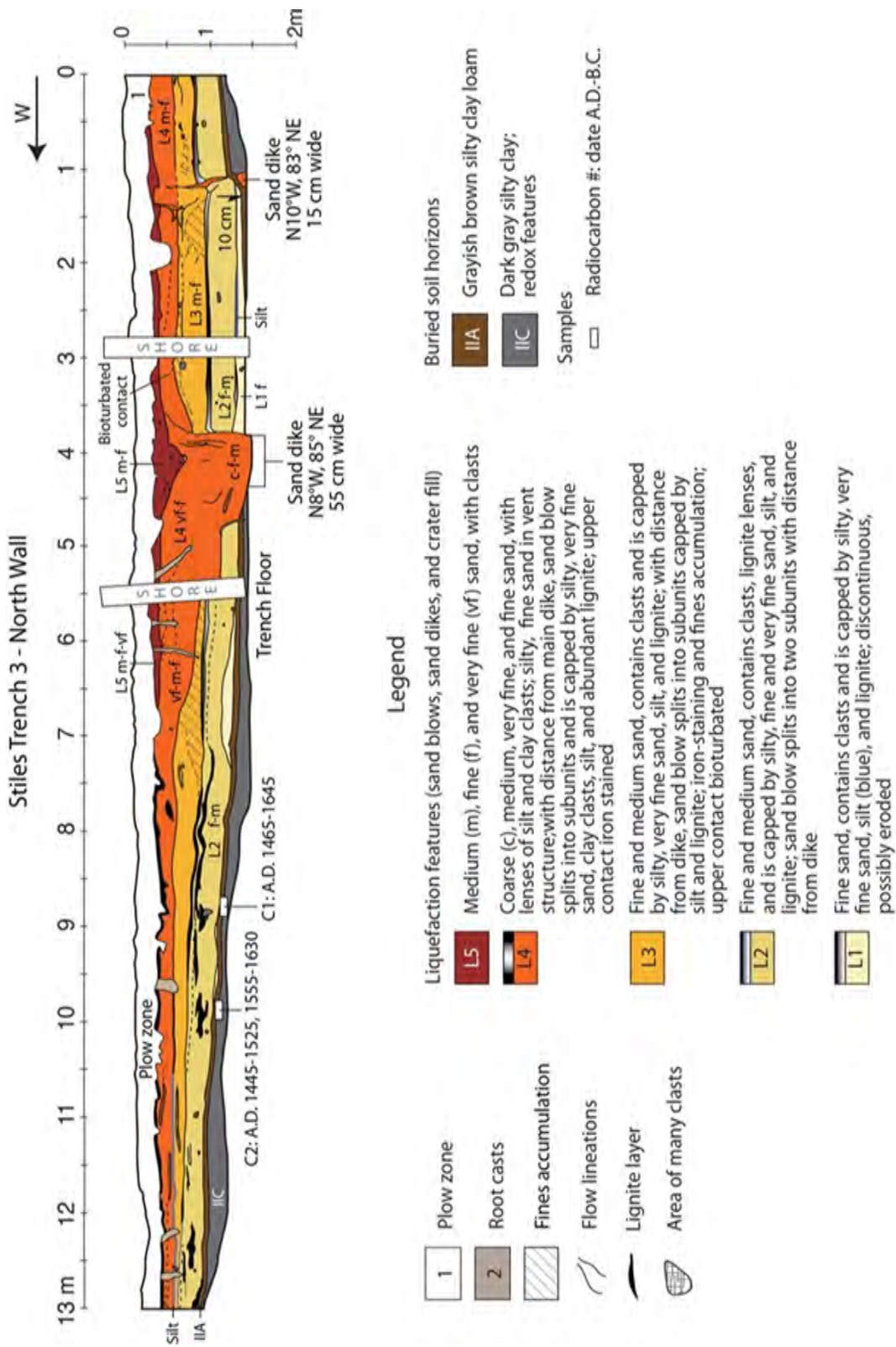


Figure 4-132 Log of Trench 3 at Stiles site, showing sand blows and related sand dikes. Radiocarbon dating of samples C1 and C2 from the top of the buried soil suggest that the overlying sand blow formed soon after A.D. 1445-1465. This compound sand blow is similar in age to compound sand blow in nearby Trench 2.

Unit L3 overlay L2, ranged up to 33 cm thick, and also changed character with distance from the main feeder dike. Adjacent to the main feeder dike, L3 was composed of fine and medium sand with clay clasts and was capped by silty very fine sand, silt, and few lenses of lignite (Figure 4-132). Towards the eastern end of the trench, unit L3 split into two subunits divided by a thin layer of silt and lignite. The upper subunit thinned and fined towards the east. Towards the western end of the trench, unit L3 split into two possibly three subunits with contacts that were difficult to track for more than 1 m. The unit thinned and fined towards the west. The upper contact of L3, as well as textural domains within the unit, were iron-stained. In addition, fines coated sand grains along these contacts. The fines probably had been washed down through the sand blow from the overlying soil by rainwater. The upper contact of unit L3 was also bioturbated in places.

Unit L4 overlay L3, ranged up to 70 cm thick adjacent to the west side of the main dike, and thins to about 20 cm on both ends of the trench (Figure 4-132). Above the main dike, the sand blow is composed of coarse, fine, and medium sand and fines upward to very fine and fine sand. A crater fill of silty, fine sand occurred at the top of L4 above the sand dike. Adjacent to the main feeder dike, L4 was composed of medium and fine sand and fines upward to very fine and fine sand. Towards the western end of the trench, the unit is composed of very fine, medium, and fine sand with lenses of silt and clay clasts, splits into 3 thin subunits separated by laminations of silty, very fine sand and lignite, and is capped by a layer up to 5 cm thick of silty, very fine sand, silt, abundant lignite, and clay clasts. Towards the eastern end of the trench, L4 is composed of medium and fine sand and appears to split into two subunits separated by a silt drape between the two dikes. East of the small dike, the unit exhibits reverse grading, coarsening upwards from fine sand with many granules of lignite to medium and fine sand. The upper contact of L4 between the two dikes is defined by silty, very fine sand and iron staining. Unit L5 overlies L4 in part and is the uppermost unit of the sequence. It was present above both dikes, where it is a crater fill, between both dikes, and for about 2 m west of the main dike. The upper part of the unit was disturbed by plowing and may have been completely destroyed towards both ends of the trench. Above the main dike, L5 was composed of medium and fine sand and contained many clasts. To either side of the main dike, the unit is discontinuous, composed of medium, fine, and very fine sand, and was disturbed by root casts.

Two feeder dikes, and associated vent areas above, were observed in the trench. The main dike exposed in the trench floor was about 55 cm wide, was composed of coarse, medium, and fine sand with clay clasts, and exhibited flow structure (Figure 4-132). Above the dike, the vent area was composed mostly of coarse, medium, and fine sand, fined upward to medium, very fine, and fine sand, contained many clay clasts, and exhibited flow structure. The strike and dip of the eastern margin of the vent structure above the main dike was N8°W and 85° NE. The smaller dike, 2.5 m east of the main dike, was 15 cm wide, observed in the trench floor and towards the lower 10 cm of the trench wall, but did not completely breach the soil to connect with the vent structure above (Figure 4-133). Flow structure was delineated by fine sand, silty very fine sand, and tiny pieces of lignite. The strike and dip of the vent structure above the smaller dike was N10°E and 83° NE.

The surface of the buried soil, as measured above the margins of the underlying smaller dike, was displaced downward by 10 cm on the west side of the dike (Figure 4-132). Similarly, the upper contact of unit L2 was displaced 10 cm across the dike, west side down whereas the upper contact of L3 was not displaced. This indicates that the ground subsided between the two dikes during the deposition of unit L3. East and west of the two sand dikes, the buried ground surface is

inclined gently towards the dikes. Above the inclined buried surface, units L2, L3, and L4 thin away from the dikes. At this site, it appears that the ground subsided as subsurface sediment vented to the surface and filled the subsided area.

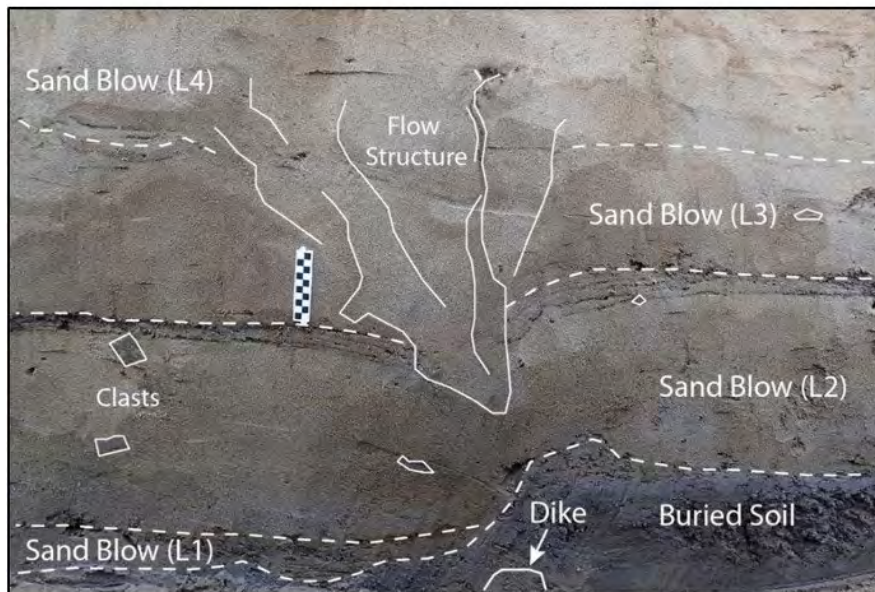


Figure 4-133 Photographs (upper - unannotated; lower - annotated) of vent area with flow structure of compound sand blow above small dike in north wall of Stiles Trench 3 (see Figure 4-132). Dike observed in trench floor and lowermost trench wall did not connect with base of sand blow. Grayish brown soil and overlying units L1 (to left of small dike) and L2 of compound sand blow were offset across dike by 10 cm. Unit L1 was capped by silt and lignite and L2 was capped by silty, fine sand and lignite that fines away from dike to silty, very fine sand, and lignite. Dashed lines represent clear contacts. Thin solid white lines indicate flow structure. On scale, each black and white interval represents 1 cm.

Radiocarbon dating was performed on two samples of charred material from the buried soil beneath the sand blow. Sample TR3-C1 collected 2 cm below the sand blow yielded a calibrated date of A.D. 1465-1645 and sample TR3-C2 collected 3 cm below the sand blow yielded a calibrated date of A.D. 1445-1525, 1555-1630 (Table 4-28). The two dates are very similar to one another and stratigraphically consistent with the date of the deeper sample being slightly older.

4.4.5.4.6 *Paleoseismic Interpretations*

Trench 1

The compound sand blow exposed in Trench 1 was composed of three depositional units separated in part by lignite and silt layers. The three units are interpreted as sand blows representing three distinct events. Dessication cracks of the upper contact of L1 suggest a short period (weeks) of subaerial exposure prior to burial by L2. Otherwise, there was no discernible soil development of the contacts separating the units. Therefore, this compound sand blow likely formed during three closely timed earthquakes, similar to some of the sand blows that formed during the A.D. 1811-1812 New Madrid earthquakes. The formation of soil lamellae in the upper 20-30 cm of the compound sand blow indicates that it is more than a few hundred years in age and did not form during the A.D. 1811-1812 earthquakes. Soil lamellae were observed in the Johnson site sand blow that formed about 1100 years ago and in several of the Marianna sand blows that are more than 5000 years old. The calibrated radiocarbon date of the soil buried by the compound sand blow provides close maximum age constraint and suggests that the liquefaction features formed soon after B.C. 1010 (or 2960 yr B.P.).

Trench 2

For the compound sand blow exposed in Trench 2, the two depositional units likely formed during two closely timed earthquakes. Subunits within L2 are probably related to changes in flow direction and velocity and/or pulsing during venting of water and sediment. The translocation of fines into the upper 10-20 cm of L2 and the accumulation of fines along the textural boundary of the two subunits of L2 suggest that the compound sand blow formed prior to A.D. 1811. The calibrated date of A.D. 1450-1640 from the upper 1 cm of buried soil provides a close maximum age and suggests that the liquefaction features formed soon after A.D. 1450.

Trench 3

The compound sand blow in Trench 3 was composed of five depositional units each capped by silty, fine and very fine sand, lignite, and silt, except for unit L5. Deposition of unit L5 might be related to reworking of unit L4 following the earthquake sequence. However, the presence of many clasts in the portion of L5 above the sand dike and the fining of L5 away from the vent suggest that it is a separate vented deposit. Of the sediment capping the four lower units, interbedded silty, fine and very fine sand, and lignite may represent the waning phase of venting whereas silt and lignite are thought to represent a post-venting deposit formed as fines settle out of vented water and lignite remains as vented water soaks into the ground or evaporates. Bioturbation of the upper contact of L3 indicates that it was exposed at the surface for a short period of time prior to burial by unit L4. Units L2, L3, and L4 divide into subunits with distance from the feeder dikes which are probably related to changes in flow direction and velocity and/or pulsing during venting of water and sediment. Accumulation of fines along the upper contact of unit L3 and the textural boundaries within L3, as well as iron-staining of upper contacts of units L2, L3, L4, suggest that the compound sand blow formed prior to A.D. 1811.

The calibrated dates of A.D. 1445-1525, 1555-1630 and A.D. 1465-1645 from 3 cm and 2 cm below the sand blow, respectively, provide close maximum age constraint and suggest that the liquefaction features formed soon after A.D. 1445-1465. This age estimate is similar to that for the nearby sand blow in Trench 2, suggesting that they formed during the same sequence of events about A.D. 1450 \pm 150 yr. Dating of the compound sand blow in this trench and Trench 2 suggest that the event occurred close to or soon after A.D. 1445.

4.4.5.5 Pritchett Site

The Pritchett site is located about 15 km west of Dyersburg, Tennessee, 10 km southeast of the Cottonwood Grove fault and near the postulated epicenter of the **M** 7.0 December 16th, 1811, aftershock (Johnston and Schweig, 1996; Hough and Martin, 2002). In addition, it is about 15 km northwest of the Eastern Reelfoot Rift Margin fault (Figure 4-18 and Figure 4-19). All of these structures may be capable of generating large earthquakes (EPRI, DOE, and NRC, 2012). The Pritchett site occurs near the mapped boundary between the Late Pleistocene valley-train deposits (level 1) to the east and Holocene meander-belt deposits to the west (Figure 4-56; Saucier, 1994). The Obion River flows along the mapped boundary of the Late Pleistocene and Holocene deposits.

The location of the **M** 7.0 December 16th, 1811, dawn aftershock is poorly constrained. Hough and Martin (2002) proposed that it occurred in western Tennessee near Calvary, a small town north-northwest of Dyersburg. This location was based on an account of the event by John Hardeman Walker, who was near a lake about 10 miles east of the Mississippi at Little Prairie (now Caruthersville) in the vicinity of the Obion River at the time of the earthquake (Cummings, 1847). According to Walker, "the soft alluvial earth was opened in many rents of great depth, in which our little lake had completely lost itself." Cummings (1847) noted that "the lake, which evidently was once the bed of the main river, is now as high and dry...and is now a beautiful prairie." On the basis of the changes to the landscape, Hough and Martin (2002) suggested that the aftershock was associated with permanent vertical deformation. In addition, they suggested the nearby southeastern segment of the Reelfoot fault as the source of the earthquake, while acknowledging uncertainty in the location.

During a previous study that involved searching for earthquake-induced liquefaction features along the Obion River, a very large sand dike containing large tabular clasts of clay and an associated sand blow were found at site OR216/603 (Figure 4-134, Figure 4-135, and Figure 4-136). The sand dike strikes \sim N35-46°E and a buried soil with *in situ* tree trunks, as well as other sedimentary layers, are offset about 1 m, east side down, across the dike. The upper part of the sand blow was apparently reworked by fluvial processes and buried (\sim 4 m) by fluvial deposits. Radiocarbon dating of a sample collected from the *in situ* tree trunk in the buried and offset soil yielded a two-sigma calibrated date of A.D. 1200-1320, AD 1350-1390, which provides a maximum age for the sand dike and related sand blow. It seems likely that these features formed during the A.D. 1450 \pm 150 yr earthquake(s).

As seen on satellite imagery, numerous lineaments occur along strike of the large sand dike at OR216/603 and define a zone that extends about 32 km from the old abandoned course of the Obion River near Midway to Chickasaw Bluffs northeast of Calvary (Figure 4-135). The lineaments include topographic and tonal lineaments, as well as large, linear sand blows like those at the Pritchett site south of OR216/603. The sand blows at the Pritchett site are reminiscent of the large, linear sand blows southwest of Marianna, AR, that appear to be the surface expression of an underlying fault zone (Tuttle et al., 2006; Odum et al., 2016). Also, the course of the Obion River also appears to have been diverted towards the south in three locations

where it encountered the zone of lineaments, including in the Midway area where the old course of the Obion River was abandoned between A.D. 1795 and 1822 according to historical maps of TN. It is not currently known, but perhaps the change in the rivers course occurred during the A.D. 1811-1812 earthquakes. Taking all these features and occurrences together, it is proposed that the Obion River zone is the surface expression of an active fault zone. The Pritchett site sand blows cross Holocene and Late Pleistocene deposits. Given the possibility that the large linear sand blows may delineate an active fault and that Late Pleistocene deposits have the potential to contain a longer record of paleoearthquakes than would Holocene deposits along the Obion, the Pritchett site was selected for paleoseismic investigation.

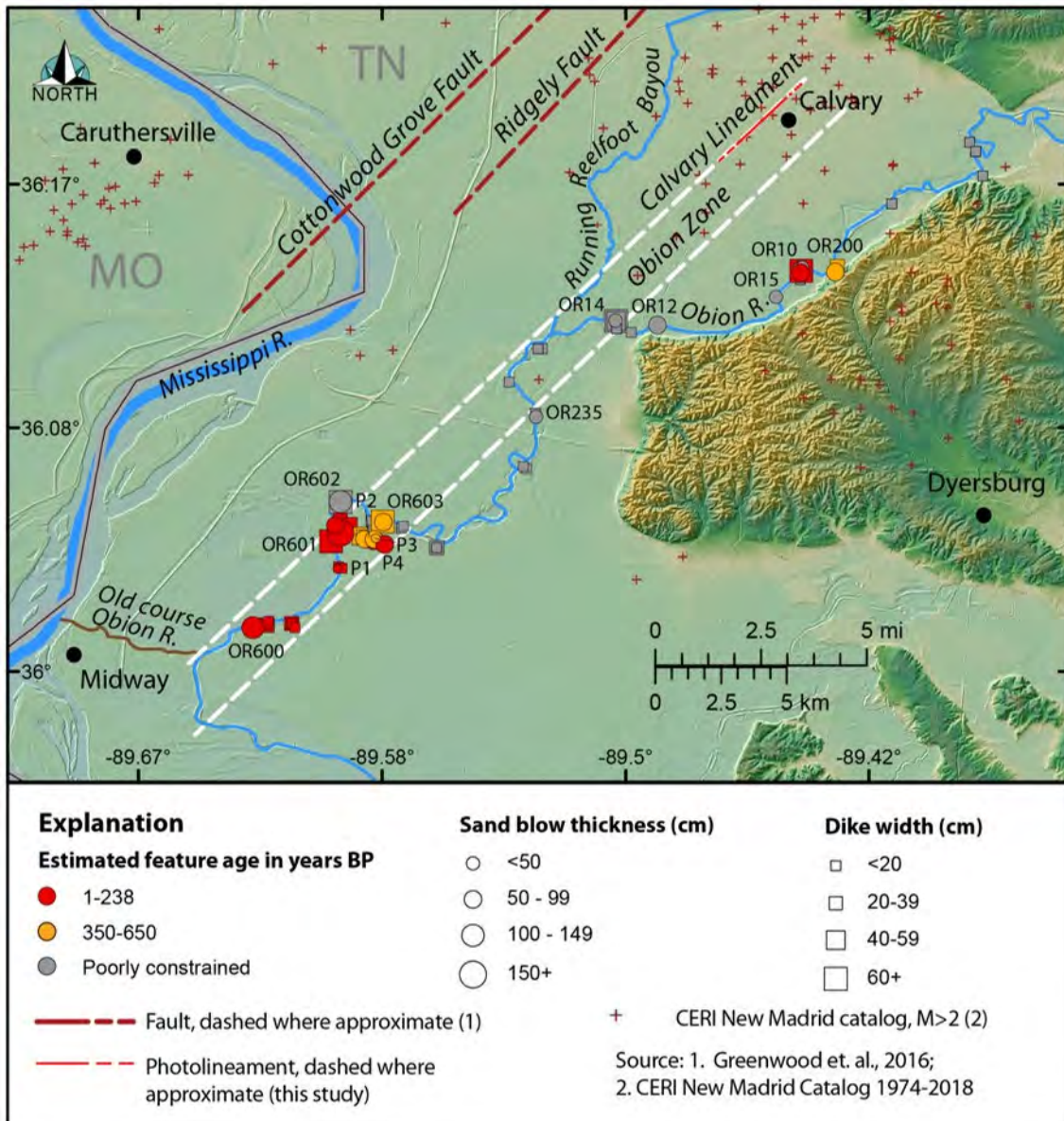


Figure 4-134 Map showing liquefaction features along the lower Obion River, including those at OR216/603 and the Pritchett site (P1-P4), previously mapped faults, including the Cottonwood Grove and Ridgely faults, and the postulated Obion River fault zone (indicated by two parallel dashed white lines).

4.4.5.5.1 Reconnaissance

The initial site visit was conducted in September 2011 primarily to field check interpretations of satellite imagery that large northeast and north-northeast oriented light-colored linear patches in are sand blows. The Pritchett site includes several open fields that have been farmed for decades (Figure 4-83). According to the owner/farmer of the property, the fields have been plowed but not graded. The plowed fields occur from 0.4 to 2.3 km from the Obion River. At the time of the initial visit, soybeans were growing in rows. There were large areas where either the soybeans were yellow and growing poorly or had died altogether. These areas corresponded with the large linear patches thought to represent sand blows, which often experience droughty soil conditions in the summer and early fall. The areas were found to be sandy at the surface in contrast to the adjacent darker-colored clayey soils typical of floodplain deposits.

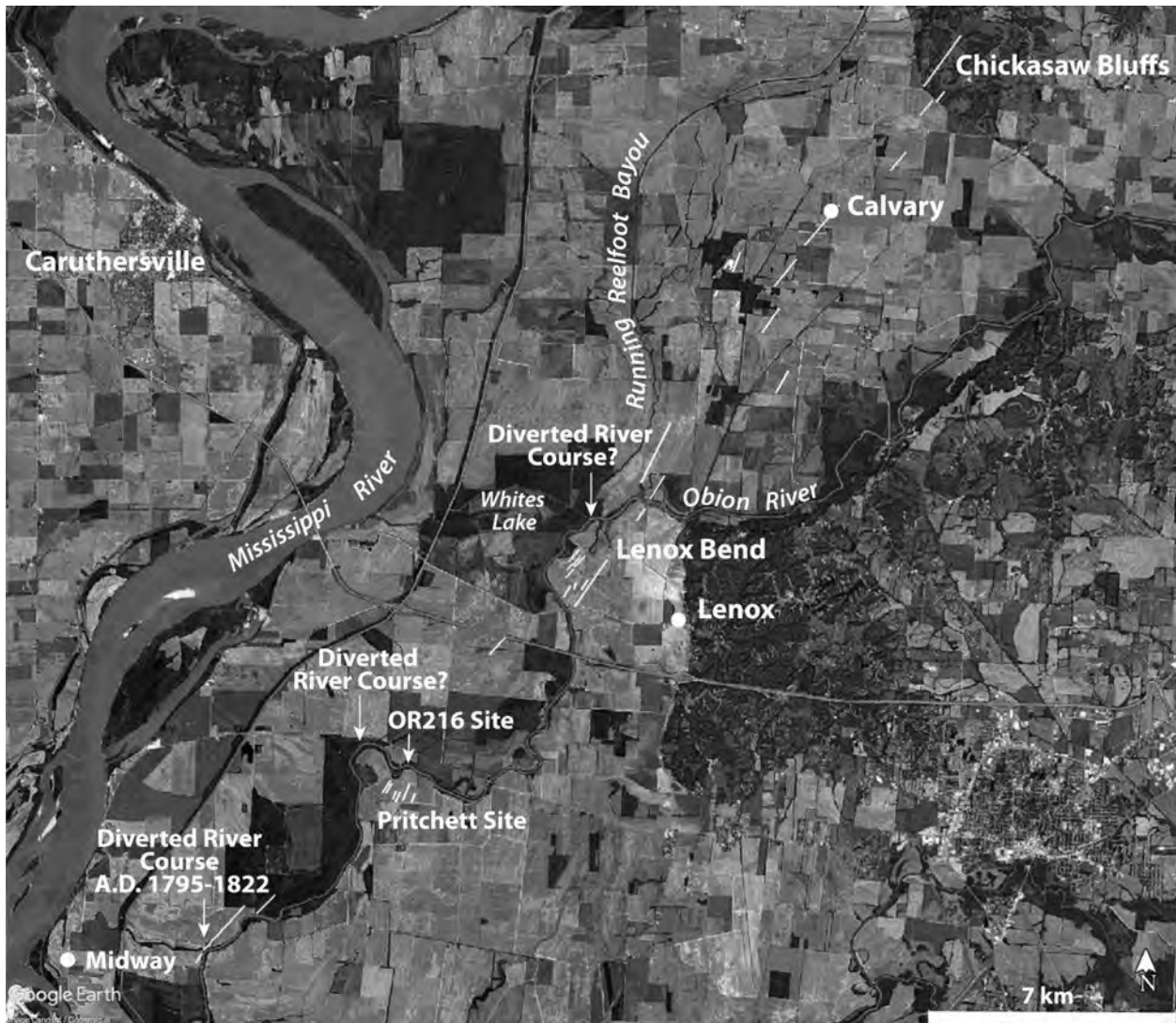


Figure 4-135 GE image showing locations of the OR216/603 and Pritchett site as well as numerous lineaments along a zone extending from the old course of the Obion River near Midway to Chickasaw Bluffs northeast of Calvary, TN.

We hand dug two soil pits in the light-colored patches to observe the sedimentological characteristics of the likely sand blow deposits (Figure 4-137). The soil pits revealed sandy layers

containing lignite and clay clasts, similar to known sand blows in the area. Both soil pits were dug in large north-northeast oriented patches. Soil pit 1 was 45 cm deep. As observed on the pit walls, the upper 20 cm were brown, massive, silty sand interpreted to be a plow zone. The lower 6 cm of the plow zone contained clay clasts and lignite. The plow zone was underlain by coarse to fine sand down to 39 cm, followed by clayey soil. The sand layer contained thin layers of lignite and clay clasts. Soil pit 2 was 60 cm deep. The upper 24 cm were brown, massive, silty sand interpreted as a plow zone. Layered lignite occurred near the base of the plow zone. The plow zone was underlain by two layers of medium to fine sand down to 54 cm below the surface. The lower few centimeters of the lower sand unit were iron-stained. Again, clayey soil was found below the sand. Field observations of large linear patches of sandy soils surrounded by clayey soils as well as subsurface sandy deposits containing lignite and clasts support the interpretation that the light-colored linear patches identified on satellite imagery are sand blows resulting from earthquake-induced liquefaction.

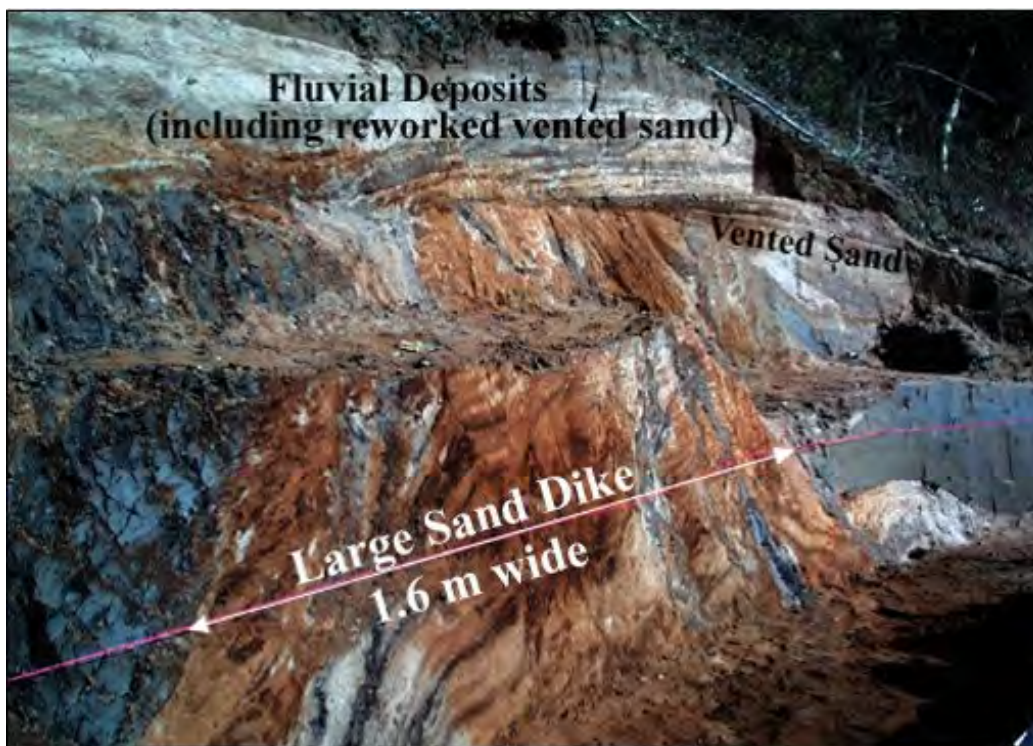


Figure 4-136 Photograph of very large sand dike striking N35-46°E and overlying sand blow buried by fluvial deposits at Obion River 216 site. *In situ* tree trunk that yielded date of A.D. 1200-1320, A.D. 1350-1390 was in top of very dark brown soil to left of dike. Liquefaction features probably formed during A.D. 1450±150 yr earthquake(s). Large linear sand blows at Pritchett site southwest of Obion River 216 occur along strike of 1.6-m-wide dike.

In order to confirm that sandy deposits are sand blows, and not some other sort of deposit such as fluvial point bar or aeolian sand dune, it is paramount to identify the feeder dike through which water and sand vented to the surface as the result of liquefaction. To assist in locating sand dikes below the sand blows, ground-penetrating radar (GPR) was used as a reconnaissance tool. GPR profiles were collected using a GSSI SIR-300 and a 400 MHz antenna with a time window of 35 ns for a penetration depth of about 1.75 m. Profiles were collected in two areas (Subareas A and B) where sand blows appear to be especially prominent (Figure 4-138 to Figure 4-139). The profiles imaged the contacts between the sand blows and the underlying clayey soil as well as

0.5-1 m wide feeder dikes that crosscut the contacts (Figure 4-140). The contacts appear to dip towards the feeder dikes and to be offset by about 0.5 m in both cases. The GPR profiles indicates that the sandy deposits are likely to be connected to feeder dikes in the depth range of 0.75-1.5 m below the surface and that the site suffered ground failure at the time the sand blows formed.

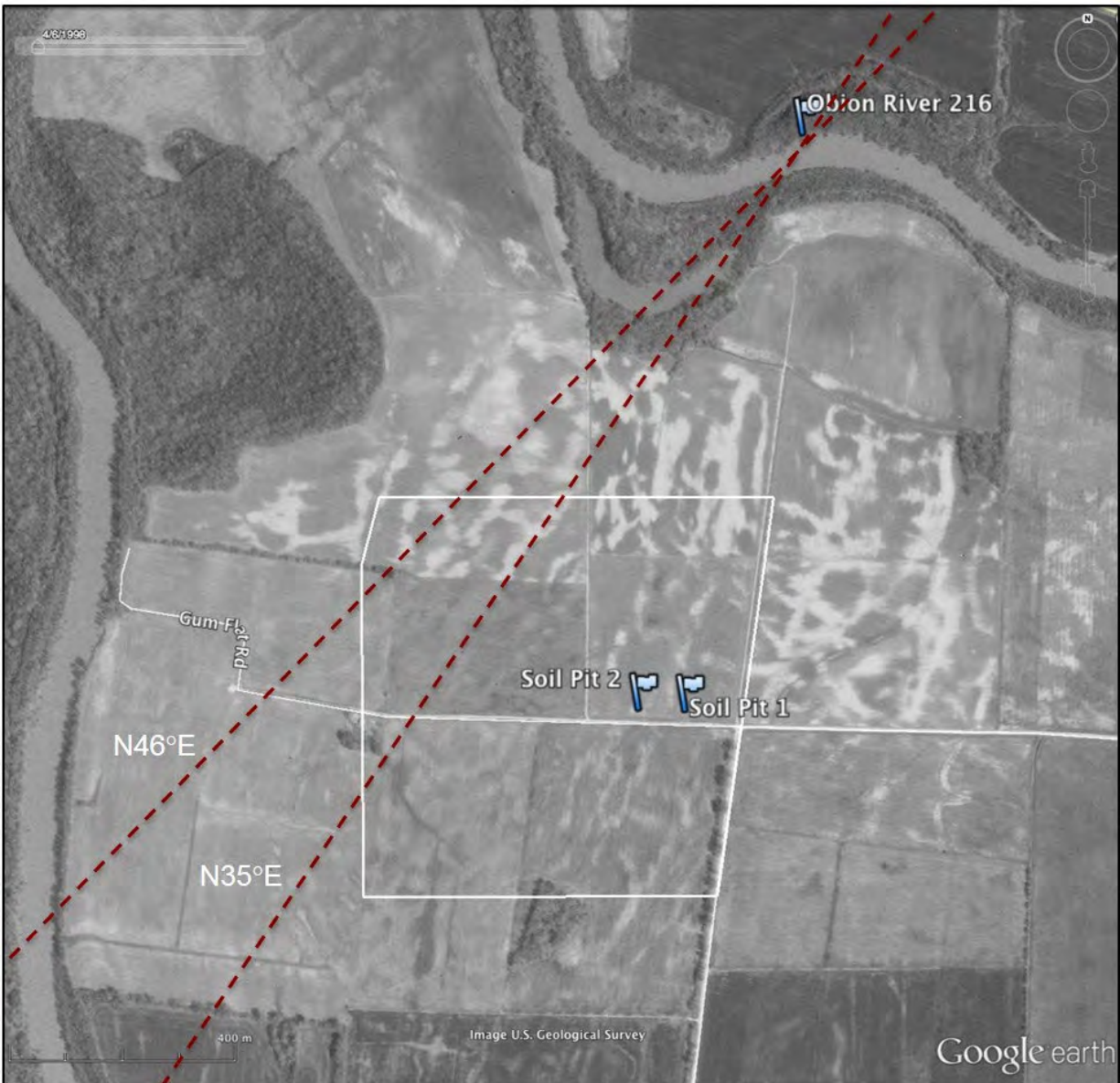


Figure 4-137 GE image showing locations of Pritchett site outlined by solid white line, soil pits excavated during initial site visit to evaluate presence of sand blows, and Obion River 216 site northeast of Pritchett site. Light-colored linear patches are large sand blows and form lineaments that cross Pritchett site. Large sand dike at Obion River 216 has similar strike (N35-46°E) to and is along trend of northeast-oriented lineaments that cross western portion of site (red dashed lines). Other lineaments with north-northeastern trend cross eastern portion of site as well as field to east. Satellite image was acquired April 6, 1998, by USDA Farm Service Agency.

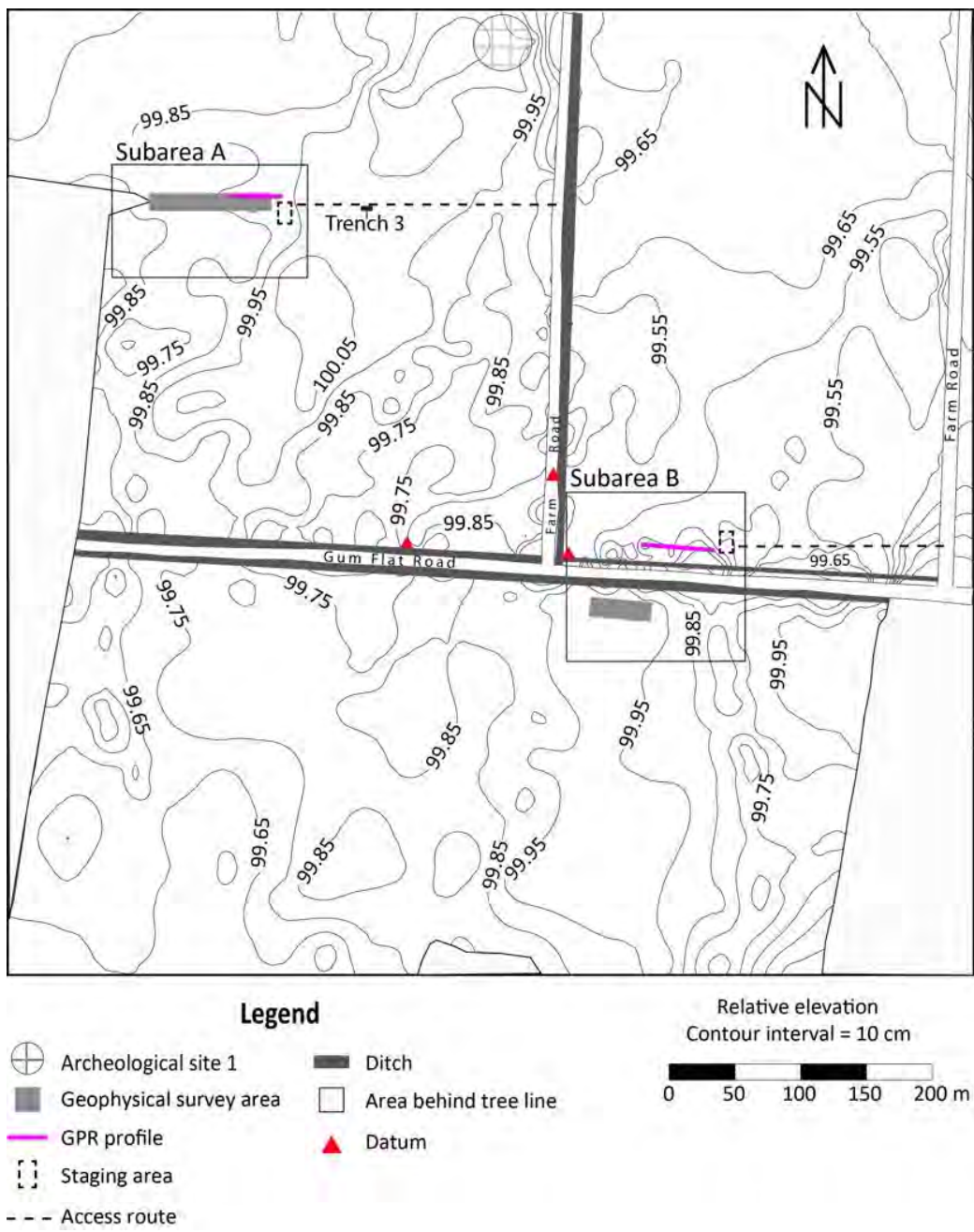


Figure 4-138 Map of Pritchett site showing locations of scatter of historical artifacts near northern edge of site; subareas A and B; geophysical survey areas and GPR profiles within those subareas; Trench 3 relocated east of subarea A; and access routes and staging areas. Enlarged maps of subareas A and B are shown in Figure 4-139.

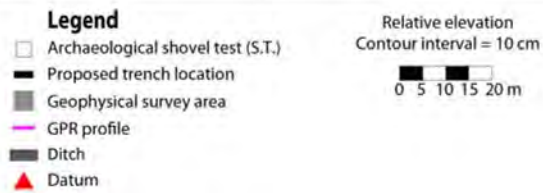
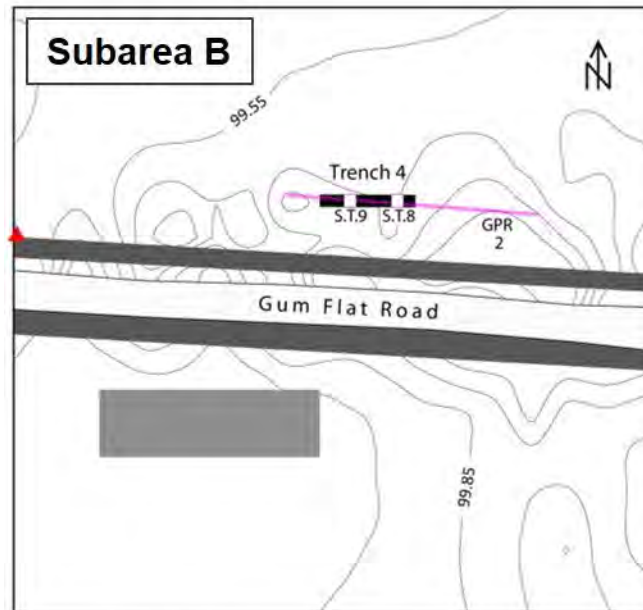
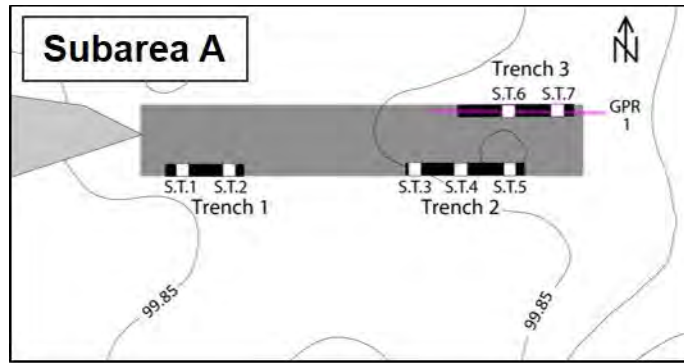


Figure 4-139 Pritchett site maps of Subareas A and B, showing locations of the geophysical survey area, GPR profiles, proposed trenches, and archaeological shovel tests. Trench 3 was located 80 m east of Trench 2 during fieldwork in fall of 2016.

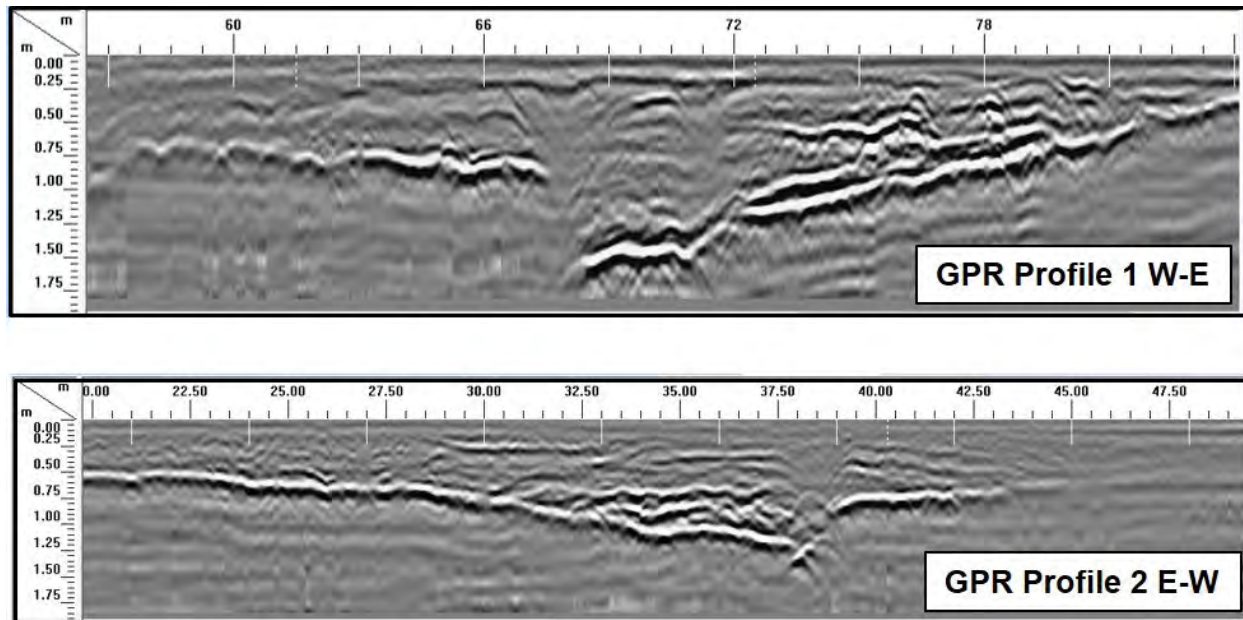


Figure 4-140 GPR profiles 1 and 2 collected across prominent sand blows at Pritchett site to verify presence of feeder dikes. On both profiles, strong dipping reflector represents contact between sand blow and underlying clayey soil and break in reflector represents feeder dike. Note ~0.5 m offsets of reflector across sand dike, which probably represents displacement of contact. Locations of profiles are shown on Figure 4-138 and Figure 4-139.

Given the likelihood that the large linear sandy patches are sand blows fed by sand dikes, arrangements were made to proceed with further site evaluation. The evaluation included (1) resistivity surveys to further map the sand blows and feeder dikes, (2) archaeological surface survey to locate any cultural sites in the site area, (3) selection of paleoseismic trenches locations based on all available information, and (4) archaeological shovel tests in the footprint of the trenches to assess the presence of absence of cultural materials.

4.4.5.5.2 *Electrical Resistivity Surveys*

In November 2015, electrical resistance tomography was used to further evaluate the Pritchett site for paleoseismological trenching. On the basis of interpretation of satellite imagery and reconnaissance at the site, two areas were selected for geophysical surveys (Figure 4-138 and Figure 4-139). Figure 4-141 shows the layout of the survey grids at the Pritchett site. Each grid consisted of multiple parallel profile lines within a rectangular area. Three east-west 96-m long profile lines were acquired in the north grid (Subarea A). Four east-west 46-m long profile lines were acquired for the south grid (Subarea B). Data were collected using an AGI SuperSting resistivity meter, with automatic electrode switching capability. Each line in the north grid consisted of 48 electrodes at 2-m spacing. Each profile line in the south grid consisted of 24 electrodes at 2-m spacing. An AGI mixed dipole array (similar to a conventional dipole-dipole configuration) was chosen for the data acquisition because this array provides optimal resolution for near-surface features and sufficient depth penetration to guide future trench excavations. Measurement errors in all surveys did not exceed 0.2%.

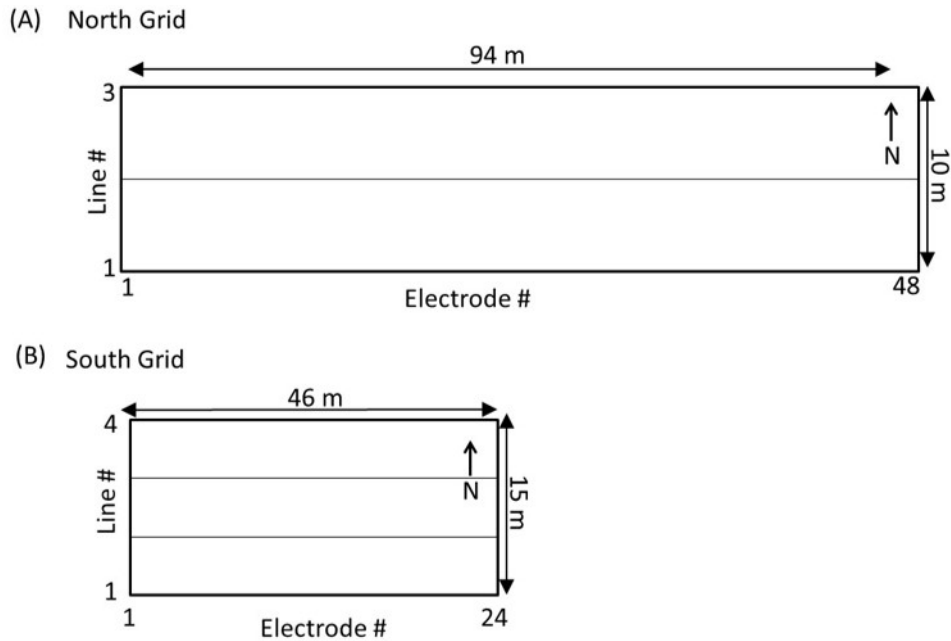


Figure 4-141 Layout of north and south resistivity survey grids at Pritchett site. (A) North survey grid (Subarea A) consisted of three 96-m parallel profile lines, spaced at 5 m apart, with 48 electrodes at 2-m spacing. (B) South survey grid (Subarea B) consisted of four profile lines spaced at 5 m, with 24 electrodes at 2-m spacing.

Raw data observations of apparent resistivity from all profile measurements were processed using AGI's 2D EarthImager software to produce cross-sections of the true subsurface resistivity distribution. The model is validated by using a forward-modeling technique to predict the apparent resistivity distribution if one assumes that the true resistivity distribution in the subsurface is correct. Statistical measures of the solution are thus obtained. The maximum RMS data error in the inversions was less than 5%.

Survey Results

North Geophysical Grid (Subarea A): Figure 4-142 contains a composite image showing the results of the electrical resistivity profile lines from the north grid at the Pritchett site. The line numbers increase to the north (see Figure 4-141 for layout). Hot colors (red-orange) represent areas of sediment with relatively high resistivity (usually indicating sandy or silty-sand deposits often associated with sand blows and sand dikes). Cool colors indicate subsurface areas that are more conductive, usually containing finer-grained sediments with varying amounts of clay. In Figure 4-142, Line 3, a moderately high resistivity anomaly is seen close to the surface at 75 m to 85 m along the profile. Small "finger-like" features at the base of the anomaly may be sand-filled dikes that connect with a narrow zone of high resistivity on the east side of the profile below 3.5 m depth. Both anomalies persist in Line 2 to the south, although they are shifted to the west. This shift suggests that the strike of the feature is northeast. A second near-surface area of moderately high resistivity is seen on the west side of the profile, between 15 m and 35 m. A zone of relatively higher conductivity separates the surface layer from a deeper zone below, which may be a sand-rich source layer. On Line 1, the two near-surface anomalies coalesce into one large high resistivity zone extending to ~2 m depth. The profile suggests an increase in sand content or coarser grained sediment. In all three profiles, a narrow zone (<2 m) appears to breach the fine-grained layer (blue layer). This feature may represent a dike, or alternatively a structural

feature. The near-surface anomalies of higher resistivity (hot colors) correlate with sandy patches observed on the surface and are attributed to sand blows.

South Geophysical Grid (Subarea B): Figure 4-143 and Figure 4-144 contain the electrical resistivity cross-sections for the south grid of the Pritchett site. Line 1, the farthest to the south, indicates a shallow (<2 m) high resistivity area on the western half of the profile. This layer decreases in resistivity to the east. The higher resistivity near-surface layer is separated from a deeper high-resistivity layer by a low resistivity zone that extends across the profile (blue region of cross-section). As seen in the north grid profiles, the deeper high-resistivity zone begins at ~ 4m below the surface. Unlike the smaller anomalies seen in the northern profiles, this large high-resistivity anomaly appears to trend north-south, although it varies slightly in width along the profile. Given its size and position relative to likely sand blows imaged in GPR profile 2 north of Gum Flat Road, this feature is interpreted as a large sand blow. In the four profiles, there is no strong evidence that the high-resistivity anomaly in the western half of the profile is connected by a dike to the zone below the high conductivity (blue) layer. However, the high-conductivity layer appears to thin towards the south, raising the possibility that a feeder dike could exist to the south of the grid.

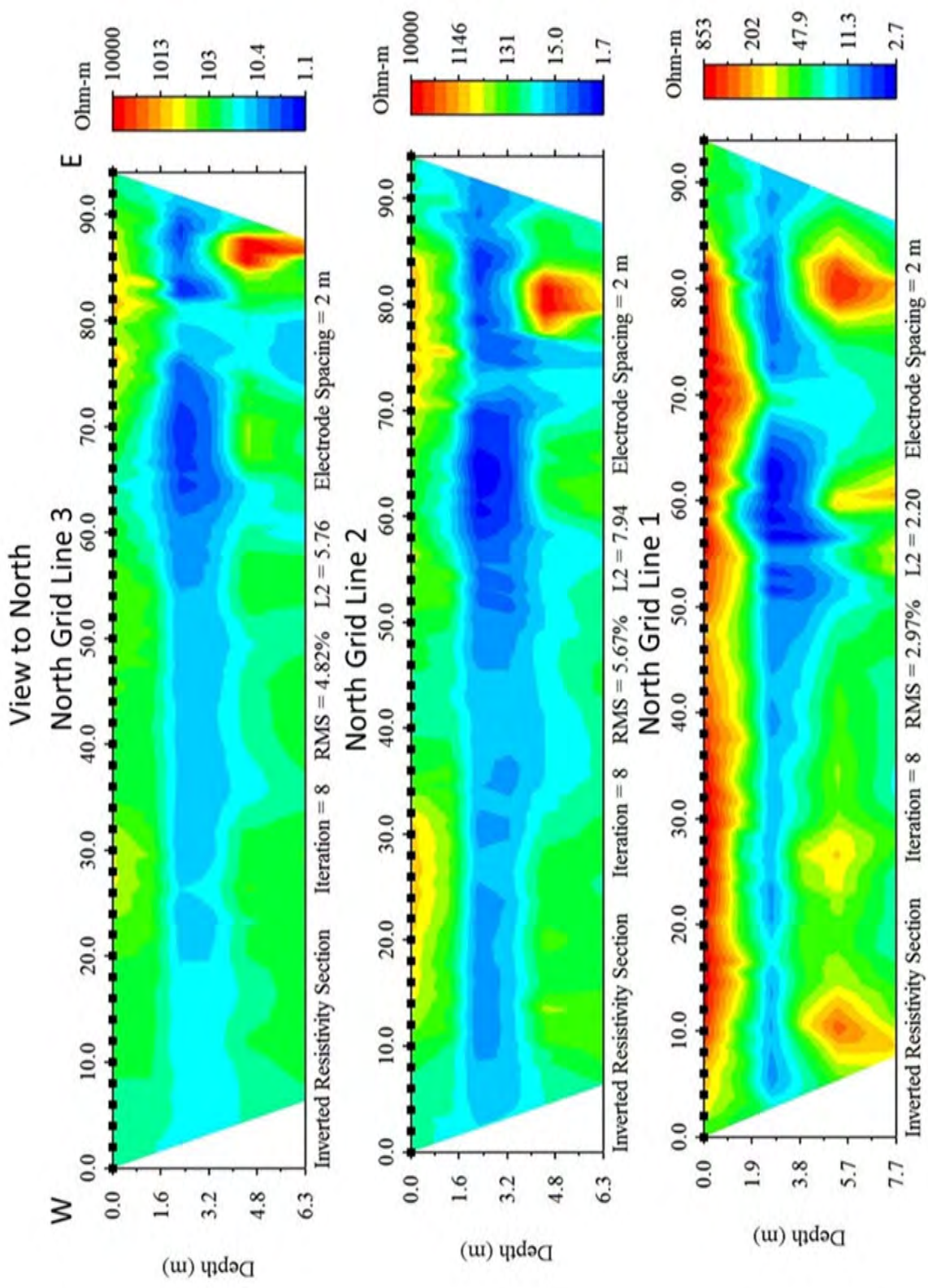


Figure 4-142 Composite Resistivity Images of Lines 1, 2 and 3 from North Grid (Subarea A) Pritchett Site

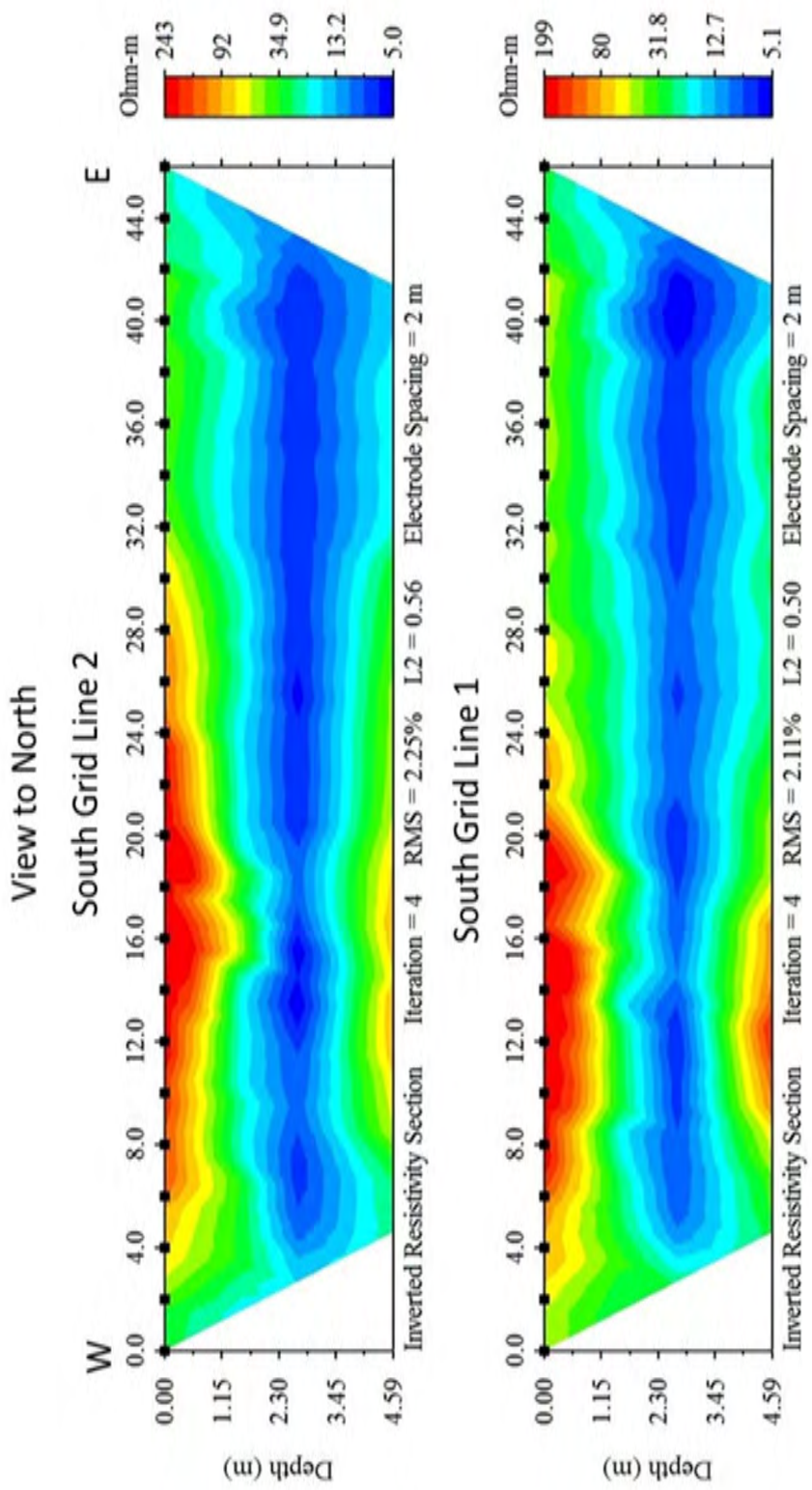


Figure 4-143 Composite Resistivity Images of Lines 1 and 2 from South Grid (Subarea B) Pritchett Site

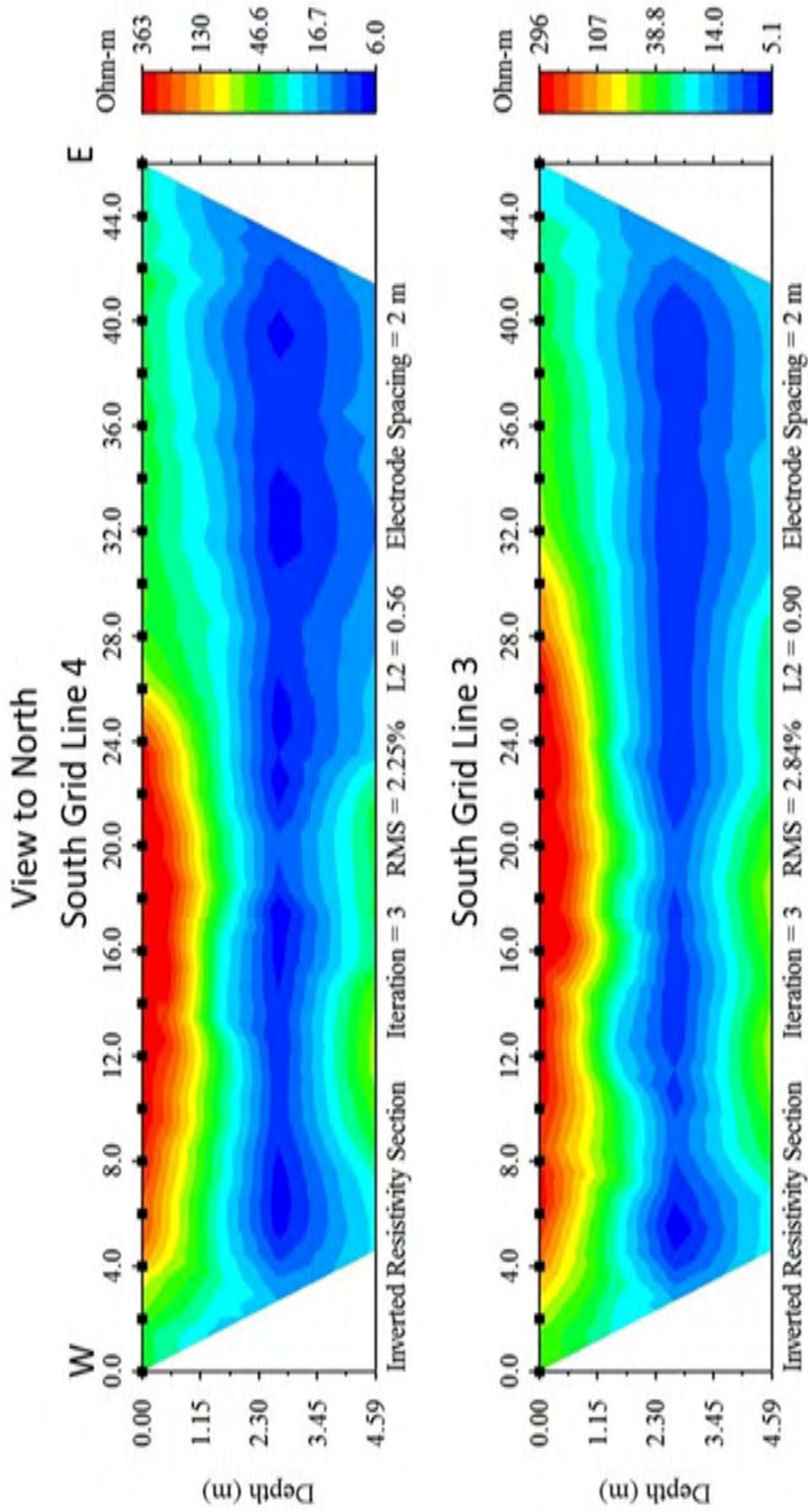


Figure 4-144 Composite Resistivity Images of Lines 3 and 4 from South Grid (Subarea B) Pritchett Site

4.4.5.5.3 Pre-Trenching Archaeological Assessment

The archaeological assessment of the Pritchett site was conducted over three days in November 2016. The assessment included a surface survey for cultural material in the site area and subsurface testing in the proposed paleoseismic trench locations. Both are reported in Tuttle et al. (2016) and summarized below.

Surface Survey

The pedestrian surface survey covered about 110 acres, encompassing and extending well beyond the proposed trench locations. At the time, crops had been harvested and visibility was moderate to poor (typically < 25%) due to soybean and milo stover (Figure 4-145). During the surface survey, three historic sites domestic sites were identified in the site vicinity. Two of the historic sites were north of the site area along the southern bank of the abandoned channel of



Figure 4-145 View west in vicinity of Trenches 1 and 2 showing moderate to poor surface visibility (typically < 25%) at time of archeological surface survey.

the Obion River. The third historic site, about 60 m in diameter, was within the Pritchett site area approximately 230 m northeast of proposed Trenches 1 and 2 (Figure 4-138). A structure is shown at this location on the 1957 Caruthersville 15' quadrangle and the 1960 air photo base (Sheet 30) for the 1965 Dyer County soil survey, but not on the 1971 Caruthersville 7.5' quadrangle. A small general surface collection of all visible material was made at the site (Table 4-29). It includes 57 items totaling 516 grams, including brick, ceramics, table and bottle glass and a few other items was made. All material collected at the site is commensurate with the mid 20th century date (1950s-1960s) indicated by the maps.

Table 4-29 Site 1 Artifacts

Item	Count	Weight (g)
ARCHITECTURE		
Brick	12	322
Pane glass	6	16
KITCHEN		
Late refined earthenware	5	10
Semiporcelain	2	2
Stoneware	1	7
Porcelain	2	2
Table glass, green	1	7
Table glass, white	1	4
Bottle glass, clear	13	73
Bottle glass, aqua	5	21
Bottle glass, white	3	23
Canning jar seal, white glass	3	9
TOYS		
Porcelain doll arm	1	3
ACTIVITIES		
File	1	9
Burned earth	1	8
TOTAL	57	516

Test Units

In Subarea A, two archaeological test units or shovel tests, designated ST1 and ST2, were excavated in the footprint of proposed Trench 1; three test units, ST3-ST5, were excavated in the footprint of Trench 2; and two test units, ST6 and ST7, were excavated in the footprint of proposed Trench 3 (Figure 4-139). In Subarea B, two archaeological test units, designated ST8 and ST9, were excavated in the footprint of proposed Trench 4 (Figure 4-139).

Test unit 1 (ST1) showed a distinct plow zone (10 YR 4/3) to about 20 cm with a plow-compacted (7.5 YR 4/4) loamy sand above the sand blow to 33 cmbs, where a redoximorphic horizon about 3 cm thick was identified (Figure 4-146). The base of the plow zone showed abundant evidence of bioturbation and leaching extending into the plow pan. The loose, coarse sand (10 YR 4/4) extended to 70 cmbs, with the lower 10 cm being saturated. The sand includes coarse quartz grains, with some mica, magnetite-hematite, and feldspar as well as small (10 YR 5/5) clayey rip-up clasts. The 2Ab horizon from 70 to 80 cmbs is slightly silty plastic clay (10 YR 6/2) with strong clay skins on blocky soil ped surfaces and prominent vertical cracks where sand has percolated down. The contact at the base of the sand blow is wavy (Figure 4-146 and Figure 4-147).

Test unit 2 (ST2) showed the plow zone extending to about 25 cmbs. The contact with the sand was irregular and heavily modified by cultivation. The homogeneous, coarse mineral sand with occasional lignite nodules and rare 2 cm x 5 cm rip-up clasts extended to 72 cmbs, with the sand being saturated at its base (Figure 4-146). The boundary with the 2Ab horizon was wavy. The buried soil was a blocky subangular silty clay with large pores, strong clay skins and red-ox features. The 2Ab was wet and plastic with some fine organic material. The only other materials noted were very occasional 0.5 cm yellow chert pea gravel in the sand horizon.

Test unit 3 (ST3) showed a loamy sand plow zone (10 YR 3/2-3/3) to about 25 cm deep, with a compacted, lamellar plow pan (10 YR 4/3) including lignite fragments to 28 cm deep, where a red-ox horizon was noted; this zone was penetrated by various root casts extending as deep as 40 cmbs. The sand blow was loose coarse sand comprised primarily of angular quartz with dark minerals and feldspars (Figure 4-148). The sand included frequent 1-2 cm fragments of lignite and 1-2 cm clayey clasts. The sand extended to 63 cmbs; the base of the stratum was wet but not saturated. The contact with the wet, plastic 2Ab was wavy. This soil was a very plastic blue clay with abundant pore space, many fine roots, incipient Fe-Mg concretions, and sandy skins between soil ped faces, which are also marked by Fe-Mn red-ox reactions.

Test unit 4 (ST4) was excavated to 100 cmbs, with water being hit at about 80 cmbs; it was too dark to draw when it was finished and the profile had collapsed by the next day. The clay substrate was not reached at 100 cmbs, but probing indicated that it is present at about 110-120 cmbs. The plow zone extended to 25 cmbs, with a wavy clear boundary at the top of the sand blow. The homogeneous, massive, loose, coarse sand included lignite and occasional pea gravel up to 1 cm in diameter (Figure 4-148).

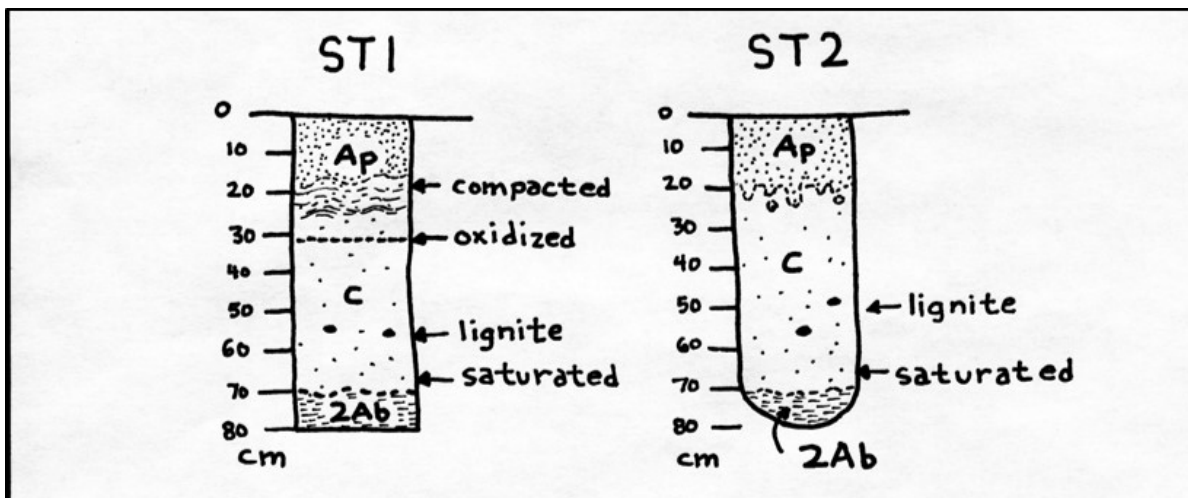


Figure 4-146 Trench 1 shovel test profiles. Soil horizons: Ap (plow zone) 10YR4/3 loamy sand; C 10YR4/4 sand with clasts 10YR5/5; 2Ab (buried soil) 10YR6/2 clay.



Figure 4-147 Photo of Shovel Test 1

Test unit 5 (ST5) was excavated to 70 cmbs (Figure 4-148 and Figure 4-149). It showed the slightly loamy sand plow zone (Ap) (10 YR 4/3) to be 22-25 cm thick, with a concretion layer at about 16 cmbs. The base of the plow zone was clear, with plow scars extending a few cm into the sand blow (10 YR 5/4 at top grading to 10 YR 5/4 at base). The sand blow had an oxidized zone (10 YR 4/6) between 30 and 40 cmbs and a thin lamella of finely divided lignite at about 45-47 cmbs, with a thicker layer of wet, abundant, larger lignite fragments between 50 and 55 cmbs.

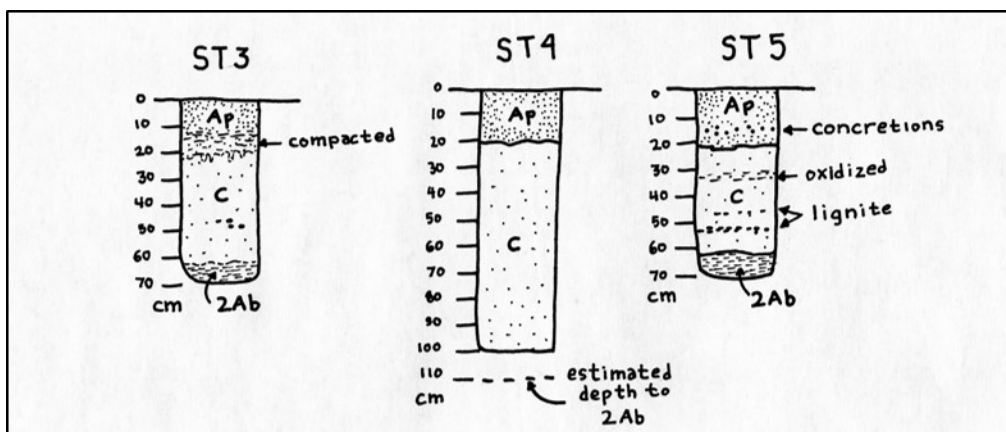


Figure 4-148 Trench 2 shovel test profiles. Soil horizons: Ap (plow zone) 10YR4/3 loamy sand; C 10YR4/4 sand with clasts 10YR5/5; 2Ab (buried soil) 10YR6/2 clay.



Figure 4-149 Photo of Shovel Test 5

The transition to the 2Ab was from 60 to 63 cmbs; this soil was a stiff, clay (60%; 2.5 YR 5/2) that is heavily mottled with red-ox features (10 YR 4/4). It has a fine to medium blocky subangular structure with sand skins evident on ped faces and in cracks and clear root traces and other finely divided organic material.

Test unit 6 (ST6) showed the base of the plow zone to be a smooth, clear transition at 18 cmbs. The sand blow extended to 59 cmbs, with a lignite lens on top of the 2Ab. The transition to the 2Ab was smooth and this soil, as in other tests in this area, was an angular to blocky clay (Figure 4-150 and Figure 4-151).

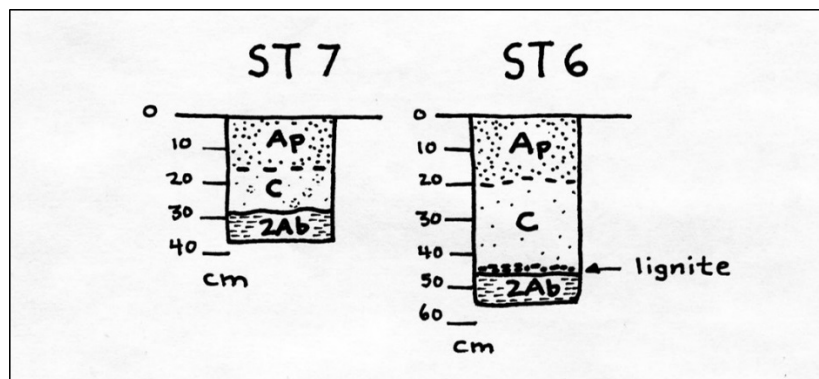


Figure 4-150 Trench 3 shovel test profiles. Soil horizons: Ap (plow zone) 10YR4/3 loamy sand; C 10YR4/4 sand with clasts 10YR5/5; 2Ab (buried soil) 10YR6/2 clay.



Figure 4-151 Photo of Shovel Test 6

Test unit 7 (ST7) was only excavated to 40 cmbs (Figure 4-150). The base of the plow zone (Ap) around 18 cmbs was indistinct; the plow zone here was slightly darker or more organic. The sand blow material was thin and modified by leaching and slightly mottled with greyer and clay films indicative of downward percolation from the topsoil (cf. a weakly developed E/B horizon). The 2Ab horizon was reached at 27 cmbs; it had a wavy clear contact with the overlying sand. The substrate was the same clay as described above. A few 0.5 cm pea gravel pebbles were noted from the sand.

Test unit 8 (ST8) was excavated to 65 cmbs (Figure 4-152 and Figure 4-153). It showed a clear lower boundary of the plow zone (between 10 YR 4/3-4/4 and 3/3-3/4), with the brown loam very cut and jumbled at base (20-30 cmbs) and the sand blow consisting of very coarse and loose material (10 YR 5/4). The base of the sand is smooth and clear at 58 cmbs. The underlying clay (2Ab; 7.5 YR 6/2) was wet and plastic, with pronounced red-ox features. The structure was again blocky subangular with heavy Fe-Mn deposition on ped faces and with abundant evidence of downward translocation of sand. The sand blow contains some pea gravel up to 1 cm in diameter.

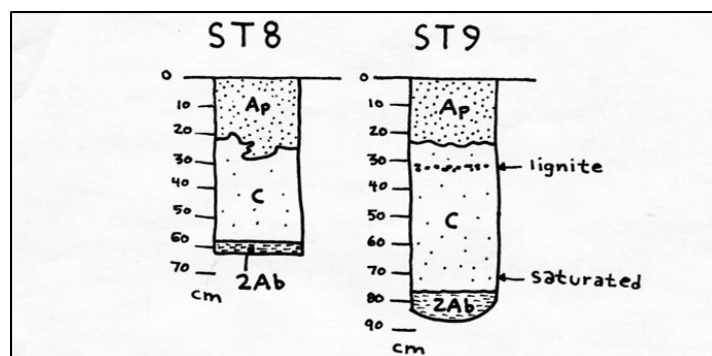


Figure 4-152 Trench 4 shovel test profiles. Soil horizons: Ap (plow zone) 10YR4/3-3/4 loamy sand; C 10YR5/4 coarse sand; 2Ab (buried soil) 7.5YR6/2-2.5YR6/0 clay.



Figure 4-153 Shovel Test 8

Test unit 9 (ST9) was excavated to 85 cmbs (Figure 4-152). The plow zone had a gradual wavy boundary at about 23 cmbs, quite unlike the jumbled plow zone soils in ST8. There was a 2 cm thick lignite lens in the sand blow at 30 cmbs. The sand blow was otherwise homogeneous. The boundary with the 2Ab was abrupt and smooth. This substrate was a wet, gleyed blue clay (bluer than 2.5 Y 6/0 grey) with a fine granular ped structure (Figure 4-154).



Figure 4-154 Shovel Test 9

Archaeological Assessment

During the pre-trenching assessment, two historic sites were identified north of the Pritchett site and a third historic site located near the northern boundary of the site. A small collection (n=57) from the third site indicated mid 20th century occupation; machine-made brick and pane glass confirm this as a structure location as indicated on a 1957 map and 1960 air photo. The site is interpreted as a tenant cabin from late in the sharecropping era. All three historic sites were well away from the trench locations.

None of the shovel tests in the areas of proposed trenching produced artifacts or any indication that an archaeological site might be present. The heavy soils and locations interior to (back of) the Obion River natural levee are taken as an indication of a low probability for prehistoric occupation in the site area. It was determined that the proposed trenches at the Pritchett site were unlikely to encounter cultural horizons or features, and therefore, that there would be no adverse effects from trenching.

4.4.5.5.4 *Siting Paleoseismic Trenches*

As described above, likely sand blows were located at the Pritchett site on the basis of interpretation of satellite imagery, field inspection including excavation of small soil pits, and GPR subsurface reconnaissance. The presence of sand blows is further supported by the results of electrical resistance tomography that imaged likely sand blows and related feeder dikes. In Subarea A, resistivity profiles number 1 and 3 provide excellent targets for paleoseismic trenching. On profile number 1 (lower profile in Figure 4-142), a highly resistive area on the surface, probably a sand blow, extends almost the entire length of the profile. In a few places, fingers of higher resistivity, likely feeder dikes, appear to crosscut somewhat less resistive zones and to connect the highly resistive area on the surface with a deeper highly resistive area, likely sandy source beds. Similar features are seen towards the eastern end of profile number 3 (upper profile in Figure 4-142). Therefore, Trench 1 was proposed from 8-22 m along resistivity profile number 1, Trench 2 was proposed from 60-82 m along profile number 1, and Trench 3 was proposed from 68-92 m along resistivity profile number 3 in order to capture the critical and diagnostic relationship between sand blows and their feeder dikes. In Subarea B, a highly resistive area on the surface probably is a sand blow. However, no feeder dikes were imaged connecting the highly resistive area on the surface with a deeper highly resistive area. Therefore, no trench was proposed in Subarea B. Trench 4 was proposed from 22-46 m along GPR Profile 2 where a breach in the strong reflector at the 38-38.5 m and at about 1 m depth is likely to be the feeder dike of a large sand blow (lower profile in Figure 4-140).

4.4.5.5.5 *Paleoseismic Observations*

In November 2016, Trenches 1, 2, and 4 were excavated in the locations as proposed in the Pritchett site evaluation report and described above. After excavating Trenches 1 and 2, it was decided to excavate Trench 3 approximately 80 m east of Trench 2 since a third trench in the vicinity of Trenches 1 and 2 was unlikely to reveal any new information. Prior to excavating Trench 3, an archaeologist, M.E. Starr, resurveyed the ground surface in that area and found no cultural material. Starr monitored excavation of all four trenches in case we encountered buried cultural materials, features, or horizons. None was encountered. Trenches 1, 2, and 3 were excavated across northeast-oriented sand blows along the N35-46°E trend of the large sand dike at Obion River 216 (Figure 4-137 to Figure 4-139). Trench 4 was excavated across a north-northeast-oriented linear sand blow that was ~350 m southeast of Trench 3. All four trenches exposed sand blows and associated sand dikes.

Trench 1

During excavation of Trench 1, the east end of the trench was extended 3 m towards the east in order to expose a large dike and, as a consequence, the west end of the trench was stopped short by 2 m. Trench 1 was 15 m long and varied from 0.9 to 1.25 m in depth (Figure 4-155). The east end was excavated deeper to expose the large sand dike.

The plow zone ranged from 15-25 cm thick. Beneath the plow zone, the sand blow, up to 77 cm thick, was composed of five depositional units, L1-L5 (Figure 4-155). Unit L1 ranged up to 32 cm thick and was composed predominantly of medium and fine sand, though a lower subunit near a small dike near meter mark 4 was composed of silty, very fine and fine sand. The unit contained a few thin stringers of lignite and clay clasts, especially adjacent to a large sand dike near meter mark 13. Most of the unit L1 exhibited fines accumulation and iron staining, especially along its upper contact. Unit L2 was overlying L1, ranged up to 30 cm thick, was composed of coarse, medium, and fine sand adjacent to the large dike towards the east end of the trench and of fine

sand adjacent to the small dike towards the western end of the trench. The unit contained clay clasts especially above the large dike and adjacent to the small dike. Unit L2 also exhibited fines accumulation and iron staining. Unit L3, overlying L2, ranged up to 30 cm thick, was composed of coarse, medium, and fine sand above the small dike, fined away from the dike to medium and fine sand, and pinched out towards the east below meter mark 11. The unit exhibited minor layering and contained clay clasts. The upper contact was silty with small pieces of lignite. Unit L3 contained many clay clasts above and adjacent to the large dike. Unit L4, above L3, ranged up to 50 cm thick above the large dike towards the eastern end of the trench, and thinned to about 5 cm towards the western end of the trench. The unit was composed of coarse, medium, and fine sand above the large dike and fined to fine and very fine sand towards the west. Above the small dike, a vent structure that appeared to be related to unit L4 contained coarse, medium, and fine sand with granules. Below meter mark 10, there was a lens of fine and very fine sand, likely to be part of a crater fill, which is labeled unit L5 on Figure 4-155. Although there is no connection to a vent structure in the trench wall, the lens is along the strike of the large sand dike and therefore may be connected to the dike via a vent structure farther to the south.

The large sand dike towards the eastern end of the trench was exposed near the bottom of the trench wall and in the trench floor. The dike was oblique to the trench wall and had a strike and dip of N54°E, 83°SE. It was about 27 cm wide, composed of medium and fine sand with many clay and sand clasts. Above the dike, there was no discernible vent structure crosscutting units L1, L2 and L4 but there were clast zones along the strike of the dike. The small dike, 9 m west of the main dike, was 5 cm wide as observed in the lower 15 cm of the trench wall (Figure 4-156). The dike was traced across the trench floor where it was discontinuous but in places up to 8 cm wide. There was no measurable vertical displacement across either dike, though the ground surface on the west side of the large dike may have dropped down by a few centimeters. The buried soil is inclined downward from west to east towards the large dike.

Radiocarbon dating was performed on two samples of charred material from the buried soil beneath the sand blow. Sample TR1-C1 collected 20 cm below the sand blow yielded a calibrated date of A.D. 1450-1640 and sample TR1-C3 collected 5 cm below the sand blow yielded a calibrated date of A.D. 1455-1645 (Table 4-30). The two dates are very similar to one another and stratigraphically consistent. One sediment sample (OSL1) collected of the soil buried by the sand blow yielded an OSL age of 7140 ± 590 (7670-6490 yr B.P.) (Table 4-31). This age is much older than the radiocarbon dates from the soil below the sand blow exposed in trench 1.

Table 4-30 Radiocarbon Dating Results for the Pritchett Site

Sample # Lab #	¹³ C/ ¹² C Ratio	Radiocarbon Age Yr B.P. ¹	Calibrated Radiocarbon Age Yr B.P. ²	Calibrated Calendar Date A.D./B.C. ²	Sample Description
PS-TR1-C1 BA-452739	-24.9	360 ± 30	500-310	AD 1450-1640	Charred material 20 cm below sand blow from gray clay
PS-TR1-C3 BA-452740	-26.9	340 ± 30	495-305	AD1455-1645	Charred material 5 cm below sand blow from gray clay
PS-TR2-C3 BA-452741	-22.9	450 ± 30	530-485	AD 1420-1465	Charred material 12 cm below sand blow from clayey soil
PS-TR3-C2 BA-453743	-24.3	400 ± 30	510-430 355-330	AD 1440-1520 AD 1595-1620	Charred material 30 cm below sand blow from clay
PS-TR4-C5 BA-452743	-25.4	170 ± 30	290-255 225-135 115-70 35-0+	AD 1660-1695 AD 1725-1815 AD 1835-1880 AD 1915-1950+	Charred material 1 cm below sand blow from silty clay

¹ Conventional radiocarbon ages in years B.P. or before present (1950) determined by Beta Analytic, Inc. Errors represent 1 standard deviation statistics or 68% probability.

² Calibrated age ranges as determined by Beta Analytic, Inc., using the Pretoria procedure (Talma and Vogel, 1993; Vogel et al., 1993). Ranges represent 2 standard deviation statistics or 95% probability.

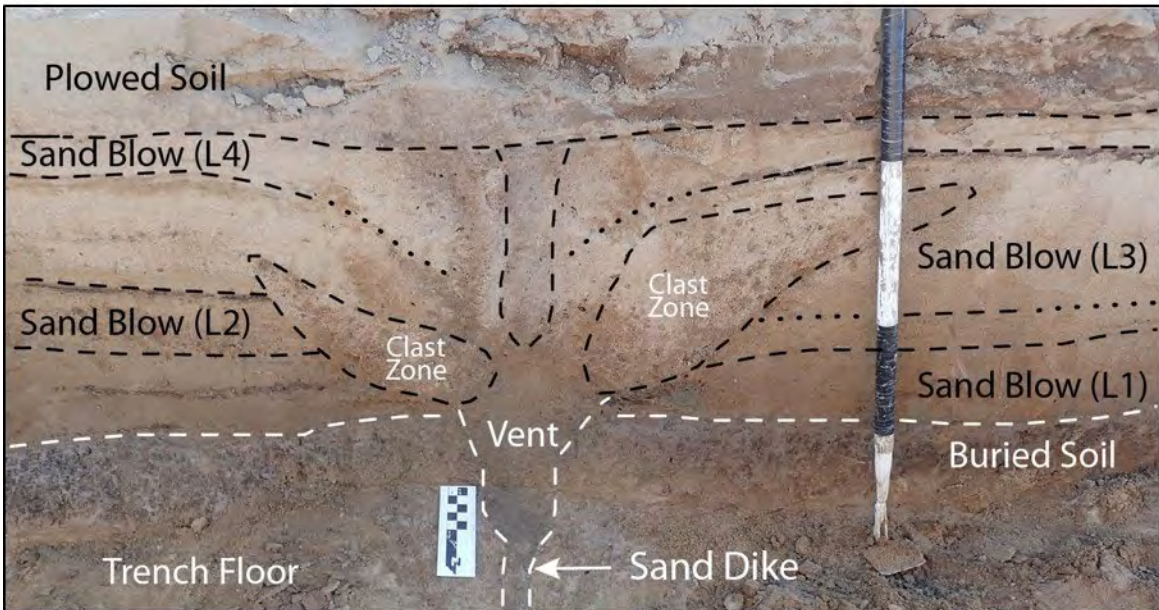


Figure 4-156 Photographs (upper - unannotated; lower - annotated) of vent area of compound sand blow above 5-cm wide dike that crosscuts clayey soil in lower portion of south wall of Trench 1 at Pritchett site (see Figure 4-155). Note clast zones in vent area above sand dike. Dashed and dotted lines represent clear and inferred contacts, respectively. On scale next to dike, small black and white intervals represent 1 cm; black and white intervals on hoe are 10 cm long.

Table 4-31 Optically Stimulated Luminescence Dating Results for the Pritchett Site

Sample Number	Lab	Cosmic Dose Rate (mGray/yr) ¹	Dose Rate (mGray/yr)	OSL Age (Yr) ²	Calendar Age (Yr) ³	Sample Description
OSL1	BG4367	0.14 ± 0.01	1.38 ± 0.07	7140 ± 590	7670-6490	From Trench 1, east end-south wall, quartz grains from upper contact of soil buried by sand blow unit L2

¹ Cosmic dose rate calculated from parameters in Prescott and Hutton (1994).

² Systematic and random errors calculated in a quadrature at one standard deviation. Datum year is A.D. 2010.

³ Years B.P. or before present (1950).

Trench 2

Trench 2, 41 m east of Trench 1, was 3 m shorter on its east end and 6 m shorter on its west end than originally proposed. It was 13 m long and varied from 0.70 to 1.25 m in depth (Figure 4-155 and Figure 4-157). The trench was deepest in the vicinity of the dike.

The plow zone ranged from 15-25 cm thick. Several plow scars extended an additional 5-10 cm into the upper part of the sand blow. Beneath the plow zone, the sand blow, up to 95 cm thick, was composed of five depositional units, L1-L5, that were similar to those observed in nearby Trench 1 (Figure 4-155). Unit L1 ranged up to 12 cm thick and was composed of fine and medium sand with clay clasts. The unit was thickest east of the large feeder dike below meter mark 7 and thinned towards the east. The unit was absent immediately west of the large feeder dike but was present from about meter mark 9 to the west end of the trench. Unit L2, overlying L1, ranged up to 48 cm thick, was composed of coarse, medium, and fine sand adjacent to the large dike and fined to fine sand towards the western end of the trench. The unit contained clay clasts and stringers of lignite. The upper 20 cm of the unit exhibited fines accumulation and iron staining, including that of a large sandy clast of L2 in the vent structure above the large dike. Unit L3, overlying L2, ranged up to 40 cm thick, was composed of predominantly coarse, medium, and fine sand with clay clasts and lignite stringers. Towards the east, the unit splits into two and then four subunits, with contacts defined by silty fine sand, lignite, and clay clasts. The uppermost of the four subunits is composed of very fine and fine sand and thickens towards the east. Towards the west, the unit thins and also fines to very fine, fine, and medium sand. The upper contact was often delineated by lignite and iron staining and had been bioturbated. Unit L4 occurred within the vent structure above the dike and was overlying L3 where it ranged up to 15 cm thick. L4 was composed mostly of medium and fine sand with a few clay clasts. A small crater fill of silty, fine sand with lignite occurred at the top of L4 above the sand dike. The unit was discontinuous west of the large dike and appeared to fill a crater above a small dike at about meter mark 8-8.5. The unit thinned towards the east and pinched out at, or was destroyed by plowing, beyond meter mark 0.5. Unit L5 occurs above unit 4 and only above the vent structure. It is composed of fine and very fine sand and is likely to be a crater fill.

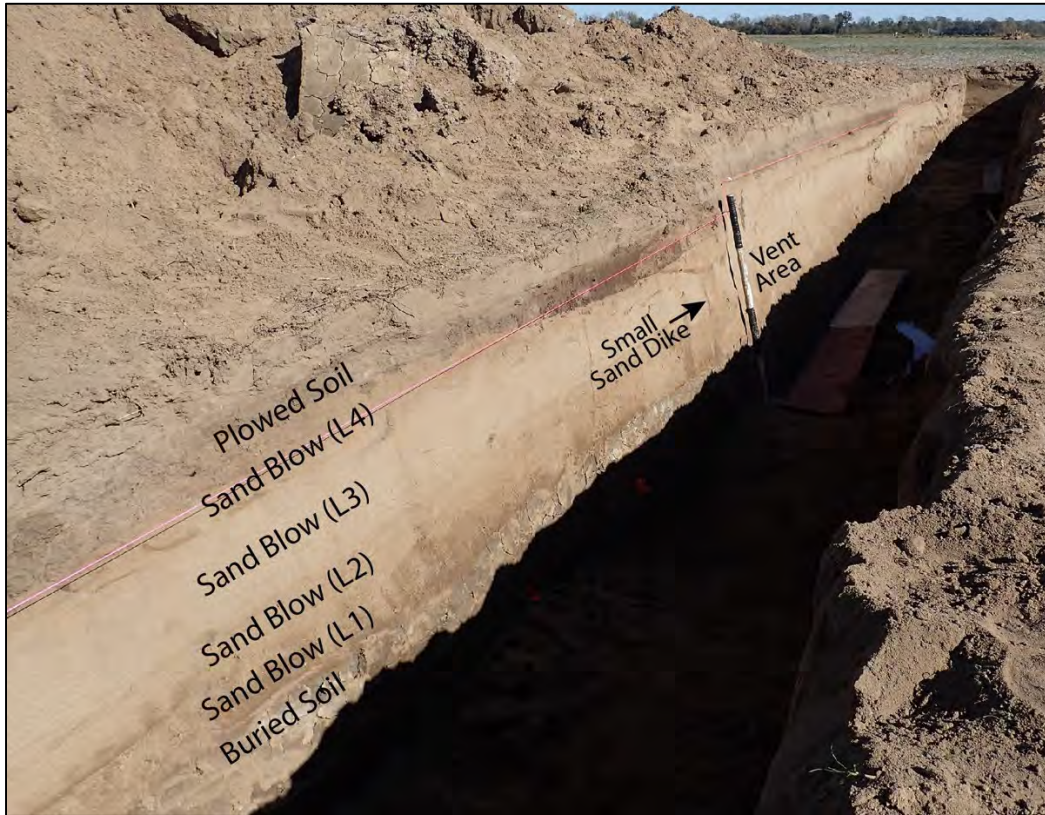


Figure 4-157 Photograph of Trench 2 at Pritchett site; view is slightly north of east. Larger dike and vent area are right (east) of hoe and smaller dike and vent area are left of hoe (see Figure 4-155). Compound sand blows are so large they are difficult to photograph in trenches. Also, low sun angle in November results in shadows in lower portion of trenches. For scale, black and white intervals on hoe are 10 cm long.

The large sand dike below meter mark 7 was exposed near the bottom of the trench wall and in the trench floor (Figure 4-155). Its western and eastern margins had strikes of N46°E and N30E, respectively, and dips of 85°SE. The dike had two components. The eastern component was 5 cm wide, was composed of fine and medium sand, and included a 2-cm wide dikelet that crosscut the overlying soil and connected with unit L1. The western component was 21 cm wide, composed of fine sand with clay clasts, and connected with the vent structure above. The vent structure was filled with mostly fine sand with clasts of clay and sand, and exhibited flow structure. The small dike, only 1 m west of the large dike, was 0.5 cm wide as observed crosscutting the clayey soil exposed in the lower 30 cm of the trench wall. The dike connected with the vent structure above filled with mostly medium sand and exhibiting flow structure.

The upper contacts of the buried soil, units L1, L2, and L3 appear to be displaced, east side down, across the large dike and overlying vent structure (Figure 4-155). The upper contacts of the buried soil and unit 1 are displaced by 30 cm whereas the upper contacts of L2 and L3 are offset by about 10 cm. This suggests that the ground subsided by about 20 cm during the deposition of L2 and by another 10 cm during the deposition of L4. This is also suggested by the greater thicknesses of units L2 and L4 on the east side compared to the west side of the vent structure. No displacement of the soil or sand blow units occurred across the small dike. In addition, the buried soil is inclined downward from both the east and the west towards the large dike.

Radiocarbon dating was performed on one sample of charred material from the buried soil beneath the sand blow. Sample TR2-C3 collected 12 cm below the sand blow yielded a calibrated date of A.D. 1420-1465 (Table 4-30). The date overlaps the lower portion of the date ranges for the two samples dated from Trench 1.

Trench 3

As mentioned above, Trench 3 was located 80 m east of Trench 2. It was 8 m long and varied from 0.40 to 0.85 m in depth (Figure 4-158). The trench was fairly shallow because the sand blow was relatively thin.

The plow zone ranged from 20-28 cm thick. Several plow scars extended an additional 5-10 cm into the upper part of the sand blow. Beneath the plow zone, the sand blow, up to 30 cm thick, was composed of two depositional units (Figure 4-158). Unit L1 ranged up to 12 cm thick and was composed of fine and medium sand with small clay clasts, except in a vent area between meter marks 6.0-6.5, where it was 20 cm thick and composed of coarse and medium sand with clay clasts. The unit thinned east of the vent area and west of the sand dike at about meter mark 1.5. The entire unit exhibited fines accumulation and iron staining, especially along its upper contact. Unit L2, overlying L1, ranged from 10-25 cm thick, was composed of medium and fine sand with few clay clasts. The unit was thickest above and adjacent to the vent area between meter marks 6.0-6.5.

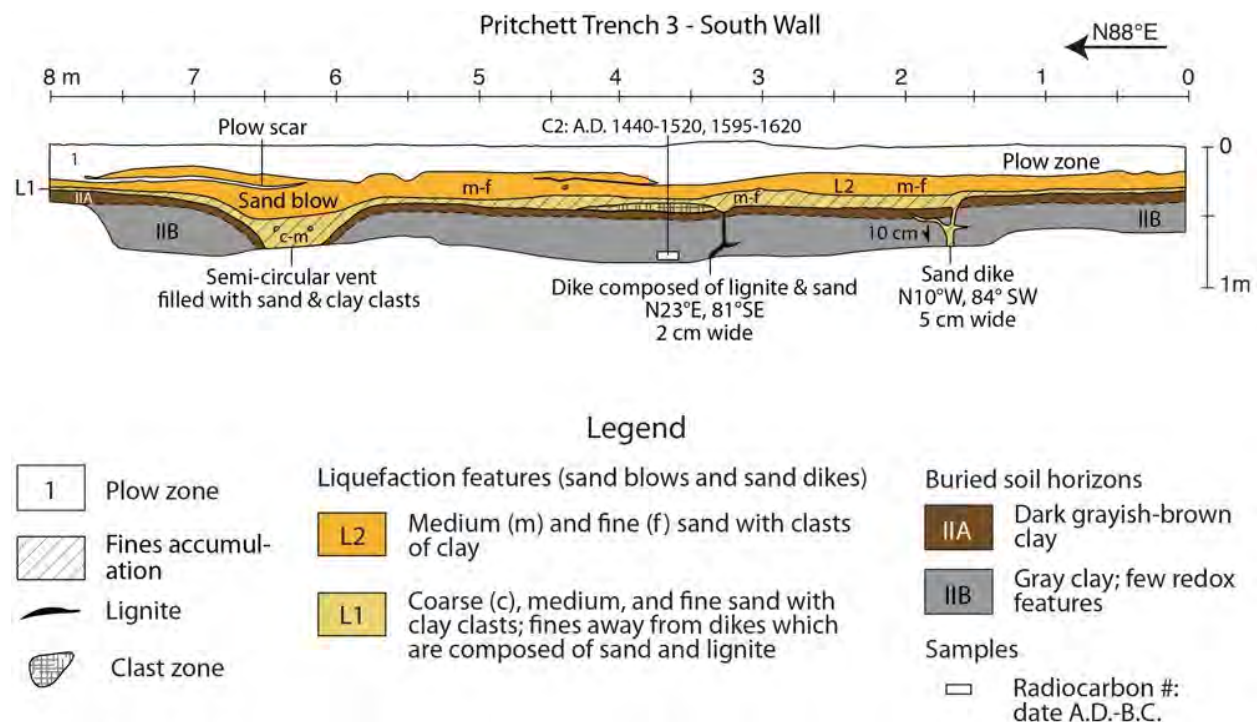


Figure 4-158 Log of Trench 3 at Pritchett site, showing compound sand blow, related sand and lignite dikes, and vent structure. Radiocarbon dating of sample TR-C2 from buried soil suggests that overlying sand blow formed after A.D. 1440.

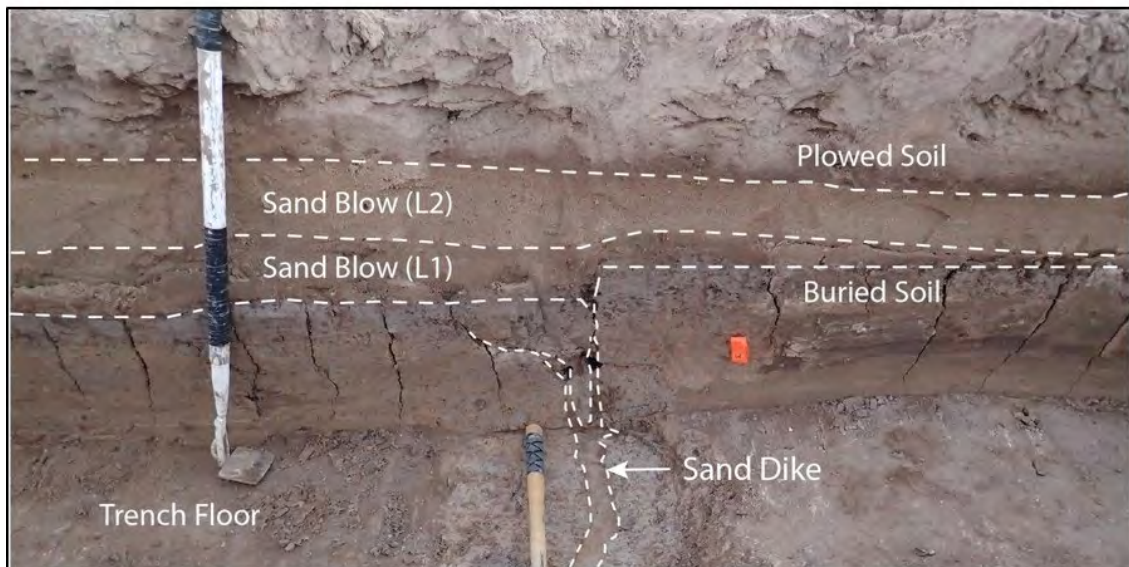


Figure 4-159 Photographs (upper - unannotated; lower - annotated) of portion of Trench 3 at Pritchett site showing sand dike crossing floor (to right of wooden handle of scarper) and lower portion of wall as well as overlying compound sand blow. Notice that clayey soil is displaced downward on left (east) side of dike relative to right side and that overlying compound sand blow, especially darker lower unit (L1), is thicker on left, filling in microtopography. Dashed lines represent clear contacts. For scale, black and white intervals on hoe are 10 cm long.

The vent area (meter marks 6.0-6.5) was exposed near the bottom of the trench wall, where the upper contact of the buried soil dips steeply into the structure. In the trench floor, the vent structure was semi-circular in plan view and filled with coarse and medium with clay clasts. The sand dike at about meter mark 1.5 was 3.5 cm wide as observed in the trench wall but widened to 5 cm as it crossed the trench floor (Figure 4-159). It was composed of fine sand and had a strike and dip of N10°W, 84°SW. A second dike, between meter marks 3-3.5, was 2 cm wide in both the trench wall and floor, was composed of lignite and fine sand, and had a strike and dip of N23°E, 81°SE.

The upper contact of the buried soil was displaced by 10 cm, east side down, across the 3.5-5.0 cm wide sand dike towards the western end of the trench (Figure 4-158). Unit L1 had vented through the dike and was thicker on the down-dropped side of the dike. The upper contact of unit 1 was displaced by 2.5 cm, east side down, above the same dike. The upper contacts of the buried soil and unit 1 might have been displaced by 2.5 cm, east side down, across the 2.0 cm wide dike.

Radiocarbon dating was performed on one sample of charred material from the buried soil beneath the sand blow. Sample TR3-C2 collected 30 cm below the sand blow yielded a calibrated date of A.D. 1440-1520, 1595-1620 (Table 4-30). The date is very similar to dates of samples collected from the clayey soil buried by sand blows at Trenches 1 and 2.

Trench 4

Trench 4 was 1 m shorter on its east end and 8 m shorter on its west end than originally proposed. The trench was centered on the sand dike that was imaged in the GPR profile. The trench was 15 m long, varied from 0.5 to 0.95 m in depth, and was deepest in the vicinity of the dike (Figure 4-160).

The plow zone ranged from 10-25 cm thick. Several plow scars extended an additional 5-15 cm into the upper part of the sand blow. Beneath the plow zone, the compound sand blow, up to 55 cm thick, was composed of four depositional units (Figure 4-160). Unit L1 ranged up to 25 cm thick and was composed of medium sand with clay clasts and lignite stringers and it fined towards the western end of the trench to silty, fine sand with lignite. The unit was thickest east of the dike below meter marks 2-5 and pinched out below meter mark 1. The unit was absent west of the same dike (below meter marks 6-7) but reappeared west of meter mark 12. Lignite occurred along portions of the upper contact of L1. There was fines accumulation in the lower centimeter of the unit. Unit L2 was 30 cm thick adjacent to the dike, where it was composed of medium and coarse sand. It thinned and fined away from the dike in both directions. Towards the east, unit L2 fined to fine and medium sand and thinned to 15 cm and thickened again to 20 cm at the end of the trench. Towards the west, it thinned to 7 cm and thickened again to 15 cm. Towards the west end of the trench, the unit split into two subunits, both of which were composed of fine sand. Silt and lignite occurred along portions of the upper contact of L2. Unit L3, above unit L2, was 15 cm thick adjacent to the dike, where it was composed of coarse, medium and fine sand. A crater fill of silty, fine sand with many clay clasts occurred at the top of L3 above the sand dike. Towards the east, unit L3 thinned to 8 cm, where it contained a stringer of clay clasts, and thickened again to 28 cm at the end of the trench, where it was also composed of coarse, medium and fine sand. Towards the west, the unit gradually thickened from 5 cm to 22 cm near a tree-root cast and then thinned until it pinched out below meter mark 14. Silt and lignite occurred along portions of the upper contact of L3, which was also slightly iron-stained and bioturbated. Unit L4, composed of coarse, medium, and fine sand with clay clasts, filled the crater above the dike between meter marks 6-7 and extended westward to about meter mark 10. The unit was discontinuous due to disturbance by plowing.

The sand dike below meter marks 6-7 was exposed near the bottom of the trench wall and in the trench floor (Figure 4-160). Its western margin had a strike and dip of N57°E, 84°SE. The dike had two components as observed in the trench floor. The main component was 12 cm wide, composed of fine sand with lignite pebbles, and connected with the vent structure in the sand blow units above. Along the eastern margin of the dike, there were discontinuous domains, up to 7 cm wide, of coarse and medium sand. There was a 1-cm wide dike about 3 m west of the

12-cm wide dike. This dike and the overlying vent structure that crosscut units L2 and L3 were filled with fine and very fine sand. The vent structure exhibited flow structure.

Radiocarbon dating was performed on one sample of charred material from the buried soil beneath the sand blow. Sample TR4-C5 collected 1 cm below the sand blow yielded a calibrated date of A.D. 1660-1695, 1725-1815, 1835-1880, A.D. 1915-1950+ (Table 4-30). There were no root casts in the vicinity of the sample to suggest that it had come from a root grown through the sand blow and thus post-dating the sand blow. The date is 200-300 years younger than all of the other samples collected below sand blows in Trenches 1, 2, and 3 suggesting that the sand blow exposed in Trench 4 is younger than the others studied at the site.

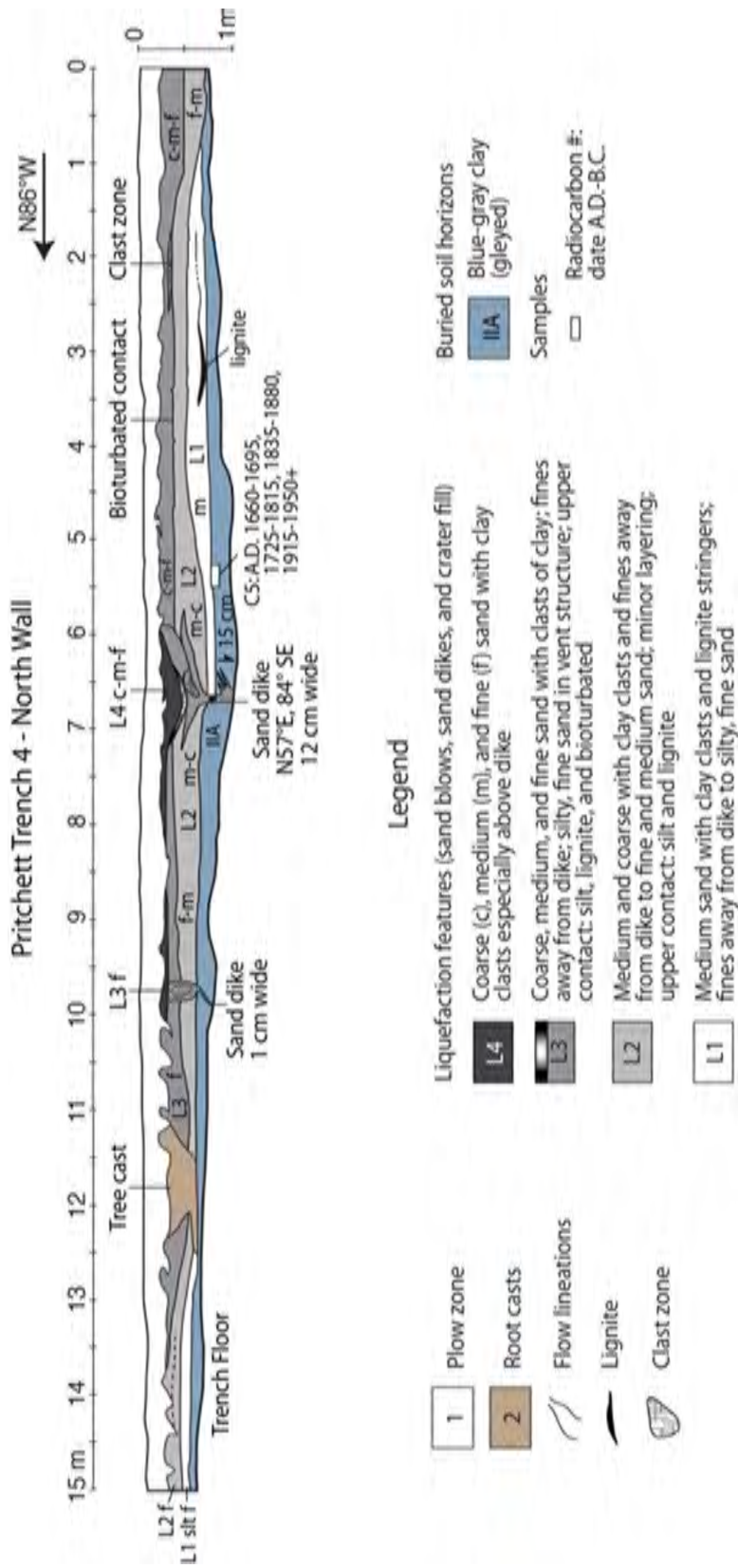


Figure 4-160 Log of Trench 4 at Pritchett site, showing compound sand blow and related sand dikes. Radiocarbon dating of sample TR4-C5 from buried soil suggests that the overlying compound sand blow formed after A.D. 1660.

4.4.5.5.6 Paleoseismic Interpretations

Trenches 1 and 2

The compound sand blows exposed in Trenches 1 and 2, only 41 m apart, are very similar to one another. They are both composed of five depositional units, exhibit fines accumulation and iron staining of sediment 0.5 m below the ground surface, and likely formed during multiple earthquakes in the same sequence. These two sand blows are also very similar to the compound sand blow exposed in Trench 3 at the Stiles site. Units L1-3 of the Pritchett sand blows are not capped by silt and lignite, but otherwise they share similar stratigraphic, sedimentological, and weathering characteristics with the Stiles sand blow, giving confidence in the interpretation that they formed during 4-5 earthquakes in the same sequence. Similar to L3 of the sand blow in Stiles Trench 3, the upper contact of L3 of the sand blow in Pritchett Trench 2 was bioturbated, indicating that it too was exposed at the surface for a short period of time prior to burial by unit L4. Accumulation of fines as well as iron staining of the lower portion of the compound sand blows in Trenches 1 and 2 suggest that they formed prior to A.D. 1811.

The calibrated dates of A.D. 1455-1645 and A.D. 1450-1640 from 5 cm and 20 cm, respectively, below the compound sand blow in Trench 1 and A.D. 1420-1465 from 12 cm below the compound sand blow in Trench 2 provide close maximum age constraint and suggest that the liquefaction features formed soon after A.D. 1420-1455. This age estimate is similar to that for the compound sand blows in Trenches 2 and 3 at the Stiles site, suggesting that they formed during the same sequence of events about A.D. 1450 \pm 150 yr, but supporting the interpretation that the event occurred close to or after A.D. 1450.

Observations of the sand blows exposed in Trenches 1 and 2 support the interpretation that these long linear sand blows may be the surface expression of an active fault. These sand blows were along strike of the very large sand dike previously documented at Obion River 216 and thought to have formed also during the A.D. 1450 \pm 150 yr event (Figure 4-136 and Figure 4-137). The sand dike below meter mark 7 in Trench 2 has a very similar strike to that of the Obion River dike. For both locations, the ground surface was displaced downward on the east side of the dike. For the dike in Trench 2, this is opposite to what would be expected if the displacement were due to lateral spreading towards the Obion River channel only 400 m to the west. There is a small abandoned creek in the field east of the Pritchett site but it is too small and far away (>600 m) to promote down-to-the-east ground failure in the vicinity of Trenches 1 and 2.

Trench 3

The compound sand blow exposed in Trench 3 likely formed during two earthquakes in the same sequence that was responsible for the compound sand blows in Trenches 1 and 2. Similar to the sand blows in Trenches 1 and 2, the sand blow in Trench 3 exhibited significant accumulation of fines and iron staining. Also, radiocarbon dating of the soil buried by the sand blow provides maximum age constraint and suggests that the sand blow formed after A.D. 1440 similar to the sand blows in Trenches 1 and 2. Correlation of the units is not certain, but on the basis of relative thickness and grain-size, L1 and L2 in Trench 3 may have formed during the same events as L2, L3, or L4 in Trenches 1 and 2. It seems unlikely that the two units in Trench 3 would correlate with units L1 and L5 in Trenches 1 and 2, which were relatively thin and fine-grained.

The Trench 3 sand blow also occurs along the projected strike of the large sand dike at Obion River 216 (Figure 4-137). In addition, one of the dikes in Trench 3 has a somewhat similar strike, N23°E, to the Obion River dike. The second dike in the trench has a northwest strike but vertical

displacement across the dike was east side down consistent with vertical displacement in Trench 2. The sand blows in Trenches, 1, 2, and 3 occur within a zone of northeast-oriented large linear sand blows that crosses the western half of the site. If the sand blows are the surface expression of faulting at depth, the zone of deformation is about 300 m wide.

Trench 4

The compound sand blow exposed in Trench 4 is composed of four depositional units and is interpreted to have formed during four earthquakes in a sequence. Units L1, L2, and L3 are not capped by silt or clay, but silt and/or lignite occur along their upper contacts, and they share other stratigraphic and sedimentological characteristics with compound sand blows along the nearby Obion River that are capped by silt or clay. There was fines accumulation in the lowest centimeter of unit L1 above a clayey soil where a perched water table would form following heavy rainstorms or floods. Also, the upper contact of L3 was slightly iron stained. Otherwise, the compound sand blow was less weathered than those exposed in Trenches 1, 2, and 3, suggesting that it is younger. This interpretation is supported by radiocarbon dating of charred material from the soil buried by the sand blow. The date provides maximum age constraint for the formation of the compound sand blow and suggests that it formed after A.D. 1660. The historical earthquake sequence of 1811-1812 is likely to have produced this compound sand blow.

The sand blow exposed in Trench 4 is one of several in a zone of north-northeast oriented large linear sand blows that crosses the eastern half of the site and the field to the east as well (Figure 4-137). If the sand blows are the surface expression of faulting at depth, the zone of deformation is about 600 m wide.

As mentioned above in Section 4.4.4.5, the **M** 7.0 December 16, 1811 dawn aftershock may have occurred near Calvary and been associated with coseismic ground deformation that caused the draining of a lake (Hough and Martin, 2002). The Reelfoot fault was suggested as the source of the earthquake. Given that Calvary occurs only 18 km to the northeast along a zone of lineaments, including the large linear sand blows at the Pritchett site, an alternative interpretation is that a fault zone beneath the Pritchett and OR216/603 sites was the source of the December 16, 1811 dawn aftershock.

4.4.6 Evaluation of Scenario Earthquakes

In this evaluation, predicted liquefaction for scenario earthquakes is compared with observed liquefaction, or lack thereof, in order to evaluate, or place limits on, possible source areas and magnitudes of paleoearthquakes that induced liquefaction. Liquefaction potential analysis is performed for scenario earthquakes of various moment magnitudes and distances to possible sources of interest. These sources might include epicenters of large historical earthquakes, delineated source areas of RLMEs or identified active faults.

4.4.6.1 Scenario Earthquakes

In this study, large historical earthquakes centered in the NMSZ, including the December 16, January 23, and February 7 main shocks of the A.D. 1811-1812 earthquake sequence as well as the January 5, 1843 and October 31, 1895 events were used as scenario earthquakes in this evaluation (Table 4-32; Figure 4-161). In addition, scenario earthquakes on the Commerce fault zone, the Eastern Reelfoot rift margin, including the north, south, and southern extension known as south river (fault) picks, and the Marianna area, were used in the analysis. The NMSZ,

Commerce fault zone, the Eastern rift margin, and Marianna area were recognized as RLMEs in the CEUS seismic source characterization project (NUREG-2115). The magnitudes of the scenario earthquakes also are taken from the CEUS seismic source characterization project. Not all values of expected magnitudes for each RLMEs zone were considered. Instead, magnitudes with heavier assigned weights were selected. For events with a large spread in expected magnitudes, a lower and an upper magnitude, and in one case several intermediate magnitudes, were selected for the evaluations (Table 4-32).

Table 4-32 Scenario Earthquakes Evaluated Using Liquefaction Potential Analysis

Source	Event	Magnitude (M)
New Madrid seismic zone	December 16, 1811	6.9, 7.6
New Madrid seismic zone	January 23, 1812	7.0, 7.5
New Madrid seismic zone	February 7, 1812	7.3, 7.8
New Madrid seismic zone	January 5, 1843	6.3
New Madrid seismic zone	October 31, 1895	6.6
Commerce fault zone	Local	6.9
Eastern rift margin-north	South of Union City, TN	6.7
Eastern rift margin-south	West of Covington, TN	6.9
Eastern rift margin-south	Northwest of Memphis, TN	6.9, 7.1
Eastern rift margin-south river (fault) picks	West of Memphis, TN	6.9, 7.1
Eastern rift margin-south river (fault) picks	Near Tunica, MS	6.9
Marianna area	Daytona Beach liquefaction sites	6.7, 6.9, 7.0, 7.25, 7.5

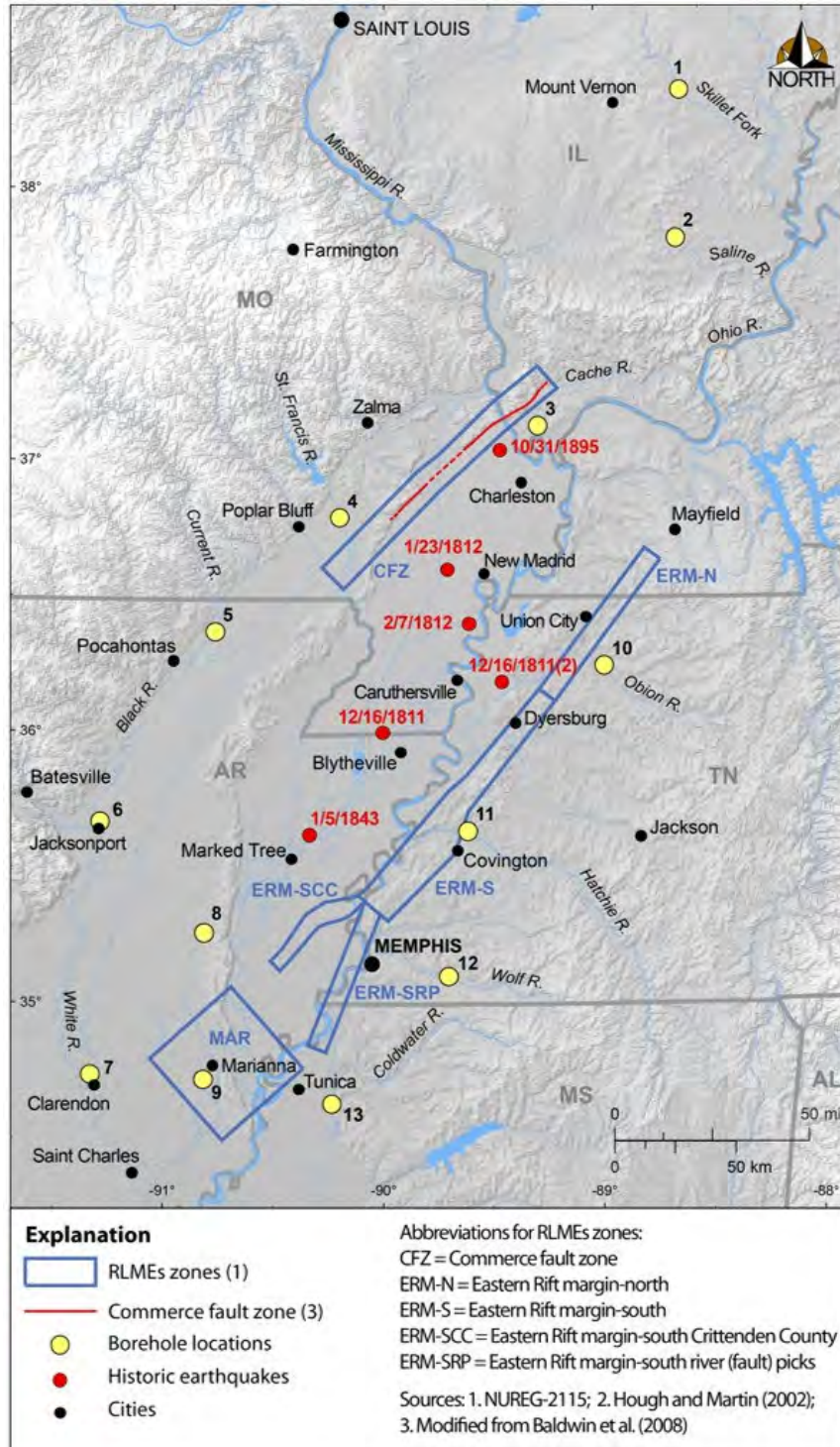


Figure 4-161 Map of NMSZ and surrounding region, showing locations of historical earthquakes and RLMEs zones (from NUREG-2115) as well as borehole locations with geotechnical data used in liquefaction potential analysis.

4.4.6.2 Liquefaction Potential Analysis

Liquefaction potential analysis was used to determine if the various scenario earthquakes are likely or not likely to induce liquefaction at the geotechnical sites along rivers searched for liquefaction features. Analysis was performed for many sites across the region, including some of the sites near or beyond the limit of the liquefaction fields. The results are then considered together to determine which scenario earthquakes best matches the observed distribution of liquefaction features generated by a particular paleoearthquake. This approach helps to constrain the locations and magnitudes of the paleoearthquakes.

As described in more detail in the Methodology section 4.2.5, the simplified, or cyclic-stress, procedure is used in this study. Regionally appropriate medium GMPEs developed during the past eight years were used to calculate peak ground accelerations or a_{max} for the scenario earthquakes. Distances between the scenario earthquakes and the geotechnical sites were measured in ArcGIS with the Point Distance tool and rounded to the nearest whole number (Table 4-33). These distances were needed to calculate peak ground acceleration generated by the various scenario earthquakes at the geotechnical sites.

Geotechnical data used in the analysis, including SPT and CPT data, sediment descriptions, and depths of water table at the time of testing, were gleaned from several sources. State Departments of Transportation in Arkansas, Illinois, Mississippi, Missouri, and Tennessee provided bridge investigation reports that contained geotechnical data including SPT measurements. Paul Mayne of Georgia Institute of Technology provided cone penetration test data for the Wolf River site east of Memphis, TN (Schneider et al., 2001). Tom Holzer of the US Geological Survey provided CPT data for the Lee1 site near Marianna, Arkansas (Table 4-34).

There are many sources of uncertainty associated with the geotechnical approach to evaluating the locations and magnitudes of paleoearthquakes, including but not limited to the following: (1) identification of the deposits that liquefied during a particular event; (2) measurements of geotechnical properties of the deposits; (3) changes in geotechnical properties due to liquefaction and to post-liquefaction effects related to compaction and weathering; and (4) short- and long-term fluctuations in the water table (NUREG-2115). In order to reflect these uncertainties, the geotechnical data were reviewed and multiple layers representative of the site and likely to be susceptible to liquefaction (e.g., within a depth range of ≤ 18 m and with blow counts of ≤ 30) selected for analysis. A water table depth of 3 m was used in the analysis, reflecting its annual average depth in the region. This seems reasonable because most New Madrid liquefaction features formed during the Late Holocene when the water table depth was similar to that of today.

In the future, evaluation of additional scenario earthquakes, using high and low GMPEs, and shallower and deeper water table depths, as well as geotechnical data collected at specific sites of liquefaction would be advantageous and would help to further constrain the interpretations of paleoliquefaction features.

Table 4-33 Distances (km) between Scenario Earthquakes or Source and Geotechnical Sites Used in analysis

Borehole Location (Map ID)	Dec 16 1811	Jan 23 1812	Feb 7 1812	Oct 31 1895	Jan 5 1843	CFZ	ERM-N	ERM-S	ERM-SRP	MA
Skillet Fork (1)	NA	219	235	NA	NA	NA	NA	NA	NA	NA
Saline River (2)	NA	166	180	NA	NA	NA	NA	NA	NA	NA
Cache River (3)	142	70	87	19	NA	NA	NA	NA	NA	NA
St. Francis River (4)	91	49	69	NA	NA	14	NA	NA	NA	NA
Current River (5)	80	99	105	NA	NA	NA	NA	NA	NA	NA
Black River (6)	120	171	169	NA	NA	NA	NA	NA	NA	NA
White River (7)	188	258	246	NA	NA	NA	NA	NA	NA	NA
Cross County Ditch (8)	103	173	160	NA	NA	NA	NA	NA	NA	NA
Marianna-Lee1 (9)	161	NA	NA	NA	NA	NA	NA	NA	NA	NA
Obion River (10)	96	76	60	NA	NA	NA	10	NA	NA	NA
Hatchie River (11)	54	107	85	NA	NA	NA	NA	10	NA	NA
Wolf River (12)	104	NA	NA	NA	NA	NA	NA	40, 60	40, 60	NA
Coldwater River (13)	154	224	205	NA	111	NA	NA	70	15, 48	55

CFZ= Commerce fault zone; ERM-N= Eastern rift margin-north; ERM-S= Eastern rift margin-south; ERM-SRP= Eastern rift margin-south river (fault) picks. NA = analysis not performed for this source.

Table 4-34 Locations of Geotechnical Data Used in Liquefaction Potential Analysis

Borehole Locations (Map ID)	Latitude (Degrees)	Longitude (Degrees)	Location Description
Skillet Fork (1)	38.36372	-88.58779	Skillet Fork Rt. 600 E, north of Wayne City, IL
Saline river (2)	37.81913	-88.61462	Saline River Ritchie Road bridge, south of Galatia, IL
Cache River (3)	37.12966	89.27271	Cache River FAS 942 bridge nar ILL 3. South of Unity, IL
St. Francis River (4)	36.79054	-90.20140	Rte. 60/3 near Fisk, MO
Current River (5)	36.37000	-90.77818	SH 328 near Reno (relief bridge), AR
Black River (6)	35.66718	-91.30056	Elgin Ferry. Elgin Road (Co Rd 37), AR
White River (7)	34.68885	-91.31642	US 79 bridge over White River, Clarendon, AR
Cross Country Ditch (8)	35.26052	-90.81944	Rte. 64 bridge over Cross County Ditch; northeast of Wynne, AR
Marianna-Lee1 (9)	34.71860	-90.81944	Marianna, AR; near large Daytona Beach sand blows
Obion River (10)	36.24585	-88.97348	SR 89 bridge over Obion River, TN
Hatchie River (11)	35.63695	-89.60966	SR 3/US 51 North of Covington, TN
Wolf River (12)	35.09949	-89.69931	East of Memphis, TN; near Collierville
Coldwater River (13)	34.62960	-90.23040	Rte. 3 bridge over Coldwater River, west of Savage, MS

4.4.6.3 Results of Analysis

To help interpret the distribution of observed liquefaction features in the New Madrid region, liquefaction potential analysis was performed for various scenario earthquakes as described above in Section 4.4.6.2. The results of the analysis are provided in Appendix G, summarized in Table 4-35 to Table 4-52, and discussed below. By comparing results of this analysis with field observations, the likely source areas and magnitudes of paleoearthquakes responsible for liquefaction features are inferred.

Liquefaction potential analysis for the **M 6.9** December 16, 1811 scenario earthquake near Blytheville, AR, predicts that liquefaction would not be likely to occur at any of the geotechnical sites considered in this study (Table 4-35; Figure 4-161). Since liquefaction features were observed in the vicinity of all of the sites, with perhaps the exception of the sites on the Black and White Rivers, this event under predicts the occurrence of liquefaction.

Table 4-35 Summary of Results for M 6.9 December 16, 1811 Scenario Earthquake

Site	Map ID#	Distance (km)	A_{max}^1	Prediction ²	Observation ³
Skillet Fork	1	NA	NA	NA	L
Saline River	2	NA	NA	NA	L
Cache River	3	142	0.07	N	L
St. Francis River	4	91	0.11	N	L
Current River	5	80	0.13	N	L
Black River	6	120	0.08	N	L/N
White River	7	188	0.05	N	L/N
Cross County Ditch	8	103	0.10	N	L
Marianna-Lee1	9	161	0.06	N	L
Obion River	10	96	0.10	N	L
Hatchie River	11	54	0.16	N	L
Wolf River	12	104	0.09	N	L
Coldwater River	13	154	0.06	N	L

¹ Derived from magnitude and distance using medium GMPE (Atkinson et. al., 2012).

² L = liquefaction likely for $\geq 50\%$ of the layers analyzed; L/N = liquefaction marginal for 1-49% of the layers analyzed; N = liquefaction likely for 0 % of the layers analyzed.

³ Observations made during this and other paleoliquefaction studies. See Appendix D - CEUS paleoliquefaction database.

In contrast, analysis for the **M 7.6** December 16, 1811 scenario earthquake predicts liquefaction at the geotechnical sites on the Cache, St. Francis, Current, and Black Rivers, Cross County Ditch, and at the Marianna site, marginal liquefaction at the geotechnical sites on the White, Obion, and Wolf Rivers, and no liquefaction at the Coldwater site (Table 4-36). In the cases of marginal liquefaction, few layers would be likely to liquefy and thus, fewer liquefaction features would be likely to form. The results of the analysis are a fairly close match to observed liquefaction, except that no Late Holocene liquefaction features produced by New Madrid events have been found in the Marianna area and only Late Holocene soft-sediment deformation structures have been found near the geotechnical site on the Black River. It seems that this scenario event may slightly overpredict the occurrence of liquefaction. Therefore, the magnitude of the earthquake that induced liquefaction across the region may have been slightly smaller than this scenario event.

Table 4-36 Summary of Results for M 7.6 December 16, 1811 Scenario Earthquake

Site	Map ID#	Distance (km)	A_{max} ¹	Prediction ²	Observation ³
Skillet Fork	1	NA	NA	NA	L
Saline River	2	NA	NA	NA	L
Cache River	3	142	0.14	L	L
St. Francis River	4	91	0.22	L	L
Current River	5	80	0.27	L	L
Black River	6	120	0.16	L	L/N
White River	7	188	0.10	L/N	L/N
Cross County Ditch	8	103	0.18	L	L
Marianna-Lee1	9	161	0.12	L	L
Obion River	10	96	0.16	L/N	L
Hatchie River	11	54	0.41	L	L
Wolf River	12	104	0.18	L/N	L
Coldwater River	13	154	0.12	N	L

¹ Derived from magnitude and distance using medium GMPE (Atkinson et. al., 2012).

² L = liquefaction likely for ≥ 50% of the layers analyzed; L/N = liquefaction marginal for 1-49% of the layers analyzed; N = liquefaction likely for 0 % of the layers analyzed.

³ Observations made during this and other paleoliquefaction studies. See Appendix D - CEUS paleoliquefaction database.

Analysis for the **M 7.0** January 23, 1812 scenario earthquake near New Madrid, MO, predicts that liquefaction would occur at the geotechnical sites on the Cache and St. Francis Rivers but at no other sites considered (Table 4-37; Figure 4-161). Therefore, this event also under predicts the occurrence of liquefaction.

Table 4-37 Summary of Results for M 7.0 January 23, 1812 Scenario Earthquake

Site	Map ID#	Distance (km)	A_{max}^1	Prediction ²	Observation ³
Skillet Fork	1	219	0.04	N	L
Saline River	2	166	0.07	N	L
Cache River	3	70	0.16	L	L
St. Francis River	4	49	0.24	L	L
Current River	5	99	0.11	N	L
Black River	6	171	0.07	N	L/N
White River	7	258	0.03	N	L/N
Cross County Ditch	8	173	0.06	N	L
Marianna-Lee1	9	NA	NA	NA	L
Obion River	10	76	0.15	N	L
Hatchie River	11	107	0.13	N	L
Wolf River	12	NA	NA	NA	L
Coldwater River	13	224	0.04	N	L

¹ Derived from magnitude and distance using medium GMPE (Atkinson et. al., 2012).

² L = liquefaction likely for ≥ 50% of the layers analyzed; L/N = liquefaction marginal for 1-49% of the layers analyzed; N = liquefaction likely for 0 % of the layers analyzed; NA = analysis not performed for this site usually because scenario event was clearly too far away to induce liquefaction.

³ Observations made during this and other paleoliquefaction studies. See Appendix D - CEUS paleoliquefaction database.

Analysis for the M 7.5 January 23, 1812 scenario earthquake predicts liquefaction at the geotechnical sites at the northern sites on Skillet Fork, Saline, Cache, St. Francis, Current, and Obion Rivers but not at the southern sites Black, White, Hatchie, Coldwater Rivers, and Cross County Ditch (Table 4-38). This would be a close match to observed liquefaction if the liquefaction field were skewed towards the northern portion of the New Madrid seismic zone.

Table 4-38 Summary of Results for M 7.5 January 23, 1812 Ccenario Earthquake

Site	Map ID#	Distance (km)	A _{max} ¹	Prediction ²	Observation ³
Skillet Fork	1	219	0.08	L/N	L
Saline River	2	166	0.10	L	L
Cache River	3	70	0.29	L	L
St. Francis River	4	49	0.40	L	L
Current River	5	99	0.16	L	L
Black River	6	171	0.10	N	L/N
White River	7	258	0.05	N	L/N
Cross County Ditch	8	173	0.10	N	L
Marianna-Lee1	9	NA	NA	NA	L
Obion River	10	76	0.27	L	L
Hatchie River	11	107	0.16	N	L
Wolf River	12	NA	NA	NA	L
Coldwater River	13	224	0.06	N	L

¹ Derived from magnitude and distance using medium GMPE (Atkinson et. al., 2012).

² L = liquefaction likely for ≥ 50% of the layers analyzed; L/N = liquefaction marginal for 1-49% of the layers analyzed; N = liquefaction likely for 0 % of the layers analyzed; NA = analysis not performed for this site usually because scenario event was clearly too far away to induce liquefaction.

³ Observations made during this and other paleoliquefaction studies. See Appendix D - CEUS paleoliquefaction database.

Analysis for the M 7.3 February 7, 1812 scenario earthquake between Caruthersville and New Madrid, MO, predicts liquefaction at the geotechnical sites on the Cache and St. Francis Rivers and only marginal liquefaction on the Saline, Current, and Obion Rivers. Liquefaction is not predicted on Skillet Fork, Black, White, Hatchie, Coldwater Rivers or Cross County Ditch (Table 4-39; Figure 4-161). This event under predict the occurrence of liquefaction as observed at distant sites.

Table 4-39 Summary of Results for M 7.3 for February 7, 1812 Scenario Earthquake

Site	Map ID#	Distance (km)	A_{max}^1	Prediction ²	Observation ³
Skillet Fork	1	235	0.05	N	L
Saline River	2	180	0.08	L/N	L
Cache River	3	87	0.15	L	L
St. Francis River	4	69	0.26	L	L
Current River	5	105	0.13	L/N	L
Black River	6	169	0.08	N	N
White River	7	246	0.03	N	N
Cross County Ditch	8	160	0.09	N	L
Marianna-Lee1	9	NA	NA	NA	L
Obion River	10	60	0.17	L/N	L
Hatchie River	11	85	0.15	N	L
Wolf River	12	NA	NA	NA	L
Coldwater River	13	205	0.06	N	L

¹ Derived from magnitude and distance using medium GMPE (Atkinson et. al., 2012).

² L = liquefaction likely for $\geq 50\%$ of the layers analyzed; L/N = liquefaction marginal for 1-49% of the layers analyzed; N = liquefaction likely for 0 % of the layers analyzed; NA = analysis not performed for this site usually because scenario event was clearly too far away to induce liquefaction.

³ Observations made during this and other paleoliquefaction studies. See Appendix D - CEUS paleoliquefaction database.

For the **M** 7.8 February 7, 1812 scenario earthquake, predicted liquefaction fairly closely matches observed liquefaction, except for the Skillet Fork, White, and Coldwater sites where liquefaction was not predicted (Table 4-40).

Table 4-40 Summary of Results for M 7.8 for February 7, 1812 Scenario Earthquake

Site	Map ID#	Distance (km)	A_{max}^1	Prediction ²	Observation ³
Skillet Fork	1	235	0.08	N	L
Saline River	2	180	0.13	L	L
Cache River	3	87	0.31	L	L
St. Francis River	4	69	0.46	L	L
Current River	5	105	0.21	L	L
Black River	6	169	0.13	L/N	L/N
White River	7	246	0.08	N	L/N
Cross County Ditch	8	160	0.14	L	L
Marianna-Lee1	9	NA	NA	NA	L
Obion River	10	60	0.52	L	L
Hatchie River	11	85	0.32	L	L
Wolf River	12	NA	NA	NA	L
Coldwater River	13	205	0.10	N	L

¹ Derived from magnitude and distance using medium GMPE (Atkinson et. al., 2012).

² L = liquefaction likely for $\geq 50\%$ of the layers analyzed; L/N = liquefaction marginal for 1-49% of the layers analyzed; N = liquefaction likely for 0 % of the layers analyzed; NA = analysis not performed for this site usually because scenario event was clearly too far away to induce liquefaction.

³ Observations made during this and other paleoliquefaction studies. See Appendix D - CEUS paleoliquefaction database.

Because New Madrid events are earthquake sequences including several large earthquakes, it makes sense to combine the results of each earthquake of a pair that provided the better match with observed liquefaction. Of these analyses, the larger magnitude earthquake of each pair - the **M** 7.6 December 16, 1811, **M** 7.5 January 23, 1812, and **M** 7.8 February 7, 1812 scenario earthquakes - provided the better match. The combined results for these three scenario earthquakes provide the best match of all with the observed liquefaction at distant sites (Table 4-41; Figure 4-161). Liquefaction is over predicted at the Black River and Marianna sites as it was for the **M** 7.6 December 16, 1811, suggesting that the magnitude of this scenario earthquake is larger than the actual earthquake that induced liquefaction across the region

Table 4-41 Combined Results for M 7.6 December 16, 1811, M 7.5 January 23, 1812, and M 7.8 for February 7, 1812 Scenario Earthquakes

Site	Map ID#	Prediction ²	Observation ³
Skillet Fork	1	L/N	L
Saline River	2	L	L
Cache River	3	L	L
St. Francis River	4	L	L
Current River	5	L	L
Black River	6	L	L/N
White River	7	L/N	L/N
Cross County Ditch	8	L	L
Marianna-Lee1	9	L	L
Obion River	10	L	L
Hatchie River	11	L	L
Wolf River	12	L/N	L
Coldwater River	13	N	L

¹ L = liquefaction likely for ≥ 50% of the layers analyzed; L/N = liquefaction marginal for 1-49% of the layers analyzed; N = liquefaction likely for 0 % of the layers analyzed; NA = analysis not performed for this site usually because scenario event was clearly too far away to induce liquefaction.

² Observations made during this and other paleoliquefaction studies. See Appendix D - CEUS paleoliquefaction database.

Because none of the A.D. 1811-1812 scenario earthquakes predicted liquefaction along the Coldwater River where liquefaction features were found during this project, the closer, though smaller, **M** 6.3 January 5, 1843 event was also considered as a scenario earthquake. However, liquefaction potential analysis for this scenario earthquake near Marked Tree, AR, also did not predict liquefaction at the geotechnical site on the Coldwater River (Table 4-42; Figure 4-161).

Table 4-42 Summary of Results for M 6.3 January 5, 1843 Scenario Earthquake

Site	Map ID#	Distance (km)	A_{max} ¹	Prediction ²	Observation ³
Coldwater River	13	111	0.05	N	L

¹ Derived from magnitude and distance using medium GMPE (Atkinson et. al., 2012).

² L = liquefaction likely for ≥ 50% of the layers analyzed; L/N = liquefaction marginal for 1-49% of the layers analyzed; N = liquefaction likely for 0 % of the layers analyzed.

³ Observations made during this and other paleoliquefaction studies. See Appendix D - CEUS paleoliquefaction database.

Liquefaction potential analysis was performed using the **M** 6.6 October 31, 1895 Charleston, MO, event as a scenario earthquake to see if it could explain the occurrence of liquefaction features along the lower Cache River in southern Illinois (Tuttle and Chester, 2005). The liquefaction features along the Cache include sand dikes, sills, and soft-sediment deformation structures, most of which formed since B.C. 2890 (4840 yr B.P.), and several of which formed since A.D. 1020

(930 yr B.P.). The results are to the affirmative suggesting that a Charleston-like event could indeed induce liquefaction in southern Illinois (Table 4-43; Figure 4-161).

In order to evaluate the Commerce fault zone as a possible source, analysis was performed for a **M** 6.9 scenario earthquake at a distance of 14 km, which represents the distance between the St. Francis River geotechnical site and the projected trend of the Commerce fault zone (Figure 4-46 and Figure 4-161). The results indicate that such an event would be likely to induce liquefaction at the geotechnical site (Table 4-44; Figure 4-46 and Figure 4-161). Therefore, if the Commerce fault zone generated a **M** 6.9 or greater earthquake in the Late Pleistocene-Late Holocene, there would likely be a liquefaction record of the event in the area.

Table 4-43 Summary of Results for M 6.6 October 31, 1895 Scenario Earthquake

Site	Map ID#	Distance (km)	A_{max}^1	Predictions ²	Observations ³
Cache River	3	19	0.30	L	L

Table 4-44 Summary of Results for M 6.9 Commerce Fault Zone Scenario Earthquake

Site	Map ID#	Distance (km)	A_{max}^1	Predictions ²	Observations ³
St. Francis River	4	14	0.93	L	L

¹ Derived from magnitude and distance using medium GMPE (Atkinson et. al., 2012).

² L = liquefaction likely for $\geq 50\%$ of the layers analyzed; L/N = liquefaction marginal for 1-49% of the layers analyzed; N = liquefaction likely for 0 % of the layers analyzed.

³ Observations made during this and other paleoliquefaction studies. See Appendix D - CEUS paleoliquefaction database.

During the CEUS seismic source characterization project, the eastern Reelfoot Rift margin (ERM) was split into four zones of repeating large magnitude earthquakes: ERM-N, ERM-S, ERM-SCC, and ERM-SRP (Figure 4-161; NUREG-2115). Liquefaction potential analysis was performed for one local (10 km) scenario event on the ERM-north, five scenario events on ERM-S (two west of Covington, TN, and three northwest of Memphis, TN), and five scenario events on ERM-SRP (three west of Memphis and two near Tunica, MS) to help evaluate whether or not earthquakes produced by the ERM would be likely to produce liquefaction features along the Obion, Hatchie, Wolf, and Coldwater Rivers.

Analysis for a local (10 km) **M** 6.7 scenario earthquake on the ERM-N predicts that liquefaction would be likely to occur at the Obion River site (Table 4-45). Similarly, a local (10 km) **M** 6.9 scenario earthquake west of Covington near the northern end of the ERM-S indicates that liquefaction would be likely to occur at the Hatchie River site (Table 4-46). Such an event also predicts marginal liquefaction at the Wolf River site near Collierville about 60 km away. Analysis for a **M** 6.9 scenario earthquake northwest of Memphis near the southern end of the ERM-S also predicts marginal liquefaction at the Wolf River site about 40 km away; whereas, analysis of a **M** 6.9 scenario earthquake with the same location does not predict liquefaction at the Coldwater River site 70 km away (Table 4-47). However, the analysis finds that a **M** 7.1 scenario event with the same location is likely to induce liquefaction at the Wolf River geotechnical site and marginal liquefaction at the Coldwater site (Table 4-48). Scenario earthquakes of **M** 6.9 and **M** 7.1 west of Memphis on the ERM-SRP produce similar results for the Wolf and Coldwater River site as did events of similar magnitudes northwest of Memphis near the southern end of the ERM-S (Table 4-49 and Table 4-50). Considering a **M** 6.9 scenario event at the southern end of the ERM-SRP near Tunica, MS, the analysis predicts marginal liquefaction at the Wolf River site 60 km away and liquefaction at the Coldwater River site only 15 km away (Table 4-51).

Table 4-45 Summary of Results for Eastern Rift Margin-North M 6.7 Scenario Earthquake South of Union City

Site	Map ID#	Distance (km)	A_{max}^1	Predictions ²	Observations ³
Obion River	10	10	0.94	L	L

Table 4-46 Summary of Results for Eastern Rift Margin-South M 6.9 Scenario Earthquakes West of Covington

Site	Map ID#	Distance (km)	A_{max}^1	Predictions ²	Observations ³
Hatchie River	11	10	1.12	L	L
Wolf River	12	60	0.19	L/N	L

Table 4-47 Summary of Results for Eastern Rift Margin-South M 6.9 Scenario Earthquakes Northwest of Memphis

Site	Map ID#	Distance (km)	A_{max}^1	Predictions ²	Observations ³
Wolf River	12	40	0.27	L/N	L
Coldwater River	13	70	0.16	N	L

Table 4-48 Summary of Results for Eastern Rift Margin-South M 7.1 Scenario Earthquakes Northwest of Memphis

Site	Map ID#	Distance (km)	A_{max}^1	Predictions ²	Observations ³
Wolf River	12	40	0.43	L	L
Coldwater River	13	70	0.18	L/N	L

Table 4-49 Summary of results for Eastern Rift margin-south river (fault) picks M 6.9 scenario earthquakes west of Memphis

Site	Map ID#	Distance (km)	A_{max}^1	Predictions ²	Observations ³
Wolf River	12	40	0.27	L/N	L

Table 4-50 Summary of Results for Eastern Rift Margin-South River (Fault) Picks M 7.1 Scenario Earthquakes West of Memphis

Site	Map ID#	Distance (km)	A_{max}^1	Predictions ²	Observations ³
Wolf River	12	40	0.43	L	L
Coldwater River	13	48	0.29	L/N	L

Table 4-51 Summary of Results for Eastern Rift Margin-South River (fault) Picks M 6.9 Scenario Earthquakes near Tunica

Site	Map ID#	Distance (km)	A_{max}^1	Predictions ²	Observations ³
Wolf River	12	60	0.19	L/N	L
Coldwater River	13	15	0.88	L	L

¹ Derived from magnitude and distance using medium GMPE (Atkinson et. al., 2012).

² L = liquefaction likely for $\geq 50\%$ of the layers analyzed; L/N = liquefaction marginal for 1-49% of the layers analyzed; N = liquefaction likely for 0 % of the layers analyzed.

³ Observations made during this and other paleoliquefaction studies. See Appendix D - CEUS paleoliquefaction database.

Although not originally planned as part of this project, Marianna scenario earthquakes were added because none of the New Madrid scenario earthquakes predicted liquefaction at the Coldwater River site. In addition, some of the liquefaction features along the Coldwater River may be similar in age to large sand blows in the Marianna area. In the liquefaction potential analysis, a **M** 6.7 scenario earthquake did not predict liquefaction at the Coldwater River site 55 km away; whereas, **M** 6.9, **M** 7.0, and **M** 7.25 events indicated marginal liquefaction; and a **M** 7.5 event predicted liquefaction (Table 4-52).

Table 4-52 Summary of Results for Marianna Area Scenario Earthquakes

Site	Map ID#	M @Distance (km)	A _{max} ¹	Predictions ²	Observations ³
Coldwater River	13	6.7 @ 55	0.159	N	L
Coldwater River	13	6.9 @ 55	0.190	L/N	L
Coldwater River	13	7.0 @ 55	0.203	L/N	L
Coldwater River	13	7.25 @ 55	0.259	L/N	L
Coldwater River	13	7.5 @ 55	0.331	L	L

¹ Derived from magnitude and distance using medium GMPE (Atkinson et. al., 2012).

² L = liquefaction likely for ≥ 50% of the layers analyzed; L/N = liquefaction marginal for 1-49% of the layers analyzed; N = liquefaction likely for 0 % of the layers analyzed.

³ Observations made during this and other paleoliquefaction studies. See Appendix D - CEUS paleoliquefaction database.

4.4.7 Summary and Discussion

This paleoliquefaction study of the New Madrid seismic zone and surrounding region was regional in scope and involved searching for and dating liquefaction features along selected rivers, conducting investigations of selected liquefaction sites, and evaluating scenario earthquakes to assist in interpreting observations in terms of likely locations and magnitudes of paleoearthquakes. The findings of the river surveys, site investigations, and evaluations of scenario events, and their implications for the timing, locations, and recurrence times of large paleoearthquakes, are discussed below.

4.4.7.1 River Surveys

Along all the rivers surveyed, Holocene deposits were inset in Late Pleistocene deposits (Figure 4-17, Figure 4-21, Figure 4-22, and Figure 4-27). Exposures were generally very good, with most exposures in Late Holocene deposits, especially those along the Obion River in western TN, and the White River near Clarendon, AR. Early to Late Holocene deposits were exposed along the St. Francis River between Chalk Bluff and Nimmons, AR, and the Coldwater River and Pompey Ditch in northwestern MS. Late Pleistocene to Late Holocene deposits were exposed along the St. Francis River between Fisk and Wilhelmina in southeastern MO, the Black River near Pochontas, Elgin, and Jacksonport, AR, areas, and the White River in the St. Charles, AR, area. The age of deposits exposed is important to note because it can limit the age of the liquefaction features found. Overall, sedimentological conditions were conducive for the formation of earthquake-induced liquefaction features.

4.4.7.1.1 *Western Lowlands – Commerce Geophysical Lineament and Western Reelfoot Rift Margin*

Large, Late Pleistocene-Early Holocene earthquakes have been proposed on the CGL in southeastern MO on the basis of liquefaction features exposed in ditches associated with the St. Francis River (Vaughn, 1994) and on fault displacements along the southeastern flank of Crowleys Ridge (Harrison and Schultz, 1994; Hoffman et al., 1996; Baldwin et al., 2006) and in the vicinity the St. Francis River near Qulin (Stephenson et al., 1999; Baldwin et al., 2014) (Figure 4-46). During this study, we found no additional liquefaction features that definitely formed during the Late Pleistocene-Early Holocene along the St. Francis River between Fisk and Wilhelmina, MO, or any of the rivers that occur within close proximity to the CGL or the western Reelfoot Rift margin (Figure 4-19; Table 4-53). The other rivers include the Black and Current Rivers near Pocahtontas, the Black River near Elgin and Jacksonport, AR, and the White River near Oil Trough. Late Pleistocene-Early Holocene deposits are exposed along all the rivers though Holocene deposits are more prevalent.

Along the St. Francis River, we found many sand dikes, and at least two generations of features, most of which formed since B.C. 3020 (4970 yr B.P.) (Figure 4-46). The Late Holocene liquefaction features at six sites were likely caused by the New Madrid events of A.D. 1811-1812, A.D. 1450, and A.D. 900, based on radiocarbon dating of host sediments and degree of weathering of the sand dikes. The dikes were small (0.2-15 cm) compared with dikes in the New Madrid seismic zone proper, which is consistent with their being distal features related to New Madrid events. Along the Black and Current Rivers near Pocahtontas, the age estimates of liquefaction features remain poorly constrained. However, the features clearly formed during the Late Holocene and may very well have formed during the same New Madrid earthquakes. No sand blows or dikes were found along the Black River near Jacksonport and Elgin, AR, or along the White River near Oil Trough, AR. However, pseudonodules were found along the Black River near Elgin that might have been caused by earthquake-induced liquefaction. If they have an earthquake origin, these soft-sediment deformation structures would suggest that ground shaking during the causative event was on the order of MMI ~VIII (Sims, 1973). Although a moderate local earthquake cannot be ruled out, one of the New Madrid events may have been responsible for these Late Holocene features. If so, the pseudonodules would represent the limit of liquefaction for that event in this area. This interpretation is supported by the apparent absence of liquefaction features along the White River near Oil Trough, which is farther away from the NMSZ and may be beyond the limit of liquefaction. Additional mapping of liquefaction features along nearby rivers somewhat closer to the New Madrid seismic zone, such as the Cache River, and dating of sediments where soft-sediment deformation structures formed, would help to increase confidence in the interpretation of a seismic origin, to better estimate the age of the features, and to further define the limit of liquefaction in this part of the Western Lowlands.

Our findings in the Western Lowlands between Fisk, MO, and Oil Trough, AR, suggest that the liquefaction field for Late Holocene New Madrid earthquakes should be extended to include the St. Francis River and the Black and Current Rivers near Pocahtontas (Figure 4-19). The pseudonodules on the Black River near Elgin might suggest that the liquefaction field should be extended to this area as well, but that would be premature given the uncertainties related to the origin and age of the features and the lack thus far of sand blows and dikes discovered in the area. The apparent absence of Late Holocene sand blows and dikes along the Black River near Jacksonport and Elgin, AR, and the White River near Oil Trough, AR, suggests that the Commerce Geophysical Lineament and western Reelfoot Rift margin fault did not produced ground shaking strong enough ($\text{MMI} \geq \text{IX}$) to induce severe and widespread liquefaction during this period.

Table 4-53 Earthquake-Induced Liquefaction Features Studied along Rivers

River Name Area	Deformation Structure	Confidence	Age Constraint year B.P.	Exposed Sediment	Likely Events¹
Western Lowlands					
St Francis-Fisk to Wilhelmina	Sand dikes SSD	High High	2 generations of sand dikes since 4970	Late Pleistocene-Late Holocene	AD 1811-1812, 1450, & 900
Current - Pocahontas	Sand dikes	High	Since 3610	Late Holocene	New Madrid events
Black River-Pocahontas	Sand dikes Sand blows	High Medium	Since 3690	Late Pleistocene-Late Holocene	New Madrid events
Black River-Jacksonport & Elgin	Pseudo-nodules	Medium	Probably since 3690	Late Pleistocene-Late Holocene	Possibly New Madrid events
White River-Oil Trough	None	NA	Since 1990	Mostly Late Holocene	NA
White River-Clarendon	Sand dike	Medium	Since 1990	Late Holocene	Possibly New Madrid events
White River-St. Charles	Pseudo-nodules	Medium	Since 720	Late Holocene & Late Pleistocene	Possibly Marianna event
St. Francis Basin					
St. Francis-Chalk Bluff to Nimmons	Sand dikes SSD	High High	2 generations of sand dikes since 11,690	Early-Late Holocene	AD 1811-1812, 1450, & 900
Locust-Creek Ditch	Sand blow Sand dike	High High	Since 270 Since 910	Late Holocene	AD 1811-1812 & 1450
Western TN					
Obion River-Obion	Sand dikes Sand blows	High High	2 generations of sand dikes since 2960	Late Holocene	AD 1811-1812 & 1450
Obion River-Midway	Sand dikes Sand blows	High High	Since 685	Late Holocene	AD 1811-1812, 1450, & possibly 900
Northwest MS					
Coldwater-Arkabutla Dam	Sand dikes Sand blow SSD	High Medium High	2, possibly 3, generations of sand dikes since 8340	Early-Late Holocene	Possibly Marianna & New Madrid events
Coldwater-Pompey Ditch	None	NA	Since 8340	Early-Late Holocene	NA

¹ New Madrid events A.D. 1811-1812 (139-138 yr B.P.), A.D. 1450 (500 yr B.P.) ± 150 yr, A.D. 900 (1050 yr B.P.) ± 150 yr, A.D. 0 (1950 yr B.P.) ± 200 yr, B.C. 1050 (3000 yr B.P.) ± 250 yr, B.C. 2350 (4300 yr B.P.) ± 200 yr. Marianna events = B.C. 2850 (4800 yr B.P.) ± 150 yr, B.C. 3550 (5500 yr B.P.) ± 150 yr, B.C. 4850 (6800 yr B.P.) ± 150 yr, B.C. 7900 (9850 yr B.P.) ± 300 yr, and one, possibly 2, Late Pleistocene events between 19-38 ka.

The apparent absence of Late Pleistocene to Middle Holocene sand blows and dikes along the rivers might suggest that neither the CGL nor the WRM produced strong ground shaking during this period either. However, exposure of Late Pleistocene to Middle Holocene deposits is more limited along the rivers, especially the White River. Also, such an interpretation would be contrary to several independent studies that proposed large Late Pleistocene to Early Holocene earthquakes in the vicinity of the St. Francis River. Given the limited exposure of Late Pleistocene-Middle Holocene deposits along rivers, we recommend an additional effort to identify and investigate sand blows on terrace surfaces of these ages. Our examination of Google Earth satellite imagery finds features that have the appearance of sand blows in fields adjacent to the St. Francis River between Fisk and Wilhelmina. These features would be good targets for additional study to improve the understanding of earthquake activity during the Late Pleistocene and Holocene and the earthquake potential of the CGL and associated faults.

4.4.7.1.2 *St. Francis Basin - New Madrid Seismic Zone and Western Reelfoot Rift Margin*

Late Holocene earthquakes centered in the New Madrid seismic zone are known to have induced liquefaction in the St. Francis Basin of northeastern AR and southeastern MO, east of Crowleys Ridge. However, most paleoliquefaction field work in the St. Francis Basin has been done in the Holocene meander belt deposits of the Mississippi River. Comparatively little paleoliquefaction field work has been conducted in the Late Pleistocene valley train deposits between Crowleys Ridge and the Holocene meander belt. Therefore, we conducted surveys along the St. Francis River between Chalk Bluff and Nimmons and Locust Creek Ditch southeast of Paragould to better understand the age and distribution of paleoliquefaction features in this area.

Along the St. Francis River, we found many sand dikes, sills, and source beds with soft-sediment deformation structures (Figure 4-36). Cross-cutting relationships indicate that there were at least two generations of dikes. On the basis of the degree of weathering of the sand dikes and radiocarbon dating at eight of the liquefaction sites, almost all of the features can be attributed to the New Madrid events of A.D. 1811-1812, A.D. 1450, and A.D. 900. The dikes were small (0.2-21 cm, except for one dike that was 41 cm wide) compared to dikes in the New Madrid seismic zone proper, but on average, slightly larger than the dikes on the St. Francis River between Fisk and Wilhelmina in the Western Lowlands.

Along Locust Creek Ditch, we found one sand blow and several dikes (5-76 cm wide). Like a sand blow previously found on Eightmile Ditch to the west (Tuttle, 1999), the sand blow, composed of two depositional units, probably formed during two earthquakes in the A.D. 1811-1812 New Madrid sequence. The largest dike was considerably more weathered than the sand blow and likely formed during the A.D. 1450 New Madrid event. It is notable that sand blows formed in this area but apparently not along the St. Francis River between Chalk Bluff and Nimmons. Also, the dikes along Locust Creek Ditch are larger than those along the St. Francis River. These differences may be related to several factors, such as liquefaction susceptibility of the sediment and distance from the seismic source.

Along both the St. Francis River and Locust Creek Ditch, we found liquefaction features that clearly formed during Late Holocene earthquakes, we found no liquefaction features that formed during pre-Late Holocene earthquakes, nor did we find evidence to suggest that the WRM has produced large earthquakes in this area at least during the Late Holocene. Although Early-Middle Holocene sediment was exposed along the northern portion of the St. Francis River immediately downstream from Chalk Bluffs, most other cutbank exposures were of inset Holocene sediment, and Late Holocene sediment at that. Therefore, the geologic record that we examined along

these two waterways was skewed towards the Late Holocene. Nevertheless, Late Holocene features were found in Early-Middle Holocene sediment, whereas older liquefaction features were not.

4.4.7.1.3 *Western Tennessee – New Madrid Seismic Zone and Eastern Reelfoot Rift Margin*

Recurrent movement during the Quaternary and repeating large-magnitude earthquakes have been proposed for the ERM in western TN, on the basis of geophysical studies along the Mississippi River and on its floodplains (e.g., Williams et al., 1995 and 2001; Hao et al., 2013) and paleoseismic and geomorphic studies in Meeman-Shelby Forest State Park northwest of Memphis, at Porter Gap southwest of Dyersburg, and near Union City (e.g., Cox et al., 2001 and 2006) (Figure 4-19). The northern segment, ERM-N, may have turned off or become less active in the Late Pleistocene-Holocene, whereas the southern segment, ERM-S, may have been active throughout the Late Pleistocene-Holocene, producing a large ($M \geq 6.5$) earthquake as recently as 2000-2,500 yr B.P. (Figure 4-161; Cox et al., 2006; NUREG-2115).

During previous paleoliquefaction studies along the Hatchie and Obion rivers near Covington and Dyersburg, TN, respectively, liquefaction features had been found that likely formed during the A.D. 1811-1812 and A.D. 1450 New Madrid events (Tuttle, 1999 and 2010; Tuttle and Schweig, 2001 and 2004). None of the liquefaction features had been dated to A.D. 900 or earlier in the Holocene or the Late Pleistocene. However, the ages of many of the liquefaction features along the two rivers were poorly constrained. We resurveyed the Obion River in the vicinity of Obion, TN, not far from the ERM-N, and in the vicinity of Midway, TN, not far from the ERM-S, to determine if any of the poorly constrained liquefaction features formed during the A.D. 900 or A.D. 0 events, or any other Late Pleistocene-Middle Holocene event (Figure 4-24). As described above, an active fault crossing the lower Obion River valley has been postulated on the basis of a very large sand dike at OR216/603 and a zone of lineaments, including large linear sand blows at the Pritchett site. Therefore, OR216/603 was revisited to collect additional material for radiocarbon dating in order to better constrain the age of the large sand dike and associated sand blow.

In the Obion area, we relocate some of the previously documented liquefaction features and also found additional features. There were clearly two generations of features that formed since B.C. 1010 (2960 yr B.P.). With additional observations and radiocarbon dating, we estimated that liquefaction features at two sites formed during A.D. 1811-1812 and A.D. 1450 New Madrid events. Sand blows were composed of only one depositional unit and ranged from 12-27 cm thick. Similarly, dikes were relatively small (1-10 cm wide). Unfortunately, a previously discovered sand blow that formed between B.C. 1680 and A.D. 1820 (3630-130 yr B.P.) had been removed by erosion.

In the Midway area, three liquefaction sites were relocated and an additional liquefaction site found. At two of the sites, sand blows and related dikes clearly formed during the A.D. 1811-1812 New Madrid event, whereas, at a third site, the liquefaction features could have formed during either the A.D. 1450 or A.D. 900 events. Also, additional dating supported the interpretation that the very large sand dike and related sand blow at OR216/603 formed during the A.D. 1450 event. Along this portion of the river, sand blows were composed of 2-5 depositional units and ranged from 95-150 cm thick. Liquefaction features in the Midway area were larger than those in the Obion area. This is due in part to the compound nature of the sand blows in the Midway area, indicating that they formed as the result of recurrent liquefaction during an earthquake sequence. This probably reflects their closer proximity to multiple seismic sources.

Our findings along the two segments of the Obion, confirm prior results that both the A.D. 1811-1812 and A.D. 1450 New Madrid events induced liquefaction along the Obion River valley. No evidence was found for liquefaction induced by earthquakes circa A.D. 900, A.D. 0, or B.C. 1050 along the river valley, though the ages of many liquefaction features remain poorly constrained. Also, no liquefaction evidence was found for pre-Late Holocene earthquakes; however, this is not surprising since most, if not all, of the exposed sediment examined is Late Holocene in age.

4.4.7.1.4 *Northwestern Mississippi and Western Lowlands –Marianna Area and Eastern Reelfoot Rift Margin*

Large earthquakes during the Late Pleistocene-Middle Holocene are thought to have occurred in the Marianna area of east-central AR (Figure 4-19), on the basis of geophysical and paleoliquefaction studies of large linear sand blows along a northwest-trending lineament (e.g., Al-Shukri et al., 2005, 2009, and 2015; Tuttle et al., 2006; Al-Qadhi, 2010). In addition, the linear sand blows and northwest-trending lineament are thought to be the surface expression of an underlying fault zone that may be related to the nearby White River fault zone. Seismic reflection surveys across the lineament imaged near-vertical faults in the 100 to 1000 meter-depth range, which likely includes Eocene through Paleozoic strata that are coincident with the lineament and associated sand blows (Odum et al., 2016). The seismic reflection study also found that fault displacement increases with depth, suggesting long-term recurrent faulting. Liquefaction potential analysis indicates that the events were at least M 6-6.5 to induce liquefaction at the Marianna sites (Al-Shukri et al., 2015). The Marianna event of B.C. 3550 (5500 yr B.P.) may have been responsible for relatively small sand blows and dikes of similar age near Marked Tree, AR, about 80 km to the north. If so, these distal features suggest that the event was $M > 7.0$ and that other liquefaction features caused by this and other Marianna events should be found within 80 km of the Marianna area. Therefore, river surveys for liquefaction features along the Coldwater River in northwestern Mississippi and along the White River in the Western Lowlands west of Marianna were undertaken to develop a better understanding of the areal distribution of liquefaction features in these areas, which in turn, would help to constrain the magnitudes of the Marianna events.

The ERM-S discussed above and the ERM-SRP are other possible sources of large earthquakes towards the southern end of the Reelfoot Rift system (Figure 4-161). The ERM-SRP is delineated from just south of Meeman-Shelby Forest State Park to about Tunica, MS, from three fault picks along a high-resolution seismic survey conducted along the Mississippi River (Hao et al., 2013). The ERM-SRP is thought to be active, based on deformation of Quaternary alluvium imaged in the survey. It is also thought to be capable of producing a M 6.9 earthquake, if it ruptured in one event. River surveys for liquefaction features along the Coldwater River are relevant for assessing the earthquake potential of the ERM-SRP.

Along the Coldwater River downstream from the Arkabutla Dam, we found one sand blow, many sand dikes and sills, as well as source beds with soft-sediment deformation structures. The sand blow was 27 cm thick and the dikes ranged from 0.2 to 24.0 cm in width. Their crosscutting relationships and weathering characteristics suggest three generations of liquefaction features. Radiocarbon dating suggests that all the features formed during the Holocene and that the features can be divided into three ages classes <8340 yr B.P., <4965 yr B. P., and <3715 yr B.P. The oldest generation of liquefaction features, including the sand blow, pre-dates earthquakes centered in the NMSZ, but is similar in age to the Marianna earthquakes (6650-6950 yr B.P. and 5350-5650 yr B.P.). The youngest generation of features post-dates the Marianna earthquakes, but is similar in age to the New Madrid earthquakes (2600-2900 yr B.P., 900-1200 yr B.P., 350-650 yr B.P.). The middle generation of features overlaps the ages of the Marianna (4650-4950 yr B.P.) and New Madrid (4150-4450 yr B.P.) earthquakes. It seems quite likely that the Early-

Middle Holocene liquefaction features formed during one or more of the Marianna earthquakes, whereas the earthquake responsible for the Late Holocene features had a different source. Earthquakes produced by the New Madrid seismic zone may be too far away to induce liquefaction along the Coldwater River. The ERM-S and ERM-SRP are much closer, and the ERM-S is thought to have produced a large earthquake between 2000-2500 yr B.P. Perhaps this event was responsible for the Late Holocene liquefaction features on the Coldwater River. Overall, the liquefaction features are relatively small, which is consistent with the interpretation that they are distal features related to large Marianna and ERM-S events. However, it is also possible that they formed during several small, local events. Additional reconnaissance for and dating of liquefaction features in northwestern MS, east-central AR, and southwestern TN, as well as further evaluation of scenario earthquakes would help to better assess locations and magnitudes of paleoearthquakes in this region.

Along the White River near Clarendon, the exposed sediment was too young to record Late Pleistocene-Middle Holocene earthquakes. However, a possible Late Holocene sand dike was found along the river. If it is an earthquake-induced liquefaction feature, the dike may have formed during one of the Late Holocene New Madrid events. The feature occurs about 120 km southwest of the southwestern end of the NMSZ and the inferred location of the **M** 6.3 1843 earthquake. It also occurs about 190 km southwest of the December 16, 1811 earthquake. According to the relationship between earthquake magnitude and distance to farthest surface expression of liquefaction (Castilla and Audemard, 2007), the sand dike occurs well within the distance range of liquefaction for either of these events. Farther south along the White River near St. Charles, pseudonodules occur within Late Pleistocene deposits. If these features are related to earthquake-induced liquefaction, they might have formed during a Late Pleistocene Marianna event. Additional reconnaissance for and dating of liquefaction features, especially within Late Pleistocene deposits, might be warranted in this area.

4.4.7.2 *Site Investigations*

In order to try to extend the NMSZ paleoearthquake chronology back in time, liquefaction sites that are located in areas of Late Pleistocene fluvial deposits were selected. From west to east, these are the Garner, Faulkner, Wildy, and Stiles sites. All occur in northeastern AR in the St. Francis Basin, between Crowleys Ridge and the Mississippi River (Figure 4-18, Figure 4-21, Figure 4-22, and Figure 4-27; Table 4-54). The Garner site is situated on the level 3 of Late Pleistocene deposits; the Faulkner and Wildy sites occur on level 2; and the Stiles site straddles the boundary between level 1 of Late Pleistocene deposits and Holocene deposits. Similarly, the Pritchett site occurs near the boundary between Late Pleistocene and Holocene deposits but east of the Mississippi River in western TN. Several of the sites are located in close proximity to structural elements that are known, or are related to known, or suspected seismic sources. The Garner site is located very close to the western Reelfoot Rift margin, the Stiles site is located above the southwestern branch of the NMSZ thought to be related to the Blytheville Arch, and the Pritchett site is located between the Cottonwood Grove fault and the eastern Reelfoot Rift margin. The latter is situated above a postulated fault zone that may have been the source of the December 16, 1811 “dawn” aftershock (Figure 4-19).

Light-colored patches suggestive of sand blows are apparent on aerial photographs and/or satellite imagery of all the sites. On imagery of the Faulkner and Stiles sites, there appeared to be two generations of sand blows based on cross-cutting relationships and relative brightness. At the Stiles, Pritchett, and Wildy sites, there appear to be large linear sand blows. The presence of sand blows was confirmed during initial site visits by hand-digging soil pits in the targeted features. In addition, Native American artifacts of the Middle Woodland culture (A.D. 400-B.C.

200) or earlier were found on the ground surface at the Faulkner, Garner, and Wildy sites, suggesting that the near-surface sediment is at least 1600 years old. Geophysical surveys were conducted at all the sites to develop depth profiles of the sand blows and to locate the feeder dikes of the sand blows. Based on these findings, trench locations were defined. Archeological assessments were conducted at all sites.

The results of initial site visits, geophysical surveys, and archeological assessments were used to develop an excavation plan of the sand blows. For the Garner, Stiles, and Pritchett sites, reports summarizing the results and the excavation plans were submitted to the US NRC for review and for submission to the Arkansas and Tennessee State Historic Preservation Offices (SHPOs). Since no objections were raised about our plans by the SHPOs, we proceeded with the excavations when weather permitted and with permission from property owners and farmers. Unfortunately, the sediment exposed in the trenches at all of the sites was Late Holocene in age. Although Late Pleistocene deposits had been mapped at the sites, it seems that periodic flooding of rivers led to deposition of overbank sediment, burying the older deposits. Even during this project, flooding of the Mississippi River and its tributaries led to flooding of some of the study sites.

Although it was disappointing that surface sediment at the study sites is Late Holocene in age, we still gathered liquefaction data that help to fill geographical and temporal gaps in information, which in turn improves estimates of timing, location, magnitude and recurrence of New Madrid paleoearthquakes and provides insight into earthquake activity along the CGL and ERM-S, and in the Marianna area.

Table 4-54 Earthquake-Induced Liquefaction Features at Study Sites

Site Name	Deformation Structure	Confidence	Age Constraint year B.P.	Exposed Sediment	Likely Events ¹
St. Francis Basin					
Faulkner	Sand blows Sand dikes	High High	2 generations; close maximums of 270 and 500	Late Holocene	AD 1811-1812 & 1450
Wildy	Sand blow Sand dikes	High High	Close maximum of 630	Late Holocene	AD 1450
Garner	Sand blows Sand dikes	High High	Close maximum Marksville culture (1750-2150); maximum 2360	Late Holocene	AD 0
Stiles	Sand blows Sand dikes	High High	2 generations; close maximums of 485 and 2960	Late Holocene	AD 1450 BC1050
Western TN					
Pritchett	Sand blows Sand dikes	High High	2 generations; close maximums of 290 and 495	Late Holocene	AD 1811-1812 & 1450

¹ New Madrid events= A.D. 1811-1812 (139-138 yr B.P.), A.D. 1450 (500 yr B.P.) ± 150 yr, A.D. 900 (1050 yr B.P.) ± 150 yr, A.D. 0 (1950 yr B.P.) ± 200 yr, B.C. 1050 (3000 yr B.P.) ± 250 yr, B.C. 2350 (4300 yr B.P.) ± 200 yr.

4.4.7.2.1 Faulkner Site

On Google Earth imagery of the Faulkner site, light-colored patches interpreted as sand blows occur along the flanks of an abandoned channel deposit. Based on their crosscutting relationships and differences in brightness of surface soils, the sand blows likely formed during two different events separated in time. During the initial site visit, potsherds of the Woodland cultural period were found on the surface of the site, suggesting that the near-surface sediments pre-dated A.D. 1000. Trenches were excavated across the sand blows, revealing two generations of liquefaction features. Based on radiocarbon dating and weathering characteristics, the older generation of liquefaction features probably formed during the A.D. 1450 New Madrid event, whereas the younger features formed during the A.D. 1811-1812 event (Figure 4-162).

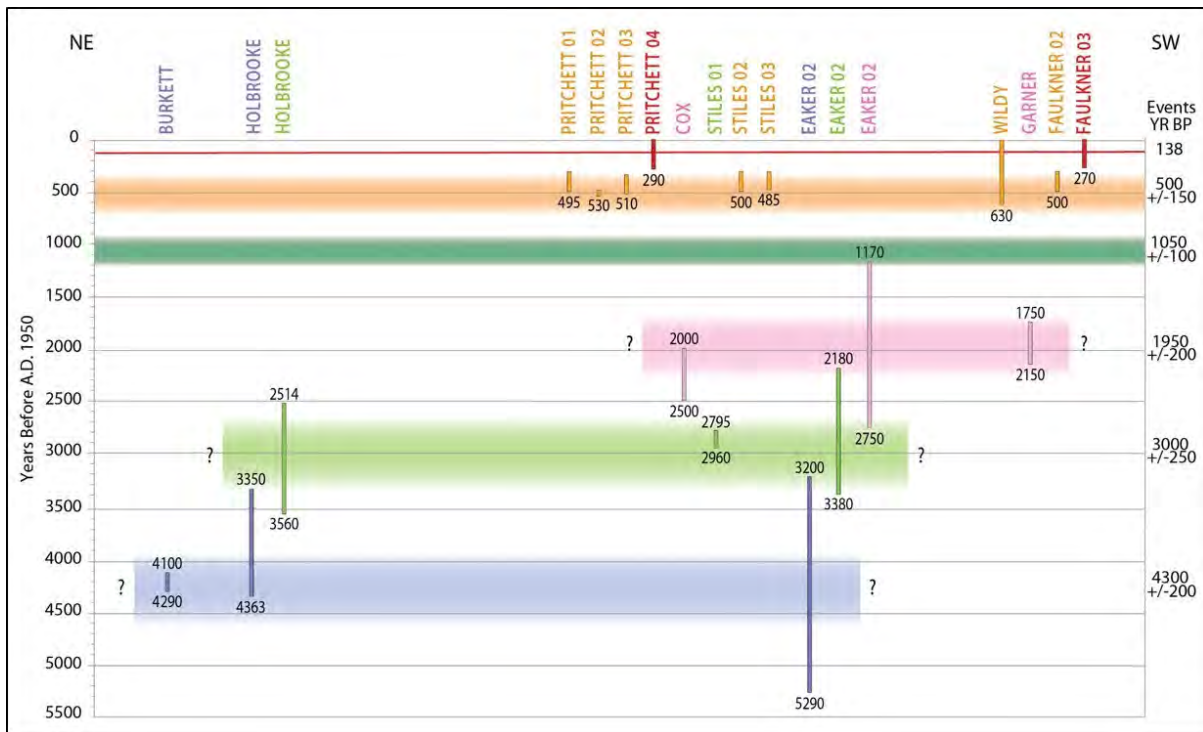


Figure 4-162 New Madrid earthquake chronology for past 5,500 years (from NUREG-2115), with events from Cox et al. (2006), Holbrooke et al. (2006), and results of site investigations from this project. New study sites listed at top across region from northeast to southwest. Vertical bars represent age estimates of individual sand blows, and horizontal bars represent event times of 138 yr BP (A.D. 1811-1812); 500 yr BP (A.D. 1450 ± 150 yr); 1,050 BP (A.D. 900 ± 150 yr); 1950 yr B.P. (A.D. 0 ± 200 yr); 3000 yr B.P. (B.C. 1050 ± 250 yr); and 4,300 yr BP (2350 B.C. ± 200 yr).

The older generation of sand blows was somewhat weathered, relatively small, and composed of two depositional units that ranged from 15-30 cm thick (Figure 4-162). One of these sand blows had accumulated within a depression, probably a partially filled tributary to the larger channel, and therefore had thicker depositional units. The feeder dikes of the older sand blows were also somewhat weathered and relatively small (0.25-7.00 cm wide), except where they intruded a large (95 cm wide) void formed by a decayed tree root system. The younger sand blow was relatively unweathered, composed of three depositional units that ranged from 12-42 cm thick, and covered a larger area than the older sand blows. Its feeder dikes were unweathered and ranged from 1-8

cm wide. Some of the dikes had intruded through tree root casts and along the contact between the soil and an *in situ* tap root. Also, a younger, unweathered dike had intruded along the margin of a weathered dike, forming a 14-cm-wide compound dike.

The size and the number of depositional units of the two generations of sand blows are consistent with other sand blows in the area that formed during the A.D. 1811-1812 and A.D. 1450 events. The number of depositional units suggest that three earthquakes were strong enough to induced liquefaction at the site during the A.D. 1811-1812, compared to two earthquakes during the A.D. 1450 event (Figure 4-163). These findings support the previous interpretation that the NMSZ produced a sequence of large earthquakes in A.D. 1450 as well as the historical sequence in A.D. 1811-1812.

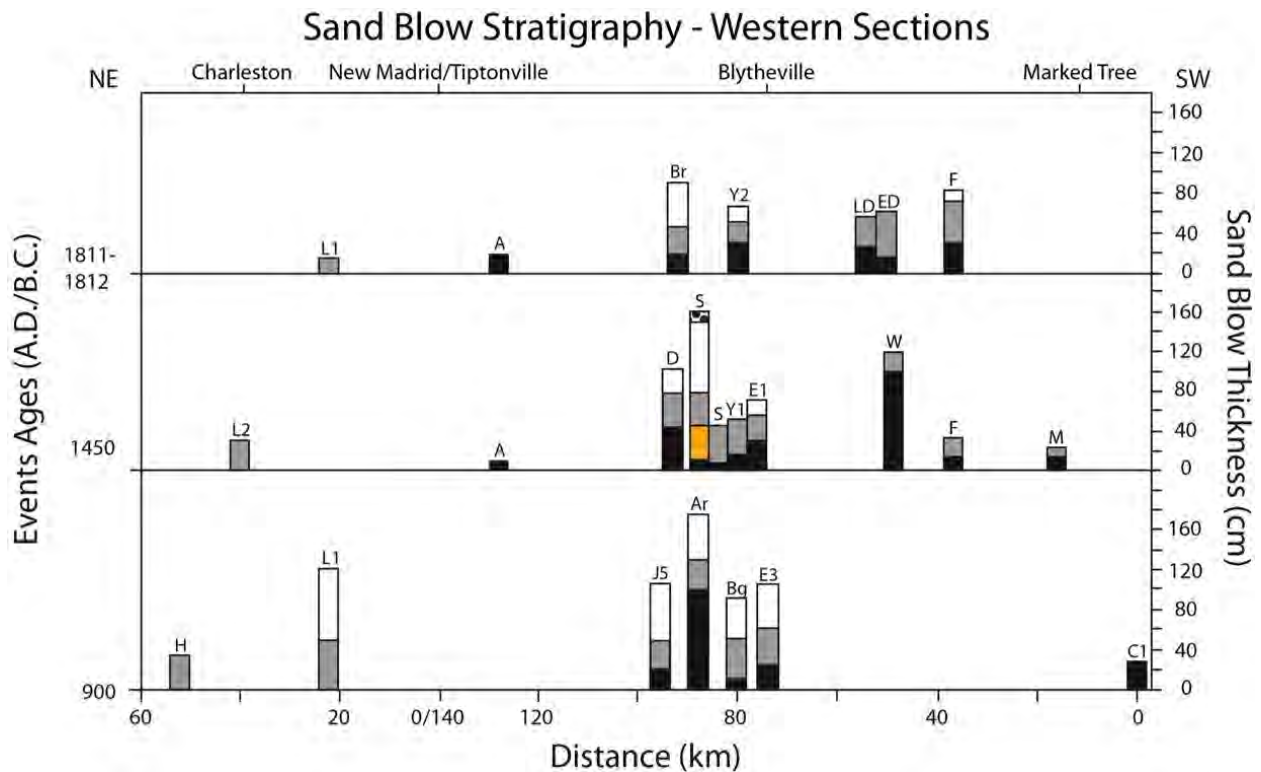


Figure 4-163 Sand blow stratigraphy showing number and thickness of depositional units at previous sites (Tuttle et al., 2002) and new study sites, Faulkner, Stiles, and Wildy, for two offset sections along the southern and northern seismicity trends from southwest of Marked Tree, AR, to northeast Tiptonville, TN and from New Madrid, MO, to northeast of Charleston, MO. Vertical bars represent depositional units of individual sand blows, and horizontal lines represent New Madrid events, circa A.D. 1811-1812, A.D. 1450, and A.D. 900. The colored depositional unit might have formed during an earthquake in western TN. Site designations: L=Li, A=Amanda, Ar=Archway, Bg=Bugg, Br=Brooke, C=Central Ditch, D=Dodd, E=Eaker, ED=Eightmile Ditch, F=Faulkner, H=Hillhouse, J=Johnson, LD=Locust Creek Ditch, M=Marked Tree, S=Stiles, Y=Yarbro, W=Wildy. Earlier events are not shown since they are represented by few sand blows.

4.4.7.2.2 *Wildy Site*

During reconnaissance, a sand blow and related sand dikes were found in a recently cleaned drainage ditch. On Google Earth imagery of the adjacent field, there was a large, linear light-colored patch that likely represented a sand blow. Potsherds of the Woodland cultural period were found in the cleaned ditch and on the surface of the field, suggesting that the near-surface sediments pre-dated A.D. 1000. Electrical resistivity profiles suggested that the linear sand blow in the field was quite thick and underlain by a wide feeder dike. A trench was excavated across the sand blow and revealed a large sand blow composed of two depositional units. Radiocarbon dating and weathering characteristics of the sand blow suggest that it formed during the A.D. 1450 event, though the A.D. 1811-1812 event cannot be ruled out (Figure 4-162).

The sand blow exposed in the trench was up to 120 cm thick, with the lower unit being 100 cm thick and the upper unit being 20 cm thick. The site had suffered asymmetrical ground failure with the ground surface being displaced downward by about 90 cm across a large (146-300 cm wide) dike, probably due to expulsion of sand from below. The lower unit of the sand blow filled the topographic low created by the ground failure. The upper unit of the sand blow was somewhat weathered, suggesting that it may be prehistoric in age. Combined with dating of the buried soil, the weathering characteristics of its upper unit suggest that the sand blow formed during the penultimate event (i.e., the A.D. 1450 New Madrid event).

The Wildy sand blow, composed of two depositional units, is interpreted to be a compound sand blow that formed during two earthquakes in a sequence. This is similar to other sand blows in the area that are thought to have formed during the A.D. 1450, like the older sand blows at the Faulkner site. The sand blow at the Wildy site is much larger than the sand blows at the Faulkner site but this may be due partly to the style of ground failure at the Wildy site. The findings at this site further support the interpretation that the A.D. 1450 event was a sequence of earthquakes and included two earthquakes that induced liquefaction in this area (Figure 4-163).

4.4.7.2.3 *Garner Site*

The Garner site was found during reconnaissance for potentially pre-A.D. 900 sand blows on the level 3 terrace of Late Pleistocene deposits. On a time series of Google Earth satellite imagery, a cluster of light-colored patches that likely represent sand blows was identified in a field north of Lighthouse Ditch. In the ditch, several sand dikes were exposed in the cutbanks, adding confidence that the light-colored patches in the adjacent field were sand blows. This was confirmed in hand-dug soil pits during the initial site visit. In addition, Late Archaic-Early Woodland (B.C. 3000-B.C. 200) artifacts were found in association with the sand blows, suggesting that they might be more than 2000 years old.

An archeological assessment determined that the site may have been periodically occupied from as early as 10 ka to about 2 ka and that cultural remains may be present in the soil buried by the sand blows. Electrical resistivity profiles imaged multiple sand blows and feeder dikes that appeared to have northeast-southwest trends. Two trenches were excavated to expose two of the sand blows and their dikes in areas of higher concentrations of cultural materials, primarily debitage and fire-cracked rock. Both sand blows were composed of only one depositional unit, very weathered, exhibiting zones of depletion and accumulation of iron and manganese, and probably formed during the same earthquake. Based on radiocarbon dating of organic material and analysis of artifacts recovered from the buried soil, the sand blows are thought to have formed between 200 B.C.-A.D. 200.

The Garner site sand blows may have formed during a New Madrid earthquake circa A.D. 0 ± 200 yr. Several other sand blows whose ages are poorly constrained also could have formed about this time. The most notable is a buried sand blow at the Eaker 2 site near Blytheville, AR, about 50 km east of the Garner site. Similar to the Garner sand blows, the Eaker 2 sand blow is 20 cm thick, composed of only one depositional unit, and formed between B.C. 800 and A.D. 780 (2750-1170 yr B.P.) (Figure 4-162). If there were a New Madrid earthquake at this time that induced liquefaction across the region, this finding would have implications for and reduce the uncertainty of recurrence times of large New Madrid events. Alternatively, the Garner and Eaker 2 sand blows might have formed as a result of a large paleoearthquake proposed for the eastern Reelfoot margin fault between 2000-2500 yr B.P. (Cox et al., 2006). This event was interpreted from fault displacements near Meeman-Shelby Forest and Porter Gap both along Chickasaw Bluffs between Memphis and Dyersburg, TN.

4.4.7.2.4 *Stiles Site*

The Stiles site is located near the epicenter of the December 16th, 1811 mainshock and is underlain by the southwestern branch of the NMSZ as well as the Blytheville Arch, a possible source of the historical and modern seismicity (Figure 4-55). The northern portion of the site is likely underlain by Late Pleistocene valley-train deposits (level 1) and the southern side of the site by Holocene meander-belt deposits of the Pemiscot Bayou, a distributary channel of the Mississippi River (Figure 4-56; Saucier, 1994). As seen during helicopter reconnaissance of the Pemiscot Bayou and on Google Earth satellite imagery, and confirmed during the initial site visit, sand blows cross the site at two orientations, sometimes intersecting one another. Two east-west-oriented sand blows on the southern side of the site may have formed along an ancestral channel of the Pemiscot Bayou. A large northwest-southeast oriented sand blow on the northern side of the site is subparallel to the drainage pattern of Late Pleistocene valley-train deposits.

An archaeological assessment of the site found no archaeological materials. Electrical resistivity imaged east-west and northwest-southeast-oriented sand blows and located their feeder dikes. On the basis of the electrical resistivity profiles, three trenches were excavated across three sand blows and related dikes, including one of the east-west-oriented sand blows and the large northwest-southeast-oriented sand blow. The third sand blow trenched was located close to the large northwest-southeast oriented sand blow but was roughly circular in plan view. The east-west oriented sand blow was composed of three major depositional units, suggesting that it formed during three earthquakes in a sequence. The upper part of the sand blow was weathered and exhibited soil lamellae, indicating that it was prehistoric in age. Based on radiocarbon dating of organic material from the buried soil beneath the compound sand blow, it is thought to have formed soon after B.C. 1010 (or 2960 yr B.P.). The northwest-southeast-oriented sand blow was also a compound sand blow, but composed of five major depositional units, suggesting that it formed during five earthquakes in a sequence. This sand blow was not weathered to the same degree as the east-west sand blow, but did exhibit iron-staining and fines accumulation, suggesting that it formed prior to A.D. 1811. Radiocarbon dating of organic material from the buried soil below the compound sand blow indicated that it formed close to or soon after A.D. 1445. The third sand blow was composed of two depositional units that likely formed during two closely timed earthquakes. Weathering characteristics and radiocarbon dating indicate the sand blow formed during the same event as the large northwest-southeast-oriented sand blow.

A New Madrid-type event about B.C. 1050 ± 250 yr was proposed by Holbrooke et al. (2006) based on the abrupt change in the channel morphology of the Mississippi River upstream of the Reelfoot fault (Figure 4-162). Given that it formed soon after B.C. 1010 (or 2960 yr B.P.), the east-west oriented sand blow at the Stiles site may have formed during this event. In addition, a

sand blow previously documented at the Eaker 2 site, about 4 km south of the Stiles site, formed between B.C. 1430-230 (or 3380-2180 yr B.P.) (Tuttle, 1999). Though not required, it seems likely that this sand blow also formed during the B.C. 1050 ± 250 yr.

The large, northwest-oriented sand blow with 5 depositional units at the Stiles site (Figure 4-163) suggests that there may be something unusual about the subsurface geology below the site. In comparison, the nearby circular sand blow that formed during the same event is composed of only two depositional units. In addition, other sand blows in the area that formed during the A.D. 1450 event, including those at Eaker 1 and Yarbro 1, are composed of 2 or 3 depositional units (Tuttle, 1999). It should be noted that large linear sand blows can be the surface expression of an underlying fault zone (Tuttle et al., 2006; Odum et al., 2016); however, there are no other indications that there is a northwest-oriented fault at this site. More likely, there is something about the sediment architecture that is influencing liquefaction and ground failure at the site. A deeper subsurface investigation would be required to understand the factors that influenced formation of this large sand blow.

Numerous compound sand blows in the New Madrid region are thought to have formed during a sequence of earthquakes about A.D. 1450 ± 150 yr. Dating of the large northwest-southeast oriented sand blow and the nearby circular sand blow indicate that they formed during this event. However, the close maximum dates based on organic material in the buried soils below the sand blows suggest that they formed close to or soon after A.D. 1450. Therefore, the maximum age, rather than the mean age for the event, is likely A.D. 1450 (500 yr B.P.).

4.4.7.2.5 *Pritchett Site*

The Pritchett site is located between the Cottonwood-Ridgely fault system and the ERM-S and along the proposed Obion River fault zone (Figure 4-24). The **M** 7.0 December 16, 1811, “dawn” aftershock may have occurred near Calvary, TN (Hough and Martin, 2002) which is located along the proposed fault zone. The proposed Obion River fault zone may have been the source of this large aftershock. The Pritchett site is south across the Obion River from OR216/603, where a buried soil was displaced downward to the east by about 1 m across a very large sand dike that formed during the A.D. 1450 New Madrid event. On satellite imagery, large linear patches likely to be sand blows are clearly visible crossing the Pritchett site. Northeast-oriented sand blows crossed the western part of the site along the trend of the very large dike at OR216/603. Other large linear patches with a north-northwest orientation crossed the eastern part of the site.

During the initial site visit, the presence of large linear sand blows was confirmed in soil pits. Geophysical surveys imaged several large sand blows and their feeder dikes and an archaeological assessment found no cultural material in the footprint of the proposed trenches. Four sand blows were excavated, three with northeast trends and one with a north-northwest trend. Two of the northeast trending sand blows were composed of five depositional units, exhibited iron staining and fines accumulation, and based on radiocarbon dating of organic material collected below the sand blow, formed soon after A.D. 1420-1455. The third northeast-oriented sand blow was composed of only two depositional units, exhibited iron staining and fines accumulation, and formed soon after A.D. 1440. The three sand blows likely formed during the A.D. 1450 event. Like the sand blows at the Stiles site that formed during the A.D. 1450 event, the close maximum constraining ages for these three Pritchett sand blows suggest that they formed close to or soon after A.D. 1450. The sand blow with the north-northwest trend on the eastern side of the site was composed of four depositional units, was less weathered than the other three sand blows, and based on radiocarbon dating, formed after A.D. 1660. Therefore, this sand blow probably formed during four earthquakes in the A.D. 1811-1812 sequence.

At the Pritchett site, the two large northeast-oriented sand blows with five depositional units likely formed during five earthquakes in a sequence in the A.D. 1450 event. With the exception of the large northwest-oriented sand blow at the Stiles site, other sand blows of this age in western TN and across the Mississippi River in AR and MO are composed of one to three depositional units (Figure 4-163 and Figure 4-164). The large north-northeast-oriented sand blow that formed during the A.D. 1811-1812 event is composed of four depositional units. Other sand blows that formed during the 1811-1812 event in western TN, including OR213, OR600, and Forked Deer 14, are composed of four to five depositional units. Other sand blows of this age in western TN and AR are composed of two to three depositional units. Therefore, the stratigraphy of the Pritchett sand blows suggests that there was one additional earthquake in the vicinity of the Pritchett site during the A.D. 1811-1812 sequence and two additional earthquakes during the A.D. 1450 sequence. This supports the interpretation that there is a seismic source very close to, possibly beneath, the site.

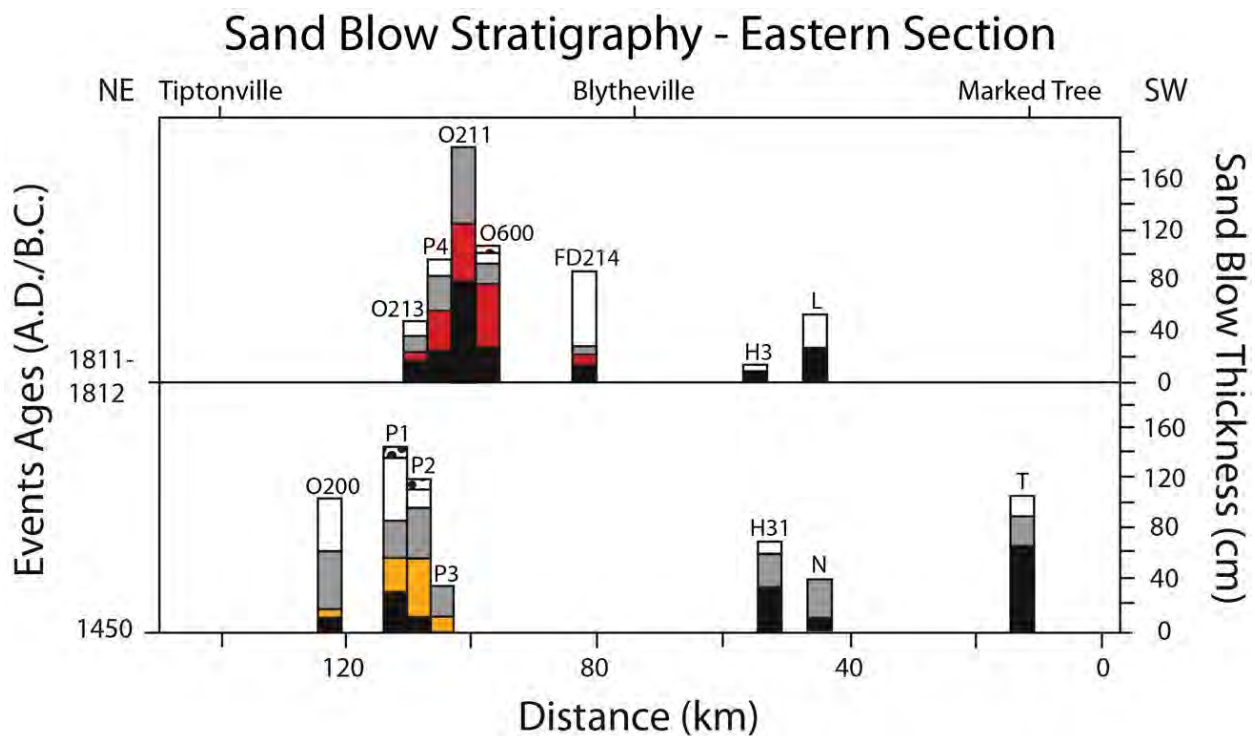


Figure 4-164 Sand blow stratigraphy showing number and thickness of depositional units at previous sites (Tuttle et al., 2002) and the Pritchett site, for a section parallel to and ~12 km east of the southern branch of the seismicity trend. Vertical bars represent depositional units of individual sand blows, and horizontal bars represent New Madrid events circa A.D. 1811-1812 and A.D. 1450. The colored depositional units might have formed during earthquakes centered in western TN. Site designations: FD=Forked Deer, L=Lowrance, H=Hatchie River, N=Nodena, O=Obion River, P=Pritchett, T=Tyrnza. To date, none of the sand blows along this section can be unequivocally attributed to the A.D. 900 event. Earlier events are not shown since they are represented by few sand blows.

If the subparallel, large linear sand blows at the site do indeed reflect faulting at depth, they suggest that the fault zone may be about 900 m wide and may have been active during both the A.D. 1450 and A.D. 1811-1812 events. Given the slightly different trends of the two sets of linear

sand blows, perhaps different segments within the fault zone ruptured during the A.D. 1450 and A.D. 1811-1812 events. If there is a fault zone beneath the site and if it ruptured in both the A.D. 1450 and A.D. 1811-1812 events, the fault zone would be a source of repeated large magnitude earthquakes. Although these observations are compelling and suggest the possible presence of an active fault zone below the Pritchett site, this interpretation requires further validation by coring and/or seismic reflection profiling of deeper geologic units at the site. In addition, investigations of other sites of large linear sand blows and other types of northeast-southwest lineaments would help to test the presence of the proposed fault zone as well as to improve our understanding of the earthquake potential of the area.

4.4.7.3 *Evaluation of Scenario Earthquakes*

A combination of New Madrid scenario events including the **M** 7.6 December 16, 1811, **M** 7.5 January 23, 1812, and **M** 7.8 February 7, 1812 events predicts liquefaction at geotechnical sites close to distal locations of observed liquefaction features. This includes the distal locations of features along the St. Francis River in southeastern MO, the Current, and possibly the Black and White Rivers in Arkansas, and the Obion, Hatchie, and the Wolf River in western Tennessee (Figure 4-19). This finding supports the interpretation that liquefaction features in those areas with age estimates similar to known New Madrid earthquakes likely formed during those events. However, it should be noted that ages are poorly constrained for all features along the Wolf River. The sole sand blow found along the river was attributed to the A.D. 1811-1812 New Madrid event based on glass and bricks in soil overlying the sand blow (Broughton et al., 2001; Van Arsdale, pers. comm., 2012).

Analysis of the New Madrid scenario events does not predict liquefaction at the Coldwater River site in northwestern MS, suggesting that a different earthquake source is responsible for observed liquefaction features along the river. Other sources of paleoearthquakes during the Middle-Late Holocene include the ERM and the Marianna area. The ERM-S is thought to have produced a large earthquake about 2000-2500 yr B.P. (Cox et al., 2006). Liquefaction potential analysis suggests that such an event, if it were of **M** 7.1, could account for Late Holocene liquefaction features on the Coldwater River. Such an event would likely produce liquefaction along the Wolf River as well and could account for some of the liquefaction features along the Wolf River.

The Marianna area produced three large earthquakes between 4650 and 6950 yr B.P. (B.C. 2700 and 5000) (Tuttle et al., 2006; Al-Shukri et al., 2009). The Marianna events are thought to be **M** \geq 6 based on liquefaction analysis performed for a local source and with geotechnical data collected in close proximity to the liquefaction sites (Al-Shukri et al., 2015). The analysis performed for this NRC study suggests that the Marianna events, if they were of **M** \geq 6.9, could have produced the Early-Middle Holocene liquefaction features along the Coldwater River. Alternatively, a **M** 7.1 on the ERM-SRP west of Memphis or a **M** 6.9 at the southern end of the ERM-SRP near Tunica could account for liquefaction on both the Coldwater and Wolf Rivers. Large uncertainties in the age estimates of liquefaction features along both rivers, limit our ability to attribute the features to any particular paleoearthquake with confidence. Therefore, additional reconnaissance for and radiocarbon dating of liquefaction features is recommended along both the Coldwater and Wolf Rivers. Well-constrained age estimates of the liquefaction features would improve correlation of features and interpretation of the location(s) and magnitude(s) of the paleoearthquake(s) responsible for their formation.

4.4.7.4 *Interpretation of Timing, Locations, Magnitudes, and Recurrence Times of Paleoearthquakes*

Fifteen years ago, following the study of liquefaction at more than 250 sites, it was recognized that New Madrid earthquake sequences similar to the historical A.D. 1811-1812 event had occurred in A.D. 1450 (500 yr B.P.) \pm 150 yr and A.D. 900 (1050 yr B.P.) \pm 100 yr. In addition, there was liquefaction evidence for at least two large earthquakes before A.D. 800, though their ages and magnitudes were poorly constrained (Tuttle et al., 2002). Several years later, a New Madrid earthquake sequence was recognized in B.C. 2350 (4300 yr B.P.) \pm 200 yr based primarily on detailed studies of liquefaction features at the Burkette archaeological site in southeastern MO and the Eaker 2 archeological site in northeastern AR (Tuttle et al., 2005). In a morphological study of the Mississippi River in the vicinity of the Reelfoot fault, channel-straightening events were found to coincide with these three New Madrid events, including the event in B.C. 2350 (4300 yr B.P.) (Holbrooke et al., 2006). In that same study, a fourth New Madrid earthquake was proposed about B.C. 1000 (3000 yr B.P.) \pm 500 yr. Since then, additional data have been accruing, mostly in the region surrounding the New Madrid seismic zone, to suggest that other structural elements of the Reelfoot Rift have produced large earthquakes during the Late Pleistocene and Holocene. These structures include the CGL and related fault zone in southeastern MO (Stephenson et al., 1999; Baldwin et al., 2006 and 2014), the ERM-N and ERM-S in western TN (e.g., Williams et al., 1995 and 2001; Cox et al., 2001 and 2006), the ERM-SRP along the Mississippi River (Hao et al., 2013), and the Marianna area at the southern end of the ERM (e.g., Al-Shukri et al., 2009 and 2015; Tuttle et al., 2006). By conducting both river surveys for and site investigations of liquefaction features in the New Madrid seismic zone and in the surrounding region, this project sought new information that would improve our understanding of the earthquake potential of New Madrid seismic zone as well as other possible earthquake sources related to the Reelfoot Rift, including the CGL, WRM, ERM, and the Marianna area.

4.4.7.4.1 *Timing of Paleoearthquakes*

Many earthquake-induced liquefaction features found during this study can be explained by the A.D. 1811-1812, A.D. 1450, and A.D. 900 earthquakes thought to be centered in the NMSZ. These features were found along rivers surveyed (Black, Current, St. Francis, Obion, White Rivers and Locust Creek Ditch) as well as those studied during site investigations (Faulkner, Pritchett, Stiles, Wildy). Regarding the timing of the previously known New Madrid events, dating of the soils buried by sand blows at the Faulkner, Stiles, and Pritchett sites suggest that the penultimate event occurred close to or soon after A.D. 1450. Therefore, perhaps A.D. 1450 (500 yr B.P.) likely represents the maximum age for the event rather than the mean age. Unfortunately, we have no new minimum constraining ages for this event. Combining new and previous age constraints, the event probably occurred between A.D. 1450 and A.D. 1600.

Some newly discovered liquefaction features probably did not form during the A.D. 1811-1812, A.D. 1450, and A.D. 900 New Madrid events. These include features at the Garner and Stiles sites in northeastern AR, as well as features along the Coldwater River in northwestern MS, and the White River near St. Charles, AR. Sand blows and related dikes at the Garner site suggest that there was a large earthquake in the New Madrid region circa A.D. 0 \pm 200 yr (1750-2150 yr B.P.). This finding is supported by several other sand blows in the region, including one at the Eaker 2 site near Blytheville, AR, whose age is less well constrained but could have formed about this time. A sand blow and related dikes at the Stiles site likely formed during the B.C. 1000 (2950 yr B.P.) event, first recognized by Holbrooke et al. (2006). Dating at the Stiles site suggests that

this event occurred in B.C. 1050 ± 250 yr (2750-3250 yr B.P.). Another sand blow at the Eaker 2 site, only a few kilometers south of the Stiles site, formed about this time, probably during the same event.

Outside the NMSZ, pseudonodules found along the White River near St. Charles, AR, may have formed during a Marianna event during the Late Pleistocene. Marianna events during the Middle Holocene may have been responsible for the formation of liquefaction features along the Coldwater River in northwest MS, since 8340 yr B.P. Some of the features probably formed during the Marianna events of B.C. 2850 (4800 yr B.P.) ± 150 yr, B.C. 3550 (5500 yr B.P.) ± 150 yr, or B.C. 4850 (6800 yr B.P.) ± 150 yr. Other Coldwater features are too young to have formed during a Marianna event, but could have formed during the proposed large earthquake on the ERM-S about 2000-2500 yr B.P. (Cox et al., 2006). As determined in the evaluation of scenario earthquakes, the New Madrid seismic zone is likely too far away to induce liquefaction along the Coldwater River.

4.4.7.4.2 *Locations and Magnitude of Paleoearthquakes*

On the basis of new data collected during this project, as well as data that have been gathered over the past fifteen years, the liquefaction fields for the A.D. 1811-1812 (138 yr B.P.), and A.D. 1450 (500 yr B.P.) New Madrid earthquake sequences have been updated (Figure 4-165). For the A.D. 1811-1812 sequence, adjustments were made to accommodate new information from the Faulkner and Locust Creek Ditch 3 sites and from the Hatchie River. New data from the Pritchett site support the interpretation of a fourth liquefaction field between Dyersburg, TN and Blytheville, AR. For the A.D. 1450 event, adjustments were made to accommodate new information from the Faulkner site and from the Hatchie River. In addition, small fourth and fifth liquefaction fields were added between Dyersburg and Blytheville to account for sand blows composed of four or five depositional units at the Pritchett site and along the Obion River. Two sites (Tyronza and Hatchie River 31) between Marked Tree, AR, and Covington, TN, are composed of three depositional units. These two sites raise the possibility of another earthquake to the southeast of the NMSZ, perhaps on the ERM-S, during the A.D. 1450 sequence; however, further work would be needed to substantiate this interpretation.

New information about compound sand blows with four or five depositional units at the Pritchett site and along the Obion River suggest that smaller earthquakes, but large enough to induce liquefaction locally, occurred between Dyersburg and Blytheville. Based on this study, one such event occurred in A.D. 1811-1812 and two such events occurred in A.D. 1450 in this area. The event in A.D. 1811-1812 may have been the December 16, 1811, “dawn” aftershock thought to have been centered near Calvary, TN. Long, linear sand blows at the Pritchett site and other lineaments seen on satellite imagery occur along a northeast-trending zone that extends from Midway, TN through Calvary to Chickasaw Bluffs. This zone may be the surface expression of a fault at depth and the source of the **M** 7.0 December 16, 1811 “dawn” aftershock. If so, it might also be the source of one or both of the events that occurred between Dyersburg and Blytheville during the A.D. 1450 sequence.

Although the distribution and stratigraphy of sand blows varies for each event, in general, they are quite similar and support the prior interpretation that the New Madrid seismic zone was the source of three very large earthquakes in A.D. 1811-1812, A.D. 1450, and A.D. 900 that caused the formation of liquefaction features across the New Madrid region (Tuttle et al., 2002). In our evaluation of scenario earthquakes, a combination of the **M** 7.6 December 16, 1811, **M** 7.5 January 23, 1812, and **M** 7.8 January 23, 1812 earthquakes predicts liquefaction at geotechnical sites close to distal sites of observed liquefaction. Although their associated uncertainties are

large (0.25-0.5), these magnitudes are in agreement with other estimates of the three mainshocks of the A.D. 1811-1812 sequence based on modeling of felt reports (Bakun and Hooper, 2002). Given the similarity in distribution and stratigraphy of sand blows that formed in A.D. 1450 and A.D. 900 with those that formed in A.D. 1811-1812, the earthquakes responsible for the A.D. 1450 and A.D. 900 features were likely similar in magnitude to the A.D. 1811-1812 earthquakes. Fewer sand blows have been documented for the A.D. 900 event, especially southwest of Blytheville, AR, along the southern branch of seismicity. For this reason, the liquefaction field in this area is smaller and therefore so is the magnitude of the causative earthquake.

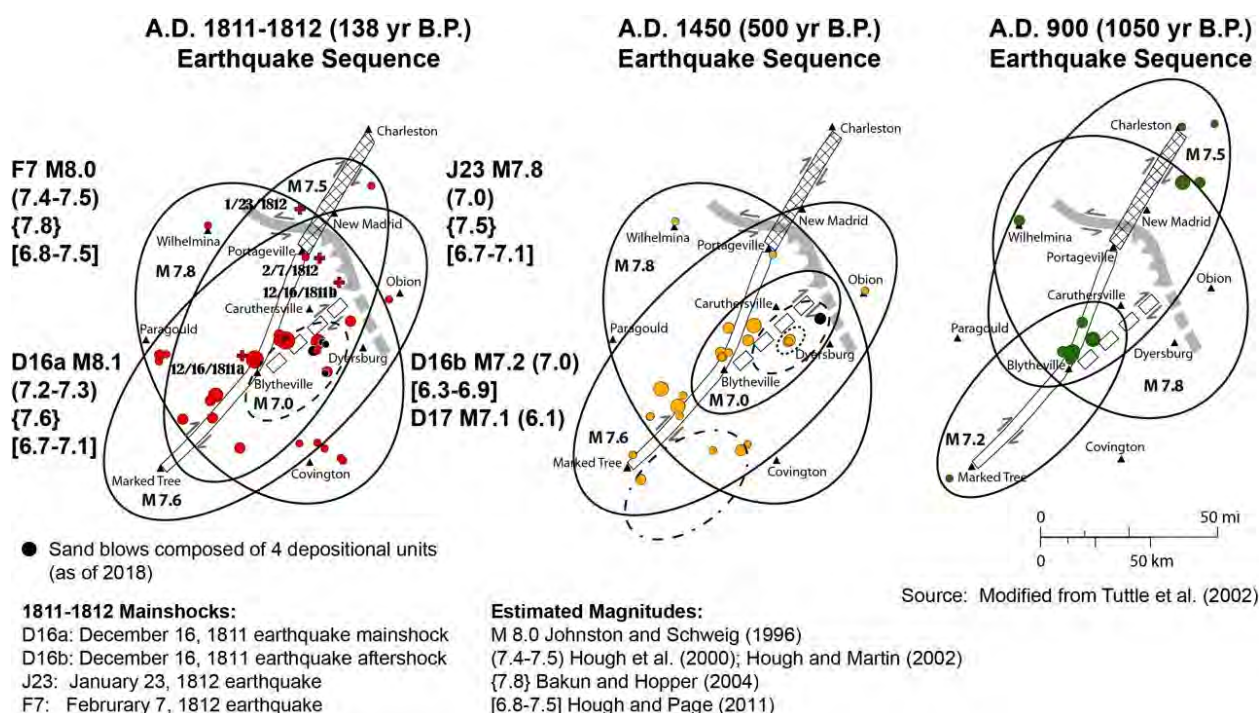


Figure 4-165 Liquefaction fields for the past three New Madrid events as interpreted from spatial distribution and stratigraphy of sand blows (modified from Tuttle et al., 2002). The colored circles represent sand blows that formed during the A.D. 1811-1812 (red), A.D. 1450 (orange), and A.D. 900 (green) events and that are shown on Figure 4-19. Black circles indicate sand blows composed of 4 depositional units. Sand blows are shown relative to the preferred fault rupture scenario for the A.D. 1811-1812 earthquake sequence (from Johnston and Schweig, 1996). Earthquake magnitudes shown within 1811-1812 ellipses are those from Bakun and Hopper (2004).

The NMSZ is the likely source of the B.C. 1050 ± 250 yr (2750-3250 yr B.P.) event that produced a compound sand blow at the Stiles site. This earthquake was first recognized by Holbrooke et al. (2006) as a channel straightening event caused by displacement on the Reelfoot fault. To produce sand blows at the Stiles and nearby Eaker 2 site 65 km away, the earthquake produced by the Reelfoot fault would have been of $M \geq 6.4$ (Castilla and Audemard, 2007). Given that the Stiles sand blow is composed of three depositional units and similar in size to historical sand blows in the area, it is likely that the B.C. 1050 event was a sequence of three large earthquakes much like the sequence of earthquakes in A.D. 1811-1812. Discovery of additional sand blows that formed during this event would help to correlate features across the region, to further define the liquefaction field, and to improve the magnitude estimate for this event.

The NMSZ is also considered the likely source of the proposed A.D. 0 ± 200 yr (1750-2150 yr B.P.) earthquake, given that the sand blows of this age, such as those found at the Garner and Eaker 2 sites, are located in the St. Francis Basin. The location of this event is poorly constrained at this time. If the Reelfoot fault were the source, the earthquake would have been of $M \geq 6.8$ to produce sand blows at the Garner site 100 km away (Castilla and Audemard, 2007). An alternative source is the ERM-S, which is thought to have produced a large earthquake between 2000-2500 yr B.P. However, this event may be a little too early to account for the sand blows at the Garner and Eaker 2 sites. If the ERM-S were the source, however, the earthquake would have been of $M \geq 6.5$ to produce sand blows at the Garner site 72 km away. Additional information about sand blows that formed circa 1.9 ka would add confidence in the interpretation of its source and magnitude.

Outside the NMSZ, the ERM-S is thought to have produced a large earthquake about 2000-2500 yr B.P. (Cox et al., 2006). According to our evaluation of scenario earthquakes, if it were of $M \geq 7.1$ and located northwest of Memphis, this event could have been responsible for the formation of Late Holocene liquefaction features along the Wolf River in southwestern TN, and the Coldwater River in northwestern MS. The Marianna area is known to be the source of repeated large magnitude earthquakes in B.C. 2850 (4800 yr B.P.) ± 150 yr, B.C. 3550 (5500 yr B.P.) ± 150 yr, and B.C. 4850 (6800 yr B.P.) ± 150 yr. If these events were of $M \geq 6.9$, they could have produced the Early-Middle Holocene liquefaction features along the Coldwater River. Although these known sources and events are likely responsible for the Coldwater liquefaction features, other sources, such as the ERM-SRP, are also possible. Additional reconnaissance for and dating of liquefaction features are needed in this area to better constrain the timing, location, and magnitude of the earthquakes responsible for the two to three generations of liquefaction features on the Coldwater River.

4.4.7.4.3 *Recurrence Times of Paleoearthquakes*

Previously, the recurrence time for New Madrid events was estimated to be about 500 years based on the liquefaction record of three New Madrid events, the A.D. 1811-1812, A.D. 1450 and A.D. 900 events in the past 1200 years (Figure 4-166; Cramer, 2001; Tuttle et al., 2002). Although paleoliquefaction features suggested earlier events, the ages of those features were poorly constrained. Recognition of the B.C. 2350 event at two paleoliquefaction sites, Burkette and Eaker 2, separated by 120 km across the New Madrid region (Tuttle et al., 2005), provided evidence for pre-A.D. 900 New Madrid events in the geologic record. The B.C. 2350 event was also recognized as a channel straightening event of the Mississippi River, as was the A.D. 900 event and an intervening event about B.C. 1000 (Holbrooke et al., 2006). Found during this study, the compound sand blow at the Stiles site that formed circa B.C. 1010, as well as a previously discovered sand blow at the Eaker 2 site, both about 65 km southwest of the Reelfoot fault, support the interpretation that there was a New Madrid event about B.C. 1000. In addition, the sand blows at the Garner site, also discovered during this study, suggest that there was a large earthquake about A.D. 0, which is also supported by another sand blow at the Eaker 2 site. These findings suggest that there may have been a New Madrid event between A.D. 900 and B.C. 1000, though additional data are needed to better define its timing, location, and magnitude. If the A.D. 0 earthquake were a New Madrid event, the average recurrence for the past five earthquake cycles is about 800 years (Figure 4-166). However, the New Madrid events are apparently much less closely spaced in time between 4400 and 1200 yr B.P. than they are for the past 1200 yr. The average recurrence time for the previous three earthquake cycles is about 1100 years compared to 500 years for the past two earthquake cycles (Figure 4-166). Given that sand blows are still being found that formed at times other than known New Madrid events, it is

quite likely that the paleoearthquake chronology is still incomplete prior to A.D. 900 and that additional events could be recognized by applying insights gained during this study. Currently, the recurrence times range from 200 to 800 years for the last two events and from 600 to 1750 years for the prior three events. This is due largely to uncertainties in the timing of the events. By narrowing the age estimates of sand blows, and thus, the estimated timing of earlier events, it would be possible to reduce the large uncertainty ranges in recurrence times.

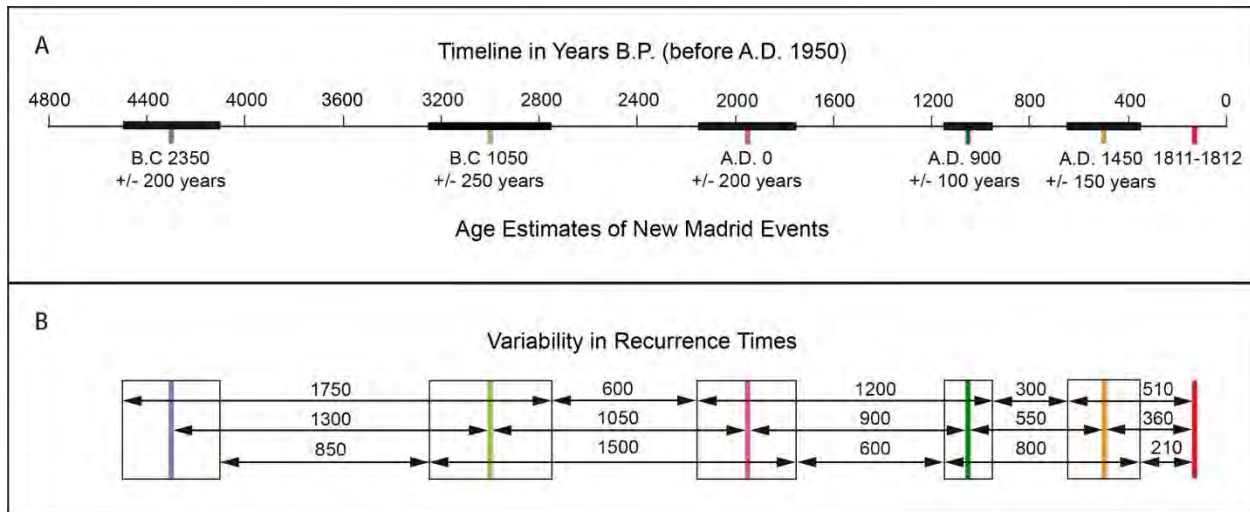


Figure 4-166 (A) Timeline showing timing of New Madrid events during the past 4,800 years. (B) Uncertainties in timing of New Madrid events leads to variability in estimates of their recurrence times. Average recurrence time for past three earthquake cycles is ~500 years and ~1100 years for the previous two earthquake cycles (modified from Tuttle et al., 2002).

The liquefaction features discovered along the Coldwater River have the potential to advance our understanding of the earthquake potential of the ERM-S fault and the Marianna area. However, more information is needed about liquefaction features in the area to better constrain the timing and location of their causative events and to estimate their recurrence times.

4.4.8 Conclusion

During this regional paleoliquefaction study, many liquefaction features were found along the St. Francis River in northeastern AR and southeastern MO that are interpreted to have formed during the New Madrid events of A.D. 1811-1812, A.D. 1450, and A.D. 900 (Figure 4-19; Table 4-53). Along Locust Creek Ditch, also in northeastern AR, and along the Obion River in western TN, liquefaction features were found that likely formed during the A.D. 1811-1812 and A.D. 1450 New Madrid events. No liquefaction features were found in the Western Lowlands in the vicinity of the CGL that predate the A.D. 900 New Madrid event or in western TN, in the vicinity of the ERM that predate the A.D. 1450 New Madrid event. However, this may be due, in part, to the prevalence of Late Holocene deposits exposed in the river cutbanks examined.

Two to three generations of liquefaction features that formed since 8340 yr B.P. were found along the Coldwater River in northwestern MS (Table 4-53). These features probably were not related to New Madrid earthquakes, but instead, may have formed during the ERM-S event of B.C. 300 and the Marianna events of B.C. 2850 ± 150 yr, B.C. 3550 ± 150 yr, or B.C. 4850 ± 150 yr. Pseudonodules along the White River near Elgin may be related to Late Holocene New Madrid

events, whereas pseudonodules along the White River near St. Charles may have formed during Late Pleistocene Marianna events. Additional study along the Coldwater and White Rivers, and on their adjacent floodplains, would likely advance our understanding of the earthquake potential of the ERM-S fault and the Marianna area.

Detailed archaeological assessments and geophysical and paleoseismic investigations were conducted at five sites (Garner, Faulkner, Wildy, Stiles, and Pritchett) that span the southern branch of the NMSZ near Paragould, AR, in the west to about Dyersburg, TN, in the east (Figures 4-18 and 4-19; Table 4-54). At the Garner site, weathered sand blows buried a soil that contained artifacts. Based on the analysis of the artifacts as well as radiocarbon dating of organic material in the soil, the sand blows formed about A.D. 0 ± 200 yr (Figure 4-162). Other sand blows, including one at the Eaker 2 site near Blytheville, AR, formed about the same time. These sand blows in the St. Francis Basin suggest that a previously unrecognized New Madrid earthquake may have occurred about A.D. 0 ± 200 yr.

At the Faulkner site, two generations of sand blows formed during the A.D. 1811-1812 and A.D. 1450 New Madrid events; at the Wildy site, a sand blow and large feeder dike formed during the A.D. 1450 New Madrid event (Figure 4-162). The Faulkner and Wildy sites provide new information about the areal distribution and stratigraphy of sand blows for these two New Madrid events. The information from the Faulkner site, in particular, helps to better constrain the liquefaction fields for the two most recent events (Figure 4-165).

At the Stiles site, two sand blows formed during the A.D. 1450 New Madrid event, one of which was very large, northwest oriented, and composed of five depositional units. A third sand blow at the site was weathered, composed of three depositional units, and formed soon after B.C. 1010 (Figure 4-162 and Figure 4-163). A large New Madrid earthquake about B.C. 1050 ± 250 yr was proposed by Holbrooke et al. (2006) based on abrupt change in the channel morphology of the Mississippi River upstream from the Reelfoot fault. The compound sand blow at the Stiles site, about 65 km southwest of the Reelfoot fault, supports the interpretation that there was a New Madrid earthquake about B.C. 1050 ± 250 yr and suggests that it was one of several large earthquakes in a sequence.

At the Pritchett site, three northeast-oriented sand blows, two of which are very large and composed of five depositional units, formed during the A.D. 1450 New Madrid event (Figure 4-162 and Figure 4-164). These sand blows are along strike with a very large sand dike exposed in the cutbank of the nearby Obion River that also formed during the A.D. 1450 event, and across which, a buried soil was displaced vertically by ~ 1 m. A fourth sand blow at the Pritchett site is north-northeast oriented, composed of four depositional units, and formed during the A.D. 1811-1812. The sand blows at the site help to define, and occur along, a 32-km long, northeast-oriented zone of lineaments that might be the surface expression of an active fault zone (Figure 4-134). The greater number of depositional units composing the Pritchett and nearby Obion River sand blows, compared to sand blows outside the area, suggest that the proposed fault zone might have been the source of a large earthquake in A.D. 1811-1812, possibly the **M** 7.0 December 16, 2011 “dawn” aftershock, and two large earthquakes in A.D. 1450. If so, this proposed fault zone would be a source of repeating large earthquakes.

The distribution and stratigraphy of sand blows continue to support the prior interpretation that the New Madrid seismic zone was the source of three very large earthquakes in A.D. 1811-1812, A.D. 1450, and A.D. 900 (Figure 4-163, Figure 4-164, and Figure 4-165; Tuttle et al., 2002). Given the similarity in distribution and stratigraphy of sand blows that formed during the A.D. 1450 and A.D. 900 events with those that formed in A.D. 1811-1812, the A.D. 1450 and A.D. 900 earthquakes

were likely similar in magnitude to the A.D. 1811-1812 earthquakes. An evaluation of scenario earthquakes found that a combination of **M** 7.6 December 16, 1811, **M** 7.5 January 23, 1812, and **M** 7.8 January 23, 1812 scenario earthquakes best predicts liquefaction observed at distal sites. Therefore, the A.D. 1450 and A.D. 900 events likely included one or more earthquakes of **M** 7.5-7.8, although it should be recognized that the associated uncertainties in magnitude are large (± 0.25 - 0.5 of a magnitude unit).

The NMSZ, including the Reelfoot fault, is thought to be the source of the B.C. 1050 ± 250 yr (2750-3250 B.P.) event that produced a compound sand blow at the Stiles site. Given that the Stiles sand blow is composed of three depositional units, the B.C. 1050 event was likely a sequence including three large earthquakes, similar to the A.D. 1811-1812 sequence. One of the B.C. 1050 earthquakes would have been of **M** ≥ 6.4 to produce sand blows at the Stiles site 65 km away from its postulated source, the Reelfoot fault.

The NMSZ is also the likely source of the A.D. 0 event 0 ± 200 yr that produced sand blows at the Garner site and the Eaker 2 site in the St. Francis Basin. If the Reelfoot fault were the source, the earthquake would have been of **M** ≥ 6.8 to produce a sand blow at the Garner site, 100 km away. An alternative source is the ERM-S, thought to have produced a large earthquake about B.C. 300 ± 250 yr (Cox et al., 2006). If the ERM-S were the source, the earthquake would have been of **M** ≥ 6.5 to produce sand blows at the Garner site 72 km away. Additional information about sand blows that formed about 1.9 ka is needed to better constrain the timing, source, and magnitude of this event.

Previously, a recurrence time of about 500 yr for the past 1200 years was estimated for New Madrid events based on the earthquake chronology of the A.D. 1811-1812, A.D. 1450 and A.D. 900 events (Cramer, 2001; Tuttle et al., 2002). The chronology is extended farther back in time with the addition of the B.C. 2350 ± 200 yr, B.C. 1050 ± 250 yr, and A.D. 0 ± 200 yr events. For the previous three earthquake cycles, the average recurrence time is about 1100 years compared to 500 years for the past two earthquake cycles (Figure 4-166). Given that sand blows are still being found that formed prior to the three most recent New Madrid earthquake sequences, it is likely that the paleoearthquake chronology is incomplete prior to A.D. 900. Recognition of additional events would further refine estimates of recurrence times of New Madrid events.

Although progress has been made during this project, additional study in the NMSZ could help to constrain the timing of recognized events, to potentially recognize additional events, and possibly extend the chronology of paleoearthquakes farther back in time. More scrutiny is needed of the paleoearthquake records of the CGL, ERM, Marianna area, all of which are thought to have produced large earthquakes in the Late Pleistocene and Holocene. Developing paleoearthquake chronologies for the NMSZ, CGL, ERM, Marianna area, all related to the Reelfoot Rift, would help to better understand long-term behavior and interaction of structural elements of the Reelfoot Rift. This understanding is likely to be relevant to other aulacogens in the CEUS and elsewhere.

4.4.9 Recommendations for Additional Research in the Greater New Madrid Region

1. Re-excavate multiple stratified sand blows at the Eaker 2 site near Blytheville, AR, and collect additional samples for dating in order to constrain the ages of the sand blows and thus the timing of paleoearthquakes. Sand blows at this site may have formed during the A.D. 0 and B.C. 1050 New Madrid events. Additional dating is needed to improve the age estimates of the sand blows. The results would add confidence in the timing of these paleoearthquakes and recurrence times of New Madrid events.
2. Continue the search for a liquefaction record of pre-A.D. 900 earthquakes in the St. Francis Basin, Western Lowlands, northwestern MS, and western TN. It is recommended that more effort be placed on finding pre-A.D. 900 sand blows on terrace surfaces of Late Pleistocene deposits rather than along river cutbanks that are dominated by Late Holocene deposits and increasingly covered by recent flood deposits. These findings will help to address whether the NMSZ activated in the Late Holocene and whether seismicity migrates along elements of the Reelfoot Rift, and if so, over what time spans.
3. Conduct additional reconnaissance for and dating of liquefaction features along the Wolf River in southwestern TN, and the Coldwater River in northwestern MS; conduct evaluation of scenario earthquakes using geotechnical data from other sites in the area. This effort will test the hypotheses that a $M \geq 7.1$ earthquake on the ERM-S and $M \geq 6.9$ earthquakes in the Marianna area produced Late Holocene and Early-Middle Holocene liquefaction features, respectively. The results will have important implications for understanding the earthquake hazard in the Memphis area as well as the long-term behavior of structural elements of the Reelfoot Rift and other aulacogens in the CEUS and elsewhere.
4. Conduct additional site investigations, both paleoseismic and geophysical, of long linear sand blows along the proposed Obion River fault zone to determine if indeed it is an active fault zone that has produced repeating large magnitude earthquakes during the Late Holocene.

5 REFERENCES

5.1 References for Main Body of Report and Archaeological Report (Appendix F)

- Aiken, M.J., *Science-Based Dating in Archaeology*, Longman Group, London and New York, 1990.
- Aitken, M.J., *An Introduction to Optical Dating: The Dating of Quaternary Sediments by the Use of Photon-Stimulated Luminescence*, Oxford University Press, 1998.
- Ambraseys, N.N., "Engineering Seismology: Earthquake Engineering and Structural Dynamics," *Journal of the International Association of Earthquake Engineering*, 17:1-105, 1988.
- Atkinson, G., and D. Boore, "Modification to Existing Ground-Motion Prediction Equations in Light of New Data," *Bulletin of the Seismological Society of America*. 101: 1121-1135, 2011.
- Atkinson, G., (with input from) J. Adams, G. Rogers, T. Onur, and K. Assatourians, "White Paper on Development of Ground Motion Prediction Equations for Canadian National Seismic hazard Maps." www.seismotoolbox.ca (*Miscellaneous Resources*), Nov. 2012
- Atkinson, G., (Project Leader), K. Assatourians, "GMPEs for National Hazard Maps." www.seismotoolbox.ca (*Miscellaneous resources*) 2012.
- Bakun, W.H., and M.G. Hooper, "Magnitudes and Locations of the 1811-1812 New Madrid, Missouri, and Charleston, South Carolina, Earthquakes," *Bulletin of the Seismological Society of America*, 94(1):64-75, 2004.
- Baldwin, J.N., R.C. Witter, J.D. Vaughn, J.B. Harris, J. Sexton, M. Lake, and S.L. Forman, "Geological Characterization of the Idalia Hill Fault Zone and Its Structural Association with the Commerce Geophysical Lineament, Idalia, Missouri," *Bulletin Seismological Society of America*, 96(6):2281-2303, 2006.
- Baldwin, J.N., R. Givler, C.C. Brossy, E.T. Elliot, J.B. Harris, 2008, "Geophysical and Paleoseismic Evaluation of the Penitentiary Fault and Its Association with the Commerce Geophysical Lineament, Tamms, Southern Illinois," National Earthquake Hazards Reduction Program, Final Technical Report to U.S. Geological Survey, Award 06-HQ-GR-0138, 34 pp, plus 10 figures and one plate, 2008.
- Baldwin, J.N., R.W. Givler, C.C. Brossy, J.B. Harris, "Geophysical and Paleoseismic Investigation of the Commerce Geophysical Lineament, Qulin, Southeast Missouri," National Earthquake Hazards Reduction Program, Final Technical Report to U.S. Geological Survey, Award No. G11AP20035, 2014.
- Berthrong, J.F., *State of Arkansas*, United States Department of the Interior, General Lands Office, Washington, 1914.
- Bollinger, G.A., M.C. Chapman, M.S. Sibol, and J.K. Costain, "An Analysis of Earthquake Focal Depth in the Southeastern U.S.," *Geophysical Research Letters*, 12:785-788, 1985.
- Boulanger, R.W. and I.M. Idriss, "CPT and SPT Based Liquefaction Triggering Procedures," Report No. UCD/CGM-14/01, Center for Geotechnical Modeling, University of California, Davis, CA, 2014.
- Boulanger, R.W. and I.M. Idriss, "Probabilistic Standard Penetration Test-Based Liquefaction: Triggering Procedure," *Journal of Geotechnical and Geoenvironmental Engineering*, 138(10):1185-1195, 2012.

- Braile, L.W., W.J. Hinze, and G.R. Keller, "New Madrid Seismicity, Gravity Anomalies, and Interpreted Ancient Rift Structures," *Seismological Research Letters*, 68:599-610, 1997.
- Branner, J.C., *Map of Crowley's Ridge and the Floodplains of Adjacent Streams*, Geological Survey of Arkansas, Little Rock, 1889.
- British Antarctic Survey Staff, "Digital Geological Data Collection System – Scientific Instrumentation," *British Antarctic Survey Website*, http://www.antarctica.ac.uk/bas_research/instruments/dgdcs.php, 2011.
- Broughton, A.T., R.B. Van Arsdale, and J.H. Broughton, "Liquefaction susceptibility mapping in the city of Memphis and Shelby County, Tennessee (in earthquake hazard evaluation in the central United States)," *Engineering Geology*, 62(1-3):207-222, 2001.
- Camp, R.J., and J.M. Wheaton, "Streamlining Field Data Collection with Mobile Apps," *Eos Trans. American Geophysical Union*, 95(49):453–454, 2014.
- Carter, M.W., "Characterizing pedogenic and potential paleoseismic features in South Anna River alluvium: epicentral region of the 2011 earthquake Central Virginia seismic zone," Presentation at the 2015 Virginia Geological Research Symposium, 2015.
- Castilla, R.A. and F.A. Audemard, "Sand Blows as a Potential Tool for Magnitude Estimation of Pre-Instrumental Earthquakes," *Journal of Seismology*, 11:473-487, 2007.
- Center for Earthquake Research and Information (CERI), *New Madrid Earthquake Catalog*, website, http://folkworm.ceri.memphis.edu/catalogs/html/cat_nm.html.
- Cetin, K.O., et al., "Standard Penetration Test-Based Probabilistic and Deterministic Assessment of Seismic Soil Liquefaction Potential," *Journal of Geotechnical and Geoenvironmental Engineering*, American Society of Civil Engineers, 1314-1340, 2004.
- Chapman, M.C., "Magnitude, Recurrence Interval, and Near-Source Ground Motion Modeling of the Mineral, Virginia, Earthquake of 23 August 2011," in J. W., Jr., Horton, M.C. Chapman, and R.A. Green, eds., *The 2011 Mineral, Virginia, Earthquake, and Its Significance for Seismic Hazards in Eastern North America*, Geological Society of America Special Paper 509: 27-45, 2015.
- Chaucer, A., and M. Stewart, "iPad Investigation – Field Mapping on an iPad 2," *Geospatial Technologies in Education Web Blog*, <http://geospatial.posterous.com/ipd-investigation-field-mapping-on-an-ipad-2>, 2012.
- Cohen, K.M., S.M. Finney, P.L. Gibbard, and J.-X. Fan, "The ICS International Chronostratigraphic Chart," *Episodes*, 36(3): 199-204, 2013.
- Colton, J.H., *Arkansas*, JH Colton & Co., New York, 1855.
- Commercial Atlas of America*. Rand McNally & Co., Chicago, 1921.
- Cox, R.T., and R.B. Van Arsdale, "Hotspot Origin of the Mississippi Embayment and Its Possible Impact on Contemporary Seismicity," *Engineering Geology*, 46:201-216, 1997.
- Cox, R.T., R.B. Van Arsdale, J.B. Harris, and D. Larsen, "Neotectonics of the Southeastern Reelfoot Rift Margin, Central United States, and Implications for Regional Strain Accommodation," *Geology*, 29(5):419-422, 2001.
- Cox, R.T., J. Cherryhomes, J.B. Harris, D. Larsen, R.B. Van Arsdale, and S.L. Forman, "Paleoseismology of the Southeastern Reelfoot Rift in Western Tennessee and Implications for Intraplate Fault Zone Evaluation," *Tectonics*, 25, TC3019, 2006.
- Cram, S.F., *Cram's Banker's and Broker's Railroad Atlas*, Geo. F Cram, Chicago, 1887.

Cram, G.F., *Unrivaled Atlas of the World*, James R Gray & Co., Chicago, 1920.

Cramer, C.H., "A Seismic Hazard Uncertainty Analysis for the New Madrid Seismic Zone," *Engineering Geology*, 62:251-266, 2001.

Csontos, R., R. Van Arsdale, R. Cox, and B. Waldron, "Reelfoot Rift and Its Impact on Quaternary Deformation in the Central Mississippi River Valley," *Geosphere*, 4:145–158, 2008.

Cummings, S., *The Western Pilot*, George Conclin, Cincinnati, Ohio, 1847.

Deeter and Davis, *Soil Survey of Craighead County, Arkansas*, United States Department of Agriculture, 1916.

DelCastello, B.G. and B.M. Butler, "Archaeological investigations at 11Js-321, Cache River Scenic Natural Area Visitor Center, Johnson County, Illinois," *Center for Archaeological Investigations Technical Report 00-1*, report submitted to Illinois Department of Natural Resources, Contract No. IDNR-9987P, Southern Illinois University, Carbondale, 2000.

Dominion, "Response to Request for Additional Information No. 3, North Anna Early Site Permit Application," Dominion Nuclear North Anna, LLC, U.S. Nuclear Regulatory Commission, Report ML042800292, 2004.

Ellsworth, W. L., K. Imanishi, J.H. Luetgert, and T.L. Pratt, "The Mw 5.8 Virginia earthquake of August 23, 2011: A High Stress Drop Event in a Critically Stressed Crust," 83rd Annual Meeting of the Eastern Section of the Seismological Society of America, October, 2011, Little Rock, Arkansas, Abstract, 2011.

Exelon Generating Company, LLC, "ESP Application for Clinton Nuclear Power Plant," USNRC document ML032721596, see Table 4.1-1 of Appendix B, 2003.

Fain, J., S. Soumana, M. Montret, D. Miallier, T. Pilleyre, and S. Sanzelle, "Luminescence and ESR Dating-Beta-Dose Attenuation for Various Grain Shapes Calculated by a Monte-Carlo Method," *Quaternary Science Reviews*, 18:231-234, 1999.

Ferguson, D.V. and J.L. Gray, *Soil Survey of Mississippi County, Arkansas*, United States Department of Agriculture, Soil Conservation Service and Arkansas Agricultural Experiment Station, 1971.

Ferguson, D.V., *Soil Survey of Craighead County, Arkansas*, United States Department of Agriculture, Soil Conservation Service and Arkansas Agricultural Experiment Station, 1979.

Fischer-Boyd, K.F., and S.A. Schumm, "Geomorphic evidence of deformation in the northern part of the New Madrid seismic zone", U.S. Geological Survey Professional Paper 1538 R, 35 p, 1995.

Forman, S., "Luminescence Dating in Paleoseismology," in M. Beer, I.A. Kougoumtzoglou, E. Patelli, and I. S.-K. Au, eds., *Encyclopedia of Earthquake Engineering*, Springer Berlin Heidelberg, 1371-1378, 2015.

Forman, S.L., J. Pierson, and K. Lepper, "Luminescence Geochronology, Quaternary Geochronology: Methods and Applications," *AGU Reference Shelf*, 4, 2000.

Fuller, M.L., "The New Madrid Earthquake," U.S. Geological Survey Bulletin 494, 1912.

GPS World Staff, "ArcGIS apps for the field launched at Esri UC," *GPS World Website*, <http://gpsworld.com/arcgis-apps-for-the-field-launched-at-esri-uc/>, 2016.

Gray, F.A., *Arkansas*, OW Gray & Son, Philadelphia, 1876.

- Green, R., et al., "Geotechnical Aspects in the Epicentral Region of the 2011 Mw 5.8 Mineral, Virginia, Earthquake," in J.W. Horton, Jr., M.C. Chapman, and R.A. Green, eds., *The 2011 Mineral, Virginia, Earthquake, and Its Significance for Seismic Hazards in Eastern North America*, Geological Society of America Special Paper 509:151-171, 2015.
- Greenwood, M. L., E. W. Woolery, R. B. Van Arsdale, W. J. Stephenson, and G L. Patterson, "Continuity of the Reelfoot fault across the Cottonwood Grove and Ridgely faults of the New Madrid seismic zone," *Bulletin of the Seismological Society of America*, 106(6):2674-2685, 2016.
- Guccione, M. J., M.F. Burford, and J.D. Kendall, "Pemiscot Bayou, a large distributary of the Mississippi River and a possible failed avulsion," *Special Publication of the International Association of Sedimentologists*, 28: 211-220, 1999.
- Hall, E.C., T.M. Bushnell, L.V. Davis, W.T. Carter, and A.L. Patrick, *Soil Survey of Mississippi County, Arkansas*, United States Department of Agriculture, Bureau of Soils, 1916.
- Hao, Y., M. Magnani, K. McIntosh, B. Waldron, and L. Guo, "Quaternary Deformation along the Meeman-Shelby Fault near Memphis, Tennessee, Imaged by High Resolution Marine and Land Seismic Reflection Profiles," *Tectonics*, 32:501-515, 2013.
- Hardesty, H.H., "New railroad and township map of Arkansas", *Hardesty's Historical and Geographical Encyclopedia*, HH Hardesty & Co., New York, 1883.
- Hargrave, M. L. and B.M. Butler, "Results of the controlled surface collection," In *Mollie Baker (11-J-964), A Woodland period site in the Kinkaid Creek drainage, Jackson County, Illinois*, by M.L. Hargrave, B.M. Butler, N. Lopinot, and T.W. Pugh, Center for Archaeological Investigations, Southern Illinois University, Carbondale, Manuscript on file 1992-3: 32-40, 1992.
- Harrison, R.W., and A. Schultz, "Strike-slip faulting at Thebes Gap, Missouri and Illinois; implications for New Madrid tectonism," *Tectonics*, 13(2):246-257, 1994.
- Hildenbrand, T. G., and J.D. Hendricks, "Geophysical Setting of the Reelfoot Rift and Relations between Rift Structures and the New Madrid seismic zone," U.S. Geological Survey, Professional Paper 1538-E, 1995.
- Hoffman, D., J. Palmer, J. D. Vaughn, and R. W. Harrison, "Late Quaternary surface faulting at English Hill in southeastern Missouri," *Seism. Res. Lett*, 67(2):41, 1996.
- Holbrooke, J., W.J. Autin, T.M. Rittenour, S. Marshak, and R.J. Goble, "Stratigraphic Evidence for Millennial-Scale Temporal Clustering of Earthquakes on a Continental-Interior Fault: Holocene Mississippi River Floodplain Deposits, New Madrid Seismic Zone, USA," *Tectonophysics*, 420:431-454, 2006.
- Horton, J.W., M.C. Chapman, and R.A. Green, "The 2011 Mineral, Virginia, Earthquake, and Its Significance for Seismic Hazards in Eastern North America-Overview and Synthesis," in J.W. Horton, Jr., M.C. Chapman, and R.A. Green, eds., *The 2011 Mineral, Virginia, Earthquake, and Its Significance for Seismic Hazards in Eastern North America*, Geological Society of America Special Paper 509:1-25, 2015.
- Hough, S. E., "Scientific overview and historical context of the 1811-1812 New Madrid earthquake sequence," *Annals of Geophysics*, 47(2/3):523-537, 2004.
- Hough, S.E., et al., "On the Modified Mercalli Intensities and Magnitudes of the 1811-1812 New Madrid Earthquakes," *Journal of Geophysical Research*, 105(B10):23,839-23,864, 2000.
- Hough, S.E., and S. Martin, "Magnitude Estimates of Two Large Aftershocks of the 16 December 1811 New Madrid Earthquake," *Bulletin of the Seismological Society of America*, 92(8):3259-3268, 2002.

Hough, S.E., and M. Page, "Toward a consistent model for strain accrual and release for the New Madrid, central United States," *Journal of Geophysical Research*, 116: B03311, doi:10.1029/2010JB007783, 2011.

Idriss, I.M. and R.W. Boulanger, "Semi-Empirical Procedures for Evaluating Liquefaction Potential during Earthquakes," *Proceedings 11th International Conference Soil Dynamics and Earthquake Engineering*, 1: 32-46, Elsevier, Berkeley, CA, 2004.

Idriss, I.M. and R.W. Boulanger, "Soil Liquefaction during Earthquakes," Earthquake Engineering Research Institute, Monograph 12, EERI MNO-12, 2008.

Idriss, I.M. and R.W. Boulanger, "SPT-Based Liquefaction Triggering Procedures, Report No. UCD/CGM – 10/02," Department of Civil and Environmental Engineering, University of California at Davis, 2010. <http://faculty.engineering.ucdavis.edu/boulanger/wp-content/uploads/sites/71/2014/09/Idriss_Boulanger_SPT_Liquefaction_CGM-10-02.pdf>. Accessed May 8, 2015.

Indexed Atlas of the World. Rand McNally & Co., Chicago, 1900.

Johnston, A.C., "Seismic Moment Assessment of Stable Continental Earthquakes, Part III: 1811-1812 New Madrid, 1886 Charleston and 1755 Lisbon," *Geophysical Journal International*, 126:314-344, 1996.

Johnston, A.C., and L.R. Kanter, "Earthquakes in Stable Continental Crust," *Scientific American*, 262:68-75, 1990.

Johnston, A.C., and E.S. Schweig, "The Enigma of the New Madrid Earthquakes of 1811-1812," *Annual Review of Earth and Planetary Sciences*, 24:339-384, 1996.

Juang, C.H. and T. Jiang, "Assessing Probabilistic Methods for Liquefaction Potential Evaluation. Soil Dynamics and Liquefaction 2000," (*Proceedings GeoDenver*), GSP 107, American Society of Civil Engineers, Reston, VA, 2000.

Juang, C.H., T. Jiang, and R.D. Andrus, "Assessing Probability-Based Methods for Liquefaction Potential Evaluation," *Journal of Geotechnical and Geoenvironmental Engineering*, 128(7):580-589, 2002.

Justice, N.D., *Stone Age Spear and Arrow Points of the Midcontinental and Eastern United States*, University of Indiana Press, Bloomington, 1987.

Justice, N.D. and S.K. Kudlaty, *Field Guide to Projectile Points of the Midwest*, University of Indiana Press, Bloomington, 1999.

Lafferty, R.H., III, "Archeological Techniques of Dating Ancient Quakes," *Geotimes*, 41(11):24-27, 1996.

Lafferty, R. H., III, M.J. Guccione, L.J. Scott, D.K. Aasen, B.J. Watkins, M.C. Sierzchula, and P.F. Baumann, "A cultural resources survey, testing, and geomorphic examination of ditches 10, 12, and 29, Mississippi County, Arkansas," Submitted to Memphis District, COE, Contract No. DACW66-86-C-0034 by MCRA Report No. 86-5, 450 p., 1987.

Lafferty, R.H. and J.E. Price, "Southeast Missouri," in C.M. McNutt, ed., *Prehistory of the central Mississippi Valley*, University of Alabama Press, Tuscaloosa, 1996.

Li, Y., et al., "Evidence for Large Prehistoric Earthquakes in the Northern New Madrid Seismic Zone, Central United States," *Seismological Research Letters*, 69(3):270-276, 1998.

- Lian, O., "Luminescence Dating, in Encyclopedia of Quarterly Science," S. A. Elias ed., Elsevier, New York, 2007.
- Liao, S.S.C., D. Veneziano, and R.V. Whitman, "Regression Models for Evaluating Liquefaction Probability," *Journal of Geotechnical Engineering*, 114(4):389–411, 1988.
- Magnani, B., and K. McIntosh, "Towards an Understanding of the Long-Term Deformation of the Mississippi Embayment," National Earthquake Hazards Reduction Program, Final Technical Report to U.S. Geological Survey, Award No. 08HQGR0089, 2009.
- McBride, J.H., T.G. Hildenbrand, W.J. Stephenson, and C.J. Potter, "Interpreting the Earthquake Source of the Wabash Valley Seismic Zone (Illinois, Indiana, and Kentucky) from Seismic-Reflection, Gravity, and Magnetic-Intensity Data," *Seismological Research Letters*, 73:660-697, 2002.
- McGahey, S.O., *Mississippi projectile point guide*, Mississippi Department of Archives and History, Jackson, 2000.
- McKeown, F.A., R.M. Hamilton, S.F. Diehl, and E.E. Glick, "Diapiric Origin of the Blytheville and Pascola Arches in the Reelfoot Rift, East-Central United States: Relations to New Madrid Seismicity," *Geology*, 18:1158-1162, 1990.
- Metzger, A.G., J.G. Armbruster, and L. Seeber, "New earthquakes from old newspapers: Improving the historical record," EOS, Transactions of the American Geophysical Union, 79(17):S340, Abstract, 1998.
- MidWest Map Co., *Highway map and guide of Arkansas*, MidWest Map Co., Aurora, Missouri, 1931.
- Mitchell, S.A., "A new map of Arkansas with its canals, roads and distances", *Mitchell's Universal Atlas*. SA Mitchell, Philadelphia, 1847.
- Moore, W.H. and M.L. Beckett, *Official map*, Arkansas Public Service Commission, Little Rock, 1946.
- Morse, D.F. and P.A. Morse, *Archaeology of the central Mississippi valley*, Academic Press, London, 1989.
- Morse, D.F. and P.A. Morse, "Northeast Arkansas," in C.M. McNutt, ed., *Prehistory of the central Mississippi Valley*, University of Alabama Press, Tuscaloosa, 1996.
- Moss, R.E.S., et al., "CPT-based Probabilistic and Deterministic Assessment of in-situ Seismic Soil Liquefaction Potential," *Journal of Geotechnical and Geoenvironmental Engineering*, 132(8):1032-1051, 2006.
- Mueller, K., S.E. Hough, and R. Bilham, "Analysing the 1811-1812 New Madrid earthquakes with recent instrumentally recorded aftershocks," *Nature*, 429:284-288, 2004.
- Obermeier, S.F., "The New Madrid Earthquakes: An Engineering-Geologic Interpretation of Relict Liquefaction Features," U.S. Geological Survey, Professional Paper 1336-B, 1989.
- Obermeier, S.F. and W.E. McNulty, "Paleoliquefaction Evidence for Seismic Quiescence in Central Virginia during Late and Middle Holocene Time," EOS, Transactions of the American Geophysical Union, 79(17), Spring Meeting Supplement, Abstract T41A-9, 1998.
- Odum, J.K., R.A. Williams, W.J. Stephenson, M.P. Tuttle, H. Al-Shukri, "Preliminary Assessment of a Previously Unknown Fault Zone Beneath the Daytona Beach Sand Blow Cluster near Marianna, Arkansas," *Seismological Research Letters*, 87(6): 1453-1464, 2016.
- Oristaglio, M. and A. Dorozynski, *A Sixth Sense*, Gerald Duckworth & Co Ltd., London, 2009.

Perino, G., *Selected Preforms, Points and Knives of the North American Indians*, I, Points and Barbs Press, Isabel, Oklahoma, 1985.

Petersen, M.D., et al., "Documentation for the 2008 Update of the United States National Seismic Hazard Maps," U.S. Geological Survey Open-File Report 2008–1128, 2008.

Petersen, M.D., et al., "Documentation for the 2014 Update of the United States National Seismic Hazard Maps," U.S. Geological Survey Open-File Report 2014–1091, 2014.

Powars, D. S., R.D. Catchings, J.W. Horton, Jr., S. Schindler, and M.J. Pavich, "Stafford fault system: 120 million year fault movement history of northern Virginia," in J.W. Horton, Jr., M.C. Chapman, and R.A. Green, eds., *The 2011 Mineral, Virginia, earthquake, and its significance for seismic hazards in eastern North America*, Geol. Soc. Am., Special Paper, 509:407-431, 2015.

Pratt T.L., C. Coruh, J.K. Costain, and L. Glover, III, "A Geophysical Study of the Earth's Crust in Central Virginia: Implication for Appalachian Crustal Structure," *Journal Geophysical Research*, 93(B6):6649-6667, 1988.

Pratt, T.L., J.W. Horton, D.B. Spears, A.K. Gilmer, and D.E. McNamara, "The 2011 Virginia M5.8 Earthquake: Insights from Seismic Reflection Imaging into Influence of Older Structures on Eastern U.S. Seismicity," in J.W. Horton, Jr., M.C. Chapman, and R.A. Green, eds., *The 2011 Mineral, Virginia, Earthquake, and Its Significance for Seismic Hazards in Eastern North America*, Geological Society of America Special Paper 509:285-293, 2015.

Prescott, J.R., and J.T. Hutton, "Cosmic Ray Contributions to Dose Rates for Luminescence and ESR Dating: Large Depths and Long-Term Time Variations," *Radiation Measurements*, 23:497-500, 1994.

Al-Qadhi, O, "Geophysical Investigation of Paleoseismological Features in Eastern Arkansas, USA," Ph.D dissertation, University of Arkansas at Little Rock, Little Rock, Arkansas, 235 pp. plus Appendix A., 2010.

Rand McNally & Co., *Enlarged Business Atlas and Shipper's Guide* Rand McNally & Co., Chicago, 1889.

Rathgeber, M., "Excavations at the Manly-Usrey site (3MS106)," Paper presented at the annual meeting of the Arkansas Archeological Society, Little Rock, Arkansas, 2012.

Robertson, P.K., "Soil Classification Using the CPT," *Canadian Geotechnical Journal*, 27(1):151-158, 1990.

Robertson, P.K., "Evaluating Soil Liquefaction and Post-Earthquake Deformations Using the CPT, Geotechnical and Geophysical Site Characterization, Vol. 1," (*Proceedings ISC-2, Porto*), Millpress, Rotterdam, 2004.

Robertson, P.K., "Interpretation of Cone Penetration Tests: A Unified Approach," *Canadian Geotechnical Journal*, 46(11):1335-1355, 2009.

Robertson, P.K. and C.E. Wride (Fear), "Evaluating Cyclic Liquefaction Potential using the Cone Penetration Test," *Canadian Geotechnical Journal*, 35(3):442-459, 1998.

Roeser, C., *State of Arkansas*. United States Department of the Interior, General Lands Office. Julius Bien, New York, 1878.

Saucier, R.T., "Effects of the New Madrid Earthquake Series in the Mississippi Alluvial Valley," *U.S. Army Corps of Engineers Waterways Experiment Station Miscellaneous Paper S-77-5*, 10, 1977.

- Saucier, R.T., "Evidence for Episodic Sand-Blow Activity during the 1811-12 New Madrid (Missouri) Earthquake Series," *Geology*, 17:103-106, 1989.
- Saucier, R., "Geoarchaeological Evidence of Strong Prehistoric Earthquakes in the New Madrid (Missouri) Seismic Zone," *Geology*, 19:296-298, 1991.
- Saucier, R.T., "Geomorphology and Quaternary Geologic History of the Lower Mississippi," *U.S. Army Corps of Engineers Waterways Experiment Station, Vols. I and II*, 1994.
- Schneider, J.A., P.W. Mayne, and T.L. Hendren, "Initial Development of an Impulse Piezovibrocone for Liquefaction Evaluation, Physics and Mechanics of Soil Liquefaction," *Proceedings of the International Workshop on the Physics and Mechanics of Soil Liquefaction, Johns Hopkins Univ., Balkema, Rotterdam*, 341-354, 1999.
- Schneider, J.A., P.W. Mayne, and G.J. Rix, "Geotechnical Site Characterization in the Greater Memphis Area using CPT," *Engineering Geology*, 62(1-3):169-184, 2001.
- Schweig, E. S., III, and R. T. Marple, "The Bootheel Lineament: A Possible Coseismic Fault of the Great New Madrid Earthquakes, *Geology*," 19:1025-1028, 1991.
- Seed, H.B. and I.M. Idriss, "Simplified Procedure for Evaluating Soil Liquefaction Potential," *Journal of the Soil Mechanics and Foundations Division (American Society of Civil Engineers)*, 97(SM9):1249-1273, 1971.
- Seed, H.B. and I.M. Idriss, "Evaluation of Liquefaction Potential of Sand Deposits based on Observations of Performance in Previous Earthquakes, Pre-Print 81-544, Session on In-situ Testing to Evaluate Liquefaction Susceptibility," ASCE National Convention, St. Louis, Missouri, October, 1981.
- Seed, H.B. and I.M. Idriss, "Ground Motions and Soil Liquefaction during Earthquakes," Earthquake Engineering Research Institute, Berkeley, CA, 1982.
- Sims, J.D., "Earthquake-Induced Structures in Sediments of Van Norman Lake, San Fernando California," *Science*, 182:161-163, 1973.
- Soller, D.R., and M.C. Reheis, "Surficial Materials in the Conterminous U.S.," U.S. Geological Survey, Open-file Report 03-275, scale 1:5,000,000, 2004.
- Al-Shukri, H., R.E. Lemmer, H.H. Mahdi, and J.B. Connelly, "Spatial and temporal characteristics of paleoseismic features in the southern terminus of the New Madrid seismic zone in eastern Arkansas," *Seismological Research Letters*, 76(4):502-511, 2005.
- Al-Shukri, H., H. Mahdi, and M. Tuttle, "Three-Dimensional Imaging of Earthquake-Induced Liquefaction Features with Ground Penetrating Radar near Marianna, Arkansas," *Seismological Research Letters*, 77:505-513, 2006.
- Al-Shukri, H., H. Mahdi, O. Al-Kadi, and M. Tuttle, "Spatial and Temporal Characteristics of Paleoseismic Features in the Southern Terminus of the New Madrid Seismic Zone in Eastern Arkansas," National Earthquake Hazards Reduction Program, Final Technical Report to U.S. Geological Survey, Award No. 07HQGR0069, 2009.
- Al-Shukri, H., H. Mahdi, M.P. Tuttle, and K. Dyer-Williams, "Geophysical and Paleoseismic Investigations of Large Sand Blows along a Northwest-Oriented Lineament near Marianna, Arkansas," National Earthquake Hazards Reduction Program, Final Technical Report to U.S. Geological Survey, Award No. G12AP20093, 2015.
- Shumway, A.M., "Focal mechanisms in the northeast New Madrid seismic zone," *Seismological Research Letters*, 79(3):469-477, 2008.

- Stephenson, W.J., J.K. Odum, R.A. Williams, T.L. Pratt, R.W. Harrison, and D. Hoffman, "Deformation and Quaternary faulting in southeast Missouri across the Commerce Geophysical Lineament," *Bulletin of Seismological Society of America*, 89(1):40-155, 1999.
- Talma, A.S. and J.C. Vogel, "A Simplified Approach to Calibrating C14 Dates," *Radiocarbon*, 35:317-322, 1993.
- Toprak, S., et al., "CPT- and SPT-based Probabilistic Assessment of Liquefaction Potential," *Proceedings of the 7th U.S.–Japan Workshop on Earthquake Resistant Design of Lifeline Facilities and Countermeasures Against Liquefaction, Seattle, WA, 19 November 1999*, MCEER, Buffalo, NY, Technical Report MCEER-99-0019, 1999.
- Tuttle, M.P., "Late Holocene Earthquakes and their Implications for Earthquake Potential of the New Madrid Seismic Zone, Central United States," Ph.D. dissertation, University of Maryland, College Park, MD, 1999.
- Tuttle, M.P., "The Use of Liquefaction Features in Paleoseismology: Lessons Learned in the New Madrid Seismic Zone, Central United States," *Journal of Seismology*, 5:361-380, 2001.
- Tuttle, M. P., "Search for and Study of Sand Blows at Distant Sites Resulting from Prehistoric and Historic New Madrid earthquakes," Collaborative Research, M. Tuttle & Associates and Central Region Hazards Team, Final Technical Report (02HQGR0097) to U.S. Geological Survey, 48 pp, 2010.
- Tuttle, M.P., "Earthquake Potential of the Central Virginia Seismic Zone," National Earthquake Hazards Reduction Program, Final Technical Report to U.S. Geological Survey, Award No. G13AP00045, 2016.
- Tuttle, M. and N. Barstow, "Liquefaction-related Ground Failure: A Case Study in the New Madrid Seismic Zone, Central United States," *Bulletin of the Seismological Society of America*, 86(3):636-645, 1996.
- Tuttle, M.P., et al., "Use of Archaeology to Date Liquefaction Features and Seismic Events in the New Madrid Seismic Zone, Central United States," *Geoarchaeology: An International Journal*, 11(6):451-480, 1996.
- Tuttle, M.P., et al., "New Evidence for a Large Earthquake in the New Madrid Seismic Zone between A.D. 1400 and 1670," *Geology*, 27(9):771-774, 1999.
- Tuttle, M.P., J.D. Sims, K. Dyer-Williams, R.H. Lafferty III, and E.S. Schweig III, "Dating of Liquefaction Features in the New Madrid Seismic Zone," U.S. Nuclear Regulatory Commission, NUREG/GR-0018, 42 pp, 2000.
- Tuttle, M.P., et al., "The Earthquake Potential of the New Madrid Seismic Zone," *Bulletin of the Seismological Society of America*, 92(6):2080-2089, 2002.
- Tuttle, M. P., and E.S. Schweig, "Towards a Paleoearthquake Chronology of the New Madrid Seismic Zone," U.S. Geological Survey, Earthquake Hazards Program, Progress Report, Award 99HQGR0022, 28 pp, 2001.
- Tuttle, M.P., and E.S. Schweig, "Search for and Study of Sand Blows at Distant Sites Resulting from Prehistoric and Historic New Madrid Earthquakes," National Earthquake Hazards Reduction Program, Annual Project Summary to U.S. Geological Survey, Award No. 1434-02HQGR0097, 2004.
- Tuttle, M.P., E.S. Schweig, J. Campbell, P.M. Thomas, J.D. Sims, and R.H. Lafferty, "Evidence for New Madrid earthquakes in A.D. 300 and 2350 B.C.," *Seismological Research Letters*, 76(4):489-501, 2005.

Tuttle, M., and J.S. Chester, "Paleoseismology Study in the Cache River Valley, Southern Illinois," National Earthquake Hazards Reduction Program, Final Technical Report to U.S. Geological Survey, Award No. HQ98GR00015), 2005.

Tuttle, M.P., H. Al-Shukri, and H. Mahdi, "Very Large Earthquakes Centered Southwest of the New Madrid Seismic Zone 5,000-7,000 years ago," *Seismological Research Letters*, 77(6):664-678, 2006.

Tuttle, M.P., R.H. Lafferty, R.F. Cande, and M.C. Sierzchula, "Impact of Earthquake-induced Ground Failure on a Mississippian Archaeological Site in the New Madrid Seismic Zone, Central USA," *Quaternary International*, 242:126-137, 2011.

Tuttle, M.P., and R. Hartleb, "Appendix E. Central and Eastern U.S. Paleoliquefaction Database, Uncertainties Associated with Paleoliquefaction Data, and Guidance for Seismic Source Characterization," in *The Central and Eastern U.S. Seismic Source Characterization for Nuclear Facilities*, Technical Report, EPRI, Palo Alto, CA, U.S. DOE, and U.S. NRC, 135 p., plus database, 2012.

Tuttle, M.P., R.H. Lafferty, III, J. Morrow, R. Scott, and L. Wolf, "Pre-Trenching Evaluation Report for the Stiles and Garner I Paleoliquefaction Site in Northeastern Arkansas," Technical report prepared for the NRC under Contact No. NRC-HQ-11-C-04-0041. April 2014, ADAMS Accession No. ML15287A206.

Tuttle, M.P., M.E. Starr, and L. Wolf, "Pre-Trenching Evaluation Report for the Pritchett Paleoliquefaction Site in Western Tennessee," Technical report prepared for the NRC under Contact No. NRC-HQ-11-C-04-0041. Unpublished. January 2016.

U.S. Geological Survey, "Preliminary geological map of the Gulf Coastal Plain of northeastern Arkansas," Water Supply Paper 399, Plate 1, 1916.

U.S. Nuclear Regulatory Commission, "Dating of Liquefaction Features in the New Madrid Seismic Zone and Implications for Earthquake Hazard," NUREG/GR-0017, September 1998.

U.S. Nuclear Regulatory Commission, "Central and Eastern United States Seismic Source Characterization for Nuclear Facilities," NUREG-2115, Vols. 1-6, February 2012, ADAMS Accession No. ML12048A776.

U.S. Nuclear Regulatory Commission, "Guidance document: Conducting paleoliquefaction studies for earthquake source characterization," NUREG/CR-7238, 185 p., 2018.

U.S. Post Office, *Post route map of the state of Arkansas*, United States Post Office Department, Washington, 1945.

Vaughn, J.D., "Paleoseismological studies in the Western Lowlands of southeast Missouri," U.S. Geological Survey Final Technical Report Award No. 14-08-0001-G1931, 1994.

Veprakas, M.J., "Redoximorphic Features for Identifying Aquic Conditions," North Carolina Agricultural Research Service, Technical Bulletin 301, 1992.

Villamor, P., P. Almond, M. Tuttle, et al., "Liquefaction Features Produced by the 2010-2011 Canterbury Earthquake Sequence in Southwest Christchurch, New Zealand and Preliminary Assessment of Paleoliquefaction Features," *Bulletin of the Seismological Society of America*, 106(4), 2016.

Vogel, J.C., et al., "Pretoria Calibration Curve for Short Lived Samples," *Radiocarbon*, 33:73-86, 1993.

- Wheeler, R.L., S. Rhea, and R.L. Dart, "Map Showing Structure of the Mississippi Valley Graben in the Vicinity of New Madrid, Missouri," U.S. Geological Survey Miscellaneous Field Studies Map MF-2264-D, 1994.
- Wheeler, R. L., E. M. Omdahl, R. L. Dart, G. D. Wilkerson, and R. H. Bradford, "Earthquakes in the central U.S., 1699-2002," U. S. Geological Survey, Geological investigations series I-2812, 2003.
- Williams, R.A., E.A. Luzietti, and D.L. Carver, "High-resolution seismic imaging of Quaternary faulting on the Crittenden County fault zone, New Madrid seismic zone, northeastern Arkansas," *Seismological Research Letters*, 66(3):42-57, 1995.
- Williams, R.A., W.J. Stephenson, J.K. Odum, and D.M. Worley, "Seismic-reflection imaging of Tertiary faulting and related post-Eocene deformation 20 km north of Memphis, Tennessee," *Engineering Geology*, 62:79-90, 2001.
- Williams, R.A., W.J. Stephenson, J.K. Odum, J. Gomberg, "Post-Eocene Deformation Observed in Seismic-Reflection Profiles Across the Southwestern Blytheville Arch and Crowley's Ridge, Arkansas," Meeting of the Seismological Society of America, Poster, 2007.
- Wintle, A.G. and A.S. Murray, "A Review of Quartz Optically Stimulated Luminescence Characteristics and Their Relevance in Single-Aliquot Regeneration Dating Protocols," *Radiation Measurements*, 41:369-391, 2006.
- Wolf, L.W., J. Collier, M. Tuttle, et al., "Geophysical Reconnaissance of Earthquake-induced Liquefaction Features in the New Madrid Seismic Zone," *Journal of Applied Geophysics*, 39:121-129, 1998.
- Wolf, L.W., M. P. Tuttle, S. Browning, et al., "Geophysical Surveys of Earthquake-induced Liquefaction Deposits in the New Madrid Seismic Zone," *Geophysics*, 71(6):B223-230, 2006.
- Youd, T.L., et al., "Liquefaction Resistance of Soils: Summary Report from the 1996 NCEER and 1998 NCEER/NSF Workshops on Evaluation of Liquefaction Resistance of Soils," *Journal of Geotechnical and Geoenvironmental Engineering*, 127(10):817-833, 2001.
- Youd, T.L. and S.K. Noble, "Liquefaction Criteria based on Statistical and Probabilistic Analyses," *Proceedings, NCEER Workshop on Evaluation of Liquefaction Resistance of Soils*, NCEER Technical Report No. 97-0022, Salt Lake City, 1997.
- Zhang, G., P.K. Robertson, and R.W.I. Brachman, "Estimating Liquefaction-Induced Ground Settlements from CPT for Level Ground," *Canadian Geotechnical Journal*, 39(5):1168-1180, 2002.

5.2 References for CEUS Paleoliquefaction Database

5.2.1 Charleston, South Carolina, Seismic Zone

- Amick, D., Gelinias, R., Maurath, G., Cannon, R., Moore, D., Billington, E., and Kemppinen, H., 1990a, Paleoliquefaction features along the Atlantic Seaboard: U.S. Nuclear Regulatory Commission Report, NUREG/CR-5613.
- Amick, D., Maurath, G., and Gelinias, R., 1990b, Characteristics of Seismically Induced Liquefaction Sites and Features Located in the Vicinity of the 1886 Charleston, South Carolina Earthquake: *Seismological Research Letters*, v. 61, no. 2, pp. 117-130.

- Hu, K., Gassman, S. L., and Talwani, P., 2002a, In-situ properties of soils at paleoliquefaction sites in the South Carolina coastal plain: *Seismological Research Letters*, v. 73, no. 6, pp. 964-978.
- Hu, K., Gassman, S. L., and Talwani, P., 2002b, Magnitudes of prehistoric earthquakes in the South Carolina coastal plain from geotechnical data: *Seismological Research Letters*, v. 73, no. 6, pp. 979-991.
- Leon, E., Gassman, S. L., and Talwani, P., 2005, Effect of soil aging on assessing magnitudes and accelerations of prehistoric earthquakes: *Earthquake Spectra*, v. 21, no. 3, pp. 737-759.
- Noller, J. S. and Forman, S. L., 1998, Luminescence Geochronology of Liquefaction Features Near Georgetown, South Carolina: in J.M. Sowers, J.S. Noller, and W.R. Lettis (eds.) *Dating and Earthquakes: Review of Quaternary Geochronology and Its Application to Paleoseismology*: U.S. Nuclear Regulatory Commission Report, NUREG/CR-5562, pp. 4.49-4.57.
- Talwani, P., and Cox, J., 1985, Paleoseismic evidence for recurrence of earthquakes Near Charleston, South Carolina: *Science*, v. 228, pp. 379-381.
- Talwani, P., Rajendran, C. P., Rajendran, K., and Madabhushi, S., 1993, Assessment of Seismic Hazard Associated with Earthquake Source in the Bluffton-Hilton Head Area: Technical Report SCUREF Task Order 41, University of South Carolina at Columbia, 85 pp.
- Talwani, P., Amick, D. C., and Schaeffer, W. T., 1999, Paleoliquefaction Studies in the South Carolina Coastal Plain: U.S. Nuclear Regulatory Commission Report NUREG/CR 6619, 109 pp.
- Talwani, P., and Schaeffer, W.T., 2001, Recurrence Rates of Large Earthquakes in the South Carolina Coastal Plain Based on Paleoliquefaction Data: *Journal of Geophysical Research*, v. 106, no. B4, p. 6621-6642.
- Talwani, P., Dura-Gomez, I., Gassman, S., Hasek, M., and Chapman, A., 2008, Studies related to the discovery of a prehistoric sandblow in the epicentral area of the 1886 Charleston SC earthquake: Trenching and geotechnical investigations: Program and Abstracts, Eastern Section of the Seismological Society of America, p. 50.
- Weems, R. E., and Obermeier, S. F., 1990, The 1886 Charleston earthquake—An overview of geological studies: in *Proceedings of the U.S. Nuclear Regulatory Commission Seventeenth Water Reactor Safety Information Meeting*, NUREG/CP-0105, volume 2, pp. 289-313.
- Weems, R.E., Obermeier, S.F., Pavich, M.J., Gohn, G.S., and Rubin, M., 1986, Evidence for three moderate to large prehistoric Holocene earthquakes near Charleston, South Carolina: in *Proceedings of the 3rd U.S. National Conference on Earthquake Engineering*, Charleston, South Carolina, v. 1, pp. 3-13.

5.2.1 New Madrid Seismic Zone

- Barnes, A. A., 2000, An interdisciplinary study of earthquake-induced liquefaction features in the New Madrid seismic zone, central United States: M.S. thesis, Auburn University, Alabama, 266 p.
- Bauer, L. M., 2006, Studies of Historic and Prehistoric Earthquake-induced Liquefaction Features in the Meizoseismal Area of the 1811-1812 New Madrid Earthquakes, Central United States: M.S. thesis, University of Memphis, Memphis, Tennessee, p. 135.
- Broughton, A. T., Van Arsdale, R. B., and Broughton, J. H., 2001, Liquefaction susceptibility mapping in the city of Memphis and Shelby County, Tennessee (in *Earthquake hazard evaluation in the central United States*): *Engineering Geology*, v. 62 (1-3), pp. 207-222.

- Browning, S. E., 2003, Paleoseismic studies in the New Madrid Seismic Zone, Central United States: M.S. thesis, Auburn University, Auburn, Alabama, 134 p.
- Buchner, C. A., Cox, R., Skinner, C. T., Kaplan, C., and Albertson, E. S., 2010, Data recovery excavations at the Laplant I Site (23NM51), New Madrid County, Missouri: Report to U.S. Army Corps of Engineers, Memphis District.
- Collier, J. W., 1998, Geophysical investigations of liquefaction features in the New Madrid seismic zone: Northeastern Arkansas and southeastern Missouri: M.S. thesis, Auburn University, Auburn, Alabama, 163 p.
- Cox, R. T., Van Arsdale, R. B., Harris, J. B., and Larsen, D., 2001, Neotectonics of the southeastern Reelfoot rift zone margin, central United States, and implications for regional strain accommodation: *Geology*, v. 29, pp. 419-422.
- Craven, J. A., 1995a, Paleoseismological Study in the New Madrid Seismic Zone Using Geological and Archeological Features to Constrain Ages of Liquefaction Deposits: M.S. thesis, University of Memphis, 51 pp.
- Craven, J. A., 1995b, Evidence of paleoseismicity within the New Madrid seismic zone at a late Mississippian Indian occupation site in the Missouri Bootheel: Geological Society of America, Abstracts with Programs, 1995 Annual Meeting, p. A-394.
- Li, Y., Schweig, E. S., Tuttle, M. P., and Ellis, M. A., 1998, Evidence for large prehistoric earthquakes in the northern New Madrid seismic zone, central United States: *Seismological Research Letters*, v. 69, no. 3, pp. 270-276.
- Liao, T., Mayne, P. W., Tuttle, M. P., Schweig, E. S., and Van Arsdale, R. B., 2002, CPT site characterization for seismic hazards in the New Madrid seismic zone: *Soil Dynamics and Earthquake Engineering*, v. 22, pp. 943-950.
- Mayne, P. W., 2001, Cone penetration testing for seismic hazards evaluation in Memphis and Shelby County, Tennessee, U.S. Geological Survey, Earthquake Hazards Program, Final Report (00HQGR0025), 21 pp.
- Saucier, R. T., 1991, Geoarchaeological evidence of strong prehistoric earthquakes in the New Madrid (Missouri) seismic zone: *Geology*, v. 19, pp. 296-298.
- Tuttle, M. P., 1999, Late Holocene Earthquakes and Their Implications for Earthquake Potential of the New Madrid Seismic Zone, Central United States: Ph.D. dissertation, University of Maryland, College Park, Maryland, 250 pp.
- Tuttle, M. P., 2008, Paleoseismological investigations at the East Site, The Gilmore/Tyronza Mitigation Project, v. 4, Data Recovery at the Tyronza Sites, Poinsett County, Arkansas, The East Site (3P0610): in Technical Report to Arkansas State Highway and Transportation Department, pp. 259-277.
- Tuttle, M. P., 2010, Search for and Study of Sand Blows at Distant Sites Resulting from Prehistoric and Historic New Madrid earthquakes: Collaborative Research, M. Tuttle & Associates and Central Region Hazards Team, U.S. Geological Survey, Final Technical Report, Award 02HQGR0097, 48 pp.
- Tuttle, M. P., and Schweig, E. S., 1995, Archeological and pedological evidence for large earthquakes in the New Madrid seismic zone, central United States: *Geology*, v. 23, pp. 253-256.
- Tuttle, M. P., Lafferty, R. H., III, and Schweig, E. S., III, 1998, Dating of liquefaction features in the New Madrid seismic zone and implications for earthquake hazard, U.S. Nuclear Regulatory Commission, NUREG/GR-0017, 77 p.

- Tuttle, M., Chester, J., Lafferty, R., Dyer-Williams, K., and Cande, B., 1999, Paleoseismology Study Northwest of the New Madrid Seismic Zone: U.S. Nuclear Regulatory Commission, NUREG/CR-5730, 98 pp.
- Tuttle, M. P., Sims, J. D., Dyer-Williams, K., Lafferty, R. H., III, and Schweig, E. S., III, 2000, Dating of Liquefaction Features in the New Madrid Seismic Zone: U.S. Nuclear Regulatory Commission, NUREG/GR-0018, 42 pp.
- Tuttle, M. P., and Schweig, E. S., 2001, Towards a Paleoearthquake Chronology of the New Madrid Seismic Zone: U.S. Geological Survey, Earthquake Hazards Program, Progress Report, Award 99HQGR0022, 28 pp.
- Tuttle, M. P., and Schweig, E. S., 2003, Search for and Study of Sand Blows at Distant Sites Resulting from Prehistoric and Historic New Madrid Earthquakes: U.S. Geological Survey, Earthquake Hazards Program, Progress Report, Award 02HQGR0097, 29 pp.
- Tuttle, M. P., and Wolf, L. W., 2003, Towards a Paleoearthquake Chronology of the New Madrid Seismic Zone: U.S. Geological Survey, Earthquake Hazards Program, Progress Report, Award 01HQGR0164, 38 pp.
- Tuttle, M. P., and Wolf, L. W., 2004, Towards a Paleoearthquake Chronology of the New Madrid Seismic Zone: U.S. Geological Survey, Earthquake Hazards Program, Final Report, Award 01HQGR0164, 36 pp.
- Tuttle, M. P., and Schweig, E. S., 2004, Search for and Study of Sand Blows at Distant Sites Resulting from Prehistoric and Historic New Madrid Earthquakes: U.S. Geological Survey, Earthquake Hazards Program, Annual Project Summary, Award 02HQGR0097, 18 pp.
- Tuttle, M. P., Schweig, E., III, Campbell, J., Thomas, P. M., Sims, J. D., and Lafferty, R. H., III, 2005, Evidence for New Madrid earthquakes in AD 300 and 2350 B.C.: *Seismological Research Letters*, v. 76, no. 4, pp. 489-501.
- Tuttle, M., and Chester, J. S., 2005, Paleoseismology Study in the Cache River Valley, Southern Illinois: U.S. Geological Survey, Earthquake Hazards Program, Final Technical Report, Award HQ98GR00015, 14 pp.
- Tuttle, M. P., Lafferty, R. H., Cande, R. F., Sierzchula, M. C., 2011, Impact of earthquake-induced liquefaction and related ground failure on a Mississippian archeological site in the New Madrid seismic zone, central USA, *Quaternary International*, DOI 10.1016/j.quaint.2011.04.043
- Tuttle, M. P., Wolf, L., Dyer-Williams, K., Starr, M. E., Lafferty, R. H., Haynes, M., Morrow, J. Scott, R., Busch, T., Moseley, C., Tucker, K., and Karrenbauer, C., 2018, Paleoliquefaction studies in moderate seismicity regions with a history of large events: U.S. Nuclear Regulatory Commission, Contract NRC-HQ-11-C-040041, this volume.
- Vaughn, J. D., 1994, Paleoseismology Studies in the Western Lowlands of Southeast Missouri: U.S. Geological Survey, Final Report, Award 14-08-0001-G1931, 27 pp.
- Wesnousky, S. G., and Johnson, D. L., 1996, Stratigraphic, paleosol, and C-14 evidence for a large pre-1811 magnitude earthquake in the New Madrid seismic zone: *Seismological Research Letters*, v. 67, no. 2, p. 60.
- Wolf, L.W., 2004, Geophysical Investigations of Earthquake-Induced Liquefaction Features in the New Madrid Seismic Zone: Earthquake Hazards Program, Final Technical Report, Award 01HQGR0003, 36 pp.

Wolf, L. W., Tuttle, M. P., Browning, S., and Park, S., 2006, Geophysical surveys of earthquake-induced liquefaction deposits in the New Madrid seismic zone, *Geophysics*, v. 71, n. 6, p. B223-230.

5.2.2 Marianna Area

Al-Qadhi, O., 2010, Geophysical Investigation of Paleoseismological Features in Eastern Arkansas, USA: Ph.D dissertation, University of Arkansas at Little Rock, Little Rock, Arkansas, 235 pp. plus Appendix A.

Al-Shukri, H., Lemmer, R. E., Mahdi, H. H., and Connelly, J. B., 2005, Spatial and temporal characteristics of paleoseismic features in the southern terminus of the New Madrid seismic zone in eastern Arkansas: *Seismological Research Letters*, v. 76, no. 4, pp. 502-511.

Al-Shukri, H., Mahdi, H., Al Qadhi, O., and Tuttle, M. P., 2009, Spatial and Temporal Characteristics of Paleoseismic Features in the Southern Terminus of the New Madrid Seismic Zone in Eastern Arkansas: U.S. Geological Survey, Earthquake Hazards Program, Final Technical Report, Award 07HQGR0069, 24 pp.

Al-Shukri, H., Mahdi, H., Tuttle, M.P., Dyer-Williams, K., 2015, Geophysical and paleoseismic investigations of large sand blows along a northwest-oriented lineament near Marianna, Arkansas, U.S. Geological Survey, Earthquake Hazards Program, Final Technical Report, Award G12AP20093, 31 p.

Tuttle, M. P., Al-Shukri, H, and Mahdi, H., 2006, Very large earthquakes centered southwest of the New Madrid seismic zone 5,000-7,000 years ago: *Seismological Research Letters*, v. 77, no. 6, pp. 664-678.

5.2.3 St. Louis Region

Tuttle, M. P., 2000, *Paleoseismological Study in the St. Louis Region*: U.S. Geological Survey, Earthquake Hazards Program, Final Technical Report (99HQGR0032), 29 pp.

Tuttle, M. P., 2005, Improving the Earthquake Chronology for the St. Louis Region: U.S. Geological Survey, Earthquake Hazards Program, Annual Project Summary, Award 05HQGR0045, 6 pp.

Tuttle, M., Chester, J., Lafferty, R., Dyer-Williams, K., and Cande, B., 1999, Paleoseismology Study Northwest of the New Madrid Seismic Zone: U.S. Nuclear Regulatory Commission, NUREG/CR-5730, 98 pp.

Tuttle, M., and Chester, J. S., 2005, Paleoseismology Study in the Cache River Valley, Southern Illinois: U.S. Geological Survey, Earthquake Hazards Program, Final Technical Report, Award HQ98GR00015, 14 pp.

5.2.4 New Madrid-Wabash Valley Region

Tuttle, M. P., 2000, *Paleoseismological Study in the St. Louis Region*: U.S. Geological Survey, Earthquake Hazards Program, Final Technical Report (99HQGR0032), 29 pp.

Tuttle, M. P., 2005, Improving the Earthquake Chronology for the St. Louis Region: U.S. Geological Survey, Earthquake Hazards Program, Annual Project Summary, Award 05HQGR0045, 6 pp.

Tuttle, M., Chester, J., Lafferty, R., Dyer-Williams, K., and Cande, B., 1999, Paleoseismology Study Northwest of the New Madrid Seismic Zone: U.S. Nuclear Regulatory Commission, NUREG/CR-5730, 98 pp.

Tuttle, M., and Chester, J. S., 2005, Paleoseismology Study in the Cache River Valley, Southern Illinois: U.S. Geological Survey, Earthquake Hazards Program, Final Technical Report, Award HQ98GR00015, 14 pp.

Tuttle, M., and Dyer-Williams, K., 2017, Filling the gap in the paleoearthquake record between the New Madrid and Wabash Valley seismic zones, U.S. Geological Survey, Earthquake Hazards Program, Final Technical Report, Award G12AP20068, 39 p., plus Appendix A.

5.2.5 Wabash Valley Seismic Zone

Exelon Generation Company, 2004, Clinton Early Site Permit Application, Response to Request for Additional Information Letter No. 7, October 11.

Green, R. A., Obermeier, S. F., and Olson, S. M., 2005, Engineering geologic and geotechnical analysis of paleoseismic shaking using liquefaction effects: Field examples: *Engineering Geology*, v. 76, pp. 263-293.

Hajic, E. R., Wiant, M. D., and Oliver, J. J., 1995, Distribution and Dating of Prehistoric Earthquake Liquefaction in Southeastern Illinois, Central U.S.: National Earthquake Hazards Reduction Program, Final Technical Report to U.S. Geological Survey under agreement no. 1434-93-G-2359, 34 pp.

McNulty, W. E. and Obermeier, S. F., 1999, Liquefaction Evidence for at Least Two Strong Holocene Paleo-Earthquakes in Central and Southwestern Illinois, USA: *Environmental and Engineering Geoscience*, v. 5, no. 2, p. 133-146.

Munson, P. J., and Munson, C. A., 1996, Paleoliquefaction Evidence for Recurrent Strong Earthquakes Since 20,000 Years BP in the Wabash Valley Area of Indiana: report submitted to the U.S. Geological Survey in fulfillment of National Earthquake Hazards Reduction Program Grant No. 14-08-0001-G2117, 137 pp.

Munson, P. J., Obermeier, S. F., Munson, C. A., and Hajic, E. R., 1997, Liquefaction evidence for Holocene and latest Pleistocene seismicity in the southern halves of Indiana and Illinois: A preliminary overview: *Seismological Research Letters*, v. 68, pp. 521-536.

Olson, S. M., Green, R. A., and Obermeier, S. F., 2005, Revised magnitude bound relation for the Wabash Valley seismic zone of the central United States: *Seismological Research Letters*, v. 76, no. 6, pp. 756-771.

Pond, E. C., and Martin, J. R., 1997, Estimated magnitudes and accelerations associated with prehistoric earthquakes in the Wabash Valley region of the central United States: in Kolata, D. R., and Hildenbrand, T. G. (editors), *Investigations of the Illinois Basin Earthquake Region: Seismological Research Letters*, v. 68, pp. 611-623.

5.2.6 Central Virginia Seismic Zone

Dominion, 2004, Response to request for additional information no. 3, North Anna Early Site Permit Application, Dominion Nuclear North Anna, LLC, U.S. Nuclear Regulatory Commission, Report ML042800292, 110 p.

Green, R., Lasley, S., Carter, M. W., Munsey, J. W., Maurer, B. W., Tuttle, M. P., 2015, Geotechnical aspects in the epicentral region of the 2011 Mw 5.8 Mineral, Virginia, earthquake, in Horton, J.W., Jr., Chapman, M.C., and Green, R.A., eds., The 2011 Mineral, Virginia, earthquake, and its significance for seismic hazards in eastern North America: Geological Society of America Special Paper 509, doi:10.1130/2015.2509(09).

Obermeier, S. F., and McNulty, W. E., 1998, Paleoliquefaction evidence for seismic quiescence in central Virginia during late and middle Holocene time, EOS, Transactions of the American Geophysical Union, v. 79, no. 17, Spring Meeting Supplement, Abstract T41A-9.

Tuttle, M.P., 2016, Earthquake Potential of the Central Virginia Seismic Zone, U.S. Geological Survey, Earthquake Hazards Program, Final Technical Report, Award G13AP00045, 32 p.

Tuttle, M. P., Wolf, L., Dyer-Williams, K., Starr, M. E., Lafferty, R. H., Haynes, M., Morrow, J. Scott, R., Busch, T., Moseley, C., Tucker, K., and Karrenbauer, C., 2018, Paleoliquefaction studies in moderate seismicity regions with a history of large events: U.S. Nuclear Regulatory Commission, Contract NRC-HQ-11-C-040041, this volume.

5.2.7 MA-NH Area

Tuttle, M., and Seeber, L., 1991, Historic and prehistoric earthquake-induced liquefaction in Newbury, Massachusetts: *Geology*, v. 19, pp. 594-597.

Tuttle, M.P., 2007, Re-evaluation of Earthquake Potential and Source in the Vicinity of Newburyport, Massachusetts: U.S. Geological Survey, Earthquake Hazards Program, Final Technical Report, Award 01HQGR0163.

Tuttle, M.P., 2009, Re-evaluation of Earthquake Potential and Source in the Vicinity of Newburyport, Massachusetts: U.S. Geological Survey, Earthquake Hazards Program, Final Technical Report, Award 03HQGR0031.

5.2.8 SE Quebec Region

Law, K.T., 1990, Analysis of soil liquefaction during the 1988 Saguenay earthquake: *Proceedings of the 43rd Canadian Geotechnical Conference, Quebec*, v. 1, pp. 189-196.

Tuttle, M.P., 1994, The Liquefaction Method for Assessing Paleoseismicity, U.S. Nuclear Regulatory Commission, NUREG/CR-6258, 38 pp.

Tuttle, M.P., Such, R., and Seeber, L., 1989, Ground failure associated with the November 25th, 1988 Saguenay earthquake in Quebec Province, Canada: in Jacob, K., ed., The 1988 Saguenay Earthquake of November 25, 1988, Quebec, Canada: Strong Motion Data, Ground Failure Observations, and Preliminary Interpretations, Buffalo, New York, National Center for Earthquake Engineering Research, pp. 1-23.

Tuttle, M., Law, T., Seeber, L., and Jacob, K., 1990, Liquefaction and ground failure in Ferland, Quebec, triggered by the 1988 Saguenay Earthquake: *Canadian Geotechnical Journal*, v. 27, pp. 580-589.

Tuttle, M. P., Cowie, P., and Wolf, L., 1992, Liquefaction induced by modern earthquakes as a key to paleoseismicity: A case study of the 1988 Saguenay earthquake: in Weiss, A., ed., Proceedings of the Nineteenth International Water Reactor Safety Information Meeting, NUREG/CP-0119, v. 3, pp. 437-462.

Tuttle, M. P., and Atkinson, G. M., 2010, Localization of large earthquakes in the Charlevoix seismic zone, Quebec, Canada during the past 10,000 years: *Seismological Research Letters*, v. 81, no. 1, pp. 18-25.

5.3 References for CEUS Radiocarbon and OSL Dating Database

5.3.1 Charleston, South Carolina, Seismic Zone

Amick, D.C., *Paleoliquefaction Investigations Along the Atlantic Seaboard with Emphasis on the Prehistoric Earthquake Chronology of Coastal South Carolina*: unpub. Ph.D. dissertation, University of South Carolina, 1990.

Amick, D., Gelinias, R., Maurath, G., Cannon, R., Moore, D., Billington, E., and Kemppinen, H., 1990a, *Paleoliquefaction features along the Atlantic Seaboard*: U.S. Nuclear Regulatory Commission Report, NUREG/CR-5613.

Amick, D., Maurath, G., and Gelinias, R., 1990b, *Characteristics of Seismically Induced Liquefaction Sites and Features Located in the Vicinity of the 1886 Charleston, South Carolina Earthquake*: *Seismological Research Letters*, v. 61, no. 2, pp. 117-130.

Noller, J. S. and Forman, S. L., 1998, *Luminescence Geochronology of Liquefaction Features Near Georgetown, South Carolina*: in J.M. Sowers, J.S. Noller, and W.R. Lettis (eds.) *Dating and Earthquakes: Review of Quaternary Geochronology and Its Application to Paleoseismology*: U.S. Nuclear Regulatory Commission Report, NUREG/CR-5562, pp. 4.49-4.57.

Schaeffer, W. T., 1996, *Paleoliquefaction investigations near Georgetown, South Carolina*, M.S. thesis, Univ. of S. C., Columbia.

Talwani, P., and Cox, J., 1985, *Paleoseismic evidence for recurrence of earthquakes Near Charleston, South Carolina*: *Science*, v. 228, pp. 379-381.

Talwani, P., Rajendran, C. P., Rajendran, K., and Madabhushi, S., 1993, *Assessment of Seismic Hazard Associated with Earthquake Source in the Bluffton-Hilton Head Area*: Technical Report SCUREF Task Order 41, University of South Carolina at Columbia, 85 pp.

Talwani, P., Amick, D. C., and Schaeffer, W. T., 1999, *Paleoliquefaction Studies in the South Carolina Coastal Plain*: U.S. Nuclear Regulatory Commission Report NUREG/CR 6619, 109 pp.

Talwani, P., and Schaeffer, W.T., 2001, *Recurrence Rates of Large Earthquakes in the South Carolina Coastal Plain Based on Paleoliquefaction Data*: *Journal of Geophysical Research*, v. 106, no. B4, p. 6621-6642.

Weems, R. E., and Obermeier, S. F., 1990, *The 1886 Charleston earthquake—An overview of geological studies*: in *Proceedings of the U.S. Nuclear Regulatory Commission Seventeenth Water Reactor Safety Information Meeting*, NUREG/CP-0105, volume 2, pp. 289-313.

Weems, R.E., Obermeier, S.F., Pavich, M.J., Gohn, G.S., and Rubin, M., 1986, *Evidence for three moderate to large prehistoric Holocene earthquakes near Charleston, South Carolina*: in *Proceedings of the 3rd U.S. National Conference on Earthquake Engineering*, Charleston, South Carolina, v. 1, pp. 3-13.

5.3.2 New Madrid Seismic Zone

Aiken, M.J., *Science-Based Dating in Archaeology*, Longman Group, London and New York, 1990.

- Barnes, A. A., 2000, An interdisciplinary study of earthquake-induced liquefaction features in the New Madrid seismic zone, central United States: M.S. thesis, Auburn University, Alabama, 266 p.
- Bauer, L. M., 2006, Studies of Historic and Prehistoric Earthquake-induced Liquefaction Features in the Meizoseismal Area of the 1811-1812 New Madrid Earthquakes, Central United States: M.S. thesis, University of Memphis, Memphis, Tennessee, p. 135.
- Broughton, A. T., Van Arsdale, R. B., and Broughton, J. H., 2001, Liquefaction susceptibility mapping in the city of Memphis and Shelby County, Tennessee (in Earthquake hazard evaluation in the central United States): *Engineering Geology*, v. 62 (1-3), pp. 207-222.
- Browning, S. E., 2003, Paleoseismic studies in the New Madrid Seismic Zone, Central United States: M.S. thesis, Auburn University, Auburn, Alabama, 134 p.
- Buchner, C. A., Cox, R., Skinner, C. T., Kaplan, C., and Albertson, E. S., 2010, Data recovery excavations at the Laplant I Site (23NM51), New Madrid County, Missouri: Report to U.S. Army Corps of Engineers, Memphis District.
- Collier, J. W., 1998, Geophysical investigations of liquefaction features in the New Madrid seismic zone: Northeastern Arkansas and southeastern Missouri: M.S. thesis, Auburn University, Auburn, Alabama, 163 p.
- Cox, R. T., Van Arsdale, R. B., Harris, J. B., and Larsen, D., 2001, Neotectonics of the southeastern Reelfoot rift zone margin, central United States, and implications for regional strain accommodation: *Geology*, v. 29, pp. 419-422.
- Craven, J. A., 1995, Paleoseismological Study in the New Madrid Seismic Zone Using Geological and Archeological Features to Constrain Ages of Liquefaction Deposits: M.S. thesis, University of Memphis, 51 pp.
- Li, Y., et al., "Evidence for Large Prehistoric Earthquakes in the Northern New Madrid Seismic Zone, Central United States," *Seismological Research Letters*, 69(3):270-276, 1998.
- Noonan, B. J., 1999, Paleoseismology study of the Cache River Valley, southern Illinois, and New Madrid Seismic Zone, southeast Missouri and Northeast Arkansas, M. S. Thesis, Texas A & M University, College Station, Texas, 91 p.
- Saucier, R. T., 1991, Geoarchaeological evidence of strong prehistoric earthquakes in the New Madrid (Missouri) seismic zone: *Geology*, v. 19, pp. 296-298.
- Tuttle, M. P., 1999, Late Holocene Earthquakes and Their Implications for Earthquake Potential of the New Madrid Seismic Zone, Central United States: Ph.D. dissertation, University of Maryland, College Park, Maryland, 250 pp.
- Tuttle, M.P., "The Use of Liquefaction Features in Paleoseismology: Lessons Learned in the New Madrid Seismic Zone, Central United States," *Journal of Seismology*, 5:361-380, 2001.
- Tuttle, M. P., 2008, Paleoseismological investigations at the East Site, The Gilmore/Tyronza Mitigation Project, v. 4, Data Recovery at the Tyronza Sites, Poinsett County, Arkansas, The East Site (3P0610): in Technical Report to Arkansas State Highway and Transportation Department, pp. 259-277.
- Tuttle, M. P., 2010, Search for and Study of Sand Blows at Distant Sites Resulting from Prehistoric and Historic New Madrid earthquakes: Collaborative Research, M. Tuttle & Associates and Central Region Hazards Team, U.S. Geological Survey, Final Technical Report, Award 02HQGR0097, 48 pp.
- Tuttle, M. P., and Schweig, E. S., 1995, Archeological and pedological evidence for large earthquakes in the New Madrid seismic zone, central United States: *Geology*, v. 23, pp. 253-256.

Tuttle, M. P., Lafferty, R. H., III, and Schweig, E. S., III, 1998, Dating of liquefaction features in the New Madrid seismic zone and implications for earthquake hazard, U.S. Nuclear Regulatory Commission, NUREG/GR-0017, 77 p.

Tuttle, M., Chester, J., Lafferty, R., Dyer-Williams, K., and Cande, B., 1999, Paleoseismology Study Northwest of the New Madrid Seismic Zone: U.S. Nuclear Regulatory Commission, NUREG/CR-5730, 98 pp.

Tuttle, M. P., Sims, J. D., Dyer-Williams, K., Lafferty, R. H., III, and Schweig, E. S., III, 2000, Dating of Liquefaction Features in the New Madrid Seismic Zone: U.S. Nuclear Regulatory Commission, NUREG/GR-0018, 42 pp.

Tuttle, M. P., and Schweig, E. S., 2001, Towards a Paleoearthquake Chronology of the New Madrid Seismic Zone: U.S. Geological Survey, Earthquake Hazards Program, Progress Report, Award 99HQGR0022, 28 pp.

Tuttle, M. P., and Schweig, E. S., 2003, Search for and Study of Sand Blows at Distant Sites Resulting from Prehistoric and Historic New Madrid Earthquakes: U.S. Geological Survey, Earthquake Hazards Program, Progress Report, Award 02HQGR0097, 29 pp.

Tuttle, M. P., and Wolf, L. W., 2003, Towards a Paleoearthquake Chronology of the New Madrid Seismic Zone: U.S. Geological Survey, Earthquake Hazards Program, Progress Report, Award 01HQGR0164, 38 pp.

Tuttle, M. P., and Wolf, L. W., 2004, Towards a Paleoearthquake Chronology of the New Madrid Seismic Zone: U.S. Geological Survey, Earthquake Hazards Program, Final Report, Award 01HQGR0164, 36 pp.

Tuttle, M. P., and Schweig, E. S., 2004, Search for and Study of Sand Blows at Distant Sites Resulting from Prehistoric and Historic New Madrid Earthquakes: U.S. Geological Survey, Earthquake Hazards Program, Annual Project Summary, Award 02HQGR0097, 18 pp.

Tuttle, M. P., Schweig, E., III, Campbell, J., Thomas, P. M., Sims, J. D., and Lafferty, R. H., III, 2005, Evidence for New Madrid earthquakes in AD 300 and 2350 B.C.: *Seismological Research Letters*, v. 76, no. 4, pp. 489-501.

Tuttle, M., and Chester, J. S., 2005, Paleoseismology Study in the Cache River Valley, Southern Illinois: U.S. Geological Survey, Earthquake Hazards Program, Final Technical Report, Award HQ98GR00015, 14 pp.

Tuttle, M.P., E.S. Schweig, J. Campbell, P.M. Thomas, J.D. Sims, and R.H. Lafferty, "Evidence for New Madrid earthquakes in A.D. 300 and 2350 B.C.," *Seismological Research Letters*, 76(4):489-501, 2005.

Tuttle, 2010, Search for and study of sand blows at distant sites resulting from prehistoric and historic New Madrid earthquakes: Collaborative Research, M. Tuttle & Associates and Central Region Hazards Team, U.S. Geological Survey, Final Technical Report to the U.S. Geological Survey Earthquake Hazards Program, Award 1434-02HQGR0097, 48 p.

Tuttle, M. P., Lafferty, R. H., Cande, R. F., Sierzchula, M. C., 2011, Impact of earthquake-induced liquefaction and related ground failure on a Mississippian archeological site in the New Madrid seismic zone, central USA, *Quaternary International*, DOI 10.1016/j.quaint.2011.04.043

Tuttle, M. P., and R. Hartleb, "Appendix E. Central and eastern U.S. paleoliquefaction database, uncertainties associated with paleoliquefaction data, and guidance for seismic source characterization," in *The Central and Eastern U.S. Seismic Source Characterization for Nuclear Facilities*, Technical Report, EPRI, Palo Alto, CA, U.S. DOE, and U.S. NRC, 135 p., plus database, 2012.

Tuttle, M. P., Wolf, L., Dyer-Williams, K., Starr, M. E., Lafferty, R. H., Haynes, M., Morrow, J. Scott, R., Busch, T., Moseley, C., Tucker, K., and Karrenbauer, C., 2018, Paleoliquefaction studies in moderate seismicity regions with a history of large events: U.S. Nuclear Regulatory Commission, Contract NRC-HQ-11-C-040041, this volume.

Vaughn, J. D., 1994, Paleoseismology Studies in the Western Lowlands of Southeast Missouri: U.S. Geological Survey, Final Report, Award 14-08-0001-G1931, 27 pp.

Wolf, L.W., 2004, Geophysical Investigations of Earthquake-Induced Liquefaction Features in the New Madrid Seismic Zone: Earthquake Hazards Program, Final Technical Report, Award 01HQGR0003, 36 pp.

5.3.3 Marianna Area

Al-Shukri, H., Lemmer, R. E., Mahdi, H. H., and Connelly, J. B., 2005, Spatial and temporal characteristics of paleoseismic features in the southern terminus of the New Madrid seismic zone in eastern Arkansas: *Seismological Research Letters*, v. 76, no. 4, pp. 502-511.

Al-Shukri, H., Mahdi, H., Al Kadi, O., and Tuttle, M. P., 2009, Spatial and Temporal Characteristics of Paleoseismic Features in the Southern Terminus of the New Madrid Seismic Zone in Eastern Arkansas: U.S. Geological Survey, Earthquake Hazards Program, Final Technical Report, Award 07HQGR0069, 24 pp.

Al-Shukri, H., Mahdi, H., Tuttle, M.P., Dyer-Williams, K., 2015, Geophysical and paleoseismic investigations of large sand blows along a northwest-oriented lineament near Marianna, Arkansas, U.S. Geological Survey, Earthquake Hazards Program, Final Technical Report, Award G12AP20093, 31 p.

Tuttle, M. P., Al-Shukri, H, and Mahdi, H., 2006, Very large earthquakes centered southwest of the New Madrid seismic zone 5,000-7,000 years ago: *Seismological Research Letters*, v. 77, no. 6, pp. 664-678.

5.3.4 St. Louis Region

Tuttle, M., and Chester, J. S., 2005, Paleoseismology Study in the Cache River Valley, Southern Illinois: U.S. Geological Survey, Earthquake Hazards Program, Final Technical Report, Award HQ98GR00015, 14 pp.

Noonan, B. J., 1999, Paleoseismology study of the Cache River Valley, southern Illinois, and New Madrid Seismic Zone, southeast Missouri and Northeast Arkansas, M. S. Thesis, Texas A & M University, College Station, Texas, 91 p.

Tuttle, M. P., 2005, Improving the Earthquake Chronology for the St. Louis Region: U.S. Geological Survey, Earthquake Hazards Program, Annual Project Summary, Award 05HQGR0045, 6 pp.

Tuttle, M., Chester, J., Lafferty, R., Dyer-Williams, K., and Cande, B., 1999, Paleoseismology Study Northwest of the New Madrid Seismic Zone: U.S. Nuclear Regulatory Commission, NUREG/CR-5730, 98 pp.

5.3.5 New Madrid-Wabash Valley Region

Tuttle, M., and Dyer-Williams, K., 2017, Filling the gap in the paleoearthquake record between the New Madrid and Wabash Valley seismic zones, U.S. Geological Survey, Earthquake Hazards Program, Final Technical Report, Award G12AP20068, 88 p.

5.3.6 Wabash Valley Seismic Zone

Exelon Generation Company, 2004, Clinton Early Site Permit Application, Response to Request for Additional Information Letter No. 7, October 11.

Hajic, E. R., Wiant, M. D., and Oliver, J. J., 1995, Distribution and Dating of Prehistoric Earthquake Liquefaction in Southeastern Illinois, Central U.S.: National Earthquake Hazards Reduction Program, Final Technical Report to U.S. Geological Survey under agreement no. 1434-93-G-2359, 34 pp.

McNulty, W. E. and Obermeier, S. F., 1999, Liquefaction Evidence for at Least Two Strong Holocene Paleo-Earthquakes in Central and Southwestern Illinois, USA: Environmental and Engineering Geoscience, v. 5, no. 2, p. 133-146.

Munson, P. J., and Munson, C. A., 1996, Paleoliquefaction Evidence for Recurrent Strong Earthquakes Since 20,000 Years BP in the Wabash Valley Area of Indiana: report submitted to the U.S. Geological Survey in fulfillment of National Earthquake Hazards Reduction Program Grant No. 14-08-0001-G2117, 137 pp.

Munson, P. J., Obermeier, S. F., Munson, C. A., and Hajic, E. R., 1997, Liquefaction evidence for Holocene and latest Pleistocene seismicity in the southern halves of Indiana and Illinois: A preliminary overview: Seismological Research Letters, v. 68, pp. 521-536.

5.3.7 Central Virginia Seismic Zone

Dominion, 2004, Response to request for additional information no. 3, North Anna Early Site Permit Application, Dominion Nuclear North Anna, LLC, U.S. Nuclear Regulatory Commission, Report ML042800292, 110 p.

Tuttle, M.P., 2016, Earthquake Potential of the Central Virginia Seismic Zone, U.S. Geological Survey, Earthquake Hazards Program, Final Technical Report, Award G13AP00045, 32 p.

5.3.8 MA-NH Area

Tuttle, M., and Seeber, L., 1991, Historic and prehistoric earthquake-induced liquefaction in Newbury, Massachusetts: Geology, v. 19, pp. 594-597.

Tuttle, M.P., J.D. Sims, and D. Roy, 2000, Paleoseismology study of the Greater Boston, Massachusetts, area, U.S. Geological Survey, Final Report, 23 pp.

Tuttle, M.P., 2007, Re-evaluation of Earthquake Potential and Source in the Vicinity of Newburyport, Massachusetts: U.S. Geological Survey, Earthquake Hazards Program, Final Technical Report, Award 01HQGR0163.

Tuttle, M.P., 2009, Re-evaluation of Earthquake Potential and Source in the Vicinity of Newburyport, Massachusetts: U.S. Geological Survey, Earthquake Hazards Program, Final Technical Report, Award 03HQGR0031.

5.3.9 SE Quebec Region

Tuttle, M.P., 1994, The Liquefaction Method for Assessing Paleoseismicity, U.S. Nuclear Regulatory Commission, NUREG/CR-6258, 38 pp.

Tuttle, M.P., 2008, Paleoseismic investigation of long term rates of large earthquakes in the Charlevoix seismic zone and proposed Rabaska site region. Report to Rabaska, Inc., Montreal, Quebec.

APPENDIX A GEOLOGIC TIME SCALES

INTERNATIONAL CHRONOSTRATIGRAPHIC CHART
 v 2016/12
 International Commission on Stratigraphy



www.stratigraphy.org

International Commission on Stratigraphy

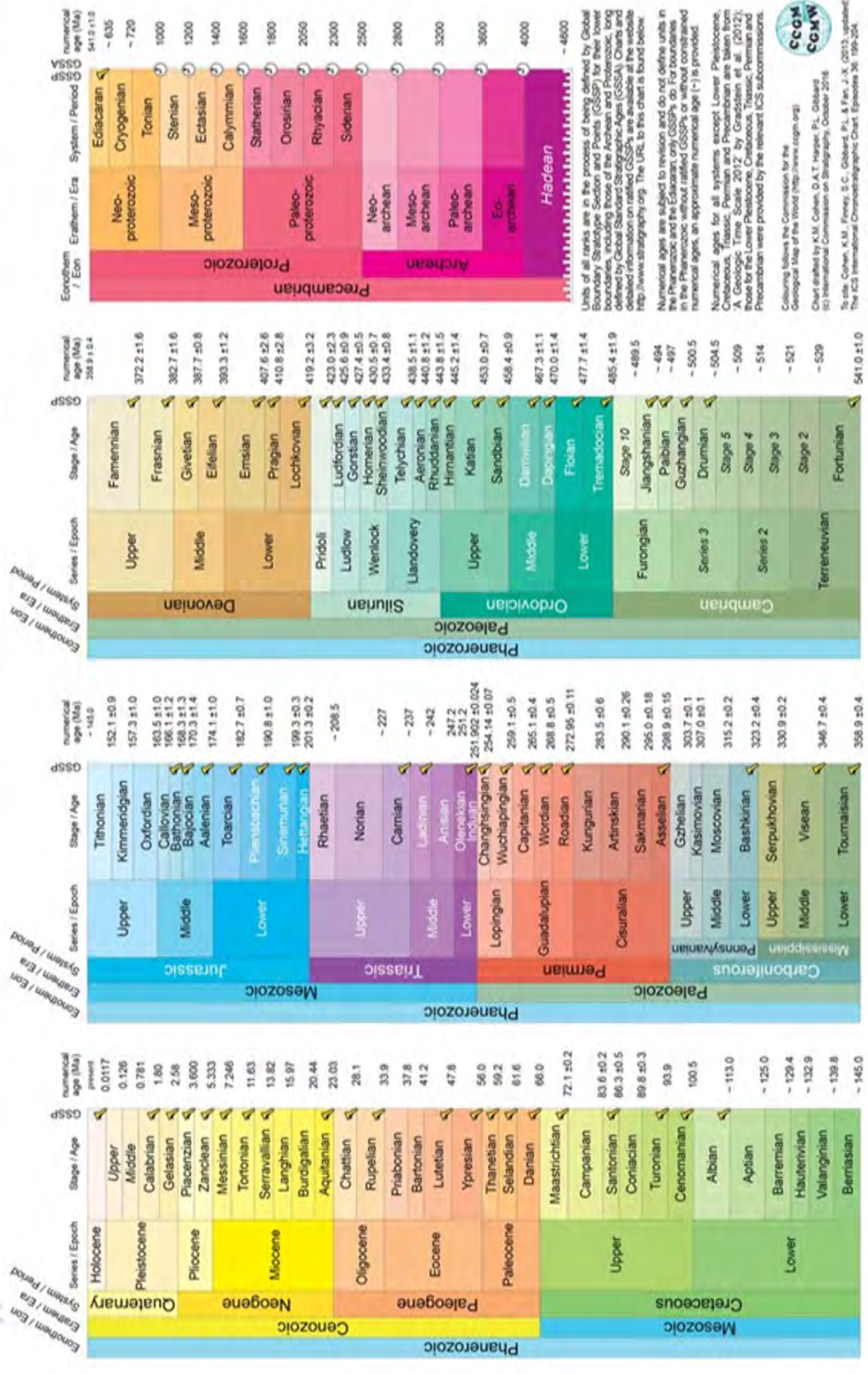
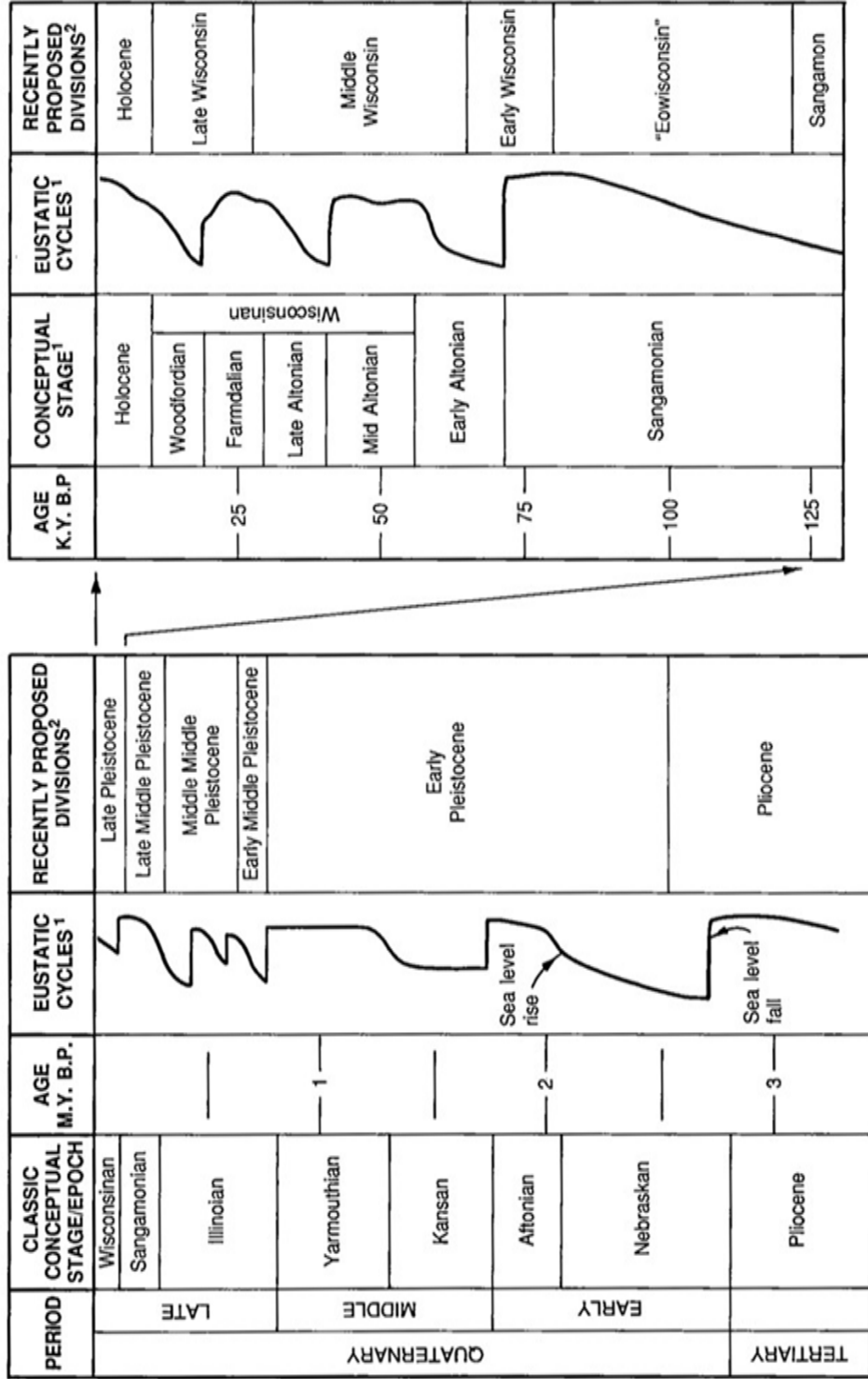


Figure A-1 Updated International Chronostratigraphic Chart (from Cohen et al., 2013)



¹ FROM BEARD, SANGREE AND SMITH (1982)

² FROM MORRISON (1991) AND RICHMOND AND FULLERTON (1986)

Figure A-2 Geologic column for the Quaternary period showing conceptual stages and generalized sea level curve indicating eustatic cycles (from Saucier, 1994).

APPENDIX B FEDERAL REGULATIONS

Federal agencies must comply with the National Environmental Policy Act and the National Historic Preservation Act when conducting or funding a paleoliquefaction field study. Compliance with the National Environmental Policy Act may require the federal agency to perform an environmental assessment and/or an environmental impact statement to assess the effects of field activities on the environment. Some federal agencies have categorical exclusions for geologic reconnaissance activities that preclude the need for performing these environmental studies. In addition, the National Historic Preservation Act requires the federal agency to comply with the section-106 process described in the Code of Federal Regulations (36 CFR 800). This process requires coordination and communication with State Historic Preservation Officers and Native American Tribes prior to initiating ground disturbing activities.

B.1 Section 106 and Investigations of Sand Blows in the New Madrid Seismic Zone

In the study region, most sand blows resulting from earthquake-induced liquefaction do not occur at archaeological sites. However, for sand blows that do occur at archaeological sites, a two-phased process was developed in order to comply with section 106 of the National Historic Preservation Act. The process involves assessing a site and developing an excavation plan for review by State and Tribal Historic Preservation Officers followed by excavating and studying sand blows and related sand dikes as well as associated archaeological deposits.

B.1.1 Phase 1

Prior to excavation, the surface of the study site is systematically surveyed to understand the areal distribution of artifacts relative to sand blow(s) previously identified during reconnaissance. If there are few artifacts, they will be flagged for later mapping. If there are many artifacts, the perimeter of the artifact scatter will be flagged. A collection of artifacts is made of the sand blow area. If the artifact density is greater than about one artifact per square meter, a controlled surface collection is made of an area at least 20 m x 20 m (400 square meters, 0.04 hectare).

Geophysical surveys, using conductivity, resistivity, magnetic gradients, and/or ground penetrating radar, are made of the sand blow area. The area surveyed is usually about 40 m x 40 m. The surveys may yield maps and/or vertical profiles of subsurface conditions. The goals of the surveys are to define the area of the sand blow(s), to locate their feeder dikes, and if possible, to identify cultural horizons and features spatially associated with the sand blow(s). This information, along with that regarding artifact distribution, is used to locate proposed trenches for subsurface study of the liquefaction features and any associated archaeological horizons or features, as well as to collect samples for dating.

Shovel testing and/or hand augering will be performed in the footprint of the proposed trenches to determine the presence or absence of archaeological deposits and to assess the impact that trenching would have on such deposits. The archaeological testing is conducted every 10 m along the line of the proposed trenches.

A topographic map is made of the study site, showing locations of individual artifacts, artifact scatters, controlled surface collections, geophysical surveys, proposed trenches, and

archaeological test units. The map also shows any modern cultural features, natural features, and datums. Finally, a site evaluation report is prepared and submitted to the appropriate State and Tribal Historic Preservation Officers for review.

B.1.2 Phase 2

Following review of the site evaluation report and acceptance of the excavation plan by the appropriate State and Tribal Historic Preservation Officers, subsurface investigation of the sand blow(s) may begin.

The locations of the proposed trenches are re-established and a backhoe is usually used to excavate the trench. It is preferable to use a 1-m wide bucket with a smooth cutting edge so that the excavation surface can be carefully monitored and that a 1-m wide trench with relatively straight walls can be excavated. If excavating in a plowed field, which is often the case in the New Madrid seismic zone, the already disturbed plow zone is carefully stripped away. The base of the plow zone is shovel-skimmed and/ or troweled to expose any archaeological features or artifacts on the surface of the undisturbed sub-plow zone. If such features or artifacts are found, they are excavated and collected by an archaeologist using recovery techniques described below.

During excavation and collection, archaeological features are thoroughly documented. The exposed portion of a feature is photographed in plan and profile views, scaled drawings of both views are made, and datum(s) may be set in the profile. Excavated matrix is bagged in 4 mil polyethylene bags and labeled per the State Plan requirements (Site #, field serial and feature numbers, depth, location, date, feature portion, stratum, and the excavators initials). Approximately half of the feature is excavated and saved for processing using the flotation recovery technique in order to obtain charred material (including charred seeds, maize kernels, wood, and insects) as small as 0.32 mm. The remainder of the excavated feature fill is examined for cultural materials (pottery, fire-cracked rock, fired clay, nut charcoals, flint tools, etc) larger than 1/16 ". Approximately one cup of soil matrix is retained for further analysis, if necessary.

Stripping continues through the sterile sand blow to the surface of the soil or sediment below. Sites of liquefaction may have suffered ground failure, including vertical and lateral displacements, during the earthquake. The ground failure may be symmetrical or asymmetrical and can vary from several to several hundred centimeters across a site. Therefore, the sand blow must be excavated relatively slowly in order to expose the surface of the buried soil or sediment. The buried surface is troweled and/or shoveled-skimmed by the archaeologist and paleoseismologist searching for artifacts, features, and other potentially datable materials. If no cultural material is found, the trench is deepened in order to expose the sand dike.

The walls of the trench reveal cross sections of the sand blow and sand dike which are logged by the paleoseismologist at a scale of 1" = 25 cm or 50 cm depending on the complexity of the geologic features. The trench also provides access to organic and sediment samples that are collected by the paleoseismologist for dating of the liquefaction features and their causative earthquake(s). If an archaeological feature is exposed in the trench wall, that portion is left *in situ* and documented in the log of the trench wall.

If an intact archaeological sheet midden or cultural horizon is found above or below the sand blow, one or more 1 m × 1 m test units are excavated. The excavated material is screened through ¼-inch hardware cloth or stainless steel pierced planking (PSP) with ¼ inch diameter openings.

All materials retained by the screen are collected, bagged, labeled, and recorded in a Field Specimen Number (FSN) log. Excavation levels within intact deposits are a maximum of 10 cm thick and at times as thin as 2 cm. The test unit(s) is excavated through the artifact-bearing cultural horizon until sterile soil is encountered.

Recovered artifacts are taken to the archaeological laboratory for identification and description. Descriptions of archaeological field and laboratory methods employed, identification of cultural materials and/or features and interpretation of the cultural periods they represent are included in a report on the paleoseismic investigation at the site.

If there are intact cultural deposits above or below the sand blow that meet Criterion d of the National Register of Historic Places (NRHP) regulations for a significant site, a report is submitted on the State Site form including documentation and analysis of samples and summary of the work accomplished.

B.2 Section 106 and Reconnaissance for Liquefaction Features Along Rivers and Ditches in the New Madrid Seismic Zone

Reconnaissance is performed along rivers and large drainage ditches across the New Madrid region in order to find and date paleoliquefaction features and to define the area of liquefaction induced by paleoearthquakes. During the reconnaissance, paleoliquefaction features are sought by examining actively eroding cutbanks of the rivers and ditches.

Few archaeological sites are likely to be encountered during reconnaissance and any sites that are encountered will not be disturbed. Due to the limited scope and minor disturbance, reconnaissance is expected to have a "no adverse effect" on historic properties. Nevertheless, the appropriate State and Tribal Historic Preservation Officers are provided a list of rivers and accompanying maps showing the portions of those rivers to be searched at least three months in advance of the fieldwork

Reconnaissance should be conducted when water levels are low and cutbanks well exposed. Therefore, in the New Madrid seismic zone reconnaissance is performed usually during the months of August through November. Reconnaissance is conducted by using a canoe or motorboat to navigate the rivers and ditches, examine the cutbanks, and access liquefaction sites to document features and collect samples for dating. Based on past experience in the region, it is likely that 2 to 14 features per 10 km stretch occur along the waterways. At locations where liquefaction features are found, the boat is anchored and 1 to 2 researchers access the shore on foot. The researchers are onshore from a few minutes to a few hours, the time required to better expose the liquefaction features, to document and photograph the features and host sediment, and in some cases, to collect samples for dating. The areas scraped in order to expose the liquefaction features and collect samples range from 17 cm x 17 cm x 2 cm to 1.3 m x 1.3 m x 5 cm. Sampling will be done by hand with a standard shovel or smaller hand tools. Samples collected may include a few organic samples such as leaves and twigs for radiocarbon dating and one or two sediment samples, approximately 2 inches in diameter by 6 inches in length, for optically luminescence dating. At some sites, no samples will be collected at all.

Liquefaction features found and documented along rivers and ditches, dating results of samples, and interpretation of the findings are included in a report on liquefaction record of past earthquakes.

APPENDIX C REVIEW OF FIELD DATA COLLECTION

As part of this project, various approaches to field data collection was reviewed (British Antarctic Survey Staff, 2011). MTA's standard field practice has been to record detailed site information using printed forms, to annotate paper copies of topographic maps, to use hand-held GPS to determine site coordinates, and to take photographs using a stand-alone digital camera. The majority of the recorded data is later manually keyed into the computer using Microsoft Excel and added to the paleoliquefaction database and using Microsoft Word to create data tables for reports. Although this approach has worked well over many years, the inefficiencies of duplicate data entry, as well as the potential for human error in paper-to-computer transfer, are good reasons to consider replacing the customary practice with digital data collection. Ideally, use of a data collector would allow site information collected in the field to be easily exported as pre-formatted text or shapefiles, along with associated image files, and then integrated into the existing paleoliquefaction database in a streamlined process. Adopting a digital methodology would also promote other useful outcomes, such as standardization of data collection and entry and more efficient processes for sharing and repurposing data.

In 2011, after online review of the most promising and reasonably priced hand-held data collectors on the market for field scientists, MTA selected, purchased, and tested the Trimble Nomad 900 GLC. When the Nomad proved difficult to use effectively to fully record site information, MTA purchased (at no cost to the contract) and tested an Apple iPad to see if using a tablet would resolve some of the problems encountered using the Nomad. The pros and cons of using the different units for data recording during fieldwork are detailed below.

C.1 Trimble Ultra-Rugged Hand-Held Nomad 900 GLC

The Trimble Nomad 900 GLC was the first unit selected and field-tested. Trimble is a long-lived company known for its rugged hand-held computers with integrated GPS. Many Trimble products are used in engineering and geology and other fields that require remote data collection. The Trimble Nomad configuration purchased by MTA included a GPS receiver (2-4 meters accuracy, WAAS corrected), a 5 megapixel-digital camera, Windows Mobile operating system running ArcPad, and Esri's mobile GIS mapping software. ArcPad supports multiple data layers, including background topographic maps and customized data entry forms, and uses the shapefile format, thus providing seamless integration with other Esri products, including ArcGIS Desktop (used by MTA).

While the functionality of the Nomad 900GLC looked promising, creating a simple data entry form that mirrored the long-used paper form proved hard to accomplish effectively. The standard site description form includes fields for information about the site as a whole, the liquefaction features found, and the samples collected for dating, as well as an area for sketching diagrams of geologic exposures and liquefaction features. In the Nomad data entry form, fields for these different elements were grouped under several tabs, and drop-down pick lists were used wherever possible to streamline data entry. Even so, the numerous data fields and small data entry display of the Nomad 900GLC made the form hard to use, and there was, not surprisingly, no functionality for field sketching. Additionally, although the camera worked well enough, the 5-megapixel resolution was not adequate quality for the detailed documentation of liquefaction features.

Pros: Reliable company, well-tested products, support available; GPS accuracy is good and well documented; easy to share shapefile data with ArcGIS; camera is integrated; customizable form; long-lived battery; rugged for outdoor use.

Cons: camera resolution too low for detailed photos; no easy way to export data in preferred format (csv text files); screen display small; form design not intuitive and requires separate software on PC; platform is PC only; relatively expensive (\$2600 in 2011 for hardware and software); unable to create site sketches.

C.2 Apple iPad 3rd Gen (Wi-Fi Only), Plus Dual XGPS 150A Bluetooth GPS

The Apple iPad was purchased to test in the field, in particular to see if it was easier to use for recording the many different kinds of data required (descriptive text, numbers, sketches, picking from dropdown lists, etc.). An online review was conducted, this time for GIS “apps” for phones and tablets designed for the collection of field data (Chaucer et al., 2012; Camp and Wheaton, 2014). The ability to add custom fields was critical. The review revealed that, while there are many GIS apps available, either free or at low cost, the majority are geared towards outdoors enthusiasts and are not robust enough in their capabilities for MTA’s use. Avenza’s PDF Maps is one example – easy to add data and background maps, but not flexible enough in terms of customization. There are also GIS enabled “form building” apps (GPS World Staff, 2016). Some of these, such as Fulcrum, which provides many templates for different kinds of field use and allows customization of data entry forms, looked promising but were not selected as they were geared towards office environments with multiple employees in the field and required a subscription. Ultimately, Garafa’s GIS Kit was purchased (\$99) for use with the iPad. As the wi-fi only iPad does not have an internal GPS, a Dual XPS bluetooth GPS receiver was purchased (\$99) in order to access GPS through iPad/GIS Kit, along with an associated app, GPS status tool, which provided accuracy readings. Creating custom forms with dropdown lists and text fields was straightforward in GIS Kit, as was adding site photos via the form. See below for two screen shots of sections of the form in use. The upper screen shot shows the location of sites on a topographic map and attribute data of liquefaction features at site SF16 selected on the map (Figure C-1). The lower screen shot shows photographs taken at site SF16 (Figure C-2).

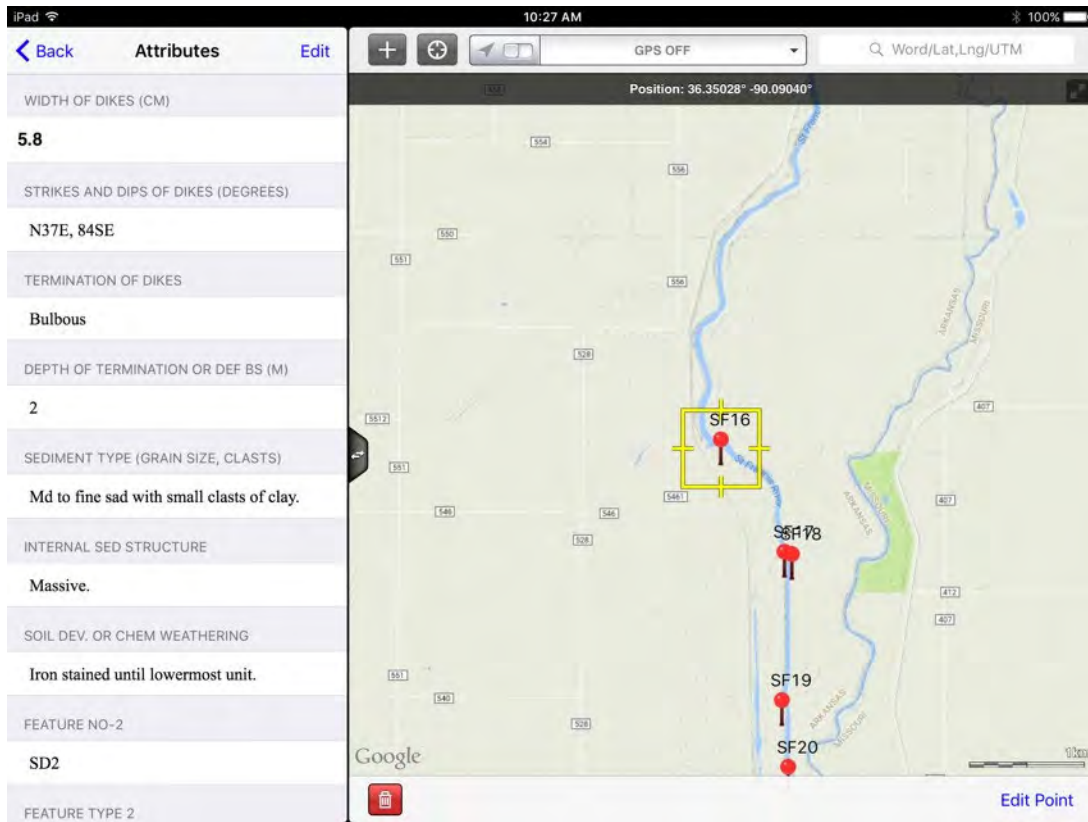


Figure C-1 Screenshot of MTA site form tested in GIS Kit app, showing site locations and attributes.

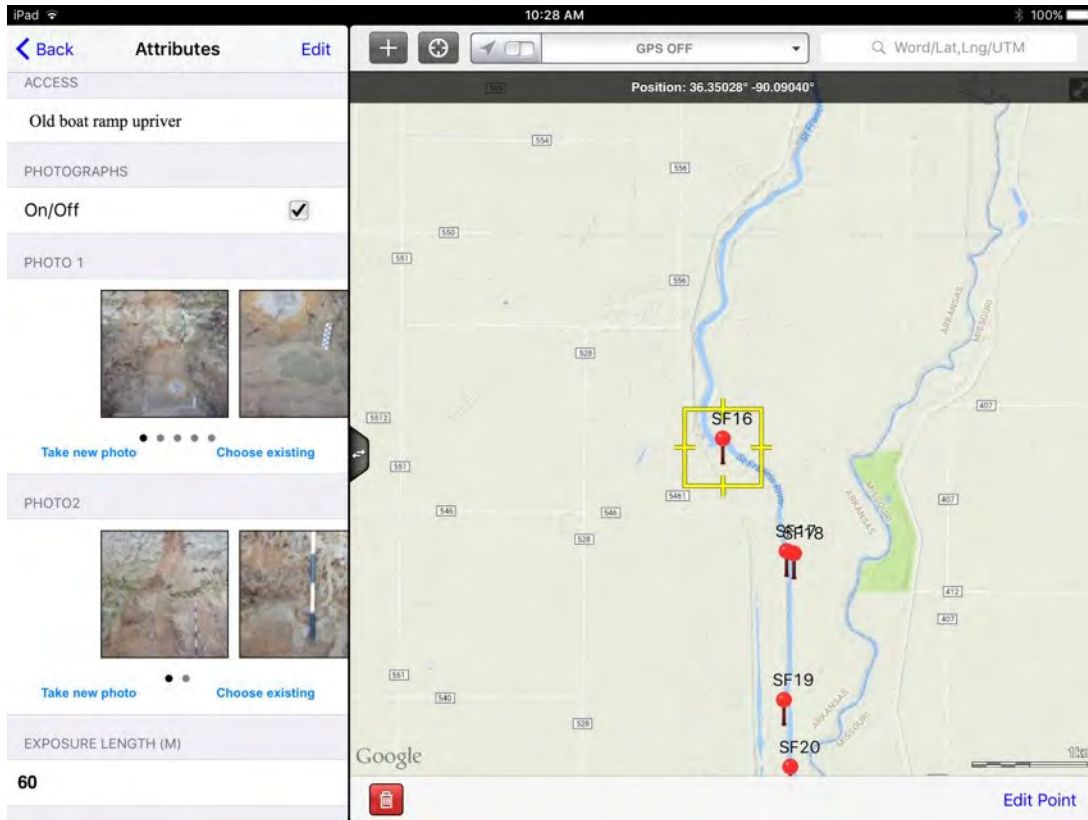



Figure C-2 Screenshot of MTA site form tested in GIS Kit app, showing site locations and geo referenced site photos.


Data import/export worked well, although for the GIS Kit version of the app, kml format is the only export option. The GIS Pro version includes many of the standard formats used in mapping software (shapefile, csv, kml, gpx etc). MTA purchased the less expensive version of the app for the purpose of testing, but would recommend the Pro version for full implementation in the field. See below for GIS Kit/GIS Pro comparison (Figure C-3):

GIS Pro vs. GIS Kit:

Feature	Kit	Pro	Feature	Kit	Pro	Feature	Kit	Pro
Import			Maps			Linear Distance		
GPX	x	x	Google Satellite	x	x	Meters	x	x
KML	x	x	Google Street	x	x	Yards	x	x
SHP	x	x	Google Hybrid	x	x	Nautical Miles	x	x
KMZ	x	x	Bing Street	x	x			
Export			Bing Topo	x	x	GPS		
GPX	x	x	Bing Satellite	x	x	Distance Filter	x	x
KML	x	x	Open Street Map	x	x	Time Filter	x	x
CSV with attributes		x	Open Topo Map	x	x	Accuracy Filter	x	x
SHP		x	Custom	x	x	Ultra Accuracy	x	x
KMZ	x	x	Offline	x	x	Compass	x	x
File Transfer			WMS		x	Feature Classes		
Mail	x	x	Raster		x	Points	x	x
iTunes	x	x	Coordinate Systems			Lines	x	x
Layers			Lat/Long	x	x	Polygons	x	x
Create	x	x	MGRS	x	x	Create/Customize	x	x
Move/Copy	x	x	USNG	x	x	Organize	x	x
Opacity	x	x	UTM	x	x	Share		x
Visibility On/Off	x	x	Area			Feature Collection		
Measure			Acres	x	x	GPS Tracking	x	x
Length	x	x	Sq Kilometers	x	x	Point Edit	x	x
Perimeter	x	x	Sq Miles	x	x	Line Edit	x	x
Area	x	x	Hectares	x	x	Polygon Edit	x	x
						Track Edit	x	x
						Pictures	x	x
						Text	x	x
						List of Values	x	x
						Custom Attributes	x	x



Using GIS Kit:
The 'Kit' version of this software is intended to allow individuals to collect accurate & sophisticated field data without being tied to an expensive server or IT unit. Anyone can easily create their own feature classes & datasets and use them to gather & interpret useful data in the field.



Using GIS Pro:
The 'Pro' version of this software gives you all the advantages of the 'Kit' version but offers more collaborative options such as SHP file export & feature class dataset sharing & WMS support. It also supports Raster data.

Figure C-3 Comparison of Features Available in Garafa's GIS Pro and GIS Kit

Pros: iPad screen size (9.7 inch) good for data entry and review; GIS Kit custom form building tool easy to use; import/export straightforward; tablet plus app more affordable than Nomad plus software; easy to cache maps to use when offline.

Cons: Not as rugged as Trimble – used sturdy case (by Lifeproof) which makes the tablet heavier and less responsive to touch; inconvenient having to use Bluetooth GPS; camera easy to use but still only 5 megapixels; unable to create site sketches within app; Apple IOS compatible only.

C.3 Summary

Unfortunately, neither of the data collecting devices evaluated proved ideal for data collection in the field as it was difficult to translate all of the information recorded on the paper form to the custom digital forms. For both devices, descriptive text was more cumbersome to add “digitally” than manually and there was no easy way to include options for sketching of exposures and features to the digital forms. The cameras, at the time of testing, were by today’s standards fairly

low resolution, producing images that were useful for basic site documentation, but not for detailed observations or inclusion in publications. However, as outlined above, the benefits of digital data collection using mobile devices are clear and the technology and tools will only improve. Based on MTA's field-testing of the Trimble and iPad, the iPad (or equivalent tablet) seems to offer the best options going forward when balancing versatility, affordability, and ease of use. In the short-term, some of the problems encountered with the iPad could be resolved by using a model with a better camera, and built in GPS which is available in all iPads with the cellular option (cellular does not need to be turned on), and by using sketching and voice-to-text-recognition apps to supplement the data collecting app. This approach would be uncomplicated, inexpensive, would not require a great deal of technical expertise to implement, and would result in born digital data that can easily be shared, analyzed, transformed, and reused.

APPENDIX D UPDATE OF CEUS PALEOLIQUEFACTION DATABASE

See Excel workbook

D.1 General Guidelines

- Column headings should be in all CAPS with no <spaces>. Use ‘underscore’ (“_”) in place of <space>, as needed.
- Column headings should be no more than 10 characters in length.
- Alphabetic field entries should have no more than 254 characters (including <spaces>), lest they be truncated.
- Numeric fields should not contain alphabetic characters or symbols.
- For fields where no data are available or that do not apply, leave field blank.

D.2 Field-Specific Guidelines

This section describes each data field and provides instruction regarding how to (and how not to) tabulate data. Each data field is described individually and in the order in which they should appear in the database.

KEY: Unique numeric designator for each entry in database. Use the following ranges for the specified priority study areas:

- 1000 – 1140: Charleston seismic zone and surrounding region (CHSZ)
- 2000 – 2871: New Madrid seismic zone and Western Lowlands (NMSZ)
- 3000 – 3090: Marianna, Arkansas Region (MAR)
- 4000 – 4122: St Louis Region (STL)
- 5000 – 5061: Region between New Madrid and Wabash Valley seismic zones (NM-WV)
- 6000 – 6232: Wabash Valley seismic zone (WVSZ)
- 7000 – 7032: Central Virginia seismic zone (CVSZ)
- 8000 – 8015: Newburyport, Massachusetts and surrounding region (MA-NH)
- 9000 – 9047: Charlevoix seismic zone and Saguenay region (SE QUEBEC)

SITE_NAME: Alphabetic. Examples: “Desha Kelso”, “Georgetown”, “Bluffton.”

FEAT_ID: Alphabetic. Unique feature identifier that combines shortened version of site name. Examples: “DK-1” for Desha Kelso-1 -or- “Bluf-2” for Bluffton-2.

XCOORD: Numeric. Longitude, in decimal degrees. All values should be negative (“-”).

YCOORD: Numeric. Latitude, in decimal degrees. All values should be positive.

COORD_ORIG: Alphabetic. Description (≤ 254 characters) of positional data, including reference shorthand (examples: “digitized from Talwani and Schaeffer (2001) Figure 1” -or- “unpublished hand-held GPS coordinates from Talwani”).

OBS_TYPE: Alphabetic. Choose from one of the following:

- trench
- cutbank
- air photo
- quarry
- field mapping
- test pit / auger

FEAT_TYPE: Alphabetic. Choose from one of the following:

- sand blow
- crater fill
- dike
- sill
- SSD [for soft sediment deformation structures that are likely to be EQ-related]

SSD_DESCR: Alphabetic. This field is only used where “SSD” is entered in the previous column. Description (≤ 254 characters) of SSD and assessment of likelihood that it is/is not EQ-related. Features that are clearly non-EQ-related are not included in the database.

FEAT_REF: Alphabetic. Reference shorthand for FEAT_TYPE and, where applicable, SSD_DESCR, listed in previous 2 columns (example: “Hall and Oates (1982)”). Multiple reference shorthand entries are acceptable, as long as total number of characters is ≤ 254 .

SB_THICK,
SB_WIDTH,
SB_LENGTH,
DK_WIDTH, and

SILL_THICK: Numeric. All dimensions are in cm. Because these dimensions typically are from limited trench exposures, values typically are minimum values (with a few exceptions). Additional descriptive info can be entered into the COMMENT field, as needed.

DIM_REF: Alphabetic. Reference shorthand for dimensional values listed in previous 5 columns (example: “Talwani and Schaeffer (2001)”).

14C_MAX: Numeric. Lower bracketing 2-sigma radiocarbon age on feature, in yrs B.P. relative to 1950 AD.

14C_MIN: Numeric. Upper bracketing 2-sigma radiocarbon age on feature, in yrs B.P. relative to 1950 AD.

14C_REF: Alphabetic. Reference shorthand for radiocarbon data listed in previous 4 columns (example: "Hall and Oates (1982)").

OSL_MAX: Numeric. Lower bracketing 2-sigma OSL age on feature, in yrs B.P. relative to 1950 AD.

OSL_MIN: Numeric. Upper bracketing 2-sigma OSL age on feature, in yrs B.P. relative to 1950 AD.

OSL_REF: Alphabetic. Reference shorthand for OSL data listed in previous 4 columns (example: "Hall and Oates (1982)").

PREFAGEEST: Numeric. In most cases, this will simply be the value midway between either: (1) 14C_MAX and 14C_MIN; and/or (2) OSL_MAX and OSL_MIN, in yrs B.P.. However, in special circumstances, this value may represent a researcher's preferred age estimate, based on specific archeological, stratigraphic or other criteria.

PREFAGEUNP: Numeric. This value represents the "+" portion of the 2-sigma "±" uncertainty value associated with the PREFAGEEST value (the final "P" in the column heading stands for "plus").

- In most cases this value will be symmetric about the PREFAGEEST value. In other words, a preferred age estimate of 600 ± 200 yrs B.P. should be entered into the database as follows: enter "600" in PREFAGEEST field, enter "200" in the PREFAGEUNP field, and enter "200" in the PREFAGEUNM field.
- In some cases, the uncertainty will be asymmetric about the PREFAGEEST (e.g., 600 +200/-150 yrs B.P.). Enter "600" in PREFAGEEST field, enter "200" in the PREFAGEUNP field, and enter "150" in the PREFAGEUNM field (described below).

PREFAGEUNM: Numeric. This value represents the "-" portion of the 2-sigma "±" uncertainty value associated with the PREFAGEEST value (the final "M" in the column heading stands for "minus"). See above.

PREFAGEREF: Alphabetic. Reference shorthand for preferred age and preferred age uncertainty data listed in previous 3 columns (example: "Hall and Oates (1982)"). Multiple reference shorthand entries are acceptable, as long as total number of characters is ≤ 254.

STRAT: Alphabetic. Description (≤ 254 characters) of qualitative age data, if any.

ARCHEO: Alphabetic. Description (≤ 254 characters) of archaeological age data, if any.

WEATHERING: Alphabetic description (≤ 254 characters) of degree of weathering of feature (NOT weathering of surrounding sediments), if available. Includes reference shorthand info as well (example: "Hall and Oates (1982)").

GEOTEC: Alphabetic. Enter “local” or “regional” for the type of geotechnical data available for the feature or site. If no geotechnical data available, leave blank.

GEOTEC_REF: Alphabetic. Reference shorthand for geotechnical data listed in previous column (example: “Green and Olson (2009)”).

COMMENT: Alphabetic. Description (\leq 254 characters) of other relevant data not captured in other fields. Note, if $>$ 254 characters required, comment can be continued in COMMENT2 and COMMENT3 fields.

APPENDIX E CEUS RADIOCARBON AND OSL DATING DATABASES

See Excel workbooks

APPENDIX F ARCHAEOLOGICAL REPORT FOR CARAWAY, WILDY, AND GARNER SITES

F.1 Introduction

Archaeological investigations were carried out at the Garner site (3CG1255) in northern Craighead County, at the Faulkner #1 and #2 sites (3CG1253 and 3CG1254) south of Caraway in extreme southeastern Craighead County, and nearby at the Wildy (3MS909) site in extreme western Mississippi County, west of Manilla. These investigations were to determine the presence or absence of intact cultural deposits at locations proposed for geological trenching, and to collect archaeological data during the excavation of geologic trenches at the Garner site. This appendix begins with background material on the natural environment as it pertains to cultural history (Section F.2) and previous archaeological investigations and land use history (Section F.3) followed by a brief description of archaeological methods used (Section F.4). The archaeological evaluations are presented (Section F.5) followed by the results of the archaeological investigations (Section F.6). Conclusions drawn from the work and recommendations in terms of the National Register of Historic Places criteria for eligibility are presented last (Section F.7).

F.2 Environment

The area of the Faulkner #1 and #2 (3CG1253 and 3CG1254) sites lies in a large tract of Amagon-Dundee poorly and somewhat poorly drained, level, loamy soils. These soils formed on low terraces and natural levees. The two adjacent sites are about 8 miles east of St. Francis River. The vicinity lies in extreme southeast Craighead County, in an area that has been extensively modified by historic drainage ditches and modern land leveling. The sites' areas are mapped as Mhoon fine sandy loam (soil code 34). The slough between these sites is mapped as Roellen silty clay loam (soil code 36). This slough was still wooded in 1977 (Ferguson 1979: Sheet 54). In contrast to much of the surrounding area with distinct sand-blow stippling, this 1977 air photo of the Faulkner vicinity shows rather more continuous sand scatter along both the east and west banks of the unnamed slough (Figure F-1). While this may be a natural distribution along an old natural levee, it is also possible that the site soils were already culturally modified by agricultural practices. The 1977 air photo forms the first of a series of air/satellite images for the project area which elucidate changes in cultural practices. In the Caraway vicinity, a farmstead, including a barn northeast of the home, lies in the southwest corner of the quarter-quarter section surveyed for this project, about 25 m west of the northwestern edge of 3CG1254. The land appears to have been cultivated in a north-south pattern as early as 40 years ago. An abandoned stream channel, identifiable from heavier, wetter soils, forms a partially wooded slough running roughly north-south through the project area. A broad, diffuse area of lighter, sandier soil in the southwestern portion of the tract appears to be a crevasse splay, but there is a white, probably purer sand spot superimposed on this pedological feature.



Figure F-1 Faulkner Vicinity in 1977 (Ferguson 1979: Sheet 54)

The February, 1997, Google Earth image (Figure F-2) shows the former slough holding water during the winter. The barn north of the farmstead is still standing. Cultivation continues in a north-south direction and most of the sand crevasse or ejecta features are indistinct.

The March, 2001, Google Earth image (Figure F-3) shows the barn near the southwest corner of the field still standing. The bankline of the old slough is clearly visible, as are distinct sand blows along the bankline and extending into the old slough. Cultivation continues in a north-south direction across the entire field including the slough and some ditching/tile features are visible in the northwest part of the field.

The October, 2010, Google Earth image (Figure F-4) shows the barn north of the farmstead having been demolished, although its site is still clear, placing the removal of the barn between 2001 and 2010. Cultivation continues in the same direction established by 1977. The old slough is indistinct, and the sand features appear to be spread, however, this image, from after the harvest season and probably before significant winter rain, shows sand spots not clear on other images.

The May, 2012, Google Earth image (not shown) shows the location of the barn fading, and other natural features are very indistinct. Even the heavier soils of the slough bed and its sandier banks are only faintly detectable. Cultivation is north-south.



Figure F-2 Google Earth Image of Faulkner (3CG1253 and 3CG1254) Vicinity, February 1997

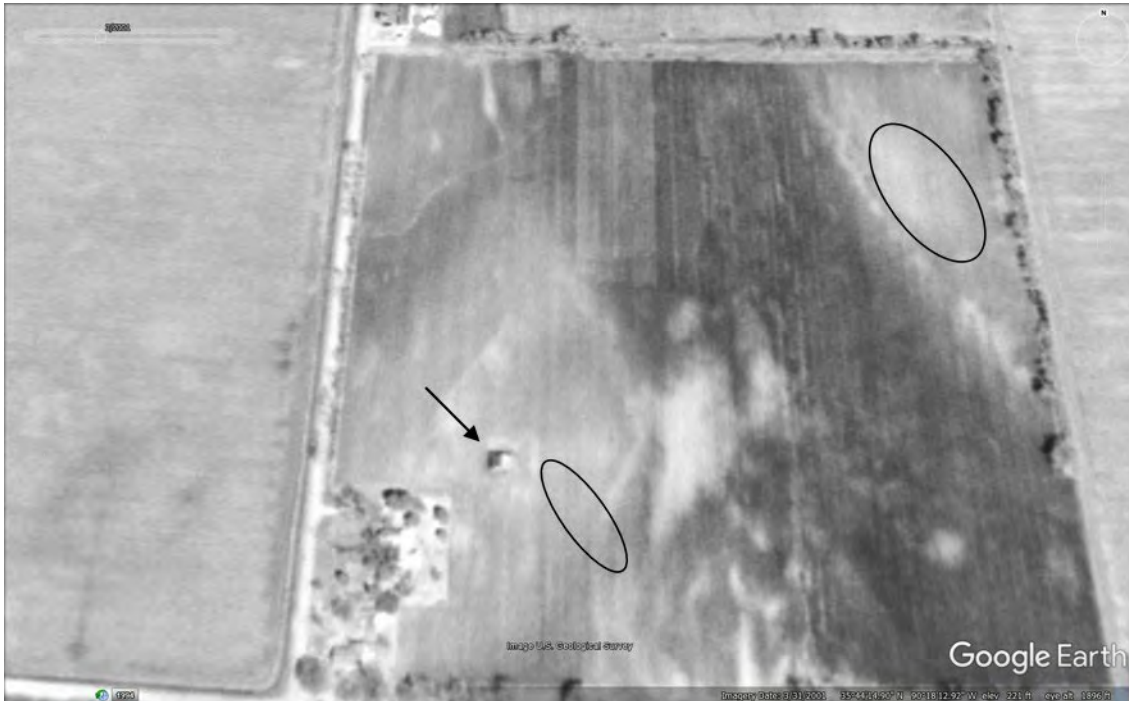


Figure F-3 Google Earth Image of Faulkner (3CG1253 and 3CG1254) Vicinity, March 2001



Figure F-4 Google Earth Image of Faulkner (3CG1253 and 3CG1254) Vicinity, October 2010



Figure F-5 Google Earth Image of Faulkner (3CG1253 and 3CG1254) Vicinity, November 2013

The November, 2013, Google Earth image (Figure F-5) after harvest shows the slough bed and its banks clearly. The location of the barn torn down between 2001 and 2010 is still evident, but being reduced by consistent north-south cultivation. Ditches/water furrows indicate a continuing problem with water in the old slough bed. Sand spots are clear along both the east and west bank lines.

The final satellite map from Google Earth for the Faulker (3CG1253 and 3CG1254) sites dates to October 2016 (not shown). This fall image appears to show a winter wheat crop. It is the only image in the series to indicate cultivation east-west, although the dominant trend, including the small grain drilling, continues in the established direction. The foundation of the barn is still faintly visible. The sand spot along the west bank of the slough, where the grain had failed, is the chief natural feature evident in this the most recent available aerial image.

The Wildy (3MS909) site (Figure F-6) lies along a ditch which parallels a gravel road and electrical transmission line. The location lies in an area of braided stream channels, with the site lying on the interfluvium between two abandoned channels east and west of the site. The area is generally flat with large, low-relief swales oriented generally north-south. Site soils are sandy and silty and have been used primarily for cotton production, with cultivation extending back at least 50 years. Northwestern Mississippi County is classified as having soils predominantly in the Amagon-Dundee-Cevasse association; these are mixed heavy and loamy soils affected by earthquake induced sand ejection. The project area lies at 225-230 feet above mean sea level, with lands along Big Lake, 5 to 6 miles to the east, are around 240' amsl. This is a generally level, low-lying area that has been improved for agriculture by the construction of parallel, east-west oriented drainage ditches which fall into the Buffalo Creek Ditch west of the project area. Buffalo Creek was channelized at some time after 1914, and possibly as late as World War II (to be discussed below) and its lateral ditches would have been excavated subsequently to prepare the landscape for cultivation. The sparse archaeological finds at this location were made in the road ditch along the south side of the county road. There was poor surface exposure in the ditch north of the road.



Figure F-6 Wildy (3MS909) Vicinity ca. 1970 (Ferguson 1971: Sheet 24)

Soils in the project vicinity are mapped as Roellen silty clay loam, a level, frequently flooded soil type typical of old stream and lake beds (soil code Rd; Ferguson, 1971). The next available air/satellite image for the area dates to 1996 (Figure F-7). This image clearly shows typical round as well as linear sand blows. This very complex pattern of sand eruption is probably indicative of the presence of buried and partially buried point bars within the braided stream surface. Note that the Buffalo Creek Ditch bottom does not show sand blows. This may be attributable to 1) heavy siltation after ca. 1900-1920, 2) lack of subsurface sand and/or extensive overburden developed since 1811-1812, or 3) land leveling. Very heavy sand (white area at northwest corner of study area) may represent ditch soil rather than a natural feature.



Figure F-7 Google Earth Image of Wildy (3MS909) Vicinity, April 1996



Figure F-8 Google Earth Image of Wildy (3MS909) Vicinity, January 2002

Between 1996 and 2002 (Figure F-8), centre pivot irrigation was installed in the project area and many other fields in the immediate vicinity. This allows for more reliable crop stands, particularly on sand-blow lands which are subject to very dry and very wet conditions within a few meters of each other. In January 2002, when the location was apparently in winter wheat, linear sand fissures are clearly visible. The January 2006, October 2010 and May 2012 Google Earth images (not shown) present similar conditions and are rather uninformative. The current (2016) Google Earth image (not shown) shows exceeding little detail, probably due to post-harvest conditions. On the 2016 image, none of the natural or cultural features of interest, besides the ditch/road and irrigation well are still visible.

The area of the Garner #1, #2 and #3 (3CG1255, 3CG1256 and 3CG1257) sites is a large tract of primarily Sharkey association poorly drained, nearly level soils. Sharkey soils formed on flood plains and slack-water flats. The vicinity lies about two miles east of the foot of Crowley's Ridge, and about 2 miles west of St. Francis River in northeastern Craighead County, in an area of low terrace. The Garner area has also been extensively modified by historic drainage ditches and modern land leveling. The specific area of these sites in the Sharkey clay-dominated vicinity is mapped as Fountain silt loam (soil code 23) in the interior part and Mhoon fine sandy loam (soil code 34) closer to Lighthouse Ditch (Figure F-9). In contrast to much of the surrounding area, which shows a stippling of discrete sand blows, as at the Faulkner sites, the Garner vicinity and other areas along the banks of Lighthouse Creek/Ditch and Big Bay Ditch, appear to have rather more extensive and contiguous sand cover in 1977 (Ferguson 1979: Sheet 6).



Figure F-9 Garner Vicinity in 1977 (Ferguson 1979: Sheet 6)

The first air/satellite image after the 1977 soil survey sheet is the February, 1994, Google Earth image, which shows that the Garner sites had been a rice field in 1993 (Figure F-10). Cultivation and grain drilling prior to throwing up the east-west trending levees was north south. Soil conditions are not clear.

The February, 2001, Google Earth image (Figure F-11) shows the Garner sites were in row crops in 2000, although surrounding fields had been in rice. Cultivation is in a north-south direction. Highly variable soils, with distinct pedon boundaries, are clearly evident in this image as very dark (wet, heavy) to very light (droughty, sandy) soils.

The January, 2006, Google Earth image (Figure F-12) shows north south cultivation as well as east-west trending rice levees. White sand spots, including in the 3CG1255 area, are very clear. The September, 2006, Google Earth image (not shown) has indistinct evidence of recent, but perhaps not 2005-06, rice cultivation. Adequate soil moisture and ground cover obscure the natural and cultural features of the field. The area of 3CG1255 is among the areas with heavy ground cover. It seems likely that some land-leveling had been done by this point, with the central, lower area of the field being filled from the north (3CG1255 vicinity).

The October, 2010, Google Earth image (Figure F-13), like that of September 2006, shows less distinct natural features, indicating the spreading and smearing of formerly distinct soil pedons. Cultivation continues north-south, and previous years' rice levees are still evident. Differential soil moisture has resulted in variable ground cover, with the 3CG1255 vicinity being more heavily vegetated, probably by wild onions and other weeds.

The September, 2015, Google Earth image (not shown) clearly shows the field to have been leveled. Natural features are no longer evident, or only faintly so. Cultivation continued in the established direction. It seems likely that the field was in corn or milo in 2015. Rice cultivation continued in some surrounding fields.



Figure F-10 Google Earth Image of Garner (3CG 1255) Vicinity, February 1994



Figure F-11 Google Earth Image of Garner (3CG 1255) Vicinity, February 2001



Figure F-12 Google Earth Image of Garner (3CG 1255) Vicinity, January 2006



Figure F-13 Google Earth Image of Garner (3CG 1255) Vicinity, October 2010

F.3 Background

Here we review the archaeological literature that pertains to the work areas, summarize the prehistory and history of the area, note previously recorded sites and National Register of Historic Places listings for the area, and make predictions concerning expected findings based on this background review.

F.3.1 Literature Review

Most work in the Mississippi Valley of Arkansas, and the St. Francis River basin in particular has focused on drainage ditches and levees. A search was made of the Arkansas Archeological Survey site files, as well of the National Register of Historic Places, for any previously recorded sites in the project vicinity. Pertinent cultural resource management reports were also reviewed. The University of Alabama library historic map archive was checked for maps pertinent to the interpretation of the natural and cultural history of the project vicinity, but no detailed historic context is presented here, as historic materials were very thinly scattered in these agricultural fields and no definite domestic or industrial sites were reported. The standard secondary source for the area is the now somewhat dated Morse and Morse (1983).

F.3.2 Prehistoric Background

The recording of prehistoric mounds and stone and ceramic artifacts began in the mid 19th century as plantations were cleared in the Arkansas Delta and continued through the mid 20th century. This work was focused on large Mississippi period sites but came to encompass earlier time periods. During the 1930s through ca. 1970 the Lower Mississippi Survey (LMS) increased knowledge of these sites while revisiting some of the earlier-reported sites and producing a stratigraphy-based chronology for the region. After ca. 1970, the style-based chronology was supplemented with an expanding radiocarbon chronology, largely thanks to cultural resources

management (CRM) rather than academic-based research. The National Historic Preservation Act (NHPA) and National Environmental Policy Act (NEPA) greatly increased the scope and intensity of archaeological investigations throughout the nation. In the project vicinity, earthquake dating work has contributed greatly to the available radiocarbon chronology (Tuttle et al., 2005, 2011). Morse and Morse (1983) summarized the state of knowledge based on the antiquarian, LMS and early CRM periods, but much work has been conducted since that time. Further reviews pertinent to the project are Morse and Morse (1996) and Lafferty and Price (1996).

Humans have been present in North America since at least 13,000 years ago, although there is very limited evidence of early occupation in the Mississippi Valley. The older land surface of the Western Lowland (west of Crowley's Ridge, which divides Greene, Craighead and Poinsett counties into eastern and western halves) was apparently heavily occupied during the Late Paleo-Indian/Early Archaic period (Dalton culture) ca. 8000 years ago. Projectile point/knives, prepared cores, adzes, formal flake tools and other lithic artifacts of this culture are widely reported in the region, and some such sites are found along the eastern foot of the ridge as well. The Middle Archaic period, 6000 to 4000 years ago, is poorly represented in the region. Various reasons for this apparent abandonment have been put forth, generally revolving around the hot-dry Altithermal/Hypsithermal climatic interval between 8000 and 3000 BC, with the apparent impact of abandonment and/or dispersal being most pronounced between 6000 and 4000 BC (Morse and Morse, 1996:124).

Elsewhere, the Middle Archaic is marked by large, crude, heavily used projectile point knives and the first stone axes, as opposed to the Dalton adze. There is evidence of a strong earthquake in the region ca. 2350 ± 200 BC (Tuttle et al., 2011), although its impact on cultural developments is unclear. By the Late Archaic/Early Woodland interval 4000-2000 years ago, the project vicinity once again saw dense, widely scattered occupation of many environmental settings as well as the beginnings of plant domestication (gourd, squash, chenopod and sunflower). The Late Archaic and Early Woodland periods are identified by a number of similar stemmed projectile point/knife forms. The early (Tchula series untempered pottery) ceramics are rarely found, so aceramic Early Woodland dating 500 BC-0 (Morse and Morse, 1996:125) sites are probably widely subsumed under a Late Archaic heading. In the Middle Woodland period (Marksville/Hopewell culture, 0-400 AD; Morse and Morse, 1996:126) sites remained widely distributed across the landscape and there is evidence in the form of more ceramics (sand and grog tempered wares), storage pits or in-ground silos and structural remains that populations were using smaller territories and camping for longer intervals on the most favored sites, while continuing to visit and create seasonal resource-extraction camps. The Marksville culture is best known from its burial mounds, which were often placed prominently on the landscape, and housing the remains of various individuals, giving rise to their interpretation as territorial markers for clans or tribes. There is considerable evidence of sedentism and incipient agriculture by the Late Woodland period (Baytown and Coles Creek cultures) and this trend continued into the Early Mississippi period, placed at 800 AD at the Zebree site (Morse and Morse, 1996:128). A strong earthquake affected the area ca. AD 900 ± 100 (Tuttle et al., 2011) and may have contributed significantly to subsequent cultural developments.

The Middle and Late Mississippi periods saw marked population growth accompanied by a contraction of population from scattered farmsteads/hamlets into larger, often fortified, towns which produced deep deposits of organic midden soils, architectural debris and intentional fills (mounds). The Mississippi period is marked by the use of shell-tempered pottery, the bow and arrow which were first introduced to the Mid-South in the Late Woodland period, and a dependence on corn-based agriculture. This population concentration was evidently occasioned by an increase in raiding or feuding in a society still accustomed to primarily achieved status, while

population concentration gave rise to social stratification based on ascribed or inherited status. These later Mississippian sites, dating 1000 to 500 years ago, concentrated their populations on large permanent streams and lakes which provided year-round water as well as fish, turtles, waterfowl and shellfish, and were bordered by sandy loam soils easily tilled with stone hoes. Another significant earthquake is documented ca. 1450 ± 150 (Tuttle et al., 2011) and its impacts are widely documented in Late Mississippian sites of the region. The fiercely competitive paramount chiefdoms of the Mississippi period were described in the four surviving accounts of the DeSoto entrada ca. AD 1540, but by the time the next European adventurers entered the Mississippi Valley in the mid seventeenth through late eighteenth centuries, decimation of the town-dwelling populations by epidemic disease had very largely depopulated the region, leaving a few villages as well as large "vacant" territories visited seasonally by hunting parties. The 1803 Louisiana Purchase transferred control of the land that became Missouri Territory in 1813 and Arkansas Territory in 1819 to the United States. During the territorial period, several remnants of eastern Indian Nations briefly settled and/or hunted in northeast Arkansas, before encroaching Euro- and Afro-American settlement pushed them further west into Indian Territory. When Arkansas acquired statehood in 1836, Crowley's Ridge had been settled but the St. Francis basin was almost entirely uninhabited.

In the absence of direct radiocarbon dates, most archaeological chronology depends upon style. This is typically broad (millennia scale) before 2000-2500 years ago, when projectile point/knife (pp/k) forms are used to estimate occupation dates. After this date, ceramic style provides a tighter (century scale) chronology. The entirety of the Central Mississippi Valley chronology need not be repeated here, but some must be presented to provide a context for the dating of the sites discovered in the course of the geological investigations.

To anticipate our results, the Garner site (3CG1255) produced two fragmentary corner-notched pp/k bases which form the main basis for the dating of the occupation covered by the sand blow that was the focus of our investigations. The chronology of known corner-notched pp/ks that might be expected in northeast Arkansas is presented below, based on standard sources (Justice, 1989; McGahey, 2000)

The earliest points in the area (Paleo-Indian and Transitional/Dalton) have "waisted" rather than notched hafting elements, but the Greenbriar Dalton variant in particular can sometimes be considered a side notched. Dalton bases are generally well thinned, resulting in an incurvate base, and the base and notches are generally heavily ground. The Greenbriar form (10,000-9000 BP; McGahey, 2000:42) is a thin, well-made Early Archaic pp/k with shallow side notches or corner removal and rounded "ears." They are also characterized by parallel blade margins, symmetrical pressure flaking and serrated blades that are sometimes beveled during resharpening. The Greenbriar base is slightly concave to straight, and always thinned and ground. These points are found in the northern half of Mississippi, on gravel cherts, with some examples on Bangor or Ft. Payne chert, indicating social affiliations in the central Tennessee River valley. McGahey (2000:31), who refuses the cluster classification of Justice (1987), places the side-notched Dalton ca. 10,000-9500 BP, and notes that it is more commonly serrated and beveled in northern Mississippi, but associated with the San Patrice variant in southern Mississippi. McGahey (2000:38) places the Geneill (another Dalton cluster form) of the Yazoo basin at 10,000-9500 BP. These well-made points have considerable morphological variation, but have concave thinned bases. Tan chert and novaculite specimens have been documented, showing that they should be identified in central Arkansas as well. The Early Archaic Stillwell (possibly also dating in the 9500-9000 BP time frame) is the first distinctly corner notched form in northwestern Mississippi (McGahey, 2000:53). Both sides have well-controlled flaking, with narrow pressure retouch and fine serration. These thin, well-made points have straight to slightly concave, carefully thinned and heavily ground bases; the depth of the notches varies greatly from shallow corner

removal to large, angled corner notches but most have wide, shallow notches. Most are made of tan gravel chert with occasional specimens on heated Tuscaloosa gravel or other non-local materials. McGahey (2000:58) cites a third Early Archaic form (which could be included in the broader Dalton cluster, or as an affine of Decatur) as the 9500-9000 BP Cave Springs point, found with and as a variant of Jude stemmed points at the Hester site in northeastern Mississippi. The Cave Springs point has considerable morphological variation, with corner removal to corner notching resulting in an expanding stem with concave base. The basal edge is usually well thinned and heavily ground. Unlike the contemporary, more eastern Decatur, Cave Springs blades are seldom beveled during resharpening and the base is almost never burinated/fractured. The type is, however, often renovated as a half-tipped endscraper after the loss of the blade. They are made on gravel pebble cores, red heat-treated Tuscaloosa gravel, and occasionally Ft. Payne and Bangor cherts (McGahey, 2000:61).

Corner notches appeared in the Early Archaic period and are found through the Middle Woodland period. While the Early Archaic Thebes cluster (Thebes, St. Charles and Lost Lake; Justice, 1987:54-59) points are primarily side notched, the somewhat later Kirk cluster (Kirk, Palmer, Charleston, Pine Tree and Decatur; Justice, 1987:71-82) forms are clearly notched from the corner, and may have excurvate, straight or incurvate basal margins, as do the St. Charles and Lost Lake forms. The early Middle Archaic St. Charles point is often made on white Burlington/Crescent chert; the two fragments from 3CG1255 are on similar materials. The Late Archaic Brewerton cluster (Justice, 1987:115) pp/ks vary from clearly corner notched to more side notched variants.

The Early Archaic (8000-6000 BC) St. Charles points, also known as "Dovetail," "fracture base," and "notch base," are lanceolate, corner-notched points with originally excurvate blade margins, biconvex cross-sections and heavily ground, straight to shallowly notched bases. These very well-made points are found across much of the eastern United States, including the Mid-South and Mid-West but are rare in the Great Lakes and Northeast (Justice, 1987:57).

In contrast, the contemporary Lost Lake cluster points, also known as Bolen and Cypress Creek I, are defined by their large, deep corner notches. These notches may curve in and up from the original corner of the biface, and are often terminated by large, conical pressure flakes. The Lost Lake blade form varies from excurvate when new to deeply incurvate after extensive, beveled and serrated resharpening, and is biconvex to rhomboidal in cross section. Many Lost Lake cluster bases are heavily ground, and the basal margin varies from straight to slightly incurvate. Projectile point/knives of the Lost Lake cluster are found over most of the Southeast, including the Ohio River valley (Justice, 1987:58).

The Lost Lake thus differs from the other Early Archaic (7500-6900 BC) Kirk Corner Notched cluster pp/ks, which have shorter, straight notches, with less basal grinding (Justice, 1987:71). The Kirk cluster includes a smaller form (Palmer) as well as the Cypress Creek II pp/k. The Early Archaic (7500-6900 BC) Palmer pp/k has a straight to slightly convex or concave, thinned and heavily ground base, biconvex cross section, and pronounced serration. The corner notches are wide and deep, resulting in barbed shoulders. Palmers are found from New England and the Great Lakes south through the Appalachians and coastal plains as far west as east Texas (Justice, 1987:78). Typical Kirk points, thought to have developed from the Palmer form, have large, triangular blades with wide, random flaking resulting in a flattened cross section lacking a distinct medial ridge. Blade sharpening and serration is bifacial, rather than beveled; this lack of variation due to degree of resharpening stands in contrast to the St. Charles and Lost Lake cluster points. Kirk cluster forms have distinct, wide shoulders with barbs that project downward. Bases are typically straight, but sometimes excurvate. Kirk cluster points are found ubiquitously through most of the United States and into southern Canada from the Atlantic westward, but are rare in

most areas west of the Mississippi River, with the exception of the Table Rock Reservoir area of Missouri, indicating that they might occasionally be found in northeast Arkansas.

The Charleston corner notched pp/k (dated 7900 BC±500 by its inclusion in a hearth at the St. Albans, West Virginia, site) typically has random flaking and asymmetrical blades from use as a knife, with extensive resharpening (Justice, 1987:79). Charleston bases are thinned by the removal of several small flakes, while the notches are created by the removal of large, conical pressure flakes. These notches, in the West Virginia sample, were 5-8 mm wide and 4-8 mm deep, leaving slightly rounded shoulder barbs or “ears.” Bases are flat to convex. The form is concentrated in the Appalachian summit and Tennessee-Ohio basin, with few identified west of the Mississippi, making this an unlikely form for our project area.

Another Early Archaic (7500-6900 BC) corner-notched form, Pine Tree, is probably identical with heavily resharped Kirk and Charleston pp/ks. The hafting areas, at least, are highly similar, with variation concentrated on the distinctly thinned cross-section, which retains its length even as the blade becomes narrower. Pine Tree bases are thinned and ground, with the basal margin generally straight, but sometimes slightly convex. The Pine Tree is found throughout the interior basin (Tennessee-Ohio valley) but like the Charleston corner notched is rare west of the Mississippi.

The Early Archaic (7500-7000 BC) Decatur corner notched point is known by many localized synonyms such as Abbott, Amos, Autauga, Barbee, Broadhead, Bynum, Church Hill, etc. (Justice, 1987:81). McGahey (2000:61) notes that the small-to-medium corner-notched Decatur points are found above Jude/Cave Springs at Hester, placing them ca. 9500-9000 BP. Decatur points have triangular blades and are flaked and resharpened in the same style as Kirk and Pine Tree, with common alternate bevels and serrations. The haft area is shortened and the base is not as wide as the shoulder, making their stems much shorter than the typical Early Archaic pp/k as well as more expanded than Cave Springs stems (Justice, 1987:81; McGahey, 2000:65). The Decatur form is also remarkable for the frequent “burin spalls” detached from the sides of the base. These burin facets may be subsequently obliterated by basal grinding, indicating that they are probably a peculiarity of knapping style and not primarily for the expedient or formal production of flakes actually intended for use as burins/gravers. The term “fracture base” is also popularly used to describe these pp/ks. However, the preform corners were prepared as striking platforms to remove these small spalls, and the removal of two such spalls results in an incurvate basal edge. The Decatur form is recognized in the central parts of the Southeast and Midwest, and so might be expected to occur occasionally in northeast Arkansas.

The Late Archaic Epps and Motley pp/k types (3500-2500 BP) from the Lower Mississippi Valley and defined for Poverty Point vicinity are large, well-made, triangular-bladed pp/ks. Motley is corner-notched but the notches are so deep and large as to create a narrow, waisted stem. Epps is a similar, contemporary, but more side-notched form, with a wider stem. Epps in particular is often associated with Boone and Crescent cherts (McGahey, 2000:176-178).

The Late Archaic (2980-1723 BC) Brewerton form includes both side-notched and corner-notched forms (Justice, 1987:115). The side-notched form may be a resharpened variant of the corner-notched, with angled notches and sharp “ears.” These are triangular, broad-bladed points with wide shoulders extending beyond the base. Blades are typically excurvate, relatively thick, and biconvex in cross-section. Serration and patterned pressure flaking are uncommon. Basal edges are typically straight but can be slightly convex and basal grinding is common. The Brewerton pp/k is part of the Laurentian tradition of the Great Lakes and New England/Ontario, so it seems an unlikely type to be found in northeast Arkansas. The Late Archaic (3200-2500 BC) Vosburg pp/k,

associated with the Brewerton form, is a small, narrow corner-notched point, with the short base having small, short notches resulting in weak shoulder barbs (Justice, 1987:116). There is sometimes weak serration of the blade, but no beveling. Bases are straight to slightly concave, and are frequently ground. This is also primarily a northeastern form, unlikely to be found in Arkansas. The Brewerton and Vosburg forms can be seen as a late, northern development or holdover of the corner-notching tradition that reached its widest use in the Early Archaic period. The Snyders (200 BC-AD 200) is a broad-bladed point with wide, sometimes expanded, corner notches. The hafting element is wide, with an expanding stem and excurvate blade with a lenticular to flattened cross-section, that may be shortened to a blunt triangular blade by resharpening. The Snyders is found from the southern Great Lakes throughout the Midwest and into the Lower Mississippi Valley (Justice, 1987:38-39). The Steuben expanding stem point is considered a late (AD 100-350) variant of Snyders, with shallow, upward-curving notches, relatively large and expanding stem, and a narrower and more ovate form than Snyders. The Steuben type is limited largely to Illinois (Justice, 1987:40-41). It should be noted that white Burlington/Crescent chert is a favored material for Snyders points.

A final corner-notched form to consider is the Jacks Reef corner-notched and Racoon side-notched Late Woodland (AD 800-1000) cluster (Justice 1987:42-43). These are made on a similar, very thin, pentagonal blade with wide irregular flake scars. The Jacks Reef form is very well thinned with wide irregular flaking and a flattened cross-section. Both have straight bases, but the Jacks Reef may have a slight basal notch or incurvate base. These types are common in New England, the Great Lakes and Midwest, but are only occasionally found in the Midwest.

F.3.3 Historic Background

Here we summarize the history of Craighead County with an emphasis on landscape evolution and settlement history. We review available maps for the county and discuss their implications for historic settlement patterns. There is an historic soils survey (1916) available for Craighead County, in addition to the current soil survey based on air photos.

Craighead County was created out of Poinsett and Greene counties in 1858. Its population has seen steady, almost uninterrupted growth since its creation (Table F-1). There was a large increase, almost a doubling, of population in these counties between 1880 and 1890, attributable to bottomland hardwood logging, and in all three counties, population continued to increase during the Great Depression and WWII, with drops only between 1950 and 1960, attributable to mechanization of agriculture. After 1970, growth in Greene and Craighead counties continued with urbanization and industrial and commercial employment, while the population of Green County has declined somewhat. Mississippi County has followed a similar trend, with a WWII-Cold war era spike due to the presence of the Blytheville AFB.

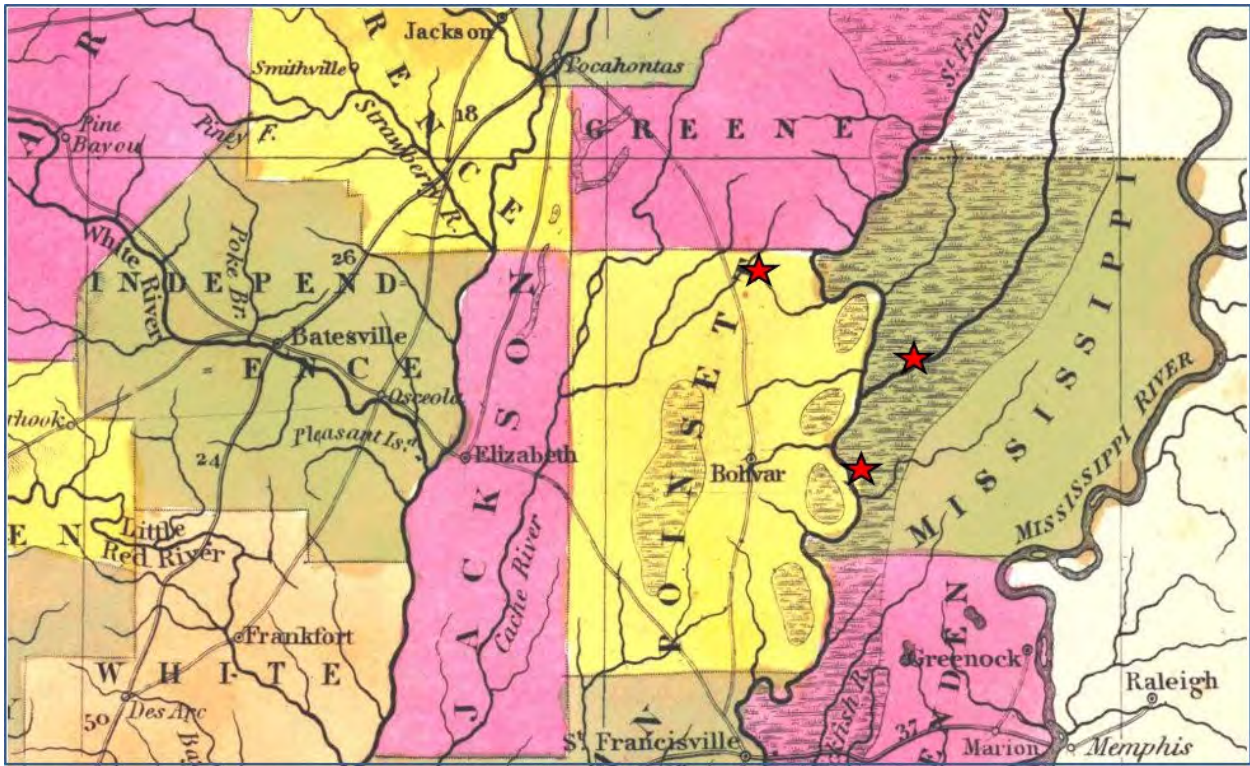


Figure F-14 Project Vicinity (Mitchell 1847)

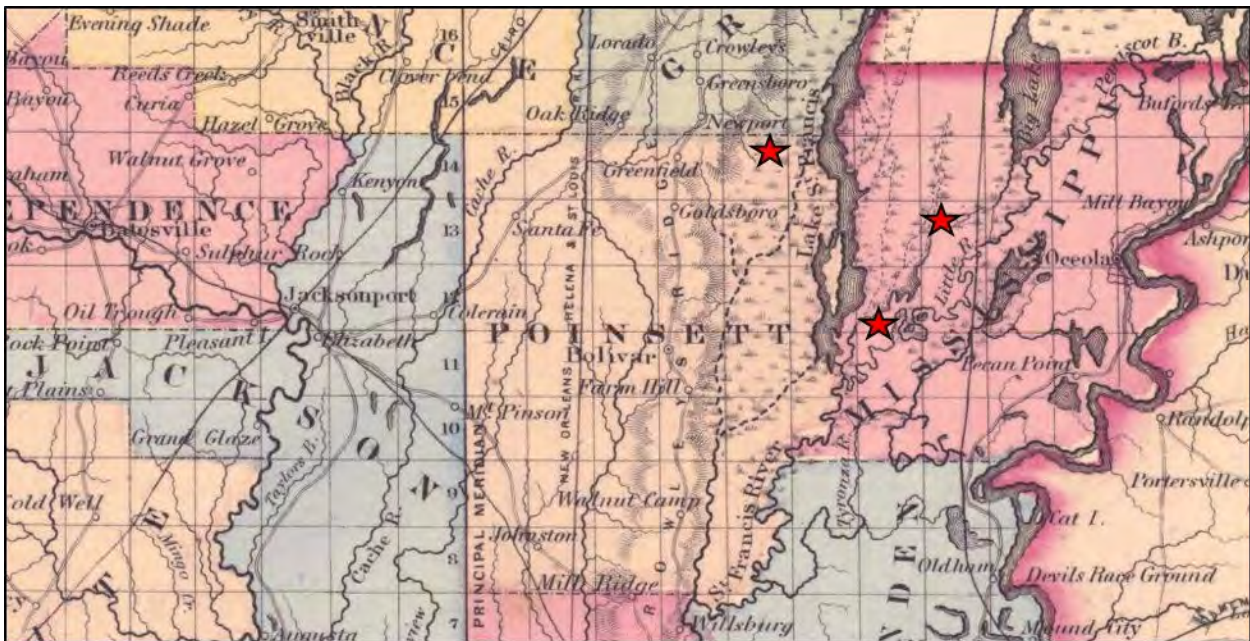


Figure F-15 Project Vicinity (Colton 1855)

Table F-1 Population History Poinsett, Craighead, Greene and Mississippi Counties, Arkansas (Wikipedia)

Census	Greene	Craighead	Poinsett	Mississippi
1840	1320		1320	1410
1850	2308		2308	2368
1860	5843	3066	3621	3895
1870	7573	4577	1720	3633
1880	7480	7037	2192	7332
1890	12,908	12,025	4272	11,635
1900	16,979	19,505	17,025	16,384
1910	23,852	27,627	12,791	30,468
1920	26,105	37,541	20,848	47,320
1930	26,127	44,740	29,695	69,289
1940	30,204	47,200	37,670	80,217
1950	29,149	50,613	39,311	82,375
1960	25,198	47,303	30,834	70,174
1970	24,765	52,068	26,822	62,060
1980	30,744	63,239	27,032	59,517
1990	31,804	68,956	24,664	57,525
2000	37,331	82,148	25,614	51,979
2010	42,090	90,443	24,583	46,780

Here we summarize the history of Craighead County with an emphasis on landscape evolution and settlement history. We review available maps for the county and discuss their implications for historic settlement patterns. There is an historic soils survey (1916) available for Craighead County, in addition to the current soil survey based on air photos.

Craighead County was created out of Poinsett and Greene counties in 1858. Its population has seen steady, almost uninterrupted growth since its creation (Table F-1). There was a large increase, almost a doubling, of population in these counties between 1880 and 1890, attributable to bottomland hardwood logging, and in all three counties, population continued to increase during the Great Depression and WWII, with drops only between 1950 and 1960, attributable to mechanization of agriculture. After 1970, growth in Greene and Craighead counties continued with urbanization and industrial and commercial employment, while the population of Green County has declined somewhat. Mississippi County has followed a similar trend, with a WWII-Cold war era spike due to the presence of the Blytheville AFB.



Figure F-16 Project Vicinity (Cram 1876)

By 1876, more than 50 years after the 1811-1812 earthquake, Craighead County had been created, and railroads now followed Crowley’s Ridge. The Cram (1876;Figure F-16) map shows Crowley’s ridge in relief, and numerous creeks originating on this upland and flowing into a much reduced swamp approximating the base of the ridge. Settlement, or at least timbering, was under way in the St. Francis swamp, and a settlement (Sunk Land or the more promising Lake City) had been created along the west bank of the river, with Mangrum on the east bank. Less swamp is also indicated east of the St. Francis, along the Pemiscot Bayou-Little River-Tyrtonza River drainage.

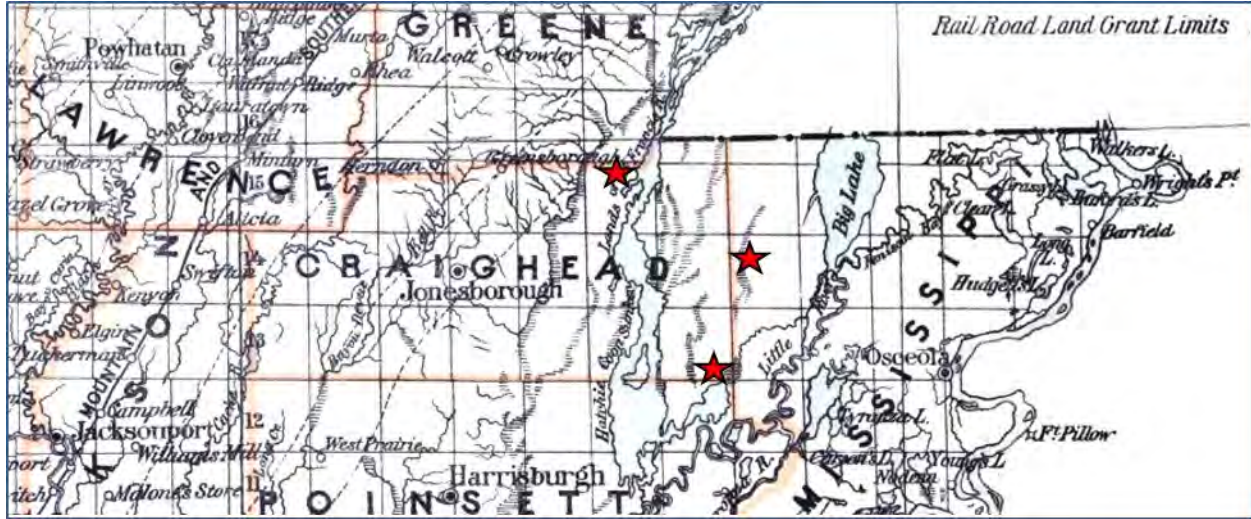


Figure F-17 Project Vicinity (Roeser 1878)

The Roeser (1878) map shows townships and improves topographic detail for the project vicinity (Figure F-17). In the Garner vicinity, short creeks from Crowley’s Ridge flow into a swamp at its base, but the land between this unnamed drainage (feature indicated by hachure) and the Hatchie Coon Sunk Lands of the St. Francis are not detailed as swamp, rather vague, swampy channels are shown in a few locations. Lighthouse Creek below the foot of Crowley’s Ridge is not indicated.

In the Caraway-Faulkner vicinity, likewise, continuous swamp is no longer indicated, but a swampy channel (Honey Cypress slough?) is shown, and the southeast corner of T13N R6E is shown as lake/swamp. The landscape of eastern Craighead County clearly continued to be dominated by water and swamp forest.



Figure F-18 Project Vicinity (Hardesty 1883)

The Hardesty (1883; Figure F-18) shows less, but similar, detail, in comparison to its contemporaries. This map is the first to indicate that settlement was proceeding into the St. Francis bottoms, with post office communities at Stottsville, Lester, Sunk Land, Mangrum's, and Bay Bridge. Lester was the nearest settlement to the Garner vicinity. The location of Bay Bridge, the town nearest the Wildy and Faulkner sites, in T13N R6E is probably in error. The Cram (1887) and subsequent maps show this community on the Memphis & Kansas City/Kansas City, Ft. Scott and Gulf Railroad.



Figure F-19 Project Vicinity (Cram 1887)

The Cram (1887; Figure F-19) map shows little relevant detail, following previous maps for lakes and swamps, and adds additional rural post office communities in the St. Francis bottom to now include Mamell; Maumell Prairie is in S14 and 15, T13N R6E (Ferguson 1979: Sheet 44) but the settlement is not otherwise attested. Bay P.O. or Big Bay Siding is shown in T13N R7E, on the KCFS&GRR.

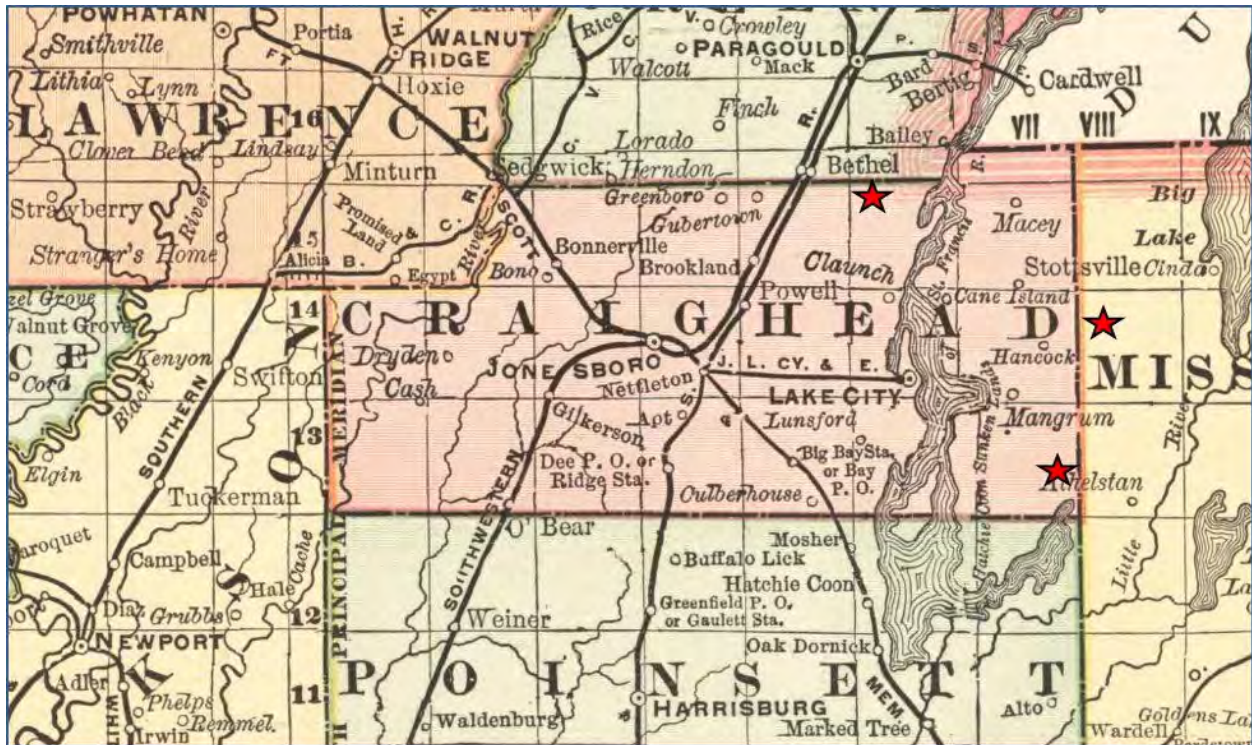


Figure F-20 Project Vicinity (Rand McNally 1889)

The Rand McNally (1889) map demonstrates increased penetration of the St. Francis bottom, with the Jonesboro, Lake City and Eastern Railroad built east from the Jonesboro rail junction to the west bank of the St. Francis at Lake City (Figure F-20). Rand McNally (1900), on the same base map, shows the JLC&E through to Leachville in northwestern Mississippi County. Other new bottom settlements included Macey, Claunch, Cane Island, Hancock, Lunsford and Culberhouse. Lester is no longer shown, replaced by Claunch, 6 miles south of the Garner sites. Bethel, a railroad station in Greene County remains the closest settlement to the Garner area. The Caraway-Faulkner area is still shown as in or near a lake, with Mangrum and Athelstan in Mississippi County being the nearest settlements. The Wildy vicinity is between Stottsville, Cane Island and Hancock.

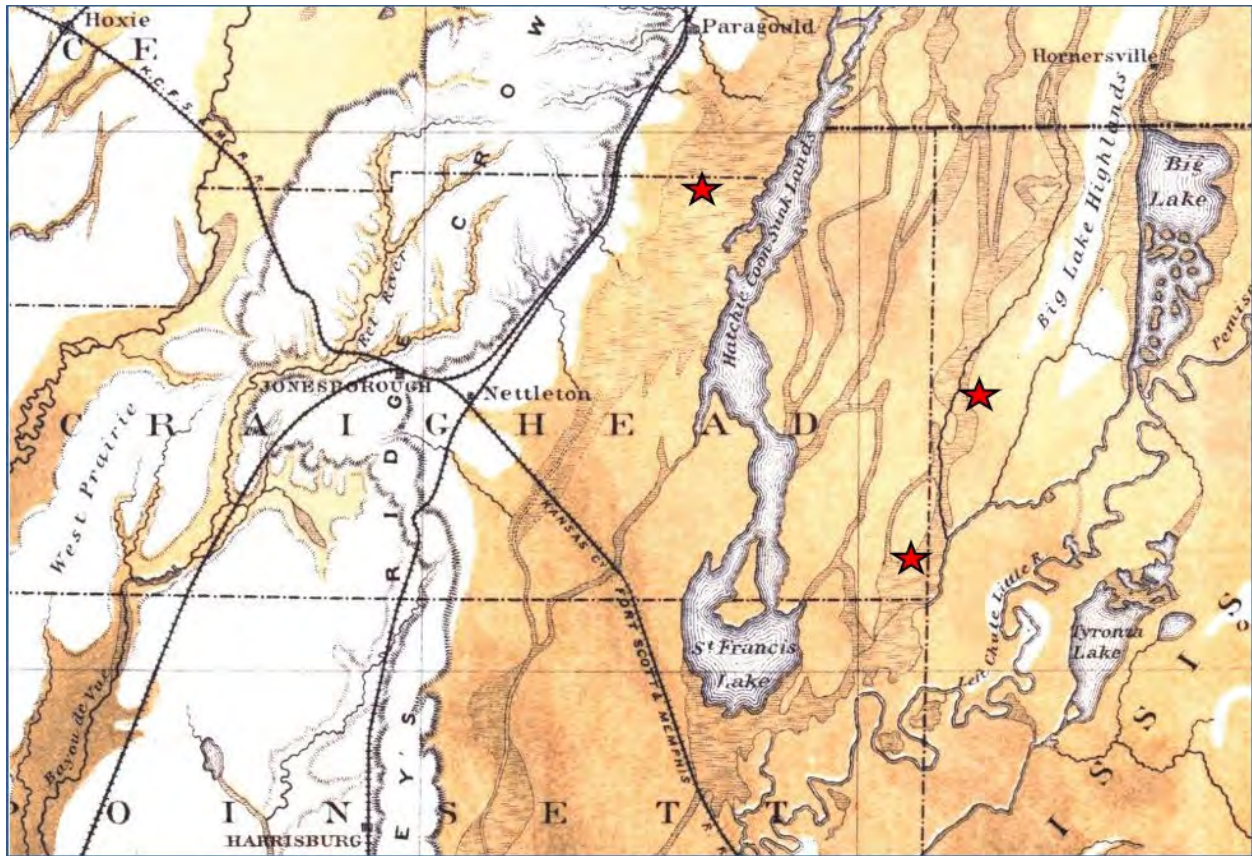


Figure F-21 Project Vicinity (Branner 1889)

While shipping and postal service had penetrated the St. Francis bottoms by the 1880s, the first geologic map of the Craighead County area (Branner, 1889) shows conditions still similar to those indicated on the Colton (1855) map, with the entire bottom from the foot of Crowley's Ridge to the St. Francis being subject to overflow, and with upland streams losing themselves in this swamp (Figure F-21). Numerous swamp channels flow into and out of the Hatchie Coon Sunk Land and St. Francis Lake. In the southeast corner of Craighead County, the Caraway-Faulkner vicinity is shown as swamps clearly occupying old channels, without distinct, mapped streams. This map does, for the first time, indicate ridges along the Left Hand Chute of Little River that were above normal overflow, as well as the similarly elevated Big Lake High Land in western Mississippi County, east of the Wildy site.

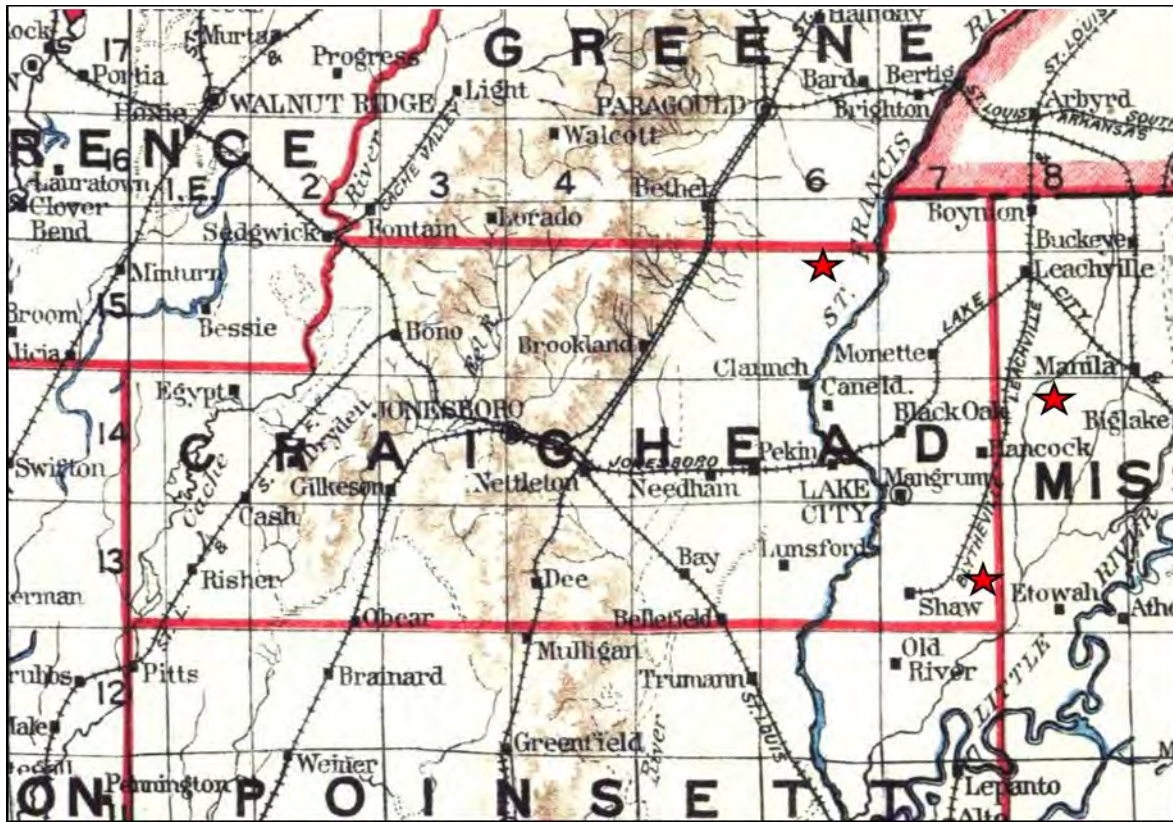


Figure F-22 Project Vicinity (Berthrong 1914)

The Berthrong (1914; Figure F-22) map shows that logging had reached the remote southeast corner of Craighead County with the construction of the Blytheville & Leachville Railroad to a terminal in T13N R6E called Shaw. This map also adds Needham and Pekin stations between Jonesboro/Nettleton, and Monette and Black Oak between Mangrum and Leachville. In the former Athelstan area of western Mississippi County there is now a village or post office called Etowah. The topographic detail is poor, but the creeks off Crowley's Ridge in the Garner vicinity are still depicted as disappearing when they reach the bottomlands.

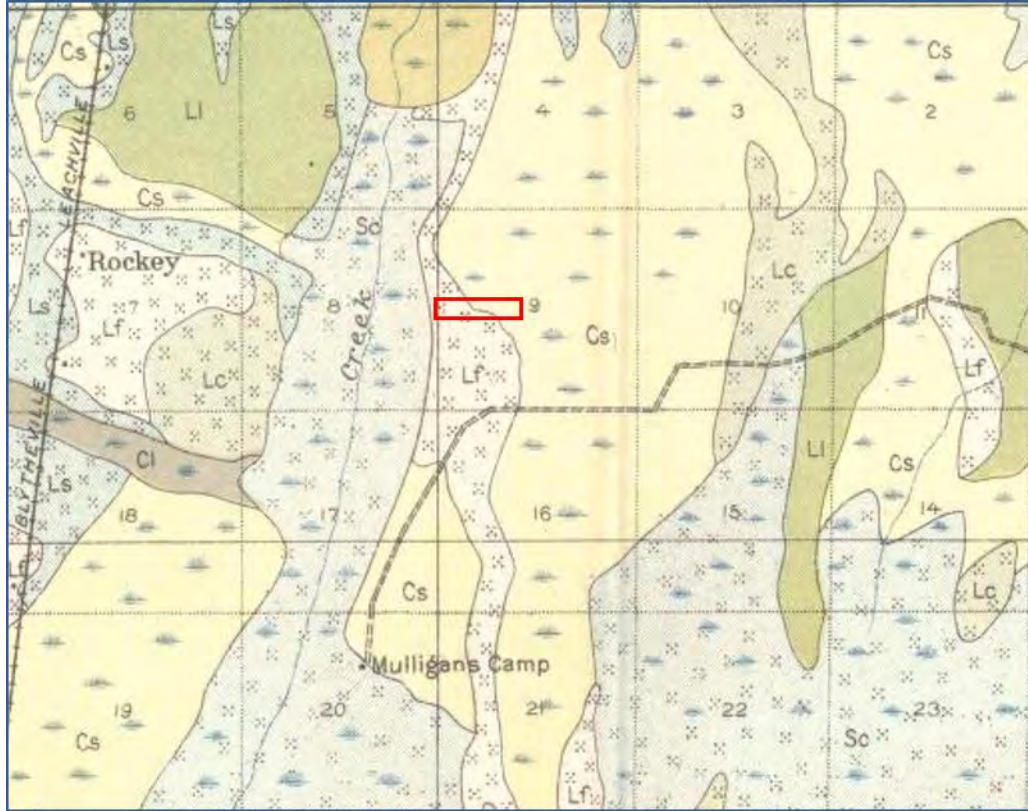


Figure F-23 Project vicinity shown on Mississippi County soil survey (1914).

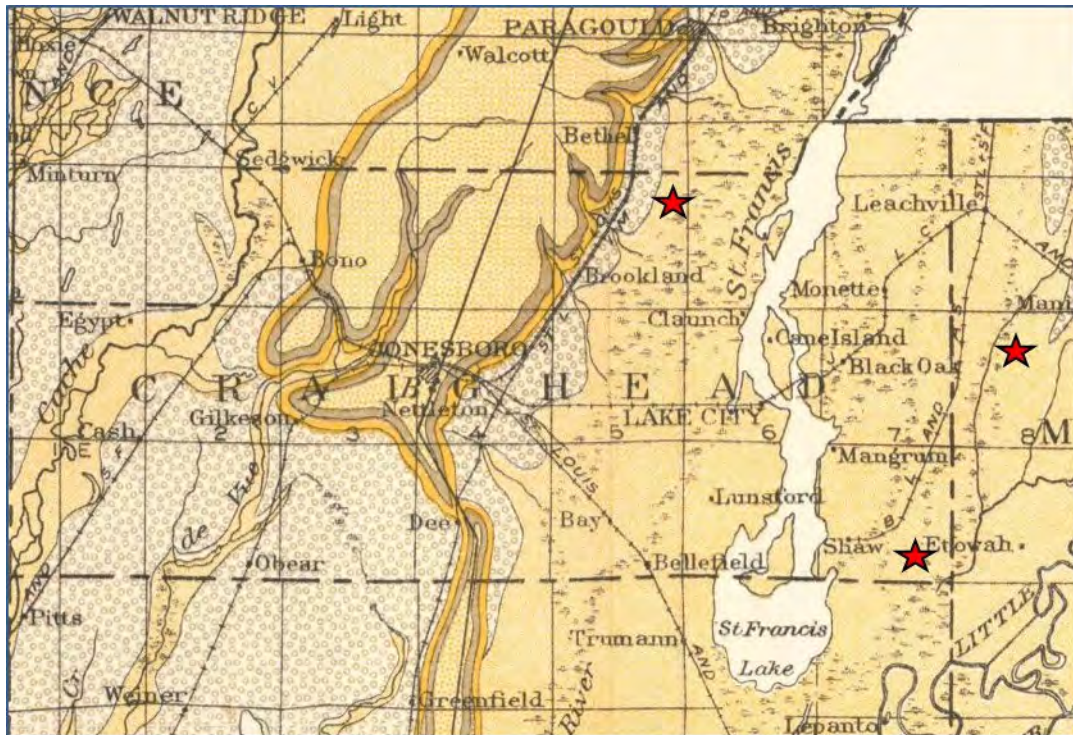


Figure F-24 Project Vicinity (USGS 1916)

The 1914 soil survey for Mississippi County (Figure F-23) shows the area of investigations at the Wildy site as Lintonia sandy loam (Lf), with sand blows, and surrounded on the east and west by swampland (Sharkey clay, Sc), including the still-unchannelized Buffalo Creek to the west. A track or wagon road leads to Mulligan's Camp, an indication that the area was still wooded or being logged ca. 1914. Mulligan's camp, being depicted as a single structure north of the Swift Point overflow, may have been a hunting rather than logging camp. At this same time, but not depicted in the section of the soil sheet shown above, the land from Manila to some five miles south, closer to Little River, was being developed as farms, with section line roads and houses.

The second available historic map that specifically addresses geology and topography is the USGS (1916) map, which is the first to clearly demarcate Crowley's Ridge and the sub-loess Plio-Pleistocene gravely material outcropping at its base (Figure F-24). One hundred years after the 1811-1812 earthquake, the St. Francis bottoms were well into the process of being transformed from swamp forest to cleared agricultural land. In the Garner vicinity, the entirety of S15N R6E is shown as swamp, fed by upland creeks. In the Caraway-Faulkner vicinity, Shaw terminal and Etowah are shown. Wildy was a stream/swamp margin south of Manilla.

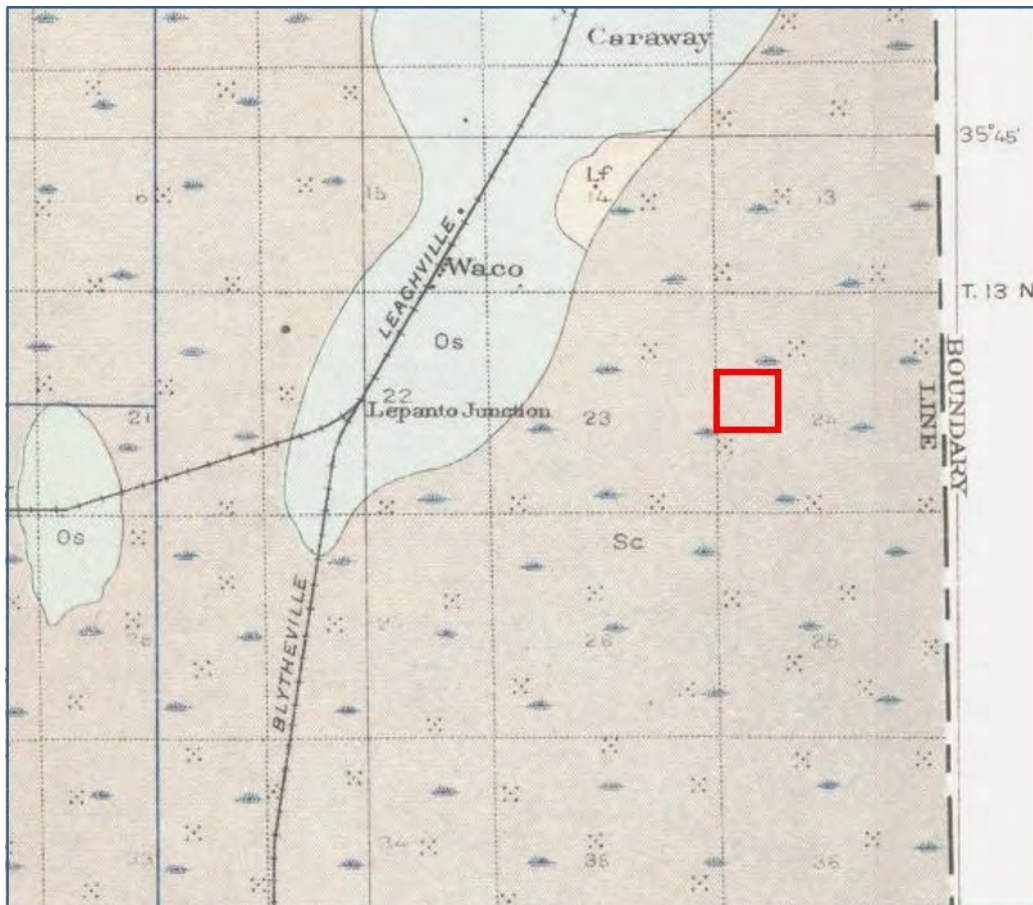


Figure F-25 Caraway-Faulkner Vicinity (USDA 1916)

The 1916 Craighead County soil survey (USDA 1916, Figure F-25) shows the Caraway vicinity sites to be located on Sharkey clay soils in swamp land with sand blows (Sc), with somewhat higher ground, where the railroad and associated settlements were located, mapped as Olivier

fine sandy loam (Os). The project area (SW ¼ NW ¼ S 24 T13N R7E) has no cultural features. The nearest identified locations are Caraway with a few houses and at Waco; no structures are shown for Lepanto Junction. Ditch No. 5, two miles west of the Faulkner project area, had been dug, indicating that logging was completed or nearing completion and the land of the vicinity was being improved for cultivation.

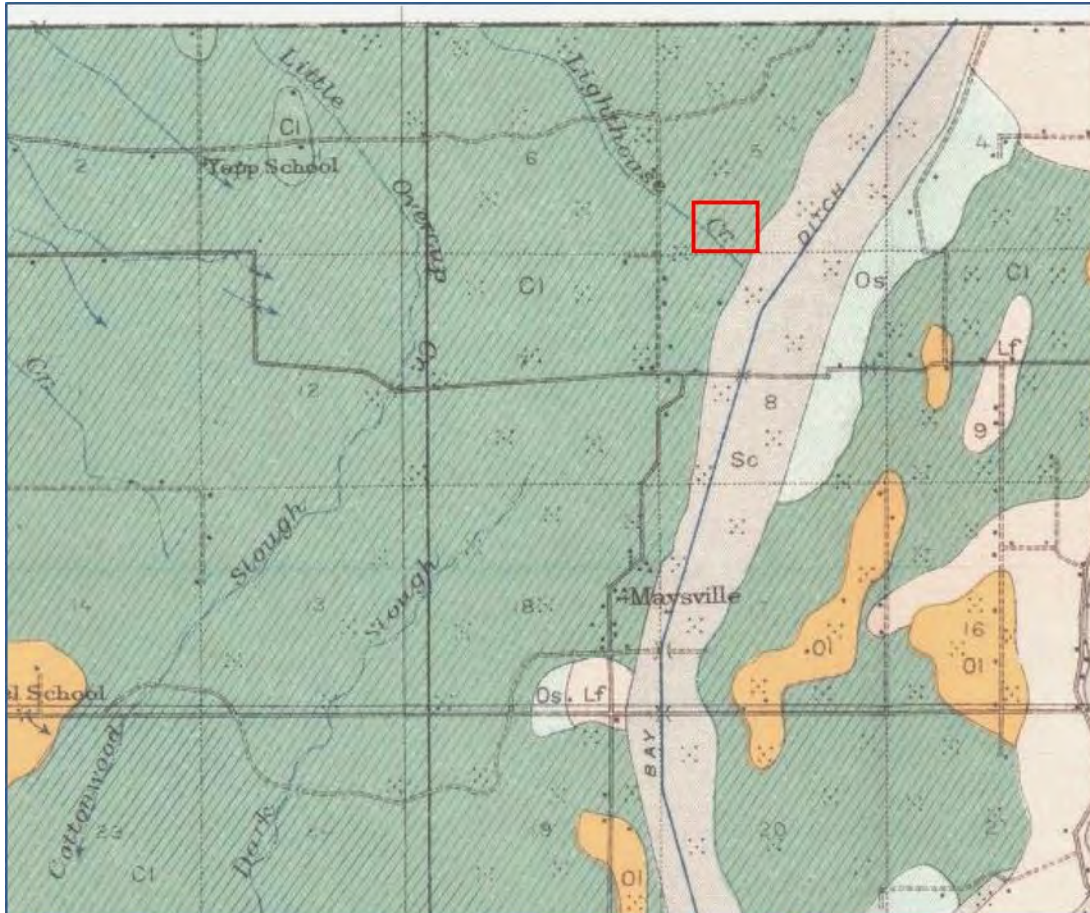


Figure F-26 Garner Vicinity (USDA 1916)

The 1916 Craighead County soil survey (USDA 1916, Figure F-26) shows Lighthouse Creek and other creeks originating on Crowley's Ridge before they were channelized. Other streams (Cottonwood Slough, Dark Slough) originated in the swamp rather than directly gathering the water of the upland streams. Big Bay Bayou had been ditched already, and the other streams would soon be connected to it by lateral ditches. The Garner sites are mapped as Calhoun silt loam, shallow phase (Cl) with sand blows but lacking the swamp symbol overlay, while the Big Bay bottom is mapped as Sharkey clay (Sc). If Lighthouse Creek is accurately depicted, 3CG1256 would have been on its south bank and 3CG1255 and 3CG1257 on the north bank. While there is no evidence on the ground today that this was the case, the description of Calhoun silt loam states that runoff from these soils found its way into "shallow troughs which frequently do not have any perceptible channel" (Deeter and Davis 1916:24). This indicates that Lighthouse Creek near Big Bay Ditch may well have been a diffuse or indistinct stream that required extensive manipulation to form it into the drainage ditch it is today. A dirt road runs along the west side of S5, with several houses along it, but the other houses and turnrows present in the later 20th century are not shown.

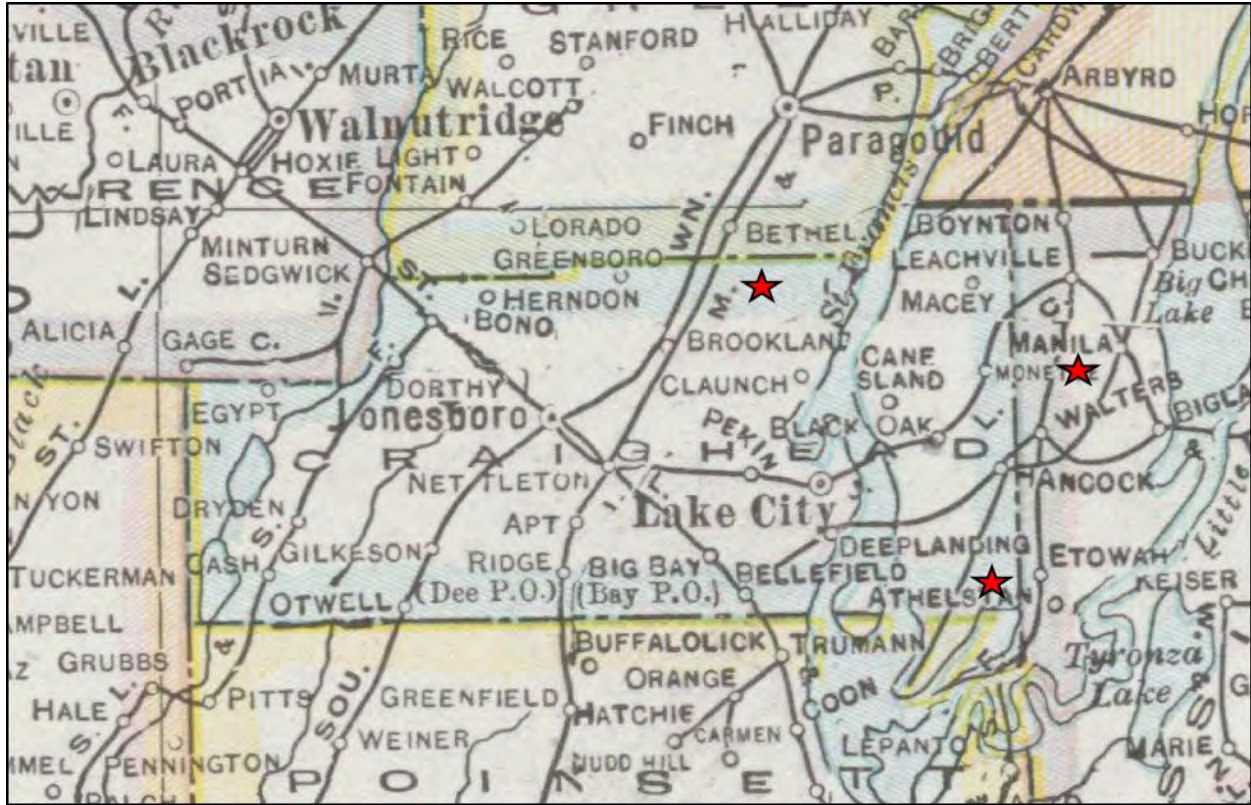


Figure F-27 Project Vicinity (Cram 1920)

The Cram (1920, Figure F-27) map shows the period of maximum penetration of the St. Francis bottom by logging and cotton-hauling railroads. The area between Bethel and Claunch appears unchanged. In the southeastern part of the county, however, additional rail lines have been constructed, so that the Blytheville & Leachville has been connected to the old mainline of the Memphis and Kansas City at Bellefield south of Big Bay. (This may be an erroneous depiction, in light of the Rand McNally 1921 map, which does not depict this second, southern rail crossing of the St. Francis.) There may have been extensive re-laying, as Shaw is no longer shown; rather Hancock and Deep Landing are shown, along with a spur to the east bank of the Hatchie Coon Sunk Lands. Both Etowah and Athelstan are shown, with another tram or spur to Etowah.

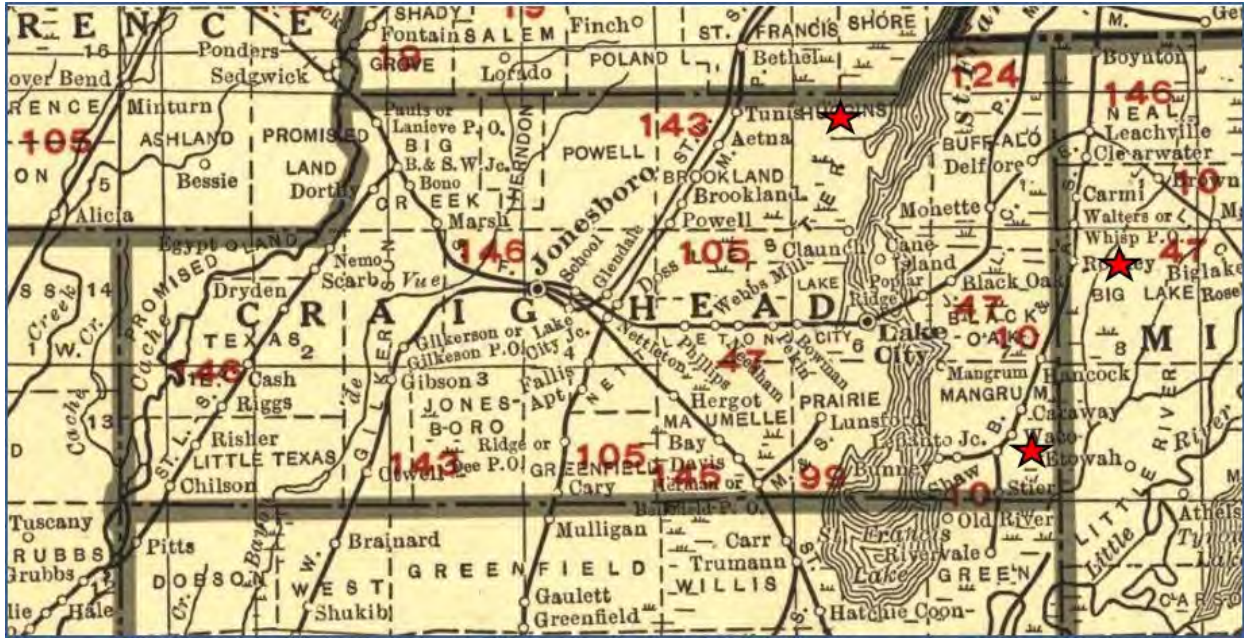


Figure F-28 Project Vicinity (Rand McNally 1921)

The Rand McNally (1921, Figure F-28) map names the townships of Craighead and Mississippi counties; the Garner sites are in Huggins and/or Lester township (T15N R6E) and the Faulkner sites are in Mangrum township (T13N R7E). Huggins township is swamp west of the St. Francis, with Claunch on its south line. Railroad stations are shown south of Bethel at Tunis and Aetna, showing increased settlement in the Garner vicinity, but probably still largely restricted to the ridge itself. Mangrum township contains the B&ASRR, with stations at Hancock, Caraway, Waco, Lepanto Junction and Stier and terminals at Bunny on St. Francis Lake and Rivervale in northeastern Poinsett County. The Faulkner site vicinity remained swamp. It is likely that both Craighead County project areas remained unsettled, uncultivated wooded or cut-over land, as they are on less desirable soils at some distance from both railroads and main highways. T12 R8 (Big Lake Township, Mississippi County) includes Buffalo Creek, which had apparently still not been channelized, although this is difficult to ascertain at this scale. The Wildy site was also marginal swamp land, served by several post offices on the Blytheville railroad.

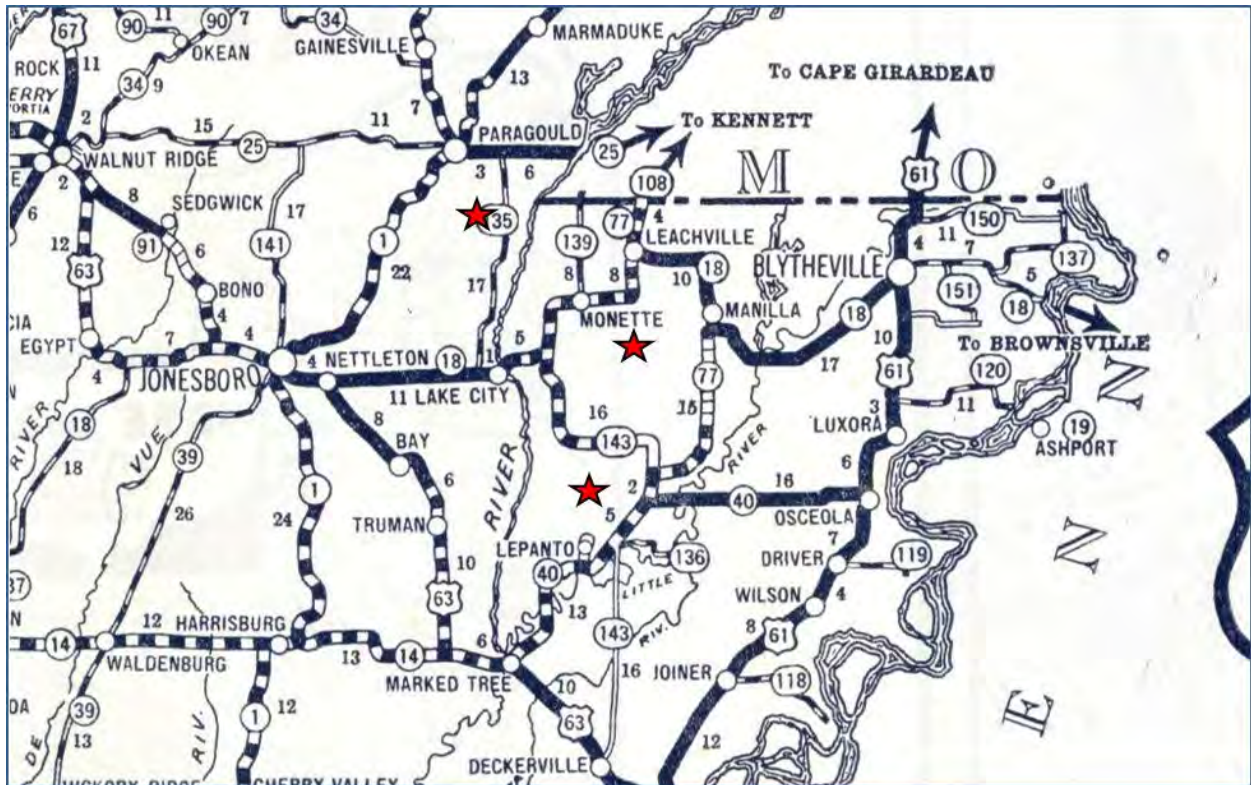


Figure F-29 Project Vicinity (MidWest Map Co. 1931)

The MidWest Map Co. (1931, Figure F-29) map is the first since the antebellum period to show roads rather than railroads. By this time, U.S. Highway 61 was paved, and a section of Arkansas Highway 18 from Jonesboro to Lake City, following the old Jonesboro and Lake City railroad, was also paved. Arkansas Highway 135, from Lake City north to the paved highway at Paragould was a minor, graveled road. This clearly indicates extensive settlement along the west bank of the St. Francis River, which has been reduced to a proper river, rather than a being shown as a vast, swampy lake. Arkansas Highway 143 (today's 158) is shown as a main, graded and graveled road to about the Caraway vicinity or the Mississippi county line, where it was still an unimproved (dirt) road. Little River and Tyronza River are similarly tamed, with the only large lake/swamp remaining being Big Lake.

The 1936 Craighead County highway map, not shown, has no cultural features in S24 T13N R7E except the drainage ditch down the centre of this row of sections from Caraway village south to Buffalo Ditch, and a similar ditch down the centre of the next row west. At this time, the railroad to Stier, Bunney and Shaw was still in existence and there was heavy settlement, including a school, along a county road along the west line of S 35, 26 and 23. In the northern part of the county, the 1936 map shows Lighthouse Ditch built trough to join Big Bay Ditch. Beyond a graded road along the west side of S 5 T15N R6E there are no other cultural features shown in the section. In 1936, both project areas apparently remained unoccupied and possibly forested.



Figure F-30 Project Vicinity (USPO 1945)

The US Postal Office route map (1945, Figure F-30) shows a cultural landscape much changed from the late nineteenth-early twentieth century era, when increased population of loggers and farmers had brought many small rural post offices into the St. Francis bottoms. Brookland on the Missouri Pacific was the mail distribution point for the Garner vicinity; any residents of the project area would have received their mail RFD by this time. The St. Louis and San Francisco, which had absorbed the J&LCRR, apparently still had a mail contract, with stops at Nettleton, Lake City, Black Oak and Monette. The Caraway and Bunney post offices had more recently been closed; their service had been from Black Oak by rail. The creation of a county road system made rural free delivery and the closing of small rural post offices possible. The loss of these crossroads store/post offices does not indicate a decrease in rural population, indeed population of Craighead County continued to increase in this decade, although there was undoubtedly a loss of rural residences and a concentration in and near Jonesboro and the few other growing towns. Any residents in or near the project areas would be expected to have located along the county roads as the dominance of the automobile over mule and wagon drew much occupation from fields to relocate beside county roads.



Figure F-31 Garner Site Project Vicinity (USGS Jonesboro 1958 and Leachville 1956)

The Leachville 15' quadrangle (USGS 1956, Figure F-31) shows the Garner vicinity still wooded. The turnrow running north-south thru S5, as well as houses/farmsteads are shown in the vicinity. Lighthouse Ditch had been dredged, with the channel in its present location by this date. This map indicates that 3CG1255, 3CG1246 and 3CG1257 have been cultivated for no more than 60 years. The three structures at the end of the field road east of the sites is believed to be the source of the very sparse historic material found in the general and controlled surface collections.

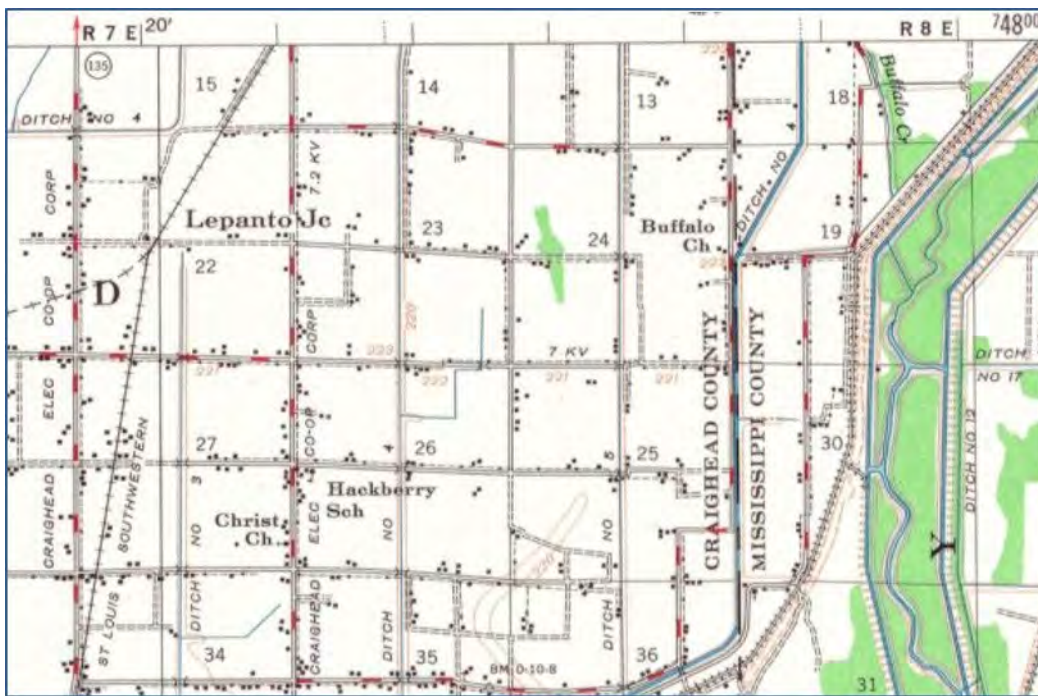


Figure F-32 Faulkner Site Project Vicinity (USGS Marked Tree 1956)

The Marked Tree 15' quadrangle (USGS 1956) shows the vicinity of the Faulkner sites as almost completely cleared cropland, with a small scope of woods separating the two sites (Figure F-32), whereas, the Manila quadrangle shows the Wildy site as entirely cleared (Figure F-33).



Figure F-33 Wildy Site Project Vicinity on Manilla 1956 Quadrangle

F.3.4 Previously Recorded Sites

An AMAZDA search of the Arkansas Archeological Survey site files shows that sites with the following reported Archaic and Woodland period components had been reported in Craighead, Green and Poinsett counties as of 2015 (Table F-2).

Table F-2 Archaic and Woodland Components in Poinsett, Craighead and Greene Counties.

Component	Craighead	%	Greene	%	Poinsett	%	Totals
Early Archaic	77	28	43	36	11	12	131
Middle Archaic	11	4	5	4	3	3	19
Late Archaic	99	36	61	51	48	53	208
Early Woodland	6	2	2	2	2	2	10
Middle Woodland	6	2	2	2	5	5	13
Late Woodland	76	28	7	6	22	24	105
Total components	275		120		91		486

This search did not include Mississippi County, which primarily has a very different physiography as well as culture history, and it did not include Mississippi period components in any of these counties. The higher totals for Craighead County are in all likelihood because of the presence of the AAS-Jonesboro station in the county. The results show Late Archaic components the most likely to be identified, followed by Early Archaic and Late Woodland. The large numbers of Early Archaic sites are in all likelihood the result of survey efforts focusing on this time period. The comparative lack of Middle Archaic and Early and Middle Woodland components may be in part an artifact of research. These periods are shorter, and also lack good diagnostics. However, the Early Archaic is also a brief period. The general lack of Middle Archaic sites has long been taken to indicate that the Delta was largely abandoned in favor of the Ozark uplands during the Hypsithermal. The lack of Early Woodland (Tchula) sites is probably because these sites are defined by the rare untempered pottery types, which may not have been present on all sites of the period, but also are marked by a continuity with the Late Archaic in projectile point types and settlement and subsistence patterns. Only some Middle Woodland (Marksville) produce diagnostic decorated ceramic types, while most sites that have components that could be attributed to the period have, with limited surface collections or shovel tests, produced only plain and cordmarked grog and/or sand tempered ceramics that were produced over a long time span within the Woodland period and so are not temporally diagnostic, and tend to be assigned to the Late Woodland period.

The significance of this gross scale data is also limited by the fact that the three counties cut across three distinct landforms: the Western Lowland, Crowley's Ridge and the Eastern Lowland. The work areas we are concerned with here are all located in the Eastern Lowland. The AMAZDA search also returned quadrangles, so the counts can be refined further to limit them to the Eastern Lowlands (Table F-3). These quadrangles are: Brookland, Cardwell, Dixie, Hatchie Coon, Joyland, Lake City, Leachville, Lepanto, Marked Tree, Monterey, Mounds, Needham, Paragould East, Rivervale, Trumann and Tyronza. This restriction shows a much different pattern. Late Archaic sites are still common, but at lower frequencies when the Crowley's Ridge and Western Lowland sections are included. The Middle Archaic, Early Woodland and Middle Woodland remain poorly represented. Late Archaic components appear to be slightly less common compared to the county at large, while Late Woodland components are distinctly more common.

Table F-3 Archaic and Woodland Components in Eastern Lowland Section of Poinsett, Craighead and Greene Counties

Component	Craighead	%	Greene	%	Poinsett	%	Totals
Early Archaic	16	13	4	17	1	3	21
Middle Archaic	2	2	1	4	0	-	3
Late Archaic	31	25	13	54	9	30	53
Early Woodland	3	3	1	4	2	7	6
Middle Woodland	2	2	0	-	4	13	6
Late Woodland	68	56	5	21	14	47	87
Total components	122		24		30		176

The Garner sites are located on the Dixie 7.5' quadrangle, while the Faulkner sites are located on the Rivervale 7.5' quadrangle. There are 17 reported archaeological surveys on the Dixie quadrangle (AMAZDA report numbers 200, 636, 680, 1287, 1317, 1606, 1755, 2179, 2742, 3363, 3482, 3588, 3880, 3966, 4225, 4231, and 5335). Most are linear surveys associated with work on the already-constructed St. Francis River levee and Eighmile Ditch as well as smaller ditches and county roads. Neither Big Bay Ditch nor Lighthouse Ditch has been the subject of archaeological survey. Also included are some farm-size blocks (AMAZDA report numbers 200, 1317, 1606, 3363, 3588, 3966, and 4225). However, most of the archaeological sites that have been reported for the area are volunteered reports from artifact collectors and Arkansas Archeological Society members working with Jonesboro station archaeologists. Two to four miles northwest of the Garner sites twelve sites have been reported, with one Early Archaic, four Late Archaic and one Late Woodland components being identified. In the five miles south of the Garner sites along Big Bay Ditch, a series of large lithic scatters on the old bankline about a quarter-mile back from the ditch have been identified, but little other evidence for these sites is available. At Dixie, in an area of about 1-mile radius (S21 and 22 T15N R6E), some 45 densely packed, typically very small, sites have been reported. Almost all date to the Late Woodland period, with limited evidence that occupation extended into the Mississippi period on a much-reduced scale.

There is less survey coverage in the vicinity of the Faulkner sites in extreme southeast Craighead County. Search of the AAS files reveals only 6 surveys (AMAZDA report numbers 7, 802, 2311, 4359, 4460 and 4461); all except #2311, which produced no sites, are linear surveys associated with the Right Hand Chute levee, Buffalo Ditch and Ditch No. 2. Twenty-one sites in Craighead County have been reported by these surveys, all identifiable components (n=9) are Late Woodland and/or Early Mississippian. There has been much less work by amateurs and survey archeologists in this remote backswamp area.

F.3.5 National Register of Historic Places Listings

There are no NRHP-listed sites in the project vicinity. Craighead County NRHP listings are primarily structures in Jonesboro, with two structures in Monett. A 142' long steel deck truss bridge over a ditch in CR 513C (built in 1942) was listed on the NRHP in 1995 (#9500614). This historic bridge is about 6 miles southeast of the Garner sites. One prehistoric archaeological site, Bay Mounds (#78000582) has been listed. The location is remote from our project.

There are 38 NRHP listings for Mississippi County. Most are historic architecture in Osceola or Blytheville, but they include the Blytheville, Leachville & Arkansas Southern Railroad depot in Leachville (listed 1992), the Jonesboro, Lake City & Eastern Railroad depot in Manilla (listed 1997) and the Herman Davis monument in Manila (listed 1995). There are also listed properties in the Wilson, Etowah, Dell, Burdett, Keiser, Dyess and Delpro areas. Mississippi County also has 4 Mississippian village sites (Chickasawba Mound, Eaker Air Force Base, Nodena and Zebree) listed on the National Register. None of these properties are near our work areas and none will be impacted by the investigations.

F.3.6 Expected Site Types

Based on previous work, the most likely site types are small lithic and/or ceramic scatters, largely or entirely confined to the plow zone. Based on the results of previous research, as just discussed, Late Archaic and Late Woodland components are the primary cultural manifestations to be expected. Sites in the area are often adversely impacted by land-leveling as well as sand blows. Prehistoric sites are typically closely associated with permanent water sources, however, the nineteenth and twentieth century land use history, in particular drainage efforts, often obscure

this relationship. Historic components are most likely to date to the latest nineteenth through middle twentieth century period of maximum dispersal on agricultural lands and represent the homesteads of share-cropping agricultural tenants, renters and resident landowners.

F.4 Archaeological Methods

Here we discuss the methods used for archaeological field and lab investigations.

F.4.1 Field Methods

The 2011 work at the Faulkner #1 and #2 sites (3CG1253 and 3CG1254) consisted of general surface collection of small, diffuse, low-density surface scatters. Site 3CG1253 was found to measure 30m x 75m while 3CG1254 measures 25m x 45m. While geological trenches were excavated on 3CG1253, all archaeological material recovered came from surface contexts except for two flakes from Soil Pit #3. A geological trench was placed downslope from 3CG1254. A topographic map of the vicinity of these sites was also produced.

The 2011 work at the Wildy (3MS909) site consisted of walking a ditch bank in search of a sand blow. A slight ceramic scatter was noted in this bank, and additional surface survey was conducted in the adjacent cultivated area. Geological trenching nearby encountered no buried, intact cultural deposits.

The 2013 and 2015 work at the Garner site (3CG1255) reported here consisted of general surface collections, test units and selected specimens collected during mechanical trenching. The 3CG1255 controlled surface collection (CSC) of 20 10m x 10m squares was conducted on 21 March 2013. Some 6 additional tools were piece-plotted within this CSC area. Two test units (or soil pits) were also excavated at 3CG1255 in 2013. TU1 was placed in the proposed Trench 1 and excavated in four levels on 20 March 2013. These levels were 0-20 cmbs, plow zone and sand; 20-30 cmbs, sand; 30-40 cmbs, sand and grey silt; and 40-50 cmbs, grey silt. TU 2 was placed in the proposed Trench 2 area on 21 March 2013. It was excavated in three levels; 0-14 cmbs, plow zone; 24-34 cmbs, grey silt, and 34-44 cmbs, grey silt. The results of the 2013 work were presented in our report of 10 April 2014 (Tuttle et al., Contract No. NRC-HQ-11-C-04-0041).

In November 2015, we returned to 3CG1255 to conduct mechanical trenching in areas investigated in 2013. Two 90-cm-wide trenches were placed on an east-west orientation. Trench 2 encountered TU 2 from 2013; the original test unit was not noted in mechanically clearing the first trench. Five 1m x 1m test units were excavated beginning below the sand blow in the previously defined "grey silt," or sealed pre-sand blow land surface. There was one unit (TU 1) in Trench 1 and four contiguous units (TU 2, 3, 4, and 5) in Trench 2.

Excavated materials were dry screened through ¼" hardware cloth, with one exception. A 50 cm x 50 cm soil column for water screening was collected from 3CG1255 TU 4; this material was processed through window screen in an unsuccessful attempt to recover charcoal from a diffuse area of burned earth. Besides finely divided burned earth, very little material was recovered from the water screen sample, but the material has been retained for potential further analysis.

F.4.2 Laboratory and Analytic Methods

Materials were washed, sorted and bagged for storage. Artifacts were sorted into standard archaeological categories. Tabular data on artifacts from site 3CG1255 are presented here as an appendix. The other locations investigated produced minimal archaeological materials, which will be presented in the descriptions of sites and investigations below.

While radiocarbon and other absolute dating methods have been used here, traditional relative or stratigraphic methods have also been applied to the materials recovered. These most importantly are projectile point/knife and biface tool typologies developed over long periods and over wide areas, as discussed above. These typologies are largely based on stratigraphic position but are occasionally tied to absolute dates.

While materials collected in 2013 have been assigned Arkansas Archeological Survey accession numbers, we acknowledge that the collections remain the property of the landowner and will be returned upon request. Materials from Wildy (3MS909) and the Faulkner #1 and #2 sites (3CG1253 and 3CG1254) have been donated to the AAS. The collections from the Garner sites (3CG1255, 3CG1256 and 3CG1257) have been de-accessioned and returned to the landowner, Greg Garner.

Updated Arkansas Archeological Survey site forms have been filed for the sites discussed here.

F.5 Results of Archaeological Evaluations

Here we discuss the results of the 2013 and 2015 geological testing and other investigations as they pertain to the archaeological deposits. Three areas are discussed: 1) two adjacent minimal manifestations in the southeast corner of Craighead County, east of the St. Francis River; 2) another minimal manifestation in adjacent Mississippi County; and 3) a cluster of large, dense, mostly Archaic occupation near the eastern flank of Crowley's Ridge and west of the St. Francis in Craighead County. More specifically, these sites are Faulkner #1 and #2 (3CG1253 and 3CG1254); Wildy (3MS909) and the Garner #1, #2 and #3 (3CG1255, 3CG1256, and 3CG1257). Sites 3CG1253 and 3CG1254 are located in a field in extreme eastern Craighead County, about 3 km north of Little River. Site 3MS909 was recorded along a ditch in extreme northwestern Mississippi County, 4.5 miles west southwest of Manila. Sites 3CG1255, 3CG1256 and 3CG1257 are three nearly contiguous scatters located in a field in extreme northern Craighead County near the junction of Lighthouse Ditch and Big Bay Ditch.

F.5.1 Sites 3CG 1253 and 3CG1254

Site 3CG1253 (Faulkner #1) was recorded by Tuttle and Haynes on 27 October 2011. The site can be located on the 1983 Rivervale 7.5' quadrangle in NW ¼ S24 T13N R7E (Figure F-34). The location is in extreme eastern Craighead County, near the Poinsett County line, in a generally level area that has been highly modified by ditching and land leveling. This site is an elongate oval prehistoric artifact scatter of 2250 square meters (75m x 30m). The location is a slight, sandy silt loam rise along an old stream channel in a cultivated field. The archaeological materials are found above an earthquake liquefaction feature. Site 3CG1253 is considered to be moderately disturbed by natural causes and agricultural activities. At the time of the 2011 field visit, the field had been harvested and surface visibility was good (51%-75%). No subsurface archaeological investigations were conducted. On 29 October 2011, geological investigations consisted of two mechanized trenches perpendicular to the old bankline and 7 scattered, hand excavated, unscreened soil pits in and near the archaeological site. Lafferty monitored the trenching, and Haynes and Morrow were on hand, but no archeological material was found in the trench. The total disturbance for the location from trenching totaled 7 m in length and approximately 1 m wide. The National Register of Historic Places eligibility of the site was not determined, but there does not at present appear to be any evidence that the site is eligible for the NRHP.

Diagnostic artifacts from 3CG1253 indicate a relatively small, low-density surface scatter with Woodland Period occupation. Material collected in the select surface collection was limited to lithics and ceramics. These were 10 pieces of chert debitage, 7 small, eroded sand tempered (Barnes series) sherds and two pieces of other fired clay (AAS accession number 2011-552). No historic artifacts were reported.

Site Faulkner #2 (3CG1254) was recorded by Lafferty, Haynes, Morrow, and Scott on 29 October 2011. The site can be located on the 1983 Rivervale 7.5' quadrangle in NW ¼ S24 T13N R7E. It is on the western side of the old river channel opposite 3CG1253, approximately 300 m southwest of the latter site. This small, elongate oval, low density prehistoric artifact scatter is of a very limited nature, as only 3 artifacts were recovered. The footing of a barn lies approximately 20 m northwest of this diffuse minimal scatter. The area where artifacts were found measures 45 m x 25 m (1125 square meters) and is limited to a low sandy silt loam rise adjacent to an abandoned stream channel. The sandy rise where artifacts were found was interpreted as a possible earthquake liquefaction feature. The site has been moderately disturbed by natural and agricultural activities and at the time of the 2011 field visit the land had been harvested but surface visibility was reportedly good (50% - 75%). No subsurface investigations, archaeological or geological, were conducted within the site boundaries as defined. Archaeological trenching with soil pits was conducted in an area sloping into the old channel 50m to 100m northeast of the artifact scatter. There were 10 hand-excavated, unscreened soil pits excavated to define the dimensions of the sand blow, and the trench measured 10 m in length. The trench was located perpendicular to the bank of the slough. Lafferty monitored the trenching, and Haynes and Morrow were on hand. However, no archaeological deposits or artifacts were encountered in the trench. The National Register of Historic Places eligibility of the site was not determined, but there does not at present appear to be any evidence that the site is eligible for the NRHP.

The 3CG1254 site is assigned to the Woodland period, based on a small sand-tempered (Barnes series) sherd as well as two non-diagnostic flakes of Crowley's Ridge gravel. These are 1) an eroded sherdlet, 1 cm x 1.7 cm and .5 cm thick; 2) a coarse tan chert gravel biface thinning flake with a shattered platform and utilized distal margin, and 3) a glossy tan gravel chert primary decortication flake with snapped distal edge and notched lateral margin. This collection of three artifacts (AAS accession number 2011-553) is considered a general (100%) collection. Topographic mapping conducted as part of the archaeological investigations show an "old foundation" 20m north of the artifact scatter. The 1983 quadrangle shows the "barn" (empty square) symbol in this area. As noted in the map review, this barn was removed between 2001 and 2010.

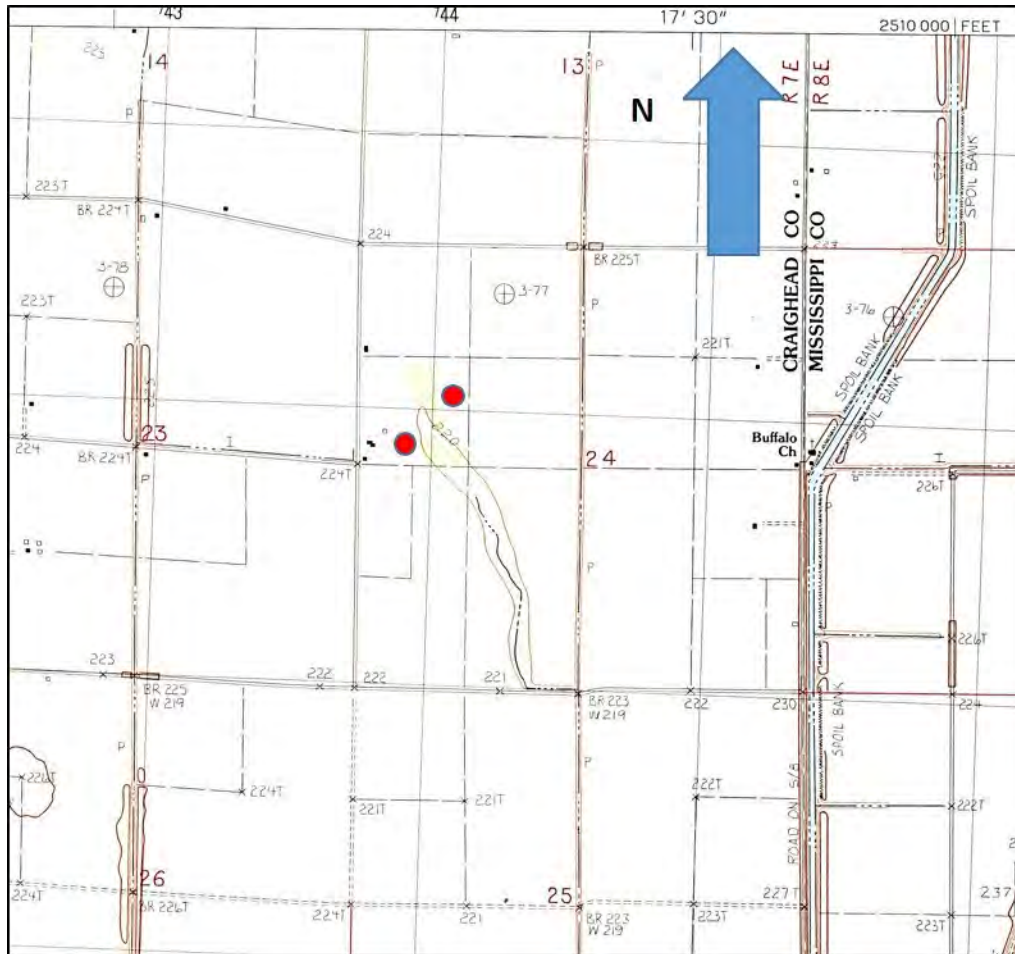


Figure F-34 Project Vicinity Shown on 1983 Rivervale 7.5' Quadrangle

F.5.2 Site 3MS909

The Wildy (3MS909) site was discovered by Tuttle and Busch on 21 September 2011 while examining ditch exposures for sand blows and related dikes. The area can be located on the Manila South (1983) 7.5' quadrangle (Figure F-35). Sand-tempered sherds were observed beneath a sand blow in the bank of a ditch running east-west through the middle of Section 9 (Figure F-36). The AAS archaeological site form reports that on 27 October 2011, the site was later recorded by Haynes, Morrow, and Scott. A surface survey by archaeologists was conducted in the south adjacent plowed field where sand blows also occurred. A small, sparse ceramic scatter was recorded in the field. All archaeological materials were recovered from a surface context. These materials held by AAS-Jonesboro were not made available for the present study. Two unscreened soil pits were excavated to assess the depth and extent of the sand blow. An area of interest was identified and subjected to electrical resistance survey. Based on the results of the survey, two trenches were placed outside the area of identified artifact scatter. Lafferty monitored the trenching, and Haynes was on hand, but no archaeological deposits or artifacts were encountered in the trench. The total area disturbed by geological trenching was 13 m long and approximately 1 m wide. A topographic map of the area of investigations was also made.

F.5.3 Sites 3CG1255, 3CG1256 and 3CG1257

These sites in Craighead County are found in a large area of prehistoric lithic scatter, east of Crowley's Ridge and near the northern (Greene) county line. Site 3CG1255 (Garner 1) is a prehistoric and historic artifact scatter in a cultivated field. It can be located on the 1983 Dixie 7.5' quadrangle in the SE ¼ S5 T15N R6E, in the Shugtown vicinity (Figure F-46). The site was discovered by Tuttle and Busch on 24 October 2012 while performing reconnaissance for sand blows on Late Pleistocene landforms east of Crowley's Ridge. Possible sand blows had been noticed on satellite imagery of the area. The archeological site was later recorded by Lafferty, Haynes, Morrow, and Scott in March 2013 during further evaluation of the site by Tuttle, Lafferty, Morrow, Scott, and Wolf, and further investigated during trenching by Tuttle, Starr, and Haynes in November 2015. The area is an "old river terrace" underlain by silty overbank and sandy channel deposits 300 m north of Lighthouse Ditch. The site is in a cultivated field where rice, corn and beans have been grown since at least the mid 20th century. The site has thus been moderately disturbed by natural causes, drainage and typical agricultural activities. In addition, the farmer indicates that this field has been lightly land leveled, with some material brought from the southern, higher part of the field and deposited across 3CG1255. The site measures 140m x 100m (14,000 square meters) based on a controlled surface collection. This intensive collection was conducted in 10m x 10m squares with diagnostic artifacts flagged and piece plotted during topographic mapping. Surface visibility during the controlled surface collection was reportedly excellent. The significance of this controlled surface collection is brought into question by the reported redeposition of material by leveling, and the plow zone and sub-sand-blow deposits appear to have little to do with each other culturally or chronologically. Indeed, it is likely that the CSC materials are out of context. Two 1ft x 2ft test pits were excavated through the sand blow in an area identified for potential mechanical trenching based on geophysical survey results. These ¼" dry screened test pits produced lithic artifacts from what appeared to be a buried, intact A horizon. As of 2013, the NRHP eligibility of site 3CG1255 was undetermined.

Artifacts reported from the 2012 and 2013 investigations at 3CG1255 were 24 chert cores, 799 pieces of debitage, 48 retouched and/or heavily utilized flakes, 3 bifaces/biface fragments, 3 projectile point/knives, 7 cobbles, 106 fire-cracked rocks and 44 pieces of burned clay, as well as 6 historic artifacts (3 ceramics, 3 container glass). These materials were accessioned by AAS-Jonesboro (accession number 2013-456, with 37 field specimen numbers for TU 1, TU2 and 20 CSC squares as well as piece plots), but the materials have been deaccessioned and returned to the landowner.

Site 3CG1256 (Garner 2) is located about 300m south of 3CG1255, along the north bank of Lighthouse Ditch in SW ¼ S5 T15N R6E. This site is a large prehistoric lithic scatter. A site form was submitted for the site by Robert Scott on 15 April 2013. Scott described the site as consisting of two or more concentrations with lighter scatter between them. He estimated the site to measure 325 m x 140 m (45,500 square meters) based on walking and flagging the area of surface finds. The tool finds were later mapped in as part of the topographic mapping around 3CG1255. The site area is considered to be a braided stream terrace with soil variously sand (sand blows), sandy silt loam and silt loam. Scott further noted that the field had been leveled with soil moved from the southwest part to the northeast part of the field. His assessment was that, while artifacts in the western part of the site "are probably not re-deposited artifacts, the ground surface artifacts are resting on in this part of the site is most likely an artifact-bearing soil horizon exposed by landleveling," as "diagnostic projectile points were found on the surface across the site...in places of significantly sandier soil than the surrounding field" (AAS site survey form 3CG1256). Diagnostic materials included Dalton points (Figure F-37, Figure F-38), early bifacial drill forms and formal cobble cores (Figure F-39, Figure F-40, and Figure F-41), large stemmed Late Archaic

pp/ks (Figure F-21, Figure F-43, Figure F-44) and crude side-notched Woodland pp/ks (Figure F-45). Besides land-leveling, the location has been moderately disturbed by natural causes, clearing, drainage and cultivation. Surface visibility conditions were excellent at the time the select surface collection was made. No subsurface investigation was made at 3CG1256. As of 2013, the NRHP status of 3CG1256 was undetermined., the location has been moderately disturbed by natural causes, clearing, drainage and cultivation. Surface visibility conditions were excellent at the time the select surface collection was made. No subsurface investigation was made at 3CG1256. As of 2013, the NRHP status of 3CG1256 was undetermined.

Artifact recovery at 3CG1256 consisted of 17 cores/core fragments, 112 pieces of debitage, 12 retouched and/or heavily utilized flakes, 12 bifaces/biface fragments, 10 projectile point/knives, 1 pitted cobble, 3 fire-cracked rock and 1 piece of burned clay. Projectile point/knives indicate occupation during the Early, Middle and Late Archaic and Early and/or Middle Woodland periods. No prehistoric ceramics or historic materials were noted. The materials were mistakenly assigned AAS accession number 2013-457 but have now been deaccessioned. This was a select or grab sample with an emphasis on tools and diagnostic art.

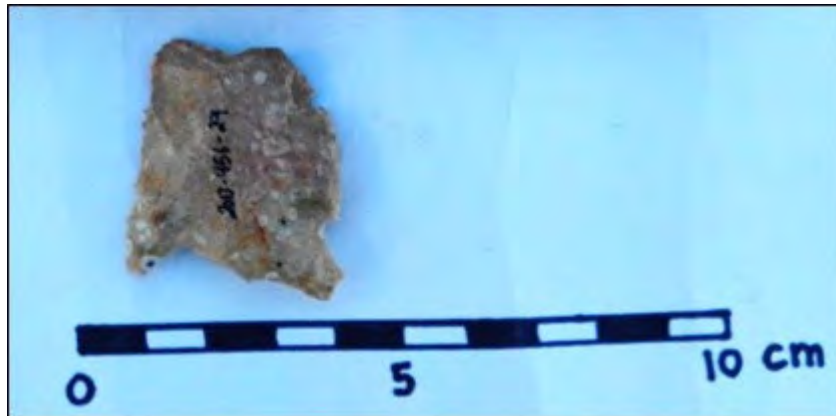


Figure F-37 Corner-Notched Base, cf. Dalton, 3CG1256



Figure F-38 Corner-Notched Dalton pp/k Base, 3CG1256



Figure F-39 Drill (Reworked pp/k?), 3CG1256



Figure F-40 Cores and Biface Preform, Archaic Period, 3CG1256, Right Possible Dalton adze



Figure F-41 Additional View of Core, 3CG1256



Figure F-42 Stemmed Points, Middle and/or Late Archaic Period, 3CG1256. Right, cf. Late Archaic Barbed



Figure F-43 Stemmed Point, Late Archaic Period, 3CG1256

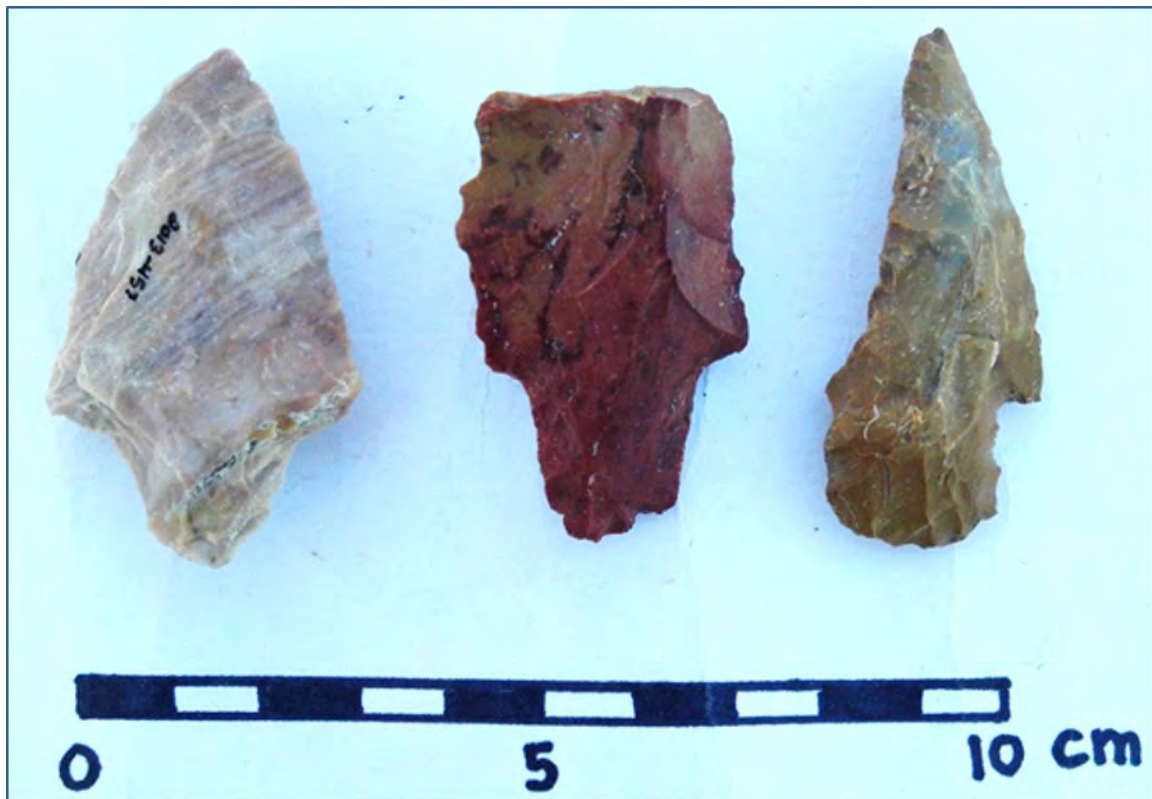


Figure F-44 Stemmed Points, Late Archaic Period, 3CG1256. Left, cf. Gary



Figure F-45 Side-Notched Woodland Period pp/ks, 3CG1256. Right, similar to Jacks Reef

Site 3CG1257 (Garner 3) is a small (50 m x 90 m or 4500 square meter) prehistoric scatter located between the larger sites 3CG1255 and 3CG1256, in SW $\frac{1}{4}$ S5 T15N R6E, on the same braided stream surface as sites 3CG1255 and CG1256. A site form was submitted for the site by Robert Scott on 15 April 2013. Scott notes that “this site was arbitrarily defined from another much larger surface scatter located immediately to the south” (i.e. 3CG1256) and that further work might demonstrate the three Garner sites to be a single contiguous archaeological area with varying density. He also entertained the possibility that this location in particular was redeposited by land-leveling. The site is judged to also be disturbed by natural causes and agriculture. Site soil is sandy silt loam. Surface visibility was excellent when the select surface collection was made. As of the 2013 surface collection, the NRHP eligibility of 3CG1257 was undetermined.

The materials recovered from 3CG1257 date to various phases of the Archaic period. Only lithics were collected. These were 1 core, 38 debitage, 1 unifacial tool, 1 biface and 1 projectile point. These materials were catalogued under AAS accession number 2013-458 but have now been deaccessioned.

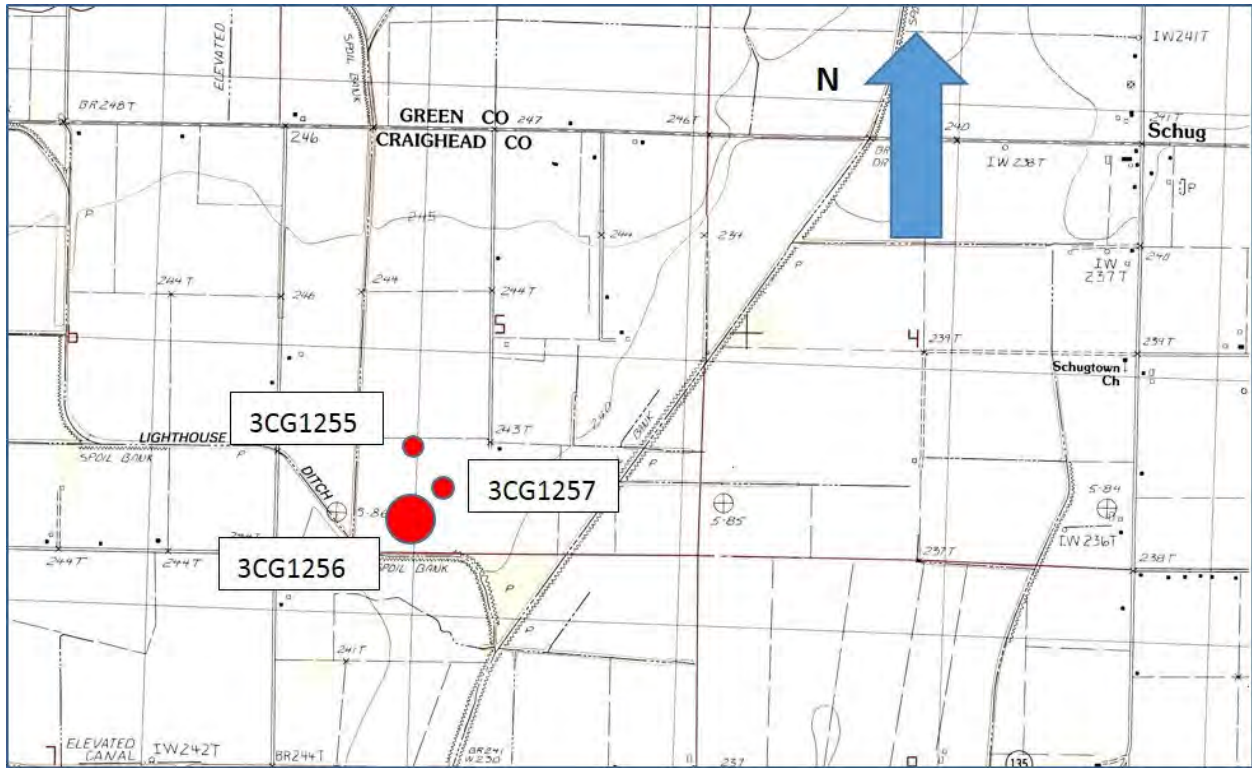


Figure F-46 Project Vicinity Shown on Dixie 7.5' Quadrangle (1983)

F.6 Archaeological Investigations

Here we discuss recent archaeological investigations carried out at the above described Craighead and Mississippi county sites.

F.6.1 Sites 3CG1253 and 3CG1254

The locality was pointed out to geologists as potentially having sand blows in combination with archaeological deposits by farmer Ron Faulkner. The Faulkner #1 and #2 archaeological sites were identified by pedestrian survey of a 40 acre cotton field by archaeologists on 11 and 27 October 2011. These small sites lie on either bank of a small, now drained and partially filled slough in an abandoned channel. The potential sand blow study areas were walked on a 2- meter interval with very little material being recovered. Stalks had been cut and surface visibility was reported at 50%. Also in October 2011, several small soil pits were hand excavated to ascertain the depth of the sand blows. These soil pits were not screened, but two flakes were recovered by hand-picking from Soil Pit 3 at 3CG1253. These soil pits were excavated to identify areas for further geological investigation; subsequent to identifying a target area for trenching, electrical resistance surveys were conducted to further refine the position of trenches. Subsequently, 7 meters of backhoe trench was excavated at 3CG1253 while a 33-meter-long trench was excavated at 3CG1254. No archaeological materials were recovered from the trench excavation and logging. A topographic map was made of the 40-acre study area.

F.6.2 Site 3MS909

Site 3MS909 was identified on 21 September 2011 when three sand-tempered (Barnes series) potsherds were recovered from beneath a sand blow that was exposed when the location was cut

through by a drainage ditch (Ditch 11) beside a county road. The material was noted to have occurred 100 cm below present ground surface and 6 to 8 cm below the base of the sand blow. After discovery of the natural and cultural material by geologists, Arkansas Archeological Survey archaeologists visited the site for surface survey. Another twenty small sand-tempered sherds (not examined by this author) were collected from the surface near the initial find. Although there is some gravel scatter from the road through/alongside of the site, no prehistoric lithic materials were recovered. It is not unusual for no stone tools or debitage to be found at small Woodland period ceramic scatters. At the time of survey, the field was planted to cotton, with 30% surface visibility. The total scatter was estimated to be less than an acre in extent and is believed to parallel Ditch 11. Subsequently, resistivity survey was conducted to map the subsurface extent of the sand blow and sand dikes and a soil probe was used to confirm the extent of the sand blow. A potential location for a trench was identified and an electrical resistance survey was conducted over the indicated area. A three foot (approximately 90 cm) wide backhoe trench was excavated based on the results of the resistivity survey. During this mechanical excavation, the plow zone was stripped and the sub-plow zone surface exposed was examined for cultural materials or features. The sand was then removed while an archaeologist monitored the excavation, and the original land surface below the sand was again examined for cultural materials or features. No additional cultural material was noted or recovered at 3MS909. A topographic map was also made of the area.

F.6.3 Site 3CG1255

In 2015, as evidently has been the case since at least 1977, the direction of cultivation of the field containing 3CG1255 was north-south. The land had been rowed up and planted to corn; when we arrived 5 November 2015, the surface was moderately obscured by corn stover. The farmer Greg Garner reports, and older aerial imagery confirms, that the land has also occasionally been used for rice cultivation. No attempt at another complete surface collection was made, but select items were collected over the course of the fieldwork and bagged as a general surface collection.

A total of 10.75 m of 90-cm-wide backhoe trench was excavated on 3CG1255. The eastern trench (Trench 1) was located based on the results of electrical resistivity survey, test pits and controlled surface collection. The trench was oriented east-west. Removal of the 15 cm thick, dark brown (10 YR 3/3) fine sandy loam plow zone failed to reveal any archaeological features intruding into the sand blow. After examination of the sub-plow zone surface, the sand blow was removed to the top of the light brownish grey (10 YR 6/2) silt below. This buried surface was marked by occasional plowscars and strong red-ox features including weak 1-2 mm Fe-Mn concretions. Chert debitage and fire cracked rock also immediately became evident as this buried surface was cleared of remaining sand. A sample of carbon (root?) was collected from a dike at 5.3 m east of west end.



Figure F-47 3CG1255, Trench 1, TU 1, 5 cm below Base of Sand Blow



Figure F-48 3CG1255, Trench 1, TU 1, 10 cm below Sand Blow, Showing Increasing Fe-Mg Concentration



Figure F-49 3CG1255, Trench 1, TU1, 15 cm below Sand Blow, Showing Fissures and/or Root Cast, with Pronounced Mottling

A test unit was laid out at 5 to 6 m east of the west end of Trench 1 and excavation began in 5 cm arbitrary levels with soil removed screened through $\frac{1}{4}$ " hardware cloth (Figure F-47). Four levels were excavated: 0-5 cm below sand, 5-10 cm, 10-15 cm and 15-20 cm. The last level was culturally sterile. Soil development in the homogeneous light brownish grey silt was weak and the concretion formation appeared to be the result of water percolating through the sand blow reaching a perched watertable formed by the rather impervious silt. In contrast to the 1-2 mm concretions at the contact, by 5-10 cmbs there were more and larger (2-4 mm) concretions (Figure F-48). By 10-15 cmbs, there were fewer concretions and the soil was heavily mottled (Figure F-49). Excavation ended at 20 cmbs, where mottling and mineral concentration were decreasing but evidence of biological activity was still clear (Figure F-50). As a potential indication of disturbance, a very small fragment of iron/steel wire was recovered from the 10-15 cm level; downward filtration of such a relatively heavy, very small, bi-pointed item is not unexpected and is not considered an indication of a significant level of disturbance. Artifacts from TU 1 are summarized below (Table F-4). Fire cracked rock (FCR) was the dominant artifact class recovered, with only 8 pieces of chert debitage.



Figure F-50 3CG1255, Trench 1, TU 1, 20 cm below Sand Blow, Fissure/Rootcast more Pronounced but Fe-Mn Concentration Decreasing

Table F-4 3CG1255, Trench 1, TU 1 artifact recovery

Level	Debitage	Other	Totals
0-5 cm	1 secondary decortication flake 1 flake fragment	14 FCR 1 quartz pebble 1 concretion	18
5-10 cm	2 biface thinning flakes 1 core fragment/shatter	23 FCR 1 quartz pebble 1 concretion	28
10-15 cm	2 biface thinning flakes 1 flake fragment	13 FCR 1 wire	17
15-20 cm			No artifacts
Totals	8debitage	50 FCR 2 pebbles 2 concretions 1 wire	63

The western trench (Trench 2) was treated in a fashion similar to Trench 1, with the plow zone removed, the sand blow surface scraped, and then the sand removed to the buried land surface, which was again scraped by shovel and trowel. Artifacts were again recovered immediately at the

contact, with a side-notched projectile point basal fragment being recovered immediately below the sand blow in the top of the old land surface (62 cmbs). Diffuse charcoal was again noted at the contact, but without any clear cultural context. There was abundant Fe-Mn concentration in small, weak concretions at the contact.

Test Unit 2 was placed at the originally mapped west end of Trench 2, which was subsequently expanded to the west. TU 2 was excavated in 5 cm thick arbitrary levels. Level 1 (0-5 cm below sand) was loamy silt noticeably darker (10 YR 5/2 greyish brown) than subsequent levels. L2 (5-10 cm, Figure F-51) and L3 (10-15 cm) were excavated through blocky subangular silt with heavy red-ox features and pronounced clay skins on ped surfaces. Concretions began at about 10 cm, where other red-ox features (mottling) were also noted. Level 4 (15-20 cm; Figure F-52) was blocky, heavily mottled grey (2.5 Y5/0) to grayish brown (2.5 Y 5/2) silt with abundant evidence of root casts and sand filled fissures. A total of 12 artifacts were collected (Table F-5).



Figure F-51 3CG1255, Trench 2, TU2, at 10cm below Sand Blow



Figure F-52 3CG1255, Trench 2, TU 2, 20 cm below Sand Blow

Table F-5 TU 2 artifact recovery

Level	Debitage	Other	Totals
0-5 cm	1 primary decortication flake 2 secondary decortications flakes 1 flake fragment	3 FCR 1 quartz pebble 1 bone	9
5-10 cm			No artifacts
10-15 cm	1 core fragment	1 FCR 1 concretion	3
15-20 cm			No artifacts
Totals	5 debitage	4 FCR 1 pebble 1 bone 1 concretion	12

Test Unit 3 was placed east of TU 2. A little partially carbonized wood and fibrous material that appeared to be Johnson grass rhizomes was noted in scraping away remnants of the sand. It is not unusual to find Johnson grass rhizomes at several meters depth. The old land surface of this unit sloped downward to the west due to collapse as sand was ejected (Figure F-53). The unit was excavated to 25 cmbs (Figure F-54). The southeast corner of this test unit contained a poorly

defined 15 cm x 15 cm concentration of oxidized, weakly fired soil interlaced with sand veins (Figure F-55). Examination of the overlying sand blow provided no indication that this ill-defined burned area extended from above. It was not evident at the surface of the old soil when excavation began was only noted at about 15 cm below the buried land surface; this material extended to 25 cm below the sand. This burned area is interpreted as a burned stump TU 3 was excavated in three 5 cm levels (0-5 cm, 5-10 cm, and 10-20 cm) as a fine waterscreen sample. An OSL column producing dates indicating burial ca. 9000 to 10,000 years ago was excavated in the north wall of this test unit; while the natural disturbance in the unit was limited to the south wall. The old land surface-sand blow contact in this unit also produced a radiocarbon date (C200) indicating carbonization ca. 410-375 B.C.



Figure F-53 3CG1255, Trench 2, TU 3, north wall and floor at 25 cm below sand blow, showing strata sloping from collapse after ejection of sand. A: modern plow zone, B: sand blow, C: buried land surface.



Figure F-54 3CG1255, Trench 2, TU3, at 25 cm below sand blow, unit excavated horizontally and so cross-cutting sloping strata, shown by differential mottling.



Figure F-55 3CG1255, Trench 2, TU 3, Southeast Corner of Completed Unit Showing Possible Tree Disturbance Originating below Sand Blow

Table F-6 TU 3 Artifact Recovery

Level	Debitage	Other	Totals
0-5 cm	1 secondary decortication flake 1 core trimming flake 2 utilized flakes		4
5-10 cm	1 biface thinning flake 2 flake fragments	9 FCR 1 burned earth	13
10-15 cm	1 biface thinning flake	1 FCR	2
15-20 cm			No artifacts
Totals	8debitage	10 FCR 1 burned earth	19

Test Unit 4 was placed east adjacent to TU3 to attempt to further define the indistinct area with weakly burned clods of clayey silt soil. Similar materials were recovered from an area extending 40 cm along the south wall of the trench and 30 cm north into the unit but again they were diffuse, poorly consolidated and not clearly of cultural origin. This “feature” is interpreted as a tree stump burned out prior to deposition of the sand blow, and prior to or perhaps contemporaneously with the deposition of the archaeological materials, rather than as a cultural feature in and of itself. It would have provided a weak spot through which sand could have been extruded upward during the sand blow’s creation. TU 4 was excavated in four 5-cm thick levels. The southwest corner of the unit (50 cm x 50 cm; Figure F-56) where burned soil was noted was bagged as a soil sample

for water screening in the same levels as the dry screen excavation; the few artifacts (1 flake) recovered from the water screening were returned to the level bags. Little or no carbon was recovered and none was noted during excavation. A further potential feature, an area of homogeneous, lighter brown (10 YR 5/4) soil was noted in the southeast corner of TU 4 Figure F-57). It was distinguished primarily by the fact that the general matrix of TU 4 from 10 cm down was markedly mottled and blocky, while this soil area was homogeneous and finely granular. No artifacts were associated with this poorly defined area. It could not be defined in the overlying sand blow. It too is interpreted as a non-cultural, pre-sand blow tree root disturbance, contemporary with or prior to the prehistoric occupation. TU 4 produced a second projectile point/knife (ppk) fragment; it is of material and manufacture similar to that recovered in clearing the top of the old land surface at 62 cm below the present surface.



Figure F-56 3CG1255, Trench 2, TU 4, showing 50 cm x 50 cm fine-screen sample column in southwest corner.



Figure F-57 3CG1255, Trench 2, TU 4, south wall, showing additional possible tree disturbance (soft, moist, dark stain in southeast corner) originating in/above sand blow.

Table F-7 TU 4 Artifact Recovery

Level	Debitage	Other	Totals
0-5 cm	1 flake fragment	3 FCR 7 burned earth 1 charcoal	12
5-10 cm	1 biface thinning flake 1 ppk base	6 burned earth 3 charcoal	11
10-15 cm	2 biface thinning flakes	5 FCR 7 burned earth	14
15-20 cm			No artifacts
Totals	4 debitage 1 ppk base	8 FCR 20 burned earth 3 charcoal	36

Test Unit 5 was placed east adjacent to TU4, to attempt to further define the possible tree stump stain. The unit was excavated in 5 cm levels to 25 cm below the sand blow (Figure F-58). The sand blow thinned over this unit, so that the old land surface was marked by plow scars diagonal to the current north-south direction of cultivation (i.e., running northwest-southeast). This unit intersected a previous 1 ft x 2 ft test unit. It also produced the deepest deposits encountered, with

materials recovered from 20-25 cm below the base of the sand blow. While adjacent units produced 5 (TU 2), 8 (TU 3) and 4 (TU 4) pieces of debitage, TU 5 produced 11 pieces of debitage.



Figure F-58 3CG1255, Trench 2, TU 5 Completed at 25 cm below Base of Sand Blow

Table F-8 TU 5 Artifact Recovery

Level	Debitage	Other	Totals
0-5 cm	2 biface thinning flakes 1 flake fragment	1 FCR 1 burned sandstone 1 pebble	6
5-10 cm	1 biface thinning flake	3 FCR 1 concretion	5
10-15 cm	1 secondary decortication flake 2 biface thinning flakes 1 flake fragment 1 ppk tip	7 FCR	12
15-20 cm	1 secondary decortications flake 1 flake fragment	8 FCR 2 burned sandstone 2 burned earth	14
20-25 cm	1 biface thinning flake	4 FCR	5
Totals	11 debitage 1 ppk tip	23 FCR 3 burned sandstone 1 pebble 1 concretion	42

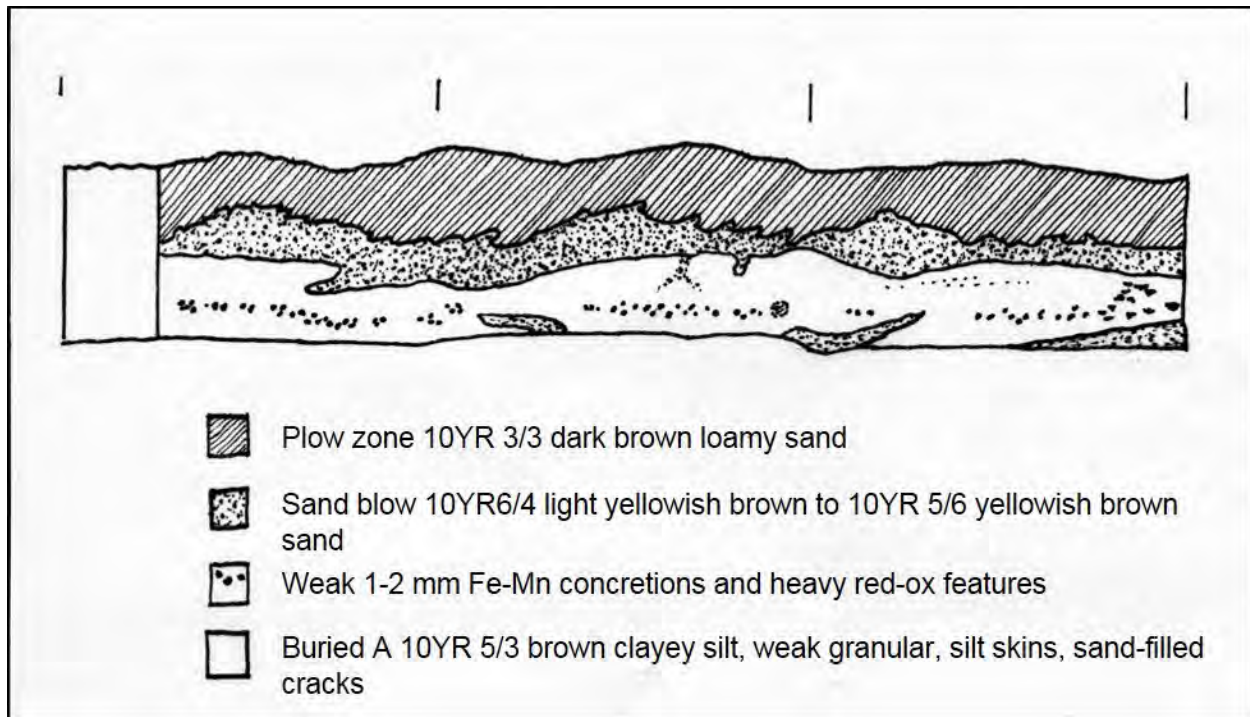


Figure F-59 Sketch of South Wall Trench 2, TU3, TU4, and TU5

In addition to the projectile point/knife base fragment recovered in clearing the sand blow base/old land surface contact in Trench 2 (Figure F-59), a second pp/k base of similar material and style was recovered from TU 4, 5-10 cm, and a nondiagnostic pp/k tip from TU 5, 10-15 cm (Figure F-60). The first specimen, from 62 cmbs, is 23 mm wide at the remaining section of blade, with a 16 mm wide stem. The notches are 4 mm wide. The basal margin is uneven, but markedly

convex. Flaking is broad and random. There is no basal grinding, but the biface has a thin (6 mm), lenticular cross-section. The material is slightly chalky, smooth, high-quality white (5 YR 8/1) chert with faint pink banding. This biface may have failed in manufacture or use, with a transverse fracture originating at one notch. The second pp/k base is a stem only, but it is also probably from a corner notched point. The stem is 25 mm wide at the convex base and 17 mm wide at the deepest preserved point of the notches and is 6 mm thick at the thickest point. The base is not ground. The material is again white (5 YR 8/1) somewhat weathered and stained, smooth, high-quality chert.

Regional projectile point morphology and chronology are discussed above in Section F 3.2 and are summarized here as it pertains to the admittedly speculative typology of the two fragmentary specimens. Notching (side, corner or intermediate) is typical of two widely separated periods: the Early Archaic and Middle Woodland. Middle Archaic and Late Archaic/Early Woodland forms in our area are almost exclusively stemmed rather than notched. First, we will discuss the Early Archaic forms. Consideration of these side-notched bases of well-thinned, white (Burlington/Crescent?) chert, along with the absence of pottery and the high density of fire-cracked rock, indicates that the sealed deposit *may* date to the Archaic period, however, it should be noted that this interpretation is open to question due to the fragmented nature of the two pp/k bases as well as the limited area investigated. The fragmentary bases resemble the St. Charles (9000-8500 BP; McGahey, 2000:68-70) form, in that they are well-thinned and have expanding, convex bases, but are atypically of the heavily ground early Archaic form in having little or no evidence of basal grinding. The Cypress Creek pp/k (8000-7500 BP; McGahey, 2000:90-95) also has wide corner notches, expanding stems and broad, random flaking but these points are typically thicker and have a straight basal margin. While our specimens are well-thinned, an identification with the Early Archaic is improbable due to the lack of highly diagnostic basal grinding.

Since Early Archaic types probably can be dismissed, another typology to consider for the notched projectile point/knife base fragments is the Middle Woodland period Hopewell-Marksville culture, Snyder cluster stems. The Snyders form (200 BC-AD 200; Justice and Kudlaty, 1999:38-39; 100 B.C.-A.D. 300; Perino, 1985) is also well thinned, with broad, random flaking; lenticular to flattened cross sections; excurvate bases on expanding stems and deep corner notches, and they too often occur on Crescent quarry type cherts and are found throughout the midcontinent from the Great Lakes to the Ozarks and Southern Plains margins. The form is allowed considerable morphological variation. The Gibson type (A.D. 250-350; Perino, 1985) is a later Snyders cluster variant with excurvate base and notched placed slightly higher (i.e. side-notched). Gibson points are typical of the Illinois Valley, eastern Missouri and regions to the north. A final type to consider is the Jack's Reef and Racoon points (Late Woodland, AD 800-1000), which are made on a very thin, flattened pentagonal biface with wide and irregular flaking. The Jack's Reef forms are considered corner-notched while the Racoon variant is side-notched (the actual difference being small and best determined from intact specimens). These last two Late Woodland notched forms are uncommon in the project area. All of these forms considered can be expected on the high-grade white cherts of the midcontinent, and all have Midwestern and Central Mississippi Valley affiliations. The lack of basal grinding is the strongest argument for a Middle Woodland rather than Early Archaic date for the 3CG1255 buried component.



Figure F-60 Projectile point/knife bases (cf. Snyders) from excavation. Left, 62 cmbs, top of old land surface; Right, TU 4, 5-10 cmbs.

While it is difficult to argue from negative evidence, it should be pointed out that no pottery was recovered from any sub-sand blow contexts in the approximately 5 square meters excavated in 2015. An aceramic component does not, however, in and of itself argue for pre-Woodland occupation, as Early and even Middle Woodland hunting and other extraction or non-habitation camps may not have required pottery. It should be noted that the records review (see Appendix F) indicated that, after Late Woodland, Late Archaic components are the most common occupation period reported for this portion of the Eastern Lowland. The fact that Early and Middle Woodland components are so poorly represented in the area may be the result of pottery being used on few sites of the period, leaving them to appear to be Archaic rather than Woodland sites. Other diagnostic artifact classes besides Tchula (Early Woodland) and Marksville (Middle Woodland) ceramics are poorly defined for the interval. Given (1) the low-density nature of the buried deposit and the sparse recovery of any material besides fire cracked rock and debitage, (2) the wide range of dates indicated by the CSC materials (Early Archaic through Middle Woodland), and (3) the ambiguous nature of our two most-diagnostic artifacts, it is difficult to assign a cultural period of the Garner site at the time of burial. Lack of pottery and local ubiquity suggests a Late Archaic/Early Woodland date, but the ppk morphology indicates a Middle Woodland date is more likely.

F.7 Recommendations Concerning Cultural Resources

The Faulkner sites (3CG1253 and 3CG1254) are small, low-density Late Woodland-transitional Mississippian scatters which lie along the banks of a now-drained slough, about a mile west of Buffalo Creek Ditch. These are diffuse surface/plow zone scatters. 3CG1253 produced 11 pieces of debitage and 5 sherds (alternatively, according to AAS site form, 10 pieces of chert debitage, 7

sand-tempered sherds and 2 fragments of other fired clay). 3CG1254 produced 2 pieces of debitage (Crowley's Ridge gravel flakes) and 1 small sand-tempered sherd. Archaeological monitoring of geological trenching failed to produce any evidence concerning the prehistoric occupation. These sites lie in an area with a very dense concentration of similar, contemporary Barnes series ceramic scatters. The backswamp location argues for these sites being of a seasonal nature, frequently and perhaps heavily occupied as camps for resource extraction and habitation. The western site, 3CG1254, in particular is a minimal manifestation, with only three artifacts reported. The area as reported of 3CG1254 also includes the foundation and other artifactual and soil remains of a barn. This barn appears on the earliest available detailed map (1977 air photo) and was removed between 2006 and 2009, based on air/satellite imagery. The site east of the former slough, 3CG1253, produced only slightly more evidence of prehistoric occupation. Neither 3CG1253 nor 3CG1254 is considered to be eligible for the NRHP. The Faulkner sites will continue to be cultivated and no further geological work is intended here. Materials from the sites (Accession # 2011-552 and 2011-553) have been donated to the AAS by the landowner.

The Wildy site (3MS909) lies a mile south of Buffalo Creek Ditch along a lateral drain. The site is a small (less than one acre) surface scatter of Late Woodland-transitional Mississippian Barnes series pottery (n=25, primarily very small, eroded, sand-tempered sherdlets), with limited evidence from a road ditch that there is also comparable material buried up to a meter deep under a sand blow. Site dimensions are unclear, due to the impact of road and ditch construction and the limited nature of the work at this site. The initial 2011 site reporting form mentioned sparse midden being present; this was the only mention of such a possibility. Archaeological monitoring of geological trenching failed to produce any further evidence concerning the prehistoric occupation. There is however still some potential for buried cultural deposits under the sand blow at 3MS909. The site will continue to be cultivated and no further geological work is planned here. Materials from the site have been donated to the AAS by the landowner (Accession # 2011-332). This small ceramic scatter was not evaluated for NRHP eligibility, but given the potential for intact, buried deposits, it should be considered potentially eligible for the NRHP, as it may contain significant information about prehistory.

Sites 3CG1256 and 3CG1257 were discovered during the course of selecting areas for geological investigations. Both sites have been impacted by land clearing, drainage, cultivation, land leveling and surface collecting. Neither site was further investigated by M.P. Tuttle and Associates, although large surface collections were obtained and catalogued by the Arkansas Archeological Survey-Jonesboro in conjunction with our work as permitted by landowner Greg Garner. These materials have been de-accessioned and returned to the landowner. Site 3CG1256 is considered to be potentially eligible for the NRHP based on density of Archaic materials, some of which appears to date to the Dalton period. Site 3CG1257 is a smaller and sparser deposit; it includes materials also associated with the Archaic period. The field containing the Garner sites has been leveled, lightly according to the landowner, but nevertheless it appears likely that the present surface distribution of artifacts results at least to some degree from this land-leveling. Mr. Garner indicated that soil had been moved from southwest to northeast across the field in 2011. The probability that the present artifact distribution across the three sites (as presently defined) results from earth moving for irrigation and texture improvement purposes is increased by the finding of plow zone artifacts in both sand blow and non-sand blow areas. Given this uncertainty, it seems best to consider 3CG1257 as also potentially significant. The three Garner sites are best considered as a complex of Archaic period occupation along Lighthouse Creek, with occasional Woodland period visits as witnessed by sparse Barnes series ceramics.

The geological work focused on the adjacent 3CG1255. The Garner #1 site (3CG1255) has been investigated by general and controlled surface collections, screened test pits, geophysical prospection, mechanical trenching and excavation of screened units below the sand blow. It should be emphasized that artifacts were recovered from the plow zone developed in the sand blow, from adjacent silty soils, and from below the sand blow. Our 2015 work demonstrated the presence of intact, sub-plow zone deposits, sealed by the sand blow, and discrete from the overlying plow zone materials, which potentially are displaced from the 3CG1256-3CG1257 area by landleveling.

While artifact recovery was quite limited, as might be expected in a low-density Archaic period lithic scatter, the pattern of fire cracked rock recovery (50 pieces weighing 125.9 g in TU 1 vs. 35 pieces weighing 73.1 g from units 2, 3, 4 and 5) indicates that there is well-preserved horizontal patterning preserved in the site. In TU 1, 2, 3 and 4, recovery was limited to 0-15 cm below the sand blow while TU 5 produced materials to 25 cm below the sand blow.

The minimal historic component is attributed to the 20th century and is believed to be field scatter from a house located about 250 m to the east along a north-south field road. The land containing the Garner sites was still wooded in 1956, indicating approximately 50 years of cultivation of the Garner sites.

Because of these well-preserved, sub-plow zone deposits, which are contained in a buried A horizon, and which appear to be limited to a single occupation, site 3CG1255 is considered to be eligible for the NRHP under criterion D, being likely to produce significant new information about prehistory. A sealed Middle Woodland occupation would be significant due to its very well-preserved nature, the sparse nature of such sites in the vicinity, and the good potential for intact horizontal patterning. Materials from the three Garner sites (3CG1255, 3CG1256 and 3CG1257) have been returned to the landowner.

No further impacts from geological investigations are anticipated at these sites. The sites will continue to be cultivated.

It should be further noted that this work demonstrates that in areas which have been land- leveled, even extensively, there is good potential for intact archaeological deposits being found sealed under sand blows. Land-leveling may obscure the pattern of sand-blows, so when searching for such sites, the oldest available winter/spring air/satellite photos should be sought. It should also be noted, concerning site deformation processes, that once a direction of cultivation is established, it tends to prevail in subsequent years unless there is a major shift in land use.

F.8 References (included in References of Main Report, Section 5.1)

Table F-9 Bag List, 3 CG1255, 2015 Field Season

Bag #	General provenience	Unit #	Level	Recovery method
1	General surface			Select
2	Trench 1	General cleaning	All	Hand picked
3	Trench 2	General cleaning	Top of old land	Hand picked
4	Trench 2	Cleaning	Top of old land	Hand picked
5	Trench 1	TU 1	0-5 cm	¼" dry screen
6	Trench 1	TU 1	5-10 cm	¼" dry screen
7	Trench 1	TU 1	10-15 cm	¼" dry screen
8	Trench 2	TU 2	5-10 cm	¼" dry screen
9	Trench 2	TU 2	10-15 cm	¼" dry screen
10	Trench 2	TU 3	0-5 cm	¼" dry screen
11	Trench 2	TU 3	5-10 cm	¼" dry screen
12	Trench 2	TU 3	10-20 cm	¼" dry screen
13	Trench 2	TU 4	0-5 cm	¼" dry screen
14	Trench 2	TU 4	5-10 cm	¼" dry screen
15	Trench 2	TU 4	10-15 cm	¼" dry screen
16	Trench 2	TU 5	0-5 cm	¼" dry screen
17	Trench 2	TU 5	5-10 cm	¼" dry screen
18	Trench 2	TU 5	10-15 cm	¼" dry screen
19	Trench 2	TU 5	15-20 cm	¼" dry screen
20	Trench 2	TU 5	20-25 cm	¼" dry screen
21	Trench 2	TU 4 50 x 50 cm	0-5 cm	Fine water screen
22	Trench 2	TU 4 50 x 50 cm	5-10 cm	Fine water screen
23	Trench 2	TU 4 50 x 50 cm	10-15 cm	Fine water screen
24	Trench 2	TU 4 50 x 50 cm	15-20 cm	Fine water screen
25	Trench 2	TU 4 50 x 50 cm	0-5 cm	Soil sample
26	Trench 2	TU 4 50 x 50 cm	5-10 cm	Soil sample
27	Trench 2	TU 4 50 x 50 cm	10-15 cm	Soil sample
28	Trench 2	TU 4 50 x 50 cm	15-20 cm	Soil sample

Table F-10 Artifact Tabulation

Count	Mass (g)	Item	Comment
Bag 1, 3CG1255, general surface			
16	123.3	Fire cracked rock	
2	66.6	Sandstone	
1	21.0	Misc. burned material	unidentified
1	10.7	Eroded prehistoric sherd	Barnes series
5	299.6	Tested pebbles/cobbles	2 heated
6	85.8	Angular shatter/core fragments	1 heated
4	53.5	Core trimming flakes	2 heated
8	58.0	Primary decortications flakes	5 heated
16	74.9	Secondary decortications flakes	6 heated
23	32.4	Biface thinning flakes	5 heated
16	36.7	Flake fragments	8 heated
1	0.9	Biface thinning flake	white chert
1	1.2	Biface fragment	stem?
1	3.1	Blade-like flake tool	heated
8	33.2	Other utilized flakes	5 heated
1	6.0	Late refined earthenware	ivory-colored, plate marley
2	11.9	Bottle glass	clear, 1 screw top jar
1	.3	Bottle glass gizzard stone	aqua
Bag 2, 3CG1255, Trench 1, general cleaning, all levels			
1	17.8	Core fragment/trimming	heated
4	13.7	Secondary decortications flake	
1	26.4	Biface thinning flake	Atypical, formal core trimming
1	2.3	Flake fragment	heated
5	56.5	Fire cracked rock	
1	0.9	Biface fragment	Blade segment, burned
Bag 3, 3CG1255, Trench 2, general cleaning, top of old land surface			
1	2.7	Secondary decortications flake	heated
1	1.0	Flake fragment	heated
7	31.7	Fire cracked rock	1 silty, grey, lime/dolostone?
Bag 4, 3 CG1255, Trench 2, top of old land, 62 cmbs, 2.3 m from west end			
1	3.3	Projectile point/knife fragment	base
Bag 5, 3CG1255, TU 1, 0-5 cm below sand; 30-35 cm below surface			
1	13.0	Secondary decortications flake	
1	0.4	Flake fragment	heated
1	1.0	Quartz pebble	14 mm max dimension
1	0.4	Fe-Mn concretion	
4	57.0	Fire cracked rock	
Bag 6, 3CG1255, TU 1, 5-10 cm			
23	45.7	Fire cracked rock	
1	1.9	Quartz pebble	15 mm max dimension
1	0.2	Fe-Mn concretion	
1	5.7	Core fragment/angular shatter	
2	0.5	Biface thinning flake	
Bag 7, 3CG1255, TU1, 10-15 cm			
1	0.3	Iron/steel wire	
2	3.8	Biface thinning flake	

Count	Mass (g)	Item	Comment
1	0.1	Flake fragment	
13	23.2	Fire cracked rock	
Bag 8, 3CG1255, Trench 2, TU 2, 5-10 cm below sand			
1	23.8	Primary decortications flake	heated
2	6.4	Secondary decortications flake	2 heated
1	1.2	Flake fragment	heated
3	8.0	Fire cracked rock	
1	0.5	Quartz pebble	
1	0.4	Bone	
Bag 9, 3CG1255, TU2, 10-15 cm			
1	12.1	Core trimming fragment	Polyhedral core
1	2.3	Fire cracked rock	
1	0.3	Fe-Mn concretion	
Bag 10, 3CG1255, TU 3, 0-5 cm			
1	7.45	Core trimming fragment	Prepared core, chalcedony like (5Y7/2 light grey)
1	0.4	Secondary decortications flake	
2	3.9	Utilized flakes	1 heated
Bag 11, 3CG1255, TU 3, 5-10 cm			
1	2.7	Biface thinning flake	heated
2	1.5	Flake fragment	1 heated
1	0.7	Burned earth	
9	31.0	Fire cracked rock	
Bag 12, 3CG1255, TU3, 15-20 cm			
1	1.9	Biface thinning flake	heated
2	2.0	Fire cracked rock	
Bag 13, 3CG1255, TU 4, 0-5 cm			
1	1.0	Flake fragment	heated
3	8.6	Fire cracked rock	
7	2.2	Burned earth	
1	0.1	Rhizome	Partly carbonized
Bag 14, 3CG1255, TU 4, 5-10 cm			
1	0.4	Biface thinning flake	heated
1	1.3	Projectile point/knife fragment	Stem, weathered, stained (5Y8/1 white)
3	0.2	Charcoal	
6	8.1	Burned earth	
Bag 15, 3CG1255, TU 4, 10-15 cm			
5	8.9	Fire cracked rock	
7	7.6	Burned earth	
2	0.9	Biface thinning flake	heated
Bag 16, 3CG1255, TU 5, 0-5 cm			
2	2.5	Biface thinning flake	
1	0.3	Flake fragment	heated
1	0.5	Chert gravel pebble	12 mm max dimension
1	2.3	Burned sandstone/hematite	
1	0.4	Fire cracked rock	

Count	Mass (g)	Item	Comment
Bag 17, 3CG1255, TU 5, 5-10 cm			
1	0.1	Biface thinning flake	White chert
1	0.4	Fe-Mn concretion	
3	2.4	Fire cracked rock	
Bag 18, 3CG1255, TU 5, 10-15 cm			
7	18.3	Fire cracked rock	
1	0.2	Flake fragment	heated
1	5.7	Secondary decortications flake	heated
1	0.5	Biface thinning flake	1 white
1	0.9	Projectile point/knife fragment	Tip, heated
Bag 19, 3CG1255, TU 5, 15-20 cm			
1	0.3	Secondary decortications flake	heated
1	2.0	Flake fragment	heated
8	21.2	Fire cracked rock	
2	7.8	Burned sandstone	
2	1.2	Burned earth	
Bag 20, 3CG1255, TU 5, 20-25 cm			
1	3.3	Biface thinning flake	
4	8.3	Fire cracked rock	

**APPENDIX G EVALUATION OF SCENARIO EARTHQUAKES
RESULTS TABLES**

Table G-1 Results of Liquefaction Potential Analysis for M 6.9 and M 7.6 December 16, 1811 Scenario Earthquake

Site/ Borehole Map ID #	Magnitude @ Distance (km)	a_{max}	Depth to Susceptible Sediment (m)	Description of Susceptible Sediment	Blow Count $N_{1(60)}$	Cyclic Stress Ratio	Results ¹
a. Results of liquefaction potential analysis for M 6.9 December 16, 1811 scenario earthquake.							
Cache River FAS 942/off ILL 3 #3	6.9@142	0.07	10	medium dense, gray sand	15	0.063	N
	6.9@142	0.07	11	medium dense, gray sand	11	0.063	N
	6.9@142	0.07	12	medium dense, gray sand	18	0.062	N
	6.9@142	0.07	13	medium dense, gray sand	10	0.062	N
St. Francis River (Geotec 9) Rt. 60/3 #4	6.9@91	0.11	5	wet, brown, silty sand, loose	5	0.087	N
	6.9@91	0.11	6	gray sand, very fine to fine with scattered thin clay layers	5	0.097	N
	6.9@91	0.11	8	gray sand, very fine to fine, medium dense to dense	15	0.102	N
	6.9@91	0.11	9	gray sand, very fine to fine, medium dense to dense	22	0.105	N
Current River @ SH 328/1 #5	6.9@80	0.13	5	Wet, loose, brown fine sand	9	0.180	N
	6.9@80	0.13	6	Wet, medium dense, brown sand	12	0.218	N
	6.9@80	0.13	8	Wet, medium dense, brown sand	18	0.296	N
	6.9@80	0.13	9	Wet, medium dense, brown to gray sand with organic matter	13	0.200	N
Black River @ Elgin Ferry/7 #6	6.9@80	0.13	11	Wet, medium dense, brown to gray sand with organic matter	9	0.154	N
	6.9@80	0.13	14	Wet, medium dense, gray sand and gravel	10	0.151	N
	6.9@120	0.08	3	Wet, medium dense, gray silty sand and gravel with some organic material (wood)	3	0.051	N
	6.9@120	0.08	5	Wet, medium dense, gray silty sand and gravel with some organic material (wood)	5	0.062	N
White River@ US 79/A #7	6.9@120	0.08	6	Wet, medium dense, gray silty sand and gravel with some organic material (wood)	13	0.069	N
	6.9@120	0.08	9	Wet, medium dense, gray silty sand and gravel	12	0.075	N
	6.9@120	0.08	12	Wet, medium dense, gray silty sand and gravel with organic material	14	0.075	N
	6.9@188	0.05	5	Moist, medium dense brown sand	8	0.037	N
	6.9@188	0.05	6	wet, loose, brown silty sand,	7	0.041	N
	6.9@188	0.05	8	Wet, loose to medium dense, brown sand	7	0.044	N
	6.9@188	0.05	9	wet, medium dense, brown sand with some gravel	22	0.045	N
	6.9@188	0.05	12	wet, medium dense brown sand with some gravel	10	0.045	N
	6.9@188	0.05	14	wet, medium dense brown sand with some gravel	20	0.043	N

Site/ Borehole Map ID #	Magnitude @ Distance (km)	a_{max}	Depth to Susceptible Sediment (m)	Description of Susceptible Sediment	Blow Count $N_{(60)}$	Cyclic Stress Ratio	Results ¹
Cross Country Ditch @ US 64/6 #8	6.9@188	0.05	15	wet, medium dense gray sand	15	0.041	N
	6.9@103	0.10	8	soft, gray fine sand	9	0.136	N
	6.9@103	0.10	11	compact sand	25	0.372	N
Obion River SR 89/1 #10	6.9@96	0.10	3	sand, grey, medium grained	10	0.065	N
	6.9@96	0.10	4	sand, grey, medium grained	6	0.077	N
	6.9@96	0.10	5	sand, grey, medium grained	16	0.084	N
	6.9@96	0.10	9	sand, grey, medium grained	19	0.094	N
	6.9@96	0.10	10	sand, grey, medium grained, silty	23	0.095	N
Hatchie Rt 51/2 #11	6.9@54	0.16	4	fine gray sand	19	0.121	N
	6.9@54	0.16	6	fine gray sand	16	0.135	N
	6.9@54	0.16	7	medium gray sand	19	0.143	N
	6.9@54	0.16	9	coarse gray sand	22	0.148	N
Coldwater US 3/7 #13	6.9@154	0.06	15	medium dense, brown and gray, fine to medium sand with fine gravel, with 2" clay layer @ bottom	23	0.054	N
	6.9@154	0.06	16	medium dense, gray, fine to medium sand, with fine gravel and clay	11	0.053	N
	6.9@154	0.06	18	dense, brown, fine to medium sand, with fine gravel	30	0.049	N
b. Results of liquefaction potential analysis for M 7.6 December 16, 1811 scenario earthquake.							
Cache River FAS 942/off ILL 3 #3	7.6@142	0.14	10	medium dense, gray sand	15	0.125	N
	7.6@142	0.14	11	medium dense, gray sand	11	0.125	L
	7.6@142	0.14	12	medium dense, gray sand	18	0.124	N
	7.6@142	0.14	13	medium dense, gray sand	10	0.123	L
St. Francis River (Geotec 9) Rt. 60/3 #4	7.6@91	0.22	5	wet, brown, silty sand, loose	5	0.174	L
	7.6@91	0.22	6	gray sand, very fine to fine with scattered thin clay layers	5	0.193	L
	7.6@91	0.22	8	gray sand, very fine to fine, medium dense to dense	15	0.204	L
	7.6@91	0.22	9	gray sand, very fine to fine, medium dense to dense	22	0.210	N
Current River @ SH 328/1 #5	7.6@80	0.27	5	Wet, loose, brown fine sand	9	0.209	L
	7.6@80	0.27	6	Wet, medium dense, brown sand	12	0.231	L
	7.6@80	0.27	8	Wet, medium dense, brown sand	18	0.244	L
	7.6@80	0.27	9	Wet, medium dense, brown to gray sand with organic matter	13	0.252	L

Site/ Borehole Map ID #	Magnitude @ Distance (km)	a_{max}	Depth to Susceptible Sediment (m)	Description of Susceptible Sediment	Blow Count $N_{(60)}$	Cyclic Stress Ratio	Results ¹
	7.6@80	0.27	11	Wet, medium dense, brown to gray sand with organic matter	9	0.254	L
	7.6@80	0.27	14	Wet, medium dense, gray sand and gravel	10	0.244	L
Black River @ Elgin Ferry/7 #6	7.6@120	0.16	3	Wet, medium dense, gray silty sand and gravel with some organic material (wood)	3	0.101	L
	7.6@120	0.16	5	Wet, medium dense, gray silty sand and gravel with some organic material (wood)	5	0.122	L
	7.6@120	0.16	6	Wet, medium dense, gray silty sand and gravel	13	0.135	N
	7.6@120	0.16	9	Wet, medium dense, gray silty sand and gravel	12	0.147	L
	7.6@120	0.16	12	Wet, medium dense, gray silty sand and gravel with organic material	14	0.146	L
	7.6@188	0.10	5	Moist, medium dense brown sand	8	0.074	N
White River @ US 79/A #7	7.6@188	0.10	6	wet, loose, brown silty sand,	7	0.082	N
	7.6@188	0.10	8	Wet, loose to medium dense, brown sand	7	0.087	L
	7.6@188	0.10	9	wet, medium dense, brown sand with some gravel	22	0.089	N
	7.6@188	0.10	12	wet, medium dense brown sand with some gravel	10	0.089	N
	7.6@188	0.10	14	wet, medium dense brown sand with some gravel	20	0.086	N
	7.6@188	0.10	15	wet, medium dense gray sand	15	0.082	N
	7.6@103	0.18	8	soft, gray fine sand	9	0.160	L
	7.6@103	0.18	11	compact sand	25	0.163	N
Obion River SR 89/1 #10	7.6@96	0.16	3	sand, grey, medium grained	10	0.105	N
	7.6@96	0.16	4	sand, grey, medium grained	6	0.122	L
	7.6@96	0.16	5	sand, grey, medium grained	16	0.134	N
	7.6@96	0.16	9	sand, grey, medium grained	19	0.150	N
	7.6@96	0.16	10	sand, grey, medium grained, silty	23	0.151	N
	7.6@54	0.41	4	fine gray sand	19	0.302	L
Hatchie Rt 51/2 #11	7.6@54	0.41	6	fine gray sand	16	0.335	L
	7.6@54	0.41	7	medium gray sand	19	0.356	L
	7.6@54	0.41	9	coarse gray sand	22	0.368	L
	7.6@154	0.12	15	medium dense, brown and gray, fine to medium sand with fine gravel, with 2" clay layer @ bottom	23	0.105	N
Coldwater US 3/7	7.6@154	0.12	16		11	0.104	N

Site/ Borehole Map ID #	Magnitude @ Distance (km)	a_{max}	Depth to Susceptible Sediment (m)	Description of Susceptible Sediment	Blow Count $N_{(60)}$	Cyclic Stress Ratio	Results ¹
	7.6@154	0.12	18	medium dense, gray, fine to medium sand, with fine gravel and clay	30	0.095	N

¹L- liquefaction likely N- liquefaction not likely

Table G-2 Results of Liquefaction Potential Analysis for M 7.0 and M 7.5 January 23, 1812 Scenario Earthquake

Site/ Borehole Map ID #	Magnitude @ Distance (km)	a_{max}	Depth to Susceptible Sediment (m)	Description of Susceptible Sediment	Blow Count $N_{1(60)}$	Cyclic Stress Ratio	Results ¹
a. Results of liquefaction potential analysis for M 7.0 January 23, 1812 scenario earthquake.							
Skillet Fork/1 RT 600 E #1	7.0 @ 219	0.04	8.2	wet, sandy loam	3	0.042	N
	7.0 @ 219	0.04	8.8	wet, sandy clay loam	2	0.042	N
	7.0 @ 219	0.04	9.8	wet, loose, fine grained sand	5	0.043	N
	7.0 @ 219	0.04	10.4	wet, sandy clay loam with sand lenses	2	0.043	N
	7.0 @ 219	0.04	11.3	wet, sandy clay loam with sand lenses	2	0.043	N
	7.0 @ 219	0.04	11.9	wet, loose, fine grained sand	5	0.043	N
	7.0 @ 219	0.04	13.4	wet, medium, fine grained sand	11	0.042	N
	7.0 @ 219	0.04	14.3	wet, loose, fine grained sand	6	0.041	N
	7.0 @ 219	0.04	15.0	wet, medium, medium grained sand with gravel	13	0.040	N
	7.0 @ 166	0.07	3.4	gray, silty sand	6	0.046	N
Saline River Richey Road/2S #2	7.0 @ 166	0.07	4.0	gray, silty sand	4	0.050	N
	7.0 @ 166	0.07	4.9	loose, brown, gravel and sand with clay binder	5	0.054	N
	7.0 @ 166	0.07	5.9	moist, gray, clay loam with gravel	3	0.058	N
	7.0 @ 166	0.07	6.4	very loose, fine gravel and sand with clay binder	2	0.060	N
	7.0 @ 166	0.07	7.0	very loose, fine gravel and sand with clay binder	1	0.061	N
	7.0 @ 166	0.07	7.9	loose fine grained sand with gravel and rotten vegetation	6	0.063	N
	7.0 @ 166	0.07	8.5	loose fine grained sand with gravel and rotten vegetation	4	0.064	N
	7.0 @ 166	0.07	9.5	medium, moist, gray, fine to coarse sand with gravel	11	0.065	N
	7.0 @ 166	0.07	10.1	medium, moist, gray, fine to coarse sand with gravel	11	0.065	N
	7.0 @ 70	0.16	10	medium dense, gray sand	15	0.144	N
Cache River FAS 942/off ILL 3	7.0 @ 70	0.16	11	medium dense, gray sand	11	0.144	L
	7.0 @ 70	0.16	12	medium dense, gray sand	18	0.143	N
	7.0 @ 70	0.16	13	medium dense, gray sand	10	0.142	L
St. Francis River (Geotec 9) Rt. 60/3 #4	7.0 @ 49	0.24	5	wet, brown, silty sand, loose	5	0.186	L
	7.0 @ 49	0.24	6	gray sand, very fine to fine with scattered thin clay layers	5	0.207	L
	7.0 @ 49	0.24	8	gray sand, very fine to fine, medium dense to dense	15	0.219	N
	7.0 @ 49	0.24	9	gray sand, very fine to fine, medium dense to dense	22	0.225	N
	7.0 @ 99	0.11	5	Wet, loose, brown fine sand	9	0.082	N

Site/ Borehole Map ID #	Magnitude @ Distance (km)	a_{max}	Depth to Susceptible Sediment (m)	Description of Susceptible Sediment	Blow Count $N_{(60)}$	Cyclic Stress Ratio	Results ¹
Current River @ SH 328/1 #5	7.0@99	0.11	6	Wet, medium dense, brown sand	12	0.091	N
	7.0@99	0.11	8	Wet, medium dense, brown sand	18	0.096	N
	7.0@99	0.11	9	Wet, medium dense, brown to gray sand with organic matter	13	0.099	N
Black River @ Elgin Ferry/7 #6	7.0@99	0.11	11	Wet, medium dense, brown to gray sand with organic matter	9	0.100	N
	7.0@99	0.11	14	Wet, medium dense, gray sand and gravel	10	0.096	N
	7.0@171	0.07	3	Wet, medium dense, gray silty sand and gravel with some organic material (wood)	3	0.042	N
	7.0@171	0.07	5	Wet, medium dense, gray silty sand and gravel with some organic material (wood)	5	0.051	N
	7.0@171	0.07	6	Wet, medium dense, gray silty sand and gravel with some organic material (wood)	13	0.056	N
	7.0@171	0.07	9	Wet, medium dense, gray silty sand and gravel	12	0.062	N
	7.0@171	0.07	12	Wet, medium dense, gray silty sand and gravel	14	0.061	N
White River @ US 79/A #7	7.0@258	0.03	5	Moist, medium dense brown sand	8	0.026	N
	7.0@258	0.03	6	wet, loose, brown silty sand,	7	0.029	N
	7.0@258	0.03	8	Wet, loose to medium dense, brown sand	7	0.030	N
	7.0@258	0.03	9	wet, medium dense, brown sand with some gravel	22	0.031	N
	7.0@258	0.03	12	wet, medium dense brown sand with some gravel	10	0.031	N
	7.0@258	0.03	14	wet, medium dense brown sand with some gravel	20	0.030	N
	7.0@258	0.03	15	wet, medium dense gray sand	15	0.029	N
Cross Country Ditch @ US 64/6 #8	7.0@173	0.06	8	soft, gray fine sand	9	0.058	N
	7.0@173	0.06	11	compact sand	25	0.059	N
Obion River SR 89/1 #10	7.0@76	0.15	3	sand, grey, medium grained	10	0.093	N
	7.0@76	0.15	4	sand, grey, medium grained	6	0.109	N
	7.0@76	0.15	5	sand, grey, medium grained	16	0.119	N
	7.0@76	0.15	9	sand, grey, medium grained	19	0.133	N
	7.0@76	0.15	10	sand, grey, medium grained, silty	23	0.135	N
Hatchie Rt 51/2 #11	7.0@107	0.13	4	fine gray sand	19	0.099	N
	7.0@107	0.13	6	fine gray sand	16	0.109	N
	7.0@107	0.13	7	medium gray sand	19	0.116	N

Site/ Borehole Map ID #	Magnitude @ Distance (km)	a_{max}	Depth to Susceptible Sediment (m)	Description of Susceptible Sediment	Blow Count $N_{(60)}$	Cyclic Stress Ratio	Results ¹
Coldwater US 3/7 #13	7.0@107	0.13	9	coarse gray sand	22	0.120	N
	7.0@224	0.04	15	medium dense, brown and gray, fine to medium sand with fine gravel, with 2" clay layer @ bottom	23	0.035	N
	7.0@224	0.04	16	medium dense, gray, fine to medium sand, with fine gravel and clay	11	0.035	N
	7.0@224	0.04	18	dense, brown, fine to medium sand, with fine gravel	30	0.032	N
b. Results of liquefaction potential analysis for M 7.5 January 23, 1812 scenario earthquake.							
Skilllet Fork RT 600 E/1 #1	7.5 @ 219	0.08	8.2	wet, sandy loam	3	0.072	L
	7.5 @ 219	0.08	8.8	wet, sandy clay loam	2	0.073	L
	7.5 @ 219	0.08	9.8	wet, loose, fine grained sand	5	0.074	N
	7.5 @ 219	0.08	10.4	wet, sandy clay loam with sand lenses	2	0.075	L
	7.5 @ 219	0.08	11.3	wet, sandy clay loam with sand lenses	2	0.075	L
	7.5 @ 219	0.08	11.9	wet, loose, fine grained sand	5	0.075	N
	7.5 @ 219	0.08	13.4	wet, medium, fine grained sand	11	0.072	N
	7.5 @ 219	0.08	14.3	wet, loose, fine grained sand	6	0.071	N
	7.5 @ 219	0.08	15.0	wet, medium, medium grained sand with gravel	13	0.069	N
	Saline River Richey Road/2S #2	7.5 @ 166	0.10	3.4	gray, silty sand	6	0.070
7.5 @ 166		0.10	4.0	gray, silty sand	4	0.075	N
7.5 @ 166		0.10	4.9	loose, brown, gravel and sand with clay binder	5	0.082	L
7.5 @ 166		0.10	5.9	moist, gray, clay loam with gravel	3	0.088	L
7.5 @ 166		0.10	6.4	very loose, fine gravel and sand with clay binder	2	0.090	L
7.5 @ 166		0.10	7.0	very loose, fine gravel and sand with clay binder	1	0.093	L
7.5 @ 166		0.10	7.9	loose fine grained sand with gravel and rotten vegetation	6	0.096	L
7.5 @ 166		0.10	8.5	loose fine grained sand with gravel and rotten vegetation	4	0.097	L
7.5 @ 166		0.10	9.5	medium, moist, gray, fine to coarse sand with gravel	11	0.099	N
7.5 @ 166		0.10	10.1	medium, moist, gray, fine to coarse sand with gravel	11	0.099	N
Cache River FAS 942/off ILL 3 #3	7.5@70	0.29	10	medium dense, gray sand	15	0.268	L
	7.5@70	0.29	11	medium dense, gray sand	11	0.268	L
	7.5@70	0.29	12	medium dense, gray sand	18	0.265	L
	7.5@70	0.29	13	medium dense, gray sand	10	0.263	L

Site/ Borehole Map ID #	Magnitude @ Distance (km)	a_{max}	Depth to Susceptible Sediment (m)	Description of Susceptible Sediment	Blow Count $N_{(60)}$	Cyclic Stress Ratio	Results ¹
St. Francis River (Geotec 9) Rt. 60/3 #4	7.5@49	0.40	5	wet, brown, silty sand, loose	5	0.310	L
	7.5@49	0.40	6	gray sand, very fine to fine with scattered thin clay layers	5	0.345	L
	7.5@49	0.40	8	gray sand, very fine to fine, medium dense to dense	15	0.365	L
	7.5@49	0.40	9	gray sand, very fine to fine, medium dense to dense	22	0.375	L
nCurret River @ SH 328/1 #5	7.5@99	0.16	5	Wet, loose, brown fine sand	9	0.126	L
	7.5@99	0.16	6	Wet, medium dense, brown sand	12	0.139	L
	7.5@99	0.16	8	Wet, medium dense, brown sand	18	0.146	N
	7.5@99	0.16	9	Wet, medium dense, brown to gray sand with organic matter	13	0.151	L
	7.5@99	0.16	11	Wet, medium dense, brown to gray sand with organic matter	9	0.153	L
Black River @ Elgin Ferry/7 #6	7.5@99	0.16	14	Wet, medium dense, gray sand and gravel	10	0.146	L
	7.5@171	0.10	3	Wet, medium dense, gray silty sand and gravel with some organic material (wood)	3	0.065	N
	7.5@171	0.10	5	Wet, medium dense, gray silty sand and gravel with some organic material (wood)	5	0.078	N
	7.5@171	0.10	6	Wet, medium dense, gray silty sand and gravel with some organic material (wood)	13	0.087	N
	7.5@171	0.10	9	Wet, medium dense, gray silty sand and gravel	12	0.095	N
	7.5@171	0.10	12	Wet, medium dense, gray silty sand and gravel with organic material	14	0.094	N
White River@ US 79/A #7	7.5@258	0.05	5	Moist, medium dense brown sand	8	0.040	N
	7.5@258	0.05	6	Wet, loose, brown silty sand,	7	0.045	N
	7.5@258	0.05	8	Wet, loose to medium dense, brown sand	7	0.048	N
	7.5@258	0.05	9	Wet, medium dense, brown sand with some gravel	22	0.049	N
	7.5@258	0.05	12	Wet, medium dense brown sand with some gravel	10	0.049	N
	7.5@258	0.05	14	Wet, medium dense brown sand with some gravel	20	0.047	N
	7.5@258	0.05	15	Wet, medium dense gray sand	15	0.045	N
Cross Country Ditch @ US 64/6 #8	7.5@173	0.10	8	soft, gray fine sand	9	0.090	N
	7.5@173	0.10	11	compact sand	25	0.092	N
Obion River SR 89/1	7.5@76	0.27	3	sand, grey, medium grained	10	0.170	L
	7.5@76	0.27	4	sand, grey, medium grained	6	0.199	L

Site/ Borehole Map ID #	Magnitude @ Distance (km)	a_{max}	Depth to Susceptible Sediment (m)	Description of Susceptible Sediment	Blow Count $N_{(60)}$	Cyclic Stress Ratio	Results ¹
#10	7.5@76	0.27	5	sand, grey, medium grained	16	0.217	L
	7.5@76	0.27	9	sand, grey, medium grained	19	0.243	L
	7.5@76	0.27	10	sand, grey, medium grained, silty	23	0.246	L
Hatchie Rt 51/2 #11	7.5@107	0.16	4	fine gray sand	19	0.116	N
	7.5@107	0.16	6	fine gray sand	16	0.129	N
	7.5@107	0.16	7	medium gray sand	19	0.137	N
	7.5@107	0.16	9	coarse gray sand	22	0.142	N
Coldwater US 3/7 #13	7.5@224	0.06	15	medium dense, brown and gray, fine to medium sand with fine gravel, with 2" clay layer @ bottom	23	0.054	N
	7.5@224	0.06	16	medium dense, gray, fine to medium sand, with fine gravel and clay	11	0.053	N
	7.5@224	0.06	18	dense, brown, fine to medium sand, with fine gravel	30	0.049	N

¹L-liquefaction likely N-liquefaction not likely

Table G-3 Results of Liquefaction Potential Analysis for M 7.3 and M 7.8 February 7, 1812 Scenario Earthquake

Site/ Borehole Map ID #	Magnitude @ Distance (km)	a_{max}	Depth to Susceptible Sediment (m)	Description of Susceptible Sediment	Blow Count $N_{r(60)}$	Cyclic Stress Ratio	Results ¹
a. Results of liquefaction potential analysis for M 7.3 February 7, 1812 scenario earthquake.							
Skilllet Fork RT 600 E/1 #1	7.3 @ 235	0.05	8.2	wet, sandy loam	3	0.049	N
	7.3 @ 235	0.05	8.8	wet, sandy clay loam	2	0.050	N
	7.3 @ 235	0.05	9.8	wet, loose, fine grained sand	5	0.051	N
	7.3 @ 235	0.05	10.4	wet, sandy clay loam with sand lenses	2	0.051	N
	7.3 @ 235	0.05	11.3	wet, sandy clay loam with sand lenses	2	0.051	N
	7.3 @ 235	0.05	11.9	wet, loose, fine grained sand	5	0.051	N
	7.3 @ 235	0.05	13.4	wet, medium, fine grained sand	11	0.049	N
	7.3 @ 235	0.05	14.3	wet, loose, fine grained sand	6	0.048	N
	7.3 @ 235	0.05	15.0	wet, medium, medium grained sand with gravel	13	0.047	N
	7.3 @ 180	0.08	3.4	gray, silty sand	6	0.053	N
Saline River Richey Road/2S #2	7.3 @ 180	0.08	4.0	gray, silty sand	4	0.057	N
	7.3 @ 180	0.08	4.9	loose, brown, gravel and sand with clay binder	5	0.062	N
	7.3 @ 180	0.08	5.9	moist, gray, clay loam with gravel	3	0.066	N
	7.3 @ 180	0.08	6.4	very loose, fine gravel and sand with clay binder	2	0.068	N
	7.3 @ 180	0.08	7.0	very loose, fine gravel and sand with clay binder	1	0.070	L
	7.3 @ 180	0.08	7.9	loose fine grained sand with gravel and rotten vegetation	6	0.072	N
	7.3 @ 180	0.08	8.5	loose fine grained sand with gravel and rotten vegetation	4	0.073	N
	7.3 @ 180	0.08	9.5	medium, moist, gray, fine to coarse sand with gravel	11	0.074	N
	7.3 @ 180	0.08	10.1	medium, moist, gray, fine to coarse sand with gravel	11	0.075	N
	7.3 @ 87	0.15	10	medium dense, gray sand	15	0.135	N
Cache River FAS 942/off ILL 3 #3	7.3 @ 87	0.15	11	medium dense, gray sand	11	0.135	L
	7.3 @ 87	0.15	12	medium dense, gray sand	18	0.134	N
	7.3 @ 87	0.15	13	medium dense, gray sand	10	0.133	L
	7.3 @ 69	0.26	5	wet, brown, silty sand, loose	5	0.201	L
St. Francis River (Geotec 9) Rt. 60/3 #4	7.3 @ 69	0.26	6	gray sand, very fine to fine with scattered thin clay layers	5	0.223	L
	7.3 @ 69	0.26	8	gray sand, very fine to fine, medium dense to dense	15	0.236	L
	7.3 @ 69	0.26	9	gray sand, very fine to fine, medium dense to dense	22	0.243	N
	7.3 @ 105	0.13	5	Wet, loose, brown fine sand	9	0.103	N
Current River @ SH 328/1	7.3 @ 105	0.13	6	Wet, medium dense, brown sand	12	0.114	N
	7.3 @ 105	0.13	8	Wet, medium dense, brown sand	18	0.121	N

Site/ Borehole Map ID #	Magnitude @ Distance (km)	a_{max}	Depth to Susceptible Sediment (m)	Description of Susceptible Sediment	Blow Count $N_{r(60)}$	Cyclic Stress Ratio	Results ¹
#5	7.3@105	0.13	9	Wet, medium dense, brown to gray sand with organic matter	13	0.124	N
	7.3@105	0.13	11	Wet, medium dense, brown to gray sand with organic matter	9	0.126	L
	7.3@105	0.13	14	Wet, medium dense, gray sand and gravel	10	0.121	N
Black River @ Elgin Ferry/7 #6	7.3@169	0.08	3	Wet, medium dense, gray silty sand and gravel with some organic material (wood)	3	0.053	N
	7.3@169	0.08	5	Wet, medium dense, gray silty sand and gravel with some organic material (wood)	5	0.065	N
	7.3@169	0.07	6	Wet, medium dense, gray silty sand and gravel with some organic material (wood)	13	0.072	N
	7.3@169	0.08	9	Wet, medium dense, gray silty sand and gravel	12	0.078	N
	7.3@169	0.08	12	Wet, medium dense, gray silty sand and gravel with organic material	14	0.078	N
	7.3@246	0.03	5	Moist, medium dense brown sand	8	0.021	N
White River@ US 79/A #7	7.3@246	0.03	6	wet, loose, brown silty sand,	7	0.023	N
	7.3@246	0.03	8	Wet, loose to medium dense, brown sand	7	0.025	N
	7.3@246	0.03	9	wet, medium dense, brown sand with some gravel	22	0.025	N
	7.3@246	0.03	12	wet, medium dense brown sand with some gravel	10	0.025	N
	7.3@246	0.03	14	wet, medium dense brown sand with some gravel	20	0.024	N
	7.3@246	0.03	15	wet, medium dense gray sand	15	0.023	N
	7.3@160	0.09	8	soft, gray fine sand	9	0.084	N
Cross Country Ditch @ US 64/6 #8	7.3@160	0.09	11	compact sand	25	0.086	N
	7.3@60	0.17	3	sand, grey, medium grained	10	0.107	N
Obion River SR 89/1 #10	7.3@60	0.17	4	sand, grey, medium grained	6	0.126	L
	7.3@60	0.17	5	sand, grey, medium grained	16	0.137	N
	7.3@60	0.17	9	sand, grey, medium grained	19	0.154	N
	7.3@60	0.17	10	sand, grey, medium grained, silty	23	0.155	N
	7.3@85	0.15	4	fine gray sand	19	0.110	N
Hatchie Rt 51/2 #11	7.3@85	0.15	6	fine gray sand	16	0.123	N
	7.3@85	0.15	7	medium gray sand	19	0.130	N
	7.3@85	0.15	9	coarse gray sand	22	0.135	N
	7.3@85	0.15	9	coarse gray sand	22	0.135	N

Site/ Borehole Map ID #	Magnitude @ Distance (km)	a_{max}	Depth to Susceptible Sediment (m)	Description of Susceptible Sediment	Blow Count $N_{r(60)}$	Cyclic Stress Ratio	Results ¹
Coldwater US 3/7 #13	7.3@205	0.06	15	medium dense, brown and gray, fine to medium sand with fine gravel, with 2" clay layer @ bottom	23	0.050	N
	7.3@205	0.06	16	medium dense, gray, fine to medium sand, with fine gravel and clay	11	0.049	N
	7.3@205	0.06	18	dense, brown, fine to medium sand, with fine gravel	30	0.045	N
b. Results of liquefaction potential analysis for M 7.8 February 7, 1812 scenario earthquake.							
Skillset Fork RT 600 E/1 #1	7.8 @ 235	0.08	8.2	wet, sandy loam	3	0.053	N
	7.8 @ 235	0.08	8.8	wet, sandy clay loam	2	0.052	N
	7.8 @ 235	0.08	9.8	wet, loose, fine grained sand	5	0.052	N
	7.8 @ 235	0.08	10.4	wet, sandy clay loam with sand lenses	2	0.052	N
	7.8 @ 235	0.08	11.3	wet, sandy clay loam with sand lenses	2	0.052	N
	7.8 @ 235	0.08	11.9	wet, loose, fine grained sand	5	0.052	N
	7.8 @ 235	0.08	13.4	wet, medium, fine grained sand	11	0.055	N
	7.8 @ 235	0.08	14.3	wet, loose, fine grained sand	6	0.059	N
Saline River Richey Road/2S #2	7.8 @ 235	0.08	15.0	wet, medium, medium grained sand with gravel	13	0.061	N
	7.8 @ 180	0.13	3.4	gray, silty sand	6	0.086	N
	7.8 @ 180	0.13	4.0	gray, silty sand	4	0.093	N
	7.8 @ 180	0.13	4.9	loose, brown, gravel and sand with clay binder	5	0.101	L
	7.8 @ 180	0.13	5.9	moist, gray, clay loam with gravel	3	0.108	L
	7.8 @ 180	0.13	6.4	very loose, fine gravel and sand with clay binder	2	0.111	L
	7.8 @ 180	0.13	7.0	very loose, fine gravel and sand with clay binder	1	0.114	L
	7.8 @ 180	0.13	7.9	loose fine grained sand with gravel and rotten vegetation	6	0.118	L
	7.8 @ 180	0.13	8.5	loose fine grained sand with gravel and rotten vegetation	4	0.120	L
	7.8 @ 180	0.13	9.5	medium, moist, gray, fine to coarse sand with gravel	11	0.121	L
Cache River FAS 942/off ILL 3 #3	7.8 @ 180	0.13	10.1	medium, moist, gray, fine to coarse sand with gravel	11	0.122	L
	7.8@87	0.31	10	medium dense, gray sand	15	0.282	L
	7.8@87	0.31	11	medium dense, gray sand	11	0.282	L
	7.8@87	0.31	12	medium dense, gray sand	18	0.280	L
St. Francis River (Geotec 9) Rt. 60/3 #4	7.8@87	0.31	13	medium dense, gray sand	10	0.278	L
	7.8@ 69	0.46	5	wet, brown, silty sand, loose	5	0.360	L
	7.8@ 69	0.46	6	gray sand, very fine to fine with scattered thin clay layers	5	0.400	L
	7.8@ 69	0.46	8	gray sand, very fine to fine, medium dense to dense	15	0.423	L
	7.8@ 69	0.46	9	gray sand, very fine to fine, medium dense to dense	22	0.435	L

Site/ Borehole Map ID #	Magnitude @ Distance (km)	a_{max}	Depth to Susceptible Sediment (m)	Description of Susceptible Sediment	Blow Count $N_{r(60)}$	Cyclic Stress Ratio	Results ¹
Current River @ SH 328/1 #5	7.8@105	0.21	5	Wet, loose, brown fine sand	9	0.164	L
	7.8@105	0.21	6	Wet, medium dense, brown sand	12	0.181	L
	7.8@105	0.21	8	Wet, medium dense, brown sand	18	0.191	L
	7.8@105	0.21	9	Wet, medium dense, brown to gray sand with organic matter	13	0.197	L
	7.8@105	0.21	11	Wet, medium dense, brown to gray sand with organic matter	9	0.199	L
	7.8@105	0.21	14	Wet, medium dense, gray sand and gravel	10	0.191	L
	7.8@169	0.13	3	Wet, medium dense, gray silty sand and gravel with some organic material (wood)	3	0.085	L
	7.8@169	0.13	5	Wet, medium dense, gray silty sand and gravel with some organic material (wood)	5	0.103	N
	7.8@169	0.13	6	Wet, medium dense, gray silty sand and gravel with some organic material (wood)	13	0.114	N
	7.8@169	0.13	9	Wet, medium dense, gray silty sand and gravel	12	0.125	N
Black River @ Elgin Ferry/7 #6	7.8@169	0.13	12	Wet, medium dense, gray silty sand and gravel with organic material	14	0.124	N
	7.8@246	0.08	5	Moist, medium dense brown sand	8	0.058	N
	7.8@246	0.08	6	wet, loose, brown silty sand,	7	0.064	N
	7.8@246	0.08	8	Wet, loose to medium dense, brown sand	7	0.068	N
	7.8@246	0.08	9	wet, medium dense, brown sand with some gravel	22	0.070	N
	7.8@246	0.08	12	wet, medium dense brown sand with some gravel	10	0.070	N
	7.8@246	0.08	14	wet, medium dense brown sand with some gravel	20	0.068	N
	7.8@246	0.08	15	wet, medium dense gray sand	15	0.065	N
	7.8@160	0.14	8	soft, gray fine sand	9	0.129	L
	7.8@160	0.14	11	compact sand	25	0.132	N
Obion River SR 89/1 #10	7.8@60	0.52	3	sand, grey, medium grained	10	0.329	L
	7.8@60	0.52	4	sand, grey, medium grained	6	0.385	L
	7.8@60	0.52	5	sand, grey, medium grained	16	0.422	L
	7.8@60	0.52	9	sand, grey, medium grained	19	0.472	L
	7.8@60	0.52	10	sand, grey, medium grained, silty	23	0.476	L
Hatchie	7.@85	0.32	4	fine gray sand	19	0.240	N

Site/ Borehole Map ID #	Magnitude @ Distance (km)	a_{max}	Depth to Susceptible Sediment (m)	Description of Susceptible Sediment	Blow Count $N_{1(60)}$	Cyclic Stress Ratio	Results ¹
Rt 51/2 #11	7. @85	0.32	6	fine gray sand	16	0.266	L
	7. @85	0.32	7	medium gray sand	19	0.283	L
	7. @85	0.32	9	coarse gray sand	22	0.293	L
Coldwater US 3/7 #13	7.8 @205	0.10	15	medium dense, brown and gray, fine to medium sand with fine gravel, with 2" clay layer @ bottom	23	0.081	N
	7.8 @205	0.10	16	medium dense, gray, fine to medium sand, with fine gravel and clay	11	0.080	N
	7.8 @205	0.10	18	dense, brown, fine to medium sand, with fine gravel	30	0.073	N

¹L- liquefaction likely N- liquefaction not likely

Table G-4 Results of Liquefaction Potential Analysis for M 6.3 January 5, 1843 Scenario Earthquake

Site/ Borehole Map ID #	Magnitude @ Distance (km)	a_{max}	Depth to Susceptible Sediment (m)	Description of Susceptible Sediment	Blow Count $N_{1(60)}$	Cyclic Stress Ratio	Results ¹
Coldwater US 3/7 #13	6.3 @ 111	0.05	10	medium dense, brown and gray, fine to medium sand with	23	0.042	N
	6.3 @ 111	0.05	11	fine gravel, with 2" clay layer @ bottom	11	0.041	N
	6.3 @ 111	0.05	12	medium dense, gray, fine to medium sand, with fine gravel and clay	30	0.038	N

¹L- liquefaction likely N- liquefaction not likely

Table G-5 Results of Liquefaction Potential Analysis for M 6.6 October, 31 1895 Scenario Earthquake

Site/ Borehole Map ID #	Magnitude @ Distance (km)	a_{max}	Depth to Susceptible Sediment (m)	Description of Susceptible Sediment	Blow Count $N_{1(60)}$	Cyclic Stress Ratio	Results ¹
Cache River	6.6 @19	0.30	10	medium dense, gray sand	15	0.279	L
	6.6 @19	0.30	11	medium dense, gray sand	11	0.279	L

Site/ Borehole Map ID #	Magnitude @ Distance (km)	a_{max}	Depth to Susceptible Sediment (m)	Description of Susceptible Sediment	Blow Count $N_{1(60)}$	Cyclic Stress Ratio	Results ¹
FAS 942/off ILL 3 #3	6.6 @ 19	0.30	12	medium dense, gray sand	18	0.277	L
	6.6 @ 19	0.30	13	medium dense, gray sand	10	0.275	L

¹L- liquefaction likely N- liquefaction not likely

Table G-6 Results of Liquefaction Potential Analysis for Commerce fault zone M 6.9 scenario earthquake

Site/ Borehole Map ID #	Magnitude @ Distance (km)	a_{max}	Depth to Susceptible Sediment (m)	Description of Susceptible Sediment	Blow Count $N_{1(60)}$	Cyclic Stress Ratio	Results ¹
St. Francis River (Geotec 9) Rt. 60/3 #4	6.9 @ 14	0.93	5	wet, brown, silty sand, loose	5	0.720	L
	6.9 @ 14	0.93	6	gray sand, very fine to fine with scattered thin clay layers	5	0.800	L
	6.9 @ 14	0.93	8	gray sand, very fine to fine, medium dense to dense	15	0.846	L
	6.9 @ 14	0.93	9	gray sand, very fine to fine, medium dense to dense	22	0.870	L

¹L- liquefaction likely N- liquefaction not likely

Table G-7 Results of liquefaction potential analysis for Eastern Rift margin-north M 6.7 scenario earthquake

Site/ Borehole Map ID #	Magnitude @ Distance (km)	a_{max}	Depth to Susceptible Sediment (m)	Description of Susceptible Sediment	Blow Count $N_{1(60)}$	Cyclic Stress Ratio	Results ¹
Obion River SR 89/1 #10	6.7 @ 10	0.94	3	sand, grey, medium grained	10	0.598	L
	6.7 @ 10	0.94	4	sand, grey, medium grained	6	0.700	L
	6.7 @ 10	0.94	5	sand, grey, medium grained	16	0.766	L
	6.7 @ 10	0.94	9	sand, grey, medium grained	19	0.857	L
	6.7 @ 10	0.94	10	sand, grey, medium grained, silty	23	0.865	L

¹L- liquefaction likely N- liquefaction not likely

Table G-8 Results of liquefaction potential analysis for Eastern Rift margin-south M 6.9 scenario earthquake west of Covington

Site/ Borehole Map ID #	Magnitude @ Distance (km)	a_{max}	Depth to Susceptible Sediment (m)	Description of Susceptible Sediment	Blow Count $N_{1(60)}$	Cyclic Stress Ratio	Results ¹
Hatchie Rt 51/2 #11	6.9 @ 10	1.14	4	fine gray sand	19	0.843	L
	6.9 @ 10	1.14	6	fine gray sand	16	0.937	L
	6.9 @ 10	1.14	7	medium gray sand	19	0.996	L
	6.9 @ 10	1.14	9	coarse gray sand	22	1.029	L

¹L- liquefaction likely N- liquefaction not likely

Table G-9 Results of liquefaction potential analysis for Eastern Rift margin-south scenario M 6.9 and M 7.1 earthquakes northwest of Memphis

Site/ Borehole Map ID #	Magnitude @ Distance (km)	a_{max}	Depth to Susceptible Sediment (m)	Description of Susceptible Sediment	Blow Count $N_{1(60)}$	Cyclic Stress Ratio	Results ¹
a. Results of liquefaction potential analysis for Eastern Rift margin-south M 6.9 scenario earthquake northwest of Memphis.							
Coldwater US 3/7 #13	6.9@70	0.16	15	medium dense, brown and gray, fine to medium sand with fine gravel, with 2" clay layer @ bottom	23	0.135	N
	6.9@70	0.16	16	medium dense, gray, fine to medium sand, with fine gravel and clay	11	0.133	N
	6.9@70	0.16	18	dense, brown, fine to medium sand, with fine gravel	30	0.122	N
b. Results of liquefaction potential analysis for Eastern Rift margin-south M 7.1 scenario earthquake northwest of Memphis							

Site/ Borehole Map ID #	Magnitude @ Distance (km)	a_{max}	Depth to Susceptible Sediment (m)	Description of Susceptible Sediment	Blow Count $N_{1(60)}$	Cyclic Stress Ratio	Results ¹
Coldwater US 3/7 #13	7.1@70	0.16	15	medium dense, brown and gray, fine to medium sand with fine gravel, with 2" clay layer @ bottom	23	0.149	N
	7.1@70	0.16	16	medium dense, gray, fine to medium sand, with fine gravel and clay	11	0.146	L
	7.1@70	0.16	18	dense, brown, fine to medium sand, with fine gravel	30	0.134	N

¹L- liquefaction likely N- liquefaction not likely

Table G-10 Results of liquefaction potential analysis for Eastern Rift margin-south river (fault) picks M 7.1 scenario earthquake west of Memphis

Site/ Borehole Map ID #	Magnitude @ Distance (km)	a_{max}	Depth to Susceptible Sediment (m)	Description of Susceptible Sediment	Blow Count $N_{1(60)}$	Cyclic Stress Ratio	Results ¹
Coldwater US 3/7 #13	7.1@48	0.29	15	medium dense, brown and gray, fine to medium sand with fine gravel, with 2" clay layer @ bottom	23	0.243	N
	7.1@48	0.29	16	medium dense, gray, fine to medium sand, with fine gravel and clay	11	0.239	L
	7.1@48	0.29	18	dense, brown, fine to medium sand, with fine gravel	30	0.219	N

¹L- liquefaction likely N- liquefaction not likely

Table G-11 Results of liquefaction potential analysis for Eastern Rift margin-south river (fault) picks M 6.9 scenario earthquake north of Tunisia

Site/ Borehole Map ID #	Magnitude @ Distance (km)	a_{max}	Depth to Susceptible Sediment (m)	Description of Susceptible Sediment	Blow Count $N_{1(60)}$	Cyclic Stress Ratio	Results ¹
Coldwater/ US 3/7 #13	6.9@15	0.88	15	medium dense, brown and gray, fine to medium sand with fine gravel, with 2" clay layer @ bottom	23	0.742	L
	6.9@15	0.88	16	medium dense, gray, fine to medium sand, with fine gravel and clay	11	0.730	L

Site/ Borehole Map ID #	Magnitude @ Distance (km)	a_{max}	Depth to Susceptible Sediment (m)	Description of Susceptible Sediment	Blow Count $N_{r(60)}$	Cyclic Stress Ratio	Results ¹
	6.9@15	0.88	18	dense, brown, fine to medium sand, with fine gravel	30	0.669	L

¹L- liquefaction likely N- liquefaction not likely

Table G-12 Results of liquefaction potential analysis for Marianna area M 6.7-M7.5 scenario earthquakes

Site/ Borehole Map ID #	Magnitude @ Distance (km)	a_{max}	Depth to Susceptible Sediment (m)	Description of Susceptible Sediment	Blow Count $N_{r(60)}$	Cyclic Stress Ratio	Results ¹
a. Results of liquefaction potential analysis for Marianna area M 6.7 scenario earthquake							
	6.7@55	0.16	15	medium dense, brown and gray, fine to medium sand with fine gravel, with 2" clay layer @ bottom	23	0.134	N
	6.7@55	0.16	16	medium dense, gray, fine to medium sand, with fine gravel and clay	11	0.132	N
	6.7@55	0.16	18	dense, brown, fine to medium sand, with fine gravel	30	0.121	N
b. Results of liquefaction potential analysis for Marianna area M 6.9 scenario earthquake							
	6.9@55	0.19	15	medium dense, brown and gray, fine to medium sand with fine gravel, with 2" clay layer @ bottom	23	0.161	N
	6.9@55	0.19	16	medium dense, gray, fine to medium sand, with fine gravel and clay	11	0.158	L
	6.9@55	0.19	18	dense, brown, fine to medium sand, with fine gravel	30	0.145	N
c. Results of liquefaction potential analysis for Marianna area M 7.0 scenario earthquake							
	7.0@55	0.20	15	medium dense, brown and gray, fine to medium sand with fine gravel, with 2" clay layer @ bottom	23	0.171	N
	7.0@55	0.20	16	medium dense, gray, fine to medium sand, with fine gravel and clay	11	0.168	L
	7.0@55	0.20	18	dense, brown, fine to medium sand, with fine gravel	30	0.154	N
d. Results of liquefaction potential analysis for Marianna area M 7.25 scenario earthquake							
	7.25@55	0.26	15	medium dense, brown and gray, fine to medium sand with fine gravel, with 2" clay layer @ bottom	23	0.219	N
	7.25@55	0.26	16	medium dense, gray, fine to medium sand, with fine gravel and clay	11	0.215	L
	7.25@55	0.26	18	dense, brown, fine to medium sand, with fine gravel	30	0.197	N

Coldwater/
US 3/7
#13

Site/ Borehole Map ID #	Magnitude @ Distance (km)	a_{max}	Depth to Susceptible Sediment (m)	Description of Susceptible Sediment	Blow Count $N_{(60)}$	Cyclic Stress Ratio	Results ¹
e. Results of liquefaction potential analysis for Marianna area M 7.5 scenario earthquake							
	7.5@55	0.33	15	medium dense, brown and gray, fine to medium sand with fine gravel, with 2" clay layer @ bottom	23	0.279	L
	7.5@55	0.33	16	medium dense, gray, fine to medium sand, with fine gravel and clay	11	0.275	L
	7.5@55	0.33	18	dense, brown, fine to medium sand, with fine gravel	30	0.252	N

¹L- liquefaction likely N- liquefaction not likely

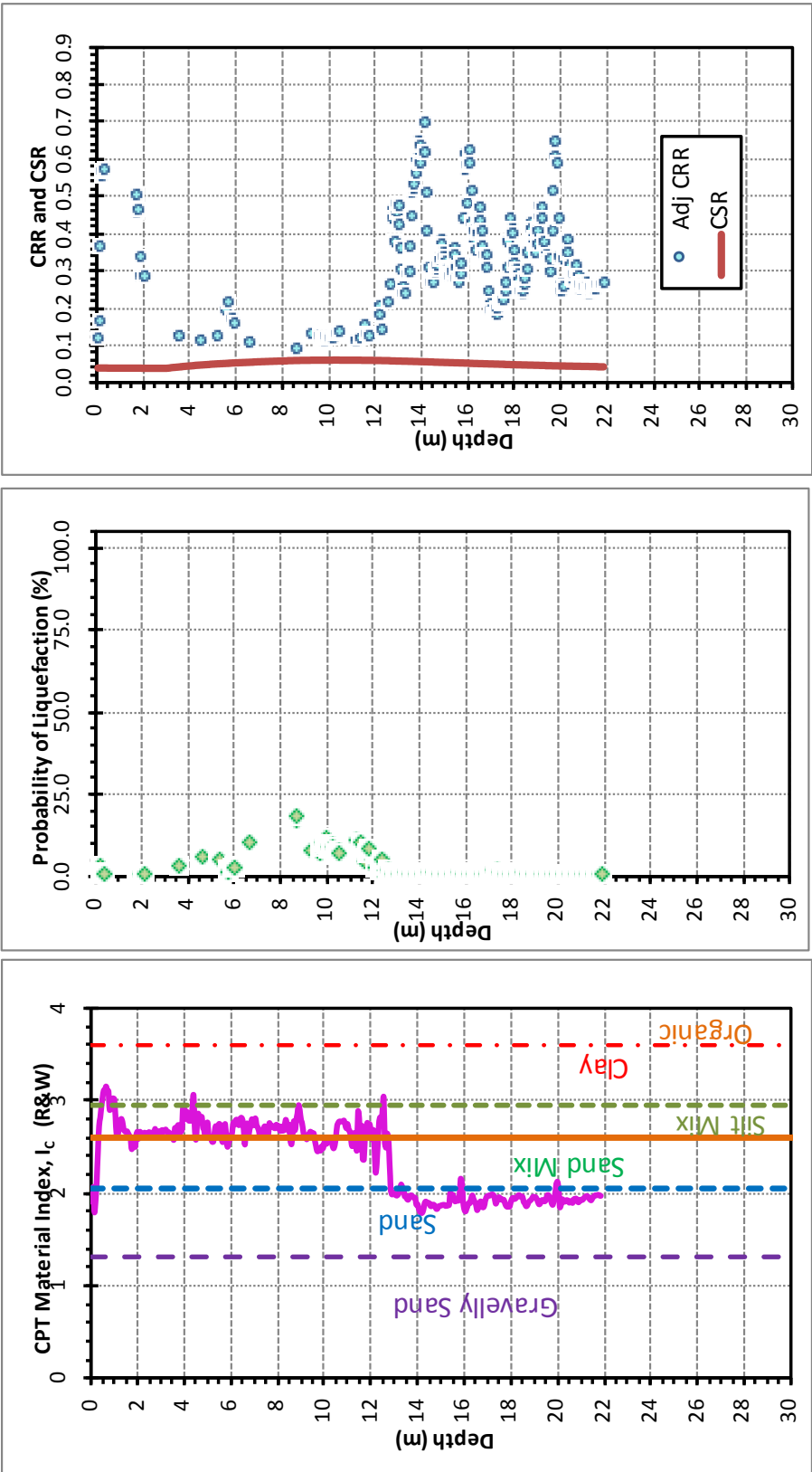


Figure G-1 Results of liquefaction potential analysis for M 6.9 December 16, 1811 scenario earthquake at Marina-Lee #1 site, distance of 161 km. Original CPT sounding used in analysis is from Holzer, U.S. Geological Survey

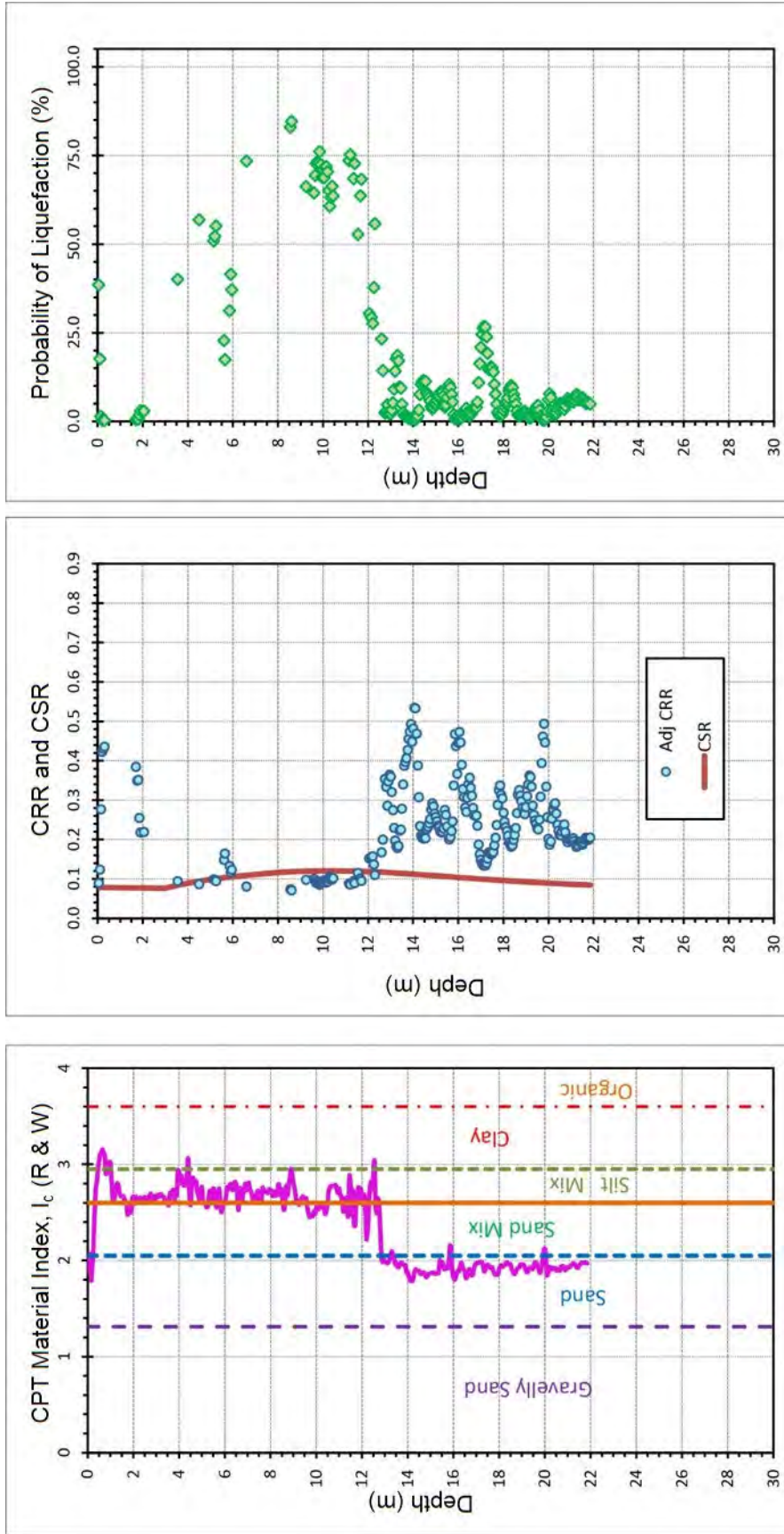


Figure G-2 Results of liquefaction potential analysis for M 7.6 December 16, 1811 scenario earthquake at Marianna-Lee1 site, at distance 161 km. Original CPT sounding used in analysis is from Holzer, U.S. Geological Survey

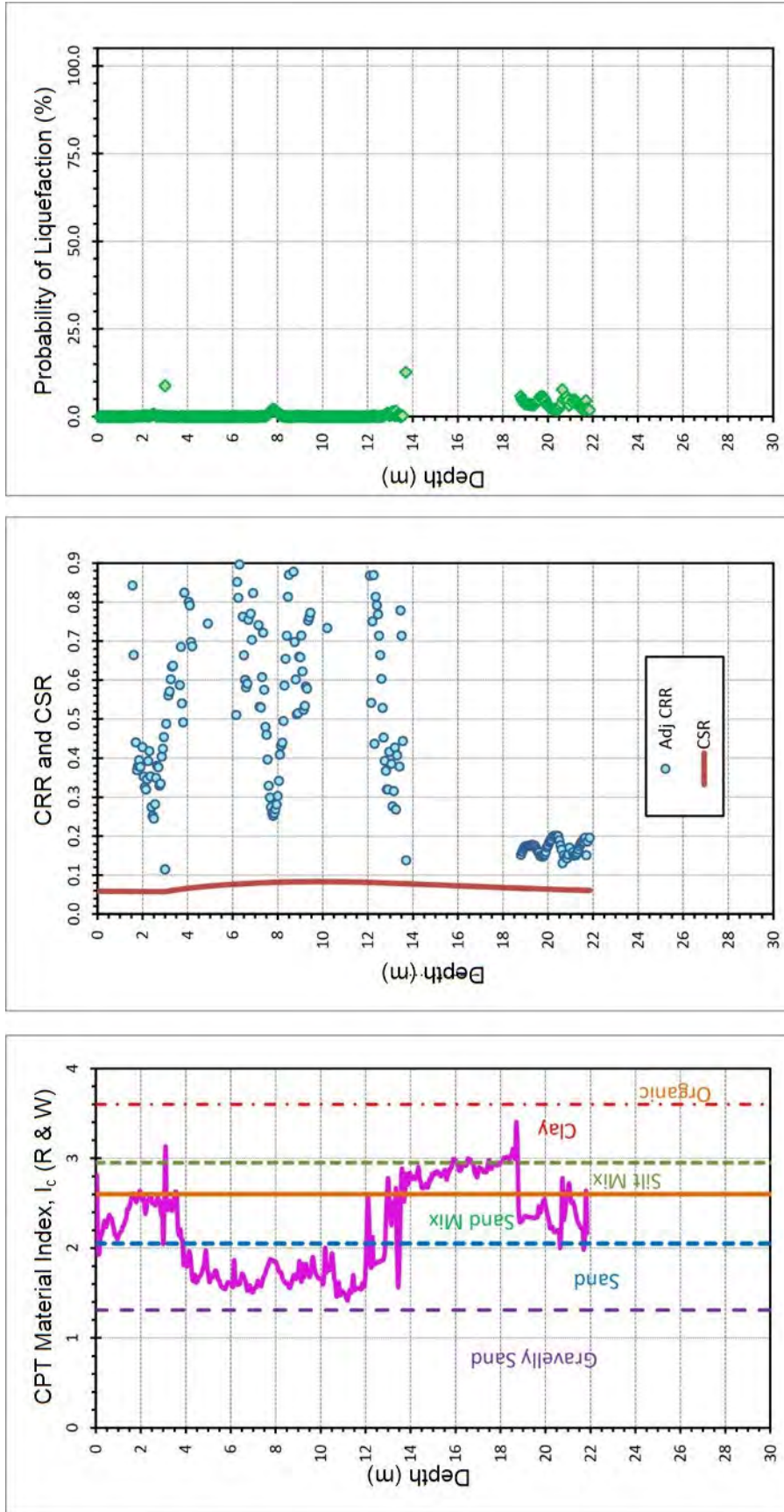


Figure G-3 Results of liquefaction potential analysis for M 6.9 December 16, 1811 scenario earthquake at Wolf River site, distance of 104 km. Original CPT sounding used in analysis is from Schneider et al., 2001

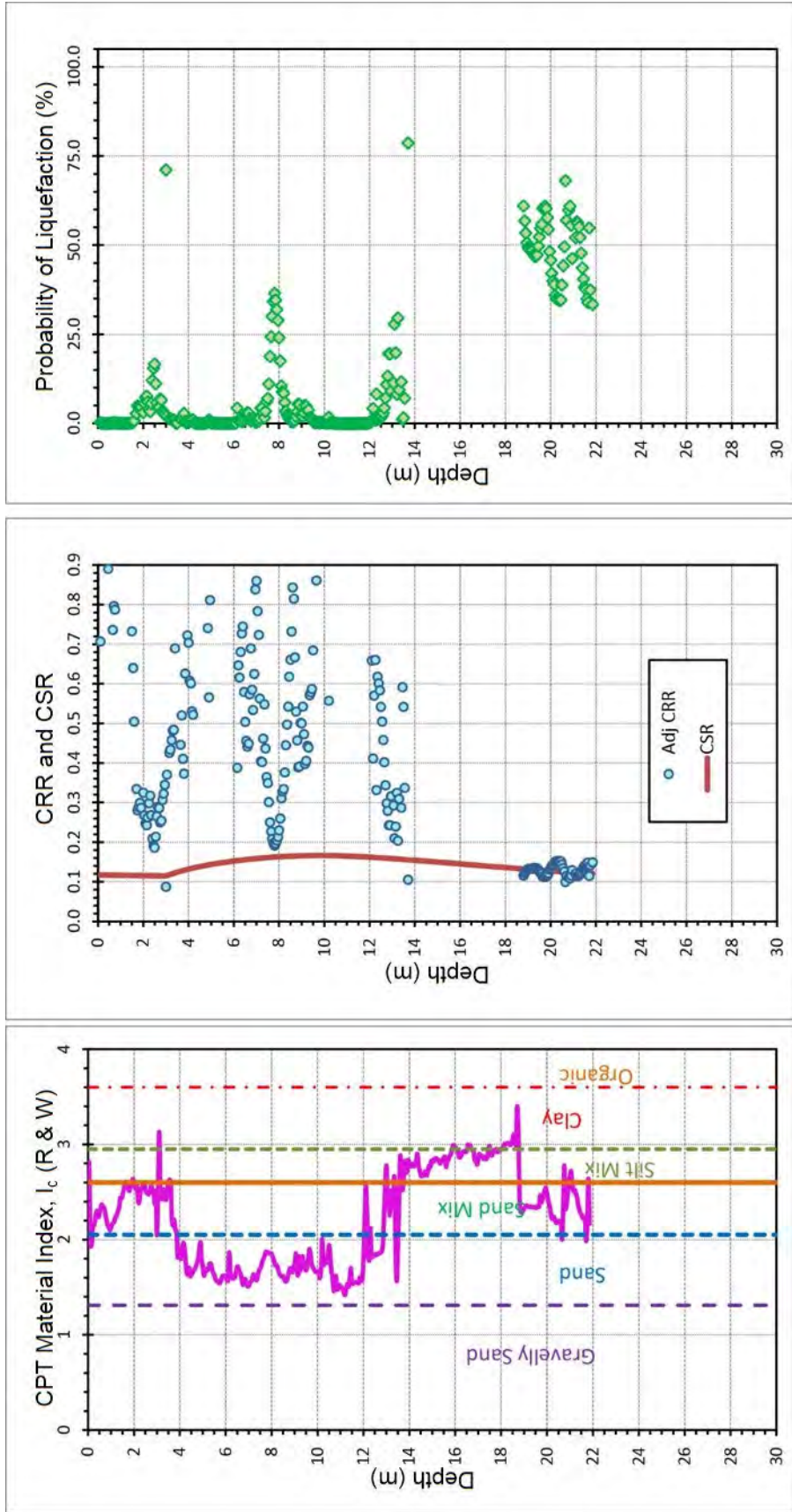


Figure G-4 Results of liquefaction potential analysis for M 7.6 December 16, 1811 scenario earthquake at Wolf River site, distance of 104 km. Original CPT sounding used in analysis is from Schneider et al., 2001

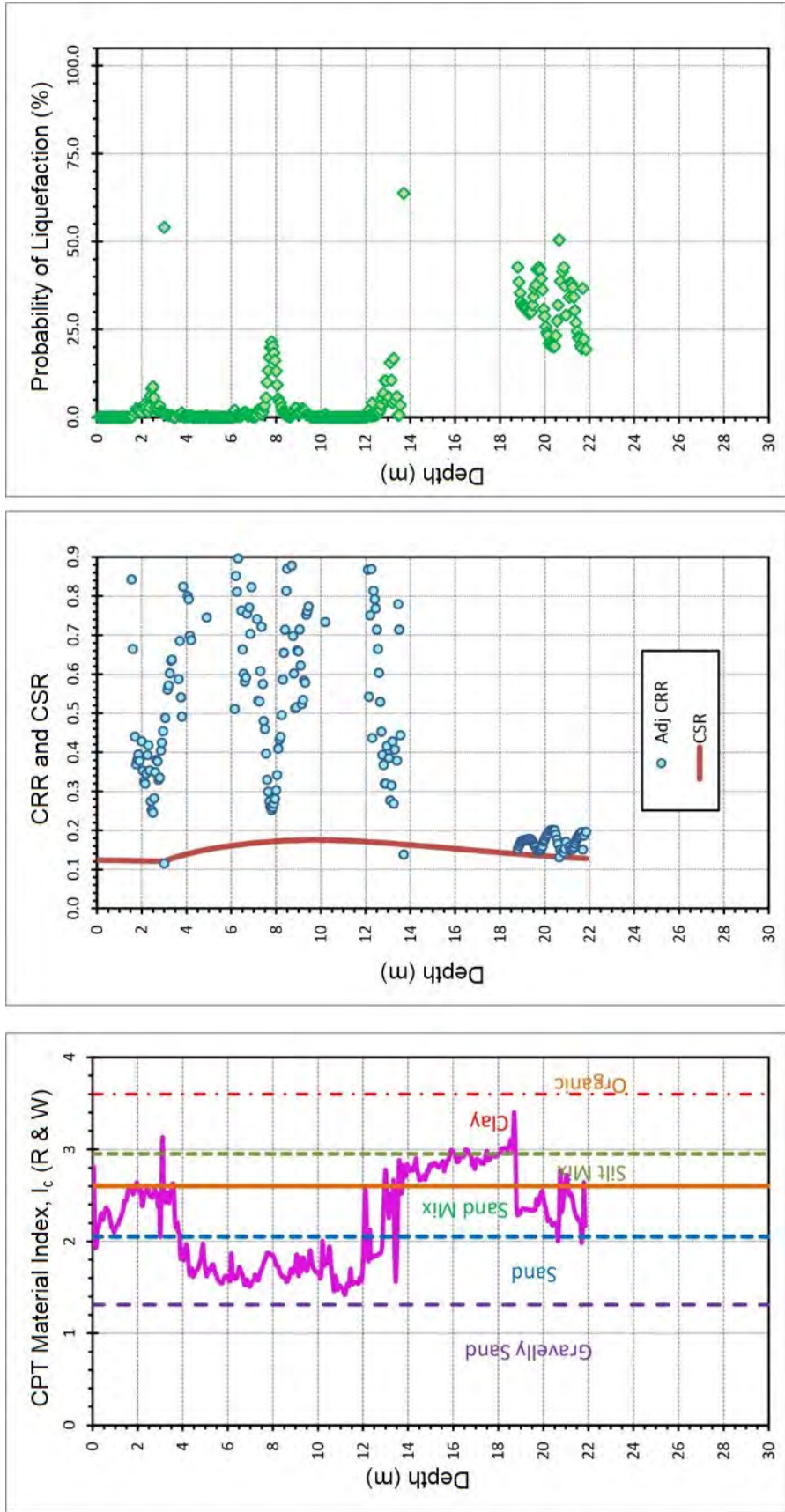


Figure G-5 Results of liquefaction potential analysis at Wolf river site for M 6.9 on Eastern Rift margin-south and south river (picks) scenario earthquake at Wolf River site, distance of 60 km. Original CPT sounding used in analysis is from Schneider et al. (2001)

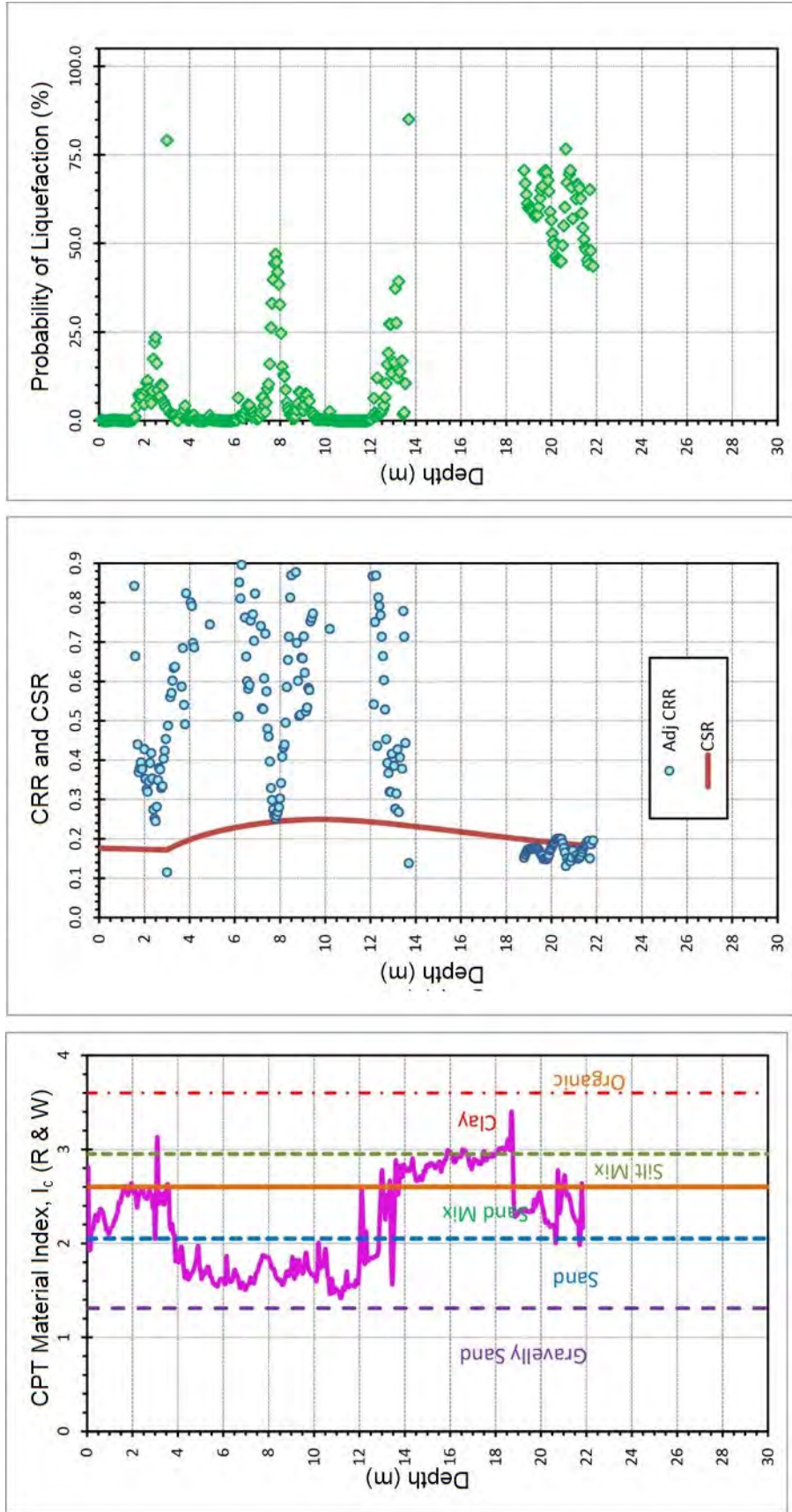


Figure G-6 Results of liquefaction potential analysis at Wolf river site for M 6.9 on Eastern Rift margin-south and south river (picks) scenario earthquakes at Wolf River site, distance of 40 km. Original CPT sounding used in analysis is from Schneider et al. (2001)

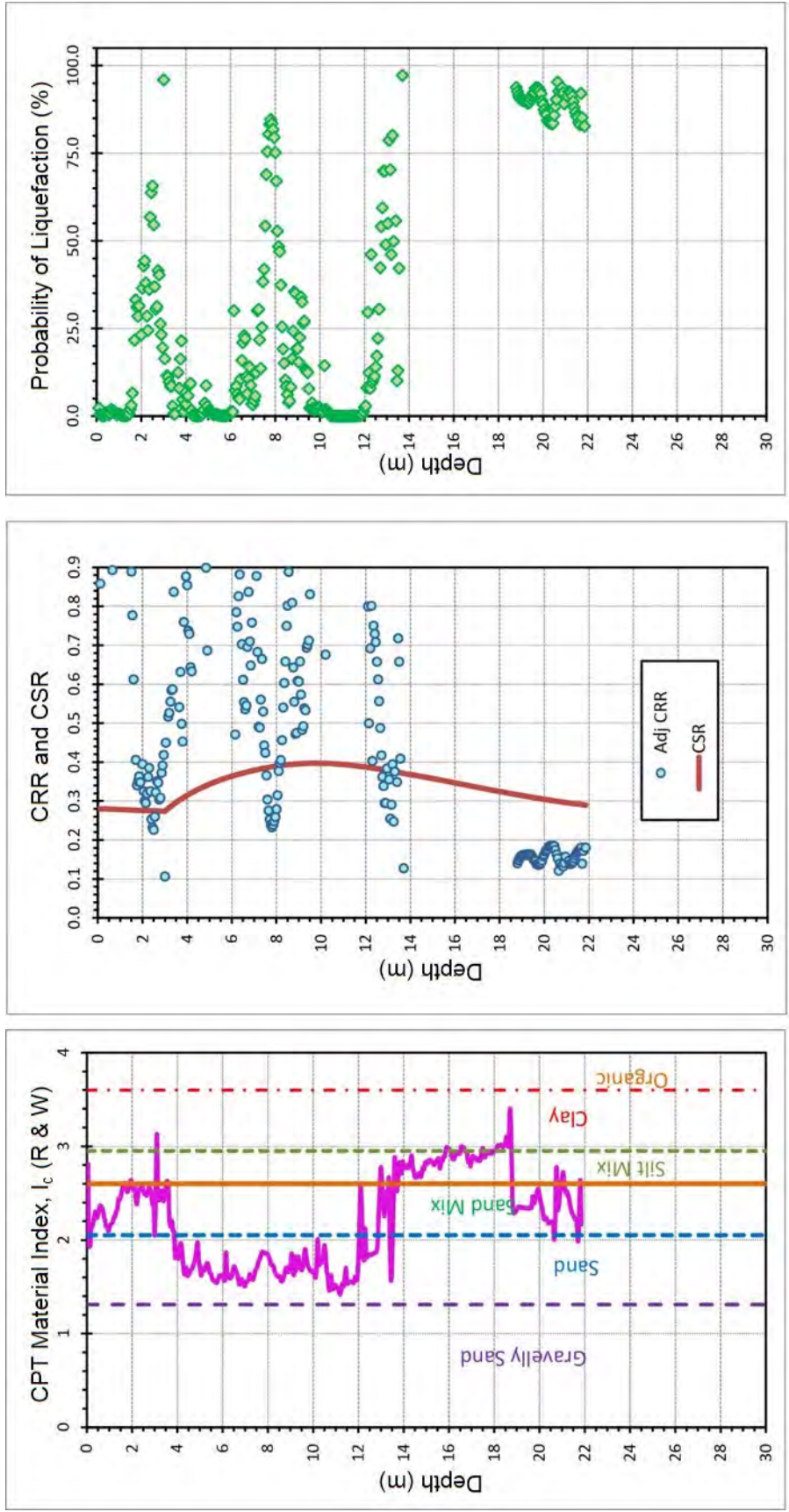


Figure G-7 Results of liquefaction potential analysis for M 7.1 on Eastern Rift margin-south and south river (fault) picks scenario earthquakes at Wolf River site, distance of 40 km. Original CPT sounding used in analysis is from Schneider et al. (2001)

BIBLIOGRAPHIC DATA SHEET

(See instructions on the reverse)

NUREG/CR-7257

2. TITLE AND SUBTITLE

Paleoliquefaction Studies in Moderate Seismicity Regions with a History of Large Events

3. DATE REPORT PUBLISHED

MONTH

June

YEAR

2019

4. FIN OR GRANT NUMBER

5. AUTHOR(S)

Tuttle, M.P., L.W. Wolf, K. Dyer-Williams, P. Mayne, R.H. Lafferty, K. Hess, M.E. Starr, M. Haynes, J. Morrow, R. Scott, T. Busch, P. Villamor, J. Dunahue, M. Rathgeber, K. Tucker, C. Karrenbauer, and C. Moseley

6. TYPE OF REPORT

Technical

7. PERIOD COVERED (Inclusive Dates)

8. PERFORMING ORGANIZATION - NAME AND ADDRESS (If NRC, provide Division, Office or Region, U. S. Nuclear Regulatory Commission, and mailing address; if contractor, provide name and mailing address.)

M. Tuttle & Associates
P.O. Box 345
Georgetown, ME 04548

9. SPONSORING ORGANIZATION - NAME AND ADDRESS (If NRC, type "Same as above", if contractor, provide NRC Division, Office or Region, U. S. Nuclear Regulatory Commission, and mailing address.)

Division of Engineering
Office of Nuclear Regulatory Research
U.S. Nuclear Regulatory Commission
Washington, DC 20555-0001

10. SUPPLEMENTARY NOTES

11. ABSTRACT (200 words or less)

This paleoliquefaction project included a paleoliquefaction study in the New Madrid seismic zone as well as post-earthquake survey for liquefaction features in the Central Virginia seismic zone following the 2011, M, 5.7 Mineral, Virginia, earthquake, development of NUREG/CR-7238 entitled, "Guidance Document: Conducting Paleoliquefaction Studies for Earthquake Source Characterization," and a training workshop on paleoliquefaction studies for U.S. Nuclear Regulatory Commission staff and other members of the nuclear regulatory community. Major discoveries in the New Madrid seismic zone include (1) a possible fault zone in western Tennessee, delineated by northeast-oriented lineaments and large linear sand blows that formed during the A.D. 1811-1812 and A.D. 1450 New Madrid events; (2) sand blows near Paragould, Arkansas, that suggest a previously unrecognized New Madrid earthquake about A.D. 0 ± 200 yr; (3) a sand blow near Blytheville, Arkansas, that supports a previously recognized New Madrid earthquake sequence about B.C. 1050 ± 250 yr; and (4) two to three generations of liquefaction features in northwestern Mississippi that may have formed during an eastern Reelfoot Rift margin event in B.C. 300 ± 250 yr and/or during the Marianna events in B.C. 2850 ± 150 yr, B.C. 3550 ± 150 yr, and B.C. 4850 ± 150 yr.

12. KEY WORDS/DESCRIPTORS (List words or phrases that will assist researchers in locating the report.)

paleoliquefaction,
paleoseismology,
New Madrid seismic zone,
Central Virginia seismic zone,
2011 Mineral Virginia earthquake,
liquefaction features,
active faults, earthquake sources,
radiocarbon dating,
geophysical surveying

13. AVAILABILITY STATEMENT

unlimited

14. SECURITY CLASSIFICATION

(This Page)

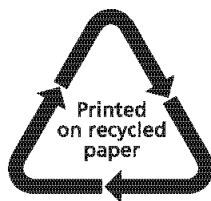
unclassified

(This Report)

unclassified

15. NUMBER OF PAGES

16. PRICE



Federal Recycling Program



UNITED STATES
NUCLEAR REGULATORY COMMISSION
WASHINGTON, DC 20555-0001

OFFICIAL BUSINESS



@NRCgov



NUREG/CR-7257

Paleoliquefaction Studies in Moderate Seismicity Regions with a History of Large Events

June 2019